INSTYTUT BIOCYBERNETYKI I INŻYNIERII BIOMEDYCZNEJ
POLSKIEJ AKADEMII NAUK

OPRACOWYWANIE, OTRZYMYWANIE I BADANIE RUSZTOWAŃ KOMÓRKOWYCH DO HODOWLI CHONDROCYTÓW LUB KOMÓREK MACIERZYSTYCH DO REGENERACJI CHRZĄSTKI STAWOWEJ

ROZPRAWA DOKTORSKA

Mgr. inż. Monika Wasyłeczko

Promotor: Prof. dr hab. inż. Andrzej Chwojnowski

WARSZAWA 2025

Podziękowania

Szczególne podziękowania kieruję do mojego Promotora prof. dr hab. inż. Pana Andrzeja Chwojnowskiego za przekazaną wiedzę, za pomoc merytoryczną, poświęcony czas, cierpliwość, oraz stworzenie zawsze życzliwej i inspirującej atmosfery. Dziękuję również za motywowanie mnie do nauki, pracy i pogłębiania wiedzy.

Wyrazy wdzięczności kieruję także do dr hab. inż. Pani Dorocie Lewińskiej za cenne uwagi i wskazówki udzielone podczas opracowywania oraz analizy niniejszej pracy doktorskiej.

Serdecznie dziękuję Wszystkim, którzy przyczynili się do powstania pracy: mgr inż. Judycie Dulnik, dr mgr inż. Wioletcie Sikorskiej, dr mgr inż. Ewie Łukowskiej oraz tym, których nie wymieniłam z imienia i nazwiska, a którzy okazali mi pomoc i życzliwość.

Dziękuję również Najbliższym – Rodzinie, Przyjaciołom i Znajomym – za wsparcie, wyrozumiałość, motywację i wiarę we mnie.

Dziękuję!

Spis treści

Wykaz publikacji zawartych w rozprawie

Publikacja 1

Monika Wasyłeczko, Wioleta Sikorska and Andrzej Chwojnowski – Review of Synthetic and Hybrid Scaffolds in Cartilage Tissue Engineering, Membranes **2020**, 10(11), 348. https://doi.org/10.3390/membranes10110348
IF: 4, 562
MNiSW: 100

Publikacja 2

Monika Wasyłeczko, Wioleta Sikorska, Małgorzata Przytulska, Judyta Dulnik, Andrzej Chwojnowski – Polyester membranes as 3D scaffolds for cell culture, Desalination and Water Treatment **2021**, 214, 181-193. https://doi.org/10.5004/dwt.2021.26658
IF: 1,383
MNiSW:100

Publikacja 3

Monika Wasyłeczko, Elżbieta Remiszewska, Wioleta Sikorska, Judyta Dulnik, Andrzej Chwojnowski – Scaffolds for Cartilage Tissue Engineering from a Blend of Polyethersulfone and Polyurethane Polymers, Molecules **2023**, 28, 1-25. https://doi.org/10.3390/molecules28073195
IF: 4,927
MNiSW: 140

Publikacja 4

Monika Wasyłeczko, Zuzanna Joanna Krysiak, Ewa Łukowska, Marcin Gruba, Wioleta Sikorska, Aleksandra Kruk, Judyta Dulnik, Jarosław Czubak, Andrzej Chwojnowski – Three-dimensional scaffolds for bioengineering of cartilage tissue, Biocybernetics and Biomedical Engineering **2022**, 42, 494– 511. https://doi.org/10.1016/j.bbe.2022.03.004
IF: 5,687
MNiSW: 200

Publikacja 5

Maciej Płończak, **Monika Wasyłeczko**, Tomasz Jakutowicz, Andrzej Chwojnowski, Jarosław Czubak – Intraarticular Implantation of Autologous Chondrocytes Placed on Collagen or Polyethersulfone Scaffolds: An Experimental Study in Rabbits, Polymers **2023**, 15, 2360. https://doi.org/10.3390/polym15102360
IF: 4,967,
MNiSW:100

Publikacja 6

Maciej Baranowski, **Monika Wasyłeczko**, Anna Kosowska, Andrzej Plichta, Sebastian Kowalczyk, Andrzej Chwojnowski, Wojciech Bielecki, Jarosław Czubak – Regeneration of Articular Cartilage Using Membranes of Polyester Scaffolds in a Rabbit Model, Pharmaceutics **2022**, 14, 1016. https://doi.org/10.3390/pharmaceutics14051016
IF: 6,321
MNiSW: 140

STRESZCZENIE

Ubytki chrząstki stawowej występują w wyniku urazów oraz procesów chorobowych. Nadal stanowią one problem w medycynie regeneracyjnej, a liczba pacjentów cierpiących rośnie w związku ze starzeniem się społeczeństwa, prowadzeniem złego trybu życia, jak również z powodu wzrostu aktywności fizycznej co ma związek z licznymi kontuzjami. Obecnie nie ma skutecznej terapii regeneracji chrząstki stawowej. Praktykowane terapie, takie jak autologiczna chondrogeneza indukowana macierzą (AMIC), mikrozłamania (MF) czy autologiczny przeszczep chondrocytów (ACI) łagodzą problem, ale tylko na jakiś czas. Regeneratem nie jest tkanka chrzęstna szklista tylko nie w pełni wartościowa tkanka szklisto-włóknista, która nie posiada odpowiednich właściwości i jest podatna na dalsze uszkodzenia. Pomocnym rozwiązaniem tego problemu w medycynie jest zastosowanie inżynierii tkankowej. Jest to dziedzina, która wykorzystuje wiedzę z medycyny, biotechnologii oraz inżynierii materiałowej. Umożliwia projektowanie oraz wytwarzanie zamienników uszkodzonych tkanek. Znajduje ona również zastosowanie w regeneracji chrząstki stawowej, gdzie wytwarzane są rusztowania komórkowe, służące jako macierz zewnątrzkomórkowa dla komórek (chondrocyty, komórki macierzyste). Rusztowania powinny spełniać odpowiednie wymagania, aby komórki mogły się w nich zasiedlić i funkcjonować. Tak więc wymagany jest dobór biokompatybilnego materiału o adekwatnych właściwościach mechanicznych oraz biochemicznych. Istotne jest również, aby cała struktura charakteryzowała się odpowiednią architekturą przestrzenną.

Rusztowania komórkowe wykorzystywane są w połączeniu z metodami ACI lub AMIC, gdzie w pierwszym przypadku są one zasiedlane izolowanymi chondrocytami, a w drugim komórkami macierzystymi.

Celem pracy było opracowanie nowych syntetycznych rusztowań do hodowli chondrocytów lub komórek macierzystych. Otrzymane konstrukcje zostały poddane analizie biologicznej i materiałowej, obejmującej testy biodegradacji w płynach fizjologicznych, ocenę właściwości mechanicznych oraz charakterystykę struktury i hydrofilowości powierzchni. Efektywność wybranych rusztowań komórkowych została zweryfikowana zarówno *in vitro*, z użyciem izolowanych chondrocytów ludzkich, jak i *in vivo* w modelu króliczym, gdzie zastosowano je do regeneracji ubytków chrząstki stawowej. Uzyskane wyniki wykazały wysoką biozgodność, skuteczność regeneracyjną oraz całkowitą biodegradację materiału bez oznak toksyczności.

Słowa kluczowe: inżynieria tkanki chrząstna; chrząstka stawowa; chrząstka szklista; rusztowania; wymagania dotyczące rusztowań; rusztowania syntetyczne; chondrocyty; inżynieria tkankowa; medycyna regeneracyjna

ABSTRACT

Articular cartilage defects occur as a result of injuries and pathological processes. They still pose a problem in regenerative medicine, and the number of affected patients is increasing due to the aging population, unhealthy lifestyles, as well as increased physical activity leading to numerous injuries. Currently, there is no effective therapy for regenerating articular cartilage. Practiced therapies such as autologous chondrocyte implantation (ACI), microfracture (MF), or autologous matrix-induced chondrogenesis (AMIC) alleviate the problem, but only temporarily. The regeneration is not hyaline cartilage tissue but rather hyaline-fibrous cartilage tissue lacking appropriate properties and susceptible to further damage. A helpful solution to this problem in medicine is the application of tissue engineering. It is a field that utilizes knowledge from medicine, biotechnology, and materials engineering, enabling the design and manufacture of substitutes for damaged tissues. It also finds application in the regeneration of articular cartilage, where scaffolds are produced to serve as extracellular matrix for cells (chondrocytes, stem cells). They should meet specific requirements for cells to inhabit and function within them. Thus, the selection of a biocompatible material with appropriate mechanical and biochemical properties is required. The scaffold should also have the appropriate spatial structure.

Scaffolds are used in combination with ACI or AMIC methods, where in the first they are seeded with isolated chondrocytes, and in the second, with stem cells.

The aim of this study was to develop novel synthetic scaffolds for the cultivation of chondrocytes or stem cells. The obtained constructs were subjected to biological and material characterization, including biodegradation tests in physiological fluids, assessment of mechanical properties, and analysis of structure and surface hydrophilicity. The performance of selected scaffolds was verified both *in vitro*, using isolated human chondrocytes, and *in vivo* in a rabbit model, where they were applied to repair articular cartilage defects. The results demonstrated high biocompatibility, regenerative effectiveness, and complete biodegradation of the material without signs of toxicity.

Key words: cartilage tissue engineering; articular cartilage; hyaline cartilage; scaffolds; requirements for scaffolds; synthetic scaffolds; chondrocytes; tissue engineering; regenerative medicine

WPROWADZENIE I CEL PRACY

Obecnie coraz więcej osób cierpi na problemy związane z uszkodzeniem chrząstki stawowej (chrząstka szklista), narządu który jest istotnym elementem aparatu ruchu i jest niezbędny do prawidłowego chodzenia. Liczba osób dotkniętych problemami z chrząstką rośnie z roku na rok. Jedną z poważniejszych chorób tkanki jest osteoartoza (OA, ang. Osteoarthritis), na którą cierpi ponad 100 milionów ludzi na świecie. OA powoduje ostry ból, ograniczenie ruchu, a nawet prowadzi do niepełnosprawności. Kolejną przyczyną uszkodzenia chrząstki są kontuzje oraz wypadki. Tak więc zagadnienie jest istotne dla osób, które uprawiają sport rekreacyjnie czy zawodowo. Prowadzenie niezdrowego trybu życia prowadzi do otyłości, która ma także wpływ na uszkodzenie chrząstki (obciążenie aparatu ruchu) [1–5].

Medycyna regeneracyjna nadal poszukuje sposobu na regenerację uszkodzonej chrząstki szklistej. Problem jest znaczący gdyż tkanka ma ograniczony potencjał regeneracyjny [6–8]. Leczenie kliniczne ma na celu złagodzenie skutków urazów, a nie naprawę uszkodzonych miejsc. Dzięki inżynierii tkankowej istnieje możliwość regeneracji chrząstki szklistej za pomocą proponowanych rozwiązań [9,10]. W związku z szybkim rozwojem wiedzy w tym zakresie pojawiły się nowe możliwości zabiegów rekonstrukcyjnych chrząstki, takich jak zastosowanie autogennych przeszczepów chondrocytów pacjenta umieszczonych na rusztowaniu (ACI, ang. Autologus Cartilage Implantation). ACI przyczynia się jedynie do otrzymania regeneratu o właściwościach zbliżonych do chrząstki szklistej [11–13]. Obiecującą metodą leczenia zmian chrzęstnych jest również autologiczna chondrogeneza indukowana macierzą (AMIC, ang. Autologous Matrix Induced Chondrogenesis) [10,13,14].

Rusztowania komórkowe (skafoldy, membrany) odgrywają główną rolę w tych metodach, działając jako tymczasowa matryca dla chondrocytów lub komórek macierzystych. Dlatego muszą być one starannie zaprojektowane, aby naśladować właściwości natywnej macierzy chrząstki szklistej. Tylko wtedy zagwarantuje to odpowiednie środowisko dla chondrocytów – do ich przyłączania się, migracji i proliferacji [15,16].

Rusztowania powinny spełniać określone wymagania, takie jak biokompatybilność, przestrzenna struktura i odpowiednie właściwości mechaniczne. Materiał rusztowania powinien być biozgodny, nie wywoływać stanów zapalnych, biodegradowalny, oraz stabilny w środowisku wodnym, aby zapewnić prawidłowy rozwój komórkom [15–19].

Ze względu na brak odpowiednich rusztowań w najbardziej obiecujących metodach terapeutycznych ACI oraz AMIC do regeneracji chrząstki szklistej, podjęłam badania, w których ustaliłam następujące cele:

- Dobór odpowiednich prekursorów (generatów) porów, które zapewnią uzyskanie w rusztowaniu makroporów ułożonych w nieregularną sieć tworzącą odpowiednie środowisko dla komórek oraz generatorów mikroporów, które zapewnią odpowiednio przepływ składników odżywczych, tlenu oraz usuwanie metabolitów w membranie. Materiał generujący makro- i mikropory powinien być łatwo rozpuszczalny w rozpuszczalnikach, które jednocześnie nie rozpuszczają biomateriału bazowego. Tak więc, w ramach otrzymania adekwatnej struktury rusztowania postanowiłam zastosować między innymi włókninę, która w strukturze ma liczne i nierównomierne ułożone włókna;
- Opracowanie sposobu otrzymania nowych rusztowań syntetycznych z biomateriałów ((kopolimer laktyd-ko-kaprolakton (PCLA) i z mieszanki biodegradowalnego poliuretanu (PUR) oraz polieterosulfonu (PES) metodą inwersji faz z dodatkiem włókniny i innych prekursorów porów;
- Otrzymanie rusztowań z PES, które zostały wcześniej opracowane w Instytucie Biocybernetyki i Inżynierii Biomedycznej (IBIB), na których przeprowadziłam hodowlę komórkową z wykorzystaniem izolowanych chondrocytów ludzkich, pozyskanych z odpadów pooperacyjnych. Wyniki z hodowli porównałam z rusztowaniem z poli-L-laktydu (PLLA).
- Przeprowadzenie badań in vivo przez współpracujących lekarzy ortopedów na otrzymanych membranach z PES oraz z PCLA w celu wykazania ich przydatności do regeneracji chrząstki stawowej.

W ramach osiągnięcia ustalonych celów, podjęłam się wykonać następujące zadania:

- Analiza struktury (wielkość, rozmieszczenie, kształt i objętość porów), ocena wytrzymałości mechanicznej, czasu degradacji i cytotoksyczności otrzymanych rusztowań;
- Przeprowadzenie degradacji rusztowań z wykorzystaniem 1M roztworu NaOH, buforowanego roztworu fizjologicznego (PBS), roztworu Hanka (HBSS) oraz sztucznego osocza (SBF);
- Ocena stopnia degradacji rusztowań oraz porównanie rusztowań przed i po degradacji;

- Testowanie wybranych rusztowań w badaniach in vitro (np. obserwacja chondrocytów, żywotność komórek, analiza elementarna, barwienie) oraz w badaniach in vivo na modelu zwierzęcym (królik) we współpracy z lekarzami ortopedami.

WYKAZ SKRÓTÓW

AC – (ang. articular cartilage) chrząstka stawowa

ACI – (ang. Autologus cartilage implantation) autologiczny przeszczep chondrocytów

AMIC – (ang. Autologous Matrix Induced Chondrogenesis) autologiczna chondro geneza indukowana macierzą

CAD – (ang. Computer-Aided Design) projektowanie wspomagane komputerowo

DMEM – (ang. Dulbecco's Modified Eagle Medium) modyfikowana pożywka Eagle'a Dulbecco

ECM – (ang. extracellular matrix) macierz zewnątrzkomórkowa

FBS – (ang. Fetal bovine serum) płodowa surowica bydlęca

GPC – (ang. Gel Permeation Chromatography) chromatografia żelowa

HA – (ang. hyaluronic acid) kwas hialuronowy

HBBS – (ang. Hanks' Balanced Salt solution) roztwór soli Hanka

IBIB – Instytut Biocybernetyki i Inżynierii Biomedycznej

IPPT – Instytut Podstawowych Problemów Techniki

LIPS – (ang. Liquid induced chase separation) inwersja faz w układzie rozpuszczalnik-nierozpuszczalnik

MF – (ang. microfracture) mikrozłamania

Mn – średnia masa molowa

MSCs – (ang. Mesenchymal stem cells) mezenchymalne komórki macierzyste

Mw – średnia wagowo masa molowa

OA – (ang. Osteoarthritis) osteoartroza

OATS – (ang. Osteochondral Autografts) przeszczepy chrzęstno-kostne

PAN – Polska Akademia Nauk

PBS – (ang. Phosphate buffered saline) buforowany roztwór soli fizjologicznej

PCL – poli-ε-kaprolakton

PCLA – poli(L-laktyd-ko-ε-kaprolakton)

PEG – poli(glikol etylenowy)

PES – polieterosulfon

PGA –poliglikolid

PLA – polilaktyd

PLLA – poli-L-laktyd

PUR – poliuretan

PVP – poliwinylopirolidon

RP – (ang. Rapid prototyping) techniki szybkiego prototypowania

RZS – reumatoidalne zapalenie stawów

SBF – (ang. stimulated body fluid) sztuczne osocze

SEM – (ang. Scanning Electron Microscopy) skaningowa mikroskopia elektronowa

TE – (ang. tissue engineering) inżynieria tkankowa

TIPS – (ang. thermal inducted phase separation) termicznie indukowana inwersja faz

3DP – (ang. 3 dimensional printing) drukowanie trójwymiarowe

PRZEGLĄD LITERATURY

1. Wprowadzenie

W ostatnich latach medycyna poczyniła znaczne postępy. Udało się znaleźć wiele rozwiązań w leczeniu chorób, tkanek, czy też narządów. Nadal istnieją nie do końca poznane, skuteczne terapie na leczenie wielu chorób oraz sposobów na regenerację uszkodzonych tkanek, narządów. Zadaniem medycyny regeneracyjnej jest opracowanie i stosowanie metod leczenia tkanek i organów, które wwyniku chorób, uszkodzeń, starzenia się lub wrodzonych wad utraciły swoją funkcję [1,20–22]. Ciało ludzkie niestety nie zawsze ma zdolność do samoleczenia. Jednym zdziałów medycyny regeneracyjnej jest inżynieria tkankowa (ang. Tissue Engineering, TE). Nauka, która łączy w sobie biologię, biotechnologię oraz inżynierię materiałową. Jej zadaniem jest naprawa tkanek, narządów poprzez wykorzystanie odpowiednich biomateriałów, komórek, czy też czynników wzrostu [20,23,24].

Zadaniem inżynierii tkankowej jest między innymi otrzymanie bio-komponentów o odpowiedniej strukturze,które będą stanowić macierz dla prawidłowego funkcjonowania komórek, tak jak w naturalnym dla nich środowisku. Wykorzystywany biomateriał powinien zapewniać odpowiednie właściwości mechaniczne, fizyczne, chemiczne, adhezję oraz proliferację komórkom. Takie podejście zapewni odpowiednie mikrootoczenie oraz zagwarantuje odtworzenie i regenerację tkanki [19,22,23,25].

Inżynieria tkankowa jest szczególnie istotna w przypadku tkanek i narządów, które nie mają możliwości do samoregeneracji. Należą do nich między innymi trzustka, wątroba czy też chrząstka szklista [1,20,23]. Ważnym aspektem inżynierii tkankowej jest rekonstrukcja tkanki chrzęstnej szklistej. Jest on istotny ze względu na częste uszkodzenia narządu w wyniku urazów, chorób i jej bardzo ograniczonej zdolności do regeneracji. Uszkodzenie chrząstki stawowej dotyczy milionów ludzi, w szczególności osób starszych (przeważnie kobiet) oraz sportowców [1–3]. Wielkość globalnego rynku naprawy chrząstki stanowiła 1,47 mld USD w 2022 roku i oczekuje się, że do 2032 roku osiągnie wartość około 4,62 mld USD [26]. Naprawa chrząstki jest wykonywana w celu wyleczenia uszkodzonej chrząstki otaczającej stawy, złagodzenia bólu i sztywności oraz odzyskania ruchomości i funkcji stawów. Ponadto może opóźnić lub zatrzymać rozwój zapalenia stawów [1–3].

Obecnie nie ma jeszcze skutecznej terapii do regeneracji chrząstki stawowej, ale najbardziej obiecujące rezultaty mają metody rekonstrukcji chrząstki, w których wykorzystywane są rusztowania trójwymiarowe (skafoldy, membrany) [9,10].

2. Chrząstka stawowa

Tkanka chrzęstna (chrząstka) to rodzaj tkanki łącznej, która jest zbudowana z komórek chrzęstnych (chondrocytów) osadzonych w istocie międzykomórkowej, bogatej we włókna kolagenowe i proteoglikany. Nie zawiera ona naczyń nerwowych, ani krwionośnych. Substancje odżywcze wnikają do niej jedynie poprzez proces dyfuzji. W zależności od jej lokalizacji i właściwości, chrząstkę można podzielić na trzy główne rodzaje [27–30]:

- Chrząstka włóknista (ang. fibrocartilage) – jest to najmniej elastyczny rodzaj tkanki chrzęstnej. Zawiera liczne włókna kolagenowe, głównie kolagen typu I, i w porównaniu do chrząstki szklistej zawiera znacznie mniej proteoglikanów. Jest obecna między innymi w dyskach międzykręgowych kręgosłupa czy też w łączeniach ścięgien z kością. Zapewnia ona trwałość i wytrzymałość [31];
- Chrząstka szklista (ang. hyaline cartilage) – najbardziej powszechny rodzaj tkanki chrzęstnej. Charakteryzuje się gładką powierzchnią i jest obecna w stawach, nosie, tchawicy, krtani i innych częściach ciała. Składa się ona głównie z kolagenu typu II i proteoglikanów w tym siarczanu chondroityny. Funkcje chrząstki szklistej obejmują amortyzację stawów, utrzymywanie kształtu struktur i uczestniczenie w procesie wzrostu kości [32];
- Chrząstka sprężysta (ang. elastic cartilage) – jest bardziej elastyczna od chrząstki szklistej, gdyż zawiera więcej włókien elastycznych. Tak więc występuje w miejscach, gdzie wymagana jest większa elastyczność, na przykład buduje małżowinę uszną, nagłośnię oraz część zewnętrznego przewodu słuchowego [33].

Jakoś życia w dużym stopniu zależy od sprawnego aparatu ruchu. Jego uszkodzenie ma wpływ na dyskomfort podczas codziennych czynności, w tym chodzenie, a nawet siedzenie. Staw kolanowy ma złożoną morfologię, gdzie właśnie chrząstka szklista spełnia bardzo ważną rolę. Tworzy ona powierzchnię stawową. Zapewnia poślizg oraz amortyzuje obciążenia w trakcie ruchu. Tkankę tworzą w około 5 procentach chondrocyty, które

zawieszone są w macierzy międzykomórkowej (~95 procent chrząstki). Chrząstka składa się z 4 warstw (Rysunek 1), które różnią się pod względem składu: włókien kolagenowych (dominujący jest kolagen typu II oraz w niewielkiej ilości kolagenu typu IX i X), ilości proteoglikanu oraz różnych proporcji chondrocytów. Naczynia krwionośne kończą się w podchrzęstnej warstwie kości, co ma wpływ na niski potencjał regeneracyjny chrząstki [8,32,34].

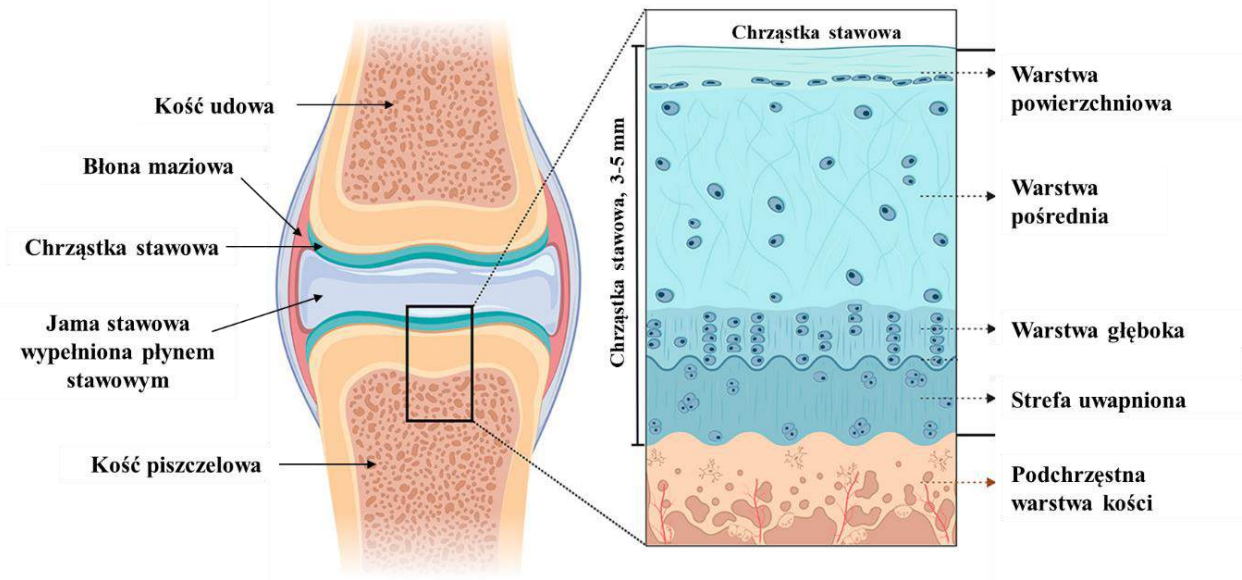

Rysunek 1. Położenie chrząstki stawowej w kolanie oraz jej warstwowa budowa. Rycina została zmodyfikowana na podstawie literatury [35].

Do uszkodzenia narządu może dojść w wyniku urazów (kontuzja, wypadki), prowadzenia nie zdrowego trybu życia (otyłość), chorób (np. osteoartroza, reumatoidalne zapalenie stawów). Uszkodzenie tkanki lub postępujący zanik chrząstki sprawia przewlekły, ostry ból, spastyczność, ograniczony zakres ruchu, a nawet doprowadzić może do niepełnosprawności. Niestety, ze względu na brak ukrwienia, naczyń limfatycznych i unerwienia chrząstka stawowa ma ograniczoną zdolność do regeneracji. Dlatego też istotne jest szybkie zdiagnozowanie uszkodzenia w celu wprowadzenia odpowiedniego leczenia [6–8].

Powszechnie występującą chorobą układu ruchu jest osteoartroza (OA, ang. osteoarthritis), która dotyka ponad 7% ludzi na całym świecie (około 528 milionów). Jest to choroba zwyrodnieniowa stawów, która przyczynia się do wtórnych zmian zwyrodnieniowych co ma wpływ na uszkodzenia tkanek budujących staw. Przewlekłe schorzenie, które z czasem objawia się znacznym ograniczeniem ruchomości stawów, obciążając jakość życia, a nawet prowadząc do niepełnosprawności. Częstość

występowania OA wzrasta wraz z przybieraniem na wadze, wiekiem, płcią żeńską i prawdopodobieństwem uprawiania sportu lub pracy, które niosą ze sobą wysokie ryzyko urazu stawu. Otyłość to kluczowy czynnik ryzyka dla rozwoju OA, potrafiący potroić ryzyko wystąpienia choroby stawu kolanowego. OA staje się coraz powszechniejsza z upływem czasu. W ciągu lat 1990-2019 jej występowanie wzrosło o 48%. Prognozy wskazują, że tendencja ta będzie się utrzymywać, zwłaszcza w krajach o silnej gospodarce rynkowej, takich jak Ameryka Północna i Europa. W tych regionach ludność starzeje się, a także coraz więcej osób cierpi na otyłość, co dodatkowo przyczynia się do wzrostu zachorowań na OA [4,5,36–38].

3. Metody leczenia chrząstki szklistej

Obecnie, mimo znacznego postępu w medycynie regeneracyjnej, wciąż brakuje sposobu na naturalne odtworzenie chrząstki szklistej. Regeneratem jest tkanka włóknisto-szklista, która ma jedynie zbliżone właściwości do chrząstki szklistej. Z czasem jest ona podatna na dalsze uszkodzenia. Ze względu na niemalże znikomą aktywność chrząstki do samoregeneracji należy szybko zastosować odpowiednie leczenie. W zależności od stopnia uszkodzenia wykorzystuje się leczenie zachowawcze i operacyjne, które mają wpływ na zahamowanie i częściową regenerację tkanki [9,10]. Leczenie zachowawcze stosuje się w przypadku drobnych, powierzchniowych uszkodzeń chrząstki. Do najbardziej popularnych należą: terapia iniekcyjna, farmakoterapia doustna, fizjoterapia, odpowiednia dieta, ortezy i inne zaopatrzenie ortopedyczne [9,38,39]. W przypadku głębszych uszkodzeń narządu wykorzystuje się metody chirurgiczne, takie jak: mikrozłamania (ang. microfracture, MF), autologiczna chondrogeneza indukowana macierzą (Autologous Matrix Induced Chondrogenesie, AMIC), autologiczny przeszczep chondrocytów (Autologous Chondrocytes Implantation, ACI), przszczepy chrzęstno-kostne (Osteochondral Autografts, OATS), czy też endoprotezy powierzchniowe. W przypadku większych zmian w chrząstce szklistej, najbardziej obiecującymi metodami są: ACI i AMIC [5,9,10,40].

W celu zwiększenia regeneracji chrząstki, opcjonalnie można dostarczyć czynników wzrostu, które są pomocne przy wspieraniu komórek naprawczych, szczególnie w przypadku problematycznego gojenia [9,24,40].

3.1. Metoda ACI

Do najbardziej obiecujących metod chirurgicznych zmierzających do odtworzenia chrząstki szklistej należą ACI i AMIC (Rysunek 2) [9,10].

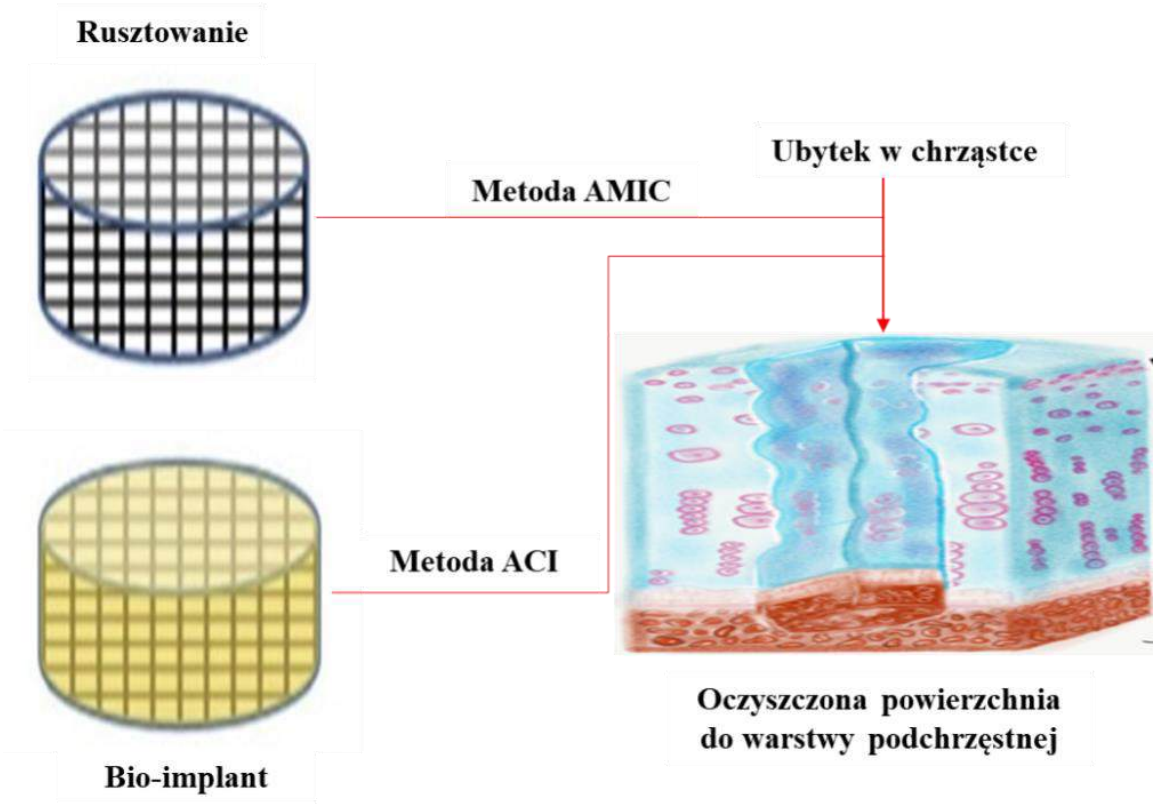

Rysunek 2. Ogólny schemat, który przedstawia wykorzystanie rusztowań w metodach ACI i AMIC. Rycina została przygotowana na podstawie literatury [41].

Metoda ACI (Rysunek 3) przebiega w dwóch etapach. W pierwszym etapie wykonuje się biopsję z nieobciążonych miejsc chrząstki pacjenta. Następnie wyizolowane komórki, z pobranej tkanki, hoduje się na matrycy w laboratorium do momentu uzyskania stosownej liczby komórek. W drugim etapie otrzymany bio-implant jest wszczepiany w odpowiednio przygotowane, oczyszczone miejsce uszkodzenia. Technika ACI wiąże się z wysokim kosztem – dwa zabiegi operacyjne, hodowla komórek, zakup macierzy (matryca, rusztowanie, membrana, podłoże), długa rehabilitacja i liczne wizyty kontrolne u specjalistów. Skuteczność metody została potwierdzona wieloma badaniami klinicznymi [11–13,41].

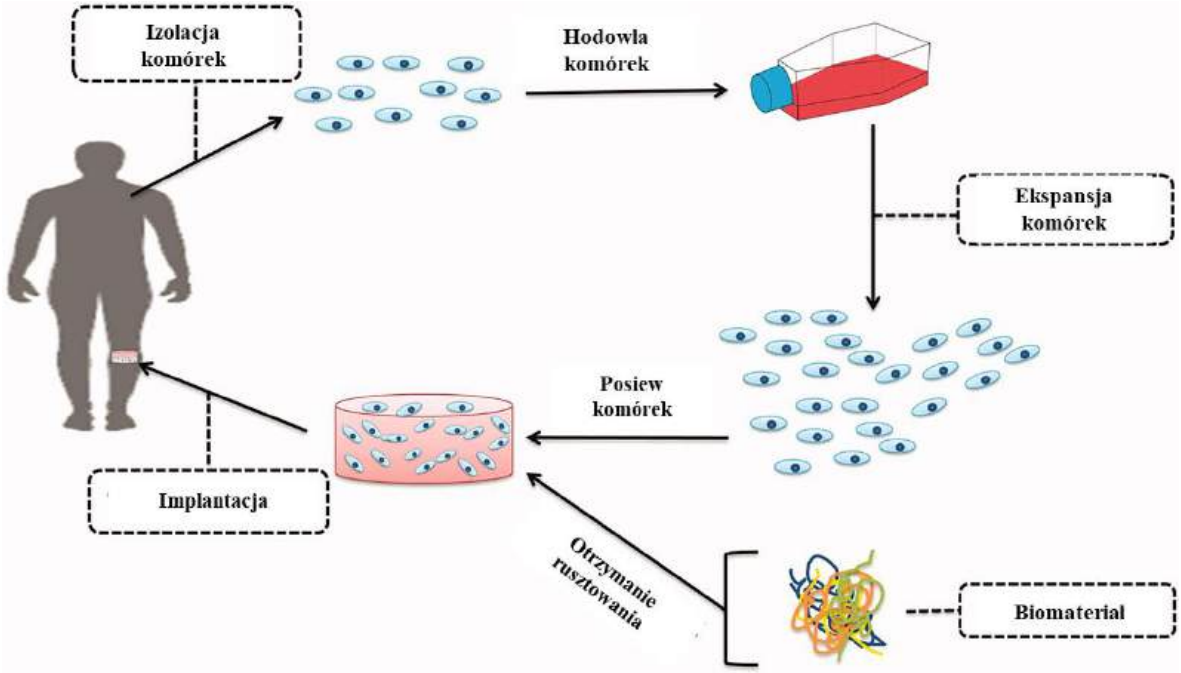

Rysunek 3. Ogólny schemat metody autologicznego przeszczepu chondrocytów (ACI) z wykorzystaniem rusztowania. Rycina zmodyfikowana została na podstawie literatury [42].

3.2. Metoda AMIC

Metoda AMIC (Rysunek 4) jest mniej inwazyjna od techniki ACI ze względu na jednoetapowość. W pierwszej kolejności, w miejscu uszkodzenia chrząstki, wykonywany jest zabieg operacyjny w celu usunięcia pozostałości uszkodzonej chrząstki do warstwy podchrzęstnej. Następnie wykonuje się technikę MF, która polega na nawiercaniu (drilling) około 10-12 otworów w celu dostania się do szpiku kostnego i wywołania krwawienia na powierzchnię ubytku [43]. Przygotowaną powierzchnię pokrywa się rusztowaniem, którego zadaniem jest stabilizacja procesu tworzenia skrzepu. Z warstwy podchrzęstnej następuje migracja wielopotencjalnych mezenchymalnych komórek progenitorowych do miejsca uszkodzenia [44,45]. Rusztowanie pełni rolę swoistej struktury, która nie tylko łączy, ale także chroni komórki, umożliwiając im przekształcenie się w chondrocyty. Te zaś są kluczowe w procesie odbudowy chrząstki szklistej [10,13,14].

Niestety, w badaniach zaobserwowano, że w metodzie AMIC (podobnie jak w metodzie ACI) możliwe jest uzyskanie jedynie tkanki włóknisto-szklistej o właściwościach zbliżonych do chrząstki szklistej [10].

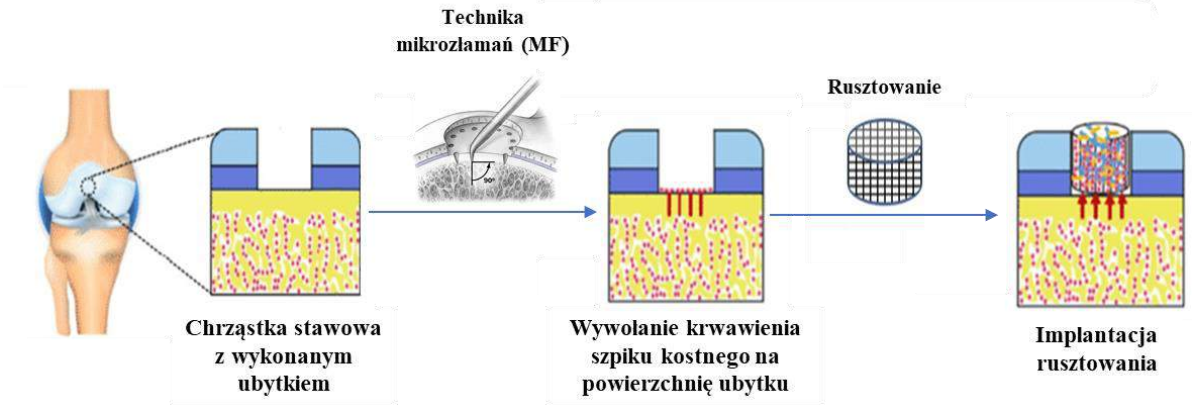

Rysunek 4. Schemat przedstawiający metodę AMIC. Rycina zmodyfikowana została na podstawie literatury [46].

Metoda AMIC posiada jednak szereg znaczących zalet. Jest zdecydowanie bardziej skuteczna od MF i bardziej ekonomiczna od metody ACI. Obecnie w metodzie wykorzystywane są komercyjnie dostępne rusztowania z kolagenu [10,13,14].

W obu metodach, ACI i AMIC bardzo ważną rolę odgrywają rusztowania, które mają służyć jako macierz podtrzymująca i zapewniająca prawidłowe funkcjonowanie komórkom (chondrocyty i komórki macierzyste).

4. Rusztowania do hodowli chondrocytów

Rusztowania do hodowli chondrocytów występują w różnych formach. W zależności od zastosowania, kluczowe jest dopasowanie odpowiedniej metody i materiału, aby mogły one wykazywać odpowiednie właściwości. Podłoża są zazwyczaj formowane w postaci rusztowań 3D, hydrożeli, nanowłókien lub ich kombinacji. W rozdziale zaprezentowane zostaną ogólne wymagania, które powinny być spełnione przez rusztowania oraz materiały polimerowe wykorzystywane zarówno do produkcji skafoldów komercyjnych, jak i rusztowań, które znajdują zastosowanie w badaniach przedklinicznych. Ponadto omówione zostaną najbardziej znane metody otrzymywania rusztowań [47–49].

4.1. Wymagania dla rusztowań

W celu zapewnienia prawidłowych warunków migracji, adhezji, wzrostu i rozmnażania komórek, rusztowania do hodowli chondrocytów czy też komórek

macierzystych powinny spełniać szereg istotnych warunków [15–18]. Poniżej zostały przedstawione niezbędne wymagania, którym powinny sprostać rusztowania:

- **Biokompatybilność** – Rusztowanie musi cechować się biokompatybilnością, co oznacza, że nie powinno wywoływać reakcji zapalnych ani aktywacji układu immunologicznego w żywym organizmie. W związku z tym istotny jest wybór odpowiedniego materiału, właściwych środków generujących pory oraz rozpuszczalników;
- **Odpowiednia struktura –** Wymagane jest aby rusztowanie naśladowało trójwymiarową strukturę tkanki chrzęstnej (natywną macierz). Pory powinny posiadać określoną wielkość i wynosić powyżej 20 μm (wielkość chondrocytów), przy czym najkorzystniejszy jest rozmiar porów około 150-250 μm dla rozwoju chondrocytów, w przypadku komórek macierzystych najbardziej odpowiednie są pory o wielkości powyżej 300 μm. Struktura powinna tworzyć spójną sieć połączonych ze sobą porów, co umożliwi migrację komórek, komunikację międzykomórkową i rozwijanie się tkanki. Dodatkowo rusztowanie powinno być półprzepuszczalne, aby umożliwić transport składników odżywczych, cząsteczek sygnałowych, tlenu i produktów przemiany materii. Górna warstwa podłoża musi być perforowana, co umożliwi komórkom penetrację do wnętrza. Natomiast dolna warstwa powinna być wystarczająco zwarta, aby zapobiec wypadnięciu komórek z membrany. Aby spełnić te wymagania należy dobrać odpowiednią metodę otrzymywania rusztowań [50];
- **Właściwości mechaniczne –** Rusztowanie powinno posiadać odpowiednie właściwości mechaniczne (elastyczność, wytrzymałość na rozciąganie), które są zbliżone do tkanki chrzęstnej szklistej aby komórki mogły rozwijać się w środowisku zbliżonym do naturalnego. Jest to istotne ze względu na ich unieruchomienie w stawie za pomocą typowych technik chirurgicznych (klejenie, szycie). Chrząstka szklista ma moduł Younga wynoszący około 10 MPa [51];
- **Kontrolowana degradacja** – Degradacja rusztowania, które ma być użyte do implantacji, powinna być powiązana z naturalnym zastąpieniem implantu nową tkanką chrzęstną. W zależności od wielkości uszkodzenia, czas regeneracji chrząstki stawowej wynosi około 12 miesięcy [52].

Przestrzenna struktura rusztowania jest niezbędna, aby zapobiec różnicowaniu chondrocytów do postaci komórek podobnych do fibroblastów. Chondrocyty hodowane na

płaskich podłożach tracą zdolność do syntezy niezbędnych białek, koniecznych do formowania chrząstki szklistej [53,54]. Ponadto, wielkość porów wynosząca około 150 μm zwiększa proliferację chondrocytów i utrzymanie fenotypu specyficznego dla chondrocytów [55]. Implant powinien być łatwy w obróbce podczas zabiegu chirurgicznego [53].

Przy projektowaniu rusztowań do regeneracji chrząstki należy uwzględnić wszystkie wyżej wymienione cechy.

4.2. Materiały wykorzystywane do produkcji rusztowań

Rusztowania powinny być wykonane z materiałów, które nie tylko są biokompatybilne, ale także ulegają biodegradacji do substancji nietoksycznych i niezapalnych dla organizmu. Dodatkowo muszą być odporne na warunki fizjologiczne, takie jak pH i temperatura ciała. Materiały stosowane do produkcji rusztowań można podzielić na dwa rodzaje: naturalne i syntetyczne polimery bądź ich kombinacja (materiały hybrydowe) [15,17,18,47,56–59]. Jako naturalne materiały wykorzystuje się przeważnie kolagen [56,60,61], kwas hialuronowy (HA) [62,63], chitozan [64,65], czy też fibrynę [44,66,67]. Są one szeroko stosowane w produkcji rusztowań do regeneracji chrząstki gdyż wykazują znaczną biokompatybilność i biodegradowalność, a większość z nich występuje naturalnie w ludzkim organizmie. Niestety, posiadają one pewne wady. Ulegają szybkiej hydrolizie co się wiąże z utratą odpowiedniej struktury rusztowania. Ich niska stabilność mechaniczna nie sprzyja utrzymaniu komórek w membranie przez dłuższy czas. Dodatkowo, metody otrzymywania rusztowań z polimerów naturalnych są ograniczone ze względu na ich słabą odporność na zmiany parametrów takich jak wysoka temperatura, ciśnienie [15,18,44,47,56,57,68–70].

Powszechnie stosowanymi materiałami syntetycznymi do rusztowań są: polilaktyd (PLA) [71–73], poliglikolid (PGA) [71,74], polieterosulfon (PES) [75–78], polikaprolakton (PCL) [79,80]. Polimery syntetyczne mogą być wykorzystywane do produkcji o różnych kształtach membran, za pomocą wielu technik, zapewniając przy tym dobre właściwości mechaniczne, fizyczne i chemiczne. Wiele z nich ulega degradacji do składników, które są metabolizowane w organizmie. Co więcej, czas degradacji można kontrolować poprzez ich łączenie w kopolimery lub mieszanki [56,57,69,70,81–91].

Materiały syntetyczne także mają wady. Ich produkty degradacji mogą powodować skutki uboczne dla organizmu gospodarza. Są to głównie kwasy powstające w efekcie

hydrolizy poliestrów. Mogą one być toksyczne dla komórek podczas hodowli lub nawet mogą wywoływać reakcję zapalną w organizmie gospodarza [19,44,50,69,70,92–94].

4.3. Metody wytwarzania rusztowań

Odpowiednią architekturę, parametry mechaniczne czy też formę skafoldu można uzyskać poprzez dobranie odpowiedniej metody produkcji rusztowań. W literaturze przedstawionych jest wiele różnych technik wytworzenia membran 3D. Wśród nich, do najpowszechniej stosowanych można zaliczyć: metody szybkiego prototypowania (ang. RP, rapid prototyping), inwersję faz, czy też elektroprzędzenie [17,50,69,70,95–98].

Metody szybkiego prototypowaniato, grupa bardziej zaawansowanych technik, które umożliwią wytwarzanie trójwymiarowych obiektów z precyzyjną kontrolą przestrzenną. Rusztowania można uzyskiwać stopniowo, warstwa po warstwie, zgodnie z projektem wygenerowanym za pomocą oprogramowania komputerowego do modelowania CAD (ang. Computer-Aided Design) lub danych z tomografii komputerowej [69,99,100]. W modelu zawarte są szczegółowe informację odnośnie rozmiaru oraz struktury rusztowania. Do najbardziej popularnej techniki RP można zaliczyć drukowanie 3D (3DP, ang. 3 dimensional printing). Polega ona na podawaniu materiału do drukarki 3D w postaci płynnej, przędzy lub proszku. Drukarka następnie kontroluje proces nanoszenia materiału, zgodnie z cyfrowym modelem, warstwa po warstwie, aż do utworzenia całego obiektu. Niezwiązany proszek jest następnie usuwany (Rysunek 5). Druk 3D można wykorzystać do precyzyjnego kontrolowania struktury rusztowań. Wymaga to jednak ścisłego monitorowania struktury materiału i właściwości mechanicznych rusztowania. Dzięki 3DP można dostosować kształt i wielkość rusztowania do regeneracji chrząstki. Metoda umożliwia precyzyjne tworzenie skafoldów z różnych materiałów w tym hydrożeli [99,101–104].

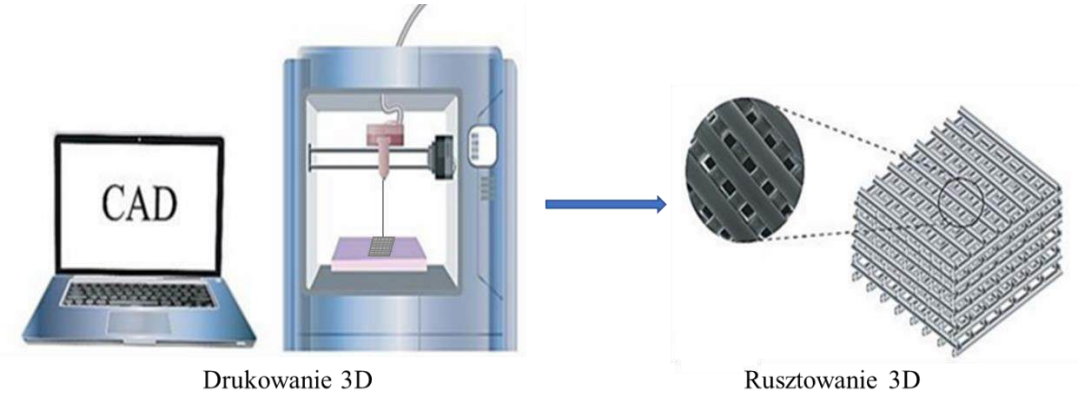

Rysunek 5. Metoda drukowania 3D rusztowań. Ilustracja została przygotowana na podstawie literatury [105].

Jedną z częściej wykorzystywanych metod do otrzymywania rusztowań do hodowli chondrocytów jest inwersja faz. Podstawowy etap tej metody polega na utworzeniu jednofazowego systemu dwuskładnikowego, zawierającego polimer i rozpuszczalnik. Następnie wprowadzany jest czynnik, który wywołuje rozdzielenie faz. Może to być temperatura, wówczas technika określana jest jako termicznie indukowana inwersja faz (TIPS, ang. Thermal inducted phase separation) [69,106–109]. Bardziej powszechną techniką jest inwersja faz w układzie rozpuszczalnik-nierozpuszczalnik (LIPS, ang. liquid-induced phase separation), gdzie separacja faz indukowana jest nierozpuszczalnikiem. Odpowiednio uformowany roztwór polimeru jest zanurzany w nierozpuszczalniku polimeru co powoduje wytrącenie polimeru. Właściwości otrzymanych rusztowań są głównie determinowane przez rodzaj użytego rozpuszczalnika i nierozpuszczalnika, stężenie polimeru i temperaturę kąpieli żelującej [105]. W metodach TIPS oraz LIPS można uzyskać membrany o różnej porowatości i wielkości porów [110–112]. Dodatkowo w metodzie LIPS można wpłynąć na strukturę rusztowania poprzez dodatek prekursora porów do wcześniej przygotowanego roztworu polimeru lub podczas tworzenia membrany. Takie podejście sprzyja tworzeniu porów o większych rozmiach i uzyskaniu wyższej porowatości. Prekursory porów są ostatecznie usuwane z rusztowania za pomocą odpowiedniego rozpuszczalnika (wymywanie prekursorów) [76,97,98,113–116]. Na rysunku poniżej (Rysunek 6) został przedstawiony schemat metody LIPS [117].

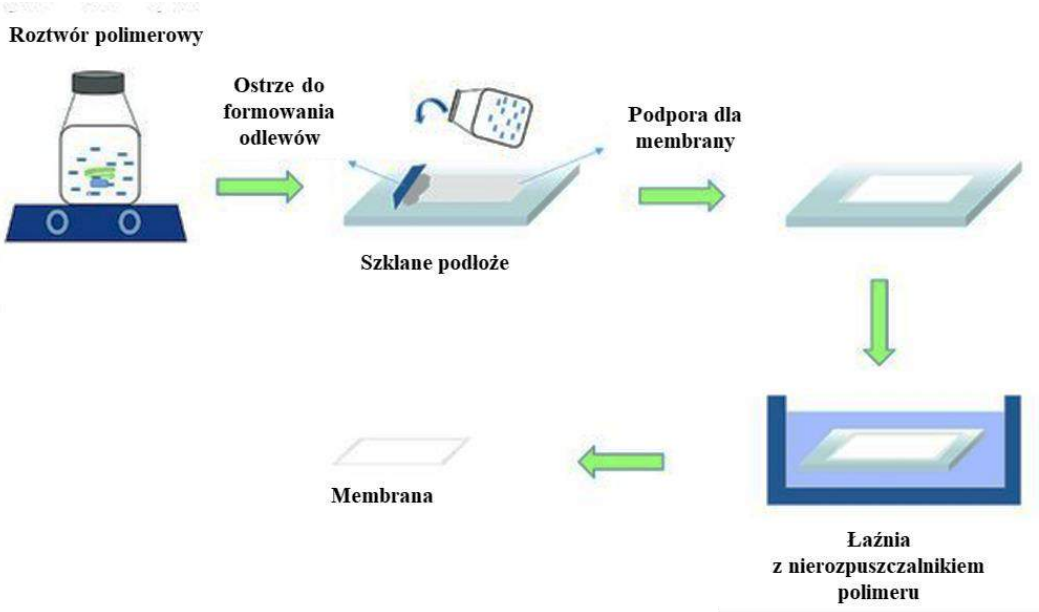

Rysunek 6. Schemat otrzymywania rusztowań metodą mokrej inwersji faz. Ilustracja została przygotowana na podstawie literatury [117].

Jako kolejną metodą wykorzystywaną do otrzymywania rusztowań do hodowli komórkowej jest technika elektroprzędzenia. Jest to prosty i efektywny sposób, który pozwala uzyskiwać włókna zarówno z naturalnych, jak i syntetycznych polimerów (Rysunek 7). W technice wykorzystuje się siły elektrostatyczne do produkcji włókien o grubości mikro i nanometrów ułożonych w mniej lub bardziej uporządkowany sposób. Uzyskane skafoldy charakteryzują się wysoką porowatością, elastycznością i dobrymi właściwościami mechanicznymi, ale jedynie w przypadku wykorzystania polimerów syntetycznych [97,118–123].

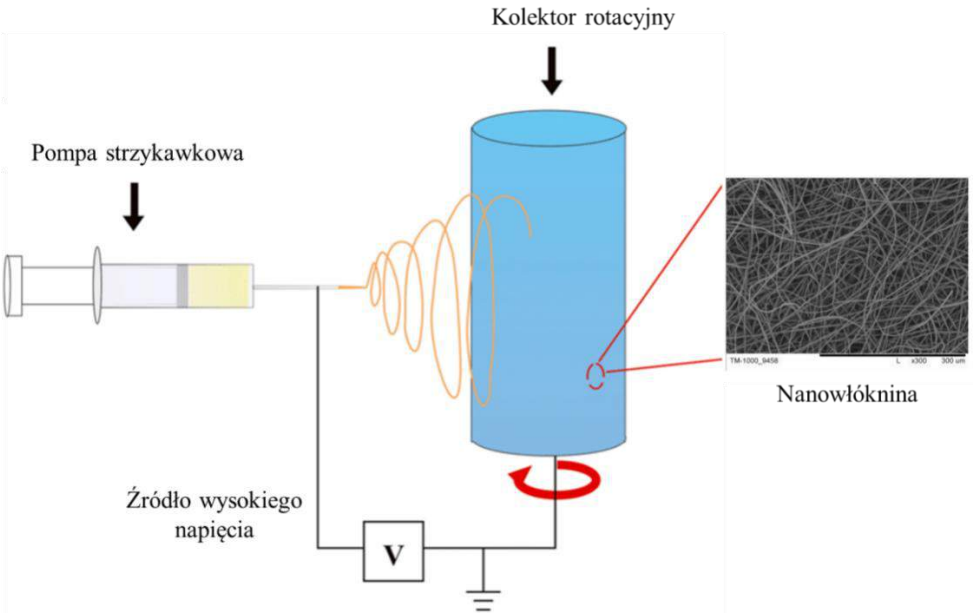

Rysunek 7. Metoda elektroprzędzenia. Obraz został przygotowany na podstawie literatury [123].

5. Rusztowania komercyjne

Obecnie wiele rusztowań przechodzi testy przedkliniczne i kliniczne. Komercyjne rusztowania stosowane w regeneracji chrząstki są zazwyczaj wykonane z naturalnych polimerów, głównie z kolagenu. Tabela 1 przedstawia przykłady komercyjnych rusztowań, w tym ich materiały i technikę implatacji. Ze względu na wspomniane wady naturalnych materiałów, rusztowania te nie spełniają odpowiednich wymagań (niska stabilność mechaniczna i szybka hydroliza). Szybko tracą swoją strukturę, ponieważ przekształcają się w formę żelową. W wyniku regeneracji uzyskuje się bezwartościową chrząstkę włóknistą, która w perspektywie jest podatna na dalsze uszkodzenia. W związku z tym, ten rodzaj membrany nie ma odpowiednich właściwości do tworzenia chrząstki szklistej [15,18,96,124–126].

Tabela 1. Rusztowania komercyjne wykorzystywane do regeneracji chrząstki stawowej.

Nazwa produktu	**Materiał**	**Metoda implatacji**
NeoCart® [53,89,126,127]	Kolagen typu I	ACI lub AMIC
ChondroGide [89,126]	Kolagen typu I / III	ACI lub AMIC
ACI-Maix™ [53,128]	Kolagen typu I / III	ACI lub AMIC
Hyalofast® [126,129,130]	Ester benzylowy kwasu hialuronowego	ACI lub AMIC
Cartipatch® [53,126,127]	Agaroza i alginian	ACI
NOVOCART® 3D – Aesculap Orthopaedics [53,56,89,126]	Kolagen typu Ii siarczan chondroityny	ACI
CaReS® [53,56,89,126]	Kolagen typu I	ACI lub AMIC
CARTISTEM® [131–133]	Kwas hialuronowy	AMIC
Chondrotissue® [126,134]	Kwas hialuronowy, poliglikolid	AMIC
BioSeed®- C [98,135]	Poliglikolid/polilaktyd, polidioksanon	ACI
MACI® [136,137] **Maix®** [138]	Kolagentypu I/III	ACI lub AMIC
Atelocollagen1® [138]	Kolagentypu I	ACI lub AMIC
BST-CarGel® [139]	chitozani β-glicerofosforan	AMIC
Agili-C™ [140–144]	Aragonit - odmiana węglanu wapnia	Wywiercanie otworu w kości, poniżej ubytku
CartiFill™ [145,146]	Kolagen typu I	AMIC
TruFit CB® [143,147,148]	Kompozyt składający się z kopolimeru glikolid-ko-laktyd, siarczanu wapnia i włókien poliglikolidowych	AMIC
MaioRegen [143,149–151]	Kolagen typu I i hydroksyapatyt wzbogacony magnezem	AMIC

Jednym z częściej stosowanych jest rusztowanie **Chondro-Gide** (Rysunek 8). Szerokoporowata membrana wykonana z kolagenu typu I / III.

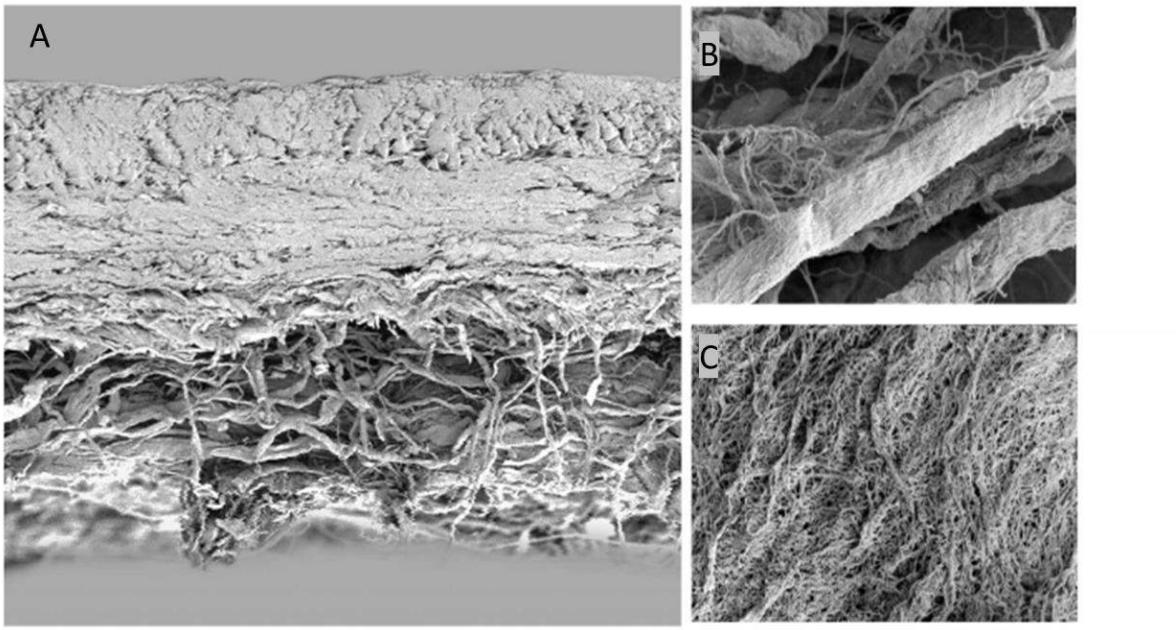

Rysunek 8. Fotomikrografy ze skaningowego mikroskopu elektronowego (SEM) rusztowania Chondro-Gide: A – przekrój poprzeczny, B – warstwa górna, C – warstwa dolna. Powiększenie: A – x100, B, C – x1500. Rysunek został przygotowany na podstawie literatury [152,153].

Rusztowanie **TruFit CB®** jest jednym z przykładów dostępnych na rynku resorbowalnych, syntetycznych implantów dwufazowych, wykonanych z opatentowanego kompozytu, w skład którego wchodzą: kopolimer glikolid-ko-laktyd, siarczan wapnia i włókna poliglikolidowe [143,147,148].

MaioRegen to wielowarstwowa matryca, która składa się z kolagenu i hydroksyapatytu (HA) wzbogaconego magnezem (Rysunek 9). Produkt naśladuje tkanki chrzęstne i kostno-chrzęstne, zarówno pod względem składu chemicznego, jak i mikro- i nanostruktury. Skafold jest dostępny w trzech różnych konfiguracjach: MaioRegenPrime, MaioRegenSlim i MaioRegen Chondro+. Reprezentują one konkretne rozwiązania w leczeniu różnych faz wczesnych patologii artretycznych: MaioRegenPrime do leczenia zmian kostno-chrzęstnych z poważnym uszkodzeniem kości podchrzęstnej, MaioRegenSlim do leczenia zmian kostno-chrzęstnych z nieznacznie uszkodzoną kością podchrzęstną i MaioRegen Chondro+ do leczenia zmian chrzęstnych [143,149–151,154].

Rysunek 9. Rusztowanie MaioRegen. Rycina została przygotowana na podstawie literatury [154].

Agili-C™ (Rysunek 10) jest implantem przeznaczonym do stosowania w ubytkach chrząstki i ubytkach kostno-chrzęstnych. Implant jest porowatym, biokompatybilnym i biodegradowalnym dwufazowym rusztowaniem, składającym się z aragonitu (odmiana węglanu wapnia) pochodzącego z oczyszczonego egzoszkieletu koralowca. W stawie kolanowym chirurg wywierca otwór w kości poniżej ubytku lub uszkodzenia chrząstki i wszczepia implant. Agili-C™ pozwala na wypełnienie ubytków w powierzchni stawu nową tkanką. Z biegiem czasu Agili-C™ stopniowo rozpada się (resorbuje) i jest zastępowany przez nową tkankę [140–144].

Rysunek 10. Implant Agili-C™. Rysunek został przygotowany na podstawie literatury [144].

6. Podsumowanie i wnioski z literatury

W przeglądzie literaturowym przedstawiłam charakterystykę i budowę chrząstki stawowej w organizmie człowieka, przyczyny jej uszkodzenia oraz najbardziej obiecujące metody do jej regeneracji, które wymagają zastosowania rusztowań do hodowli komórek. Opisałam strukturę rusztowań, rodzaj materiałów i metody najczęściej wykorzystywane do otrzymywania skafoldów. Na zakończenie zaprezentowałam komercyjne rusztowania stosowane do regeneracji chrząstki stawowej.

Przeprowadzony przegląd literatury wskazuje, że choć badania w dziedzinie regeneracji chrząstki stawowej są intensywne i obiecujące, wciąż brakuje rusztowań, które skutecznie regenerują chrząstkę szklistą. Prace nad opracowaniem efektywnych technologii i materiałów wspomagających regenerację chrząstki nadal trwają.

Przegląd literatury naukowej wskazuje, że rusztowania do hodowli komórkowej wykazują największy potencjał w metodach ACI i AMIC. Struktury te umożliwiają odtworzenie naturalnej macierzy pozakomórkowej, co stanowi fundamentalne wsparcie fizyczne dla komórek, zwiększając szanse na skuteczną regenerację chrząstki stawowej.

CEL PRACY ORAZ TEZY BADAWCZE

Celem mojej pracy było opracowanie nowych rusztowań komórkowych do hodowli chondrocytów lub komórek macierzystych. Przydatność opracowanych i otrzymanych rusztowań przetestowałam w badaniach in vitro (hodowla chondrocytów ludzkich). Wybrane rusztowania zostały również przebadane w badaniach in vivo (regeneracja ubytków chrząstki w kolanach królika) przez współpracujących lekarzy ortopedów.

Aby zrealizować cel badawczy, sformułowałam dwie tezy:

- **TEZA 1 – Możliwe jest opracowanie sposobu otrzymywania nowych, syntetycznych rusztowań komórkowych do hodowli chondrocytów lub komórek macierzystych;**
- **TEZA 2 – Opracowane i otrzymane syntetyczne rusztowania komórkowe mogą znaleźć zastosowanie do hodowli chondrocytów i regeneracji ubytków chrząstki stawowej.**

7. Omówienie prac własnych

W medycynie regeneracyjnej chrząstki stawowej nadal poszukiwany jest skuteczny sposób leczenia. Wytwarzanie rusztowań znajduje zastosowanie w najbardziej obiecujących metodach ACI i AMIC. Rozdział 7 zawiera przegląd wyników uzyskanych w badaniach własnych, które zostały uporządkowane według tez badawczych. Kluczowe wyniki są zwięźle opisane, z naciskiem na najważniejsze rezultaty w odniesieniu do głównego celu mojej rozprawy doktorskiej.

W badaniach własnych, jako grupę materiałów przeznaczonych do produkcji rusztowań, wybrałam biokompatybilne polimery syntetyczne. Materiały, które mają odpowiednie właściwości mechaniczne i z których można łatwo formować dowolne kształty membran. Następnym krokiem był dobór metody, gdzie zastosowałam technikę inwersji faz w układzie rozpuszczalnik-nierozpuszczalnik z wymywaniem poroforów. Największym wyzwaniem był dobór prekursorów porów. Od nich zależy odpowiednia sieć wzajemnie połączonych porów oraz mikroporowata struktura. Po wstępnych badaniach, które wykazały bardzo obiecujące wyniki zdecydowałam się wykorzystać włókniny z żelatyny i z poliwinylopirolidonu oraz krystaliczny NaCl, których zadaniem było wytworzenie odpowiednich makroporów. W zależności od rodzaju prekursorów porów, dobierałam odpowiednie rozpuszczalniki i nierozpuszczalniki polimerów i prekursorów porów.

7.1. Przegląd rusztowań syntetycznych i hybrydowych w inżynierii tkanki chrzęstnej

W Publikacji 1: „Review of Synthetic and Hybrid Scaffolds in Cartilage Tissue Engineering” przedstawiłam przegląd rozwiązań jakie oferuje inżynieria tkanki chrzęstnej do regeneracji chrząstki stawowej.

Na początku przedstawiłam ogólne informacje dotyczące chrząstki stawowej. Następnie omówiłam kliniczne strategie leczenia ubytków chrząstki. Zwróciłam uwagę na to, że dzięki postępowi w medycynie możliwe jest pobieranie komórek macierzystych nie tylko z krwi pępowinowej, endometrium czy szpiku kostnego, ale także z dorosłych tkanek każdego organizmu, zwłaszcza z tkanki tłuszczowej, której główną zaletą jest jej dostępność. Zaznaczyłam, że w metodach klinicznych pomocne są czynniki wzrostu dla komórek macierzystych, co sprzyja regeneracji chrząstki (Rysunek 11). Omówiłam wpływ czynników wzrostu na chondrogenezę i utrzymanie właściwego fenotypu komórek.

Mediatory polipeptydowe, takie jak transformujący czynnik wzrostu (TGF), insulinopodobny czynnik wzrostu (IGF) oraz czynnik wzrostu fibroblastów (FGF), stymulują proliferację komórek chrząstki i stabilizują ich ekspresję fenotypową oraz proces chondrogenezy. Działając pod wpływem tych czynników, tworzona tkanka wykazuje budowę histologiczną i właściwości biochemiczne zbliżone do chrząstki szklistej. Ponadto przyspieszają one gojenie się ubytku chrząstki i zwiększają zawartość kolagenu typu II w porównaniu z kolagenem typu I.

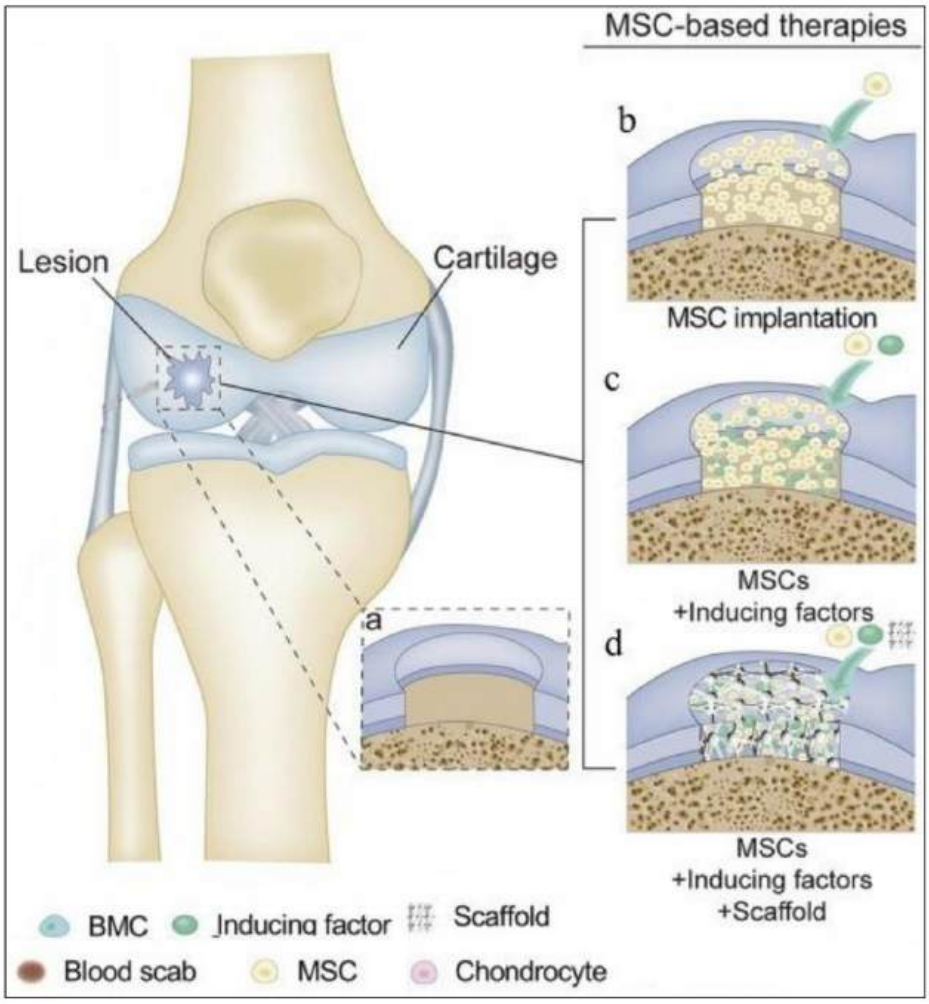

Rysunek 11. Metody naprawy chrząstki za pomocą terapii opartych na mezenchymalnych komórkach macierzystych (MSC): (a) uszkodzenie chrząstki o pełnej grubości; (b-d) terapie z wykorzystaniem MSC i odpowiednich dodatków. Reprodukcja z Publikacji 1.

W artykule opisałam także metodę ACI, jako bardzo obiecującą technikę terapeutyczną w regeneracji chrząstki stawowej (Rysunek 12).

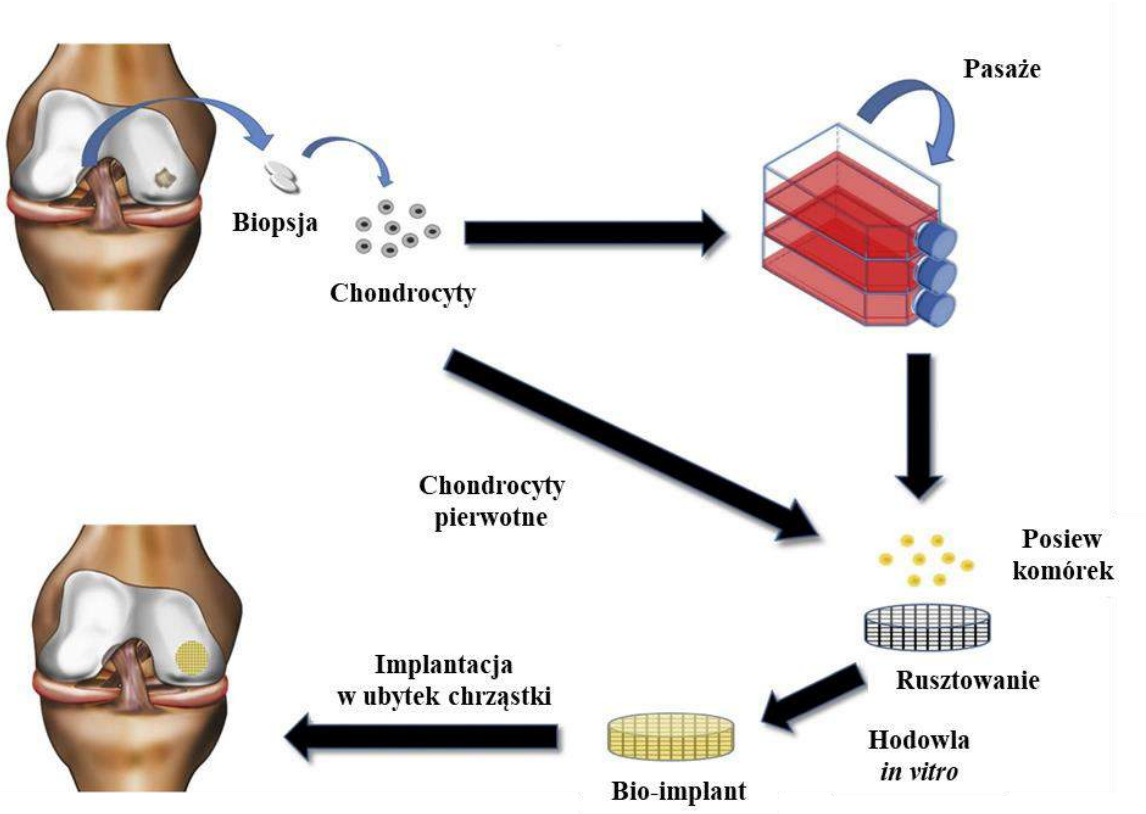

Rysunek 12. Ogólny schemat metody ACI z wykorzystaniem rusztowania. Reprodukcja z Publikacji 1.

W kolejnej części artykułu skoncentrowałam się na rusztowaniach, które są kluczowym elementem w procesie regeneracji chrząstki, zwłaszcza w metodzie ACI. Omówiłam, jakie cechy powinny mieć rusztowania, na przykład ich kształt, materiał i właściwości mechaniczne. Dodatkowo wspomniałam o tym, że wielkość porów w rusztowaniu oraz sposób hodowli mają duże znaczenie, w zależności od rodzaju komórek MSC i chondrocytów (Rysunek 13).

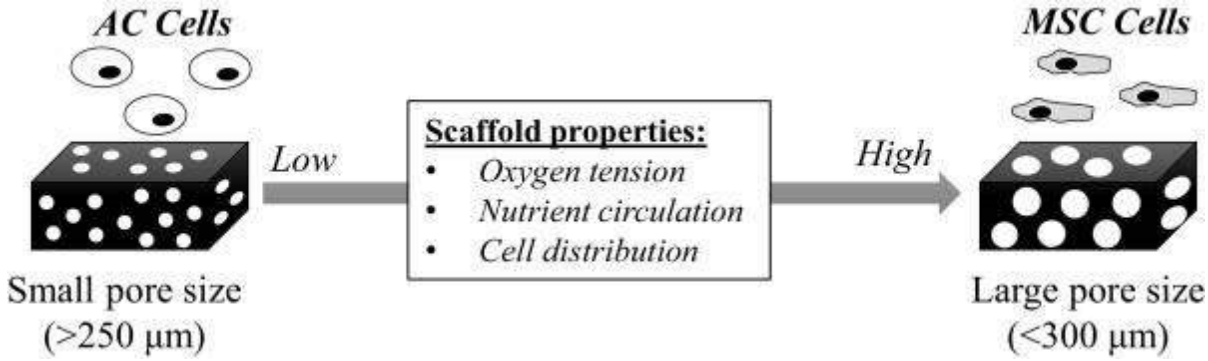

Rysunek 13. Ogólna demonstracja właściwości rusztowania i warunków panujących w trakcie hodowli dla odpowiedniego wzrostu chondrocytów (ACs) i MCS. Reprodukcja z Publikacji 1.

Następnie omówiłam biomateriały stosowane do otrzymywania rusztowań, w tym zarówno polimery naturalne, jak i syntetyczne. Przedstawiałam ich zalety i wady, a także wspomniałam o materiałach hybrydowych, które łączą korzyści obu rodzajów polimerów, gwarantując lepsze właściwości rusztowania. W kolejnym etapie wymieniłam i opisałam różne techniki wytwarzania rusztowań, które dostarczają różnorodne formy konstrukcyjne skafoldów. Dodatkowo zilustrowałam schematycznie główne struktury rusztowań, uwzględniając ich obrazy z mikroskopu elektronowego (Rysunek 14).

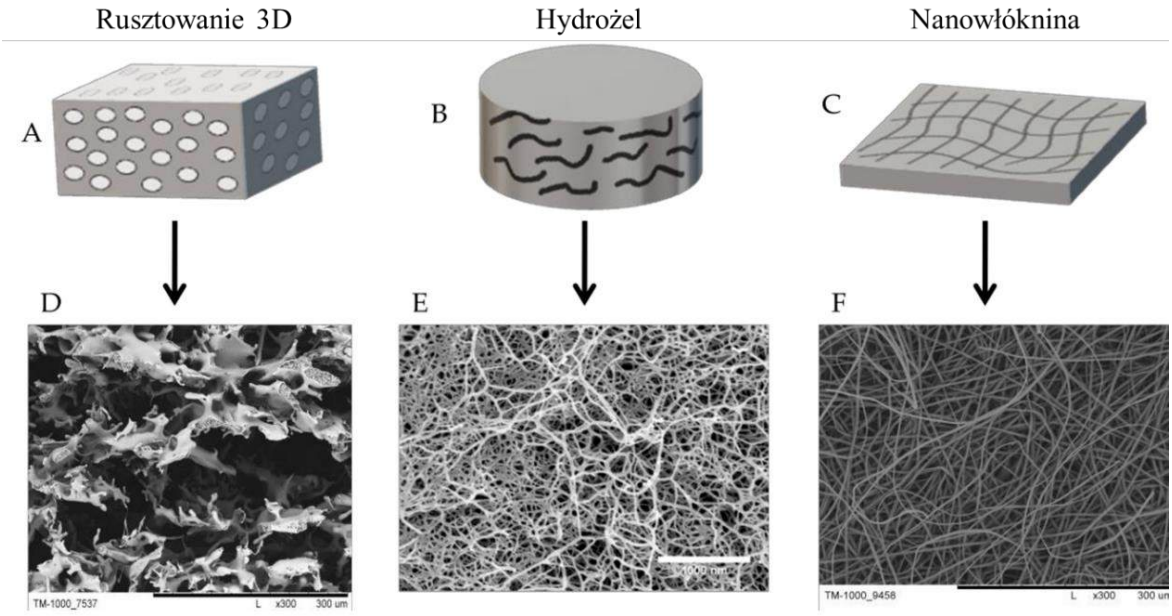

Rysunek 14. Schematyczna ilustracja głównych form rusztowań dla inżynierii tkanki chrzęstnej: A, D – rusztowanie 3D; B, E – hydrożel; C, F – nanowłóknina. Paski skali: D – 300 µm; E – 1000 nm; F – 300 µm. Reprodukcja z Publikacji 1.

W zakończeniu artykułu omówiłam różne rodzaje rusztowań wykonanych z naturalnych, syntetycznych i hybrydowych materiałów, które były lub są testowane w badaniach klinicznych lub przedklinicznych. W mojej rozprawie doktorskiej rozszerzyłam ten przegląd o dodatkowe i bardziej aktualne informacje.

7.2. Opracowanie i otrzymanie syntetycznych rusztowań do hodowli chondrocytów lub komórek macierzystych

W badaniach własnych koncentrowałam się na opracowaniu rusztowań przestrzennych na bazie biokompatybilnych polimerów syntetycznych do hodowli chondrocytów i komórek macierzystych. Opracowałam pięć rusztowań, które przedstawiłam w podrozdziałach 7.2.1. i 7.2.2.

7.2.1. Rusztowania komórkowe z kopolimeru kaprolaton-ko-polilaktyd (PLCA) (na podstawie Publikacji 2)

W ramach pracy otrzymałam dwa rodzaje przestrzennych rusztowań wykonanych z biodegradowalnego kopolimeru poli(L-laktyd-ko-ε-kaprolakton) (PLCA). Otrzymałam je metodą mokrej inwersji faz przy użyciu różnych rozpuszczalników i generatorów (prekursorów) porów. W jednym przypadku zastosowałam włókninę z poliwinylopirolidonu 1,3 MDa (PVP) i polimeru Pluronic 127-F w celu uzyskania odpowiednio makro- i mikroporów (PCLA1) (Rysunek 15). W drugim przypadku wykorzystałam włókninę z żelatyny i polimer PVP 10 kDa jako prekursory odpowiednio makro- i mikroporów (Rysunek 16). W zależności od generatorów porów uzyskałam różne struktury membran. Według literatury, tego typu rusztowania nie zostało wcześniej otrzymane.

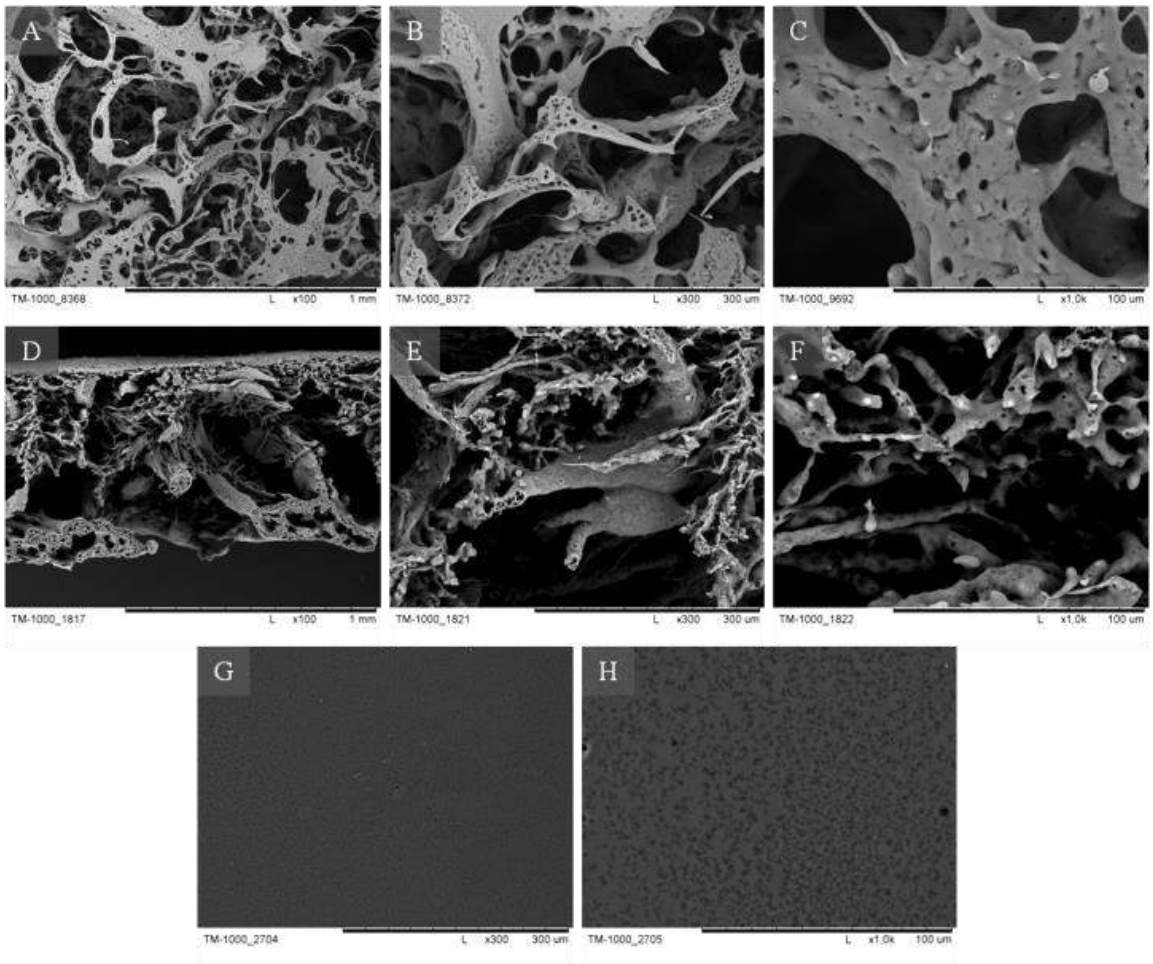

Rysunek 15. Obrazy SEM rusztowania PLCA1: A-C wierzchnia strona rusztowania; D-F przełom membrany, G-H spodnia warstwa rusztowania. Paski skali: : A, D – 1 mm; B, E, G - 300 μm; C, F, H - 100 μm. Reprodukcja z Publikacji 2.

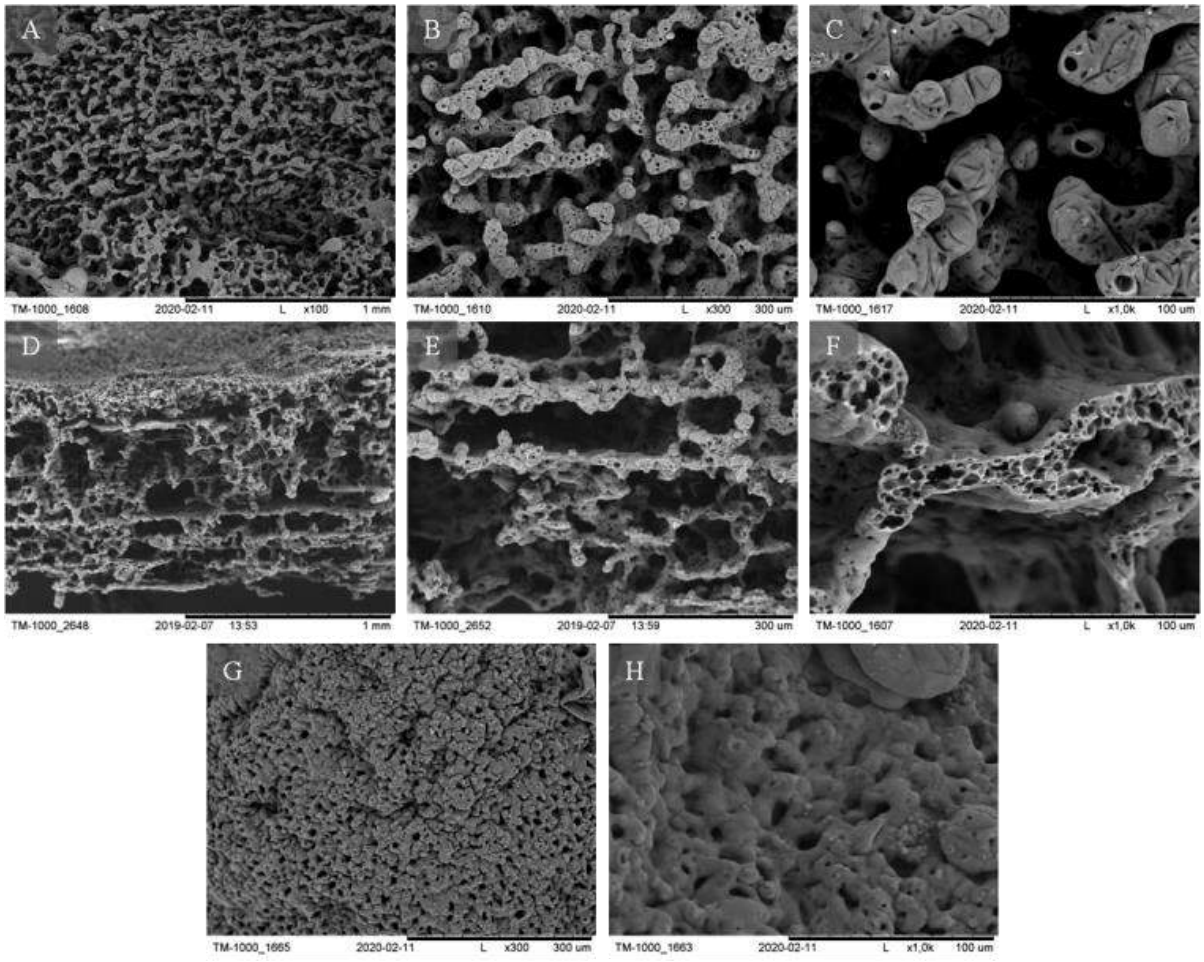

Rysunek 16. Obrazy SEM rusztowania PLCA2: A-C wierzchnia strona rusztowania; D-F przełom membrany, G-H spodnia warstwa rusztowania. Paski skali: A, D – 1 mm; B, E, G - 300 μm; C, F, H - 100 μm. Reprodukcja z Publikacji 2.

Uzyskałam rusztowania, które charakteryzują się odpowiednią strukturą: warstwa górna posiada średnicę porów powyżej 20 μm, czyli tyle ile mają chondrocyty ludzkie; wymiar porów w przełomie wynosi powyżej 300 μm co zapewni swobodne funkcjonowanie komórkom; natomiast spód membrany jest zwarty co zapobiega wypadnięciu komórek i cząsteczek białka poza rusztowanie. Wnętrze obu membran ma nieregularną sieć połączonych ze sobą porów, co zapewnia odpowiednie środowisko do migracji, proliferacji i adhezji komórek. Gwarantuje to produkcję białek macierzy zewnątrzkomórkowej (ECM). Wykazałam, że poprzez wybór nieklasycznego prekursora porów – włókniny, można kontrolować rozmiar i ilość makroporów oraz grubość ścian między porami. Pomimo podobnej struktury włóknin z PVP i włókniny z żelatyny (Rysunek 17), różnice w strukturze membran są znaczące (Rysunek 15 i Rysunek 16). Ponadto struktura obu rusztowań jest mikroporowata, co zapewnia dostęp substancji

odżywczych, tlenu, czy też umożliwia usuwanie produktów przemiany materii z wnętrza rusztowań.

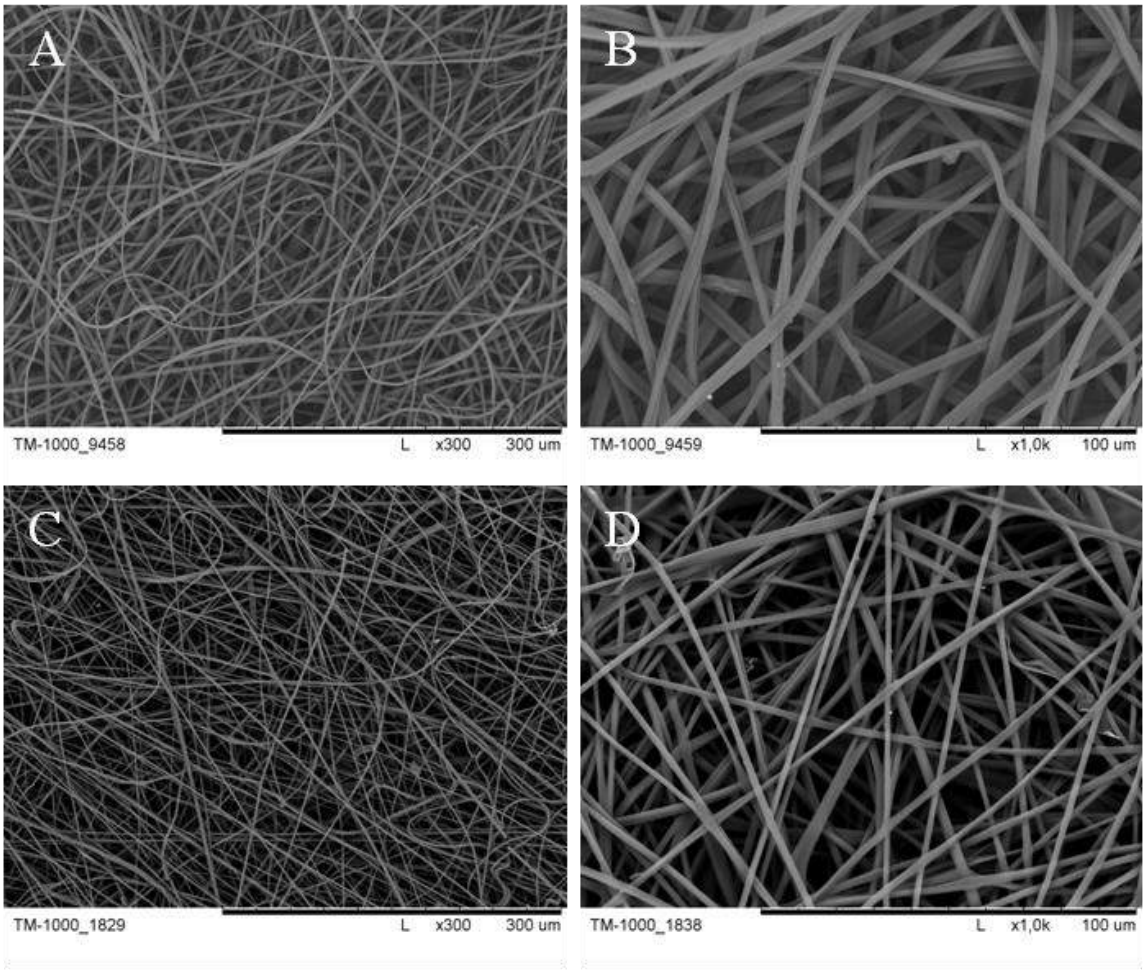

Rysunek 17. Fotomikrografy włókniny z żelatyny wieprzowej (A, B) i włókniny z PVP 1,3 MDa (C, D) otrzymanych metodą elektroprzędzenia. Powiększenie 300x (A, C) i 1000x (B, D). Reprodukcja z Publikacji 2.

Rozmiar porów badałam także za pomocą MeMoExplorer™, zaawansowanego oprogramowania przeznaczonego do komputerowej analizy obrazów ze skaningowego mikroskopu elektronowego (SEM). Celem programu jest precyzyjny pomiar powierzchni porów obecnych w membranach. Dzięki czemu możliwe jest obiektywne oszacowanie rozkładu wielkości porów oraz przygotowanie danych do dowolnych analiz statystycznych, które można przeprowadzić za pomocą zewnętrznych narzędzi, takich jak Excel, Origin. Wyniki pokazują średni procent występowania porów o odpowiednim rozmiarze (8 klas wielkości porów) lub współczynnik porowatości – średni procent wszystkich porów (Total) w stosunku do całego rozmiaru obrazu SEM (Tabela 2). Analiza wykazała, że w obu typach rusztowań najczęściej występowały pory o powierzchni większej niż 300 μm^2.

Tabela 2. Klasy wielkości porów.

Klasa wielkości porów	1	2	3	4	5	6	7	8	9
Rozmiar [µm^2]	0÷3	3÷8	8÷20	20÷80	80÷100	100÷150	150÷300	>300	Total

Ponadto komputerowa analiza danych z MeMoExplorer^{TM} umożliwia ocenić powtarzalność uzyskiwanych struktur rusztowań (współczynnik niestabilności). Jest on obliczany jako stosunek odchylenia standardowego (SD) uśrednionej wartości współczynnika porowatości do uśrednionej wartości współczynnika porowatości. Powtarzalność struktur badałam również po degradacji w płynach fizjologicznych – w zbuforowanym roztworze soli fizjologicznej (PBS) i zrównoważonym roztworze soli Hanka (HBSS).

W badaniach zmierzyłam także porowatość rusztowań przed i po degradacji. Rusztowania charakteryzowały się wysoką porowatością, około 95%. Po degradacji wartość ta wzrosła do 99%, szczególnie dla PLCA2 w HBSS.

Bardzo ważnym parametrem rusztowań do inżynierii tkanki chrzęstnej jest biodegradacja. Aby symulować warunki fizjologiczne, do określenia szybkości degradacji rusztowań wykorzystałam PBS i HBSS, który ma podobny skład jonów nieorganicznych do osocza krwi. Po 28 dniach degradacji rusztowań zaobserwowałam wzrost utraty masy w płynie PBS do 49% dla PLCA2, a dla PLCA1 tylko do 12%, (Rysunek 18). Utrata masy rusztowań po 4 tygodniach w płynie HBSS (Rysunek 19) dla PLCA2 wyniósł około 71%, a dla PLCA1 5 razy mniej, około 14%. Po degradacji wykazałam także zwiększenie powierzchni porów.

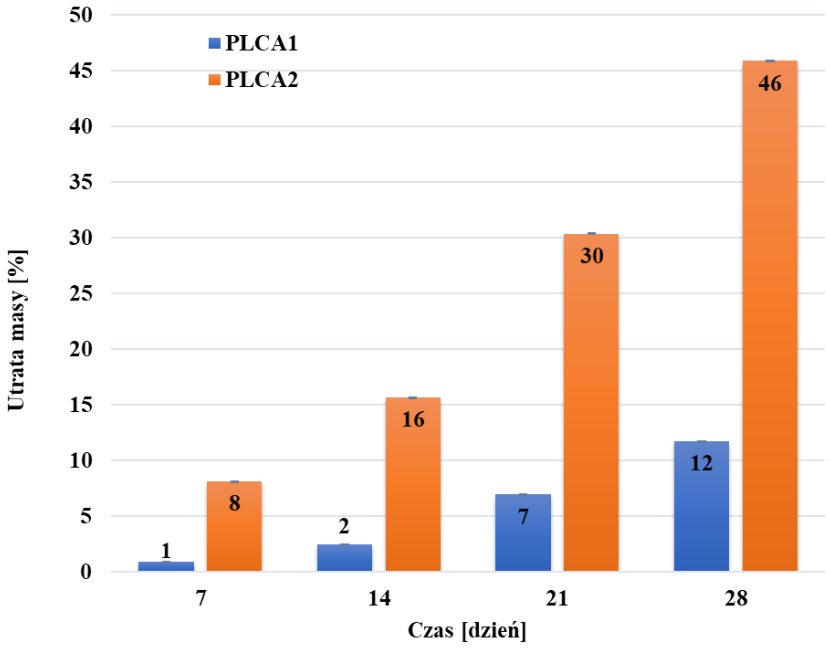

Rysunek 18. Utrata masy rusztowań PLCA1 i PLCA2 w funkcji czasu w płynie PBS.

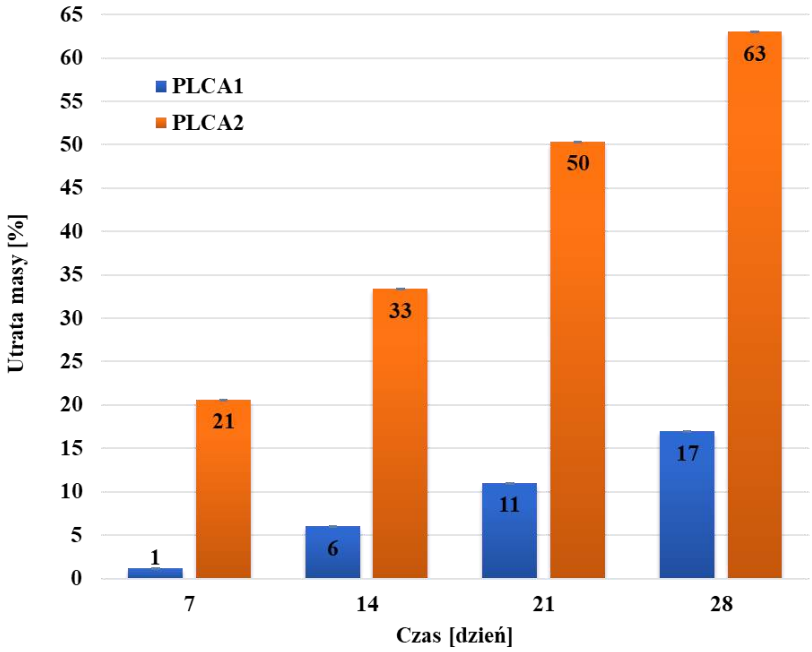

Rysunek 19. Utrata masy rusztowań PLCA1 i PLCA2 w funkcji czasu w płynie HBSS.

W pracy wykazałam, że rusztowania PCLA1 oraz PCLA2 posiadają odpowiednie parametry, którymi powinny charakteryzować się rusztowania do hodowli komórek macierzystych, co też jest udowodnieniem **Tezy 1: Możliwe jest opracowanie sposobu otrzymywania nowych, syntetycznych rusztowań komórkowych do hodowli chondrocytów lub komórek macierzystych**.

7.2.2. Rusztowania komórkowe z mieszanki polimerów (na podstawie Publikacji 3)

W trakcie kontynuacji moich badań zdecydowałam się na zastosowanie innego materiału biokompatybilnego. Ponadto, postanowiłam poeksperymentować z prekursorami makroporów oraz rozszerzyć zakres przeprowadzanych analiz (Rysunek 20). Poszerzenie badań miało na celu uwydatnienie dodatkowych cech, które powinny być obecne w strukturach rusztowań przeznaczonych do hodowli chondrocytów i komórek macierzystych. Według literatury, do tej pory nie udało się uzyskać tego typu rusztowań.

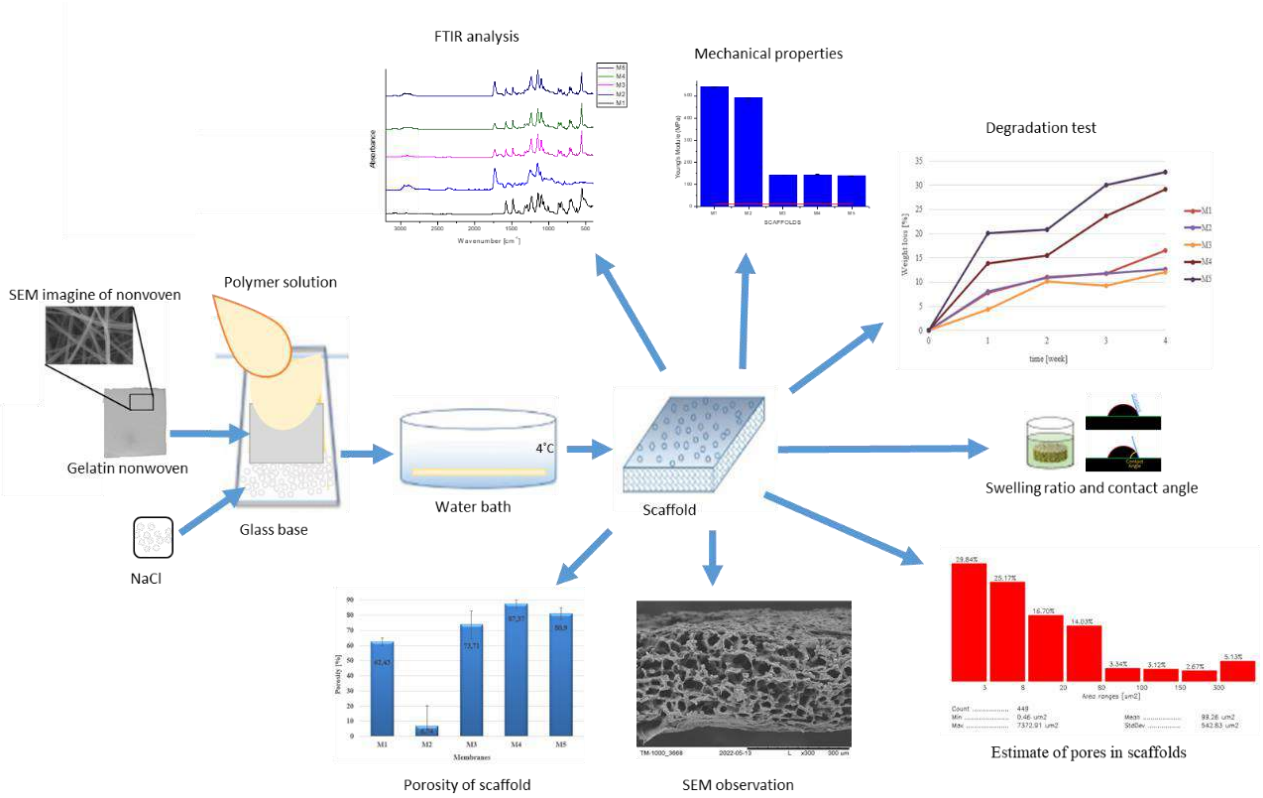

Rysunek 20. Schemat otrzymania rusztowań oraz przeprowadzone analizy. Reprodukcja z Publikacji 3.

W pracy przedstawiłam oraz szczegółowo omówiłam trzy rodzaje rusztowań, które otrzymałam metodą mokrej inwersji faz z biokompatybilnych polimerów, a mianowicie z PES i poliuretanu (PUR). Polimery stosowane były w różnych proporcjach wagowych (PES:PUR –2:1 dla M3; 1:1 dla M4; 1:2 dla M5). Celowe zastosowanie polimeru PUR, otrzymanego na drodze syntezy, wynikało z jego struktury, zawierającej wiązanie estrowe, które jest podatne na hydrolizę [155,156]. W celu uzyskania makroporów w strukturze rusztowań, zastosowałam włókninę z żelatyny, z którą miałam już kontakt w moich poprzednich badaniach. Dodatkowo, jako nowy porofor zastosowałam krystaliczny chlorek sodu (NaCl).

Podobnie jak w poprzednich badaniach, uzyskane membrany M3-M5 prezentowały odpowiednią strukturę (Rysunek 21). Wykorzystanie NaCl miało kluczowe znaczenie dla uzyskania perforowanej górnej warstwy, charakteryzującej się porami o średnicy powyżej 20 µm. Włóknina pełniła istotną rolę w kształtowaniu trójwymiarowej sieci makroporów, które łączyły się ze sobą. Jednocześnie dolna warstwa zachowała swoją nieprzepuszczalność dla komórek i białka.

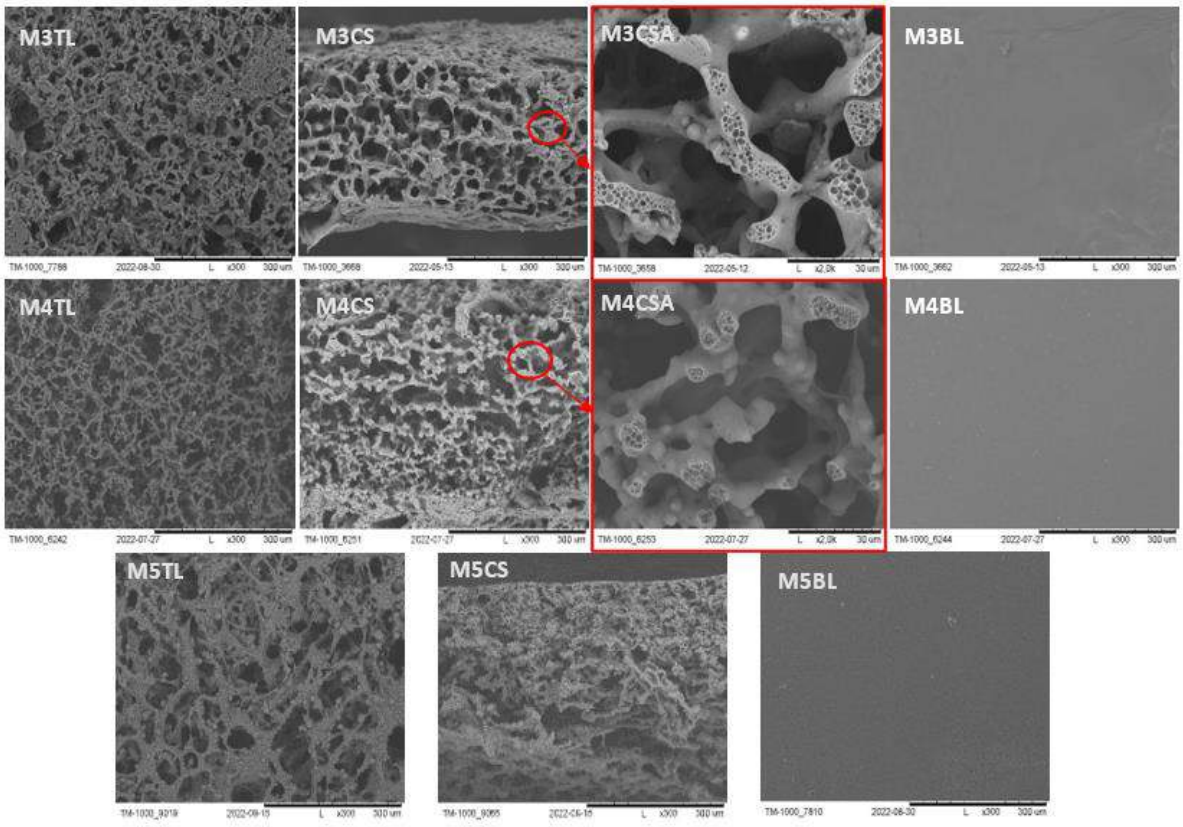

Rysunek 21. Fotomikrografy SEM rusztowań M3 – M5. Na obrazach M3CSA i M4CSA przedstawiono powiększenie mikroporów wścianach przekrojów poprzecznych (czerwony kolor). TL - warstwa górna; CS - przekrój poprzeczny; BL - warstwa dolna. Paski skali: 2000 µm – M3CSA, M4CSA; 300 µm – pozostałe obrazy. Reprodukcja z Publikacji 3.

Strukturę membran przeanalizowałam także za pomocą oprogramowania MeMoExplorer™. Przeprowadzona analiza wykazała, że w rusztowaniach najczęściej występowały pory o powierzchni przekraczającej 300 µm^2 (Rysunek 22).

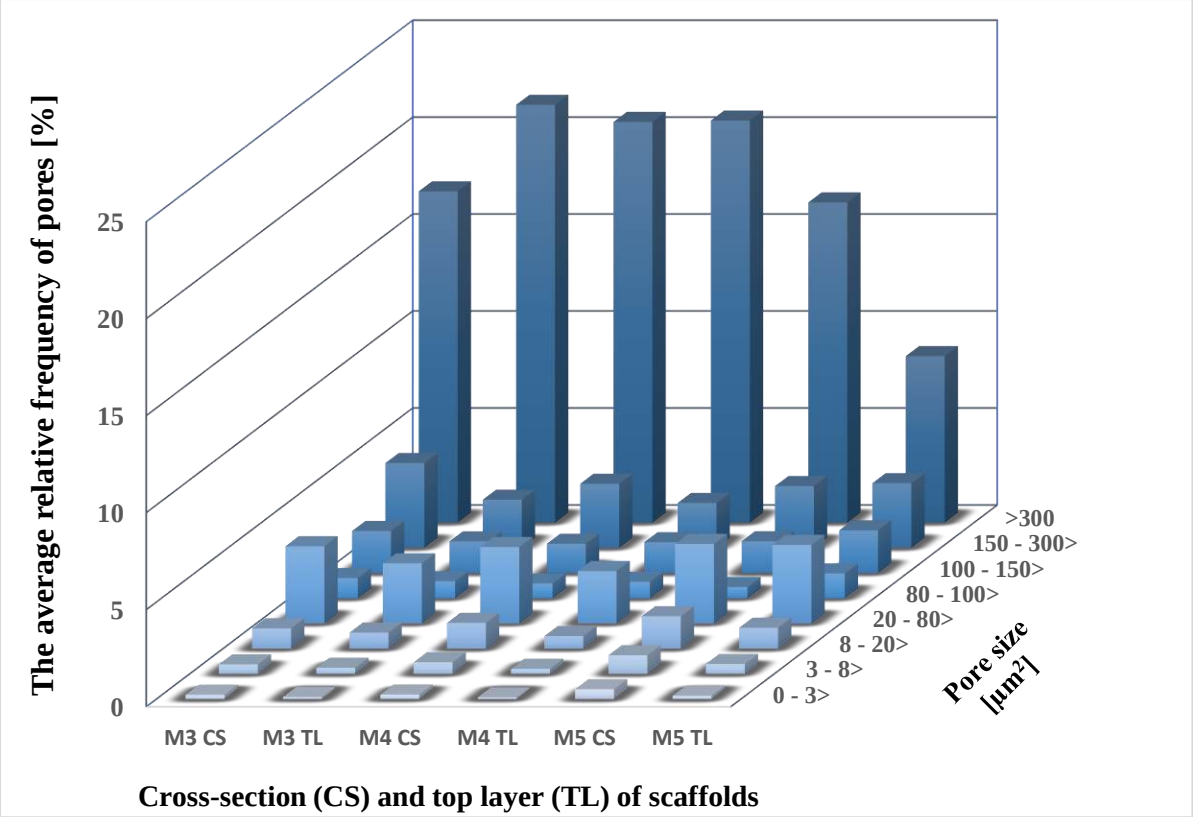

Rysunek 22. Średnia częstotliwość występowania porów w ośmiu klasach wielkości dla przekroju poprzecznego (CS) i górnej warstwy (TL) rusztowań M3-M4. Reprodukcja z Publikacji 3.

Istotną cechą rusztowań komórkowych jest hydrofilowość. Parametr, który określa możliwość migracji płynów ustrojowych, wody i składników odżywczych do wnętrza rusztowań, a tym samym umożliwia funkcje życiowe rozwijających się w nich komórek. Badania zwilżalności (kąt zwilżania, nasiąkliwość) wykazały hydrofilowy charakter rusztowań. Skafoldy M3-M5 uzyskały bardzo dobre nasycenie substancją hydrofilową PBS, natomiast kąt zwilżania rusztowań potwierdził hydrofilowy charakter membran. Wykazałam w ten sposób, że dodatki używane podczas wytwarzania rusztowań (prekursory porów), znacząco zmieniają strukturę membran. Zaobserwowałam wzrost zarówno rozmiaru, liczby, jak i całkowitej porowatości skafoldów. Te modyfikacje wpłynęły również na poprawę właściwości hydrofilowych rusztowań, co zwiększyło ich zdolność do absorpcji płynów fizjologicznych i wywarło istotny wpływ na tempo degradacji materiału.

Kolejnym istotnym parametrem rusztowań są właściwości mechaniczne, które powinny być zbliżone do wytrzymałości naturalnej tkanki. Wartość modułu Younga ludzkiej chrząstki stawowej przy rozciąganiu wynosi około 10 MPa. Otrzymane podłoża

wykazały właściwości mechaniczne powyżej 10 MPa. Oznacza to, że z pewnością wytrzymałyby one warunki występujące w stawie kolanowym.

Rusztowania poddałam także badaniu degradacji w symulowanym płynie ustrojowym (SBF, ang. simulated body fluid) w inkubatorze, w temperaturze 36 ± 1˚C. Dla każdej z membran odnotowałam utratę masy (Rysunek 23). Największy procent utraty masy był dla rusztowania M5, w którym występowała dwukrotna przewaga masy PUR nad PES. Ponadto, w trakcie badań zauważyłam degradację PES, co stanowi nową obserwację, nie odnotowaną dotąd w literaturze. W pracy wykazałam różne szybkości degradacji rusztowań M3-M5 pokazując, że przy odpowiednim doborze stosunków wagowych polimerów można kontrolować czas degradacji.

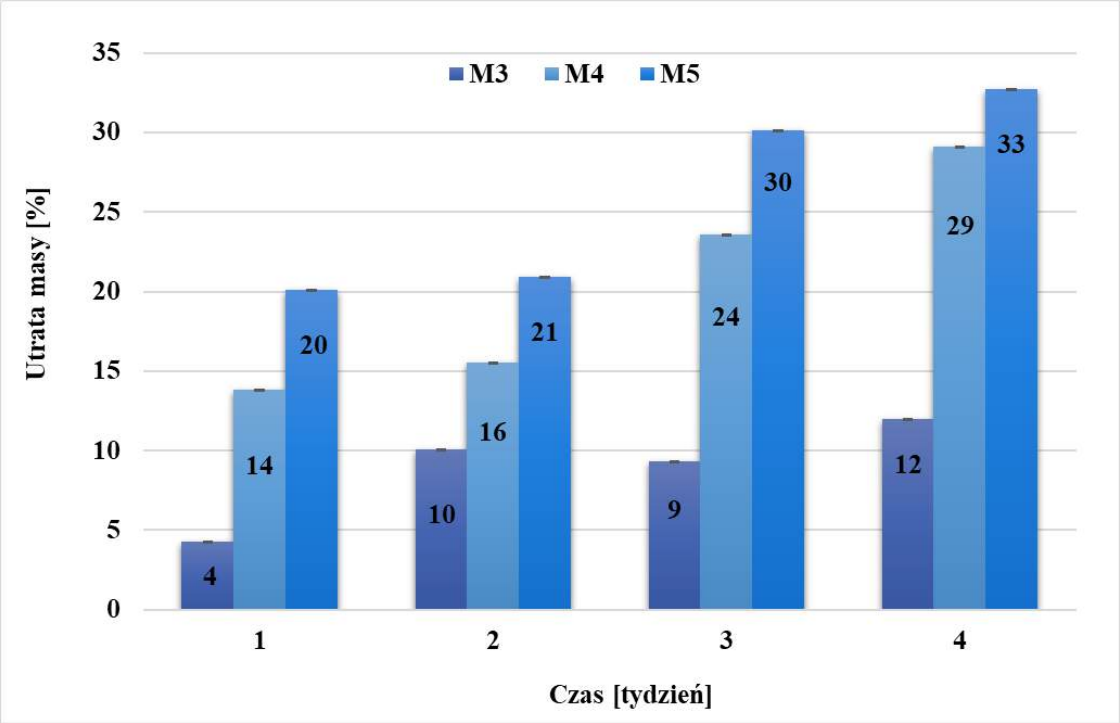

Rysunek 23. Utrata masy rusztowań podczas degradacji w SBF.

W pracy, przedstawiłam także wzrost zarówno porowatości, jak i powierzchni porów dla rusztowań po degradacji. Są to istotne cechy, niezbędne do zwiększenia przestrzeni dla produktów komórkowych, takich jak białko tworzące chrząstkę szklistą.

Hydrolizę polimeru PUR potwierdziłam także za pomocą analizy spektroskopii w podczerwieni z transformacją Fouriera (FT-IR), w której po degradacji zauważalny jest zanik wiązań estrowych przy długości fali około 1730 cm^{-1}.

Opracowane i otrzymane przeze mnie membrany posiadają odpowiednie właściwości jakie powinny spełniać rusztowania dla inżynierii chrząstki stawowej. Takie

membrany mogą być kolonizowane zarówno przez chondrocyty (metoda ACI) jak i komórki macierzyste (technika AMIC).

Publikacja 2 i Publikacja 3, których opis przedstawiłam w rozdziale 7.2, przedstawiają wyniki, które stanowią udowodnienie postawionej **TEZY 1: Możliwe jest opracowanie sposobu otrzymywania nowych, syntetycznych rusztowań komórkowych do hodowli chondrocytów lub komórek macierzystych**.

7.3. Testowanie membran w badaniach in vitro oraz in vivo

Aby sprawdzić przydatność rusztowań do regeneracji chrząstki stawowej, niezbędne jest przeprowadzenie odpowiednich badań in vitro oraz in vivo. Przeprowadziłam badania in vitro z wykorzystaniem ludzkich chondrocytów na rusztowaniach komórkowych z PES i z poli-L-laktydu (PLLA). Dodatkowo opracowane i otrzymane przeze mnie rusztowania zostały przebadane in vivo na modelu zwierzęcym (królik) przez współpracujących lekarzy ortropedów. Otrzymane wyniki przedstawiłam w kolejnych podrozdziałach.

7.3.1. Badania in vitro z wykorzystaniem ludzkich chondrocytów (na podstawie Publikacji 4)

W niniejszej publikacji przedstawiłam perspektywę prowadzenia hodowli izolowanych chondrocytów ludzkich na rusztowaniach z PES oraz z PLLA. Badania in vitro są kluczowe w kontekście przygotowań do badań klinicznych. Przeprowadziłam analizę porównawczą struktury rusztowań z PES i z PLLA oraz ich przydatność do wzrostu ludzkich chondrocytów.

Badania przeprowadziłam na rusztowaniu PES, które zostało opracowane w Instytucie Biocybernetyki i Inżynierii Biomedycznej Polskiej Akademii Nauk (IBIB PAN) [76]. Proces uzyskiwania membrany z PES wymaga zastosowania bibuły (prekursor makroporów), która jest trawiona przez okres czterech tygodni, co czyni ten proces czasochłonnym i złożonym. Jako membranę porównawczą wykorzystałam rusztowanie z PLLA, które również zostało opracowane i otrzymane w IBIB PAN [157,158]. Jego produkcja jest zdecydowanie szybsza i prostsza, gdyż do uzyskania makroporów wykorzystuje się włókninę z żelatyny. Oba rusztowania otrzymałam metodą mokrej inwersji faz (Rysunek 6). Charakterystyka struktury obu rusztowań spełniała niezbędne cechy skafoldów do hodowli chondrocytów (Rysunek 24). Oba rusztowania mają

perforowaną warstwę górną z porami o średnicy ponad 20 µm, co umożliwia chondrocytom penetrację do wnętrza skafoldu. Wnętrze obu membran ma sieć połączonych ze sobą makroporów, co zapewnia odpowiednie warunki do rozwoju chondrocytów i gwarantuje przestrzeń dla ich produktów. Struktura mikroporów zapewnia transport tlenu, produktów odżywczych i metabolicznych. Dolna warstwa rusztowań jest zbita, co uniemożliwia komórkom wydostanie się z rusztowań.

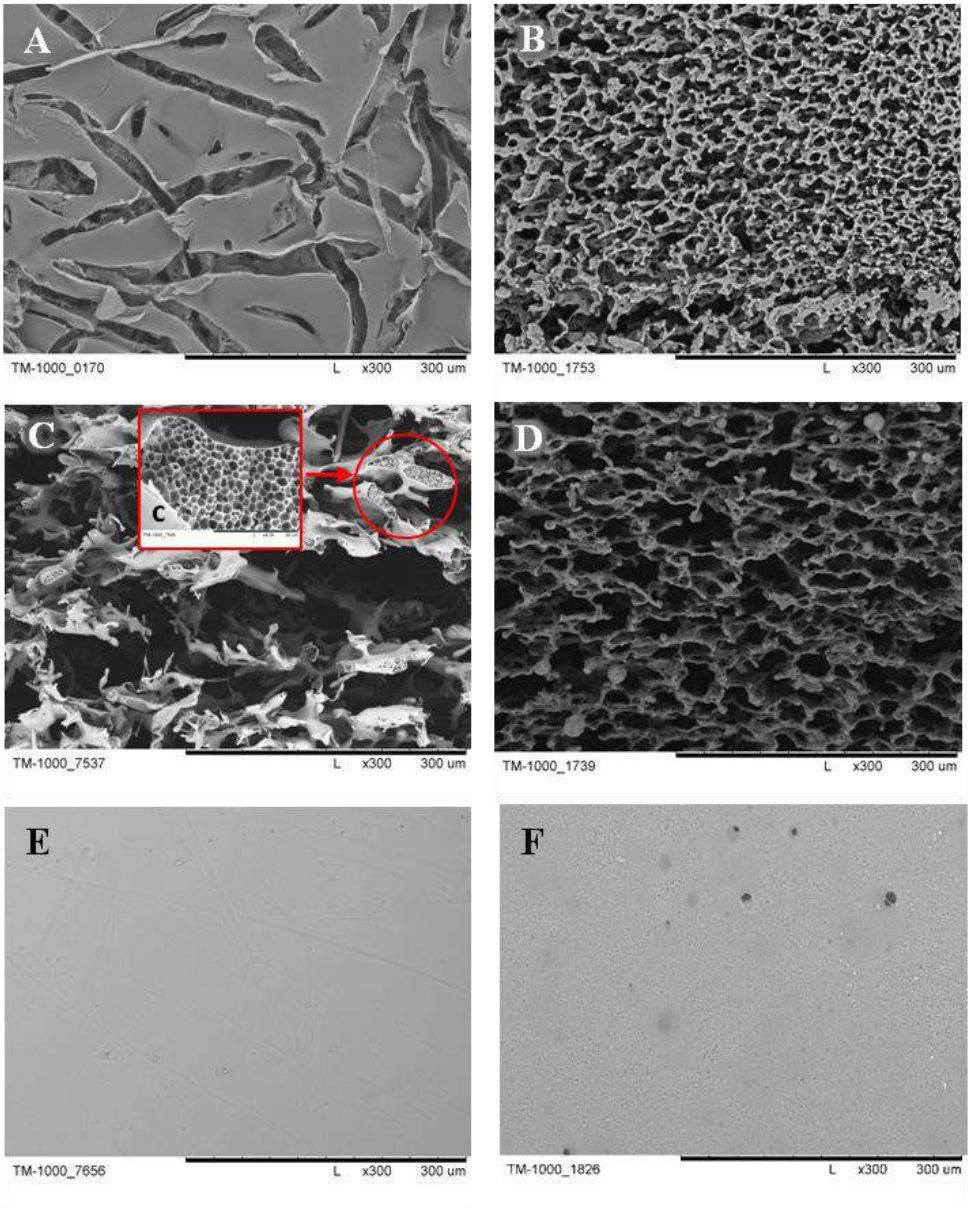

Rysunek 24. Obrazy SEM rusztowańz PES i z PLLA. A – perforowana warstwa rusztowania z PES; B – perforowana warstwa rusztowania z PLLA; C – przekrój rusztowania z PES; c- struktura mikroporów rusztowania z PES; D – przekrój rusztowania z PLLA; E –dolna warstwa rusztowania z PES; F – dolna warstwa rusztowania z PLLA. Paski skali: A, B, C, D, E, F – 300 µm, c – 20 µm. Reprodukcja z Publikacji 4.

Ważnym i wymagającym etapem w badaniach było opracowanie procedury (czas i płyn) izolacji chondrocytów z chrząstki pozyskiwanej z odpadów pooperacyjnych od pacjentów hospitalizowanych w Szpitalu Ortopedycznym im. prof. Adama Grucy w Otwocku. Izolowane, pierwotne (bez pasażu) komórki były wysiane na perforowane warstwy membran z PES oraz z PLLA. Strukturę rusztowań przed, w trakcie i po procesie hodowli, morfologię komórek, obecność jąder komórkowych, oraz produkty komórek analizowałam z wykorzystaniem SEM oraz mikroskopu odwróconego (Rysunek 25).

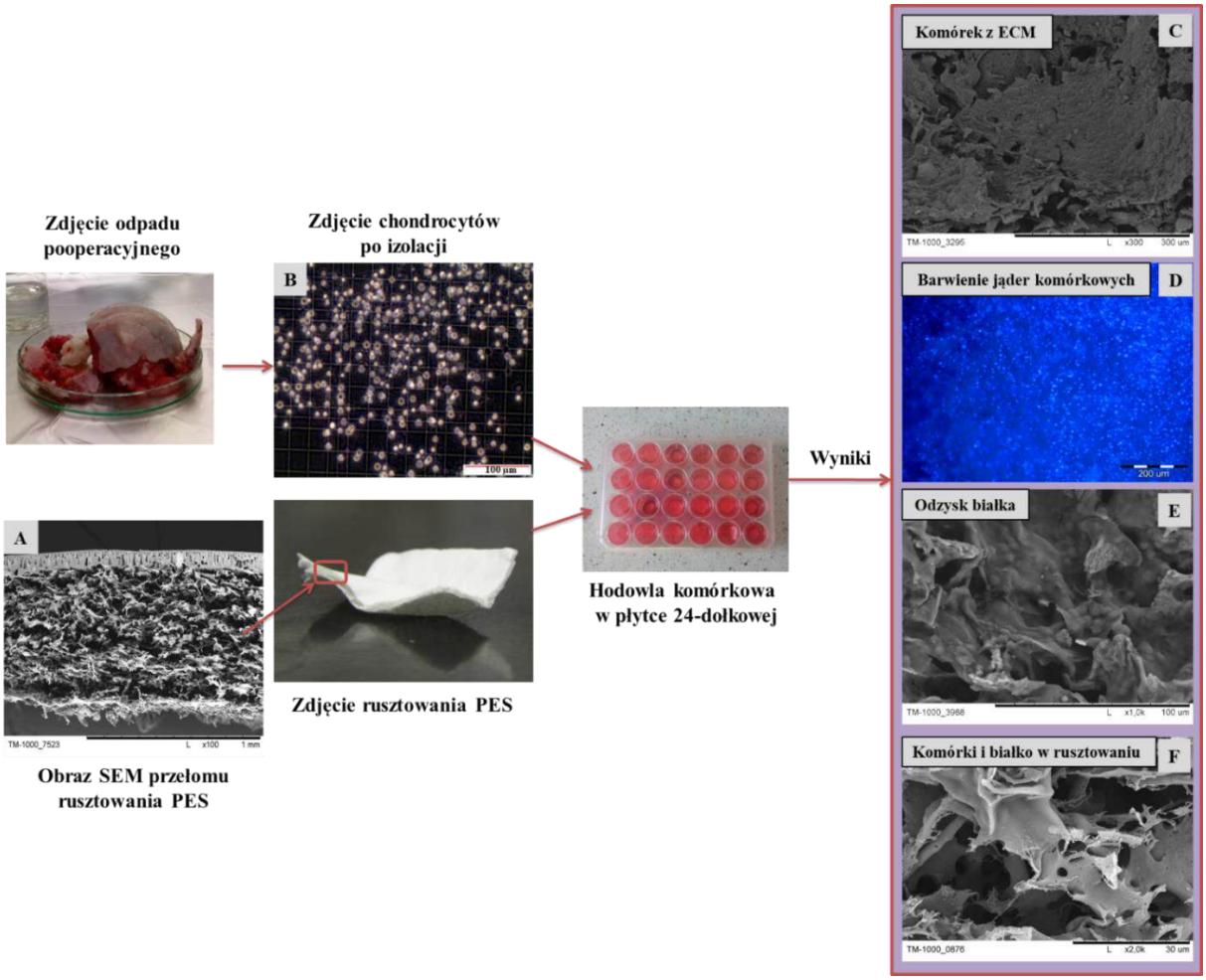

Rysunek 25. Ogólny schemat przedstawiający zarówno procedurę wykonywanych badań jak i otrzymane rezultaty przed (A, B) w trakcie (C, D, F) oraz po zakończeniu hodowli (E). Paski skali: F – 30 µm, B, E – 100 µm, D – 200 µm, C – 300 µm, A – 1 mm. Obrazy A, C, E, F zostały wykonane za pomocą SEM. Zdjęcia B i D – wykonano z użyciem mikroskopu odwróconego. Reprodukcja z Publikacji 4.

Żywotność komórek oceniłam za pomocą testu MTT (bromek 3-[4,5-dimetylotiazolo-2-yl]-2,5-difenylu). Wykonałam także barwienie jąder komórkowych z wykorzystaniem barwnika Hoechst (Rysunek 25 D). Rusztowanie z PES uzyskało wyższą aktywność komórek oraz większą zawartość białek w porównaniu z rusztowaniami z

PLLA, czemu dowiodły wyniki testu MTT oraz analiza pierwiastkowa, która wykazała znacznie wyższą zawartość azotu w rusztowaniu z PES. Zawartość azotu jest obiektywnym i wiarygodnym wskaźnikiem ilości białek w badanej próbce. Dowodzi to, że skafold z PES zapewnia lepsze środowisko dla wzrostu chondrocytów i produkcji białek. Inną zaletą materiału z PES są grupy siarczanowe [$-SO^2$] w łańcuchu polimeru, które występują także w macierzy chrząstki szklistej (siarczan chondroityny). Może to warunkować podobieństwo do naturalnego środowiska chondrocytów. Ponadto, rusztowanie z PES można sterylizować różnymi dostępnymi technikami, takimi jak etanol, promienie gamma lub promieniowanie β oraz można je łatwo przechowywać. Oba rusztowania mają odpowiednią strukturę oraz właściwości mechaniczne jako rusztowania do hodowli chondrocytów. Niestety, ze względu na krótki czas degradacji materiału z PLLA, rusztowanie okazało się niestabilne. Po 2 tygodniach hodowli, skafold z PLLA był kruchy i ulegał rozpadowi (degradacja). Ponadto w trzecim tygodniu hodowli zaobserwowałam spadek żywotności komórek w rusztowaniach z PLLA. Można to wytłumaczyć negatywnym wpływem kwasu mlekowego na chondrocyty i zmniejszoną strukturą materiału w wyniku degradacji. Dowodzi to, że badane rusztowania z PLLA nie są odpowiednie aby zapewnić właściwe warunki dla komórek na czas hodowli i regeneracji chrząstki. Natomiast rusztowanie z PES, nawet po 7 tygodniach hodowli, wykazywało odpowiednią strukturę i można było zaobserwować znacznie więcej wybarwionych jąder komórkowych (białe punkty) (Rysunek 26). Badania wykazały znaczną przewagę rusztowań z PES nad rusztowaniami z PLLA w hodowli chondrocytów ludzkich.

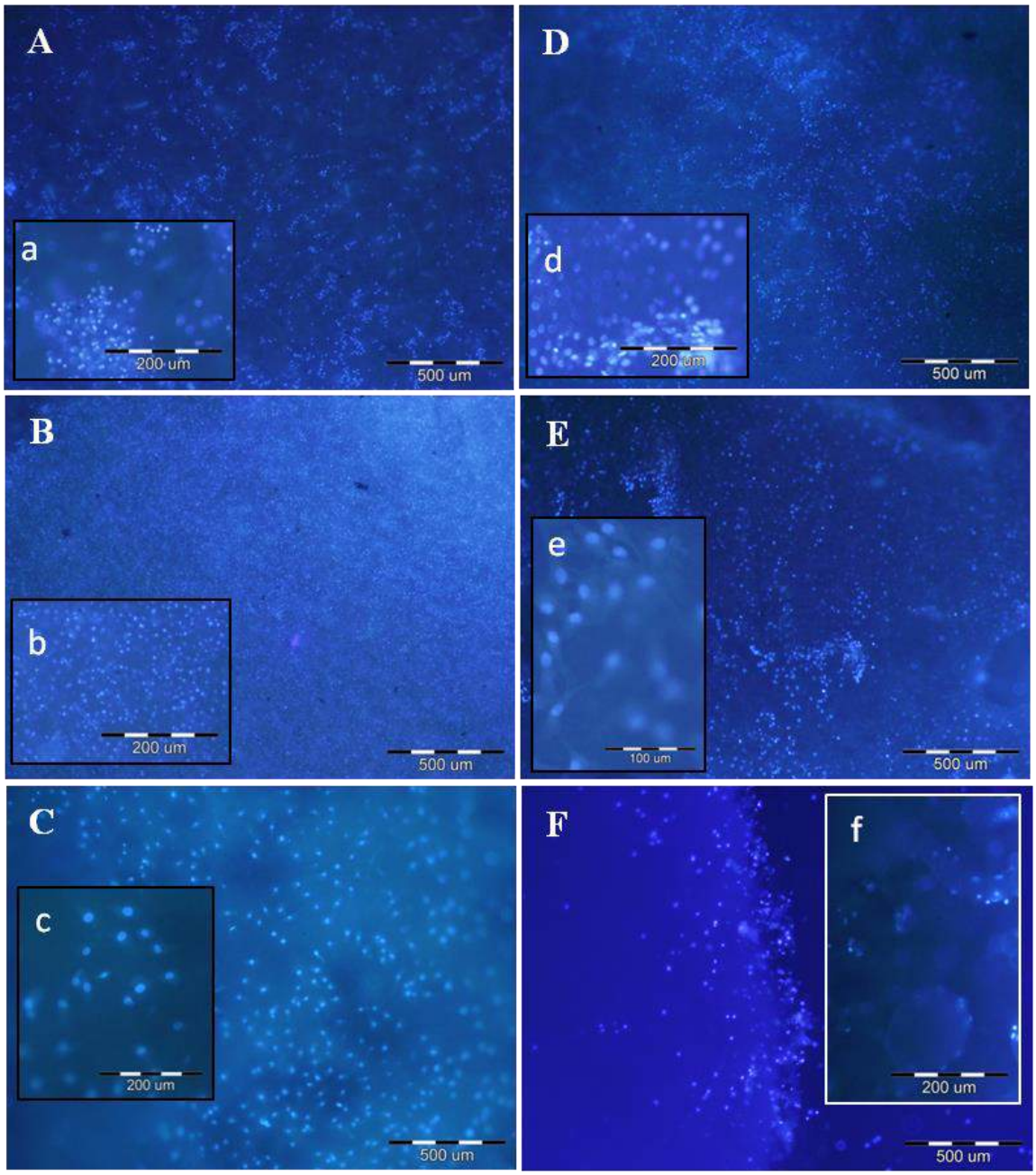

Rysunek 26. Barwienie barwnikiem Hoechst jąder komórkowych. A, B, C – rusztowania z PES odpowiednio po 72 godzinach, 3 tygodniach i 7 tygodniach hodowli; D, E, F – rusztowania z PLLA odpowiednio po 72 godzinach, 3 tygodniach i 7 tygodniach hodowli. Zdjęcia a-f pokazują przybliżenie zdjęć A-F. Paski skali: A-F – 500 µm; a-d, f – 200 µm; e – 100 µm. Reprodukcja z Publikacji 4.

Ponadto, w trakcie prac badawczych opracowano i następnie opatentowano sposób na odzyskanie białka z rusztowań, poprzez rozpuszczenie membran (polimeru) po hodowli w odpowiednim rozpuszczalniku, który nie narusza białka [159]. Za pomocą SEM wykazałam, że odzyskane białka miały strukturę podobną do natywnej tkanki chrzęstnej (Rysunek 27).

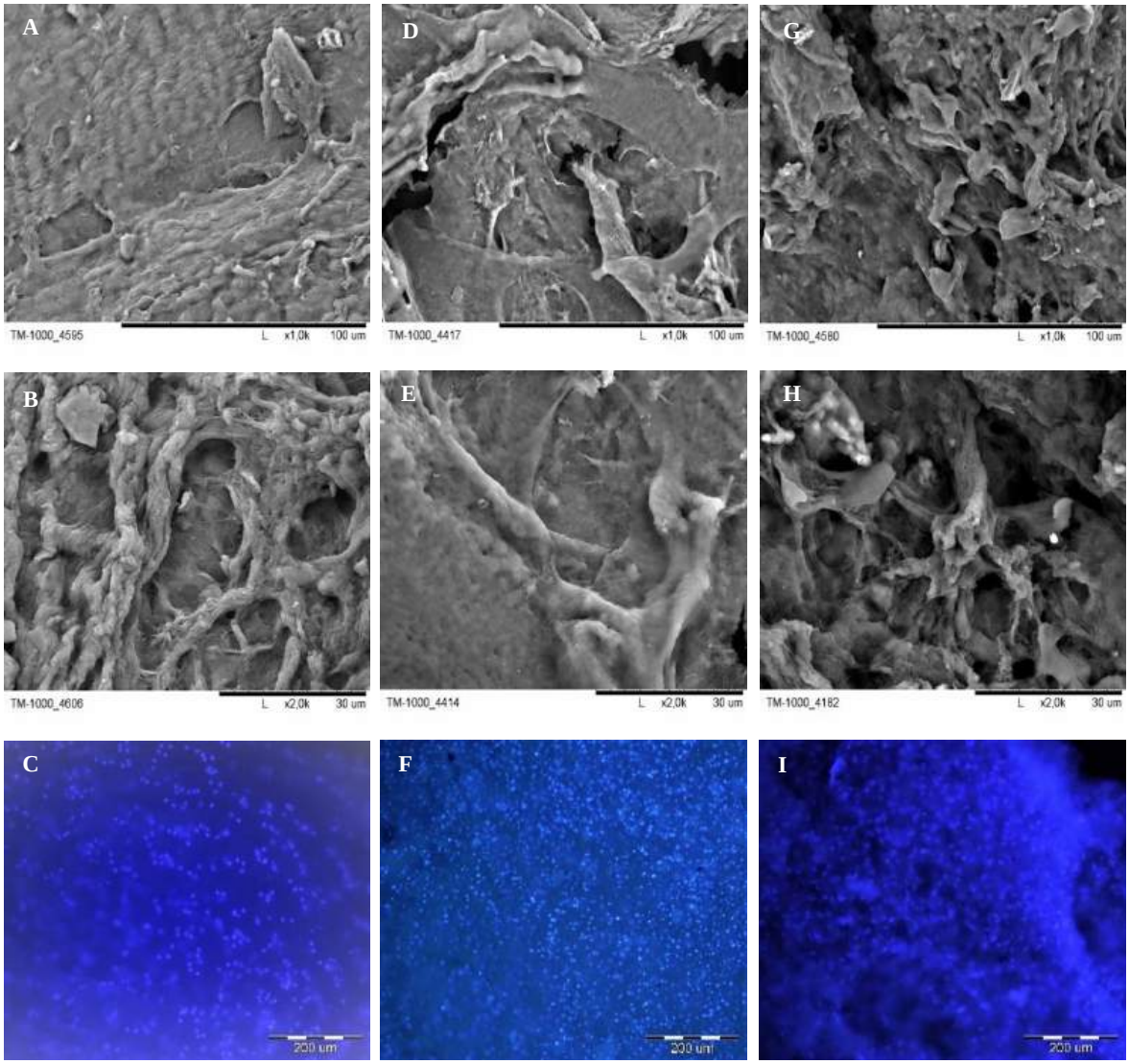

Rysunek 27. Obrazy SEM chrząstki natywnej i odzysków uzyskanych z rusztowań (A, B, D, E, C, H) oraz wybarwienie jąder komórkowych za pomocą barwnika Hoechst (C, F, I), gdzie A-B przedstawia chrząstkę natywną, D-E odzysk z rusztowania z PES po 3 i 7 tygodniach; G-H – odzysk z rusztowania z PLLA po 3 i 7 tygodniach. Barwienie jąder barwnikiem Hoechst odpowiednio dla C – chrząstki natywnej, F – odzysków z rusztowania z PES po 3 tygodniach hodowli, I – odzysk z rusztowania z PLLA po 3 tygodniach hodowli. Zdjęcia C, F, I zostałe wykonane z użyciem mikroskopu odwróconego. Paski skali: C, F, I – 200 µm, A, D, C – 100 µm oraz B, E, H – 30 µm. Reprodukcja z Publikacji 4.

W niniejszej publikacji wykazałam, że otrzymane przeze mnie rusztowania PES znajdują zastosowanie do prowadzenia hodowli chondrocytów ludzkich, co też stanowi udowodnienie **TEZY 2: Opracowane i otrzymane syntetyczne rusztowania komórkowe mogą znaleźć zastosowanie do hodowli chondrocytów i regeneracji ubytków chrząstki stawowej.**

7.3.2. Badania in vivo z wykorzystaniem modelu zwierzęcego (na podstawie Publikacji 5)

Publlikacja przedstawia wykorzystanie metody terapeutycznej ACI na dwóch różnych rusztowaniach w leczeniu uszkodzeń chrząstki stawowej królika. Pierwsza z nich to dostępna na rynku membrana Chondro-Gide, która wykonana jest z kolagenu typu I i typu III. Drugie rusztowanie to otrzymane przeze mnie syntetyczne rusztowanie z PES (Rysunek 28), które otrzymałam także do hodowli izolowanych ludzkich chondrocytów (rozdział 7.3.1). Nowość tego badania polega na zastosowaniu syntetycznej membrany z PES, która została wykorzystana po raz pierwszy na modelu zwierzęcym oraz jej porównaniu względem komercyjnej membrany Chondro-Gide.

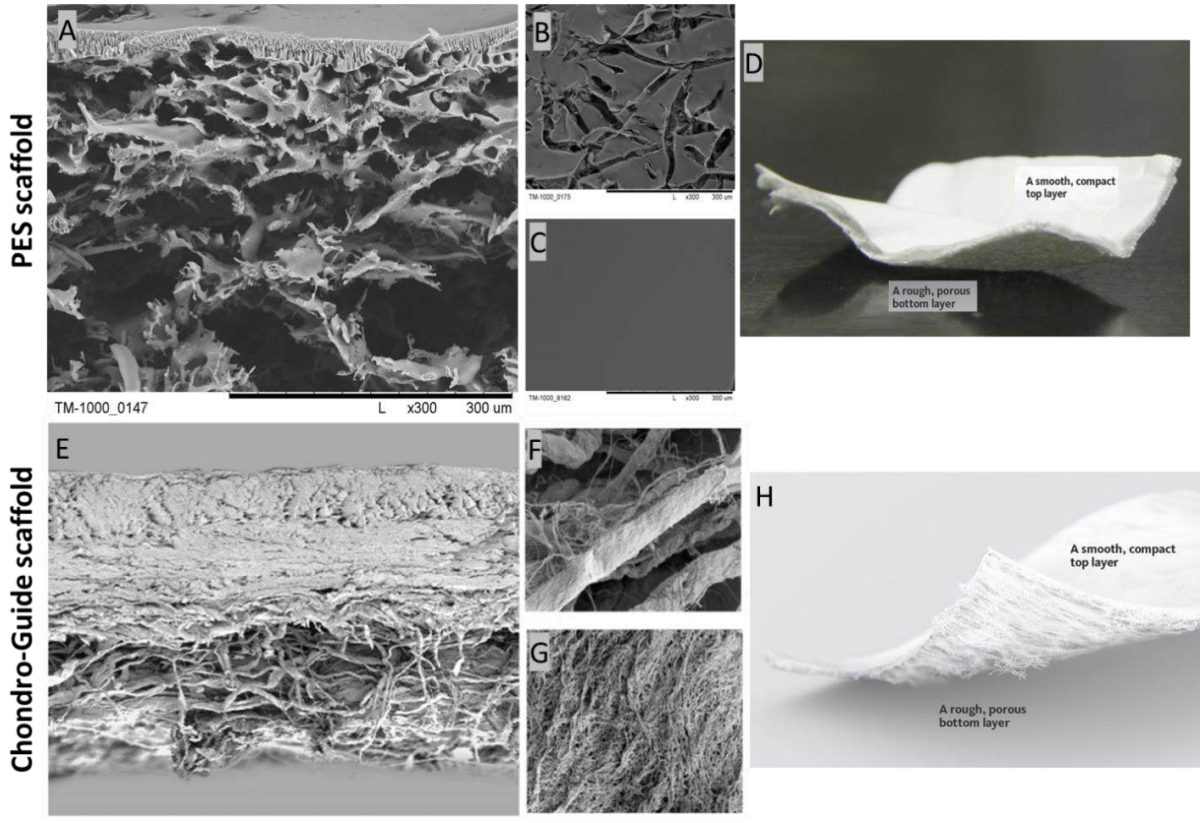

Rysunek 28. Schemat, na którym zostały przedstawione obrazy SEM rusztowania z PES (A – przełom rusztowania, B – warstwa górna, C –warstwa dolna) oraz membrana Chondro-Gide (E – przełom rusztowania, F – warstwa górna, G – warstwa dolna). Na zdjęciach zostały odpowiednio przedstawione skafoldy: D – rusztowanie z PES i H – membrana Chondro-Gide. Powiększenie: (A–C) x300; (E) x100; (F,G) x1500. Reprodukcja z Publikacji 5.

Do badania wykorzystano prawe i lewe kolano 64 królików rasy białej nowozelandzkiej o masie ciała około 3 kg w wieku 4 miesięcy. We wszystkich stawach

kolanowych wykonano ubytki pełnej grubości, penetrujące do warstwy podchrzęstnej. Wytworzone zmiany zostały wypełnione „bez" lub „z" chondrocytami po dwóch tygodniach hodowli na rusztowaniach kolagenowych lub skafoldach z PES (Rysunek 29). Uzyskano łącznie pięć grup z nastepujęcym podziałem:

I. Wszczepienie rusztowania Chondro-Gide z chondrocytami;
II. Wszczepienie rusztowania PES z chondrocytami;
III. Wszczepienie rusztowania Chondro-Gide bez chondrocytów;
IV. Wszczepienie rusztowania PES bez chondrocytów;
V. Ubytek bez implantu, umożliwiający przedostanie się komórek ze szpiku do zregenerowanej tkanki (grupa kontrolna).

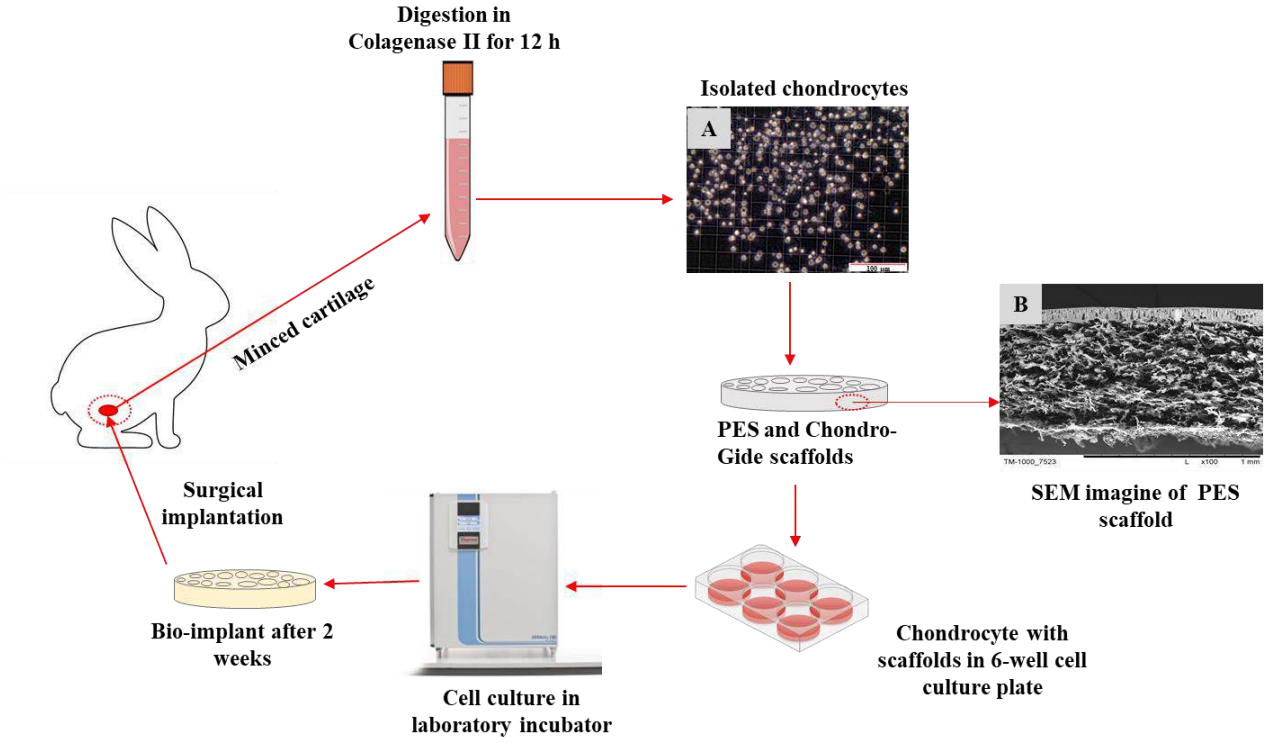

Rysunek 29. Schemat przedstawiający procedurę przeprowadzonych badań. Paski skali: A – 100 µm, B – 1 mm. Reprodukcja z Publikacji 5.

Tkankę reparacyjną analizowano makroskopowo i histologicznie po operacji w 12, 25 i 52 tygodniu. W pracy oceniono ekspresję genu (analiza RT-PCR mRNA) kodującego prokolagen typu II, który jest typowy dla chrząstki szklistej oraz przeprowadzono analizę

pierwiastkową w celu oszacowania masy tkanki wyhodowanej na membranach. Ze względu na materiał tworzący Chondro-Gide (kolagen typu I i III) test RT-PCR i analiza elementarna została przeprowadzona wyłącznie dla rusztowań z PES.

Badanie RT-PCR wyizolowanego mRNA z komórek oderwanych od rusztowania PES wykazało ekspresję prokolagenu typu II. Analiza elementarna membrany PES po 2 tygodniach hodowli z chondrocytami królika wykazała 0,23 mg tkanki.

Ocena makroskopowa i mikroskopowa udowodniła, że jakość zregenerowanej tkanki była podobna po przeszczepieniu komórek umieszczonych na membranach z PES lub Chondro-Gide. Zregenerowana tkanka w ubytkach osiągnęła dojrzałość po 12 tygodniach i wykazywała morfologię chrząstki szklistej nawet po 52 tygodniach. W badaniu uzyskano ponad 95% całkowitej regeneracji ubytków chrząstki w kolanach króliczych. Ponadto w próbkach histopatologicznych nie stwierdzono pozostałości fragmentów rusztowania PES. Badania dowiodły, że membrana PES spełniła swoje zadanie i może być wykorzystana do dalszych badań.

Przeprowadzone badania udowadniają **TEZĘ 2: Opracowane i otrzymane syntetyczne rusztowania komórkowe mogą znaleźć zastosowanie do hodowli chondrocytów i regeneracji ubytków chrząstki stawowej.**

7.3.3. Badania in vivo z wykorzystaniem modelu zwierzęcego (na podstawie Publikacji 6)

Spośród opracowanych i otrzymanych przeze mnie rusztowań wytypowałam dwa skafoldy z poliestru – rusztowania PLCA1 i PLCA2 (Publikacja 2, Rozdział 7.2.1), które przekazałam do dalszych badań in vivo na modelu zwierzęcym (królik) w celu sprawdzenia ich skuteczności w regeneracji chrząstki stawowej. W Publikacji 6, rusztowanie PLCA1, do otrzymania którego użyto włókniny z PVP zostało nazwane „PVP" (Rysunek 30, Rysunek 15), natomiast skafold PLCA2, gdzie zastosowałam włókninę z żelatyny, nazwano jako rusztowanie „Z" (Rysunek 31, Rysunek 16). Rusztowania zostały wytypowane do badań ze względu na perforowaną warstwę wierzchnią z porami o średnicy powyżej 20 μm oraz sieć wzajemnie połączonych makroporów o średnicy większej niż 300 μm w przełomie membran. Cechy te są niezbędne do chondrogenezy MSCs.

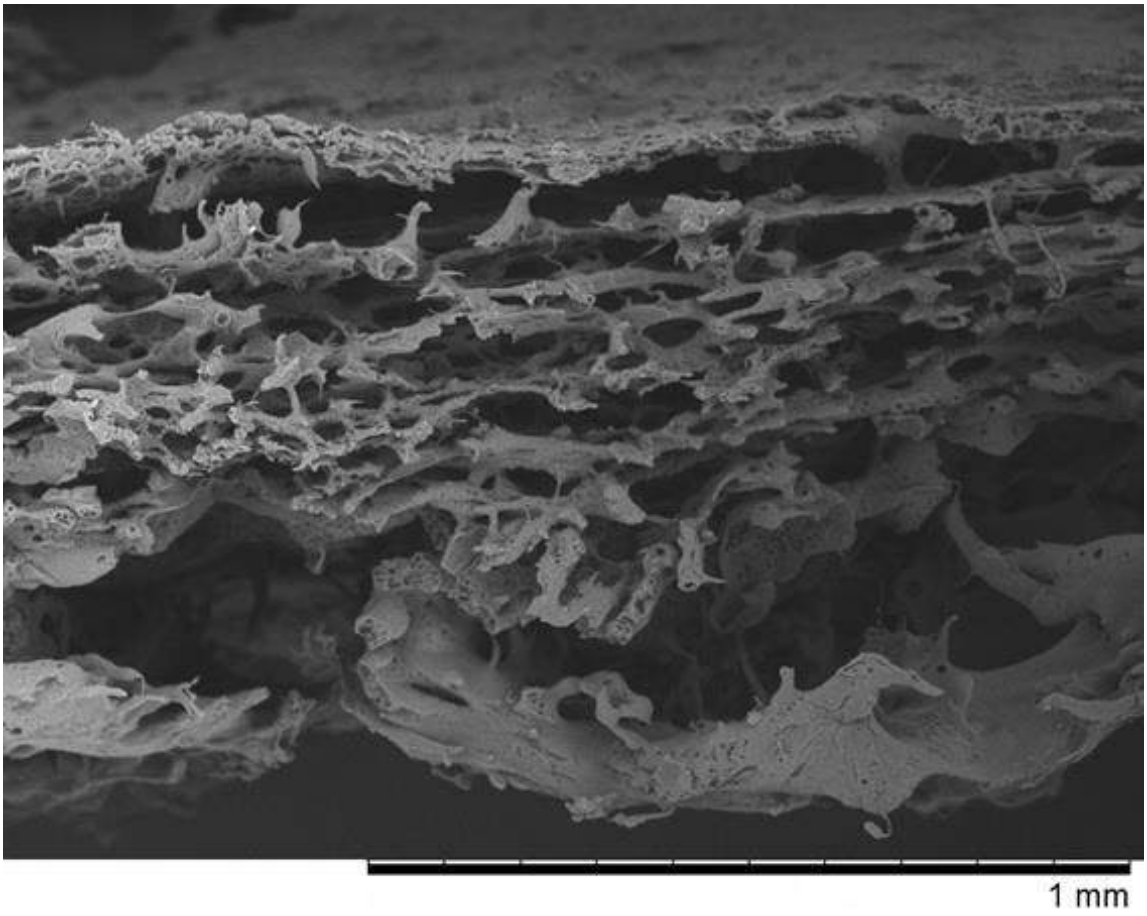

Rysunek 30. Rusztowanie "PVP". Pasek skali 1 mm. Reprodukcja z Publikacji 6.

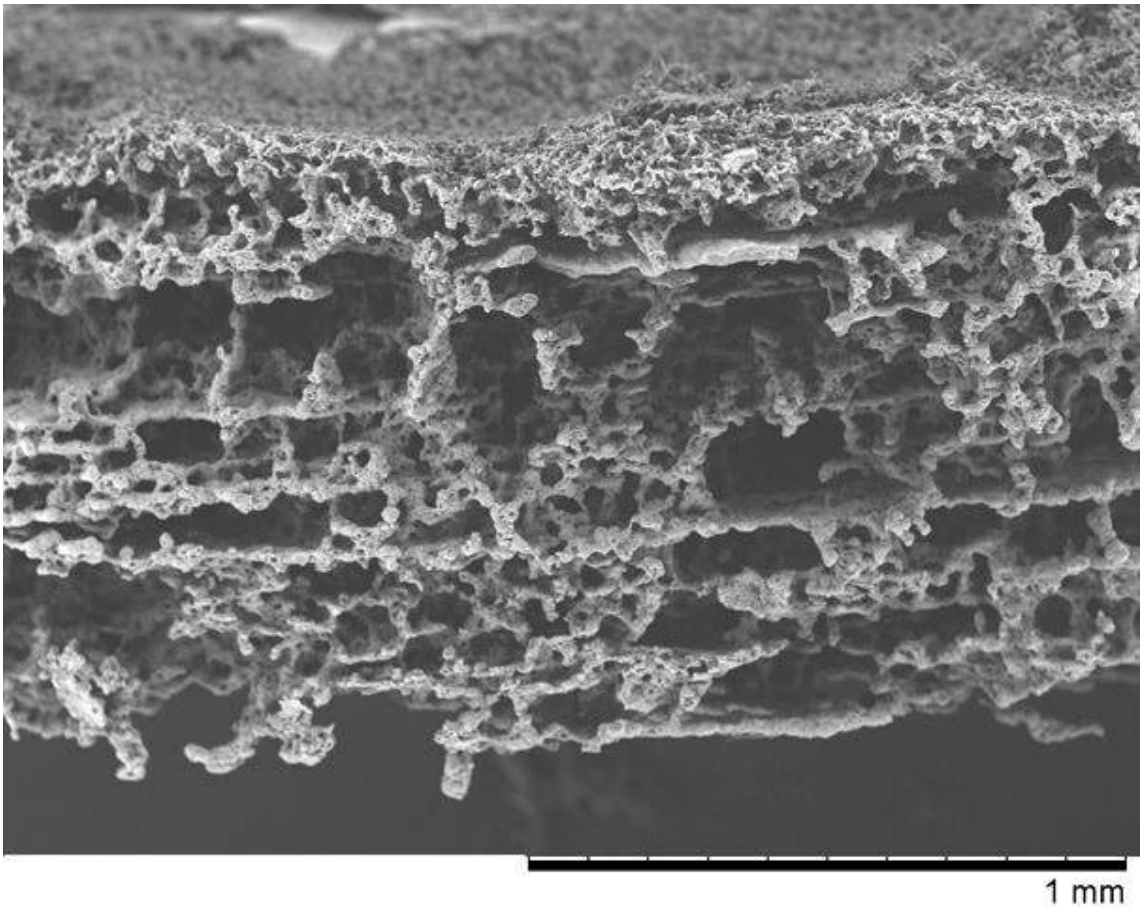

Rysunek 31. Rusztowanie "Z". Pasek skali 1 mm. Reprodukcja z Publikacji 6.

Do badania użyto prawe i lewe kolano 27 samców królików rasy białej nowozelandzkiej o masie około 3,5 kg w wieku około 4 miesięcy. W badaniu została wykorzystana metoda terapeutyczną AMIC. We wszystkich stawach kolanowych wykonano ubytki do warstwy podchrzęstnej, które następnie były poddawane procedurze MF. Wytworzone zmiany zostały wypełnione rusztowaniami lub pozostawione bez wypełnienia (grupa kontrolna) (Rysunek 32).

Uzyskano łącznie trzy grupy z nastepujęcym podziałem:

I) Wszczepienie rusztowań „PVP”;

II) Wszczepienie rusztowań „Z”;

III) Ubytki bez implantu (grupa kontrolna).

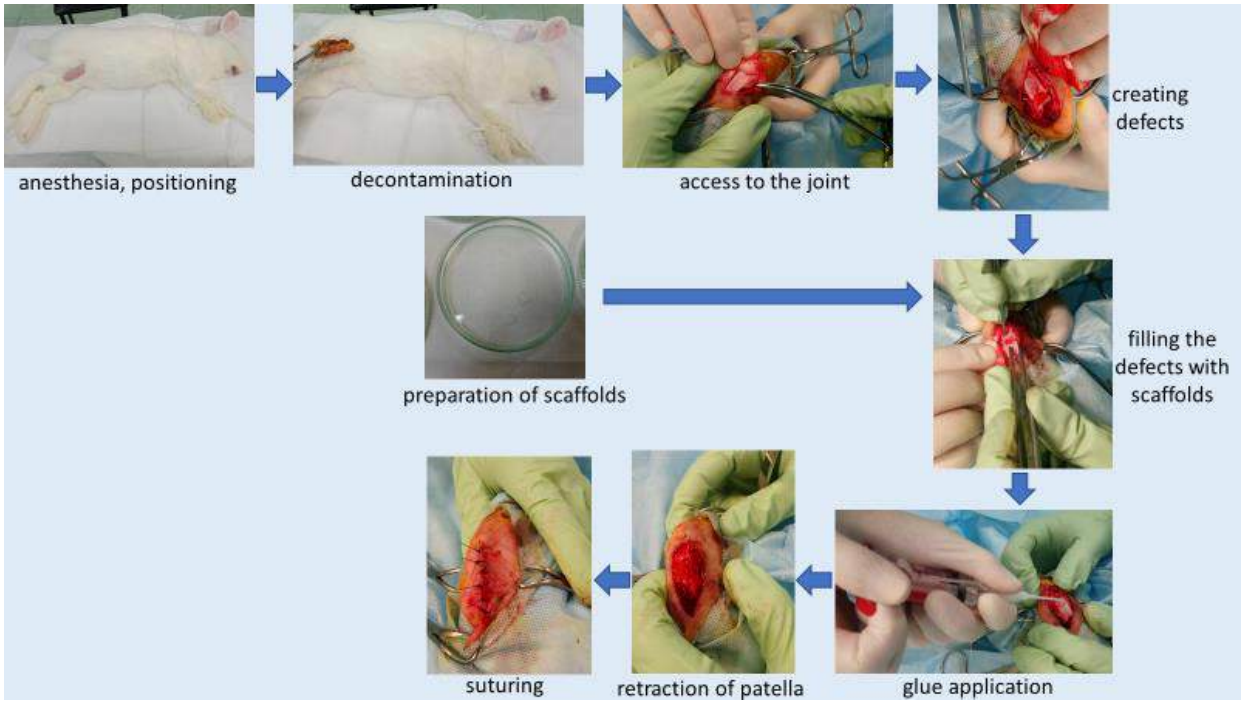

Rysunek 32. Schemat implatacji rusztowań. Reprodukcja z Publikacji 6.

Po 8, 16 i 24 tygodniach przeprowadzono badania histopatologiczne i chromatografię żelową (GPC) (Rysunek 33).

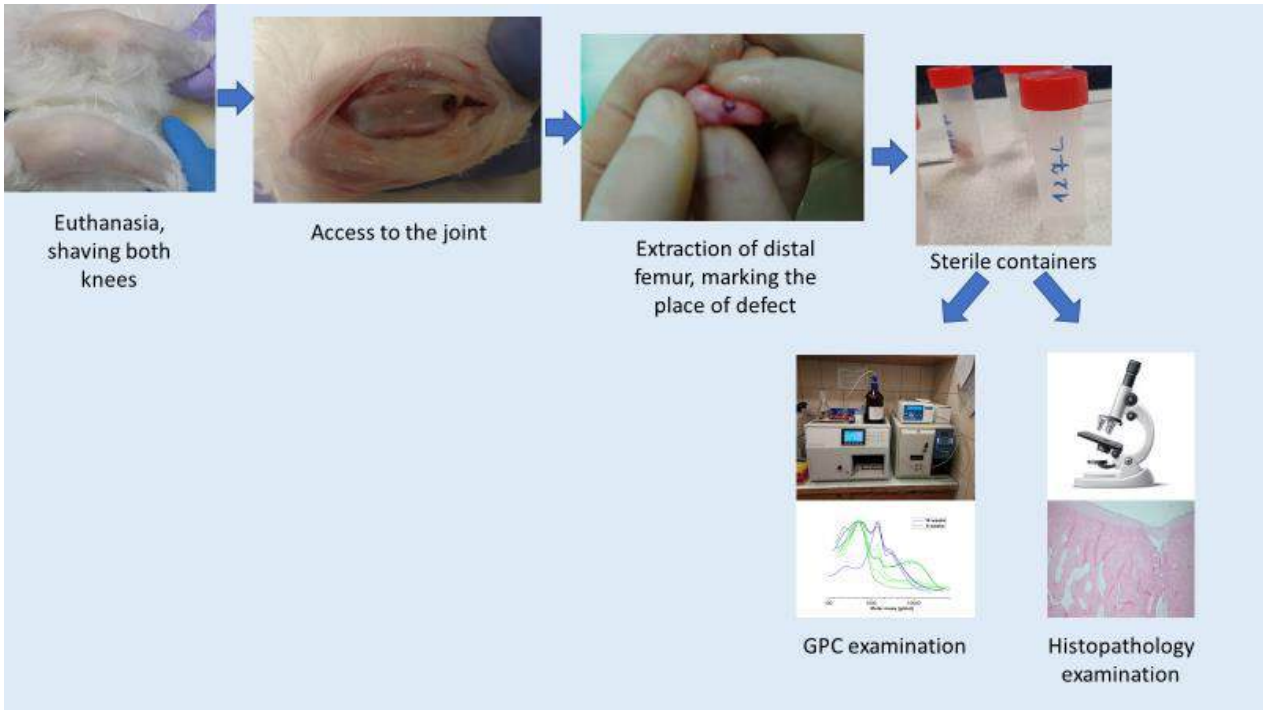

Rysunek 33. Badania GPC oraz histologiczne po terminacji zwierząt. Reprodukcja z Publikacji 6.

Testy GPC wykazały, że proces biodegradacji postępuje wykładniczo, powodując degradację membran w odpowiednim czasie. Zastosowana technika chirurgiczna nie

powodowała migracji membran po implantacji. Po terminacji, w próbkach nie znaleziono żadnych fragmentów rusztowań w badaniach GPC oraz nie stwierdzono żadnych widocznych pozostałości wszczepionego materiału w próbkach histopatologicznych. Prawdopodobnie poliester został zdegradowany do postaci bardzo krótkich łańcuchów polimerowych, które zostały łatwo i całkowicie zdegradowane do produktów CO_2 i H_2O, które mogą być usuwane przez organizm.

Wydłużony czas obserwacji pokazał, że wyniki regeneratów w grupie kontrolnej były gorsze w porównaniu do grup I) i II), które z czasem ulegały poprawie. Prawdopodobnie komórki macierzyste w grupie kontrolnej osiadły jedynie powierzchownie wokół wady. Dodatkowo w badaniach wykazano, że membrana "PVP" jest lepsza ze względu na fakt, że po 24 tygodniach obserwacji wystąpił statystyczny trend dla wyższych ocen histologicznych. Była ona także łatwiejsza do implantacji ze względu na mniejszą kruchość niż membrana "Z".

W badaniach wykazano, że opracowane i otrzymane przeze mnie rusztowania poliestrowe wspierają regenerację chrząstki stawowej w modelu króliczym, co też udowadnia **TEZĘ 2**.

W badaniach, które przedstawiłam w rozdziale 7.3, wykazałam, że otrzymane rusztowania znajdują zastosowanie do hodowli chondrocytów i regeneracji chrząstki stawowej, co też stanowi udowodnienie **TEZY 2: Opracowane i otrzymane syntetyczne rusztowania komórkowe mogą znaleźć zastosowanie do hodowli chondrocytów i regeneracji ubytków chrząstki stawowej.**

8. Dyskusja

Regeneracja chrząstki stawowej pozostaje jednym z wyzwań współczesnej inżynierii tkankowej, głównie ze względu na jej ograniczoną zdolność do samoregeneracji. W literaturze naukowej coraz większą uwagę poświęca się projektowaniu rusztowań komórkowych spełniających kluczowe wymagania dla regeneracji chrząstki stawowej, takie jak odpowiednie właściwości mechaniczne, strukturalne, biodegradacyjne. Poniżej przedstawiłam szczegółową analizę i dyskusję uzyskanych wyników na tle najnowszych doniesień literaturowych.

Głównym celem badań było opracowanie rusztowań syntetycznych, umożliwiających hodowlę chondrocytów lub komórek macierzystych. W tym kontekście sformułowano dwie tezy badawcze, z których pierwsza zakładała możliwość otrzymania rusztowań komórkowych poprzez odpowiedni dobór materiałów i metod wytwarzania.

Metody wytwarzania rusztowań komórkowych

Tradycyjne metody**,** takie jak inwersja faz, liofilizacja czy elektroprzędzenie, nadal pozostają konkurencyjne w kontekście otrzymywania rusztowań o odpowiedniej strukturze i kontrolowanej porowatości. Dupuy S. i wsp. [160] w artykule przeglądowym przedstawiają zalety tego rodzaju metod, a mianowicie niska cytotoksyczność oraz prostota wykonania, co czyni je atrakcyjnymi dla zastosowań. Jednak pomimo swojej skuteczności często brakuje im możliwości precyzyjnej kontroli architektury rusztowania i właściwości mechanicznych. Niemniej jednak postępy w projektowaniu materiałów wykazały potencjał pokonania tych ograniczeń. Na przykład wykazano, że elektroprzędzone rusztowania łączące nanowłókna żelatyny i siarczanu chondroityny z mechanicznie wytrzymałym polikaprolaktonem (PCL) skutecznie wspomagają chondrogenezę bez konieczności stosowania pożywek różnicujących. Z kolei Wang Y. i wsp. [161] wykazali, że elektroprzędzone, trójwymiarowe struktury cechują się doskonałą biozgodnością, odpowiednią porowatością oraz zdolnością wspierania i różnicowania komórek chrzęstnych. Podkreślono również ich potencjał do pełnienia roli funkcjonalnych rusztowań w ortopedii regeneracyjnej, co potwierdza zasadność dalszego rozwijania i adaptacji tych tradycyjnych technik w kontekście klinicznym. Jednak metoda elektroprzędzenia ma ograniczenia w otrzymywaniu grubszych rusztowań przy jednoczesnym zachowaniu jednolitej struktury porowatej. Choć nowoczesne metody, takie jak druk 3D, zyskują na znaczeniu w inżynierii tkankowej, nadal napotykają istotne

ograniczenia. W literaturze podkreśla się trudności związane z uzyskaniem odpowiednich bioinków (biotuszów), wysokie koszty, długi czas wytwarzania, problemy z biodegradacją materiałów oraz ograniczoną stabilność mechaniczną rusztowań. Wang Y. i wsp. w artykule [162] przedstawiają przegląd rusztowań z biokompatybilnych materiałów drukowanych 3D. Autorzy zwrócili uwagę na wymagania bioników o określonych właściwościach reologicznych lub braku kontroli nad biodegradacją. Dodatkowo zaznaczają, że syntetyczne bioinki mogą być niekompatybilne, a druk 3D z materiałów naturalnych jest niestabilny. Autorzy podkreślają, że w metodzie nadal brakuje danych klinicznych, a większość sukcesów dotyczy badań na modelu zwierzęcym. Wymagana jest konieczność dalszych badań i optymalizacji zanim metoda zostanie powszechnie wdrożona klinicznie. Na ograniczenia w dostępnych materiałach drukarskich, w szczególności w przypadku biotuszy z komórkami wskazali autorzy Lin X. i wsp. [163]. W artykule dokonany został przegląd rusztowań wielowarstwowych, których zadaniem powinno być lepsze naśladowanie architektury chrząstki szklistej w porównaniu do jednolitych rusztowań. Jednak zwrócono uwagę na to, że metoda druku 3D jest czasochłonna, kosztowna i wymaga dokładnej kontroli nad strukturą porów i warstw. Dodatkowo Wu X. i wsp. [164] w artykule przeglądowym zaznaczyli, że bioinki wymagają precyzyjnego doboru lepkości, szybkości procesu żelowania oraz sił ścinających, aby zapewnić drukowalność i przeżywalność komórek. Dodatkowo zwrócili uwagę na to, że częstymi problemami podczas biodruku hydrożeli jest zatykanie dysz, brak spójności rusztowań czy rozwarstwianie materiału. Mimo dynamicznego rozwoju technologii biodruku 3D oraz obiecujących wyników badań in vitro i *in vivo*, większość rusztowań komórkowych uzyskanych tą metodą nie została jak dotąd dopuszczona do badań klinicznych. Fakt ten wskazuje na istotne ograniczenia tej technologii. Tym samym podkreślona zostaje przewaga klasycznych, dobrze przebadanych metod wytwarzania rusztowań, które mimo mniejszej innowacyjności nadal stanowią bardziej praktyczną alternatywę w kontekście zastosowań klinicznych. W przeprowadzonych badaniach wykazałam, że klasyczne metody, takie jak inwersja faz z wykorzystaniem odpowiednich prekursorów porów, pozostają konkurencyjne względem nowoczesnych technologii. Wykorzystałam metodę, która charakteryzuje się prostotą, niskim kosztem oraz krótkim czasem wykonania. W przeciwieństwie do bardziej złożonych metod, takich jak druk 3D, nie wymaga specjalistycznych materiałów ani aparatury, co czyni ją atrakcyjną alternatywą, szczególnie na etapie badań przedklinicznych.

Struktura rusztowań komórkowych

Architektura rusztowań komórkowych, w tym rozkład porów, ich średnica oraz połączenia między nimi, odgrywa kluczową rolę w rozwoju komórek chrzęstnych. Rusztowania komórkowe o porowatości w zakresie 65–90% oraz średnicy porów 50–300 μm wykazują parametry uznawane w literaturze za optymalne dla wzrostu i różnicowania komórek, co potwierdzili m.in. Lin X. i wsp. [163]. Chen i wsp. [165] oraz Wu X. i wsp. [164] w artykułach wskazują, że odpowiednia porowatość i sieć wzajemnie połączonych porów są niezbędne dla efektywnej migracji komórek, dyfuzji składników odżywczych oraz usuwania metabolitów. Struktury tego typu sprzyjają unaczynieniu i skutecznej regeneracji tkanki. W badaniach własnych otrzymałam rusztowania o porowatości w zakresie 75-98,5 % i średnicy porów 50–400 μm, poprzez zastosowanie prekursorów porów, takich jak włókniny polimerowe i kryształy soli NaCl. Parametry te pozostają zgodne z wartościami uznawanymi w literaturze za optymalne dla wzrostu chondrocytów i komórek macierzystych. Pory w rusztowaniach były wzajemnie połączone, co jest niezbędne do wspierania hodowli komórkowej oraz ułatwiania wymiany składników odżywczych.

Właściwości mechaniczne rusztowań komórkowych

Właściwości mechaniczne rusztowań stanowią kluczowy czynnik determinujący ich przydatność w regeneracji chrząstki stawowej. Rusztowania powinny być elastyczne i odporne na ucisk, aby wytrzymać obciążenia występujące w stawie i zapewniać stabilność do czasu odbudowy tkanki [166]. W literaturze można wyszukać informację odnośnie hydrożeli, które stanowią atrakcyjny materiał do regeneracji chrząstki stawowej, gdyż są biokompatybilne, wykazują podobieństwo do macierzy zewnątrzkomórkowej oraz umożliwiają wbudowanie w ich strukturę komórek i czynników bioaktywnych. Jednak z tego względu, że są one głównie otrzymywane z biopolimerów naturalnych mają one niską wytrzymałość mechaniczną, co ogranicza ich użycie w miejscach, w których występuje wysokie obciążenie. Autorzy Wu X. i wsp. [164] zaznaczają, że zwiększenie stabilności materiału wymaga zastosowania dodatków, takich jak inne polimery, włókien, co komplikowałoby skład biotuszów w procesie druku 3D. Mimo wysokiego potencjału hydrożeli w regeneracji chrząstki stawowej mają one ograniczenia w produkcji oraz niską wytrzymałość mechaniczną. Z tego względu użyte materiały mają znaczący wpływ na właściwości mechaniczne rusztowań komórkowych. Lin X. i wsp. [163], Chen M. i wsp. [167] oraz Li C-S. [168] w artykułach podkreślają, że naturalne polimery mają niską

wytrzymałość mechaniczną oraz słabą stabilność i są podatne na hydrolizę. Natomiast materiały syntetyczne mimo dobrej wytrzymałości mają zasadniczą wadę, mogą ulegać przedwczesnej biodegradacji co ma wpływ na osłabienie właściwości mechanicznych i utratą odpowiedniej struktury rusztowania, niezbędnej do rozwoju komórek w rusztowaniu. Wu X. i wsp. [164] wykazali, że zbyt szybki rozpad rusztowania uniemożliwia regenerację, natomiast zbyt wolny blokuje odbudowanie tkanki. W badaniach własnych, do otrzymania rusztowań zastosowałam biokompatybilne polimery syntetyczne, które zapewniły odpowiednią wytrzymałość mechaniczną przy zachowaniu elastyczności materiału. W badaniach potwierdziłam również, że łączenie polimerów o zróżnicowanej podatności na biodegradację pozwala na projektowanie rusztowań o kontrolowanym czasie rozkładu. Szczególnie istotnym wynikiem było zaobserwowanie stopniowej biodegradacji polietersulfonu w stymulowanym płynie fizjologicznym, co pozostaje w sprzeczności z dotychczasowymi doniesieniami literaturowymi, według których PES uznawany był za materiał trwały i nieulegający biodegradacji. Wyniki te mogą mieć znaczenie w kontekście indywidualizacji terapii poprzez dostosowanie właściwości materiału do wieku pacjenta i tempa regeneracji tkanki.

Kolejnym etapem w pracy dyplomowej było potwierdzenie, że otrzymane rusztowania syntetyczne zapewnią odpowiednie warunki do wzrostu komórek chrzęstnych i mogą wspierać regenerację chrząstki stawowej. Dlatego też druga teza badawcza zakładała, że otrzymane rusztowania komórkowe mogą znaleźć zastosowanie do hodowli chondrocytów i regeneracji ubytków chrząstki stawowej.

W ostatnich latach zauważalny jest dynamiczny rozwój nowatorskich strategii w projektowaniu wielowarstwowych rusztowań do regeneracji chrząstki, szczególnie tych, które łączą właściwości mechaniczne z wysoką bioaktywnością i integrujących właściwości zarówno tkanki chrzęstnej, jak i podchrzęstnej. Przykładem tego trendu jest rusztowanie opracowane przez Lewisa i wsp. [169], które łączy supramolekularny polimer wiążący czynnik wzrostu TGFβ-1 z mikrożelami kwasu hialuronowego. Badania w modelu owcy wykazały, że rusztowanie to wykazuje wysoką stabilność in situ, nawet w warunkach mechanicznego obciążenia stawu, a także znacząco wspiera regenerację chrząstki szklistej w porównaniu do samego czynnika wzrostu. Obiecujące wyniki uzyskali autorzy Yanga i wsp. [170], gdzie zaprojektowali dwuwarstwowe rusztowanie złożone z chitozanu i jedwabiu w warstwie chrząstkowej oraz drukowanego 3D porowatego tantalu jako warstwy podchrzęstnej. Unikalnym elementem tej konstrukcji było zastosowanie egzosomów z modyfikowanym miR-29a, które silnie promowały różnicowanie

chondrocytów i regenerację tkanki. Badania *in vivo* w modelu szczura z ubytkami pełnej grubości wykazały skuteczną integrację z otaczającą tkanką oraz jednoczesną regenerację chrząstki i kości podchrzęstnej. Kolejnym przykładem jest trójwarstwowe rusztowanie opracowane przez Zhong i wsp. [171], składające się z metakrylowanych kompozytów hydrożelowych GelMA (metakrylowana żelatyna) i nHAMA (metakrylowany hydroksyapatyt), które odwzorowuje strukturę osteochondralną. W modelu zwierzęcym autorzy potwierdzili skuteczną regenerację zarówno chrząstki, jak i kości, z dobrym utrzymaniem integralności warstw i integracją z otaczającą tkanką. Dodatkowo, autorzy Xu i wsp. [172] udowodnili wysoki potencjał rusztowań opartych na zdecelularyzowanej macierzy zewnątrzkomórkowej (dECM) w połączeniu z komponentami syntetycznymi. Uzyskane kompozyty, charakteryzujące się wysoką bioaktywnością, wykazały w testach *in vivo* skuteczne pobudzanie regeneracji tkanek, szczególnie dzięki obecności naturalnych składników ECM oraz możliwości dostosowania właściwości mechanicznych do konkretnej lokalizacji tkankowej.

W kontekście projektowania zaawansowanych rusztowań komórkowych warto równocześnie zwrócić uwagę na rozwiązania o prostszej konstrukcji, które pomimo braku aktywnych składników biologicznych mogą przynosić istotne korzyści kliniczne. Przykładem są dwuwarstwowe, bezkomórkowe implanty takie jak MaioRegen Chondro+, które zostały ocenione w badaniu Gudas i wsp. [173] w ramach 2-letniej obserwacji klinicznej. Implantacja przeprowadzona metodą artroskopową wykazała znaczną poprawę funkcji stawu już po 6 miesiącach, utrzymującą się w dłuższej perspektywie. Chociaż rusztowania tego typu nie zawierają komórek ani czynników wzrostu, potwierdzono ich bezpieczeństwo i skuteczność w leczeniu uszkodzeń chrząstki.

Tabela 3 przedstawia zestawienie rusztowań opisywanych zarówno w rozprawie doktorskiej (Publikacje 3–6), jak i w najnowszej literaturze światowej (2024–2025), z uwzględnieniem ich rodzaju, bioaktywności, metody otrzymywania oraz danych dotyczących porowatości i wielkości oporów.

Tabela 3. Rusztowania komórkowe do regeneracji chrząstki stawowej.

Rodzaj rusztowania	**Bioaktywność, badania**	**Właściwości mechaniczne**	**Metoda otrzymania**	**Porowatość**	**Wielkość porów**
Supramolekularne + mikrożele HA [169]	Zawiera peptydy wiążące TGF-β1; wspiera różnicowanie chondrogeniczne MSCs. Badania *in vitro* i *in vivo* (owca)	~5 kPa (moduł sprężystości)	Pasta iniekcyjna (samozestalenie w kontakcie z Ca^{2+})	Brak danych	Brak danych
Dwuwarstwowe rusztowanie hybrydowe: chitozan/jedwab i tantal [170]	Zawiera egzosomy z miR-29a; badania *in vivo* (szczur)	Brak danych	Druk 3D (tantal), liofilizacja, sieciowanie (chitozan/jedwab)	~75%	80–160 µm (dla warstwy chitozan/ jedwab)
Trójwarstwowe rusztowanie z metakrylowej żelatyny (GelMA) i metakrylowanego hydroksyapatytu (nHAMA) [171]	Dobra biokompatybilność i właściwości chodrogenne prowadzące do regeneracji osteochondralnej	Wytrzymałość 181 kPa	Fotoutwardzanie warstwowe	Struktura porowata z gradientem	Brak danych
Rusztowanie komercyjne MaioRegen Chondro+ [173]	Badanie kliniczne 2-letnie, skuteczna odbudowa chrząstki	Brak danych	Liofilizacja	Brak danych	Brak danych
Kompozytowe rusztowanie z decelurozowaną macierzą zewnątrzkomórkową (dECM) [172]	Naturalna bioaktywność	Brak danych	Liofilizacja, odlewanie	Brak danych	100–200 µm
Rusztowanie z mieszanki polimerów PES/PUR (Publikacja 3)	Biokompatybilne polimery	Wytrzymałość >10 MPa	Inwersja faz + prekursory porów (włóknina i kryształy NaCl)	Do 87%	50–300 µm
Rusztowanie PES z izolowanymi chondrocytami ludzkimi (Publikacja 4)	Badania *in vitro* (chondrocyty ludzkie)	Wytrzymałość >10 MPa	Inwersja faz + prekursory porów (włóknina polimerowa)	98,50%	60-300 µm µm

Rusztowanie PES z chondrocytami królika (Publikacja 5)	Badania *in vivo* (królik)	Wytrzymałość >10 MPa	Inwersja faz + prekursory porów (włóknina polimerowa)	98,50%	60-300 µm µm
Rusztowanie z kopolimeru PCLA, bez komórek (Publikacja 6)	Badania *in vivo* (królik)	Brak danych	Inwersja faz + prekursory porów (włóknina polimerowa)	75-95%	50-400 µm
Rusztowanie z PES z komórkami auto- i allogenicznymi [174]	Badania *in vivo* (królik)	Wytrzymałość >10 MPa	Inwersja faz + prekursory porów (włóknina polimerowa)	98,50%	60-300 µm

Na tle opisywanych w literaturze światowej zaawansowanych rozwiązań, opracowane w ramach niniejszej rozprawy doktorskiej syntetyczne rusztowania wykazały porównywalny, a w wielu aspektach konkurencyjny potencjał. Wszystkie uzyskane wyniki wskazują, że zaprojektowane rusztowania mogą stanowić realną alternatywę zarówno dla komercyjnych implantów, jak i eksperymentalnych konstrukcji. Kluczową przewagą zaprezentowanych rozwiązan jest nie tylko potwierdzona skuteczność biologiczna, ale także wysoka powtarzalność procesu wytwarzania, łatwość produkcji oraz przewidywalna biodegradacja materiału. W badaniach *in vitro* potwierdziłam, że rusztowania z PES wspierają proliferację i rozwój ludzkich chondrocytów w stopniu wyraźnie lepszym niż porównawcze rusztowania z polilaktydu. Z kolei w modelu zwierzęcym (króliczym) zaobserwowano powstawanie tkanki o strukturze zbliżonej do chrząstki szklistej oraz dobrą integrację rusztowania z otaczającą tkanką, co potwierdziły oceny histologiczne i ekspresja markerów chondrogenezy (Publikacje 4–6). Istotnym uzupełnieniem danych własnych są doniesienia literaturowe [174,175], które potwierdzają potencjał polimeru PES jako materiału biomedycznego oraz badania przedstawione w artykule autorstwa Jakutowicz i wsp., które wykazały, że rusztowania z PES przedstawia porównywalną skuteczność regeneracyjną przy zastosowaniu zarówno chondrocytów autologicznych, jak i allogenicznych, co otwiera perspektywy rozwoju terapii opartych na allogenicznych przeszczepach komórkowych. Na tym tle syntetyczne rusztowania opracowane w ramach pracy cechuje przewaga w zakresie prostoty technologicznej, stabilności strukturalnej, możliwości produkcji na większą skalę oraz elastyczności w projektowaniu właściwości degradacyjnych. Ich parametry mechaniczne, biozgodność i efektywność regeneracyjna czynią je obiecującym rozwiązaniem w kontekście zastosowań klinicznych.

Uzyskane wyniki potwierdzają, że opracowane w ramach rozprawy rusztowania syntetyczne wykazują wysoką efektywność w regeneracji chrząstki stawowej, zarówno w warunkach *in vitro,* jak i *in vivo*. Zastosowane materiały zapewniły korzystne właściwości mechaniczne, biokompatybilność oraz możliwość dostosowania struktury do potrzeb klinicznych, co czyni je konkurencyjnymi wobec obecnych rozwiązań komercyjnych i ksperymentalnych. Jednocześnie należy zauważyć, że pomimo dynamicznego rozwoju materiałów bioaktywnych oraz nowoczesnych strategii inżynierii tkankowej, regeneracja chrząstki nadal napotyka na istotne wyzwania. Obejmują one m.in. trudności z integracją rusztowań z otaczającą tkanką, ograniczoną wytrzymałość długoterminową, brak standaryzacji materiałów oraz niewystarczające dane kliniczne, mimo obiecujących wyników badań przedklinicznych. W związku z powyższym, przyszłe kierunki badań powinny koncentrować się na dalszym udoskonalaniu rusztowań pod względem ich bioaktywności, trwałości i potencjału translacyjnego. Kluczowe będzie także rozwijanie strategii łączących prostotę i bezpieczeństwo sprawdzonych rozwiązań z zaawansowanymi właściwościami biologicznymi, co może stanowić realną drogę do skutecznej i dostępnej terapii uszkodzeń chrząstki stawowej.

9. Podsumowanie

Dotychczas nie opracowano skutecznych rusztowań do regeneracji chrząstki stawowej w metodach ACI i AMIC, które byłyby stabilne w organizmie w czasie niezbędnym do odbudowy tkanki. Obecnie wzrasta liczba pacjentów cierpiących na schorzenia chrząstki stawowej, w tym chorobę zwyrodnieniową (osteoartrozę), które mogą prowadzić nawet do inwalidztwa. Jest to poważny i nadal nierozwiązany problem medycyny regeneracyjnej w zakresie leczenia tego typu urazów.

Celem pracy było opracowanie i ocena syntetycznych rusztowań komórkowych do regeneracji ubytków chrząstki stawowej. W ramach badań otrzymałam rusztowania na bazie polimerów syntetycznych PES, PUR i PLCA, które charakteryzowały się korzystnymi właściwościami mechanicznymi, biozgodnością i kontrolowaną biodegradacją. Opracowałam rusztowania o zróżnicowanym czasie degradacji, zależnym od składu materiałowego, co umożliwia dostosowanie ich do potrzeb klinicznych, względem wieku pacjenta, wielkości ubytku czy stopnia zaawansowania zmian zwyrodnieniowych.

Wybrane rusztowania przebadałam *in vitro* oraz *in vivo* we współpracy z lekarzami ortopedami. W hodowli z izolowanymi ludzkimi chondrocytami rusztowania z PES wykazały wyższą skuteczność niż porównawcze rusztowania z polimeru PLLA. Z kolei badania *in vivo* na modelu króliczym wykazały wysoką jakość regeneratu chrząstki w przypadku rusztowań z PLCA oraz rusztowań z PES, które porównywalne było z komercyjnym implantem Chondro-Gide. W badaniach potwierdzona została całkowita biodegradacja rusztowań z poliestru bez oznak toksyczności. Szczególnie istotnym wynikiem było zaobserwowanie biodegradacji rusztowań z PES, uznawanego dotąd za materiał trwały, co stanowi nową obserwację o dużym znaczeniu badawczym.

Uzyskane wyniki potwierdzają, że syntetyczne rusztowania komórkowe opracowane i otrzymane w ramach pracy spełniają wymagania stawiane materiałom dla potrzeb inżynierii tkanki chrzęstnej. W perspektywie mogą one znaleźć zastosowanie nie tylko w regeneracji chrząstki stawowej w metodach ACI i AMIC, lecz także w rekonstrukcji pourazowej w obrębie twarzy (nos).

Bibliografia

[1] Coffman JA, Rieger S, Rogers AN, Updike DL, Yin VP. Comparative biology of tissue repair, regeneration and aging. Npj Regenerative Medicine 2016;1:1–5. https://doi.org/10.1038/npjregenmed.2016.3.

[2] Patel J, Chen S, Katzmeyer T, Pei YA, Pei M. Sex-dependent variation in cartilage adaptation: from degeneration to regeneration. Biology of Sex Differences 2023;14:1–28. https://doi.org/10.1186/s13293-023-00500-3.

[3] Kjennvold S, Randsborg PH, Jakobsen RB, Aroen A. Fixation of Acute Chondral Fractures in Adolescent Knees. Cartilage 2021;13:293S-301S. https://doi.org/10.1177/1947603520941213.

[4] Courties A, Kouki I, Soliman N, Mathieu S, Sellam J. Osteoarthritis year in review 2024: Epidemiology and therapy. Osteoarthritis and Cartilage 2024;32:1397–404. https://doi.org/10.1016/j.joca.2024.07.014.

[5] Makaram NS, Simpson AHRW. Disease-modifying agents in osteoarthritis: where are we now and what does the future hold? Bone and Joint Research 2023; 12:654–6. https://doi.org/10.1302/2046-3758.1210.BJR-2023-0237.

[6] Chu CR. Articular Cartilage: Injury, Restoration, and Preservation. Operative Techniques in Orthopaedics 2022; 32:100964. https://doi.org/10.1016/j.oto.2022.100964.

[7] Li M, Yin H, Yan Z, Li H, Wu J, Wang Y, et al. The immune microenvironment in cartilage injury and repair. Acta Biomaterialia 2022;140:23–42. https://doi.org/10.1016/j.actbio.2021.12.006.

[8] Nischal N, Iyengar KP, Herlekar D, Botchu R. Imaging of Cartilage and Chondral Defects: An Overview. Life 2023;13. https://doi.org/10.3390/life13020363.

[9] Daou F, Cochis A, Leigheb M, Rimondini L. Current advances in the regeneration of degenerated articular cartilage: A literature review on tissue engineering and its recent clinical translation. Materials 2022;15. https://doi.org/10.3390/ma15010031.

[10] Cong B, Sun T, Zhao Y, Chen M. Current and Novel Therapeutics for Articular Cartilage Repair and Regeneration. Therapeutics and Clinical Risk Management 2023;19:485–502. https://doi.org/10.2147/TCRM.S410277.

[11] Smith L, Jakubiec A, Biant L, Tawy G. The biomechanical and functional outcomes of autologous chondrocyte implantation for articular cartilage defects of the knee: A systematic review. Knee 2023;44:31–42.

https://doi.org/10.1016/j.knee.2023.07.004.

[12] Migliorini F, Eschweiler J, Prinz J, Weber CD, Hofmann UK, Hildebrand F, et al. Autologous chondrocyte implantation in the knee is effective in skeletally immature patients: a systematic review. Knee Surgery, Sports Traumatology, Arthroscopy 2023; 31:2518–25. https://doi.org/10.1007/s00167-022-07212-y.

[13] Schneider S, Kaiser R, Uterhark B, Holz J, Ossendorff R, Salzmann G. Autologous surface repair: autologous matrix-induced chondrogenesis and minced cartilage implantation. Journal of Cartilage and Joint Preservation 2023; 3:100111. https://doi.org/10.1016/j.jcjp.2023.100111.

[14] Migliorini F, Schenker H, Maffulli N, Eschweiler J, Lichte P, Hildebrand F, et al. Autologous matrix induced chondrogenesis (AMIC) as revision procedure for failed AMIC in recurrent symptomatic osteochondral defects of the talus. Scientific Reports 2022;12:1–7. https://doi.org/10.1038/s41598-022-20641-6.

[15] Ahmadi F, Giti R, Mohammadi-Samani S, Mohammadi F. Biodegradable Scaffolds for Cartilage Tissue Engineering GMJ. Gmj 2017; 6:70–80. https://doi.org/10.22086/GMJ.V6I2.696.

[16] Flores-Jiménez MS, Garcia-Gonzalez A, Fuentes-Aguilar RQ. Review on porous scaffolds generation process: A tissue engineering approach. ACS Appl Bio Mater. 2023; 6(1):84–99. doi:10.1021/acsabm.2c00740

[17] Bružauskaitė I, Bironaitė D, Bagdonas E, Bernotienė E. Scaffolds and cells for tissue regeneration: different scaffold pore sizes—different cell effects. Cytotechnology 2016; 68:355–69. https://doi.org/10.1007/s10616-015-9895-4.

[18] Kalkan R, Nwekwo CW, Adali T. The Use of Scaffolds in Cartilage Regeneration. Eukaryotic Gene Expression 2018 ;28:343–8.

[19] Todros S, Todesco M, Bagno A. Biomaterials and their biomedical applications: From replacement to regeneration. Processes 2021;9. https://doi.org/10.3390/pr9111949.

[20] Altyar AE, El-Sayed A, Abdeen A, Piscopo M, Mohamed MA, Alghamdi MA, et al. Future regenerative medicine developments and their therapeutic applications. Biomed Pharmacother. 2023; 158:114114. doi:10.1016/j.biopha.2022.114114

[21] Hynds RE, Magin CM, Ikonomou L, Aschner Y, Beers MF, Burgess JK, Heise RL, Hume PS, Krasnodembskaya A, Mei SHJ, Misharin AV, Park JA, Reynolds SD, Tschumperlin DJ, Tanneberger AE, Vaidyanathan S, Ryan AL, Weiss DJ. Stem cells, cell therapies, and bioengineering in lung biology and diseases 2023. Am J Physiol Lung Cell Mol Physiol. 2024;327(6):L327–L340. doi:10.1152/ajplung.00052.2024.

[22] Goldie K. The evolving field of regenerative aesthetics. Journal of Cosmetic Dermatology 2023; 22:1–7. https://doi.org/10.1111/jocd.15556.

[23] Shafiee A, Atala A. Tissue Engineering: Toward a New Era of Medicine. Annual Review of Medicine 2017; 68:29–40. https://doi.org/10.1146/annurev-med-102715-092331.

[24] Shakoor S, Kibble E, El-Jawhari JJ. Bioengineering Approaches for Delivering Growth Factors: A Focus on Bone and Cartilage Regeneration. Bioengineering 2022; 9. https://doi.org/10.3390/bioengineering9050223.

[25] Cao NT, Muthukumaran S, Chen X. Market of tissue engineering in Canada from 2011 to 2020. Frontiers in Bioengineering and Biotechnology 2023;11:1–7. https://doi.org/10.3389/fbioe.2023.1170423.

[26] Cartilage Repair Market - Global Industry Analysis, Size, Share, Growth, Trends, Regional Outlook, and Forecast 2023-2032 n.d. https://www.precedenceresearch.com/cartilage-repair-market.

[27] Chang L, Marston G, Martin A. Anatomy , Cartilage 2022:2–4.

[28] Walter SG, Ossendorff R, Schildberg FA. Articular cartilage regeneration and tissue engineering models: a systematic review. Archives of Orthopaedic and Trauma Surgery 2019;139:305–16. https://doi.org/10.1007/s00402-018-3057-z.

[29] Nordberg RC, Bielajew BJ, Takahashi T, et al. Recent advancements in cartilage tissue engineering innovation and translation. Nat Rev Rheumatol. 2024; 20(6):323–346. doi:10.1038/s41584-024-01118-4.

[30] Sophia Fox AJ, Bedi A, Rodeo SA. The basic science of articular cartilage: Structure, composition, and function. Sports Health 2009; 1:461–8. https://doi.org/10.1177/1941738109350438.

[31] Chen S, Fu P, Wu H, Pei M. Meniscus, articular cartilage and nucleus pulposus: a comparative review of cartilage-like tissues in anatomy, development and function. vol. 370. 2017. https://doi.org/10.1007/s00441-017-2613-0.

[32] Loy BN, Zimel M, Gowda AL, Tooley TR, Maerz T, Bicos J, et al. A Biomechanical and Structural Comparison of Articular Cartilage and Subchondral Bone of the Glenoid and Humeral Head. Orthopaedic Journal of Sports Medicine 2018; 6:1–7. https://doi.org/10.1177/2325967118785854.

[33] Safshekan F, Tafazzoli-Shadpour M, Abdouss M, Shadmehr MB. Viscoelastic Properties of Human Tracheal Tissues. Journal of Biomechanical Engineering 2017;139:1–9. https://doi.org/10.1115/1.4034651.

[34] Kopf S, Sava MP, Stärke C, Becker R. The menisci and articular cartilage: a life-long fascination. EFORT Open Reviews 2020;5:652–62. https://doi.org/10.1302/2058-5241.5.200016.

[35] Chen L, Wei L, Su X, Qin L, Xu Z, Huang X, et al. Preparation and Characterization of Biomimetic Functional Scaffold with Gradient Structure for Osteochondral Defect Repair. Bioengineering 2023; 10. https://doi.org/10.3390/bioengineering10020213.

[36] Lee DH, Kim SJ, Kim SA, Ju G ik. Past, present, and future of cartilage restoration: from localized defect to arthritis. Knee Surgery and Related Research 2022;34:1–8. https://doi.org/10.1186/s43019-022-00132-8.

[37] Leifer VP, Katz JN, Losina E. The burden of OA-health services and economics. Osteoarthritis and Cartilage 2022; 30:10–6. https://doi.org/10.1016/j.joca.2021.05.007.

[38] Householder NA, Raghuram A, Agyare K, Thipaphay S, Zumwalt M. A Review of Recent Innovations in Cartilage Regeneration Strategies for the Treatment of Primary Osteoarthritis of the Knee: Intra-articular Injections. Orthopaedic Journal of Sports Medicine 2023; 11:1–20. https://doi.org/10.1177/23259671231155950.

[39] Steinmetz RG, Guth JJ, Matava MJ, Smith M V., Brophy RH. Global Variation in Studies of Articular Cartilage Procedures of the Knee: A Systematic Review. Cartilage 2022; 13. https://doi.org/10.1177/19476035221098169.

[40] Zheng MH, Willers C, Kirilak L, Yates P, Xu J, Wood D, et al. Matrix-Induced Autologous Chondrocyte Implantation (MACI®): Biological and histological assessment. Tissue Engineering 2007; 13:737–46. https://doi.org/10.1089/ten.2006.0246.

[41] Chondromalacja – częsty problem, niestety! n.d. https://biegajacyortopeda.pl/porady-ortopedy/chondromalacja-czesty-problem/.

[42] Rahmani Del Bakhshayesh A, Babaie S, Tayefi Nasrabadi H, Asadi N, Akbarzadeh A, Abedelahi A. An overview of various treatment strategies, especially tissue engineering for damaged articular cartilage. Artificial Cells, Nanomedicine and Biotechnology 2020;48:1089–104. https://doi.org/10.1080/21691401.2020.1809439.

[43] Mirza U, Shubeena S, Shah MS, Zaffer B. Microfracture : A technique for repair of chondral defects 2018;6:1092–7.

[44] Zhao Z, Fan C, Chen F, Sun Y, Xia Y, Ji A, et al. Progress in Articular Cartilage Tissue Engineering : A Review on Therapeutic Cells and Macromolecular Scaffolds 2019; 1900278:1–13. https://doi.org/10.1002/mabi.201900278.

[45] Le H, Xu W, Zhuang X, Chang F, Wang Y, Ding J. Mesenchymal stem cells for cartilage regeneration. Journal of Tissue Engineering 2020; 11. https://doi.org/10.1177/2041731420943839.

[46] Lu J, Shen X, Sun X, Yin H, Yang S, Lu C, et al. Increased recruitment of endogenous stem cells and chondrogenic differentiation by a composite scaffold containing bone marrow homing peptide for cartilage regeneration. Theranostics 2018;8:5039–58. https://doi.org/10.7150/thno.26981.

[47] Zhao Z, Fan C, Chen F, Sun Y, Xia Y, Ji A, et al. Progress in Articular Cartilage Tissue Engineering: A Review on Therapeutic Cells and Macromolecular Scaffolds. Macromolecular Bioscience 2020;20:1–13. https://doi.org/10.1002/mabi.201900278.

[48] Zhao T, Wei Z, Zhu W, Weng X. Recent Developments and Current Applications of Hydrogels in Osteoarthritis. Bioengineering 2022;9:1–21. https://doi.org/10.3390/bioengineering9040132.

[49] McGivern S, Boutouil H, Al-Kharusi G, Little S, Dunne NJ, Levingstone TJ. Translational application of 3D bioprinting for cartilage tissue engineering. Bioengineering 2021;8:1–21. https://doi.org/10.3390/bioengineering8100144.

[50] Loh QL, Choong C. Three-dimensional scaffolds for tissue engineering applications: Role of porosity and pore size. Tissue Engineering - Part B: Reviews 2013;19:485–502. https://doi.org/10.1089/ten.teb.2012.0437.

[51] Lai YS, Chen WC, Huang CH, Cheng CK, Chan KK, Chang TK. The effect of graft strength on knee laxity and graft in-situ forces after posterior cruciate ligament reconstruction. PLoS ONE 2015; 10: 1–11. https://doi.org/10.1371/journal.pone.0127293.

[52] Bilal M. Barkatali. How does cartilage regeneration repair damaged or lost knee cartilage? n.d. https://www.topdoctors.co.uk/medical-articles/how-does-cartilage-regeneration-repair-damaged-or-lost-knee-cartilage.

[53] Huang BJ, Hu JC, Athanasiou KA. Cell-based tissue engineering strategies used in the clinical repair of articular cartilage. Biomaterials 2016;98:1–22. https://doi.org/10.1016/j.biomaterials.2016.04.018.

[54] Takahashi T, Ogasawara T, Asawa Y, Mori Y, Uchinuma E, Takato T, et al. Three-dimensional microenvironments retain chondrocyte phenotypes during proliferation culture. Tissue Engineering 2007;13:1583–92. https://doi.org/10.1089/ten.2006.0322.

[55] Hollister SJ. Porous scaffold design for tissue engineering. Nature Materials 2005;4:518–24. https://doi.org/10.1038/nmat1421.

[56] Irawan V, Sung TC, Higuchi A, Ikoma T. Collagen Scaffolds in Cartilage Tissue Engineering and Relevant Approaches for Future Development. Tissue Engineering and Regenerative Medicine 2018;15:673–97. https://doi.org/10.1007/s13770-018-0135-9.

[57] Armiento AR, Stoddart MJ, Alini M, Eglin D. Biomaterials for articular cartilage tissue engineering: Learning from biology. Acta Biomaterialia, vol. 65, Acta Materialia Inc; 2018, p. 1–20. https://doi.org/10.1016/j.actbio.2017.11.021.

[58] Panadero JA, Lanceros-Mendez S, Ribelles JLG. Differentiation of mesenchymal stem cells for cartilage tissue engineering: Individual and synergetic effects of three-dimensional environment and mechanical loading. Acta Biomaterialia 2016;33:1–12. https://doi.org/10.1016/j.actbio.2016.01.037.

[59] Setayeshmehr M, Esfandiari E, Rafieinia M, Hashemibeni B, Taheri-kafrani A, Samadikuchaksaraei A. Hybrid and Composite Scaffolds Based on Extracellular 2019;25. https://doi.org/10.1089/ten.teb.2018.0245.

[60] Zhang Y, Li X, Wang Y, et al. Construction of ultrasonically treated collagen/silk fibroin composite scaffolds with enhanced porosity and mechanical properties for cartilage regeneration. Sci Rep. 2023;13:123456. doi:10.1038/s41598-023-43397-z.

[61] Rares H, Benea C, Earar K, Lattanzi W, Quercia V, Berce C, et al. Collagen Scaffold and Lipoaspirate Fluid - derived Stem Cells for the Treatment of Cartilage Defects in a Rabbit Model 2015:515–20.

[62] Gobbi A, Whyte GP. Long-term Clinical Outcomes of One-Stage Cartilage Repair in the Knee With Hyaluronic Acid – Based Scaffold Embedded With Mesenchymal Stem Cells Sourced From Bone Marrow Aspirate Concentrate 2019:1621–8. https://doi.org/10.1177/0363546519845362.

[63] Lin H, Beck AM, Fritch MR, Tuan RS, Deng Y, Kilroy EJ, et al. Optimization of photocrosslinked gelatin / hyaluronic acid hybrid scaffold for the repair of cartilage defect 2019:1–12. https://doi.org/10.1002/term.2883.

[64] Wen S, Hung K, Hsieh K, Chen C, Tsai C, Hsu S. In vitro and in vivo evaluation of chitosan – gelatin scaffolds for cartilage tissue engineering. Materials Science & Engineering C 2013;33:2855–63. https://doi.org/10.1016/j.msec.2013.03.003.

[65] Mittal H, Sinha S, Singh B, Kaur J, Sharma J, Alhassan SM. Recent progress in the structural modification of chitosan for applications in diversified biomedical fields. European Polymer Journal 2018; 109: 402–34. https://doi.org/10.1016/j.eurpolymj.2018.10.013.

[66] Filardo G, Drobnic M, Perdisa F, Kon E, Hribernik M, Marcacci M. Fibrin glue improves osteochondral scaffold fi xation : study on the human cadaveric knee exposed to continuous passive motion. Osteoarthritis and Cartilage 2014;22:557–65. https://doi.org/10.1016/j.joca.2014.01.004.

[67] Kim J, Hyung T, Lim D, Yeon S, Lee Y, Koh Y, et al. Biochemical and Biophysical Research Communications Chondrogenic differentiation of human ASCs by stiffness control in 3D fi brin hydrogel. Biochemical and Biophysical Research Communications 2020;522:213–9. https://doi.org/10.1016/j.bbrc.2019.11.049.

[68] Demoor M, Ollitrault D, Gomez-Leduc T, Bouyoucef M, Hervieu M, Fabre H, et al. Cartilage tissue engineering: Molecular control of chondrocyte differentiation for proper cartilage matrix reconstruction. Biochimica et Biophysica Acta - General Subjects 2014;1840:2414–40. https://doi.org/10.1016/j.bbagen.2014.02.030.

[69] Eltom A, Zhong G, Muhammad A. Scaffold Techniques and Designs in Tissue Engineering Functions and Purposes: A Review. Advances in Materials Science and Engineering 2019; 2019. https://doi.org/10.1155/2019/3429527.

[70] Welsh BL, Sikder P. Advancements in Cartilage Tissue Engineering: A Focused Review. Journal of Biomedical Materials Research - Part B Applied Biomaterials 2025;113. https://doi.org/10.1002/jbm.b.35520.

[71] Asghari F, Samiei M, Adibkia K, Akbarzadeh A, Davaran S. Biodegradable and biocompatible polymers for tissue engineering application: a review. Artificial Cells, Nanomedicine and Biotechnology 2017; 45: 185–92. https://doi.org/10.3109/21691401.2016.1146731.

[72] Singhvi MS, Zinjarde SS, Gokhale DV. Polylactic acid: synthesis and biomedical applications. J Appl Microbiol. 2019;127(6):1612–1626. doi:10.1111/jam.14290

[73] Silva D, Kaduri M, Poley M, Adir O, Krinsky N, Shainsky-roitman J, et al. Mini Review Biocompatibility , biodegradation and excretion of polylactic acid (PLA) in medical implants and theranostic systems. Chemical Engineering Journal 2018. https://doi.org/10.1016/j.cej.2018.01.010.

[74] Budak K, Sogut O, Sezer UA. A review on synthesis and biomedical applications of polyglycolic acid 2020: 1–19.

[75] Mahboudi H, Soleimani M, Enderami SE, Kehtari M, Hanaee- Ahvaz H, Ghanbarian H, et al. The effect of nanofibre-based polyethersulfone (PES) scaffold on the chondrogenesis of human induced pluripotent stem cells. Artificial Cells, Nanomedicine and Biotechnology 2018; 46: 1948–56. https://doi.org/10.1080/21691401.2017.1396998.

[76] Dudziński K, Chwojnowski A, Gutowska M, Płończak M, Czubak J, Łukowska E, et al. Three dimensional polyethersulphone scaffold for chondrocytes cultivation - The future supportive material for articular cartilage regeneration. Biocybernetics and Biomedical Engineering 2010;30:65–76.

[77] Mahboudi H, Kazemi B, Soleimani M, et al. Enhanced chondrogenesis of human bone marrow mesenchymal stem cells on nanofiber-based polyethersulfone (PES) scaffold. *Gene*. 2018;643:98–106. doi:10.1016/j.gene.2017.11.073.

[78] Irfan M, Idris A. Overview of PES biocompatible/hemodialysis membranes: PES-blood interactions and modification techniques. Materials Science and Engineering C 2015;56:574–92. https://doi.org/10.1016/j.msec.2015.06.035.

[79] Janmohammadi M, Nourbakhsh MS. Electrospun polycaprolactone scaffolds for tissue engineering : a review. International Journal of Polymeric Materials and Polymeric Biomaterials 2018; 0:1–13. https://doi.org/10.1080/00914037.2018.1466139.

[80] Dao TT, Vu NB, Pham LH, Bui T, Le PT, Pham P Van. In Vitro Production of Cartilage Tissue from Rabbit Bone Marrow-Derived Mesenchymal Stem Cells and Polycaprolactone Scaffold 2017. https://doi.org/10.1007/5584.

[81] He Y, Wang WR, Ding JD. Effects of L-lactic acid and D,L-lactic acid on viability and osteogenic differentiation of mesenchymal stem cells. Chinese Science Bulletin 2013;58:2404–11. https://doi.org/10.1007/s11434-013-5798-y.

[82] Xu Y, Kim C, Saylor DM, Koo D. Review Article Polymer degradation and drug delivery in PLGA-based drug – polymer applications : A review of experiments and theories 2016:1–25. https://doi.org/10.1002/jbm.b.33648.

[83] Jiang L, Xu L, Ma B, Ding H, Tang C. Effect of component and surface structure on poly (L -lactide-co- ε - caprolactone) (PLCA) -based composite membrane. Composites Part B 2019; 174:107031. https://doi.org/10.1016/j.compositesb.2019.107031.

[84] Prasanna S, Narayan B, Rastogi A, Srivastava P. Design and evaluation of chitosan / poly (L -lactide)/ pectin based composite scaffolds for cartilage tissue regeneration. International Journal of Biological Macromolecules 2018;112:909–20. https://doi.org/10.1016/j.ijbiomac.2018.02.049.

[85] Nofar M, Sacligil D, Carreau PJ, Kamal MR, Heuzey MC. Poly (lactic acid) blends: Processing, properties and applications. International Journal of Biological Macromolecules 2019;125:307–60. https://doi.org/10.1016/j.ijbiomac.2018.12.002.

[86] Jafari M, Paknejad Z, Rad MR, Motamedian SR, Eghbal MJ, Nadjmi N, et al. Polymeric scaffolds in tissue engineering: a literature review. Journal of Biomedical Materials Research - Part B Applied Biomaterials 2017;105:431–59. https://doi.org/10.1002/jbm.b.33547.

[87] Sikorska W, Wojciechowski C, Przytulska M, Rokicki G, Wasyłeczko M, Kulikowski JL, et al. Polysulfone–polyurethane (PSf-PUR) blend partly degradable hollow fiber membranes: Preparation, characterization, and computer image analysis. Desalination and Water Treatment 2018;128. https://doi.org/10.5004/dwt.2018.23101.

[88] Ye H, Zhang K, Kai D, Li Z, Loh XJ. Polyester elastomers for soft tissue engineering. Chemical Society Reviews 2018;47:4545–80. https://doi.org/10.1039/c8cs00161h.

[89] Jeuken RM, Roth AK, Peters RJRW, van Donkelaar CC, Thies JC, van Rhijn LW, et al. Polymers in cartilage defect repair of the knee: Current status and future prospects. Polymers 2016;8. https://doi.org/10.3390/polym8060219.

[90] Daranarong D, Techaikool P, Intatue W, Daengngern R, Thomson KA, Molloy R, et al. Effect of surface modification of poly(L-lactide-co-ε-caprolactone) membranes by low-pressure plasma on support cell biocompatibility. Surface and Coatings Technology 2016;306:328–35. https://doi.org/10.1016/j.surfcoat.2016.07.058.

[91] Guo C, Cai N, Dong Y. Duplex surface modification of porous poly (lactic acid) scaffold. Materials Letters 2013; 94:11–4. https://doi.org/10.1016/j.matlet.2012.11.092.

[92] Lv J, Wu Y, Cao Z, Liu X, Sun Y, Zhang P, Zhang X, Tang K, Cheng M, Yao Q. Enhanced Cartilage and Subchondral Bone Repair Using Carbon Nanotube-Doped Peptide Hydrogel–Polycaprolactone Composite Scaffolds. Pharmaceutics. 2023;15(8):2145. doi:10.3390/pharmaceutics15082145

[93] Zhang X, Wu Y, Pan Z, Sun H, Wang J, Yu D, et al. The effects of lactate and acid on articular chondrocytes function: Implications for polymeric cartilage scaffold design. Acta Biomaterialia 2016; 42:329–40. https://doi.org/10.1016/j.actbio.2016.06.029.

[94] Sun K, Liu B, Wang DA. Editorial: Focus issue on biomaterials approaches to the repair and regeneration of cartilage tissue. Biomedical Materials (Bristol) 2023;18:16–9. https://doi.org/10.1088/1748-605X/acc560.

[95] Zhao P, Gu H, Mi H, Rao C, Fu J, Turng L sheng. Fabrication of scaffolds in tissue engineering: A review. Frontiers of Mechanical Engineering 2018;13:107–19. https://doi.org/10.1007/s11465-018-0496-8.

[96] Medvedeva E V., Grebenik EA, Gornostaeva SN, Telpuhov VI, Lychagin A V., Timashev PS, et al. Repair of damaged articular cartilage: Current approaches and future directions. International Journal of Molecular Sciences 2018;19. https://doi.org/10.3390/ijms19082366.

[97] Li Y. Techniques for fabrication and construction of three-dimensional scaffolds for tissue engineering 2013:1–14.

[98] Dutta RC, Dey M, Dutta AK, Basu B. Competent processing techniques for scaffolds in tissue engineering. Biotechnology Advances 2017;35:240–50. https://doi.org/10.1016/j.biotechadv.2017.01.001.

[99] Yan Q, Dong H, Su J, Han J, Song B, Wei Q, et al. A Review of 3D Printing Technology for Medical Applications. Engineering 2018;4:729–42. https://doi.org/10.1016/j.eng.2018.07.021.

[100] Abdelaal OAM, Darwish SMH. Review of Rapid Prototyping Techniques for Tissue Engineering Scaffolds Fabrication 2013. https://doi.org/10.1007/978-3-642-31470-4.

[101] Li K, Wang D, Zhao K, Song K, Liang J. Electrohydrodynamic jet 3D printing of PCL/PVP composite scaffold for cell culture. Talanta 2020:120750. https://doi.org/10.1016/j.talanta.2020.120750.

[102] Daly AC, Freeman FE, Gonzalez-fernandez T, Critchley SE, Nulty J, Kelly DJ. 3D Bioprinting for Cartilage and Osteochondral Tissue Engineering 2017;1700298:1–20. https://doi.org/10.1002/adhm.201700298.

[103] Seung J, Sang H, Jung H, Lee H, Hong H, Jin Y, et al. 3D-printable photocurable bioink for cartilage regeneration of tonsil-derived mesenchymal stem cells. Additive Manufacturing 2020;33:101136. https://doi.org/10.1016/j.addma.2020.101136.

[104] Marycz K, Smieszek A, Targonska S, Walsh A, Szustakiewicz K, Wiglusz RJ. Three dimensional (3D) printed PLA with nano-hydroxyapatite doped with europium(III) ions (nHAp-PLLA@Eu3+) composite for osteochondral defect regeneration and theranostics. Materials Science & Engineering C 2020:110634. https://doi.org/10.1016/j.msec.2020.110634.

[105] Zarei M, Shabani Dargah M, Hasanzadeh Azar M, Alizadeh R, Mahdavi FS, Sayedain SS, et al. Enhanced bone tissue regeneration using a 3D-printed poly(lactic acid)/Ti6Al4V composite scaffold with plasma treatment modification. Scientific Reports 2023; 13:1–19. https://doi.org/10.1038/s41598-023-30300-z.

[106] Mannella GA, Conoscenti G, Pavia FC, Carrubba V La, Brucato V. Preparation of polymeric foams with a pore size gradient via Thermally Induced Phase Separation (TIPS). Materials Letters 2015;160:31–3. https://doi.org/10.1016/j.matlet.2015.07.055.

[107] Buzarovska A, Gualandi C, Parrilli A, Scandola M. Effect of TiO2 nanoparticle loading on Poly(L-lactic acid) porous scaffolds fabricated by TIPS. Composites Part B 2015. https://doi.org/10.1016/j.compositesb.2015.07.016.

[108] Sultana N, Hassana MI, Ridzuana N, Ibrahima Z, Soonc CF. Fabrication of Gelatin Scaffolds using Thermally Induced Phase Separation Technique 2018;31:1302–7.

[109] Conoscenti G, Schneider T, Stoelzel K, Carfì Pavia F, Brucato V, Goegele C, et al. PLLA scaffolds produced by thermally induced phase separation (TIPS) allow human chondrocyte growth and extracellular matrix formation dependent on pore size. Materials Science and Engineering C 2017;80:449–59. https://doi.org/10.1016/j.msec.2017.06.011.

[110] Structure MM, Mechanical H, Kim J, Shin K, Koh Y, Hah MJ, et al. Production of Poly(ε -Caprolactone)/Hydroxyapatite Composite Scaffolds with a Tailored Macro/Micro-Porous Structure, High Mechanical Properties, and Excellent Bioactivity n.d. https://doi.org/10.3390/ma10101123.

[111] Georgiadou S, Katsogiannis KAG, Vladisavljevic GT. Porous electrospun polycaprolactone (PCL) fibres by phase separation 2015; 69: 284–95. https://doi.org/10.1016/j.eurpolymj.2015.01.028.

[112] Huang C, Thomas NL. Fabricating Porous Poly(lactic acid) Fibres via Electrospinning. European Polymer Journal 2017. https://doi.org/10.1016/j.eurpolymj.2017.12.025.

[113] Chwojnowski A, Kruk A, Wojciechowski C, Łukowska E, Dulnik J, Sajkiewicz P. The dependence of the membrane structure on the non-woven forming the macropores in the 3D scaffolds preparation. Desalination and Water Treatment 2017;64:324–31. https://doi.org/10.5004/dwt.2017.11394.

[114] Prasad A, Sankar MR, Katiyar V. State of Art on Solvent Casting Particulate Leaching Method for Orthopedic ScaffoldsFabrication 2017;4:898–907.

[115] Plisko T V, Penkova A V, Burts KS, Bildyukevich A V, Dmitrenko ME, Melnikova GB, et al. Effect of Pluronic F127 on porous and dense membrane structure formation via non-solvent induced and evaporation induced phase separation. Journal of Membrane Science 2019;580:336–49. https://doi.org/10.1016/j.memsci.2019.03.028.

[116] Gadomska-Gajadhur A, Kruk A. Original method of imprinting pores in scaffolds for tissue engineering 2020:1–13. https://doi.org/10.1002/pat.5091.

[117] Nayab SS, Abbas MA, Mushtaq S, Niazi BK, Batool M, Shehnaz G, et al. Anti-foulant ultrafiltration polymer composite membranes incorporated with composite activated carbon/chitosan and activated carbon/thiolated chitosan with enhanced hydrophilicity. Membranes 2021; 11. https://doi.org/10.3390/membranes11110827.

[118] Sharifi F, Irani S, Azadegan G, Pezeshki-modaress M. Co-electrospun gelatin-chondroitin sulfate / polycaprolactone nanofibrous scaffolds for cartilage tissue engineering. Bioactive Carbohydrates and Dietary Fibre 2020;22:100215. https://doi.org/10.1016/j.bcdf.2020.100215.

[119] Zhou Y, Chyu J, Zumwalt M. Recent Progress of Fabrication of Cell Scaffold by Electrospinning Technique for Articular Cartilage Tissue Engineering 2018;2018.

[120] Girão AF, Semitela Â, Ramalho G, Completo A, Marques PAAP. Mimicking nature-Fabrication of 3D anisotropic electrospun polycaprolactone scaffolds for cartilage tissue engineering applications. Composites Part B 2018. https://doi.org/10.1016/j.compositesb.2018.08.001.

[121] Bdikin I, Marques PAAP. Electrospinning of bioactive polycaprolactone-gelatin nanofibres with increased pore size for cartilage tissue engineering applications 2020. https://doi.org/10.1177/0885328220940194.

[122] Canton TT, Kunert LR, Suellen B, Ana I, Serafini P. Nonwoven membranes for tissue engineering : An overview of cartilage , Nonwoven membranes for tissue engineering : an overview of cartilage , epithelium , and bone regeneration. Journal of Biomaterials Science, Polymer Edition 2019;30:1026–49. https://doi.org/10.1080/09205063.2019.1620592.

[123] Liu Q, Chen Z, Pei X, Guo C, Teng K, Hu Y, et al. Review: applications, effects and the prospects for electrospun nanofibrous mats in membrane separation. Journal of Materials Science 2020;55:893–924. https://doi.org/10.1007/s10853-019-04012-7.

[124] Demoor M, Ollitrault D, Gomez-Leduc T, Bouyoucef M, Hervieu M, Fabre H, et al. Cartilage tissue engineering: Molecular control of chondrocyte differentiation for proper cartilage matrix reconstruction. Biochimica et Biophysica Acta - General Subjects 2014;1840:2414–40. https://doi.org/10.1016/j.bbagen.2014.02.030.

[125] Armiento AR, Stoddart MJ, Alini M, Eglin D. Biomaterials for articular cartilage tissue engineering: Learning from biology. Acta Biomaterialia 2018; 65:1–20. https://doi.org/10.1016/j.actbio.2017.11.021.

[126] Bistolfi A, Ferracini R, Galletta C, Tosto F, Sgarminato V, Digo E, et al. Regeneration of articular cartilage : Scaffold used in orthopedic surgery . A short handbook of available products for regenerative joints surgery 2017;1:1–7. https://doi.org/10.15761/CSRR.1000101.

[127] Urbanek O, Kołbuk D, Wróbel M. International Journal of Polymeric Materials and Articular cartilage : New directions and barriers of scaffolds development – review. International Journal of Polymeric Materials and Polymeric Biomaterials 2018;0:1–15. https://doi.org/10.1080/00914037.2018.1452224.

[128] Follow-up F, Randomized P, Brittberg M, Recker D, Ilgenfritz J. Matrix-Applied Characterized Autologous Cultured Chondrocytes Versus Microfracture 2018:1–9. https://doi.org/10.1177/0363546518756976.

[129] Tan SI, Jun S, Tho W, Tho KS. Biological resurfacing of grade IV articular cartilage ulcers in knee joint with Hyalofast 2020;28:1–7. https://doi.org/10.1177/2309499020905158.

[130] Sofu H, Camurcu Y, Ucpunar H, Ozcan S, Yurten H, Sahin V. Clinical and radiographic outcomes of chitosan-glycerol phosphate / blood implant are similar with hyaluronic acid-based cell-free scaffold in the treatment of focal osteochondral lesions of the knee joint. Knee Surgery, Sports Traumatology, Arthroscopy 2019;27:773–81. https://doi.org/10.1007/s00167-018-5079-z.

[131] Lam ATL, Reuveny S, Oh SKW. Human mesenchymal stem cell therapy for cartilage repair: Review on isolation, expansion, and constructs. Stem Cell Research 2020;44:101738. https://doi.org/10.1016/j.scr.2020.101738.

[132] Surgery O, Surgery O, Cartilage I, Society R. Cartilage Regeneration in Osteoarthritic Patients by a Composite of Allogeneic Umbilical Cord Blood-Derived Mesenchymal Stem Cells and Hyaluronate Hydrogel : Results from Trial for Safety and Results From a a Clinical Clinical Trial for Safety and Concept 2017.

[133] Negoro T, Takagaki Y, Okura H, Matsuyama A. Trends in clinical trials for articular cartilage repair by cell therapy. Npj Regenerative Medicine 2018;3. https://doi.org/10.1038/s41536-018-0055-2.

[134] Siclari A, Mascaro G, Kaps C, Boux E. A 5-Year Follow-Up After Cartilage Repair in the Knee Using a Platelet- Rich Plasma-Immersed Polymer-Based Implant 2014:346–54.

[135] Müller S. Repair of Focal Cartilage Defects With Scaffold-Assisted Autologous Chondrocyte Grafts 2015. https://doi.org/10.1177/0363546511403279.

[136] Bartlett W, Skinner JA, Gooding CR, Carrington RWJ, Flanagan AM, Briggs TWR, et al. Autologous chondrocyte implantation versus matrix-induced autologous chondrocyte implantation for osteochondral defects of the knee. A prospective, randomised study. Journal of Bone and Joint Surgery - Series B 2005;87:640–5. https://doi.org/10.1302/0301-620X.87B5.15905.

[137] Gigante A, Enea D, Greco F, Bait C, Denti M, Schonhuber H, et al. Distal realignment and patellar autologous chondrocyte implantation: Mid-term results in a selected population. Knee Surgery, Sports Traumatology, Arthroscopy 2009;17:2–10. https://doi.org/10.1007/s00167-008-0635-6.

[138] Vinatier C, Guicheux J. Cartilage tissue engineering: From biomaterials and stem cells to osteoarthritis treatments. Annals of Physical and Rehabilitation Medicine 2016;59:139–44. https://doi.org/10.1016/j.rehab.2016.03.002.

[139] Steinwachs MR, Waibl B, Mumme M. Arthroscopic treatment of cartilage lesions with microfracture and BST-Cargel. Arthroscopy Techniques 2014;3:e399–402. https://doi.org/10.1016/j.eats.2014.02.011.

[140] Chubinskaya S, Di Matteo B, Lovato L, Iacono F, Robinson D, Kon E. Agili-C implant promotes the regenerative capacity of articular cartilage defects in an ex vivo model. Knee Surgery, Sports Traumatology, Arthroscopy 2019;27:1953–64. https://doi.org/10.1007/s00167-018-5263-1.

[141] Kon E, Di Matteo B, Verdonk P, Drobnic M, Dulic O, Gavrilovic G, et al. Aragonite-Based Scaffold for the Treatment of Joint Surface Lesions in Mild to Moderate Osteoarthritic Knees: Results of a 2-Year Multicenter Prospective Study. American Journal of Sports Medicine 2021;49:588–98. https://doi.org/10.1177/0363546520981750.

[142] Van Genechten W, Vuylsteke K, Struijk C, Swinnen L, Verdonk P. Joint Surface Lesions in the Knee Treated with an Acellular Aragonite-Based Scaffold: A 3-Year Follow-Up Case Series. Cartilage 2021;13:1217S-1227S. https://doi.org/10.1177/1947603520988164.

[143] Longley R, Ferreira AM, Gentile P. Recent Approaches to the Manufacturing of Biomimetic Multi-Phasic Scaffolds for Osteochondral Regeneration 2018. https://doi.org/10.3390/ijms19061755.

[144] Briickner R, Rearrangement W. Agili-C 2022:2–9.

[145] Heng CHY, Snow M, Dave LYH. Single-Stage Arthroscopic Cartilage Repair With Injectable Scaffold and BMAC. Arthroscopy Techniques 2021;10:e751–6. https://doi.org/10.1016/j.eats.2020.10.065.

[146] Silva AN, Lim WAJ, Cheok JWG, Gatot C, Tan HCA. Autologous collagen-induced chondrogenesis versus microfracture for chondral defects of the knee: Surgical technique and 2-year comparison outcome study. Journal of Orthopaedics 2020;22:294–9. https://doi.org/10.1016/j.jor.2020.06.008.

[147] Melton JTK, Wilson AJ, Chapman-Sheath P, Cossey AJ. TruFit CB® bone plug: Chondral repair, scaffold design, surgical technique and early experiences. Expert Review of Medical Devices 2010;7:333–41. https://doi.org/10.1586/erd.10.15.

[148] Di Cave E, Versari P, Sciarretta F, Luzon D, Marcellini L. Biphasic bioresorbable scaffold (TruFit Plug®) for the treatment of osteochondral lesions of talus: 6- to 8-year follow-up. Foot 2017;33:48–52. https://doi.org/10.1016/j.foot.2017.05.005.

[149] D'Ambrosi R, Valli F, De Luca P, Ursino N, Usuelli FG. Maioregen osteochondral substitute for the treatment of knee defects: A systematic review of the literature. Journal of Clinical Medicine 2019;8. https://doi.org/10.3390/jcm8060783.

[150] Perdisa F, Filardo G, Sessa A, Busacca M, Zaffagnini S, Marcacci M, et al. One-Step Treatment for Patellar Cartilage Defects with a Cell-Free Osteochondral Scaffold: A Prospective Clinical and MRI Evaluation. American Journal of Sports Medicine 2017;45:1581–8. https://doi.org/10.1177/0363546517694159.

[151] Kon E, Filardo G, Brittberg M, Busacca M, Condello V, Engebretsen L, et al. A multilayer biomaterial for osteochondral regeneration shows superiority vs microfractures for the treatment of osteochondral lesions in a multicentre randomized trial at 2 years. Knee Surgery, Sports Traumatology, Arthroscopy 2018;26:2704–15. https://doi.org/10.1007/s00167-017-4707-3.

[152] Geistlich. Arthroscopic Hip Technique Chondral Lesions in the Hip Joint. https://www.geistlich.com/orthopedic/cartilage-regeneration/amic-chondro-gide/amic-hip

[153] M. Steinwachs. Collagen Membrane for Articular Cartilage Repair: Chondro-Gide, Geistlich: n.d.

[154] Kon E, Delcogliano M, Filardo G, Busacca M, Di Martino A, Marcacci M. Novel nano-composite multilayered biomaterial for osteochondral regeneration: A pilot clinical trial. American Journal of Sports Medicine 2011;39:1180–90. https://doi.org/10.1177/0363546510392711.

[155] Sikorska W, Milner-Krawczyk M, Wasyłeczko M, Wojciechowski C, Chwojnowski A. Biodegradation process of PSF-PUR blend hollow fiber membranes using escherichia coli Bacteria—evaluation of changes in properties and porosity. Polymers 2021;13. https://doi.org/10.3390/polym13081311.

[156] Sikorska W, Wasyłeczko M, Przytulska M, Wojciechowski C, Rokicki G, Chwojnowski A. Chemical degradation of PSF-PUR blend hollow fiber membranes-assessment of changes in properties and morphology after hydrolysis. Membranes 2021;11. https://doi.org/10.3390/membranes11010051.

[157] Kruk A, Gadomska-Gajadhur A, Ruśkowski P, Chwojnowski A, Dulnik J, Synoradzki L. Preparation of biodegradable semi-permeable membranes as 3D scaffolds for cell cultures. Desalination and Water Treatment 2017;64:317–23. https://doi.org/10.5004/dwt.2017.11415.

[158] Gadomska-Gajadhur A, Kruk A, Synoradzki L, Chwojnowski A. Patent PL 229497 B1; Method for producing three-dimensional polylactide scaffolds, 2015.

[159] Chwojnowski Andrzej, Łukowaska Ewa, Wojciechowski Cezary, Wasyłeczko Monika, Sikorska Wioleta KZ. PL238140B1_Sposób wyodrębniania białka z hodowli komórkowych prowadzonych na rusztowaniach komórkowych.pdf, 2021.

[160] Dupuy S, Salvador J, Morille M, Noël D, Belamie E. Control and interplay of scaffold-biomolecule interactions applied to cartilage tissue engineering. Biomaterials Science 2025:1871–900. https://doi.org/10.1039/d5bm00049a.

[161] Wang Y, Shen N, Zhu Z, Liu J, Qi X, Liu Z, et al. Electrospun 3D nanofibrous materials and their applications in orthopaedics. vol. 8. Springer International Publishing; 2025. https://doi.org/10.1007/s42114-024-01120-0.

[162] Wang M, Wu Y, Li G, Lin Q, Zhang W, Liu H, et al. Articular cartilage repair biomaterials: strategies and applications. Materials Today Bio 2024;24:100948. https://doi.org/10.1016/j.mtbio.2024.100948.

[163] Lin X, Zhang Y, Li J, Oliver BG, Wang B, Li H, et al. Biomimetic multizonal scaffolds for the reconstruction of zonal articular cartilage in chondral and osteochondral defects. Bioactive Materials 2025;43:510–49. https://doi.org/10.1016/j.bioactmat.2024.10.001.

[164] Wu X, Cheng X, Kang M, Dong R, Zhao J, Qu Y. Natural polysaccharide-based hydrogel bioprinting for articular cartilage repair. Frontiers in Materials 2024;10:1–14. https://doi.org/10.3389/fmats.2023.1204318.

[165] Hu X, Wu Z, Zhang Z, Yao H, Wang DA. Type II collagen scaffolds for tissue engineering. Communications Materials 2024;5:1–17. https://doi.org/10.1038/s43246-024-00598-x.

[166] Yang C, Chen R, Chen C, Yang F, Xiao H, Geng B, et al. Tissue engineering strategies hold promise for the repair of articular cartilage injury. vol. 23. BioMed Central; 2024. https://doi.org/10.1186/s12938-024-01260-w.

[167] Chen M, Jiang Z, Zou X, You X, Cai Z, Huang J. Advancements in tissue engineering for articular cartilage regeneration. Heliyon 2025;10:e25400. https://doi.org/10.1016/j.heliyon.2024.e25400.

[168] Li CS, Xu Y, Li J, Qin SH, Huang SW, Chen XM, et al. Ultramodern natural and synthetic polymer hydrogel scaffolds for articular cartilage repair and regeneration. Biomedical Engineering Online 2025;24:13. https://doi.org/10.1186/s12938-025-01342-3.

[169] Lewis JA, Namke B, Luc Y, Satherb NA, T. MM, Mullend M, et al. A bioactive supramolecular and covalent polymer scaffold for cartilage repair in a sheep model. Proceedings of the National Academy of Sciences 2024;121:2017. https://doi.org/10.1073/pnas.

[170] Yang F, Wang Z, Wu M, Xu J, Li J, Liu J, et al. Application of miR-29a-Exosome and multifunctional scaffold for full-thickness cartilage defects. Extracellular Vesicle 2024;4:100055. https://doi.org/10.1016/j.vesic.2024.100055.

[171] Zhong Y, Cao X, Huang M, Lei Y, Liu AL. Biomimetic bone cartilage scaffolds based on trilayer methacrylated hydroxyapatite/GelMA composites for full-thickness osteochondral regeneration. International Journal of Biological Macromolecules 2025;298:139860. https://doi.org/10.1016/j.ijbiomac.2025.139860.

[172] Xu P, Kankala RK, Wang S, Chen A. Decellularized extracellular matrix-based composite scaffolds for tissue engineering and regenerative medicine. Regenerative Biomaterials 2024;11. https://doi.org/10.1093/rb/rbad107.

[173] Gudas R, Staškūnas M, Mačiulaitis J, Gudaitė E, Aleknaite-Dambrauskiene I. Arthroscopic Implantation of a Cell-Free Bilayer Scaffold for the Treatment of Knee Chondral Lesions: A 2-Year Prospective Study. Cartilage 2024. https://doi.org/10.1177/19476035241232061.

[174] Jakutowicz T, Wasyłeczko M, Płończak M, Wojciechowski C, Chwojnowski A, Czubak J. Comparative Study of Autogenic and Allogenic Chondrocyte Transplants on Polyethersulfone Scaffolds for Cartilage Regeneration, 2024. https://doi.org/10.3390/ijms25169075.

[175] Wasyłeczko M, Wojciechowski C, Chwojnowski A. Polyethersulfone Polymer for Biomedical Applications and Biotechnology 2024:37–42. https://doi.org/10.3390/ijms25084233

PUBLIKACJE ZAWARTE
W ROZPRAWIE DOKTORSKIEJ

PUBLIKACJA 1

Review of Synthetic and Hybrid Scaffolds in Cartilage Tissue Engineering

Monika Wasyłeczko, Wioleta Sikorska and Andrzej Chwojnowski

Membranes **2020**, 10(11), 348.
https://doi.org/10.3390/membranes10110348
IF= 4, 562
MNiSW: 100

membranes

MDPI

Review

Review of Synthetic and Hybrid Scaffolds in Cartilage Tissue Engineering

Monika Wasyłeczko *, Wioleta Sikorska and Andrzej Chwojnowski

Nałęcz Institute of Biocybernetics and Biomedical Engineering, Polish Academy of Sciences, Trojdena 4 str., 02-109 Warsaw, Poland; wsikorska@ibib.waw.pl (W.S.); achwoj@ibib.waw.pl (A.C.)

* Correspondence: mwasyleczko@ibib.waw.pl

Received: 28 September 2020; Accepted: 11 November 2020; Published: 17 November 2020

Abstract: Cartilage tissue is under extensive investigation in tissue engineering and regenerative medicine studies because of its limited regenerative potential. Currently, many scaffolds are undergoing scientific and clinical research. A key for appropriate scaffolding is the assurance of a temporary cellular environment that allows the cells to function as in native tissue. These scaffolds should meet the relevant requirements, including appropriate architecture and physicochemical and biological properties. This is necessary for proper cell growth, which is associated with the adequate regeneration of cartilage. This paper presents a review of the development of scaffolds from synthetic polymers and hybrid materials employed for the engineering of cartilage tissue and regenerative medicine. Initially, general information on articular cartilage and an overview of the clinical strategies for the treatment of cartilage defects are presented. Then, the requirements for scaffolds in regenerative medicine, materials intended for membranes, and methods for obtaining them are briefly described. We also describe the hybrid materials that combine the advantages of both synthetic and natural polymers, which provide better properties for the scaffold. The last part of the article is focused on scaffolds in cartilage tissue engineering that have been confirmed by undergoing preclinical and clinical tests.

Keywords: cartilage tissue engineering; articular cartilage; scaffolds; scaffold obtaining methods; materials for scaffolds; scaffold requirements; synthetic and hybrid scaffolds; chondrocytes; mesenchymal stem cells; tissue engineering; regenerative medicine

1. Introduction

Most human tissues and organs have a limited capacity to properly self-regenerate. Moreover, they are often exposed to damage as a result of injuries, accidents, and various diseases involving tissue dysfunction or devastating deficits [1,2]. Many surgical strategies have been developed to ameliorate these problems, including the transplantation of artificial substitutes, such as joint prostheses, heart valves, kidneys, or even tissues and organs [3–5]. Unfortunately, the main obstacles for organ transplantation are the deficit of donor organs and the necessity of lifelong immunosuppression. Nonbiological components can cause particular problems, such as a lack of biocompatibility, the development of serious infections, and limited durability [6,7]. Therefore, regenerative medicine including tissue engineering (TE) is a promising domain of research that can offer not only tissues and organs for transplantation but can also provide new perspectives for the treatment of many diseases [8]. This is due to the combination of biological sciences and material engineering methods enabling the development and acquisition of biological substitutes [2,9]. At present, regenerative medicine offers methods for treating various tissues, including the skin, musculoskeletal tissue, the liver, gastrointestinal tissue, nervous system tissue, and cardiovascular tissue [9–12] and can even treat diseases such as diabetes [13,14]. Currently, scaffolds are increasingly

popular substitutes in TE. Scaffolds can be used for in vitro cultures of appropriate cells, which can be implanted into the body as a bio-implant after a suitable amount of time and can also be transplanted directly into the organism as a medium for the colonization of host stem cells [15–18]. Scaffolds should be three-dimensional with a network of an interconnected pore structure and tunable sizes that depend on the kinds of cells. A scaffold needs to be biocompatible and provide appropriate mechanical stability and shape properties to resist stresses during cultivation and after being implanted into the body [19–21].

An example of a tissue with limited regenerative capacity is cartilage, due to its lack of vascularization and innervations [22]. Scientists and doctors are still looking for an effective method to regenerate cartilage, and the most promising method is to use scaffolds [22–25].

This review article presents a general description of articular cartilage, the problems faced by this organ, and the current methods for its treatment. Next, the requirements and materials for scaffolds in cartilage engineering are presented, along with general methods for their preparation. In this section, the requirements for scaffolds using chondrocytes and stem cells are also highlighted. The last section of the article presents scaffolds made of synthetic polymers and their combinations with natural materials (hybrid scaffolds). This work focuses on research fromthe last decade, taking into consideration scaffolds that are currently under development as well as those that have undergone or are undergoing clinical research.

2. Articular Cartilage and Clinical Strategies for Treatment

Cartilage is a skeletal connective tissue classified into three types, for which hyaline is necessary to enable proper movement [23,26]. Cartilage is still a still problem for regenerative medicine because there is no effective treatment for its reconstruction. Currently, supportive treatment methods are used. Articular cartilage and its general treatment methods are briefly discussed in this section.

2.1. Articular Cartilage: Characteristics, Roles, Joint Diseases, and Traumatic Lesions

Articular cartilage (AC) is a type of hyaline cartilage. It is a hard and elastic tissue located between the bones. AC is composed of spheroid cells called chondrocytes and is 10 to 13 µm in diameter [23]. These cells constitute about 2% of the total volume of AC and produce an extracellular matrix (ECM) that is rich, among others, in collagen type II and proteoglycans. As a solid phase, AC is porous and permeable. The main component of the fluid phase of AC is water with inorganic ions such as sodium, chloride, and potassium. Cells are protected by the surrounding ECM from damaging forces. Cartilage is an avascular and aneural tissue, so it has no ability to transfer nutrients to cells (ECM helps transfer nutrients to chondrocytes via diffusion from the synovial fluid). This means that cartilage does not have a self-repair ability, which is why the role of doctors and scientists in cartilage tissue engineering/regenerative medicine is important. The principle functions of AC are, among others, to protect the ends of the bones from damage caused by movement (acting as a shock absorber). AC provides the mechanical ability to withstand loads and impacts and also provides a low-friction gliding surface. Trauma, an unhealthy lifestyle, traffic accidents, or various diseases (e.g., gene mutations and autoimmune disorders) can damage the cartilage, causing pain, movement limitations, stiffness, swelling, and even disability [23,26–29]. Examples of joint-damaging diseases include obesity and osteoporosis. This leads to an abrasion of the cartilage, which loses its elasticity and resistance to friction. Initially, this process is painless due to the lack of innervation and blood supply in the cartilage (it cannot be regenerated). Cartilage wear involves slow joint death, which is a consequence of aging and the accumulation of injuries from youth. Many people with knee ligament or meniscus damage have damaged cartilage after a few years [28,30]. Another type of cartilage damage occurs due to the disease osteochondritis dissecans, in which the bone dies and is secreted into the joint with the cartilage covering it. This bone and cartilage can then fracture and become loose [31]. Next, juvenile idiopathic arthritis (JIA) is the most common type of childhood arthritis. This autoimmune disease is a chronic inflammatory process that damages the articular cartilage,

induces bone epiphysis, and is responsible for extra-articular symptoms and systemic complications. This disease can occur at any stage of developmental age and its very wide symptomatology creates diagnostic problems, especially in the initial stages of the disease development [29,32]. The most common disease connected with articular cartilage defects is osteoarthritis (OA). This is the most common musculoskeletal disorder resulting from the degradation of cartilage and leads to a poor quality of life and disability. It can affect any joints in the body, including those in the knees, hips, spine, or fingers. Factors that can affect the development of this disease include genetic factors, obesity, inflammation, trauma, occupational factors, or metabolic syndrome. Moreover, OA progresses with age and mainly affects women. Without treatment, no recovery can be achieved [30,33–36].

2.2. Treatment Methods for Cartilage Regeneration

Despite much research on the matter, there are no effective treatments for OA. Current clinical methods focus mostly on pain treatment and are not satisfactory [37]. Many clinical techniques to repair/regenerate cartilage are known. Which method will be used depends on factors such as the area of damage, the depth, location, associated damage, chronicity, and age, as well as the physical activity of the patient. The depth or degree of cartilage damage is a key factor that determines the choice of treatment method. In classifying the degree of damage, many divisions are used to describe both the depth and the area of damage. The most widely used system is the Outerbridge classification, which takes into account size and depth (Table 1) [38,39].

Table 1. Outerbridge classification of articular cartilage lesions.

Grade of Damage	Description
Grade 0	Normal AC with a smooth surface
Grade I	Soft and swollen cartilage with a reduced amount of proteoglycans and increased water content.
Grade II	The surface is cracked up to half the thickness of the cartilage, a so-called "Blemish" of cartilage. Swelling or fraying is visible via Magnetic Resonance Imaging (MRI) imaging. The area of the damage does not exceed 1.25 cm^2 (less than 50%) of the surface. This corresponds to damage of an intermediate thickness.
Grade III	The damage exceeds half the thickness of the cartilage and may reveal the subchondral bone; the surface of the damage exceeds 1.25 cm^2. The deep defect comprises more than 50%.
Grade IV	Full thickness defect(s). Destruction with complete exposure of the subchondral bone.

In grades I and II, conservative treatments, such as patient education, reduction of BMI, rehabilitation, or the application of pharmacological treatment and dieting, usually give good results. Surgical interventions are recommended for grades III or IV. The most commonly used surgical methods are the microfracture (MF) method, chondroplasty surgery, osteochondral transplantation, and mosaicplasty, as well as cell-based approaches, such as autologous chondrocyte implantation (ACI). The microfracture technique is used much more frequently than other techniques but is not satisfactory. In recent years, the progress of cartilage tissue engineering has provided great hope for the regeneration of damaged cartilage. In every case, the doctor must decide which method is appropriate to choose. Each method has its own indicators and limitations, as well as advantages and disadvantages. The most appropriate management should be implemented at every stage of cartilage damage. The more extensive and serious the damage is, the more difficult and complicated the therapy will be, and the lower the chance of a full recovery [22,24,25,40].

MF is a safe, minimally invasive, and cheap method for cartilage repair. MF is a subchondral bone marrow stimulation method where a blood clot fills the defect. This provides a suitable environment

for tissue regeneration. Unfortunately, the MF technique promotes regeneration to fibrocartilage tissue with inferior biomechanical properties compared to hyaline cartilage [37,41].

More promising methods for the treatment of chondral lesion are cell-based approaches. These techniques enable the implantation of articular chondrocytes (ACs) from the patient in place of the defect. ACI with or without a scaffold is used in routine clinical practice. Three-dimensionalscaffolds serve as a temporary matrix for chondrocytes isolated from a healthy non-load-bearing area of the patient's cartilage. Generally, the therapeutic cells are cultured in vitro on scaffolds. Then, a bio-implant is transplanted into the tissue defect. The scaffold is gradually degraded along with cartilage formation (Figure 1) [22,25,40,42,43]. The schema in Figure 2 presents the ACI method with a scaffold, showing a version where ACs can be passaged to multiply them or placed directly in the scaffold for an in vitro culture.

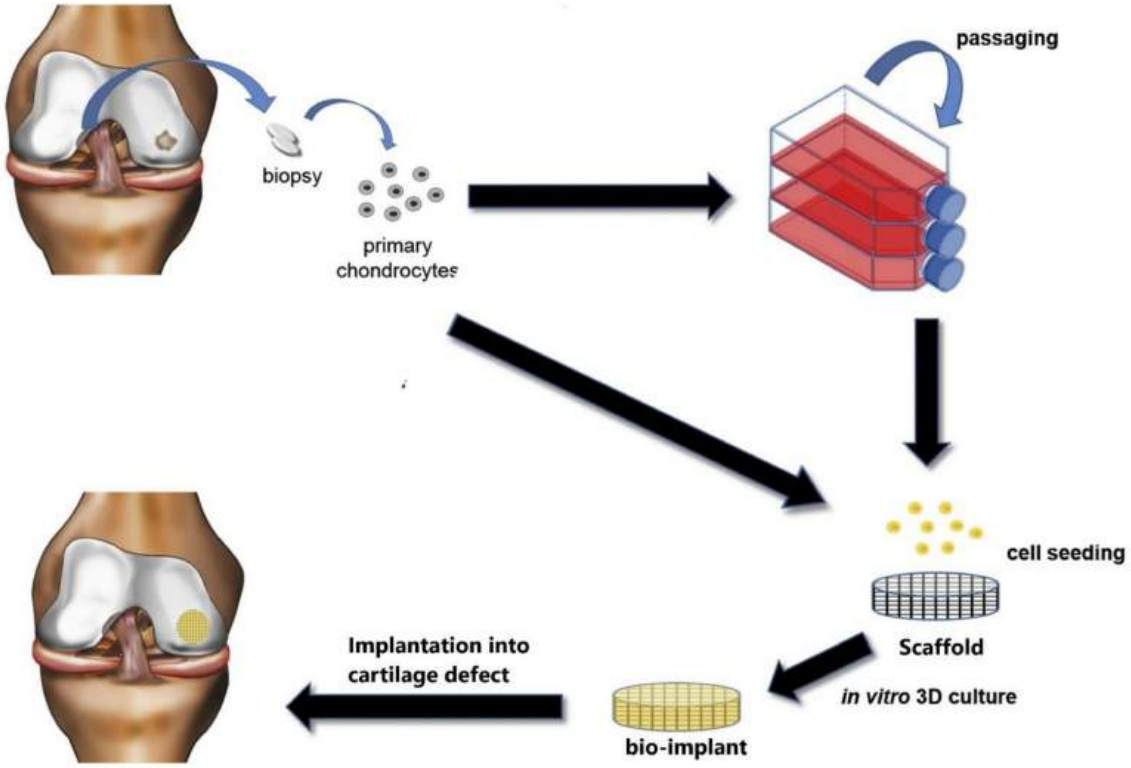

Figure 1. General schema of the autologous chondrocyte implantation (ACI) method with a 3D scaffold. This schema was modified according to a previous article [44].

Compared to MF, ACI allows the repair of larger cartilage defects. Moreover, studies indicate better results for ACI compared to MF [40,45]. Unfortunately, no current treatment for articular cartilage repair has recreated native hyaline cartilage. Current approaches reconstruct fibrocartilage, which is susceptible to further damage. However, combining different approaches, including advanced scaffolds, growth factors, or alternative cell types, such as mesenchymal stem cells (MSCs), provides an alternative for obtaining an effective cartilage treatment method. MSCs can be obtained from different sources, such as adipose tissue and bone marrow with the potential to differentiate into ACs. In addition, this approach can avoid the invasion of the joint for the initial harvesting of ACs [22,25,40,43,46–51].

Scaffolds can also serve as carriers of chondrogenic cells, MSCs, and the bioactive factors influencing chondrocyte growth and differentiation (growth factors) or their combinations. Recent treatments have indicated possibilities to regenerate articular cartilage using the surgical implantation of MSCs into articular cartilage lesions (Figure 2). Scaffolds for MSCs should meet the appropriate parameters described in Section 3.1.

Thanks to advances in medicine, it is now possible to collect stem cells not only from umbilical cord blood, endometrium, or bone marrow [46,47,49] but also from the adult tissues of each organism, especially from adipose tissue (AT) [47,52,53]. The main advantage of AT is its availability and abundance. Studies show that there are many times more stem cells in AT than in bone marrow. MSCs obtained from their own AT have a significant advantage over bone marrow cells due to their availability and large number. The collection procedure itself is also less painful and invasive for the patient [47,52,54,55].

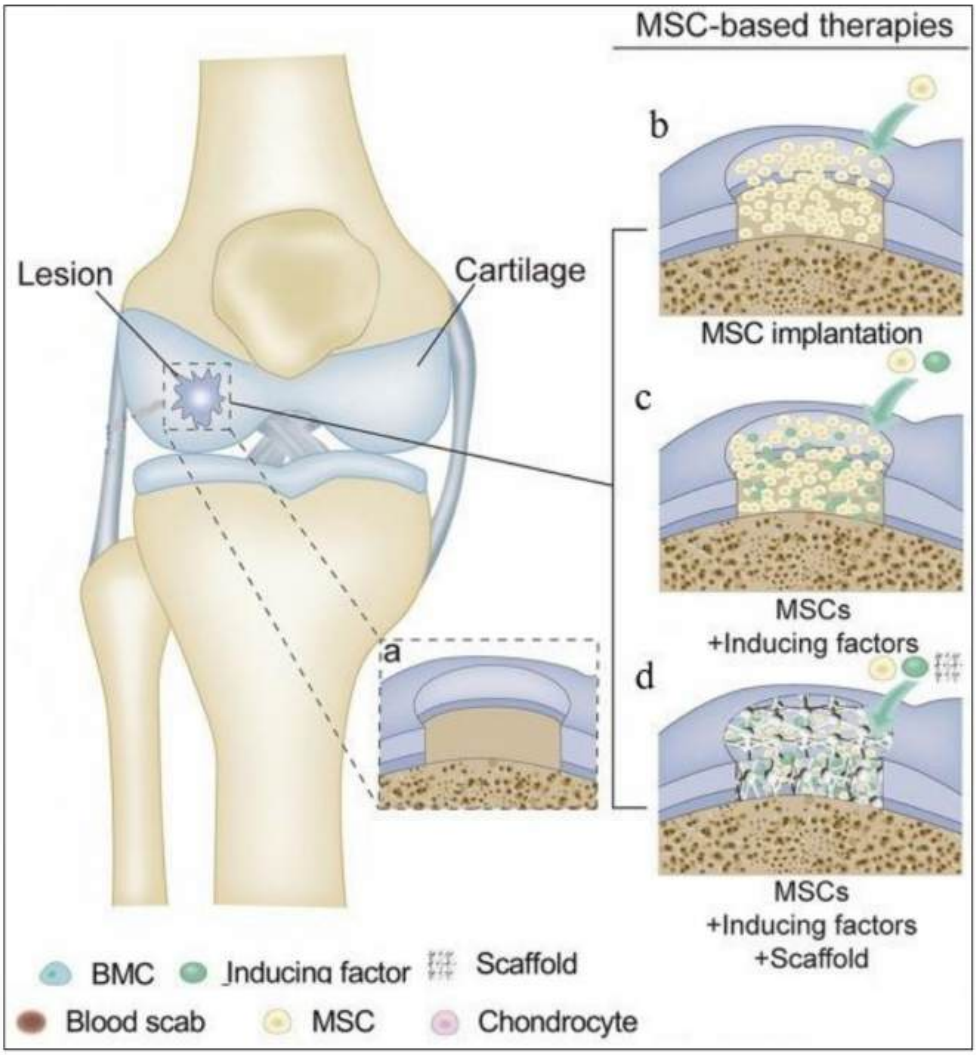

Figure 2. Cartilage repair methods via mesenchymal stem cell (MSC)-based therapies: (**a**) full-thickness cartilage injury; (**b**–**d**) therapies using MSCs and appropriate additives. The schema was modified from a previous article [53].

In clinical methods, growth factors for ACs and MSCs are helpful. Studies have shown the effects of growth factors on chondrogenesis and the maintenance of the correct phenotypes of cells. These growth factors can be added to the medium or scaffold during cultivation. Polypeptide mediators, such as transforming growth factor β (TGF-β), insulin-like growth factor (IGF), and fibroblast growth factor (FGF), stimulate the proliferation of cartilage cells and stabilize their phenotypic expression and chondrogenesis. It has been shown that the therapeutic potential of growth factors in the process of cartilage regeneration is significant. Under the influence of these factors, tissue is formed, the histological structure and biochemical properties of which are similar to hyaline cartilage. Moreover, they hasten the healing of the defect and increase the content of type II collagen compared to I [46,53,56].

3. Scaffold for Articular Cartilage Repair: Requirements, Materials, and Method for Obtaining

The role of scaffolds in cartilage tissue engineering is to provide a suitable environment for cells and guarantee success in the tissue regeneration process; this is possible by providing an environment similar to native articular cartilage. Therefore, scaffolds must possess adequate parameters, such as correct architecture, biocompatibility, degradability, or specific chemical and physical properties. This can be achieved through the choice of appropriate materials, additives, such as pore precursors, and manufacturing methods [17,57].

This section presents the requirements for scaffolds in tissue cartilage engineering, the available materials, and techniques for obtaining said scaffolds.

3.1. Requirements for Scaffolds

Scaffolds for cartilage tissue engineering should provide an appropriate environment and enable cell adhesion, migration, and development by having an appropriate architecture, controlled degradability, adequate mechanical parameters, and good biocompatibility. Many structural features, including porosity, pore size, interconnectivity, and permeability, play a meaningful role in AC development and cartilage regeneration [15,17,51,57]. A three-dimensional design for scaffolds is necessary to prevent the dedifferentiation of chondrocytes into fibroblast-like cells or the chondrogenesis of MSCs [50,58–60]. Chondrocytes cultivated on flat surfaces lose their ability to produce particular proteins that are necessary to the formation of hyaline cartilage [61,62]. A highly porous membrane with an interconnected macro-pore network can improve cell seeding, cell migration, cell development, and tissue ingrowth [19,50]. Moreover, the membrane's structure should be micro-porous to ensure the diffusion of oxygen, nutrients, and metabolism products. Regulated and controlled biodegradation are relevant to the formation of newly regenerating tissue cartilage and mainly depend on the materials used. The products released during degradation should be non-toxic to the body and easily removable. Scaffolds should maintain appropriate parameters in their stiffness, strength, and flexibility, conducive to integration and further tissue development. These parameters are important during cultivation and especially after implantation into the body due to the conditions in the knee [15,19,44,50,51,57–59,63–65]. Moreover, the parameters of scaffolds should be adapted to the types of cells. The sizes of the macro-pores must also be properly adjusted to the types of cells [15,17,19,64]. Pore sizes of about 150–250 µm are desirable for ACs, whereas large pore sizes of more than 300 µm are adequate for MSCs. Using the right pore sizes will support cell proliferation, the preservation of an appropriate phenotype, and chondrogenic differentiation (Figure 3) [17,20,64,66–70].

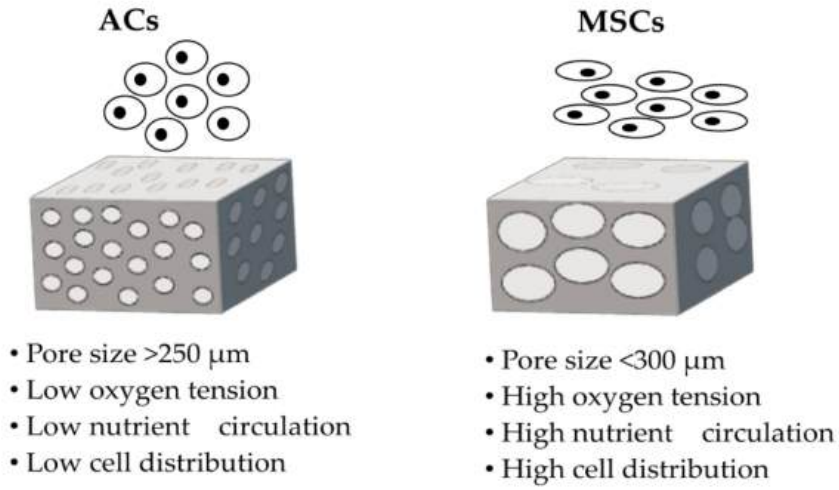

Figure 3. General schematic demonstration of the scaffold properties for the appropriate growth of articular chondrocytes (ACs) and mesenchymal stem cells (MSCs).

To obtain an appropriate scaffold structure depends on the relevant methods, materials, and pore precursors. One way to obtain suitable pores is the use of nonwovens produced by the electrospinning method. Depending on the nonwoven used, pores of 150 µm or greater can be produced [71,72]. To obtain information on the sizes of the pores in scaffolds, specialized programs can be used. One such program is MeMoExplorer™, an advanced membrane morphology software that analyzes SEM images. This software enables the contouring of pores and the measurement of their surfaces. These pores are partitioned into various size-classes, and measurements of the total areas (porosity coefficients) are provided [73,74]. Moreover, using pore precursors such aspoly(vinyl pyrrolidone) or poly(ethylene glycol) can improve the hydrophilicity and mechanical properties of membranes. This is important due to the hydrophobic nature of most synthetic polymers used for scaffold manufacturing [67,75]

Thus, physical parameters such as stiffness, the structures of scaffolds (e.g., pore size, interconnection, and porosity), and culture conditions are important for the fate of the cells. The different conditions for ACs and MSCs are presented above.

3.2. Materials Intended for Scaffolds

Materials for scaffolds should be biocompatible, exhibit adequate mechanical parameters, and be biodegradable into non-toxic and non-inflammatory components in the host organism. These materials should also be resistant to the conditions in the body, such as pH and body temperature. Therefore, appropriate materials for the production of scaffolds should be selected. Such materials can be made of synthetic or natural polymers or a combination of both (i.e., hybrid materials (hybrid)) [17,25,51,57,64,76]. Natural materials such as collagen [64,69,77], hyaluronic acid (HA) [78,79], chitosan (CH) [80,81], chondroitin sulfate (CS) [82,83], and fibrin [25,84,85] are widely used in the production of scaffolds for cartilage regeneration. These materials are characterized by their high biocompatibility and bioactivity. Due to their origins, these materials have properties similar to those of native tissues, and most of such materials naturally occur in the human body. These materials support cell attachment and stimulate the production of the ECM. Unfortunately, natural materials have disadvantages. Because of their rapid hydrolysis, natural materials quickly lose their properties suitable for the scaffold structure. Their low mechanical stability is also not adequate to support cells, and their products are thus insufficient for the regeneration of tissue. Moreover, the methods for obtaining such materials are limited due to the low resistance of natural polymers to changes in process parameters, such as high temperatures [25,50,51,57,59,64,76,86].Synthetic polymers, such as poly(ethylene glycol) (PEG) [87,88], polycaprolactone (PCL) [89,90], polylactic acid (PLA) [87,91,92], polyurethane [93,94], poly(glycolic acid) (PGA) [87,95], polyethersulfone (PES) [96–99], and polysulfone [100,101], are more diverse and promising. Some of these materials have been approved by the FDA for clinical human use [49,51,57,102–105]. Unfortunately, decisions of the FDA may be overturned. This change is associated with a new validation request, which is a long and difficult process. Unlike natural materials, synthetic polymers can be used to produce various shapes of membranes via many techniques and provide cell attachment, as well as good mechanical, physical, and chemical properties that can be modified to improve the parameters of the material. Most of these polymers degrade into components that are metabolized in the body. Moreover, the mechanical properties and degradation time can be controlled by combining these polymers (as copolymers or blends) [20,59,64,74,76,86,102,106–113].

Synthetic materials, like natural materials, have some disadvantages. One of them is an unexpected degradation time, which can cause brittleness of the scaffolds, even during culturing [59]. One example is PLA, which can be influenced by the use of a PLA copolymer with PCL or PEG and will affect the quality of the material [107,110,114]. Synthetic materials also lack desirable biological properties [115]. Moreover, the degradation products can result in side-effects for the host organism. These side-effects mostly involve acids that can be toxic to cells during cultivation or even elicit an inflammatory response in the host organism [59,86,103,116].

To date, studies have been conducted to obtain hybrid materials. Hybrid scaffolds combine the advantages of both synthetic and natural materials, allowing one to obtain membranes with defined

mechanical properties featuring the retained bio-functionality and tunable degradation necessary for the regeneration of cartilage [51,57,58,115].

3.3. Methods for Obtaining Scaffolds

The desired architecture, mechanical parameters, and forms of a scaffold can be obtained by selecting appropriate scaffold production methods. Scaffolds can be formed into 3D membranes (sponges), hydrogels, nonwovens (nanofibers) (Figure 4), or combinations thereof.

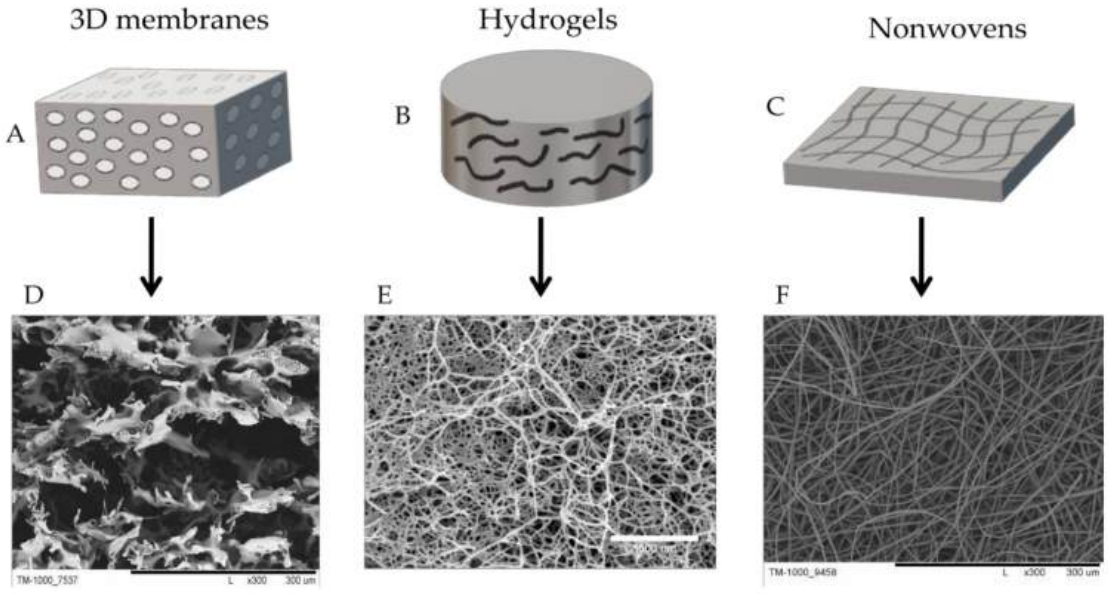

Figure 4. Schematic illustration of the main forms of scaffolds for cartilage tissue engineering: (**A**,**B**) hydrogels; (**C**,**D**) sponges; (**E**,**F**) nonwoven (nanofibers). Scale bars: D—300 µm; E—1000 nm; F—300 µm.

The literature describes many methods for producing a network of connected pores offering control over the mechanical properties and the time of scaffold degradation. This section will present the most popular techniques for obtaining synthetic and hybrid scaffolds for cartilage tissue engineering [17,19,21,40,59,86,117,118].

One of the most frequently used methods is phase inversion. Depending on the factor that induces the phase separation of the polymer solution, phase inversion can be carried out in two ways. One such method involves the temperature. This method is called thermal-induced phase separation (TIPS) and can be performed in liquid–liquid and liquid–solid systems, where the temperature of the process is appropriately selected. This method can obtain large and small pores with different membrane porosities [59,66,119–121]. In the second case, the phase inversion factor is non-solvent. This is the so-called non-solvent induced phase separation (NIPS) method. Here, the properly formed polymer solution is immersed into a non-solvent of the polymer. The phase inversion then produces a membrane. In these cases, like with the TIPS method, membranes with different porosities and pore sizes can be obtained [122–124]. A variant of this method involves adding a pore precursor to a previously prepared polymer solution or during the formation of a membrane. This approach promotes the formation of larger pore sizes and higher porosity. Pore precursors are ultimately removed from the scaffold by an appropriate solvent (porogen-leaching) [71,97,117,118,125–127]. Another similar method is solvent-casting particulate leaching (SCPL). This method involves dispersing salt particles in a biocompatible polymer solution. The solvent used to dissolve the polymer is then evaporated to obtain a polymer/salt composite membrane. Then, the salt is leached out by dipping the membrane into water or other salt solvents (not polymer solvents). The obtained membrane is dried to produce a

porous compatible membrane. The most commonly used pore precursors are sodium bicarbonate, sodium chloride, and a sodium acetate preparation of polycaprolactone [128].

The freeze-drying technique is a method that uses the sublimation process. In the first step, the polymer is dissolved in a suitable solvent, and then the polymer solution is cooled to its freezing point. In this way, by means of sublimation, the solid solvent is evaporated to obtain a scaffold with multiple pores. With this technique, the dissolved substances can be separated in the ice phase and a small porous structure can be obtained. The final scaffolds are then formed after the final drying. The advantage of this method is its application in biomedical contexts due to the use of water and ice crystals instead of organic solvents in the preparation of the scaffolds. One is also able to control the sizes of the pores by changing the freezing method. The disadvantages of this method are its high energy consumption and a long preparation process [21,59,117,118].

Another common method used to obtain scaffolds is electrospinning. This is a simple and effective technique that can obtain nonwovens from both natural and synthetic polymers. In this method, electrostatic forces are used to produce fibers or spheres with different morphologies and sizes at the micrometer and nanometer scales. Electrospun scaffolds can be characterized by their high porosity, good mechanical properties, and flexibility [117,129–132]. Moreover, the fibers can be modified using this method, e.g., by functionalizing the fiber surface via enzyme immobilization [133,134]. Therefore, the fibers obtained by the electrospinning technique have wide biomedical applications in addition to their use as scaffolds in tissue engineering [129–131,135].

The aforementioned methods are considered conventional. A group of more advanced methods, known as rapid prototyping (RP) techniques, enable the production of three-dimensional objects with precise spatial control over the polymer structure. In this way, scaffolds can be obtained gradually, layer by layer, according to computerized data, such as computer-aided design (CAD) or computed tomography (CT) data [5,59,136]. The most common and popular RP techniques involve 3D printing (3DP). As mentioned above, 3DP consists of creating tools and prototype functions directly from computer models. This technique is carried out by applying powdered material in layers and selectively fusing the powder through "inkjet printing" the adhesive. Then, after the layers are deposited, the unbound powder is removed and a 3D object is obtained. Three-dimensional printing can be used to precisely control the structures of the scaffolds at the micron level; however, it requires close monitoring of the tissue structure and the mechanical properties of the scaffold. The 3DP technique also includes bioprinting [5,137–140]. Another RP method is selective laser sintering (SLS), where a laser is the power source used to sinter the powdered material. The advantage of this technique is the excellent control it offers over the microstructures of the obtained scaffolds by adjusting the process parameters, e.g., the percentage composition of the mixed polymer/composite powder blend. Moreover, this method can use ultra-high molecular weights of polyethylene. Unfortunately, in this process, an additional procedure is required to remove the injected powder, which, in addition to its high operating temperature, is the main disadvantage of SLS [5,141]. In addition to RP, relevant methods include stereolithography (SLA) [142–144] and fused deposition modeling (FDM) for creating an object through the controlled deposition of molten material [5,145,146].

The scaffold material, biological factors, and even cells can be used in RP methods. These elements make it possible to obtain a construct with a precise, controllable, and complex internal structure featuring appropriate mechanical properties [59,118,136,137,147,148]. A combination of the above methods can obtain hybrid membranes, which are important due to the sensitivity of some materials to technological conditions, such as temperature. This approach can obtain scaffolds with appropriate mechanical properties as well as appropriate biological parameters. For example, it is possible to combine electrospinning techniques with 3D printing [118,149–151].

Cross-linking should also be mentioned as a common method used for the preparation of hybrid scaffolds. Cross-linking can be done in essentially two ways: (1) the formation of a multi-functional molecule with a low molecular weight, resulting in higher molecular weight branched structures and, ultimately, continuous cross-linked structures, and (2) obtaining a networked structure by bonding long

linear polymer molecules. Cross-linked polymers have properties that give them numerous applications, including their (1) resistance to solvents, (2) common high softening and heat-distortion temperatures, and (3) excellent dimensional stability. In freeze-drying and cross-linking techniques, it is possible to cross-link polymers during freeze-drying fabrication. [152–154]. Cross-linking polymerization is commonly used to produce hydrogels using hydrophilic monomers with cross-linkers. The components can be of both natural and synthetic origin [155]. Table 2 presents the advantages and disadvantages of the methods for obtaining scaffolds.

Table 2. Rapid prototyping (RP) and conventional methods for obtaining scaffolds for tissue engineering cartilage.

Technique	Advantages	Disadvantages
3D printing (3DP)	• Possibility of using hydrogels and cells	• Low precision • Long-standing process • Poor mechanical properties
Selective laser sintering (SLS)	• Smart process • High precision • No need for support • Construction	• High temperature • Rough surface
Stereolithography (SLA)	• High precision • Smart process • Soft surface	• Risk of high process temperature • Untreated • Material may be cytotoxic • high costs
Fused deposition modeling (FDM)	• Good mechanical properties	• Poor precision • High temperature • Narrow range of parameters • Limits in application to biodegradable polymers
Bioprinting	• High precision • Low costs • High speed of printing • Possibility of supporting high cell viability	• Depends on the cell's existence
Electrospinning	• Standard technique for obtaining nanofibrous scaffolds	• Toxicity of using solvents • Depends on many factors • Obtaining 3D structure or/and adequate pore sizes for biomedical applications can be problematic
Freeze-drying	• Capability of controlling the pore size • Possibility of obtaining high temperatures • Used for multiple purposes	• Toxicity when using solvents • High energy consumption • Irregular obtained size pores

Table 2. *Cont.*

Technique	Advantages	Disadvantages
Thermal-induced phase separation (TIPS)	• Possibility of using a low temperature • Very high porosity surface-to-volume ratio • Scaffolds obtained from a thermoplastic crystalline polymer	• Used only for thermoplastics
Solvent-casting particulate leaching (SCPL)	• High porosity • Low costs • Can be used for fabricating thin membranes of thin-wall 3D specimens	• High toxicity when using solvents • Time consuming for thin membranes

4. Scaffolds for Cartilage Treatment

Scaffolds for cartilage regeneration can be made of synthetic or natural polymers or acombination of both (a hybrid scaffold). Commercial scaffolds for regenerative cartilage are mainly made of natural materials, such as collagen or hyaluronic acid [40,44,156]. Due to the disadvantages of natural materials, research is underway to obtain scaffolds from synthetic and hybrid materials with the addition of biological components—membranes where the advantages of both synthetic and natural materials are taken into account [40,51,64]. This section presents scaffolds made of natural, synthetic, and hybrid materials, along with a short description of them (Table 3).

Table 3. Synthetic and hybrid scaffolds for cartilage regeneration.

Scaffold Name [Ref.]	Component	Method	Properties (Porosity (%), Pore Size (μm), Mechanical Properties)	Cell Source/Animal Model	Results
Synthetic scaffolds					
BioSeed®-C (Biotissue) [156,157]	PGA/PLA, PDS	Thermoplastic process	Good mechanical properties and adequate structure for cells	Human articular chondrocytes	Assessed in clinical trials. In the results, the scaffolds featured significantly improved final postoperative values. This highlights their effectiveness in cartilage regeneration.
Spongy PU scaffold [158]	PU	Freeze-drying	96.9% 126–186 μm Storage modulus: ~60.36 kPa	Chondrocytes, human MSCs	Biodegradable PU scaffold had better outcomes than PLA 3D membranes during culturing.
NSP-PCL scaffold [159]	PCL	Freeze-drying	The porosity of the scaffold was designed to promote cartilage ingrowth	Rabbit articular chondrocytes	The NSP-PCL scaffold indicated better results during in vitro and in vivo studies compared to the Chondro-Gide® scaffold.
RO45 3DHC [160]	PCL	3D printing	**RO45:** 84.6% 135–285 μm Compressive modulus: 25.6 MPa **3DHC** 83.8% 150–700 μm Compressive modulus: 3 MPa	Human adipose-derived MSCs	The RO45 scaffold was preferable for chondrogenic differentiation compared to 3DHC, which indicated better cell proliferation, scaffold penetration, and more favorable mechanical properties in the final construct.
Polysulphonic scaffold [97,98,161,162]	PES	Non-solvent induced phase separation and porogen- leaching	98.5% 60–300 μm	Rabbit model and human articular chondrocytes	A study with a rabbit model suggested that the scaffold is effective in repairing articular cartilage defects. In vitro study with human cells gave promise results.
PLLA-100 scaffolds [66]	PLLA	Thermally induced phase separation	93% 100 ± 20 μm	Human articular chondrocytes	The scaffold promoted the secretion of chondrogenic genes. It was better than the PLLA scaffold with larger pores (~200 μm).
PLCL-2 scaffold [163]	PLCL	Gel-pressing	80% 300–500 μm Young's modulus: ~0.7 MPa	Rabbit articular chondrocytes and mice model	The adequate structure of the scaffold showed that chondrocytes did not change their phenotypes during the in vitro study. The in vivo study indicated that the scaffold would maintain mechanical integrity and guide cartilaginous tissue formation.

Table 3. *Cont.*

Scaffold Name [Ref.]	Component	Method	Properties (Porosity (%), Pore Size (μm), Mechanical Properties)	Cell Source/Animal Model	Results
			Hybrid scaffold		
Chondrotissue® (Biotissue) [156,164]	PGA, HA	Freeze-drying		Platelet-rich plasma and bone marrow concentrate	The one-step cartilage repair method is available for clinical use. Treatment results follow up to 5 years of good outcomes with the potential for future benefits.
IC scaffold [153]	PLGA, COL	Freeze-drying and cross-linking	99.1% 50–400 μm Young's modulus: ~9 kPa	Bovine articular chondrocytes (BACs) and mice model	IC scaffold promoted cartilaginous gene expression, chondrocyte proliferation, and the regeneration of cartilage tissue with high mechanical properties. It seems to be promising for cartilage tissue applications.
Gel/PCEC-TGFβ1 hydrogel scaffold [165]	Gelatin, PCEC, TGFβ1	Cross-linking, freeze-drying	~150 μm Young's modulus: ~0.65 MPa	Human adipose tissue (AD)-MSCs	The study showed the potential for the growth and differentiation of h-AD-MSCs and could be a promising scaffold for cartilage tissue engineering.
PLCL-COLI [166]	PLCL, COL	3D printing	~85% ~10 μm; ~450 μm Young's modulus: ~0.21 MPa	Rabbit articular chondrocytes	Scaffold with a controlled structure, good biocompatibility, elasticity, and mechanical properties, as well as potential in cartilage regeneration.
C2C1H scaffold [167]	PLA, COL, CH	Freeze-drying and melt-spun	>85% Young's modulus: 52.3 kPa	Bovine articular cartilage chondrocytes	A hybrid scaffold with high porosity, good mechanical strength, and interconnected pore network. It has potential as a scaffold for cartilage tissue engineering.
ECM-PLGA scaffold [168,169]	PLGA, ECM	SCPL	90%	Rat mesenchymal stem cells (MSCs) and rat model	The in vitro study showed good properties of attachment, proliferation, and differentiation of the MSCs. Involved the implantation of a cell with MSCs and type II collagen mRNA expression. The in vivo study indicated the regeneration of tissue to hyaline cartilage. The scaffold could be promising for cartilage regeneration therapy.

Table 3. *Cont.*

Scaffold Name [Ref.]	Component	Method	Properties (Porosity (%), Pore Size (μm), Mechanical Properties)	Cell Source/Animal Model	Results
PCL/COL1 [170]	PCL, COL	Selective laser sintering	82.98% Young's modulus: 3.75 MPa	Pig articular chondrocytes and nude mice model	Scaffold with high porosity and repetitive pore structure. In vitro and in vivo study showed good outcomes compared to the PCL membrane. The addition of collagen ensured the proper development of chondrocytes.
CH/PLLA/PC scaffold [110]	PLLA, CH, PC	Freeze-drying and cross-linking	79–84% 49–170 μm	Rabbit articular chondrocytes	Outcomes from the in vivo study showed the suitability of the scaffold for cartilage tissue regeneration.
Chitosan-modified PLCL scaffold [171]	PLCL, CH	Porogen-leaching, lyophilization, and cross-linking	~85% 200–500 μm Young's modulus: 0.04 MPa	Pig articular chondrocytes	Biodegradable scaffolds with high porosity, good mechanical strength, and interconnected pore structure. Supplied a good environment for chondrocyte adhesion, proliferation, differentiation, and ECM secretion. The results were good but still require further research.
CSMA/PECA/GO (S2) scaffold [172]	CSMA, MPEG-PCL-AC (PECA), GO		~70% Mean 175.2 μm Compressive modulus: 0.48 MPa	Rabbit articular chondrocytes	Scaffold with an appropriate structure with biological components; provided an adequate environment for cells. The in vivo results were promising with great potential for the future.

CH—chitosan; COL—collagen, PU—polyurethane; PC—pectin based; PDS—poly-p-dioxanone; CS—chondroitin sulfate; CSMA—methacrylated chondroitin sulfate; HA—hyaluronic acid; PEG—poly(ethylene glycol); PCL—polycaprolactone; PLA—polylactic acid; PLLA—poly(l-lactide); PGA—poly(glycolic acid); PES—polyethersulfone; PLGA—polylactic-co-glycolic acid; PCEC—polycaprolactone-polyethylene glycol; ECM—extracellular matrix; PLCL—poly(l-lactide-co-ε-caprolactone); SCPL—solvent casting and particulate leaching method; AC—acryloyl chloride; GO—graphene oxide; PECA—poly(ethylene glycol) methyl ether-ε-caprolactone-acryloyl chloride.

4.1. Natural Scaffolds

Natural scaffolds are characterized by high bioactivity, biocompatibility, and biodegradability to non-toxic components. Due to their composition of natural materials, these scaffolds are similar to native tissue, which means that their presence creates an ideal environment for cells. Thus, the main advantage of natural polymers is their similarity to cartilage's ECM components. Their presence appropriately stimulates chondrogenesis and the maintenance of the cellular phenotypes of chondrocytes. These scaffolds affect the adhesion and proliferation of the cell and cell proliferation. Therefore, products used in cartilage regenerative medicine are mainly made of natural materials. Table 4 shows examples of commercial scaffolds, including their materials and basic characteristics. Scaffolds are mostly made of collagen, the main component of cartilage ECM. Unfortunately, these scaffolds often do not meet the necessary requirements, as they quickly lose their structure (sensitivity to an aquatic environment) and transform into a gel-like form. They are also not mechanically strong enough to support the cells and regenerated tissue. Thus, this kind of membrane does not have suitable properties to create hyaline cartilage. As a result of regeneration, non-valuable fibrous cartilage is obtained, which is susceptible to future damage [40,50,51,57,76,111,156,173].

Table 4. Natural scaffolds approved for medical use for cartilage tissue engineering.

Product (Company)	Materials	Characteristic
Hyalofast®(Anika) [110,154,174,175]	Benzyl ester of hyaluronic acid	A bioresorbable3D scaffold used through a one-step procedure aftera microfracture. It can be used even for deep cartilage lesions. The scaffold's non-woven structure allows it to be cut and adaptively matched into uneven lesions.
NeoCart®(Histogenics) [44,110,154]	Bovine type I collagen	Bioresorbableelectrospun scaffold used in MACI, a two-step procedure. The patient's chondrocytes are expanded into scaffolds. Then, they are incubated in the Tissue Engineering Processor (TEP), which simulates the variation of mechanical forces and reduces oxygen pressure, allowing the maintenance of the chondrocyte phenotype forming the appropriate proteins of the ECM.
ChondroGide(Geistlich) [110,154]	Type I/III collagen	The first described matrix for the ACI method. It is used in a one-step procedure. ChondroGide's role is to support and promote the chondrogenic differentiation of MSCs released after the microfracture method.
ACI-Maix™ (MACI) [44,45]	Type I/III collagen	The procedure is a two-step process. Expanded autologous chondrocytes (2 or 3 passage) are cultured into the scaffold for 3 or 4 days before implantation into the patient.
Cartipatch®(Xizia Biotech) [44,156,173]	Agarose and alginate	The cylindrical scaffold of a single layer of hydrogel with expanded cartilage cells. The clinical procedure is the same as that for the two-step method. The alginate polymer provides elasticity to the matrix, which facilitates handling during the surgical procedure.
NOVOCART® 3D—AesculapOrthopaedics (BBraun) [44,64,111,156]	Type I collagen, chondroitin sulfate	A sponge scaffold with a bilayer structure and interconnected pores, used in a two-step procedure. This scaffold is desirable in young patients,<16 years old, to avoid eventual secondary injuries, such as early osteoarthritis.

Table 4. *Cont.*

Product (Company)	Materials	Characteristic
CaReS®(Arthrokinetics) [44,64,111,156]	Type I collagen gel	The scaffold is used in a two-step clinical procedure. Isolated autologous chondrocytes are mixed with a fluid matrix. Then, after 14 days, it is set in the lesion using fibrin glue. The height, thickness, and size of the hydrogel can be easily adjusted to the lesion.
CARTISTEM® (Medipost) [49,176,177]	Hyaluronic acid	Allogeneic human umbilical cord blood (hUCB)-derived MSCs and HA hydrogel products for cartilage regeneration for repeated traumas or degenerative osteoarthritis. A 7-year follow-up study of 104 patients showed promising efficacy in terms of durable cartilage regeneration with no significant adverse effects.

Because natural materials usually have poor mechanical properties, they are often insufficient to regenerate a given tissue. An additional disadvantage is their limited processing methods resulting from the low resistance of the materials to changes in process parameters (e.g., pH, high-temperature, and pressure). For this reason, natural scaffolds do not have the desired parameters. Additionally, the regenerated cartilage is not hyaline cartilage but fibrocartilage with inferior properties.

4.2. Hydrogel Scaffolds

Scaffolds of a hydrogel formare of great interest in cartilage regenerative engineering. These scaffolds are formed as a result of the cross-linking of natural and synthetic (or both) polymers and are characterized by their ability to absorb water or biological fluids. All these features make such scaffolds very similar to natural cartilage ECM [155,178,179].

Unfortunately, like natural scaffolds, hydrogel scaffolds have one major disadvantage. Due to their solubility in aquatic conditions, these scaffolds have low mechanical strength, which makes them difficult to handle [105,178]. Intensive studies are currently underway on the development of hydrogels from synthetic and hybrid materials [49,53,176,177,180]. Yang etal. obtained a synthetic hydrogel scaffold with the strength and modulus of native cartilage. This scaffold was composed of a bacterial cellulose (BC) nanofiber network with a PVA–poly(2-acrylamido-2-methyl-1-propanesulfonic acid sodium salt) (PAMPS) double-network hydrogel. BC was chosen as the nanofiber network due to its high tensile strength, biocompatibility, and lack of the enzymes necessary to degrade cellulose in the human body. Moreover, BC mimics collagen. The second layer of the PVA hydrogel provides elasticity, viscoelastic energy dissipation, and tensile resistance by allowing the BC fibers to share the load in the composite framework. This is an example of a scaffold with promising performance for further research in cartilage tissue engineering [180].An example of a hybrid hydrogel scaffold is gelatin/polycaprolactone–polyethylene glycol (Gel/PCEC-TGFβ1) (Table 3).This scaffold uses both natural and synthetic polymers and growth factors. It was prepared and evaluated for human mesenchymal stem cells derived from adipose tissue (h-AD-MSCs). During the study, the tests indicated the expression of cartilage-specific genes, such as collagen type II and aggrecan, showing promising results and potential for further research on cartilage regeneration [165].

So-called injectable hydrogels have gained interest in medicine for local deformation in cartilage. In this process, a mixture of the patient's expanded cells with the hydrogel is injected into the cartilage-damaged area. In the body, cells gradually multiply and the hydrogel is degraded. The advantage of this method is its low invasiveness and the possibility of its precise adjustment to the defect [49,53,179]. There are numerous ongoing/recruiting clinical trials using sealant gel-based MSC constructs for cartilage regeneration [49,176]. Some of them (CARTISTEM®, CaReS®, and Cartipatch®)were approved for clinical usage (Table 4) [49,176,177].

4.3. Synthetic Scaffolds

Research on using synthetic scaffolds for the regeneration of cartilage has been described in numerous studies. These scaffolds are characterized by their biocompatibility, biodegradability, and good mechanical properties and can be obtained by various methods due to their better resistance to physicochemical properties compared to natural membranes. Currently, few synthetic scaffolds are being tested in clinical trials for their use in cartilage regeneration [51].

An example of a commercial scaffold made from synthetic materials is the BioSeed®-C (Biotissue) membrane. This membrane is composed of PGA/PLA and PDS materials and is characterized by bioresorbability, elasticity, and the ability to be cut without fraying. This membrane's adequate 3D structure and the stability of the environment during culturing stimulate the patient's cells to differentiate [156]. The clinical outcomes at 4 years after implantation showed promising curativeresults for cartilage defects of the knee [157].

The most commonly used synthetic materials for the production of scaffolds for cartilage repair are PLA [66,181,182], PCL [91,159,160,183,184], and copolymers such as PLGA [185–188] and PLCA [154,163,189]. Christensen et al. used a nanostructured porous polycaprolactone (NSP-PCL) scaffold [159] and compared its in vivo and in vitro outcomes in a rabbit model with a commercial Chondro-Gide® scaffold. The observation time was 13 weeks, and the results were better for the synthetic scaffolds than the commercial ones. This scaffold had higher chondrogenic markers during the in vitro study and better in vivo histological scores. Thus, NSP-PCL seems to be an adequate scaffold for cartilage repair [159]. Research was also conducted with other synthetic materials, such as a spongy PU scaffold [160]. Scaffolds made from PU material had good hydrophilicity and porosity with interconnected pores and adequate mechanical strength. In a previous study, a PU scaffold was compared with a conventional PLA scaffold. The suitability of the scaffold for cartilage regeneration was evaluated during culturing with chondrocytes and human mesenchymal stem cells (MSCs). The chondrocytes grew better and secreted more glycosaminoglycan in the PU scaffolds than in the PLA scaffolds. Moreover, the human MSCs showed greater chondrogenesis in the PU scaffolds than in the PLA membranes. Degradable PU scaffolds thus have potential in cartilage tissue engineering applications [158]. Another example is PES materials. Polysulphonic membranes are an example of scaffolds that offer promising results for the regeneration of cartilage, as these membranes have an interconnected pore network, good elasticity, and excellent mechanical properties [97,98,161,162]. A study with a rabbit model showed that this membrane was better than a commercial Chondro-Gide® scaffold [162]. Unfortunately, the main disadvantage of synthetic polymers is their degradation, which leads to the release of acids. This can cause inflammation in the body. Additionally, in some cases, the degradation is too fast, causing the membranes to break or even crumble; moreover, the membranes do not have adequate biological properties. Therefore, research is being done to obtain scaffolds with a combination of synthetic and natural materials [59,86,103,111,115,116].

4.4. Hybrid Scaffolds

Considering the advantages of synthetic and natural materials, scaffolds with good mechanical and biological properties can be obtained. Currently, hybrid scaffolds are one direction of research in pursuit of a suitable implant for articular cartilage regeneration. The membranes of such scaffolds can be improved by inserting other biologically active additives, such as growth factors, and through a selection of appropriate kinds of cells [25,40,49–51,64,115,190]. This section presentsand discusses scaffolds made of hybrid materials. Some of these scaffolds are outlined in Tables 3 and 4.

Currently, few hybrid scaffolds have undergone clinical trials. One of them is Chondrotissue® (Biotissue) [158,166]. This resorbable membrane is composed of PGA and HA and is used in clinical contexts through a one-step treatment method. This membrane's elasticity is due to the addition of autologous platelet-rich plasma (PRP) or serum enriched with platelets. This method relieves pain, improves mobility, and supports cartilage regeneration. Five years of clinical trials confirmed the good

outcomes of this one-step procedure with Chondrotissue®, which provides stable results with future potential in hyaline cartilage regeneration.

Rofiqoh et al. developed an IC hybrid scaffold composed of PLGA and collagen. This scaffold features a high porosity membrane with an interconnected pore network and good mechanical properties. The studies were carried out with the use of bovine articular chondrocytes and invivo implantation into mice. The results showed the regeneration of cartilage-like tissue with high potential for further work [153]. Another example of a hybrid scaffold is PLCL-COLI. In a previous study, a PLCL membrane was printed, treated with alkali, and coated with collagen type I (COLI). The obtained scaffold had high porosity with a controlled structure. This scaffold provided good biocompatibility and elastic and mechanical properties. The compressive modulus of the membrane was, moreover, 0.21 MPa (similar to human cartilage). This scaffold provides good outcomes and has promise as an implant in cartilage repair [166]. Next, a C2C1H scaffold was obtained and characterized by Haaparanta et al. This scaffold was composed of collagen, chitosan, and PLA. A synthetic polymer used as a 3D mesh gave the scaffold good mechanical strength, and the natural components mimicked an appropriate environment for chondrocytes. The researchers studied eight scaffolds, determining C2C1H to be the best. This scaffold had a highly porous structure with interconnected pores and good mechanical strength with appropriate stiffness. A culture with isolated bovine chondrocytes showed promising results, with promise for further work towards cartilage regeneration [167]. Another example is the ECM-coated polylactic-co-glycolic acid (ECM-PLGA) scaffold designed by Nogami et al. In this scaffold, a synthetic polymer established the appropriate mechanical properties, while the use of ECM provided an appropriate environment for the cells. This scaffold's structure achieved the relevant properties for cartilage regeneration. The in vitro study showed attachment, growth, and differentiation of the MSCs. In the invivo study, cell-free scaffolds were implanted into the osteochondral defects of rat knees. Research workers demonstrated that the scaffolds promoted the regeneration of hyaline-like cartilage, which was better than the cartilage in the empty control group. An ECM-PLGA implant may be a good component for use in a one-step method for cartilage regeneration, but more research is required [168,169].

In the literature, there are many examples of hybrid scaffolds used for cartilage tissue engineering, where a biodegradable synthetic polymer provides the housing framework. Mainly, these scaffolds use porous membranes to provide the necessary mechanical properties to support tissue growth, while the additives include natural composites (bioactive fillers). These fillers produce bioactive signals that supply the required information for chondrogenesis and maintain the proper phenotypes of the chondrocytes [25,49,51,110,115,190–192]. These are mostly components that naturally occur in the cartilage, such as HA [156,164,193,194], CS [172], COL [64,151,153,167,170,195,196], and ECM [168,197].

5. Conclusions

Currently, the most promising method for cartilage regeneration is the transplantation of implants with or without cells in the area with the damage. Therefore, research is underway to obtain an appropriate scaffold. There are many commercial scaffolds used in orthopedics, which, unfortunately, do not completely fulfill their proper roles in the regeneration of hyaline cartilage. New solutions are constantly being sought, including new scaffolds, growth factors, and sources of cells, as well as methods for delivering the implants to damaged areas. Currently, according to the literature, hybrid scaffolds provided the most promising results in research on articular cartilage regeneration. A combination of synthetic materials to ensure adequate mechanical strength and natural components to ensure proper chondrogenesis and preserve the phenotype has the greatest probability of obtaining hyaline cartilage in a damaged area. In addition, the literature provides information on the search for an appropriate method/improvement of current methods for scaffolding production. Boosters that can be added to the scaffolds or the medium (e.g., growth factors) are also being sought. The selection of appropriate types of cells is also under investigation, mainly focusing on MSCs and human autologous chondrocytes. Proper selection of all the above-mentioned factors could ensure that the appropriate

articular cartilage regeneration is obtained. The problems to be solved are significant due to the number of people with cartilage problems, such as osteoarthritis. There are several scaffolds designed for orthopedics, but no one solution can guarantee the reconstruction of hyaline cartilage, as most interventions yield fibrocartilage, which is susceptible to further damage. Thus, patients eventually return to the starting point. Consequently, it is important to obtain an appropriate scaffold and method for the regeneration of hyaline cartilage.

Ultimately, two important conclusions can be highlighted. Thus far, no scaffolds have been obtained that achieve the optimal conditions for the regeneration of articular cartilage. The obtained results suggest that due to our poor ability to modify natural materials, hybrid scaffolds and composite ones combining the properties and advantages of several natural and synthetic materials are the most promising options.

Funding: This work did not receive any specific grant from funding agencies in the public, commercial, or not-for-profit sectors.

Conflicts of Interest: The authors declare no conflict of interest in relation to the writing of this article.

References

1. Gurtner, G.C.; Werner, S.; Barrandon, Y.; Longaker, M.T. Wound repair and regeneration. *Nature* **2008**, *453*, 314–321. [CrossRef] [PubMed]
2. Dzobo, K.; Thomford, N.E.; Senthebane, D.A.; Shipanga, H.; Rowe, A.; Dandara, C.; Pillay, M.; Motaung, K.S.C.M. Advances in regenerative medicine and tissue engineering: Innovation and transformation of medicine. *Stem Cells Int.* **2018**, *2018*. [CrossRef] [PubMed]
3. Duan, B. State-of-the-Art Review of 3D Bioprinting for Cardiovascular Tissue Engineering. *Ann. Biomed. Eng.* **2017**, *45*, 195–209. [CrossRef] [PubMed]
4. Scarritt, M.E.; Pashos, N.C.; Bunnell, B.A. A review of cellularization strategies for tissue engineering of whole organs. *Front. Bioeng. Biotechnol.* **2015**, *3*, 43. [CrossRef]
5. Yan, Q.; Dong, H.; Su, J.; Han, J.; Song, B.; Wei, Q.; Shi, Y. A Review of 3D Printing Technology for Medical Applications. *Engineering* **2018**, *4*, 729–742. [CrossRef]
6. Giwa, S.; Lewis, J.K.; Alvarez, L.; Langer, R.; Roth, A.E.; Church, G.M.; Markmann, J.F.; Sachs, D.H.; Chandraker, A.; Wertheim, J.A.; et al. The promise of organ and tissue preservation to transform medicine. *Nat. Biotechnol.* **2017**, *35*, 530–542. [CrossRef]
7. Popoola, J.; Greene, H.; Kyegombe, M.; MacPhee, I.A. Patient involvement in selection of immunosuppressive regimen following transplantation. *Patient Prefer. Adherence* **2014**, *8*, 1705–1712. [CrossRef]
8. Feinberg, A.W. Engineered tissue grafts: Opportunities and challenges in regenerative medicine. *Wiley Interdiscip. Rev. Syst. Biol. Med.* **2012**, *4*, 207–220. [CrossRef]
9. Park, K.M.; Shin, Y.M.; Kim, K.; Shin, H. Tissue Engineering and Regenerative Medicine 2017: A Year in Review. *Tissue Eng. Part B Rev.* **2018**, *24*, 327–344. [CrossRef]
10. Murphy, S.V.; Atala, A. Organ engineering—Combining stem cells, biomaterials, and bioreactors to produce bioengineered organs for transplantation. *BioEssays* **2013**, *35*, 163–172. [CrossRef]
11. Mazza, G.; Al-Akkad, W.; Rombouts, K.; Pinzani, M. Liver tissue engineering: From implantable tissue to whole organ engineering. *Hepatol. Commun.* **2018**, *2*, 131–141. [CrossRef] [PubMed]
12. Tarassoli, S.P.; Jessop, Z.M.; Al-Sabah, A.; Gao, N.; Whitaker, S.; Doak, S.; Whitaker, I.S. Skin tissue engineering using 3D bioprinting: An evolving research field. *J. Plast. Reconstr. Aesthetic Surg.* **2018**, *71*, 615–623. [CrossRef] [PubMed]
13. Farina, M.; Alexander, J.F.; Thekkedath, U.; Ferrari, M.; Grattoni, A. Cell encapsulation: Overcoming barriers in cell transplantation in diabetes and beyond. *Adv. Drug Deliv. Rev.* **2019**, *139*, 92–115. [CrossRef] [PubMed]
14. Liu, Y.; Luo, J.; Chen, X.; Liu, W.; Chen, T. *Cell Membrane Coating Technology: A Promising Strategy for Biomedical Applications*; Springer: Singapore, 2019; Volume 11, ISBN 0123456789.
15. Hollister, S.J. Porous scaffold design for tissue engineering. *Nat. Mater.* **2005**, *4*, 518–524. [CrossRef] [PubMed]
16. O'Brien, F.J. Biomaterials & scaffolds for tissue engineering. *Mater. Today* **2011**, *14*, 88–95. [CrossRef]

17. Bružauskaitė, I.; Bironaitė, D.; Bagdonas, E.; Bernotienė, E. Scaffolds and cells for tissue regeneration: Different scaffold pore sizes—Different cell effects. *Cytotechnology* **2016**, *68*, 355–369. [CrossRef]
18. Dhandayuthapani, B.; Yoshida, Y.; Maekawa, T.; Kumar, D.S. Polymeric scaffolds in tissue engineering application: A review. *Int. J. Polym. Sci.* **2011**, *2011*. [CrossRef]
19. Loh, Q.L.; Choong, C. Three-dimensional scaffolds for tissue engineering applications: Role of porosity and pore size. *Tissue Eng. Part B Rev.* **2013**, *19*, 485–502. [CrossRef]
20. Jafari, M.; Paknejad, Z.; Rad, M.R.; Motamedian, S.R.; Eghbal, M.J.; Nadjmi, N.; Khojasteh, A. Polymeric scaffolds in tissue engineering: A literature review. *J. Biomed. Mater. Res. Part B Appl. Biomater.* **2017**, *105*, 431–459. [CrossRef]
21. Zhao, P.; Gu, H.; Mi, H.; Rao, C.; Fu, J.; Turng, L. Fabrication of scaffolds in tissue engineering: A review. *Front. Mech. Eng.* **2018**, *13*, 107–119. [CrossRef]
22. Walter, S.G.; Ossendorff, R.; Schildberg, F.A. Articular cartilage regeneration and tissue engineering models: A systematic review. *Arch. Orthop. Trauma Surg.* **2019**, *139*, 305–316. [CrossRef] [PubMed]
23. Zhang, L.; Hu, J.; Athanasiou, K.A. The role of tissue engineering in articular cartilage repair and regeneration. *Crit. Rev. Biomed. Eng.* **2009**, *37*, 1–57. [CrossRef] [PubMed]
24. Kwon, H.; Brown, W.E.; Lee, C.A.; Wang, D.; Paschos, N.; Hu, J.C.; Athanasiou, K.A. Surgical and tissue engineering strategies for articular cartilage and meniscus repair. *Nat. Rev. Rheumatol.* **2019**, *15*, 550–570. [CrossRef] [PubMed]
25. Zhao, Z.; Fan, C.; Chen, F.; Sun, Y.; Xia, Y.; Ji, A.; Wang, D.A. Progress in Articular Cartilage Tissue Engineering: A Review on Therapeutic Cells and Macromolecular Scaffolds. *Macromol. Biosci.* **2020**, *20*, 1900278. [CrossRef]
26. Sophia Fox, A.J.; Bedi, A.; Rodeo, S.A. The basic science of articular cartilage: Structure, composition, and function. *Sports Health* **2009**, *1*, 461–468. [CrossRef]
27. Bhosale, A.M.; Richardson, J.B. Articular cartilage: Structure, injuries and review of management. *Br. Med Bull.* **2008**, *87*, 77–95. [CrossRef]
28. Collins, K.H.; Herzog, W.; Macdonald, G.Z.; Reimer, R.A. Obesity, Metabolic Syndrome, and Musculoskeletal Disease: Common Inflammatory Pathways Suggest a Central Role for Loss of Muscle Integrity. *Front. Physiol.* **2018**, *9*. [CrossRef]
29. Krishnan, Y.; Grodzinsky, A.J. Cartilage diseases. *Matrix Biol.* **2018**, *71–72*, 51–69. [CrossRef]
30. Oliveira, M.C.; Ph, D.; Vullings, J.; van de Loo, F.A.J.; Ph, D. Osteoporosis and osteoarthritis are two sides of the same coin paid for obesity. *Nutrition* **2020**, *70*, 110486. [CrossRef]
31. Accadbled, F.; Vial, J.; Gauzy, J.S. De Osteochondritis dissecans of the knee. *Orthop. Traumatol. Surg. Res.* **2018**, *104*, S97–S105. [CrossRef]
32. Barendregt, A.M.; Mazzoli, V.; Van Den Berg, J.M.; Kuijpers, T.W.; Maas, M. T 1 ρ-mapping for assessing knee joint cartilage in children with juvenile idiopathic arthritis—Feasibility and repeatability. *Pediatric Radiol.* **2020**, *50*, 371–379. [CrossRef] [PubMed]
33. Brody, L.T. Knee osteoarthritis: Clinical connections to articular cartilage structure and function. *Phys. Ther. Sport* **2015**, *16*, 301–316. [CrossRef] [PubMed]
34. Silverwood, V.; Blagojevic-Bucknall, M.; Jinks, C.; Jordan, J.L.; Protheroe, J.; Jordan, K.P. Current evidence on risk factors for knee osteoarthritis in older adults: A systematic review and meta-analysis. *Osteoarthr. Cartil.* **2015**, *23*, 507–515. [CrossRef] [PubMed]
35. Johnson, C.I.; Argyle, D.J.; Clements, D.N. In vitro models for the study of osteoarthritis. *Vet. J.* **2016**, *209*, 40–49. [CrossRef]
36. Appleton, C.T. Osteoarthritis year in review 2017: Biology. *Osteoarthr. Cartil.* **2018**, *26*, 296–303. [CrossRef]
37. Armiento, A.R.; Alini, M.; Stoddart, M.J. Articular fibrocartilage—Why does hyaline cartilage fail to repair? *Adv. Drug Deliv. Rev.* **2019**, *146*, 289–305. [CrossRef]
38. Bs, C.S.; Kweon, C.Y. Classifications in Brief: Outerbridge Classification of Chondral Lesions. *Clin. Orthop. Relat. Res.* **2018**, 2101–2104. [CrossRef]
39. Posadzy, M.; Desimpel, J.; Vanhoenacker, F. Staging of Osteochondral Lesions of the Talus: MRI and Cone Beam CT. *J. Belg. Soc. Radiol.* **2017**. [CrossRef]
40. Medvedeva, E.V.; Grebenik, E.A.; Gornostaeva, S.N.; Telpuhov, V.I.; Lychagin, A.V.; Timashev, P.S.; Chagin, A.S. Repair of damaged articular cartilage: Current approaches and future directions. *Int. J. Mol. Sci.* **2018**, *19*, 2366. [CrossRef]

41. Mirza, U.; Shubeena, S.; Shah, M.S.; Zaffer, B. Microfracture: A technique for repair of chondral defects. *J. Entomol. Zool. Stud.* **2018**, *6*, 1092–1097.
42. Dunkin, B.S.; Lattermann, C. New and emerging techniques in cartilage repair: Matrix-induced autologous chondrocyte implantation. *Oper. Tech. Sports Med.* **2013**, *21*, 100–107. [CrossRef] [PubMed]
43. Brittberg, M. Symposium Scaffold based Autologous Chondrocyte Implantation: The Surgical Technique. *Asian J. Arthrosc.* **2019**, *4*, 23–26. [CrossRef]
44. Huang, B.J.; Hu, J.C.; Athanasiou, K.A. Cell-based tissue engineering strategies used in the clinical repair of articular cartilage. *Biomaterials* **2016**, *98*, 1–22. [CrossRef] [PubMed]
45. Brittberg, M.; Recker, D.; Ilgenfritz, J.; Saris, D.B.F. Matrix-Applied Characterized Autologous Cultured Chondrocytes Versus Microfracture: Five-Year Follow-up of a Prospective Randomized Trial. *Am. J. Sports Med.* **2018**, *46*, 1343–1351. [CrossRef]
46. Fahy, N.; Alini, M.; Stoddart, M.J. Mechanical stimulation of mesenchymal stem cells: Implications for cartilage tissue engineering. *J. Orthop. Res.* **2018**, *36*, 52–63. [CrossRef]
47. Mastrolia, I.; Foppiani, E.M.; Murgia, A.; Candini, O.; Samarelli, A.V.; Grisendi, G.; Veronesi, E.; Horwitz, E.M.; Dominici, M. Challenges in Clinical Development of Mesenchymal Stromal/Stem Cells: Concise Review. *Stem Cells Transl. Med.* **2019**, *8*, 1135–1148. [CrossRef]
48. Charlier, E.; Deroyer, C.; Ciregia, F.; Malaise, O.; Neuville, S.; Plener, Z.; Malaise, M.; de Seny, D. Chondrocyte dedifferentiation and osteoarthritis (OA). *Biochem. Pharmacol.* **2019**, *165*, 49–65. [CrossRef]
49. Lam, A.T.L.; Reuveny, S.; Oh, S.K.W. Human mesenchymal stem cell therapy for cartilage repair: Review on isolation, expansion, and constructs. *Stem Cell Res.* **2020**, *44*, 101738. [CrossRef]
50. Demoor, M.; Ollitrault, D.; Gomez-Leduc, T.; Bouyoucef, M.; Hervieu, M.; Fabre, H.; Lafont, J.; Denoix, J.M.; Audigié, F.; Mallein-Gerin, F.; et al. Cartilage tissue engineering: Molecular control of chondrocyte differentiation for proper cartilage matrix reconstruction. *Biochim. Et Biophys. Acta Gen. Subj.* **2014**, *1840*, 2414–2440. [CrossRef]
51. Ahmadi, F.; Giti, R.; Mohammadi-Samani, S.; Mohammadi, F. Biodegradable Scaffolds for Cartilage Tissue Engineering. *Galen Med. J.* **2017**, *6*, 70–80. [CrossRef]
52. Zhang, R.; Ma, J.; Han, J.; Zhang, W.; Ma, J. Mesenchymal stem cell related therapies for cartilage lesions and osteoarthritis. *Am. J. Transl. Res.* **2019**, *11*, 6275–6289. [PubMed]
53. Le, H.; Xu, W.; Zhuang, X.; Chang, F.; Wang, Y.; Ding, J. Mesenchymal stem cells for cartilage regeneration. *J. Tissue Eng.* **2020**, *1*, 1–22. [CrossRef] [PubMed]
54. Koh, Y.G.; Choi, Y.J.; Kwon, O.R. Second-Look Arthroscopic Evaluation of Cartilage Lesions after Mesenchymal Stem Cell Implantation in Osteoarthritic Knees. *Am. J. Sports Med.* **2014**, *42*, 1628–1637. [CrossRef] [PubMed]
55. Francis, S.L.; Duchi, S.; Onofrillo, C.; Bella, C.D.; Choong, P.F.M. Adipose-Derived Mesenchymal Stem Cells in the Use of Cartilage Tissue Engineering: The Need for a Rapid Isolation Procedure. *Stem Cells Int.* **2018**, *2018*, 13–16. [CrossRef]
56. Augustyniak, E.; Trzeciak, T. The role of growth factors in stem cell-directed chondrogenesis: A real hope for damaged cartilage regeneration. *Int. Orthop.* **2015**, *39*, 995–1003. [CrossRef]
57. Kalkan, R.; Nwekwo, C.W.; Adali, T. The Use of Scaffolds in Cartilage Regeneration. *Eukaryot. Gene Expr.* **2018**, *28*, 343–348. [CrossRef]
58. Panadero, J.A.; Lanceros-Mendez, S.; Ribelles, J.L.G. Differentiation of mesenchymal stem cells for cartilage tissue engineering: Individual and synergetic effects of three-dimensional environment and mechanical loading. *Acta Biomater.* **2016**, *33*, 1–12. [CrossRef]
59. Eltom, A.; Zhong, G.; Muhammad, A. Scaffold Techniques and Designs in Tissue Engineering Functions and Purposes: A Review. *Adv. Mater. Sci. Eng.* **2019**, *2019*. [CrossRef]
60. Okubo, R.; Asawa, Y.; Watanabe, M.; Nagata, S.; Nio, M. Proliferation medium in three-dimensional culture of auricular chondrocytes promotes effective cartilage regeneration in vivo. *Regen. Ther.* **2019**, *11*, 306–315. [CrossRef]
61. Takahashi, T.; Ogasawara, T.; Asawa, Y.; Mori, Y.; Uchinuma, E.; Takato, T.; Hoshi, K. Three-Dimensional Microenvironments Retain Chondrocyte Phenotypes During Proliferation Culture. *Tissue Eng.* **2007**, *13*, 1583–1592. [CrossRef]

62. Schulze-Tanzil, G.; De Souza, P.; Villegas Castrejon, H.; John, T.; Merker, H.J.; Scheid, A.; Shakibaei, M. Redifferentiation of dedifferentiated human chondrocytes in high-density cultures. *Cell Tissue Res.* **2002**, *308*, 371–379. [CrossRef] [PubMed]
63. Koh, Y.G.; Lee, J.A.; Kim, Y.S.; Lee, H.Y.; Kim, H.J.; Kang, K.T. Optimal mechanical properties of a scaffold for cartilage regeneration using finite element analysis. *J. Tissue Eng.* **2019**, 10. [CrossRef] [PubMed]
64. Irawan, V.; Sung, T.C.; Higuchi, A.; Ikoma, T. Collagen Scaffolds in Cartilage Tissue Engineering and Relevant Approaches for Future Development. *Tissue Eng. Regen. Med.* **2018**, *15*, 673–697. [CrossRef] [PubMed]
65. Lai, Y.S.; Chen, W.C.; Huang, C.H.; Cheng, C.K.; Chan, K.K.; Chang, T.K. The effect of graft strength on knee laxity and graft in-situ forces after posterior cruciate ligament reconstruction. *PLoS ONE* **2015**, 10. [CrossRef]
66. Conoscenti, G.; Schneider, T.; Stoelzel, K.; Carfì Pavia, F.; Brucato, V.; Goegele, C.; La Carrubba, V.; Schulze-Tanzil, G. PLLA scaffolds produced by thermally induced phase separation (TIPS) allow human chondrocyte growth and extracellular matrix formation dependent on pore size. *Mater. Sci. Eng. C* **2017**, *80*, 449–459. [CrossRef]
67. Zhao, Y.; Tan, K.; Zhou, Y.; Ye, Z.; Tan, W.S. A combinatorial variation in surface chemistry and pore size of three-dimensional porous poly(ε-caprolactone) scaffolds modulates the behaviors of mesenchymal stem cells. *Mater. Sci. Eng. C* **2016**, *59*, 193–202. [CrossRef]
68. Nava, M.M.; Draghi, L.; Giordano, C.; Pietrabissa, R. The effect of scaffold pore size in cartilage tissue engineering. *J. Appl. Biomater. Funct. Mater.* **2016**, *14*, e223–e229. [CrossRef]
69. Zhang, Q.; Lu, H.; Kawazoe, N.; Chen, G. Pore size effect of collagen scaffolds on cartilage regeneration. *Acta Biomater.* **2014**, *10*, 2005–2013. [CrossRef]
70. Matsiko, A.; Gleeson, J.P.; O'Brien, F.J. Scaffold mean pore size influences mesenchymal stem cell chondrogenic differentiation and matrix deposition. *Tissue Eng. Part A* **2015**, *21*, 486–497. [CrossRef]
71. Chwojnowski, A.; Kruk, A.; Wojciechowski, C.; Łukowska, E.; Dulnik, J.; Sajkiewicz, P. The dependence of the membrane structure on the non-woven forming the macropores in the 3D scaffolds preparation. *Desalin. Water Treat.* **2017**, *64*, 324–331. [CrossRef]
72. Kruk, A.; Gadomska-Gajadhur, A.; Ruśkowski, P.; Chwojnowski, A.; Dulnik, J.; Synoradzki, L. Preparation of biodegradable semi-permeable membranes as 3D scaffolds for cell cultures. *Desalin. Water Treat.* **2017**, *64*, 317–323. [CrossRef]
73. Przytulska, M.; Kulikowski, J.L.; Wasyłeczko, M.; Chwojnowski, A.; Piętka, D. The evaluation of 3D morphological structure of porous membranes based on a computer-aided analysis of their 2D images. *Desalin. Water Treat.* **2018**, 128. [CrossRef]
74. Sikorska, W.; Wojciechowski, C.; Przytulska, M.; Rokicki, G.; Wasyłeczko, M.; Kulikowski, J.L.; Chwojnowski, A. Polysulfone–polyurethane (PSf-PUR) blend partly degradable hollow fiber membranes: Preparation, characterization, and computer image analysis. *Desalin. Water Treat.* **2018**, 128. [CrossRef]
75. Malik, T.; Razzaq, H.; Razzaque, S.; Nawaz, H.; Siddiqa, A.; Siddiq, M.; Qaisar, S. Design and synthesis of polymeric membranes using water-soluble pore formers: An overview. *Polym. Bull.* **2019**, *76*, 4879–4901. [CrossRef]
76. Armiento, A.R.; Stoddart, M.J.; Alini, M.; Eglin, D. Biomaterials for articular cartilage tissue engineering: Learning from biology. *Acta Biomater.* **2018**, *65*, 1–20. [CrossRef]
77. Rares, H.; Benea, C.; Earar, K.; Lattanzi, W.; Quercia, V.; Berce, C.; Mohan, A. Collagen Scaffold and Lipoaspirate Fluid—Derived Stem Cells for the Treatment of Cartilage Defects in a Rabbit Model. *Rev. Chim.* **2015**, *69*, 515–520.
78. Gobbi, A.; Whyte, G.P. Long-term Clinical Outcomes of One-Stage Cartilage Repair in the Knee With Hyaluronic Acid—Based Scaffold Embedded With Mesenchymal Stem Cells Sourced From Bone Marrow Aspirate Concentrate. *Am. J. Sports Med.* **2019**, *47*, 1621–1628. [CrossRef]
79. Lin, H.; Beck, A.M.; Fritch, M.R.; Tuan, R.S.; Deng, Y.; Kilroy, E.J.; Tang, Y.; Alexander, P.G. Optimization of photocrosslinked gelatin/hyaluronic acid hybrid scaffold for the repair of cartilage defect. *J. Tissue Eng. Regen. Med.* **2019**, *13*, 1418–1429. [CrossRef]
80. Wen, S.; Hung, K.; Hsieh, K.; Chen, C.; Tsai, C.; Hsu, S. In vitro and in vivo evaluation of chitosan—Gelatin scaffolds for cartilage tissue engineering. *Mater. Sci. Eng. C* **2013**, *33*, 2855–2863. [CrossRef]
81. Mittal, H.; Sinha, S.; Singh, B.; Kaur, J.; Sharma, J.; Alhassan, S.M. Recent progress in the structural modification of chitosan for applications in diversified biomedical fields. *Eur. Polym. J.* **2018**, *109*, 402–434. [CrossRef]

82. Chen, S.; Chen, W.; Chen, Y.; Mo, X.; Fan, C. Chondroitin sulfate modified 3D porous electrospun nano fi ber scaffolds promote cartilage regeneration. *Mater. Sci. Eng. C* **2020**, *118*, 1–12. [CrossRef]
83. Zhou, F.; Zhang, X.; Cai, D.; Li, J.; Mu, Q.; Zhang, W.; Zhu, S. Silk fibroin-chondroitin sulfate scaffold with immuno-inhibition property for articular cartilage repair. *Acta Biomater.* **2017**, *63*, 64–75. [CrossRef] [PubMed]
84. Filardo, G.; Drobnic, M.; Perdisa, F.; Kon, E.; Hribernik, M.; Marcacci, M. Fibrin glue improves osteochondral scaffold fi xation: Study on the human cadaveric knee exposed to continuous passive motion. *Osteoarthr. Cartil.* **2014**, *22*, 557–565. [CrossRef] [PubMed]
85. Kim, J.; Hyung, T.; Lim, D.; Yeon, S.; Lee, Y.; Koh, Y.I. Biochemical and Biophysical Research Communications Chondrogenic differentiation of human ASCs by stiffness control in 3D fi brin hydrogel. *Biochem. Biophys. Res. Commun.* **2020**, *522*, 213–219. [CrossRef]
86. Chung, C.; Burdick, J.A. Engineering cartilage tissue. *Adv. Drug Deliv. Rev.* **2008**, *60*, 243–262. [CrossRef]
87. Asghari, F.; Samiei, M.; Adibkia, K.; Akbarzadeh, A.; Davaran, S. Biodegradable and biocompatible polymers for tissue engineering application: A review. *Artif. Cells Nanomed. Biotechnol.* **2017**, *45*, 185–192. [CrossRef]
88. Fan, C.; Wang, D. A biodegradable PEG-based micro-cavitary hydrogel as scaffold for cartilage tissue engineering. *Eur. Polym. J.* **2015**, *72*, 651–660. [CrossRef]
89. Janmohammadi, M.; Nourbakhsh, M.S. International Journal of Polymeric Materials and Electrospun polycaprolactone scaffolds for tissue engineering: A review. *Int. J. Polym. Mater. Polym. Biomater.* **2018**, 1–13. [CrossRef]
90. Dao, T.T.; Vu, N.B.; Pham, L.H.; Bui, T.; Le, P.T.; Van Pham, P. In Vitro Production of Cartilage Tissue from Rabbit Bone Marrow-Derived Mesenchymal Stem Cells and Polycaprolactone Scaffold. *Adv. Exp. Med. Biol.* **2017**, *1804*, 45–60. [CrossRef]
91. Singhvi, M.S. Polylactic acid: Synthesis and biomedical applications. *J. Appl. Microbiol.* **2012**, *127*, 1612–1626. [CrossRef]
92. Silva, D.; Kaduri, M.; Poley, M.; Adir, O.; Krinsky, N.; Shainsky-roitman, J.; Schroeder, A. Mini Review Biocompatibility, biodegradation and excretion of polylactic acid (PLA) in medical implants and theranostic systems. *Chem. Eng. J.* **2018**. [CrossRef]
93. Wen, Y.; Dai, N.; Hsu, S. Acta Biomaterialia Biodegradable water-based polyurethane scaffolds with a sequential release function for cell-free cartilage tissue engineering. *Acta Biomater.* **2019**, *88*, 301–313. [CrossRef] [PubMed]
94. Hung, K.; Tseng, C.; Hsu, S. Synthesis and 3D Printing of Biodegradable Polyurethane Elastomer by a Water-Based Process for Cartilage Tissue Engineering Applications. *Adv. Healthc. Mater.* **2014**, 1578–1587. [CrossRef] [PubMed]
95. Budak, K.; Sogut, O.; Sezer, U.A. A review on synthesis and biomedical applications of polyglycolic acid. *J. Polym. Res.* **2020**, *27*, 1–19. [CrossRef]
96. Mahboudi, H.; Soleimani, M.; Enderami, S.E.; Kehtari, M.; Hanaee-Ahvaz, H.; Ghanbarian, H.; Bandehpour, M.; Nojehdehi, S.; Mirzaei, S.; Kazemi, B. The effect of nanofibre-based polyethersulfone (PES) scaffold on the chondrogenesis of human induced pluripotent stem cells. *Artif. Cells Nanomed. Biotechnol.* **2018**, *46*, 1948–1956. [CrossRef]
97. Dudziński, K.; Chwojnowski, A.; Gutowska, M.; Płończak, M.; Czubak, J.; Łukowska, E.; Wojciechowski, C. Three dimensional polyethersulphone scaffold for chondrocytes cultivation—The future supportive material for articular cartilage regeneration. *Biocybern. Biomed. Eng.* **2010**, *30*, 65–76.
98. Płończak, M.; Czubak, J.; Hoser, G.; Chwojnowskl, A.; Kawiak, J.; Dudzińskp, K.; Czumińska, K. Repair of articular cartilage full thickness defects with cultured chondrocytes placed on polysulphonic membrane—Experimental studies in rabbits. *Biocybern. Biomed. Eng.* **2008**, *28*, 87–93.
99. Irfan, M.; Idris, A. Overview of PES biocompatible/hemodialysis membranes: PES-blood interactions and modification techniques. *Mater. Sci. Eng. C* **2015**, *56*, 574–592. [CrossRef]
100. Filimon, A.; Olaru, N.; Doroftei, F.; Logigan, C.; Dunca, S. Design of Biologically Active Surfaces Based on Functionalized Polysulfones by Electrospinning. *Proceedings* **2019**, *41*, 35. [CrossRef]
101. Filimon, A.; Avram, E.; Dunca, S. Surface and Interface Properties of Functionalized Polysulfones: Cell-Material Interaction and Antimicrobial Activity. *Polym. Eng. Sci.* **2015**, *55*, 2184–2894. [CrossRef]
102. Ye, H.; Zhang, K.; Kai, D.; Li, Z.; Loh, X.J. Polyester elastomers for soft tissue engineering. *Chem. Soc. Rev.* **2018**, *47*, 4545–4580. [CrossRef] [PubMed]

103. Puppi, D.; Chiellini, F.; Piras, A.M.; Chiellini, E. Progress in Polymer Science Polymeric materials for bone and cartilage repair. *Prog. Polym. Sci.* **2010**, *35*, 403–440. [CrossRef]
104. Chen, F.M.; Liu, X. Advancing biomaterials of human origin for tissue engineering. *Prog. Polym. Sci.* **2016**, *53*, 86–168. [CrossRef] [PubMed]
105. Janoušková, O. Synthetic Polymer Scaffolds for Soft Tissue Engineering. *Physiol. Res.* **2018**, *67*, S335–S348. [CrossRef]
106. He, Y.; Wang, W.R.; Ding, J.D. Effects of L-lactic acid and D,L-lactic acid on viability and osteogenic differentiation of mesenchymal stem cells. *Chin. Sci. Bull.* **2013**, *58*, 2404–2411. [CrossRef]
107. Xu, Y.; Kim, C.; Saylor, D.M.; Koo, D. Polymer degradation and drug delivery in PLGA-based drug—Polymer applications: A review of experiments and theories. *J. Biomed. Mater. Res. Part B Appl. Biomater.* **2016**, *105*, 1692–1716. [CrossRef]
108. Jiang, L.; Xu, L.; Ma, B.; Ding, H.; Tang, C. Effect of component and surface structure on poly (L-lactide-co-ε-caprolactone) (PLCA)-based composite membrane. *Compos. Part B* **2019**, *174*, 107031. [CrossRef]
109. Prasanna, S.; Narayan, B.; Rastogi, A.; Srivastava, P. Design and evaluation of chitosan/poly (L-lactide)/pectin based composite scaffolds for cartilage tissue regeneration. *Int. J. Biol. Macromol.* **2018**, *112*, 909–920. [CrossRef]
110. Nofar, M.; Sacligil, D.; Carreau, P.J.; Kamal, M.R.; Heuzey, M.C. Poly (lactic acid) blends: Processing, properties and applications. *Int. J. Biol. Macromol.* **2019**, *125*, 307–360. [CrossRef]
111. Jeuken, R.M.; Roth, A.K.; Peters, R.J.R.W.; van Donkelaar, C.C.; Thies, J.C.; van Rhijn, L.W.; Emans, P.J. Polymers in cartilage defect repair of the knee: Current status and future prospects. *Polymers* **2016**, *8*, 219. [CrossRef]
112. Daranarong, D.; Techaikool, P.; Intatue, W.; Daengngern, R.; Thomson, K.A.; Molloy, R.; Kungwan, N.; Foster, L.J.R.; Boonyawan, D.; Punyodom, W. Effect of surface modification of poly(L-lactide-co-ε-caprolactone) membranes by low-pressure plasma on support cell biocompatibility. *Surf. Coat. Technol.* **2016**, *306*, 328–335. [CrossRef]
113. Guo, C.; Cai, N.; Dong, Y. Duplex surface modification of porous poly (lactic acid) scaffold. *Mater. Lett.* **2013**, *94*, 11–14. [CrossRef]
114. Tsurumi, T.; Fuse, M. Enhancement of apatite precipitation on an alkaline hydrolyzed poly (lactic acid-ε-Caprolactone) film in simulated body fluid. *J. Hard Tissue Biol.* **2014**, *23*, 15–19. [CrossRef]
115. Setayeshmehr, M.; Esfandiari, E.; Rafieinia, M.; Hashemibeni, B.; Taheri-kafrani, A.; Samadikuchaksaraei, A. Hybrid and Composite Scaffolds Based on Extracellular. *Tissue Eng. Part B Rev.* **2019**, *25*, 202–224. [CrossRef]
116. Zhang, X.; Wu, Y.; Pan, Z.; Sun, H.; Wang, J.; Yu, D.; Zhu, S.; Dai, J.; Chen, Y.; Tian, N.; et al. The effects of lactate and acid on articular chondrocytes function: Implications for polymeric cartilage scaffold design. *Acta Biomater.* **2016**, *42*, 329–340. [CrossRef]
117. Lu, T.; Li, Y.; Chen, T. Techniques of fabrication and construction three-dimensional scaffold. *Int. J. Nanomed.* **2013**, *8*, 337–350. [CrossRef]
118. Dutta, R.C.; Dey, M.; Dutta, A.K.; Basu, B. Competent processing techniques for scaffolds in tissue engineering. *Biotechnol. Adv.* **2017**, *35*, 240–250. [CrossRef]
119. Mannella, G.A.; Conoscenti, G.; Pavia, F.C.; Carrubba, V.L.; Brucato, V. Preparation of polymeric foams with a pore size gradient via Thermally Induced Phase Separation (TIPS). *Mater. Lett.* **2015**, *160*, 31–33. [CrossRef]
120. Buzarovska, A.; Gualandi, C.; Parrilli, A.; Scandola, M. Effect of TiO_2 nanoparticle loading on Poly(L-lactic acid) porous scaffolds fabricated by TIPS. *Compos. Part B* **2015**. [CrossRef]
121. Sultana, N.; Hassana, M.I.; Ridzuana, N.; Ibrahima, Z.; Soonc, C.F. Fabrication of Gelatin Scaffolds using Thermally Induced Phase Separation Technique. *Int. J. Eng.* **2018**, *31*, 1302–1307. [CrossRef]
122. Structure, M.M.; Mechanical, H.; Kim, J.; Shin, K.; Koh, Y.; Hah, M.J.; Moon, J.; Kim, H. Production of Poly(ε-Caprolactone)/Hydroxyapatite Composite Scaffolds with a Tailored Macro/Micro-Porous Structure, High Mechanical Properties, and Excellent Bioactivity. *Materials* **2017**, *10*, 1123. [CrossRef]
123. Georgiadou, S.; Katsogiannis, K.A.G.; Vladisavljevic, G.T. Porous electrospun polycaprolactone (PCL) fibres by phase separation. *Eur. Polym. J.* **2015**, *69*, 284–295. [CrossRef]
124. Huang, C.; Thomas, N.L. Fabricating Porous Poly(lactic acid) Fibres via Electrospinning. *Eur. Polym. J.* **2017**. [CrossRef]

125. Prasad, A.; Sankar, M.R.; Katiyar, V. ScienceDirect State of Art on Solvent Casting Particulate Leaching Method for Orthopedic Scaffolds Fabrication. *Mater. Today Proc.* **2017**, *4*, 898–907. [CrossRef]
126. Plisko, T.V.; Penkova, A.V.; Burts, K.S.; Bildyukevich, A.V.; Dmitrenko, M.E.; Melnikova, G.B.; Atta, R.R.; Mazur, A.S.; Zolotarev, A.A.; Missyul, A.B. Effect of Pluronic F127 on porous and dense membrane structure formation via non-solvent induced and evaporation induced phase separation. *J. Membr. Sci.* **2019**, *580*, 336–349. [CrossRef]
127. Gadomska-Gajadhur, A.; Kruk, A.; Ruśkowski, P.; Sajkiewicz, P.; Dulnik, J.; Chwojnowski, A. Original method of imprinting pores in scaffolds for tissue engineering. *Polym. Adv. Technol.* **2020**, 1–13. [CrossRef]
128. Taylor, P.; Yang, Q.; Chen, L.; Shen, X.; Tan, Z. Preparation of Polycaprolactone Tissue Engineering Scaffolds by Improved Solvent Casting/Particulate Leaching Method Preparation of Polycaprolactone Tissue Engineering Scaffolds by Improved Solvent Casting/Particulate Leachin. *J. Macromol. Sci. Part B Phys.* **2006**, *45*, 1171–1181. [CrossRef]
129. Sharifi, F.; Irani, S.; Azadegan, G.; Pezeshki-Modaress, M. Bioactive Carbohydrates and Dietary Fibre Co-electrospun gelatin-chondroitin sulfate/polycaprolactone nanofibrous scaffolds for cartilage tissue engineering. *Bioact. Carbohydr. Diet. Fibre* **2020**, *22*, 100215. [CrossRef]
130. Zhou, Y.; Chyu, J.; Zumwalt, M. Recent Progress of Fabrication of Cell Scaffold by Electrospinning Technique for Articular Cartilage Tissue Engineering. *Int. J. Biomater.* **2018**, *2018*. [CrossRef]
131. Girão, A.F.; Semitela, Â.; Ramalho, G.; Completo, A.; Marques, P.A.A.P. Mimicking nature- Fabrication of 3D anisotropic electrospun polycaprolactone scaffolds for cartilage tissue engineering applications. *Compos. Part B* **2018**. [CrossRef]
132. Bdikin, I.; Marques, P.A.A.P. Electrospinning of bioactive polycaprolactone-gelatin nanofibres with increased pore size for cartilage tissue engineering applications. *J. Biomater. Appl.* **2020**, *35*, 459–470. [CrossRef]
133. Wang, Z.; Wan, L.; Liu, Z.; Huang, X.; Xu, Z. Enzymatic Enzyme immobilization on electrospun polymer nanofibers: An overview. *J. Mol. Catal. B* **2009**, *56*, 189–195. [CrossRef]
134. Yang, Z.; Si, J.; Cui, Z.; Ye, J.; Wang, X.; Wang, Q.; Peng, K.; Chen, W.; Chen, S. Biomimetic composite scaffolds based on surface modification of polydopamine on electrospun poly (lactic acid)/cellulose nanofibrils. *Carbohydr. Polym.* **2017**, *174*, 750–759. [CrossRef] [PubMed]
135. Canton, T.T.; Kunert, L.R.; Suellen, B.; Ana, I.; Serafini, P. Nonwoven membranes for tissue engineering: An overview of cartilage, Nonwoven membranes for tissue engineering: An overview of cartilage, epithelium, and bone regeneration. *J. Biomater. Sci. Polym. Ed.* **2019**, *30*, 1026–1049. [CrossRef]
136. Abdelaal, O.A.M.; Darwish, S.M.H. Review of Rapid Prototyping Techniques for Tissue Engineering Scaffolds Fabrication. In *Characterization and Development of Biosystems and Biomaterials*; Springer: Berlin/Heidelberg, Germany, 2013; Volume 29, pp. 33–54. [CrossRef]
137. Li, K.; Wang, D.; Zhao, K.; Song, K.; Liang, J. Electrohydrodynamic jet 3D printing of PCL/PVP composite scaffold for cell culture. *Talanta* **2020**, 120750. [CrossRef]
138. Daly, A.C.; Freeman, F.E.; Gonzalez-Fernandez, T.; Critchley, S.E.; Nulty, J.; Kelly, D.J. 3D Bioprinting for Cartilage and Osteochondral Tissue Engineering. *Adv. Healthc. Mater.* **2017**, *6*, 1700298. [CrossRef]
139. Seung, J.; Sang, H.; Jung, H.; Lee, H.; Hong, H.; Jin, Y.; Ji, Y.; Joo, O.; Hee, S.; Hum, C. 3D-printable photocurable bioink for cartilage regeneration of tonsil-derived mesenchymal stem cells. *Addit. Manuf.* **2020**, *33*, 101136. [CrossRef]
140. Marycz, K.; Smieszek, A.; Targonska, S.; Walsh, A.; Szustakiewicz, K.; Wiglusz, R.J. Three dimensional (3D) printed PLA with nano-hydroxyapatite doped with europium(III) ions (nHAp-PLLA@Eu3+) composite for osteochondral defect regeneration and theranostics. *Mater. Sci. Eng. C* **2020**, 110634. [CrossRef]
141. Wu, J.; Yang, R.; Zheng, J.; Pan, L.; Liu, X. Fabrication and improvement of PCL/alginate/PAAm scaffold via selective laser sintering for tissue engineering. *Micro Nano Lett.* **2019**, *14*, 852–855. [CrossRef]
142. Aisenbrey, E.A.; Tomaschke, A.; Kleinjan, E.; Muralidharan, A.; Pascual-Garrido, C.; Mcleod, R.R.; Ferguson, V.L.; Bryant, S.J. A Stereolithography-Based 3D Printed Hybrid Scaffold for In Situ Cartilage Defect Repair. *Macromol. Biosci.* **2017**, *18*, 1–8. [CrossRef]
143. Gauvin, R.; Chen, Y.; Woo, J.; Soman, P.; Zorlutuna, P.; Nichol, J.W.; Bae, H.; Chen, S.; Khademhosseini, A. Biomaterials Microfabrication of complex porous tissue engineering scaffolds using 3D projection stereolithography. *Biomaterials* **2012**, *33*, 3824–3834. [CrossRef] [PubMed]
144. Chartrain, N.A.; Williams, C.B.; Whittington, A.R. A review on fabricating tissue scaffolds using vat photopolymerization. *Acta Biomater.* **2018**, *74*, 90–111. [CrossRef] [PubMed]

145. Longley, R.; Ferreira, A.M.; Gentile, P. Recent Approaches to the Manufacturing of Biomimetic Multi-Phasic Scaffolds for Osteochondral Regeneration. *Int. J. Mol. Sci.* **2018**, *19*, 1755. [CrossRef] [PubMed]
146. Mohanty, A.K. Improving the Impact Strength and Heat Resistance of 3D Printed Models: Structure, Property, and Processing Correlationships during Fused Deposition Modeling (FDM) of Poly(Lactic Acid). *ACS Omega* **2018**. [CrossRef]
147. Murphy, S.V.; Atala, A. 3D bioprinting of tissues and organs. *Nat. Biotechnol.* **2014**, *32*, 773–785. [CrossRef]
148. Cheng, A.; Schwartz, Z.; Kahn, A.; Li, X.; Shao, Z.; Sun, M.; Ao, Y.; Boyan, B.D.; Chen, H.; Antonio, S.; et al. Advances in Porous Scaffold Design for Bone and Cartilage Tissue Engineering and Regeneration. *Tissue Eng. Part B Rev.* **2018**, *25*, 14–29. [CrossRef]
149. Chen, W.; Xu, Y.; Liu, Y.; Wang, Z.; Li, Y.; Jiang, G.; Mo, X.; Zhou, G. Three-dimensional printed electrospun fi ber-based scaffold for cartilage regeneration. *Mater. Des.* **2019**, *179*, 107886. [CrossRef]
150. Garrigues, N.W.; Little, D.; Sanchez-Adams, J.; Ruch, D.S.; Guilak, F. Electrospun cartilage-derived matrix scaffolds for cartilage tissue engineering. *J. Biomed. Mater. Res. Part A* **2014**, *59784*, 28–30. [CrossRef]
151. Xu, T.; Binder, K.W.; Albanna, M.Z.; Dice, D.; Zhao, W.; Yoo, J.J.; Atala, A. Hybrid printing of mechanically and biologically improved constructs for cartilage tissue engineering applications. *Biofabrication* **2013**, *5*, 1–11. [CrossRef]
152. Nielsen, L.E. Polymer Reviews Cross-Linking—Effect on Physical Properties of Polymers. *J. Macromol. Sci. Part C* **2008**, *3*, 69–103. [CrossRef]
153. Rofiqoh, N.; Putri, E.; Wang, X.; Chen, Y.; Li, X.; Kawazoe, N.; Chen, G. Preparation of PLGA-collagen hybrid scaffolds with controlled pore structures for cartilage tissue engineering. *Prog. Nat. Sci. Mater. Int.* **2020**. [CrossRef]
154. Laurent, P. Suitability of a PLCL fibrous scaffold for soft tissue engineering applications: A combined biological and mechanical characterisation. *J. Biomater. Appl.* **2018**, *32*, 1–13. [CrossRef] [PubMed]
155. Ahmed, E.M. Hydrogel: Preparation, characterization, and applications: A review. *J. Adv. Res.* **2015**, *6*, 105–121. [CrossRef] [PubMed]
156. Bistolfi, A.; Ferracini, R.; Galletta, C.; Tosto, F.; Sgarminato, V.; Digo, E.; Vernè, E.; Massè, A. Regeneration of articular cartilage: Scaffold used in orthopedic surgery. A short handbook of available products for regenerative joints surgery. *Clin. Sci. Res. Rep.* **2017**, *1*, 1–7. [CrossRef]
157. Müller, S. Repair of Focal Cartilage Defects With Scaffold-Assisted Autologous Chondrocyte Grafts. *Am. J. Sports Med.* **2011**, *39*, 1697–1705. [CrossRef]
158. Tsai, M.; Hung, K.; Hung, S.; Hsu, S. Evaluation of biodegradable elastic scaffolds made of anionic polyurethane for cartilage tissue engineering. *Colloids Surf. B Biointerfaces* **2015**, *125*, 34–44. [CrossRef]
159. Borsøe, B.; Casper, C.; Foldager, B.; Møller, O.; Lind, M. A novel nano-structured porous polycaprolactone scaffold improves hyaline cartilage repair in a rabbit model compared to a collagen type I/III scaffold: In vitro and in vivo studies. *Knee Surg. Sports Traumatol. Arthrosc.* **2012**, *20*, 1192–1204. [CrossRef]
160. Theodoridis, K.; Aggelidou, E.; Vavilis, T.; Manthou, M.E.; Tsimponis, A.; Demiri, E.C.; Boukla, A.; Salpistis, C. Hyaline cartilage next generation implants from adipose—Tissue—Derived mesenchymal stem cells: Comparative study on 3D—Printed polycaprolactone scaffold patterns. *J. Tissue Eng. Regen. Med.* **2019**, 342–355. [CrossRef]
161. Płończak, M.; Czubak, J. Culture of Human Autologous Chondrocytes on Polysulphonic Membrane—Preliminary Studies. *Biocybern. Biomed. Eng.* **2012**, *32*, 63–67. [CrossRef]
162. Płończak, M. The Value of Autogenous Cartilage Cell Transplants in the Experimental Treatment of Articular Cartilage Defects in Rabbits. Ph.D. Thesis, Medical Centre of Postgraduate Education in Warsaw, Warsaw, Poland, 28 May 2008.
163. Taylor, P.; Jung, Y.; Kim, S.H.; You, H.J. Application of an elastic biodegradable poly (L-lactide-co-ε-caprolactone) scaffold for cartilage tissue regeneration. *J. Biomater. Sci. Polym. Ed.* **2012**, 1073–1085. [CrossRef]
164. Siclari, A.; Mascaro, G.; Kaps, C.; Boux, E. A 5-Year Follow-Up After Cartilage Repair in the Knee Using a Platelet—Rich Plasma-Immersed Polymer-Based Implant. *Open Orthop. J.* **2014**, *8*, 346–354. [CrossRef] [PubMed]
165. Asadi, N.; Alizadeh, E.; Rahmani, A.; Bakhshayesh, D.; Mostafavi, E.; Akbarzadeh, A.; Davaran, S. Fabrication and in Vitro Evaluation of Nanocomposite Hydrogel Sca ff olds Based on Gelatin/PCL—PEG—PCL for Cartilage Tissue Engineering. *ACS Omega* **2019**, *4*, 449–457. [CrossRef]

166. He, Y.; Liu, W.; Guan, L.; Chen, J.; Duan, L.; Jia, Z.; Huang, J.; Li, W.; Liu, J.; Xiong, J.; et al. A 3D-Printed PLCL Scaffold Coated with Collagen Type I and Its Biocompatibility. *Biomed Res. Int.* **2018**, *2018*, 1–10. [CrossRef] [PubMed]
167. Haaparanta, A.; Ja, E.; Fatih, I.; Ville, C.; Kiviranta, I.; Kelloma, M. Preparation and characterization of collagen/PLA, chitosan/PLA, and collagen/chitosan/PLA hybrid scaffolds for cartilage tissue engineering. *J. Mater. Sci. Mater. Med.* **2014**, *25*, 1129–1136. [CrossRef] [PubMed]
168. Nogami, M.; Kimura, T.; Seki, S.; Matsui, Y.; Yoshida, T.; Koike-Soko, C.; Okabe, M.; Motomura, H.; Gejo, R.; Nikaido, T. A human amnion derived extracellular matrix coated cell free scaffold for cartilage repair: In vitro and in vivo studies. *Tissue Eng. Part A* **2016**, *22*, 680–688. [CrossRef] [PubMed]
169. Yamanaka, K.; Yamamoto, K.; Sakai, Y.; Suda, Y.; Shigemitsu, Y. Seeding of mesenchymal stem cells into inner part of interconnected porous biodegradable scaffold by a new method with a filter paper. *Dent. Mater. J.* **2015**, *34*, 78–85. [CrossRef] [PubMed]
170. Chen, C.; Shyu, V.B.; Chen, J.; Lee, M. Selective laser sintered poly-ε-caprolactone scaffold hybridized with collagen hydrogel for cartilage tissue engineering. *Biofabrication* **2014**, 015004. [CrossRef]
171. Taylor, P.; Li, C.; Wang, L.; Yang, Z.; Kim, G. A Viscoelastic Chitosan-Modified Three-Dimensional Porous Poly (L-Scaffold for Cartilage Tissue Engineering. *Biomater. Sci.* **2012**, 405–424. [CrossRef]
172. Liao, J.; Qu, Y.; Chu, B.; Zhang, X.; Qian, Z. Biodegradable CSMA/PECA/Graphene Porous Hybrid Scaffold for Cartilage Tissue Engineering. *Sci. Rep.* **2015**, *5*, 9879. [CrossRef]
173. Urbanek, O.; Kołbuk, D.; Wróbel, M. International Journal of Polymeric Materials and Articular cartilage: New directions and barriers of scaffolds development—Review. *Int. J. Polym. Mater. Polym. Biomater.* **2018**, 1–15. [CrossRef]
174. Tan, S.I.; Jun, S.; Tho, W.; Tho, K.S. Biological resurfacing of grade IV articular cartilage ulcers in knee joint with Hyalofast. *J. Orthop. Surg.* **2020**, *28*, 1–7. [CrossRef] [PubMed]
175. Sofu, H.; Camurcu, Y.; Ucpunar, H.; Ozcan, S.; Yurten, H.; Sahin, V. Clinical and radiographic outcomes of chitosan-glycerol phosphate / blood implant are similar with hyaluronic acid-based cell-free scaffold in the treatment of focal osteochondral lesions of the knee joint. *Knee Surg. Sports Traumatol. Arthrosc.* **2019**, *27*, 773–781. [CrossRef] [PubMed]
176. Park, Y.B.; Ha, C.W.; Lee, C.H.; Yoon, Y.C.; Park, Y.G. Cartilage Regeneration in Osteoarthritic Patients by a Composite of Allogeneic Umbilical Cord Blood-Derived Mesenchymal Stem Cells and Hyaluronate Hydrogel: Results from Trial for Safety and Results From a a Clinical Clinical Trial for Safety and Concept. *Stem Cells Transl. Med.* **2017**, *6*, 613–621.
177. Negoro, T.; Takagaki, Y.; Okura, H.; Matsuyama, A. Trends in clinical trials for articular cartilage repair by cell therapy. *NPJ Regen. Med.* **2018**. [CrossRef]
178. Hoffman, A.S. Hydrogels for biomedical applications. *Adv. Drug Deliv. Rev.* **2012**, *64*, 18–23. [CrossRef]
179. Ren, K.; He, C.; Xiao, C.; Li, G.; Chen, X. Injectable glycopolypeptide hydrogels as biomimetic scaffolds for cartilage tissue engineering. *Biomaterials* **2015**, *51*, 238–249. [CrossRef]
180. Yang, F.; Zhao, J.; Koshut, W.J.; Watt, J.; Riboh, J.C.; Gall, K.; Wiley, B.J. A Synthetic Hydrogel Composite with the Mechanical Behavior and Durability of Cartilage. *Adv. Funct. Mater.* **2020**, *30*, 1–8. [CrossRef]
181. Rosenzweig, D.H.; Carelli, E.; Steffen, T.; Jarzem, P.; Haglund, L. 3D-printed ABS and PLA scaffolds for cartilage and nucleus pulposustissue regeneration. *Int. J. Mol. Sci.* **2015**, *16*, 15118–15135. [CrossRef]
182. Cristian, M.; Conde, M.; Demarco, F.F.; Alcazar, J.C.; Nör, J.E.; Beatriz, S. Influence of Poly-L-Lactic Acid Scaffold ' s Pore Size on the Proliferation and Differentiation of Dental Pulp Stem Cells. *Braz. Dent. J.* **2015**, *26*, 93–98.
183. Oh, S.H.; Kim, T.H.; Im, G.I.; Lee, J.H. Investigation of pore size effect on chondrogenic differentiation of adipose stem cells using a pore size gradient scaffold. *Biomacromolecules* **2010**, *11*, 1948–1955. [CrossRef]
184. Moura, C.S.; Silva, J.C.; Fernandes, P.R.; Lobato, C.; Manuel, J.; Cabral, S.; Linhardt, R.; Bártolo, P.J.; Ferreira, F.C. Chondrogenic differentiation of mesenchymal stem/stromal cells on 3D porous poly (ε-caprolactone) scaffolds: Effects of material alkaline treatment and chondroitin sulfate supplementation. *J. Biosci. Bioeng.* **2020**, *129*, 756–764. [CrossRef] [PubMed]
185. Sonomoto, K.; Yamaoka, K.; Kaneko, H.; Yamagata, K. Spontaneous Differentiation of Human Mesenchymal Stem Cells on Poly-Lactic-Co-Glycolic Acid Nano-Fiber Scaffold. *PLoS ONE* **2016**, *11*, e0153231. [CrossRef] [PubMed]

186. He, A.; Liu, L.; Luo, X.; Liu, Y.; Liu, Y.; Liu, F.; Wang, X. Repair of osteochondral defects with in vitro engineered cartilage based on autologous bone marrow stromal cells in a swine model. *Sci. Rep.* **2017**, 1–12. [CrossRef]
187. Zhang, Y.; Yang, F.; Liu, K.; Shen, H.; Zhu, Y.; Zhang, W.; Liu, W.; Wang, S.; Cao, Y.; Zhou, G. The impact of PLGA scaffold orientation on in vitro cartilage regeneration. *Biomaterials* **2012**, *33*, 2926–2935. [CrossRef] [PubMed]
188. Duan, P.; Pan, Z.; Cao, L.; He, Y.; Wang, H.; Qu, Z.; Dong, J. The effects of pore size in bilayered poly (lactide-co -glycolide) scaffolds on restoring osteochondral defects in rabbits. *J. Biomed. Mater. Res. Part A Off. J. Soc. Biomater. Jpn. Soc. Biomater. Aust. Soc. Biomater. Korean Soc. Biomater.* **2013**, *102*, 180–192. [CrossRef] [PubMed]
189. Jonnalagadda, J.B.; Rivero, I.V.; Dertien, J.S. In vitro chondrocyte behavior on porous biodegradable poly (e-caprolactone)/polyglycolic acid scaffolds for articular chondrocyte adhesion and proliferation. *J. Biomater. Sci.* **2015**, 37–41. [CrossRef]
190. Safinsha, S.; Ali, M.M. Composite scaffolds in tissue engineering. *Mater. Today Proc.* **2020**, *24*, 2318–2329. [CrossRef]
191. Li, L.; Li, J.; Guo, J.; Zhang, H.; Zhang, X.; Yin, C. 3D Molecularly Functionalized Cell-Free Biomimetic Scaffolds for Osteochondral Regeneration. *Adv. Funct. Mater.* **2019**, *29*, 1807356. [CrossRef]
192. Setayeshmehr, M.; Esfandiari, E.; Hashemibeni, B.; Hossein, A. Chondrogenesis of human adipose-derived mesenchymal stromal cells on the [devitalized costal cartilage matrix/poly (vinyl alcohol)/fi brin] hybrid scaffolds. *Eur. Polym. J.* **2019**, *118*, 528–541. [CrossRef]
193. Tavakoli, E.; Mehdikhani-Nahrkhalaji, M.; Hashemi-Beni, B.; Zargar-Kharazi, A. Preparation, Characterization and Mechanical Assessment of Poly (Lactide-Co-Glycolide)/Hyaluronic Acid/Fibrin/Bioactive Glass Nano-Composite Scaffolds for Cartilage Tissue Engineering Applications. *Procedia Mater. Sci.* **2015**, *11*, 124–130. [CrossRef]
194. Mintz, B.R.; Cooper, A.C., Jr. Hybrid hyaluronic acid hydrogel/poly (e-caprolactone) scaffold provides mechanically favorable platform for cartilage tissue engineering studies. *J. Biomed. Mater. Res. Part A* **2013**, *102*, 2918–2926. [CrossRef] [PubMed]
195. He, X.; Fu, W.; Feng, B.; Wang, H.; Liu, Z.; Yin, M.; Wang, W. Electrospun collagen—poly (l-lactic acid-co-e-caprolactone) membranes for cartilage tissue engineering. *Regen. Med.* **2013**, *8*, 425–436. [CrossRef] [PubMed]
196. Paatela, T.; Meller, A.; Muhonen, V.; Salonius, E.; Haaparanta, A.; Elina, J. Articular Cartilage Repair With Recombinant Human Type II Collagen/Polylactide Scaffold in a Preliminary Porcine Study. *J. Orthop. Res.* **2016**, *34*, 745–753. [CrossRef]
197. Levorson, E.J.; Hu, O.; Mountziaris, P.M.; Kasper, F.K.; Mikos, A.G. Cell Derived Polymer / Extracellular Matrix Composite Scaffolds for Cartilage Regeneration, Part 2: Construct Devitalization and Determination of Chondroinductive Capacity. *Tissue Eng. Part C Methods* **2014**, *20*, 358–372. [CrossRef] [PubMed]

PUBLIKACJA 2

Polyester membranes as 3D scaffolds for cell culture

Monika Wasyłeczko, Wioleta Sikorska,
Małgorzata Przytulska, Judyta Dulnik,
Andrzej Chwojnowski.
Desalination and Water Treatment **2021**, 214, 181-193.
https://doi.org/10.5004/dwt.2021.26658
IF: 1,383
MNiSW: 100

Desalination and Water Treatment
www.deswater.com

doi: 10.5004/dwt.2021.26658

214 (2021) 181–193
February

Polyester membranes as 3D scaffolds for cell culture

Monika Wasyłeczko[a,*], Wioleta Sikorska[a], Małgorzata Przytulska[a], Judyta Dulnik[b], Andrzej Chwojnowski[a]

[a]*Department of Biomaterials and Biotechnological Systems, Nałęcz Institute of Biocybernetics and Biomedical Engineering, Polish Academy of Sciences, Trojdena 4 str., 02-109 Warsaw, Poland, emails: mwasyleczko@ibib.waw.pl (M. Wasyłeczko), wsikorska@ibib.waw.pl (W. Sikorska), mprzytulska@ibib.waw.pl (M. Przytulska), achwojnowski@ibib.waw.pl (A. Chwojnowski)*
[b]*Laboratory of Polymers and Biomaterials, Institute of Fundamental Technological Research, Polish Academy of Sciences, Pawińskiego 5B str., 02-106 Warsaw, Poland, email: jdulnik@ippt.pan.pl*

Received 9 April 2020; Accepted 25 May 2020

ABSTRACT

The study presents two types of three-dimensional membranes made of the biodegradable copolymer. They were obtained by the wet-phase inversion method using different solvent and pore precursors. In one case, a nonwoven made of gelatin and polyvinylpyrrolidone (PVP) as precursors of macropores and small pores, respectively, were used. In the second case, PVP nonwovens and Pluronic were used properly for macro- and micro-pores. As the material, a biodegradable poly(L-lactide-co-ε-caprolactone) is composed of 30% ε-caprolactone and 70% poly(L-lactic acid) was used. Depending on the pore precursors, different membrane structures were obtained. The morphology of pores was studied using the MeMoExplorer™, an advanced software designed for computer analysis of the scanning electron microscopy images. The scaffolds were degraded in phosphate-buffered saline and Hank's balanced salt solutions at 37°C. Moreover, the porosity of the membranes before and after hydrolysis was calculated.

Keywords: 3D scaffolds; Poly(L-lactide-co-ε-caprolactone); Porosity of membrane; Phase inversion method; Degradation of scaffolds

1. Introduction

Semipermeable membranes are used in various areas of technology like chemical (including petrochemical), food and drink industry, water purification, pharmaceutical, and biomedical application including tissue engineering [1–10]. Tissue engineering as a scientific discipline proposes new alternatives for the treatment by transplantation of biological material that would replace, maintain, or restore function to damaged tissues or whole organs [11,12]. Depending on the application, the membrane should have appropriate properties such as biocompatibility, morphology, mechanical properties, non-toxicity, and even bioresorbability. For the tissue regeneration process, it is necessary to obtain appropriate porous scaffolds as a support for cells during *in vitro* culture with various growth factors. The use of spatial structures determines the functioning of cells and facilitates obtaining the desired tissue [13–17].

One of the most important parameters of the scaffolds for cell culture is morphology and more precisely – porosity. The size and number of pores have a huge impact on cell penetration into the membrane, their migration, proliferation, production of extracellular matrix (ECM), as well as diffusion of nutrients, oxygen, and removal of metabolites outside the scaffold [14,18,19]. To obtain the adequate pore size, the pore precursors such as salts [20], polymers [21,22–24], and nonwovens [25,26] are used. The size of the pore is properly defined by the purpose of the research,

* Corresponding author.

among other for which kind of cells they will be intended [14,16,18]. For example, working with chondrocytes requires smaller pores than working with stem cells for chondrogenesis [25,27,28]. It will be different from hepatocytes [29] or with osteoblasts [28,30]. Moreover, to obtain adequate morphology of the membranes the various methods are used, such as 3D print, phase separation, gas foaming, particulate leaching, selective laser sintering, electrospinning, or freeze-drying [13,18,26,27,31,32].

Further important parameter during the production of scaffolds is material. It should be characterized by biocompatibility, appropriate strength properties (modulus of elasticity, compressive, and tensile strength, stiffness, etc.), biodegradability (the speed must be carefully selected for the formation of a new tissue structure), or bioresorbability. The degradation products should not be toxic to the body and need to be excreted from the body. The most commonly biomaterials used for scaffolds are natural and synthetic polymers, or their combination. Examples of natural materials for scaffolds are gelatine, chitosan, alginate, and hyaluronic acid. They are characterized by high biocompatibility and biodegradability but their drawback is among other solubility in an aquatic environment and not enough mechanical strength [15,19,33–35]. The most common synthetic materials are the aliphatic polyesters: polylactide (PLA), polycaprolactone (PCL), polyglycolide (PGA), or their copolymers like poly(L-lactide-co-ε-caprolactone) (PLCA). Polyesters are biocompatible polymers with good mechanical strength which degrade to non-toxic products that are easily removed from the organism [15,33,35–38].

The article presents the formation of biocompatible, semipermeable, three-dimensional scaffolds of degradable co-polyester PLCA. Depending on the micro-, macropores precursors used a different membranes morphology was obtained. Structure analysis was performed by using scanning electron microscopy (SEM). The porosity assessment was made by a computer program, the MeMoExplorer™ used to analyzing SEM images. The usage and description of the program have been presented in previous works [39–41]. Furthermore, the degradation assessment of the scaffolds was performed in simulated physiological conditions using phosphate-buffered saline (PBS) and Hank's balanced salt solution (HBSS) at 37°C. Weight loss, pH of media, and SEM of samples were used to monitor the degradations.

Such membranes can be used in tissue engineering, in which scientists are still looking for new scaffolds for cell culture.

2. Experimental

2.1. Materials

Copolymer of L-lactide and ε-caprolactone in a 70/30 molar ratio was purchased from Corbion. Polyvinylpyrrolidone (PVP) 10 kDa, phosphate buffer solution (PBS), Pluronic® F127, sodium bicarbonate, sodium azide (NaN_3), sodium chloride, potassium chloride, phenol red, monopotassium phosphate (KH_2PO_4), D-glucose, disodium phosphate, magnesium sulfate, and calcium chloride were purchased from Sigma-Aldrich. 1,4-Dioxane,chloroform were procured from POCh SA. Methanol and ethanol were purchased from Linegal Chemicals. The pork gelatin and PVP nonwovens (Fig. 1) were obtained by an electrospinning method in the Institute of Fundamental Technological Research PAS.

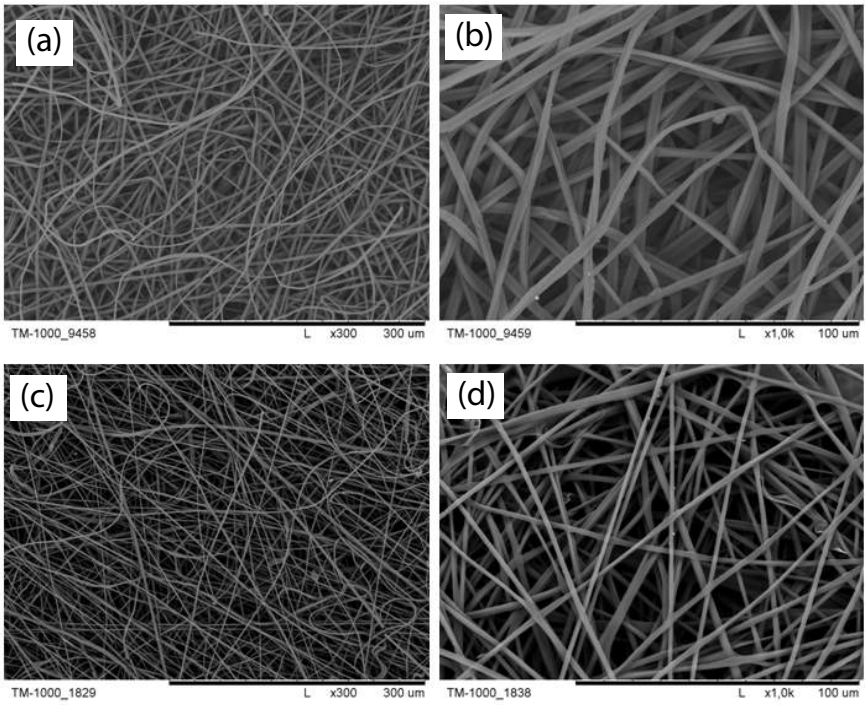

Fig. 1. Photomicrographs of pork gelatin (a and b) and PVP nonwovens (c and d) obtained by an electrospinning method. Magnification 300× (a and c) and 1,000× (b and d).

The deionized water (18.2 MΩ cm conductivity) was obtained using Mili-Q apparatus (Milipore).

2.2. Preparation of scaffold using PVP nonwoven (PLCA1)

The PLCA and pluronic polymers were dissolved in dioxane with constant stirring to obtain 10 wt.% concentration with 4:1 ratio of PLCA:Pluronic. A polymer mixture was poured onto the cooled glass base (4°C) and its thickness was set to 2 nm, after which the PVP layer was laid. Then another portion of polymers was poured to saturate the nonwoven, again a second slice of nonwoven and third layer of membrane forming solution were added. All layers were pressed and the air was removed using a Teflon roller. Received membrane was gelled in a bath with deionized water with ice (about 4°C). The prepared membranes were stored in 70% ethanol. It is important to protect the PVP nonwoven from water to prevent its dissolving.

2.3. Preparation of scaffold using gelatin nonwoven (PLCA2)

The PLCA and PVP polymers were dissolved in chloroform with constant stirring to obtain 10 wt.% concentration with 4:1 ratio of PLCA:PVP. The scaffold was made analogous to PLCA1 preparation. The only difference was that the gelation bath contained cooled methanol at 4°C and the obtained membrane was treated with warm water (50°C) to removed gelatin nonwoven. Similarly to PLCA1 scaffold, the prepared membranes were stored in 70% ethanol and the gelatin nonwoven need to be protected from water.

2.4. SEM observation

Morphology of top and bottom layers, and cross-section of scaffolds before and after hydrolysis were examined using a SEM (Hitachi TM – 1000) with an accelerator voltage of 15 kV. The samples were immersed into the ethanol for at least 15 min and then they were removed and put into liquid nitrogen in order to fracture them into pieces. Afterwards, the samples were dried and coated with a 7 nm layer of gold using a sputter coater (EMITECH K550X).

2.5. Estimate of pores in scaffolds by computer analysis of SEM images

For the analysis, the thirty SEM photomicrographs of cross-section and top layer of both scaffolds, before and after hydrolysis, were taken according to the description in section 2.4 (SEM observation). SEM images were taken with the same size (1,280 × 950 = 1,216,000 px = 182,681 μm^2, 100 μm = 258 pixels) with microscope magnification of ×300. Then they were analyzed by the MeMoExplorer software which involved selection and contouring of pores, measurement of their surfaces, partition of pores into various size, classes, and measurement of total areas (porosity coefficients) covered by pores of given classes. The received data can be processed statistically to obtaining parameters like average (Ave), standard deviation (SD), and instability coefficients (SD/Ave). That can be done by using a suitable software like Microsoft Excel.

2.6. Degradation of scaffolds at simulated physiological condition

The degradation of the scaffolds was performed in simulated physiological condition using PBS and HBSS. Both liquids were prepared in the laboratory. The PBS was prepared by dissolving the tablets in deionized water, while HBSS was prepared according to the method given in literature [42]. The scaffolds were cut into rectangles, which were measured (length, width, and thickness) using caliper and SEM tools and weighed by electronic balance (MATTLER TOLEDO KA-52c). The shape of membranes was different due to their specific structure and incapability to cut them out of a similar size. The weight of each sample was about 0.014 g. Samples of scaffolds (n = 6) were immersed into small, plastic cubs filled with 40 mL of PBS at pH 7.26 and HBSS at pH 7.78 (it was increased after the addition of sodium azide – bacteriostatic agent) for five (PLCA1) and four (PLCA2) weeks at 37°C. The time for PLCA2 has been shortened due to its rapid hydrolysis. Every week specimens were washed in deionized water, dried, weighed, and the pH-values of PBS and HBSS were monitored using an electrolyte-type pH meter (METTLER TOLEDO MP225). The mass loss was calculated from the following equation [43]:

$$\text{Weight loss} = \frac{\left(M_0 - M_t\right)}{M_0} \times 100\% \quad (1)$$

where M_0 and M_t with subscript 0 and t are masses at the immersion time of 0 and t, respectively. All the values presented were the average of six samples.

2.7. Porosity of scaffolds

The porosity of the scaffolds was determined by measuring the mass and dimensions of the scaffolds before and after hydrolysis, as described by Ho and Hutmacher [44]. It was calculated with the following formula:

$$\text{Porosity} = \frac{D_p - D_{\text{ap}}}{D_p} \times 100\% \quad (2)$$

where D_p is the density of PLCA (1.621 g/cm^3), D_{ap} is the apparent density (scaffold mass/apparent scaffold cube volume). The calculations were carried out in 10 repetitions for both scaffolds before hydrolysis and five repetitions after hydrolysis.

All data were expressed as average (Ave) ± standard deviation (SD).

3. Results and discussion

The main aim in preparation of scaffolds for cell culture is to use appropriate biocompatible material and obtain an adequate three-dimensional network of interconnected macropores. The top layer of scaffolds need to be perforated to enable cells to enter the membrane and the bottom surface should be dense to prevent them from leaving the membrane. Moreover, membrane (including the inner pore walls) need to be semipermeable which is obtained

by using micropores precursor like PVP or Pluronic. Small pores are necessary for migration of nutrients, oxygen, or metabolites.

3.1. Characterization of PLCA1 and PLCA2 scaffolds

Advantage of nonwovens used as non-classical pore precursors, is that they are located during preparation in the whole volume of the membrane-forming solution, which guarantees even distribution of macropores, throughout the scaffold. Depending on the pore precursors used, different size of pores were obtained.

The SEM micrographs of PLCA1 scaffold present an irregular structure with macropores, obtained using PVP nonwovens (Fig. 2). The perforation gaps of PLCA1 surface (Figs. 2a–c) are from 20 to 400 μm size. The interior (Figs. 2d–f) is a three-dimensional network of interconnected macropores from 20 to even 500 μm diameter.

The inner walls of membrane are porous and have uneven surface with protruding parts of the polymer that can facilitate cell adhesion. The addition of Pluronic affects microporous morphology. The bottom layer of PLCA1 is compact with nano-sized micropores (Figs. 2d–h). Likewise to the PLCA1, the SEM images of the PLCA2 scaffolds show a three-dimensional structure (Fig. 3).

The top layer contains many pores from 30 to 150 μm size (Figs. 3a–c). The cross-section creates a network of interconnected macropores between 50 and 350 μm length and from 20 to 250 μm width (Figs. 3d–f). They are smaller and definitely more numerous compared to the PLCA1 scaffold. Visible microporous structure (Figs. 3c, f, and h) is due to the addition of 10 kDa PVP. The bottom layer is dense with visible small pores up to 15 μm diameter (Figs. 3g–f). The average thickness of both scaffolds is about 700–1,200 μm and it depends on the thickness of the used nonwovens.

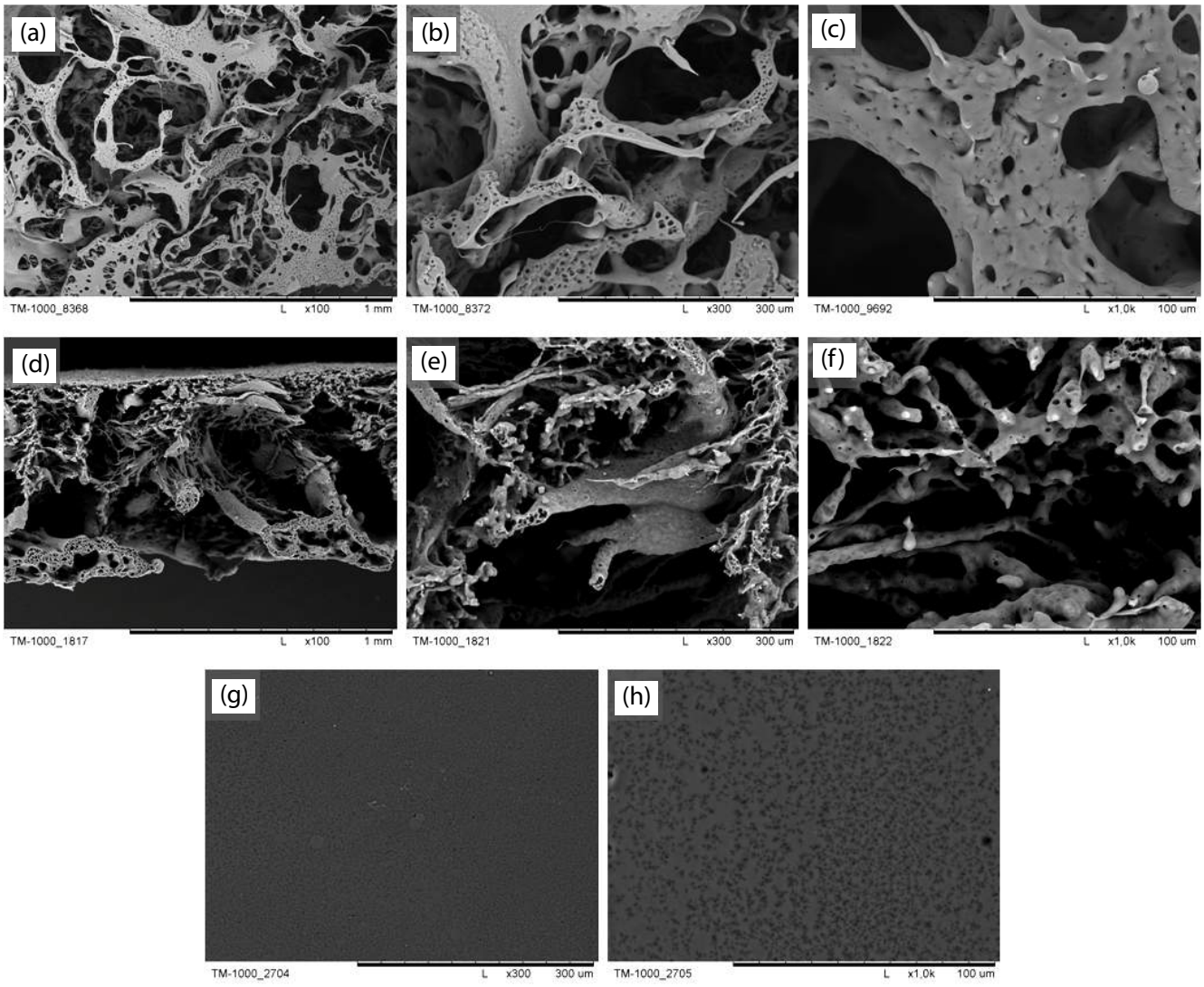

Fig. 2. SEM photomicrographs of the PLCA1 scaffold: (a–c) perforated skin layer; (d–f) cross-section; (g–h) dense bottom layer. Scale bars: (a and d) 1 mm; (b, e, and g) 300 μm; (c, f, and h) 100 μm.

Both scaffolds have a perforated skin layer that allows cells to enter them. The interior of both membranes has an irregular network of interconnected macropores that provides an appropriate environment for migration, proliferation, and adhesion of cells and is suitable for the production of ECM, protein. The selection of the nonwoven material as a pore precursor determines the shape of pores in the membrane. Through the choice of nonwovens, it is possible to control the size of the macropores, the thickness of the walls between pores, and width of scaffolds. Despite similar nonwovens structure of PVP and gelatin, the differences in membranes structures are significant. The larger pores with many protruding polymer parts are obtained using PVP nonwoven for PLCA1 membrane (Fig. 2). On the other hand, PCLA2 scaffold, where macropore precursor is gelatin nonwoven, has smaller, more numerous, and repeatable pores (Fig. 3). Microporous structure of both scaffolds results from using PVP 10 kDa and Pluronic to membrane-forming solution. Such construction ensures access to nutritious substances, oxygen, or allows for the removal of metabolic products from the interior of scaffolds. The bottom skin layer is compact that prevents cells and protein particles to get away out from scaffolds.

3.2. Hydrolysis of scaffolds at simulated physiological condition

To simulate physiological conditions, the PBS and HBSS fluids were used to determine the degradation rate of scaffolds. Especially, the Hank's balanced salt solution has a similar inorganic ion composition compared to blood plasma [45]. The samples for degradation were different in size due to the various construction of the scaffolds. For PLCA1 average size was 0.66 cm × 1.2 cm × 0.08 cm and for PLCA2 was 0.9 cm × 1.2 cm × 0.11 cm. The weight for PLCA1 was approximately 0.013 g and for PLCA20.015 g. The hydrolysis time for PLCA1 was 5 weeks but for PLCA2, it was only 4 weeks due to faster destruction of the PLCA2 sample at 37°C.

After hydrolysis in HBSS, in both scaffolds numerous cracks and enlargement of pores were visible (Figs. 4 and 5).

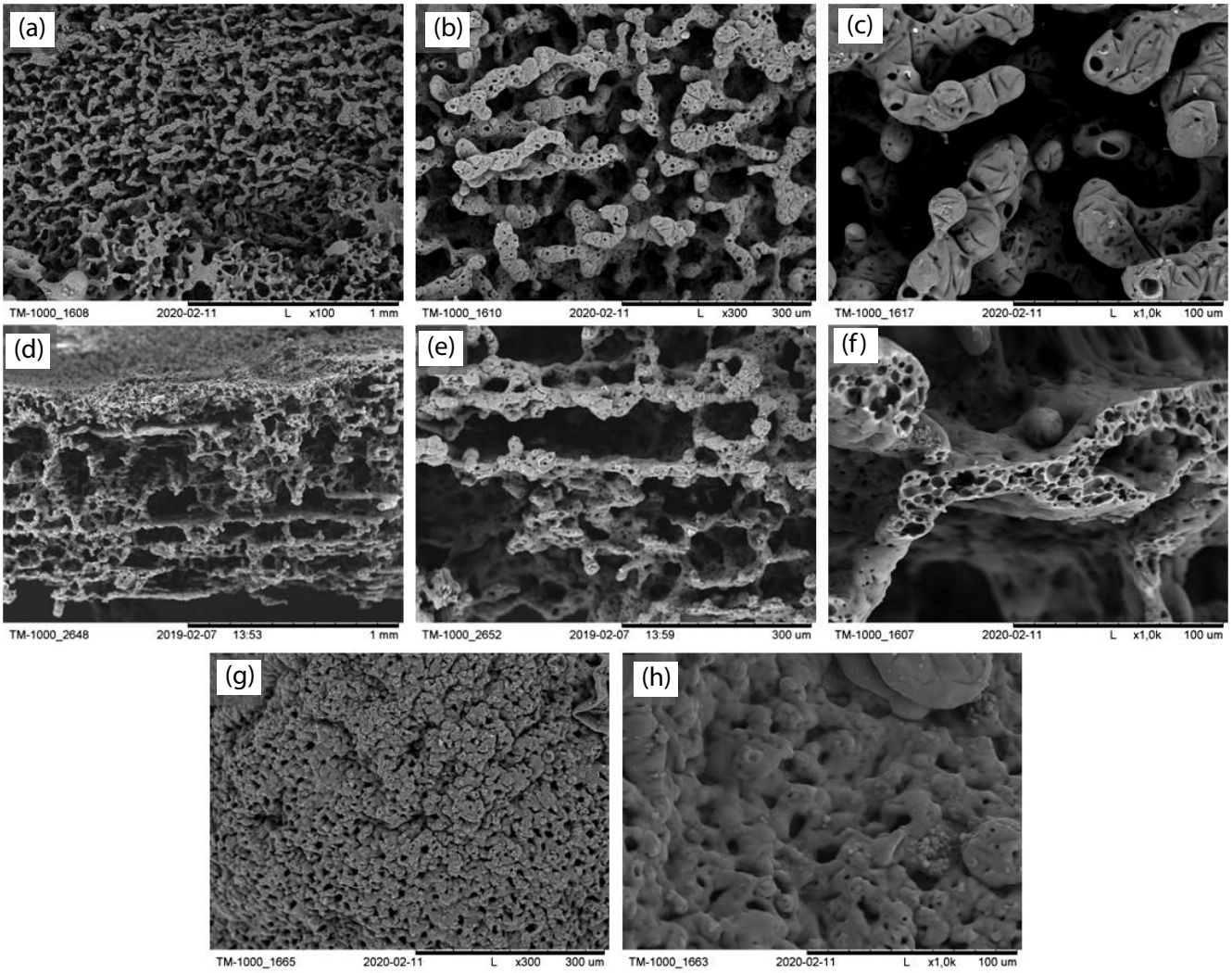

Fig. 3. SEM photomicrographs of the PLCA2 scaffold: (a–c) perforated skin layer; (d–f) cross-section; (g–h) dense bottom layer. Scale bars: (a and d) 1 mm; (b, e, and g) 300 μm; (c, f, and h) 100 μm.

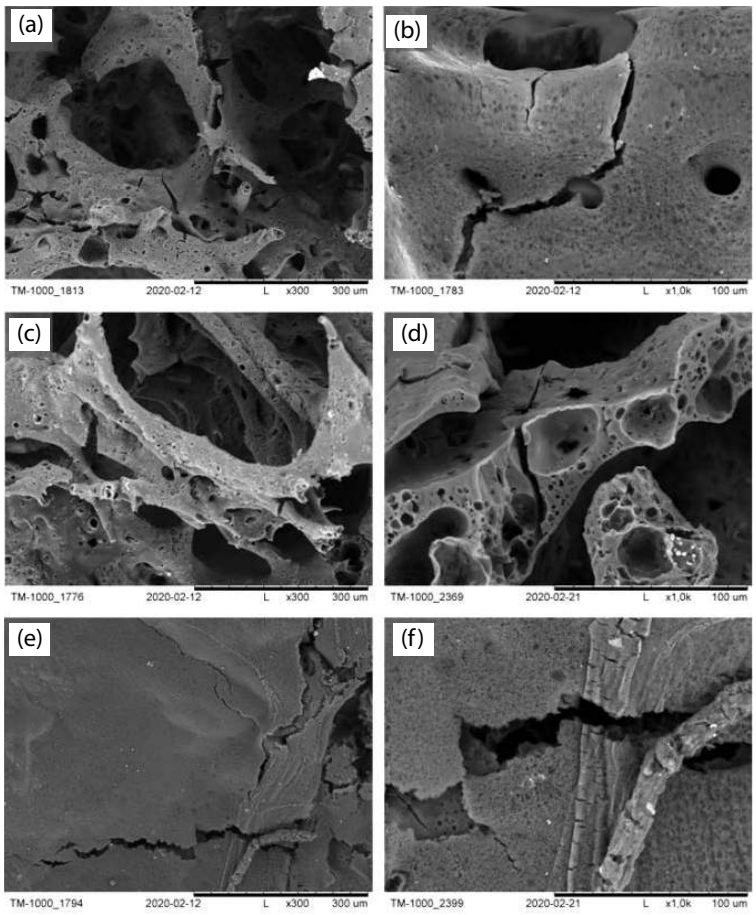

Fig. 4. SEM photomicrographs of the PLCA1 after hydrolysis in HBSS: (a and b) perforated skin layer; (c and d) cross-section; (e and f) dense bottom layer. Scale bars: (a, c, and e) 300 μm; (b, d, and f) 100 μm.

Similar breaks are noticeable on the SEM images in both scaffolds after hydrolysis in PBS (Figs. 6 and 7). However, more cracks can be observed after degradation in HBSS.

Fig. 8 shows the changes in pH medium during hydrolytic degradation in PBS and HBSS media. In both cases, there was a decrease of pH, which can be explained by the presence of the lactic and/or caproic acids formed as a result of polyester hydrolysis. The scaffolds' masses were evaluated before and after hydrolysis to check the impact of the PBS and HBSS medium on membranes (Figs. 9 and 10).

The percentage of weight loss in PBS up to the second week was initially slow, especially for PLCA1, only about 2% and 15% for PLCA2 and then significantly activated. On 28th day, an increase in weight loss can be seen for PLCA2 up to 49%, while for PLCA1 only to 12%, where it increases to 17% after 5 weeks. Definitely slower degradation is in the case of the PLCA1 scaffold. The weight loss of scaffolds in HBSS fluid is higher than was observed in the PBS medium, especially for PLCA2 (Fig. 10). After 4 weeks, the degradation rate of PLCA2 is about 71% and for PLCA1 five times less, about 14% and it increases to around 20% in 35 d. For both membranes, an increase in weight loss can be seen especially after 3 weeks.

The resume results of weights change before and after hydrolysis are shown in Table 1.

The weights are presented as an average of all samples before (n = 12) and after (n = 6) hydrolysis. The loss of weight is observed for both membranes in the range from 17 to 72 of the weight percentage. Due to the similar composition of HBSS to blood plasma [45], it can be stated that the degradation of the PLCA2 scaffold in the body can occur earlier than for PLCA1. It can also be seen that the decrease in pH is not rapid (Fig. 8), which should not have a negative effect on the body like the occurrence of inflammation.

3.3. Pore distributions for scaffolds before and after hydrolysis

The aim of MeMoExplorer™ is a precise measurement of pores present in the membranes for estimation of their size distribution and preparation of data for a statistical analysis that can be performed using software like the Microsoft Excel. The size of the pores was analyzed based on thirty SEM images for each cross-section and top layer of both scaffolds. In Table 2, the area of pores in eight size classes is presented. The results show the average percentage of appropriate pore size in relation to the whole SEM photomicrographs size.

In both scaffolds, the largest number of pores are those of an area over 300 μm^2. This is noticeable for cross-section and surface of both membranes. Above 1% or even about

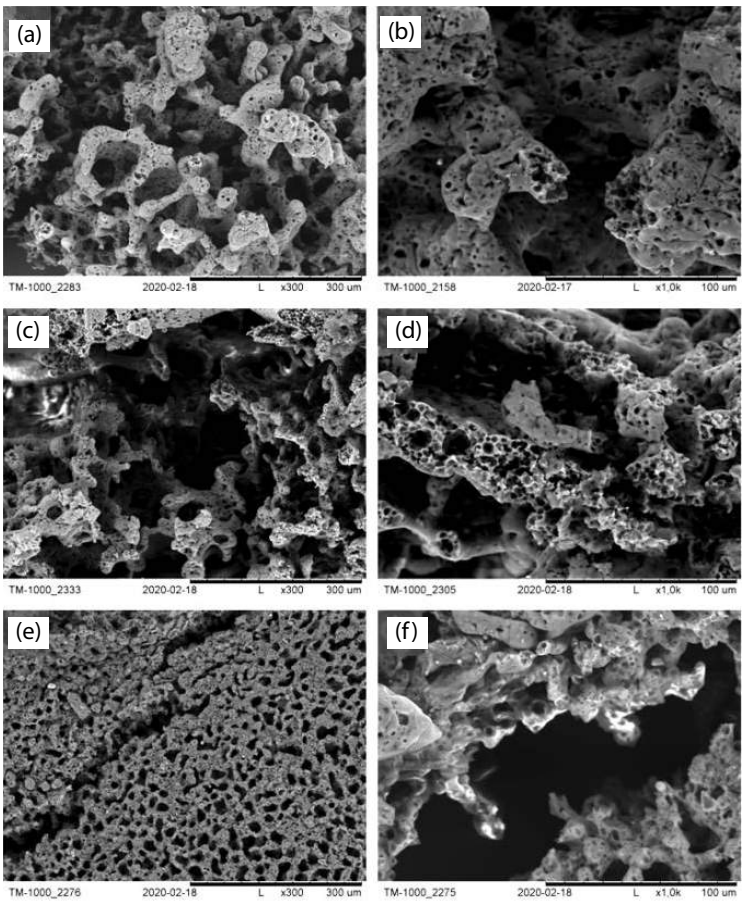

Fig. 5. SEM photomicrographs of the PLCA2 after hydrolysis in HBSS: (a and b) perforated skin layer; (c and d) cross-section; (e and f) dense bottom layer. Scale bars: (a, c, and e) 300 μm; (b, d, and f) 100 μm.

Table 1
Average weights of scaffolds before and after hydrolysis

Scaffold/medium	Weight before hydrolysis (g)	Weight after hydrolysis (g)	Weight loss after hydrolysis (%)
PLCA1/PBS	0.0129 ± 0.0030	0.0107 ± 0.0030	17
PLCA2/PBS	0.0143 ± 0.0023	0.0073 ± 0.0014	50
PLCA1/HBSS	0.0142 ± 0.0043	0.0113 ± 0.0043	20
PLCA2/HBSS	0.0128 ± 0.0030	0.0037 ± 0.0012	72

2% are the pores with 20–80 μm^2, while about 1% are the pores with 150–300 μm^2. Furthermore, the program provides data on the total number of pores (porosity coefficient). The porosity values for top-layers and cross-sections of scaffolds and also the difference between them are presented in Table 3. In addition, a comparison of pores after hydrolysis in PBS and HBSS was made.

The porosity coefficient in the cross-section before and after hydrolysis is higher for PLCA1 compared to PLCA2 membrane. The difference is not significant (0.42%). It is different for the top layer, where the areas of pores are higher even up to 1% for PLCA2. An increase in pore surface is noticeable in each case after hydrolysis, especially in HBSS medium. The most appreciable change is for the top layer of the PLCA2 where the increase is by almost 7%.

3.4. Coefficients of dissimilarity of pore size of scaffolds

Furthermore, computer analysis of the obtained SEM images is intended to evaluate the reproducibility of obtaining parameters in scaffolds production process (instability coefficient). It is calculated by the ratio of standard deviation (SD) of the porosity coefficient to averaged value (Ave) of the porosity coefficient estimated in the set of SEM images. The pore repeatability was also studied after hydrolysis. In Fig. 11 coefficients of dissimilarity, before and

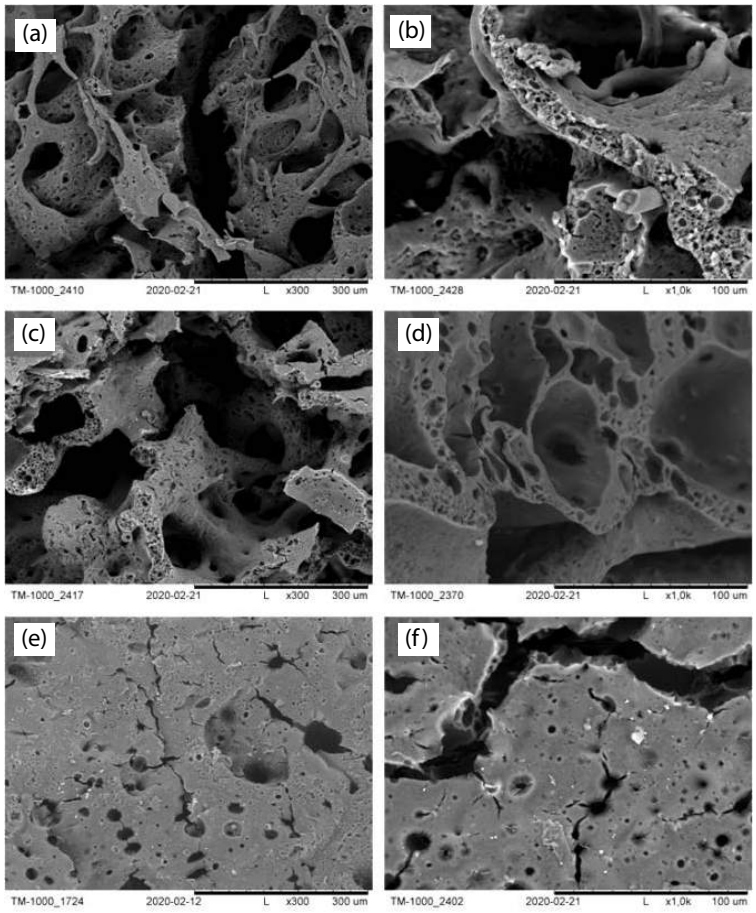

Fig. 6. SEM photomicrographs of the PLCA1 after hydrolysis in PBS: (a and b) perforated skin layer; (c and d) cross-section; (e and f) dense bottom layer. Scale bars: (a, c, and e) 300 μm; (b, d, and f) 100 μm.

after hydrolysis, of cross-section for both membranes are presented.

In Fig. 12, the instability coefficient, before and after degradation, for the top layer of both membranes is presented.

The cross-section and top layer of PLCA2 scaffold appeared to be the best one from the stability point of view. The instability coefficient is the smallest for this sample and it is only about 0.15. A stabilizing effect is observed in each case for both membranes, before and after hydrolysis, indicating the repeatability of the pore size. It is generally low and does not exceed 0.17 for cross-section and 0.30 for the top layer of both scaffolds.

3.5. Porosity of membrane

For biomedical applications pore size and porosity of scaffolds are critical factors to consider. Depending on the obtained parameters, it is possible to select appropriate cells for the experiment. In the study, the porosity of scaffolds was measured before and after hydrolysis (Fig. 13, Table 4). Results show that membranes obtained with addition of PVP nonwoven with pluronic (PLCA1) and gelatin nonwoven with PVP pore precursors (PLCA2) are characterized by a high porosity, about 95%. The higher value of this parameter was observed for membranes obtained with gelatin nonwoven and PVP 10 kDa added to polymeric solution. But this difference was not significant, just only about 2%. After degradation this value is increases, especially for PLCA2 in HBSS.

In Fig. 13, the abbreviation Diff means difference between porosity of PLCA1 or PLCA2 before and after degradation in PBS and HBSS media. The largest dissimilarity in porosity is observed in HBSS medium for PLCA2 and it is 2.61%, where as for PLCA1 it is 1.44%. In the case of degradation in PBS, the porosity difference is higher for PLCA2 again and equals 1.63%, while for PLCA1 it is only 0.38% that is more than four times less than for PLCA2 hydrolysis in PBS. In Table 4, the porosity values before and after degradation of the scaffolds are presented. In addition, the difference between the PLCA1 and PLCA2 are calculated.

The difference in the increase in porosity between PLCA2/HBSS and PLCA1/HBSS is over 3.1% as a result of its faster degradation.

Such scaffolds could be used for culture of microorganisms with the possibility of using in biotechnology. For example, as immobilization carrier to support the formation of biofilms in membrane reactors for water purification. Due to the presence of microbial cells, it is possible to significantly increase the efficiency of microbiological processes for removal or bioremediation of organic contaminants. In

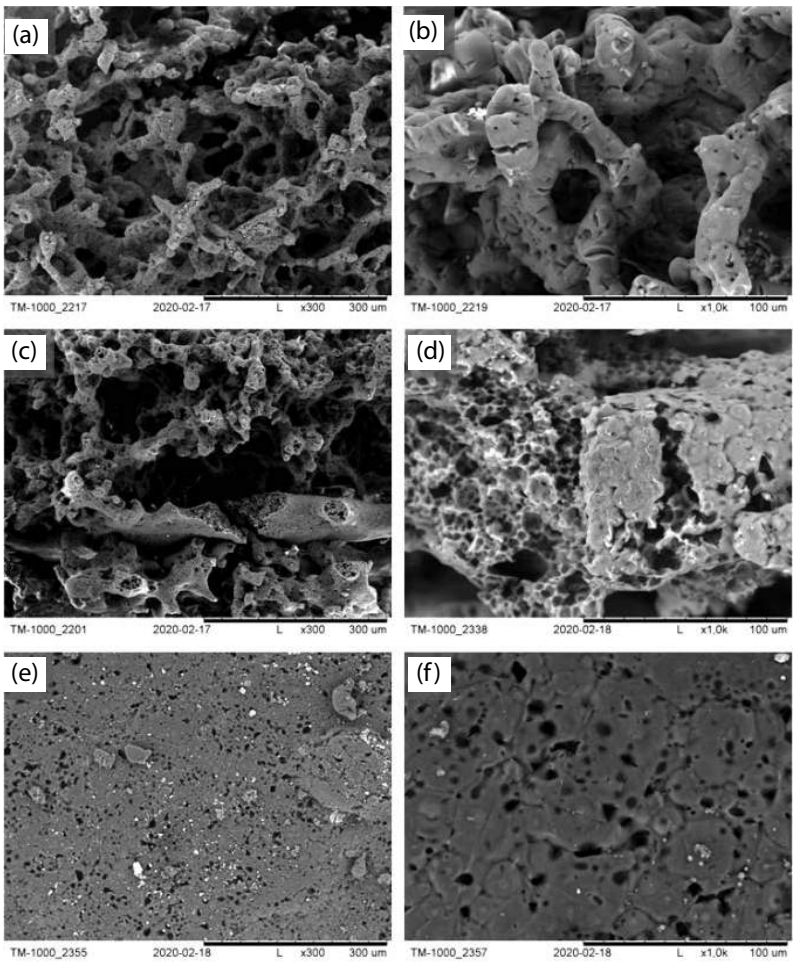

Fig. 7. SEM photomicrographs of the PLCA2 after hydrolysis in PBS: (a and b) perforated skin layer; (c and d) cross-section; (e and f) dense bottom layer. Scale bars: (a, c, and e) 300 μm; (b, d, and f) 100 μm.

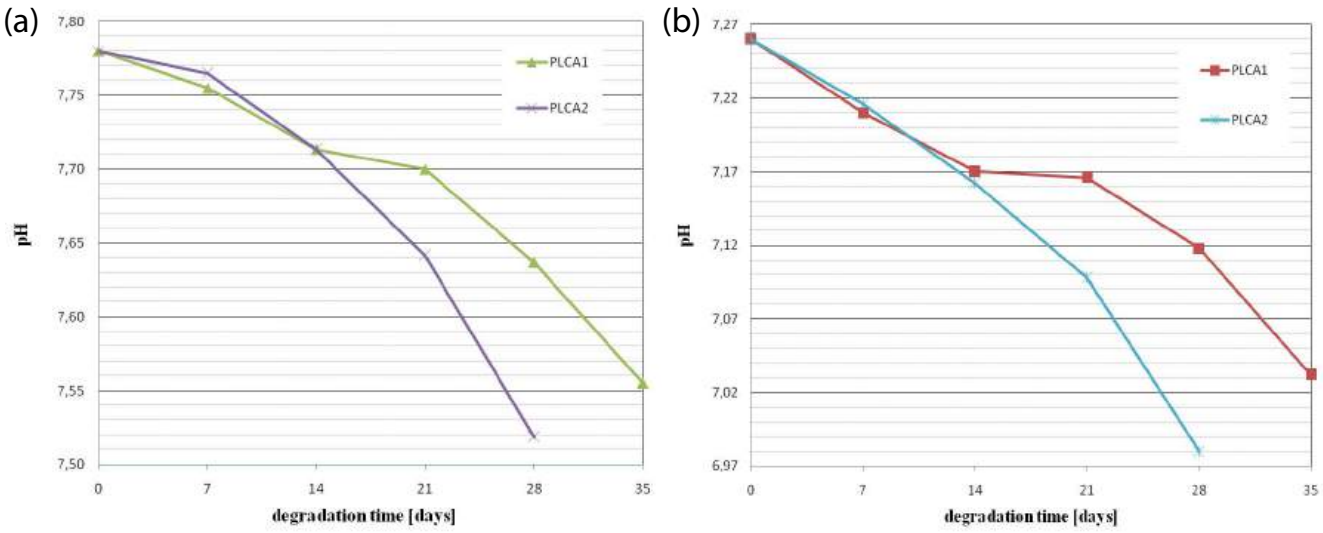

Fig. 8. Change in pH of HBSS (a) and PBS (b) medium during degradation of the PLCA1 and PLCA2 scaffolds.

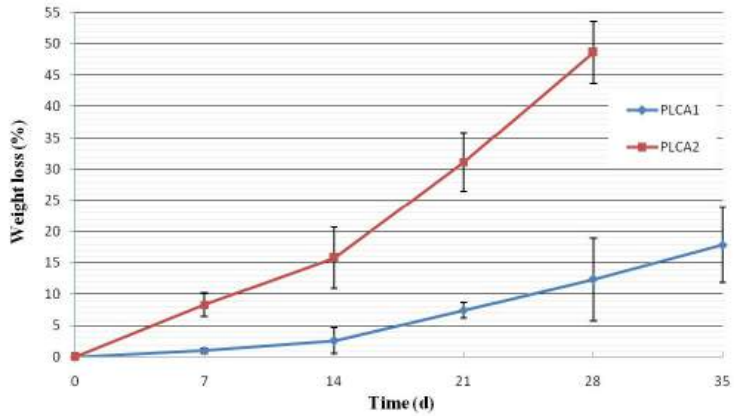

Fig. 9. Weight loss of PLCA1 and PLCA2 scaffolds as a function of degradation time in PBS medium.

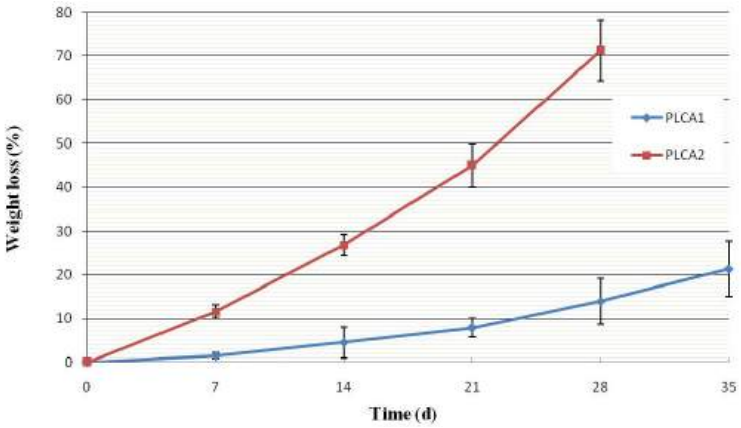

Fig. 10. Weight loss of PLCA1 and PLCA2 scaffolds as a function of degradation time in HBSS media.

Table 2
Average relative frequency of pores in eight size classes

Pore size (μm²)	0–3	3–8	8–20	20–80	50–100	100–150	150–300	>300
	(%)							
Cross-section of PCLA1	0.06 ± 0.02	0.20 ± 0.07	0.51 ± 0.21	1.63 ± 0.85	0.40 ± 0.25	0.73 ± 0.47	0.92 ± 0.53	42.73 ± 8.95
Cross-section of PCLA2	0.06 ± 0.03	0.18 ± 0.09	0.41 ± 0.23	1.14 ± 0.61	0.28 ± 0.17	0.54 ± 0.26	0.78 ± 0.40	43.37 ± 8.06
Top layer of PLCA1	0.07 ± 0.04	0.24 ± 0.11	0.55 ± 0.26	1.86 ± 0.96	0.55 ± 0.37	0.91 ± 0.50	1.19 ± 0.73	27.98 ± 8.43
Top layer of PLCA1	0.10 ± 0.03	0.34 ± 0.08	0.71 ± 0.15	1.51 ± 0.57	0.33 ± 0.29	0.71 ± 0.71	1.38 ± 1.02	29.26 ± 7.11

Table 3
Total areas of pores in relation to the whole SEM image size for cross-section and top layer of scaffolds

Scaffold/difference	Porosity coefficients before hydrolysis (%)	Porosity coefficients after hydrolysis in PBS (%)	Porosity coefficients after hydrolysis in HBSS (%)
Cross-section of PLCA1	47.18 ± 7.37	50.34 ± 8.08	51.32 ± 7.80
Cross-section of PLCA2	46.76 ± 7.04	47.38 ± 7.91	48.60 ± 7.40
Diff. between cross-section of scaffolds	0.42	2.95	2.72
Top layer of PLCA1	33.35 ± 7.05	36.41 ± 6.48	38.72 ± 6.67
Top layer of PLCA2	34.35 ± 5.36	40.15 ± 9.52	41.15 ± 11.56
Diff. between top layer of scaffolds	0.99	3.74	2.43

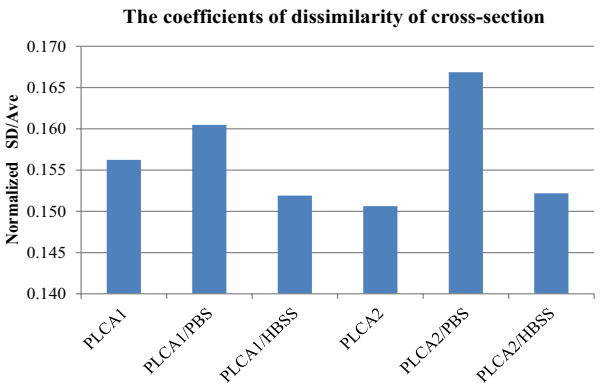

Fig. 11. Instability coefficients in cross-section of obtained scaffolds before and after hydrolyze.

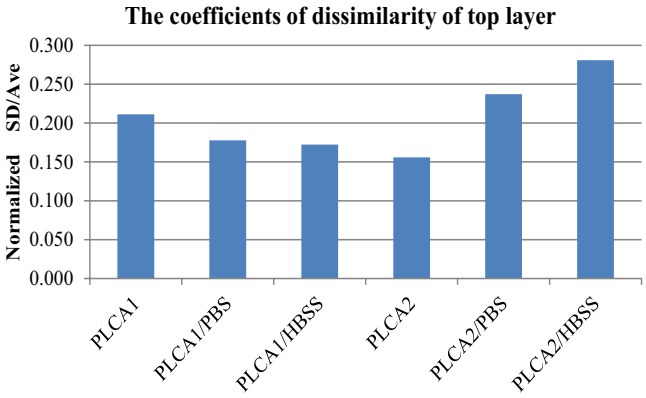

Fig. 12. Instability coefficients in the surface of obtained scaffolds before and after hydrolyze.

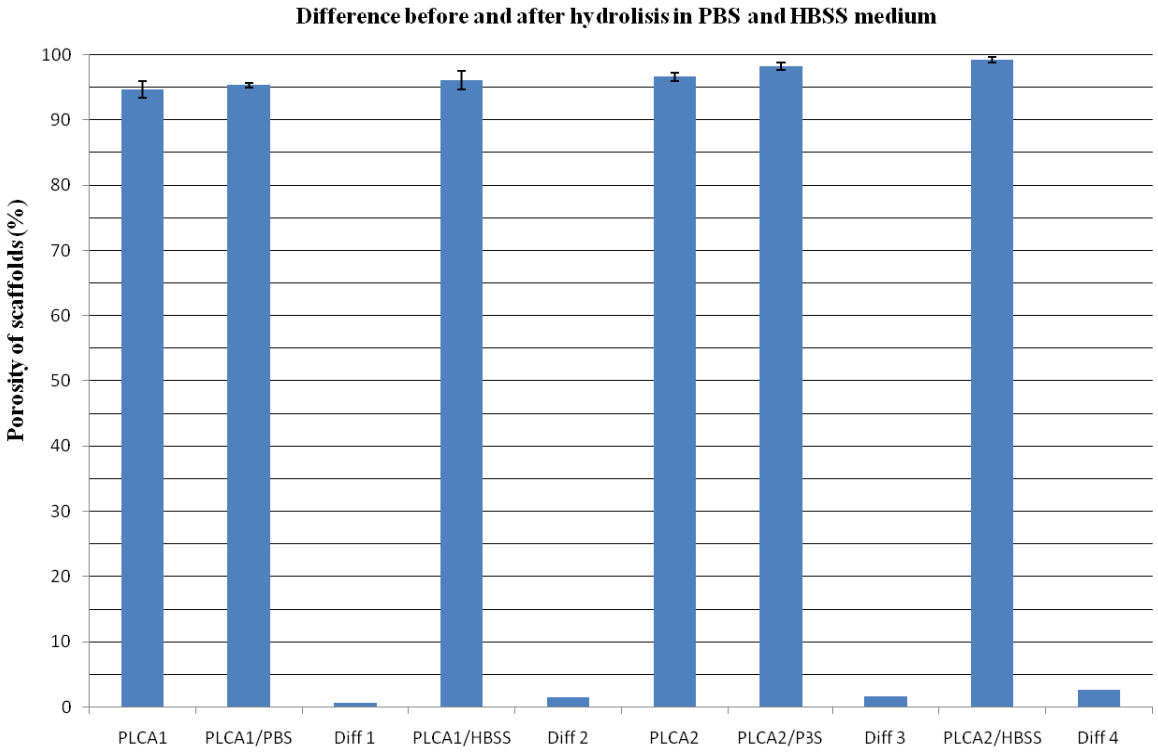

Fig. 13. Porosity of scaffold before degradation and difference between membranes of the same type after hydrolysis.

Table 4
Difference in porosity of scaffolds, before and after hydrolysis between PLCA1 and PLCA2

Scaffold/difference	Porosity before hydrolysis (%)	Porosity after hydrolysis in PBS (%)	Porosity after hydrolysis in HBSS (%)
PLCA1	94.67 ± 1.28	95.34 ± 0.38	96.11 ± 1.44
PLCA2	96.60 ± 0.68	98.23 ± 0.59	99.21 ± 0.44
Diff. between scaffolds	1.93	2.89	3.10

addition, microorganisms on a solid support are not leaching out of the bioreactor along with the flowing liquid. Porous membranes may also affect the selective delivery of substances, gases or removal of metabolites from the stream. Furthermore, polyester based biofilm carriers could be a carbon source to promote the growth of microorganisms [46–48].

4. Conclusion

The aim of this study was to obtain highly porous scaffolds for cell culture. Membranes were received by wet phase inversion using biocompatible PLCA material composed of 30% PCL and 70% PLA. The appropriate structure was achieved by the addition of selected macro- and micropore precursors. In both cases, the addition of PVP and gelatin nonwovens ensured a network of interconnected macropores, while Pluronic and PVP 10 kDa assured the microporous structure of both membranes. The scaffolds were hydrolyzed at simulated physiological conditions in PBS and HBSS, where weight loss, an increase of porosity, and a change in the structure and size of the pores were noted. The results are much more favorable after degradation in HBSS, especially in the case of PLCA2 in which gelatin nonwoven and PVP 10 kDa were used. Additionally, on the basis of computer analysis using the MeMoExplorer™ software, coefficients of dissimilarity of pore size were calculated. In each case is lower than 0.30, which indicates the repeatability in structure of scaffolds before and after degradation. However, the better and more promising results are for the PLCA2 scaffold, which can be used for further *in vitro* cellular studies.

References

[1] X. Zhenga, Z. Zhang, D. Yu, X. Chen, R. Cheng, S. Min, J. Wang, Q. Xiao, J. Wang, Overview of membrane technology applications for industrial wastewater treatment in China to increase water supply, Resour. Conserv. Recycl., 105 (2015) 1–10.

[2] A.K. Pabby, S.S.H. Rizvi, A.M.S. Requena, Membrane Separations - Chemical, Pharmaceutical, Food, and Biotechnological Applications, 2nd ed., CRC Press, New York, NY, 2015.

[3] N.L. Le, S.P. Nunes, Materials and membrane technologies for water and energy sustainability, Sustainable Mater. Technol., 7 (2016) 1–28.

[4] C. Xu, V.S. Thiruvadi, R. Whitmore, H. Liu, Delivery systems for biomedical applications: basic introduction, research frontiers and clinical translations, Biomater. Transl. Med., 5 (2019) 93–116.

[5] M. Takht Ravanchi, T. Kaghazchi, A. Kargari, Application of membrane separation processes in petrochemical industry: a review, Desalination, 235 (2009) 199–244.

[6] H. Lin, W. Gao, F. Meng, B.-Q. Liao, K.-T. Leung, L. Zhao, J. Chen, H. Hong, Membrane bioreactors for industrial wastewater treatment: a critical review, Crit. Rev. Environ. Sci. Technol., 42 (2012) 677–740.

[7] A. Ciechanowska, D. Schwanzer-Pfeiffer, E. Rossmanith, S. Sabalinska, C. Wojciechowski, J. Hartmann, K. Hellevuo, A. Chwojnowski, P. Foltynski, D. Falkenhagen, J.M. Wojcicki, Artificial vessel as a basis for disease related cell culture model, Int. J. Artif. Organs, 29 (2006) 1–4.

[8] M. Farina, J.F. Alexander, U. Thekkedath, M. Ferrari, A. Grattoni, Cell encapsulation: overcoming barriers in cell transplantation in diabetes and beyond, Adv. Drug Deliv. Rev., 139 (2019) 92–115.

[9] Y. Liu, J. Luo, X. Chen, W. Liu, T. Chen, Cell Membrane Coating Technology: A Promising Strategy for Biomedical Applications, Nano Microlett., 11 (2019) 1–46, doi: 10.1007/s40820-019-0330-9.

[10] G. Orive, D. Emerich, A. Khademhosseini, S. Matsumoto, R.M. Hernández, J.L. Pedraz, T. Desai, R. Calafiore, P. de Vos, Engineering a clinically translatable bioartificial pancreas to treat type I diabetes, Trends Biotechnol., 36 (2018) 445–456.

[11] K.M. Park, Y.M. Shin, K. Kim, H. Shin, Tissue Engineering and Regenerative Medicine 2017: A Year in Review, Tissue Eng. Part B, 24 (2018) 327–344.

[12] F. Berthiaume, T.J. Maguire, M.L. Yarmush, Tissue engineering and regenerative medicine: history, progress, and challenges, Annu. Rev. Chem. Biomol. Eng., 2 (2011) 403–430.

[13] A.A. Chaudhari, K. Vig, D.R. Baganizi, R. Sahu, S. Dixit, V. Dennis, S.R. Singh, S.R. Pillai, Future prospects for scaffolding methods and biomaterials in skin tissue engineering: a review, Int. J. Mol. Sci., 17 (2016) 1–31, doi: 10.3390/ijms17121974.

[14] I. Bružauskaitė, D. Bironaitė, E. Bagdonas, E. Bernotienė, Scaffolds and cells for tissue regeneration: different scaffold pore sizes—different cell effects, Cytotechnology, 68 (2016) 355–369.

[15] M.P. Nikolova, M.S. Chavali, Recent advances in biomaterials for 3D scaffolds: a review, Bioact. Mater., 4 (2019) 271–292.

[16] S.J. Hollister, Porous scaffold design for tissue engineering, Nat. Mater., 4 (2005) 518–524.

[17] F. Ahmadi, R. Giti, S. Mohammadi-Samani, F. Mohammadi, Biodegradable scaffolds for cartilage tissue engineering, Galen Med. J., 6 (2017) 70–80.

[18] Q.L. Loh, C. Choong, Three-dimensional scaffolds for tissue engineering applications: role of porosity and pore size, Tissue Eng. Part B, 19 (2013) 485–502.

[19] F.J. O'Brien, Biomaterials and scaffolds for tissue engineering, Mater. Today, 14 (2011) 88–95.

[20] X. Liang, Y. Qi, Z. Pan, Y. He, X. Liu, S. Cui, J. Ding, Design and preparation of quasi-spherical salt particles as water-soluble porogens to fabricate hydrophobic porous scaffolds for tissue engineering and tissue regeneration, Mater. Chem. Front., 2 (2018) 1539–1553.

[21] W. Zhao, Y. Su, C. Li, Q. Shi, X. Ning, Z. Jiang, Fabrication of antifouling polyethersulfone ultrafiltration membranes using Pluronic F127 as both surface modifier and pore-forming agent, J. Membr. Sci., 318 (2008) 405–412.

[22] B. Chakrabarty, A.K. Ghoshal, M.K. Purkait, Preparation, characterization and performance studies of polysulfone membranes using PVP as an additive, J. Membr. Sci., 315 (2008) 36–47.

[23] A.V. Bildyukevich, T.V. Plisko, A.S. Liubimova, V.V. Volkov, V.V. Ususky, Hydrophilization of polysulfone hollow fiber membranes via addition of polyvinylpyrrolidone to the bore fluid, J. Membr. Sci., 524 (2016) 537–549.

[24] G. Arthanareeswaran, D. Mohan, M. Raajenthiren, Preparation, characterization and performance studies of ultrafiltration membranes with polymeric additive, J. Membr. Sci., 350 (2010) 130–138.

[25] K. Dudziński, A. Chwojnowski, M. Gutowska, M. Płończak, J. Czubak, E. Łukowska, C. Wojciechowski, Three dimensional polyethersulphone scaffold for chondrocytes cultivation - the future supportive material for articular cartilage regeneration, Biocybern. Biomed. Eng., 30 (2010) 65–76.

[26] A. Chwojnowski, A. Kruk, C. Wojciechowski, E. Łukowska, J. Dulnik, P. Sajkiewicz, The dependence of the membrane structure on the non-woven forming the macropores in the 3D scaffolds preparation, Desal. Water Treat., 64 (2017) 324–331.

[27] G. Conoscenti, T. Schneider, K. Stölzel, F. Carfì Pavia, V. Brucato, C. Goegele, V. Carrubba, G. Schulze-Tanzil, PLLA scaffolds produced by thermally induced phase separation (TIPS) allow human chondrocyte growth and extracellular matrix formation dependent on pore size, Mater. Sci. Eng., C, 80 (2017) 449–459.

[28] M.J. Gupte, W.B. Swanson, J. Hu, X. Jin, H. Ma, Z. Zhang, Z. Liu, K. Feng, G. Feng, G. Xiao, N. Hatch, Y. Mishina, P.X. Ma, Pore size directs bone marrow stromal cell fate and tissue regeneration in nanofibrous macroporous scaffolds by mediating vascularization, Acta Biomater., 82 (2018) 1–11.

[29] P.L. Lewis, R.M. Green, R.N. Shah, 3D-printed gelatin scaffolds of differing pore geometry modulate hepatocyte function and gene expression, Acta Biomater., 69 (2018) 63–70.

[30] G. Turnbull, J. Clarke, F. Picard, P. Riches, L. Jia, F. Han, B. Li, W. Shu, 3D bioactive composite scaffolds for bone tissue engineering, Bioact. Mater., 3 (2018) 278–314.
[31] P. Denis, J. Dulnik, P. Sajkiewicz, Electrospinning and structure of bicomponent polycaprolactone/gelatin nanofibers obtained using alternative solvent system, Int. J. Polym. Mater. Polym. Biomater., 64 (2015) 354–364.
[32] R. Sakai, B. John, M. Okamoto, J.V. Seppälä, J. Vaithilingam, H. Hussein, R. Goodridge, Macromol. Mater. Eng. 1/2013, Macromol. Mater. Eng., 298 (2013) 45–52, doi: 10.1002/mame.201370001.
[33] R. Song, M. Murphy, C. Li, K. Ting, C. Soo, Z. Zheng, Current development of biodegradable polymeric materials for biomedical applications, Drug Des. Dev. Ther., 12 (2018) 3117–3145.
[34] L.S. Nair, C.T. Laurencin, Biodegradable polymers as biomaterials, Prog. Polym. Sci., 32 (2007) 762–798.
[35] F. Asghari, M. Samiei, K. Adibkia, A. Akbarzadeh, S. Davaran, Biodegradable and biocompatible polymers for tissue engineering application: a review, Artif. Cells Nanomed. Biotechnol., 45 (2017) 185–192.
[36] T. Urbánek, E. Jäger, A. Jäger, M. Hrubý, Selectively biodegradable polyesters: nature-inspired construction materials for future biomedical applications, Polymers, 11 (2019) 1–21, doi: 10.3390/polym11061061.
[37] D. Daranarong, P. Techaikool, W. Intatue, R. Daengngern, K. Thomson, R. Molley, N. Kungwan, L. Foster, D. Boonyawan, W. Punyodom, Effect of surface modification of poly(L-lactide-co-ε-caprolactone) membranes by low-pressure plasma on support cell biocompatibility, Surf. Coat. Technol., 306 (2016) 328–335.
[38] T. Li, L. Tian, S. Liao, X. Ding, S.A. Irvine, S. Ramakrishna, Fabrication, mechanical property and *in vitro* evaluation of poly(L-lactic acid-co-ε-caprolactone) core-shell nanofiber scaffold for tissue engineering, J. Mech. Behav. Biomed. Mater., 98 (2019) 48–57.
[39] W. Sikorska, C. Wojciechowski, M. Przytulska, G. Rokicki, M. Wasyłeczko, J.L. Kulikowski, A. Chwojnowski, Polysulfone–polyurethane (PSf-PUR) blend partly degradable hollow fiber membranes: preparation, characterization, and computer image analysis, Desal. Water Treat., 128 (2018) 383–391.
[40] M. Przytulska, J.L. Kulikowski, M. Wasyłeczko, A. Chwojnowski, D. Piętka, The evaluation of 3D morphological structure of porous membranes based on a computer-aided analysis of their 2D images, Desal. Water Treat., 128 (2018) 11–19.
[41] M. Przytulska, A. Kruk, J.L. Kulikowski, C. Wojciechowski, A. Gadomska-Gajadhur, A. Chwojnowski, Comparative assessment of polyvinylpyrrolidone type of membranes based on porosity analysis, Desal. Water Treat., 75 (2017) 18–25.
[42] W. Chrzanowski, E. Ali, A. Neel, D. Andrew, J. Campbell, Effect of surface treatment on the bioactivity of nickel – titanium, Acta Biomater., 4 (2008) 1969–1984.
[43] M. Ara, M. Watanabe, Y. Imai, Effect of blending calcium compounds on hydrolytic degradation of poly(DL-lactic acid-co-glycolic acid), Biomaterials, 23 (2002) 2479–2483.
[44] S.T. Ho, D.W. Hutmacher, A comparison of micro CT with other techniques used in the characterization of scaffolds, Biomaterials, 27 (2006) 1362–1376.
[45] J. Gonzalez, R.Q. Hou, E.P.S. Nidadavolu, R. Willumeit-Römer, F. Feyerabend, Magnesium degradation under physiological conditions – best practice, Bioact. Mater., 3 (2018) 174–185.
[46] Y. Zhao, D. Liu, W. Huang, Y. Yang, M. Ji, L.D. Nghiem, Q.T. Trinh, N.H. Tran, Insights into biofilm carriers for biological wastewater treatment processes: current state-of-the-art, challenges, and opportunities, Bioresour. Technol., 288 (2019) 1–14.
[47] Z.B. Bouabidi, M.H. El-Naas, Z. Zhang, Immobilization of microbial cells for the biotreatment of wastewater: a review, Environ. Chem. Lett., 17 (2019) 241–257.
[48] D. Lu, H. Bai, F. Kong, S.N. Liss, B. Liao, Recent advances in membrane aerated biofilm reactors, Crit. Rev. Environ. Sci. Technol., 50 (2020) 1–55, doi: 10.1080/10643389.2020.1734432.

PUBLIKACJA 3

Scaffolds for Cartilage Tissue Engineering from a Blend of Polyethersulfone and Polyurethane Polymers

Monika Wasyłeczko, Elżbieta Remiszewska, Wioleta Sikorska, Judyta Dulnik, Andrzej Chwojnowski – Molecules **2023**, 28, 1-25.
https://doi.org/10.3390/molecules28073195
IF: 4,927
MNiSW: 140

molecules

MDPI

Article

Scaffolds for Cartilage Tissue Engineering from a Blend of Polyethersulfone and Polyurethane Polymers

Monika Wasyłeczko [1,*], Elżbieta Remiszewska [1], Wioleta Sikorska [1], Judyta Dulnik [2] and Andrzej Chwojnowski [1]

[1] Nalecz Institute of Biocybernetics and Biomedical Engineering, Polish Academy of Sciences, Trojdena 4, 02-109 Warsaw, Poland; achwojnowski@ibib.waw.pl (A.C.)
[2] Institute of Fundamental Technological Research Polish Academy of Sciences, Laboratory of Polymers and Biomaterials, Pawińskiego 5b, 02-106 Warsaw, Poland
* Correspondence: mwasyleczko@ibib.waw.pl

Abstract: In recent years, one of the main goals of cartilage tissue engineering has been to find appropriate scaffolds for hyaline cartilage regeneration, which could serve as a matrix for chondrocytes or stem cell cultures. The study presents three types of scaffolds obtained from a blend of polyethersulfone (PES) and polyurethane (PUR) by a combination of wet-phase inversion and salt-leaching methods. The nonwovens made of gelatin and sodium chloride (NaCl) were used as precursors of macropores. Thus, obtained membranes were characterized by a suitable structure. The top layers were perforated, with pores over 20 µm, which allows cells to enter the membrane. The use of a nonwoven made it possible to develop a three-dimensional network of interconnected macropores that is required for cell activity and mobility. Examination of wettability (contact angle, swelling ratio) showed a hydrophilic nature of scaffolds. The mechanical test showed that the scaffolds were suitable for knee joint applications (stress above 10 MPa). Next, the scaffolds underwent a degradation study in simulated body fluid (SBF). Weight loss after four weeks and changes in structure were assessed using scanning electron microscopy (SEM) and MeMoExplorer Software, a program that estimates the size of pores. The porosity measurements after degradation confirmed an increase in pore size, as expected. Hydrolysis was confirmed by Fourier-transform infrared spectroscopy (FT-IR) analysis, where the disappearance of ester bonds at about 1730 cm^{-1} wavelength is noticeable after degradation. The obtained results showed that the scaffolds meet the requirements for cartilage tissue engineering membranes and should undergo further testing on an animal model.

Keywords: articular cartilage; cartilage tissue engineering; hydrolysis process; materials for scaffolds; partly degradable scaffolds; polyethersulfone–polyurethane scaffolds; polyurethane degradation; regenerative medicine; scaffold requirements; tissue engineering

Citation: Wasyłeczko, M.; Remiszewska, E.; Sikorska, W.; Dulnik, J.; Chwojnowski, A. Scaffolds for Cartilage Tissue Engineering from a Blend of Polyethersulfone and Polyurethane Polymers. *Molecules* **2023**, *28*, 3195. https://doi.org/10.3390/molecules28073195

Academic Editors: Bruce P. Lee and Matthias Schnabelrauch

Received: 16 February 2023
Revised: 29 March 2023
Accepted: 31 March 2023
Published: 3 April 2023

1. Introduction

Membranes are increasingly used in regenerative medicine, including tissue engineering (TE). A development of new membranes permits the replacement of transplants or provides new alternative methods allowing the treatment of damaged tissues or even diseases such as diabetes [1–3]. For example, flat membranes can be used for skin regeneration [4,5], the spatial form of membranes (scaffolds) are used for cell support during cultivation [6–9], and hollow fiber membranes (HFMs) are used in dialysis [10]. Membranes are also used to encapsulate active ingredients/cells in a drug delivery system (DDS) [1,11,12].

Tissue damage is a serious problem affecting many people of all ages. It can be caused by trauma, an unhealthy lifestyle, degenerative changes, or inflammatory diseases [2,13–17]. Some tissues, such as hyaline cartilage, due to its lack of vascularization and innervations, show limited regenerative capacity [18–20]. Articular cartilage is necessary to ensure proper

movement [20,21]. Therefore, cartilage damage requires medical intervention, such as the microfracture (MF) method, or cell-based approaches, for example, autologous chondrocyte implantation (ACI). None of these methods produce sufficient results because they promote regeneration to fibrocartilage tissue which has inferior biomechanical properties and is susceptible to further damage [19,22–24]. The MF method involves stimulating the subchondral bone marrow, where a blood clot fills the defect [19,23–25]. The ACI method enables the implantation of the patient's articular chondrocytes (ACs) in place of the cartilage lesions. Cells are either delivered directly to the damaged site or are delivered in a scaffold that acts as a temporary matrix [19,23,26,27]. Studies show better results for ACI compared to MF [23,28]. Doctors and scientists are still looking for an effective method to regenerate cartilage. A promising solution for restoring hyaline cartilage is to combine well-known methods such as the MF technique with scaffolds, which will provide the right conditions for mesenchymal stem cells [8,21,27,29]. Therefore, scaffolds tailored for cartilage needs deserve special attention.

The architecture of scaffolds suitable for this application should be characterized by a strongly developed three-dimensional spatial structure with a network of interconnected pores of the right size. It is important since such construction mimics the environment of a living organism (native tissue) much better, compared to two-dimensional membranes [30–33]. It affects the settlement and migration of cells, as well as their products, which consequently leads to cartilage regeneration. It requires the presence of micropores, which will be responsible for both supplying nutrients and oxygen to cells, and also for removing metabolism products outside the membrane [8,9,34,35]. Moreover, scaffolds should be characterized by biocompatibility and degradability. This can be achieved by selecting, carefully, the method of preparation, materials, and additives, such as pore precursors [9,35,36]. Depending on the application (cell selection), a scaffold with the appropriate pore size should be selected. Namely, stem cells are required correspondingly to their size, with larger pores inside the membrane [8,9,37,38]. What is more, the scaffold's parameters such as mechanical strength, stiffness, and flexibility are essential during cell cultivation and after implantation into the body [30–32,35,39]. A desirable feature of scaffolds is controlled degradability in conditions that are present in the human body. The degradation time should not be too long or short and be proportional for tissue regeneration [35,40,41].

By properly selecting the scaffold material, both the degradation time, as well as its mechanical properties, can be easily controlled [6,9,27,34,35,41–44]. Natural polymers such as sugar and protein compounds such as collagen (COL) [45,46], hyaluronic acid (HA) [47], chondroitin sulfate (CS) [48,49], and fibrin [50] could be used to develop materials for cartilage regeneration. Natural materials are characterized by high bioactivity and biocompatibility, and they have properties similar to those of native tissues. Although they have many advantages, they are not the easiest materials for scaffold production. They are usually sensitive to elevated temperatures, pressure, and varying pH. Membranes made solely of these polymers have poor mechanical strength, and their rapid hydrolysis (sensitivity to an aquatic environment) causes a loss of the proper structure of the scaffold [27,30,32,35,44,45]. Synthetic polymers, compared to natural polymers, have better mechanical resistance and durability under various conditions. The most commonly used synthetic polymers in scaffold development are polylactic acid (PLA) [51,52], polycaprolactone (PCL) [53,54], polyurethane (PUR) [55,56], and polyethersulfone (PES) [7,57–59]. Due to their good mechanical, physical, and chemical properties, they can be used to produce various scaffold shapes using different techniques. Those which are biodegradable break down into components that are non-toxic for the host and metabolized in the body. In addition, their mechanical properties and degradation time can be controlled by combining two or more polymers (as copolymers or blends) [29,32,44,60–66]. It is worth noting that some synthetic materials do not have adequate biological properties, and sometimes degradation products, such as acids, can cause side effects on the host organism, for example, induce an inflammatory response [32,67,68]. Considering the advantages of synthetic and natural polymers, hybrid membranes with good biological and mechanical properties can

be obtained, which is the current direction of scientists [23,27,30,41,67,69,70]. Moreover, noteworthy are membranes made of a blend of polymers, one of which is biodegradable. The disappearance of one of them that happens over time improves fluid transport and separation properties. For instance, increasing porosity/pore size will affect the release of space for regeneration, while the more stable polymer will preserve the scaffold skeleton [42,43,60,62,64,70].

Many scaffolds are undergoing preclinical and clinical tests. Commercial scaffolds used in cartilage regeneration are generally made of natural polymers (mainly collagen). Due to the mentioned disadvantages of natural materials, these scaffolds do not meet the necessary requirements (low mechanical stability and rapid hydrolysis). They quickly lose their structure because they turn into a gel-like form. This leads to the regenerated non-valuable fibrocartilage, which is susceptible to further damage [23,30,35,41,44,71].

This study aimed to obtain partially degradable scaffolds for cartilage tissue engineering. Three membranes were obtained from a blend of PES and synthesized PUR polymers, in different weight ratios. The PES–PUR blend was chosen because of the biocompatibility of PES and PUR (important for biomedical applications), the good solubility of both polymers in the same solvents (important for manufacturing), and the presence of ester bonds in PUR (hydrolysis in physiological fluid). Water-soluble substitutes were used to obtain micro- and macropores in the scaffold (adequate structure of membranes). The scaffolds were prepared using a combination of wet phase separation and salt leaching techniques. In this work, the possibility of partial degradation using simulated body fluid (SBF) at a temperature of 36 $\pm$ 2 °C (in vitro degradation) was evaluated. The mechanical, morphological, and physical properties of the scaffolds were determined, among others, by scanning electron microscope (SEM), Fourier-transform infrared spectroscopy (FT-IR), and contact angle examination.

2. Results and Discussion

2.1. Morphology Characterization of the Membranes before Degradation

Scaffolds as a temporary cellular environment allow cells to function as in a native tissue. However, they should meet a certain set of requirements, including the suitable architecture, or physicochemical and biological properties. This is essential for proper cell growth, which involves adequate tissue regeneration [30–32,35,39,43]. The morphology of the membranes was characterized by SEM, which made it possible to obtain information regarding both the surface and cross-section of each membrane.

The SEM images of M1-M5 membranes are shown in Figures 1 and 2. The reference membranes M1–M2 were made by the phase inversion method, without the addition of NaCl or nonwoven gelatin. Their structure was compact, and this was particularly noticeable for M2. They were made to observe pure PES and PUR polymers without adding macropores generators. In contrast, the M3–M5 (Figure 2) scaffolds adequately met the conditions necessary for cell culture. They were made using a macropore generator—NaCl and gelatin nonwoven. The top layer was perforated, allowing cells to enter the membrane. Their cross-section was characterized by a unique spatial structure formed by an interconnected network of pores [7,36,62]. Their main task, in addition to keeping cells in space, is to provide an environment as similar as possible to that naturally occurring in the human body. It is expected that using a scaffold of proper architecture will ensure that the cells cultured within the scaffold will have the right shape, and their metabolism and vital functions will be normal. The bottom layer, on the other hand, was compact, which should prevent cells from escaping. In addition, micropores were visible in the cross-section of a membrane formed by an addition of PVP 10 kDa and Pluronic F127 precursors of pores (Figure 2: M3CSA, M4CSA). They affect oxygen and nutrient permeation and metabolite removal [8,9,34,35].

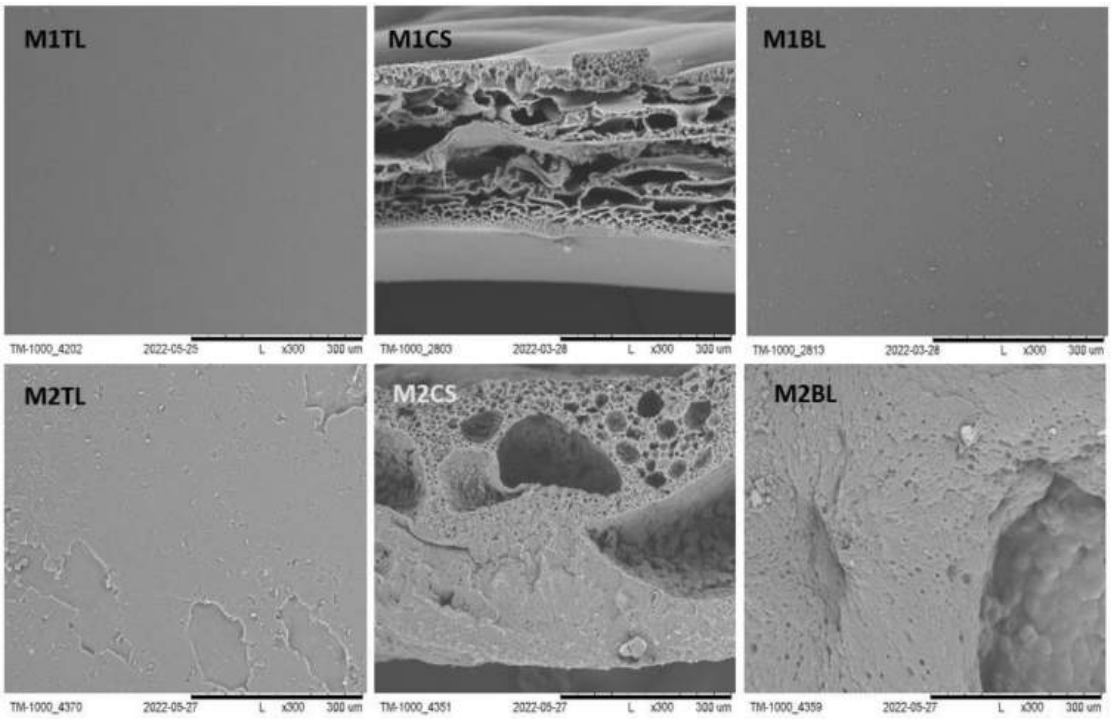

Figure 1. The SEM photomicrographs of the M1 and M2 membranes. TL—Top layer; CS—Cross section; BL—Bottom layer. Scale bars: 300 µm.

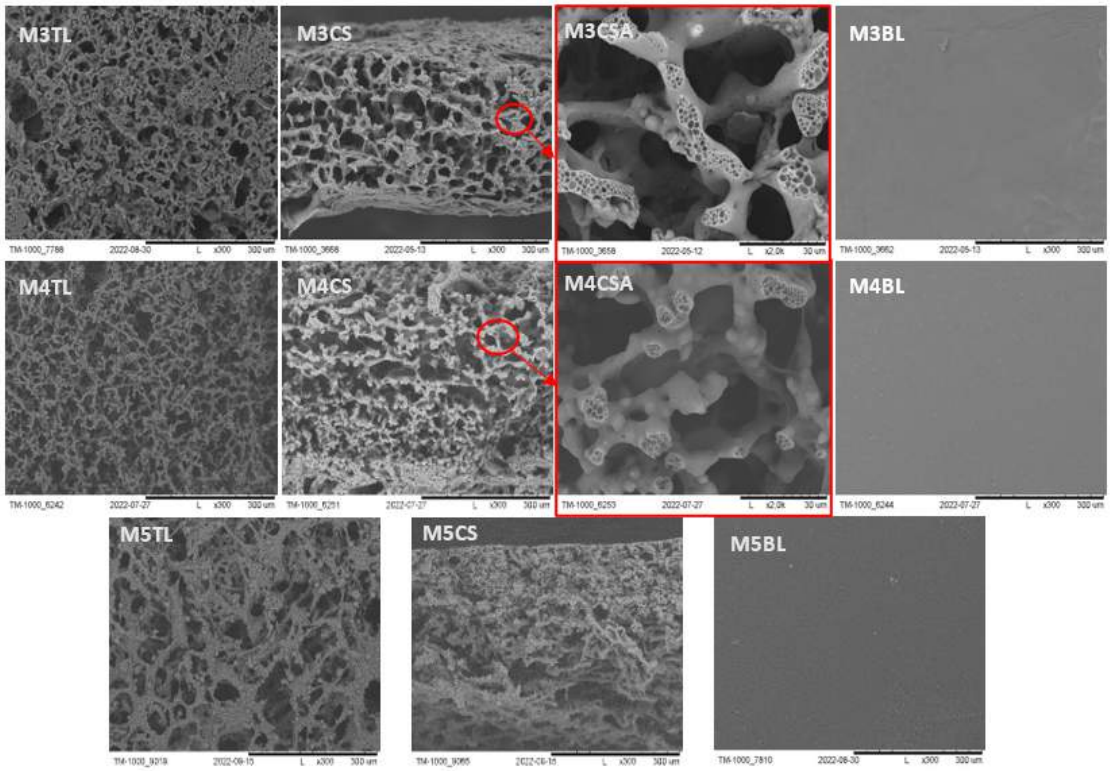

Figure 2. The SEM photomicrographs of the M3 and M5 scaffolds. The imagines of M3CSA and M4CSA show a magnification of the micropores that occur in the walls in cross-section (red circles). TL—Top layer; CS—Cross section; BL—Bottom layer. Scale bar: 2000 µm—M3CSA, M4CSA; 300 µm—others.

2.2. Degradation Studies

2.2.1. SEM Imaging and pH Measurement during and after Degradation

In vivo experiments using an animal model are not always available to elucidate the mechanism of membrane degradation. Instead, various in vitro experiments have been designed to simulate membrane's degradation in vivo. In this work, hydrolytic degradation was carried out using three fluids. The study investigated how the degradation of the obtained membranes proceeds. Whether it is possible and how it proceeds over four weeks in different liquids.

Degradation was performed in 1 M NaOH, Hank's balanced salt solution (HBSS), and a simulated body fluid (SBF). It was carried out in an incubator, at 36 ± 1 °C. Membrane weight tests were performed weekly (Figures 3–5, while FT-IR (Section 2.7), pH (Table 1), and SEM observations were performed after 2 and 4 weeks. The SEM photomicrographs of the membranes after 2 and 4 weeks of degradation are available in the Supplementary Materials (Table S2). For the facilitation of discussion, the abbreviations of MxYy were used, where x denoted the membrane number, Y denoted the degradation fluid (where Y for SBF was B; for HBSS, H; and for NaOH, N), and y denoted the number of the week. For example, M1B2 indicates the degradation of the membrane M1 in SBF after two weeks.

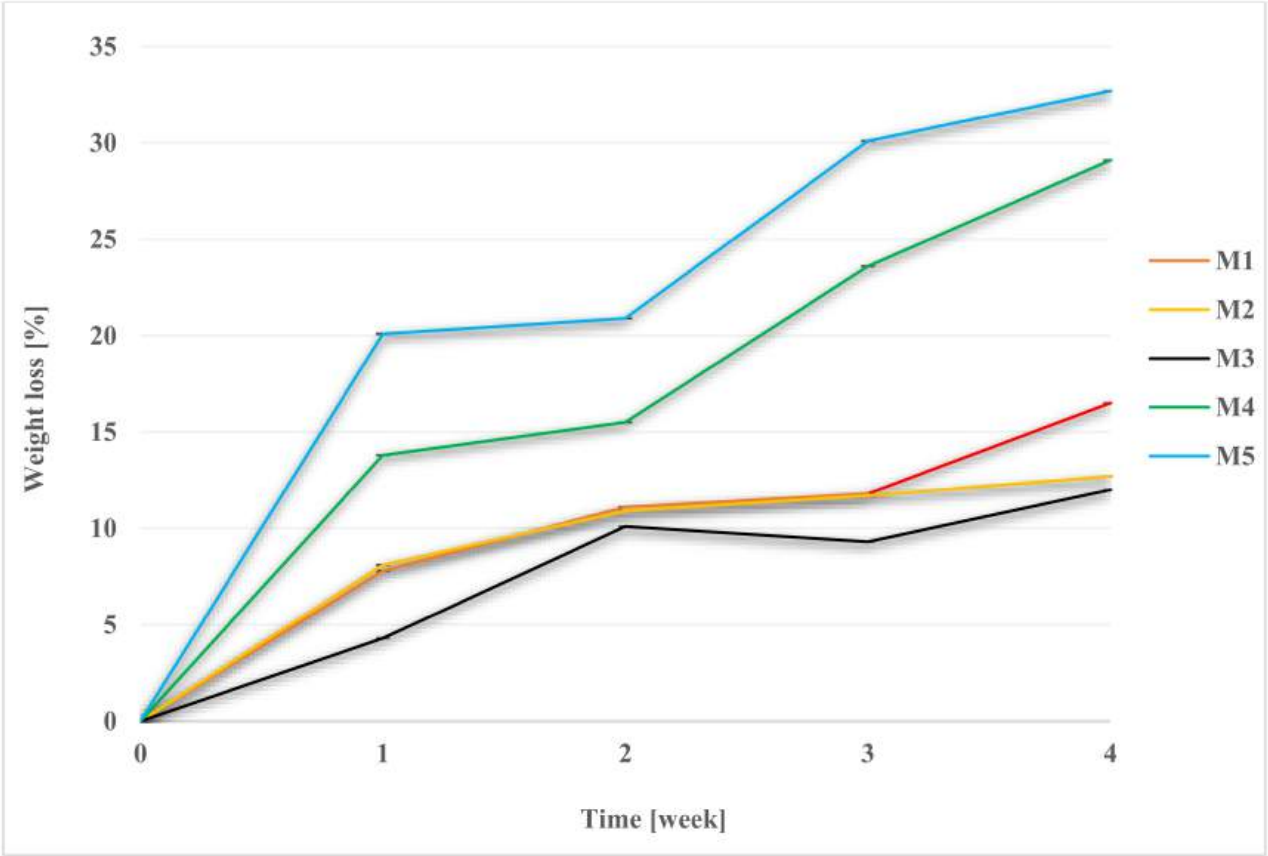

Figure 3. Weight loss of membranes during degradation in SBF.

After 2 weeks, cracks were noticeable on the membranes, with the exception for the M5H2 and M5B2 scaffolds, where no changes were found. After 4 weeks, changes were visible in all cases, especially for M2N4, M3N4, and M5N4, where destruction had occurred almost completely. Small fragments and crumbs remained of these scaffolds. Even the membranes made of PES (M1) and the M4 scaffold, with twice the advantage of PES over PUR, were very brittle after 4 weeks, and they were prone to fracture.

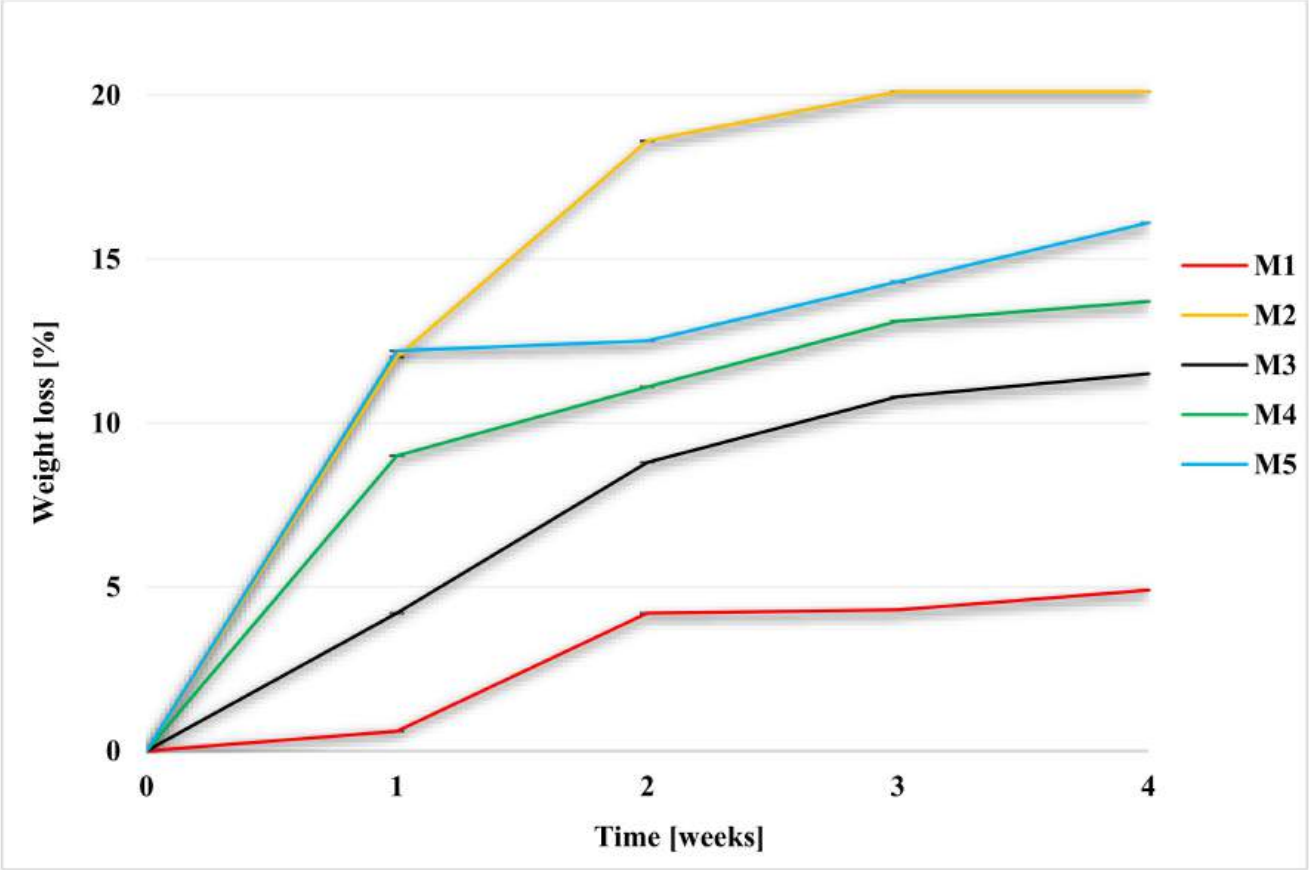

Figure 4. Weight loss of membranes during degradation in HBSS.

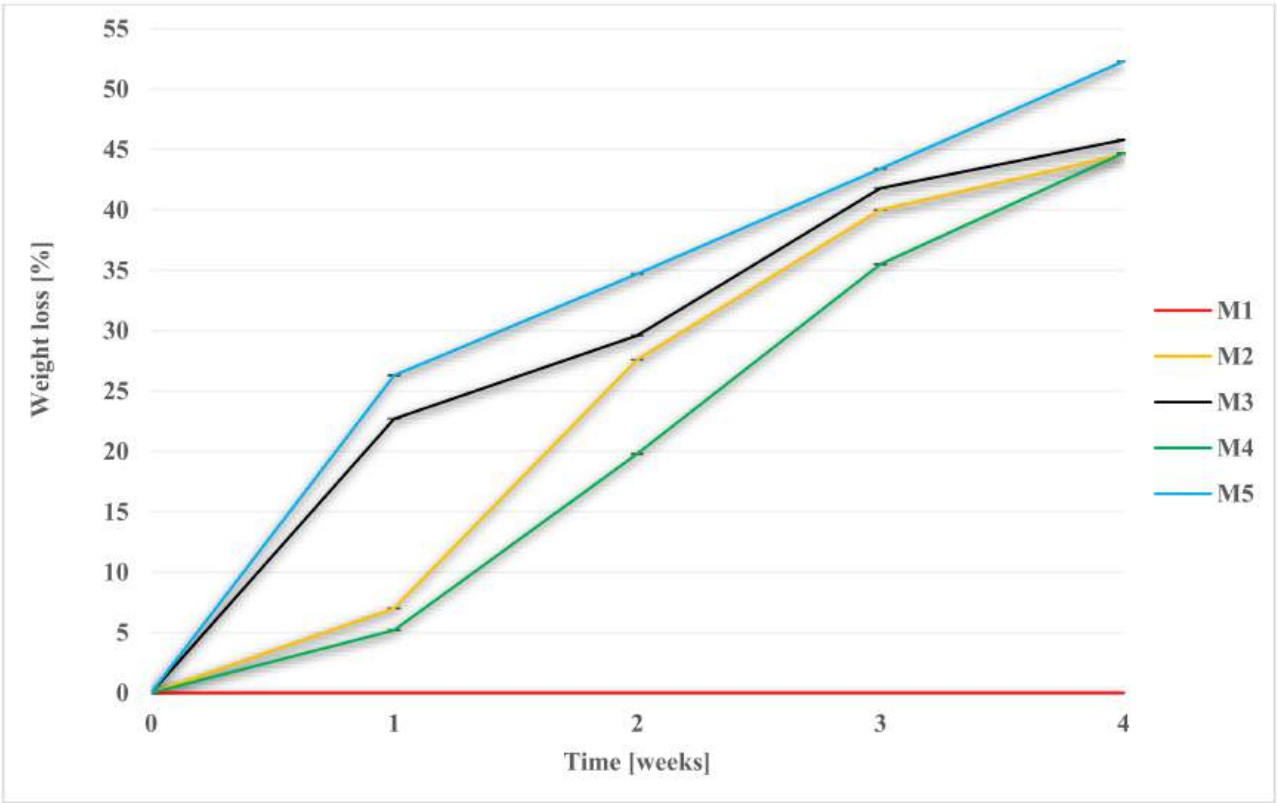

Figure 5. Weight loss of membranes during degradation in NaOH.

Table 1. The pH of degradation media before and after 2 and 4 weeks of degradation.

Fluid	SBF					HBSS					NaOH				
Membranes	**M1**	**M2**	**M3**	**M4**	**M5**	**M1**	**M2**	**M3**	**M4**	**M5**	**M1**	**M2**	**M3**	**M4**	**M5**
Initial pH			7.31					7.54					13.50		
Average pH after 2 weeks	7.42	7.47	7.67	7.05	7.30	7.39	7.26	7.10	7.58	6.98	13.80	13.89	13.99	13.78	13.84
Average pH after 4 weeks	7.68	7.66	7.35	7.47	7.50	7.37	7.49	6.87	7.24	7.84	13.52	13.47	13.77	13.57	13.45

As can be seen in Table 1, the pH changed during and after degradation. No high decreases or increases in pH were noted, which could affect the organism [72–74].

During SEM observations, attention was focused on the presence of spheroids on the membranes after 4 weeks of degradation in SBF and HBSS, where by far the highest amount was observed for the M4 scaffold (Figure 6). From the literature review, it was noted that these spheroids could be a result of apatite formation on the membranes [75–78].

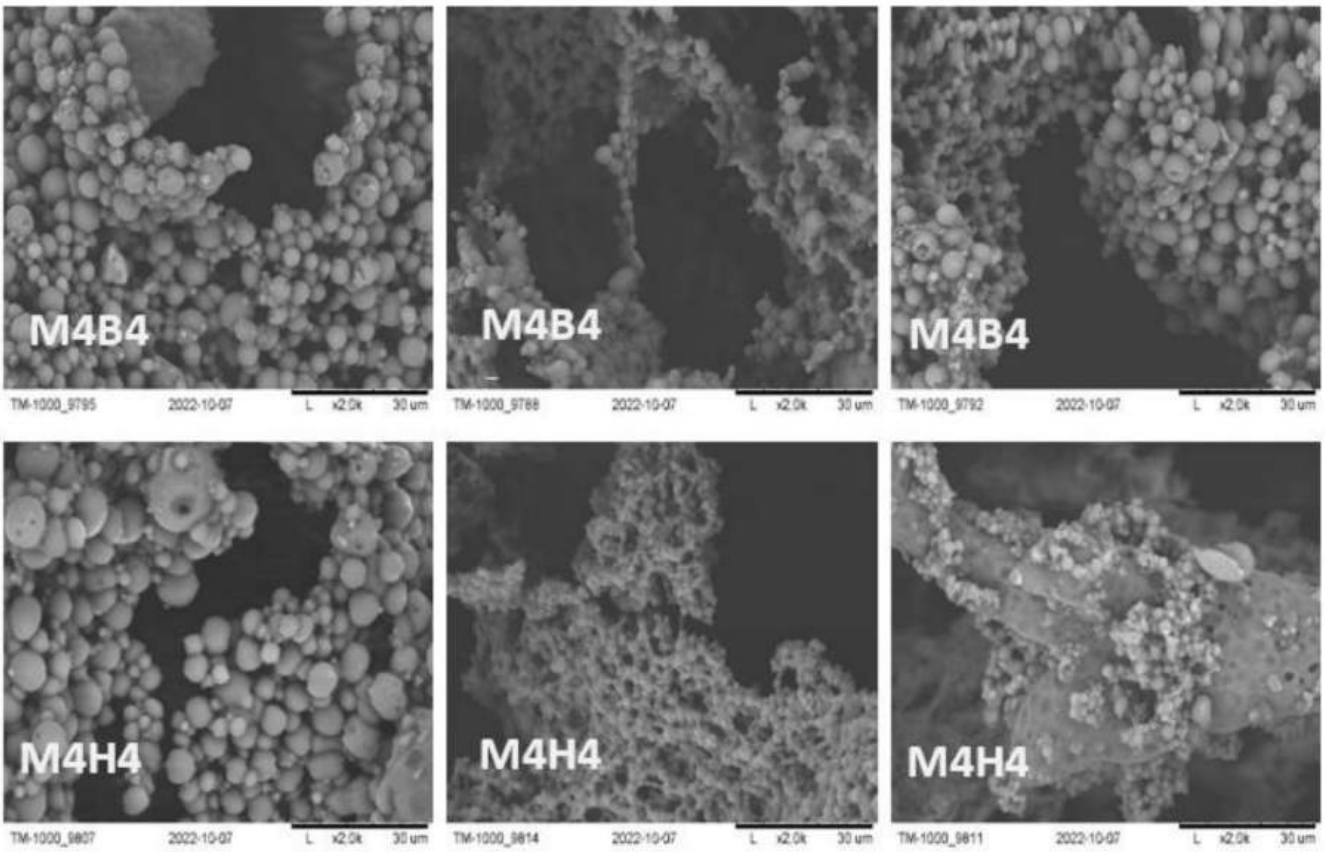

Figure 6. SEM micrographs of spheroids on scaffold M4 after 4 weeks degradation in SBF and HBSS.

2.2.2. Weight Loss during Degradation

Scaffold weights were measured each week. After removal from the medium, the samples were properly rinsed in redistilled water and dried at 30 °C. The graphs (Figures 4–6) show the percentage of mass loss of the membranes during four weeks of degradation in each media.

For each of the membranes, a weight loss during degradation was noted. The results for M2 membrane, made of PES, were far from expected, as even a mass loss of up to 12.7% ± 0.0002 in SBF was noted for it, while for HBSS it was 4.9% ± 0. Moreover, the M4 scaffold, in which the weight ratio of PES was twice that of PUR, showed significant

weight loss: 29.1% ± 0.001 in SBF and 13.7% ± 0.001 in HBSS. Among the M3–M5 scaffolds, the lowest percentage of mass loss was for M3—12% ± 0.001 in SBF and 11.5% ± 0.0001 in HBSS.

The highest percentage of mass lost during degradation was recorded for scaffold M5, in which there was a two-times weight ratio advantage of PUR over PES. In the SBF medium, it was 32.7% ± 0.0007, while in HBSS, it was 16.1% ± 0.0004. In a previous study in a Ph.D. thesis by Tomasz Jakutowicz, the absence of a PES scaffold was observed during animal model testing after 6 months of implantation into the joint [79]. The study observed PES degradation in SBF and HBSS, where there is no information on that topic in the literature. The degradation time in SBF, which is most closely related in composition to blood plasma, showed different degradation rates for scaffolds of different material composition. This showed that with the proper selection of the weight ratio of polymers, the degradation time can be controlled [42,43].

The situation was different for the hydrolysis experiment in 1 M NaOH. The highest percentage of sample mass loss caused by hydrolysis after 4 weeks was observed for the M5 scaffold, and it was 52.3% ± 0.0014, whereas for M1, no change in mass was observed. For M2, M3, and M4 membranes, the mass loss was 44.6% ± 0.0034, 45.8 ± 0.0029, and 44.7 ± 0.0172, respectively. M3 and M5 scaffolds were completely deconstructed after 4 weeks. Small pieces and crumbs remained of the membranes. Changes in the membranes were noticeable in the case of each material. After 4 weeks, membranes were brittle and friable, even in the case of M1.

Hydrolysis and biodegradation of capillary membranes made of a mixture of PUR and polysulfone (PSf) have been performed in previous works using 1 M NaOH [60,63] and *E. coli* [64]. The (bio)degradability of synthesized PUR was demonstrated. In this work, in vitro biodegradation was presented using simulated physiological fluids, which have not been used before relative to PES, and this kind of PUR materials, which shows the novelty of this research. Further research should be conducted in this direction.

2.3. Estimate of Pores in Scaffolds by Computer Analysis of SEM Images

2.3.1. Pore Distributions and the Total Aera of Pores for Scaffolds before Degradation

It is impossible to determine exactly what numerical changes occur in pore size by evaluating SEM images analyzed by comparing two pictures with the human eye. It is not a precise method. Therefore, to more accurately assess changes in pore size, SEM micrographs were analyzed using MeMoExplorer ™ Software [80].

Figure 7 presents the area of pores in eight size classes for the cross-section (CS) and the top layer (TL) of scaffolds. The results show the average percentage of appropriate pore size to the whole SEM photomicrographs size.

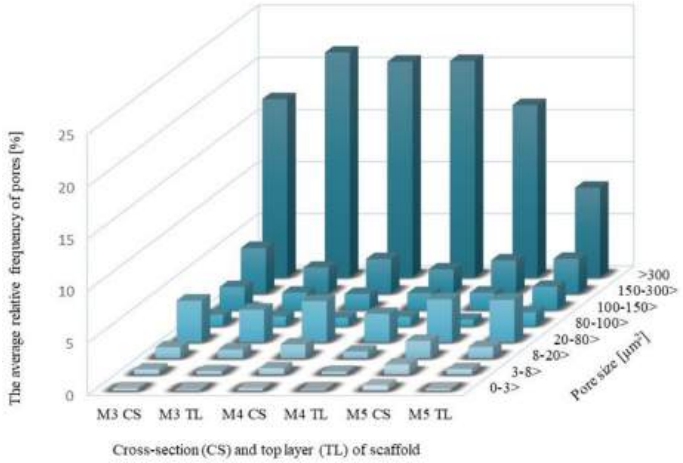

Figure 7. The average relative frequency of pores in eight size classes for cross-section (CS) and the top layer (TL) of scaffolds.

In each scaffold, the largest number of pores were of those with an area over 300 μm^2. This was noticeable in the case of cross-section (CS) and the top layer (TP). The highest percentage of these pores was recorded for the top layer of M3, 21.54% ± 10.89, and for the cross-section of M4, 20.66% ± 11.22, while the top layer for M4 was 20.73% ± 9.49. In contrast, the result for cross-section for M3 was lower than M4 at 17.08% ± 5.61. The lowest percentage of pores above 300 μm^2 was recorded for M5, 16.51% ± 7.72 for cross-section, and 8.58% ± 5.46 for the top layer. The 150–300 μm^2 range of pores were relatively frequent at 2.48–4.37%, and the 20–80 μm^2 pores were in the range of 4.1–2.7%. The pores with an area of 0–3 μm^2 turned out to be the least common, ranging from 0.09–0.51%.

2.3.2. Total Area of Pores after Degradation

Next, the data on the total area of pores for scaffolds before and after degradation (Figures 8–10) were calculated. The highest percentage of the total area of pores before degradation was obtained for the M4 scaffold cross-section (32.33% ± 2.56), while for the surface, it was recorded for M3 (30.88% ± 9.04). The total area of pores for M4 on the top layer was slightly lower than M3 (29.18% ± 5.94), while the percentage for the M3 cross-section was 30.38% ± 3.76. The lowest percentage of the total area of pores was for M5: for the surface, it was 21.20% ± 4.69, and for the cross-section, it was 29.14% ± 5.42.

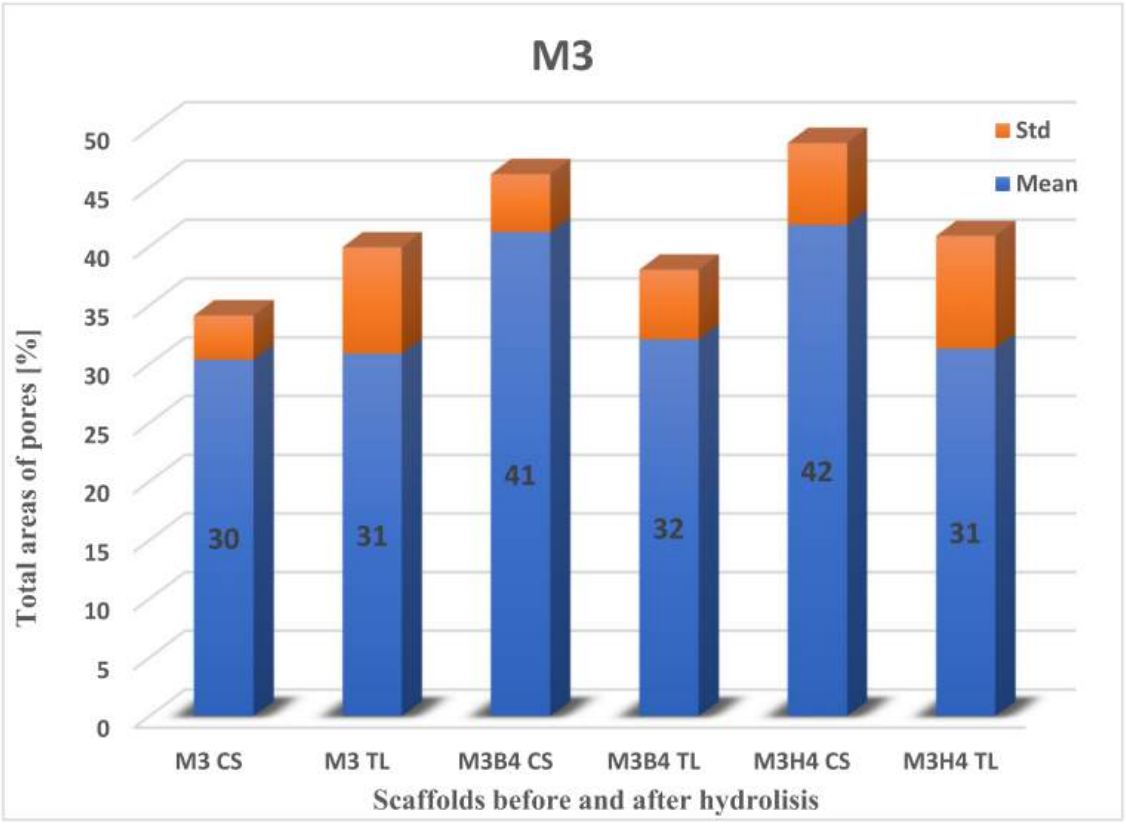

Figure 8. The total area of pores to the whole SEM image size for cross-section (CS) and the top layer (TL) of the M3 scaffold. B—degradation in SBF; H—degradation in HBSS.

The largest change in the area of pores was recorded during hydrolysis in 1 M NaOH. For the cross-section of the M4 scaffold, 55.79% ± 17.40 (23.46% increase) was obtained, and for the top layer, 47.96% ± 12.47 (18.78% increase). Unfortunately, a comparison of the M4 scaffold against the M3 and M5 membranes was not obtained, because of their destruction. The difference in the change in the number of pores in the surface and cross-section is shown in Table 2.

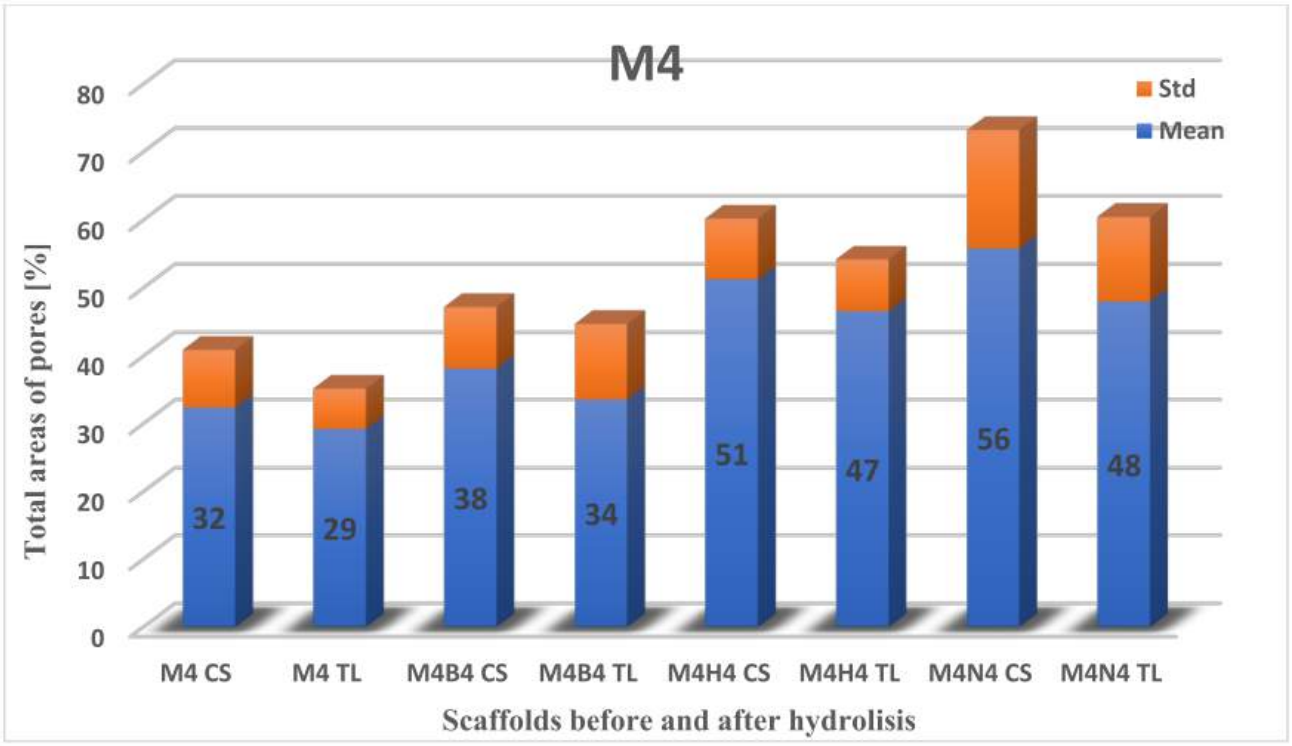

Figure 9. The total area of pores to the whole SEM image size for cross-section (CS) and the top layer (TL) of the M4 scaffold. B—degradation in SBF; H—degradation in HBSS; N—degradation in NaOH.

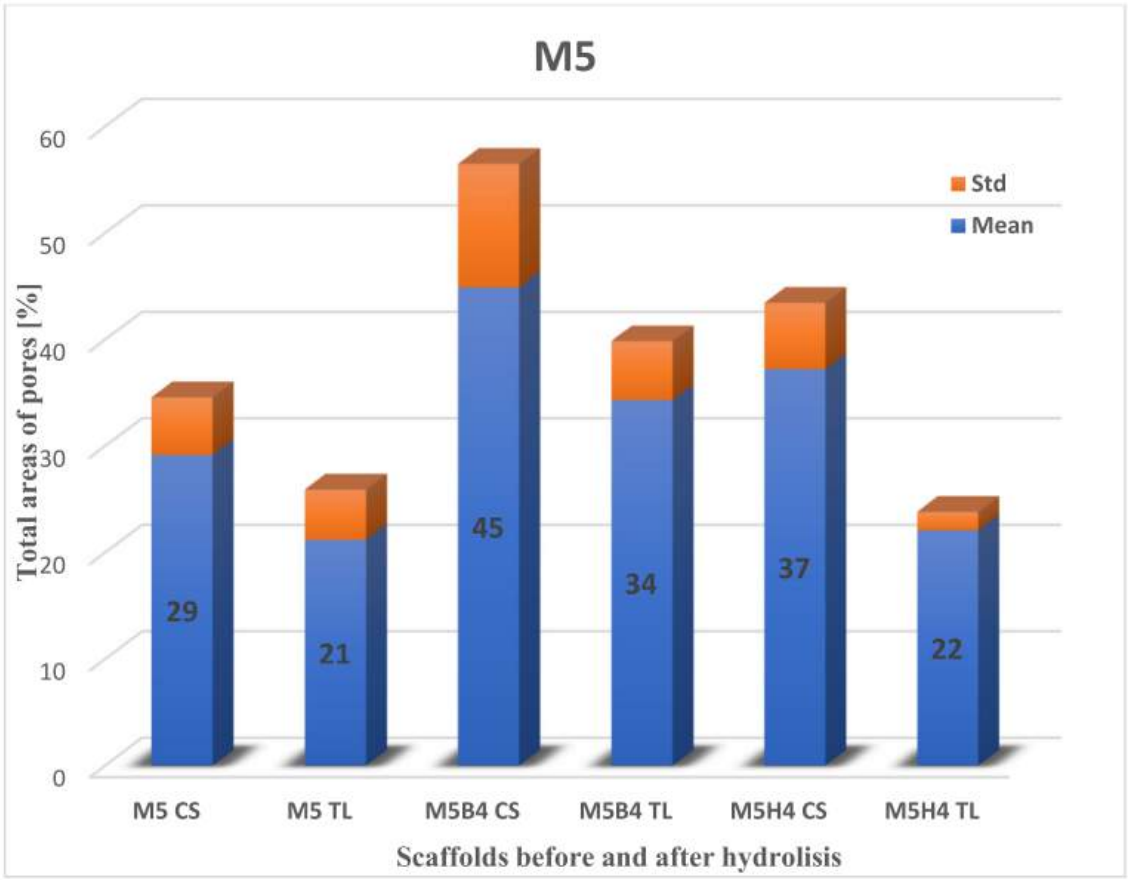

Figure 10. The total area of pores to the whole SEM image size for cross-section (CS) and the top layer (TL) of the M4 scaffold. B—degradation in SBF; H—degradation in HBSS.

Table 2. The difference in the total area of pores [%] for scaffolds before and after degradation in SBF and HBSS fluids.

Scaffold	Difference in HBSS Medium [%]	Difference in SBF Medium [%]
M3 CS	11.47	10.84
M3 TL	1.01	1.23
M4 CS	18.89	5.80
M4 TL	17.36	4.33
M5 CS	8.06	15.75
M5 TL	0.89	13.10

The highest difference in the total area of pores was noticed for scaffold M4 in HBSS fluid for the cross-section and the top layer. The situation was different for the SBF medium, where it was observed for scaffold M5 (Table 2). The lowest difference was for the cross-section of the M4 scaffold in SBF (5.80) and the top layer of the M5 scaffold in HBSS (0.89).

A comparison of the area of pores > 300 um in the cross-section was made before and after degradation in physiological fluids (Table 3). The difference was noticeable mainly in the M5 scaffold in SBF. The increase in pores area was twofold. This information suggests that space was freed up in the scaffolds as a result of increased surface area in the largest pores. The difference was mainly noticeable for the M5 scaffold in SBF. The increase in pore area was twofold. In contrast, it was the smallest for the M4 scaffold in SBF [43].

Table 3. Total areas of pores > 300 μm^2 before and after degradation.

Scaffold	Total Area of Pores > 300 μm^2 before and after Degradation		
	Before Degradation	After Degradation in HBSS	After Degradation in SBF
M3 CS	17.08 ± 5.61	32.11 ± 9.11	31.39 ± 6.26
M4 CS	20.66 ± 11.22	44.75 ± 10.46	24.82 ± 13.68
M5 CS	16.51 ± 7.72	27.33 ± 7.72	36.50 ± 9.12

2.4. Porosity of Membranes

The study also determined the porosity of the membranes before and after degradation. The diagram (Figure 11) shows the porosity of the membranes before degradation. The calculations were made using Equation (2). The highest porosity was recorded for scaffold M4 (87.37% ± 2.74), while the lowest porosity was obtained for membrane M2, which was only 6.74 ± 13.54.

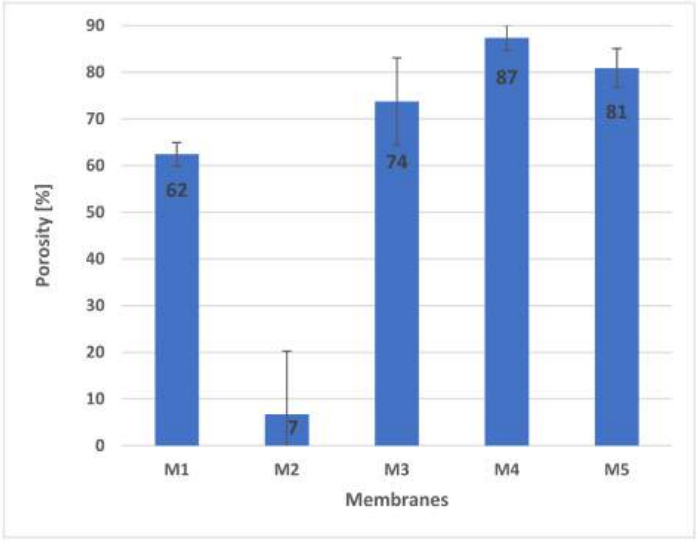

Figure 11. Porosity of membranes before degradation.

Figure 12 shows the porosity of the membranes after degradation and the difference (Diff) that was measured before and after degradation. The highest porosity was recorded for the M4 scaffold in NaOH (94.99% ± 0.88), where the difference was 7.62%. The largest difference in porosity was calculated for the M2 membrane in NaOH, where the porosity was 80.73% ± 4.45. The increase in porosity was 53.99%. There was a slight increase in porosity for M3H4 and M4B4, by 0.39% and 0.75%, respectively. Changes in pore size after degradation were shown in porosity and SEM image analysis. This is very important information, as it indicates that during degradation, space is released for newly forming tissue [60,62,64,70].

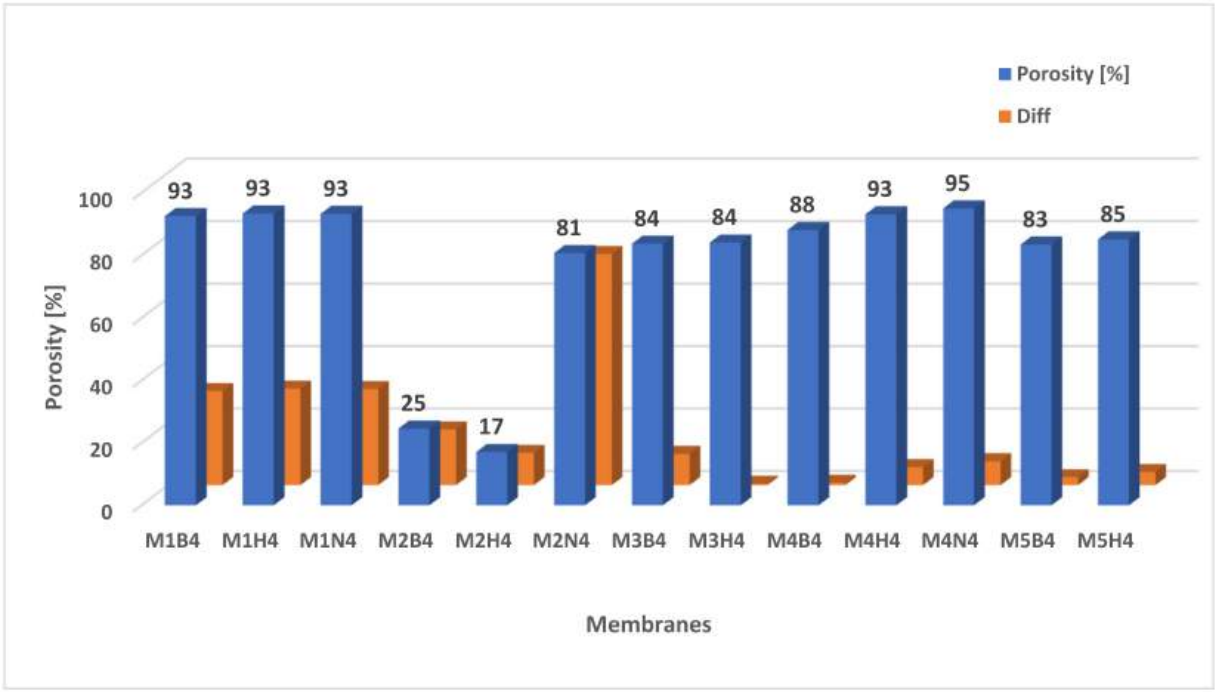

Figure 12. The porosity of membranes after degradation and difference (Diff) between membranes before and after hydrolysis.

2.5. Wettability of Membranes

An essential feature of cellular scaffolds is their hydrophilicity. This parameter determines the possibility of migration of body fluids, water, and nutrients into the interior of the scaffolds, and it thus defines the vital functions of the cells developing in them [81–83]. PUR and PES polymers, due to their chemical structure, are hydrophobic. Because of a concern that the scaffolds would also be hydrophobic, it was decided to test their swelling ratio using PBS and the contact angle using deionized water. The M1 and M2 reference membranes and M3, M4 and M5 scaffolds were investigated, which from the point of view of cell culture would meet the requirements for cell culture.

2.5.1. Swelling Ratio

Scaffolds M3–M5 showed very good saturation with hydrophilic substance PBS in contrast to reference membranes M1 and M2 (Figure 13).

This shows that the additives used during the preparation of the scaffolds (pore precursors) not only increased the size and number of pores and porosity, but also the property of the scaffolds. The number of pores and their size increases the absorbency of the samples, which has an impact on degradation. The highest swelling ratio was observed in scaffold M4: 506.02% ± 60.31 after 3 h and 550.70% ± 57.03 after 24 h. Scaffold M3 (494% ± 77.83 after 3 h and 502.38% ± 62.70 after 24 h) showed similar absorbability. The M5 scaffold showed a swelling ratio of 263.81% ± 36.46 after 3 h and 293.43% ± 28.08

after 24 h. The lowest saturation value came out for reference membranes M1 and M2 (57.11% ± 10.35 and 82.44% ± 11.85, respectively, after 3 h), which were obtained without the use of non-woven gelatin and NaCl. In these tests, the results after 3 h and 24 h were similar. These studies confirm the correlation between scaffold morphology and saturation, which also has an impact on scaffold degradation. Namely, the porosity and swelling ratio were the highest for M4, which also resulted in its increased porosity and size of pores after degradation (Figures 11–13) [81–83].

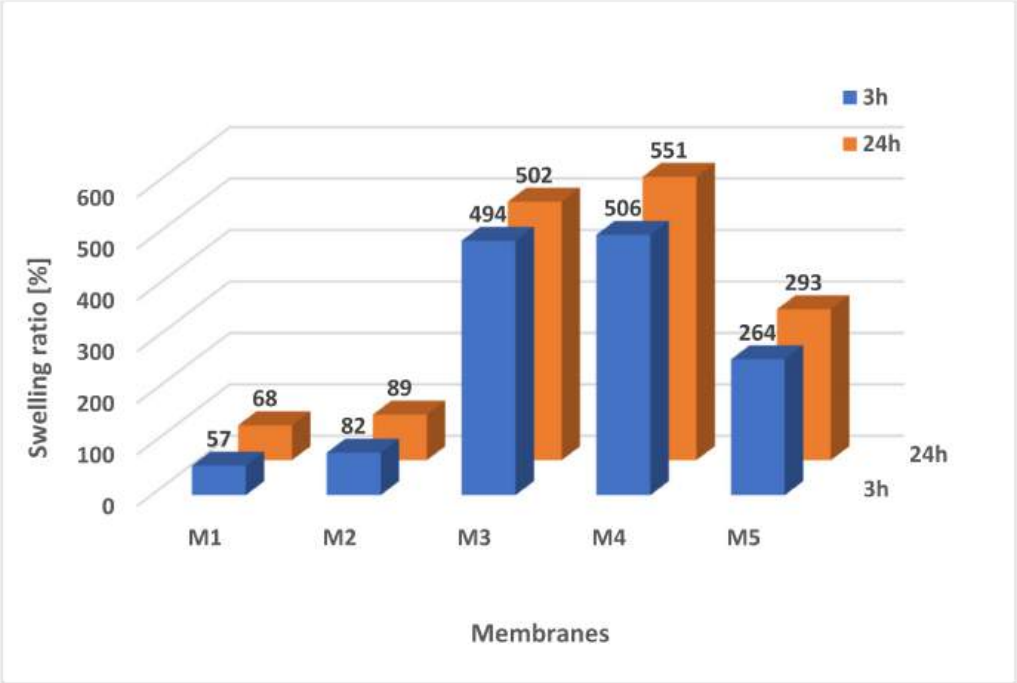

Figure 13. Swelling ratio of membranes in PBS after 3 and 24 h.

2.5.2. Contact Angle

The nature of the membrane surface was studied by measuring the contact angle. Figure 14 presents a diagram showing the average wetting angle (Ave) for the membranes along with the standard deviation (SD). In addition, photos of the membrane surface with a water droplet are presented above the diagram. The contact angles of all the membranes were below 62°, which means that each membrane had a hydrophilic surface.

For M1 and M2 membranes, the wetting angle was 54.45° ± 1.40 and 55.67 ± 1.12, respectively. According to the literature, the value of the pristine PES membrane is 60–65 [84,85]. In the study, the M1 membrane had a smaller contact angle because using the pore precursors (poly(vinylpyrrolidone) and Pluronic) improves hydrophilicity. This is often used to refine the hydrophilic properties of membranes [8,85]. The higher contact angle was obtained for M5 (61.84 ± 0.81). The most hydrophilic scaffold proved to be M4, 51.26° ± 1.06, and M3, which was 30.02 ± 1.10. These results were similar to the swelling ratio (Section 2.5.1), where the lowest outcome was for M5.

Measurements were also made for the membranes after degradation. In each case, the water droplet was soaked in very quickly (Figure 15). Adsorption of water by the scaffold determines the permeation of proteins, the improved release of nutrient ions (cell nutrition), or cell-surface adhesion. This is essential for regulating cell metabolic functions. In addition, polymer degradation is dependent on the surface properties of the polymer. Hydrolytic degradation does not occur until water enters the scaffold [86–88].

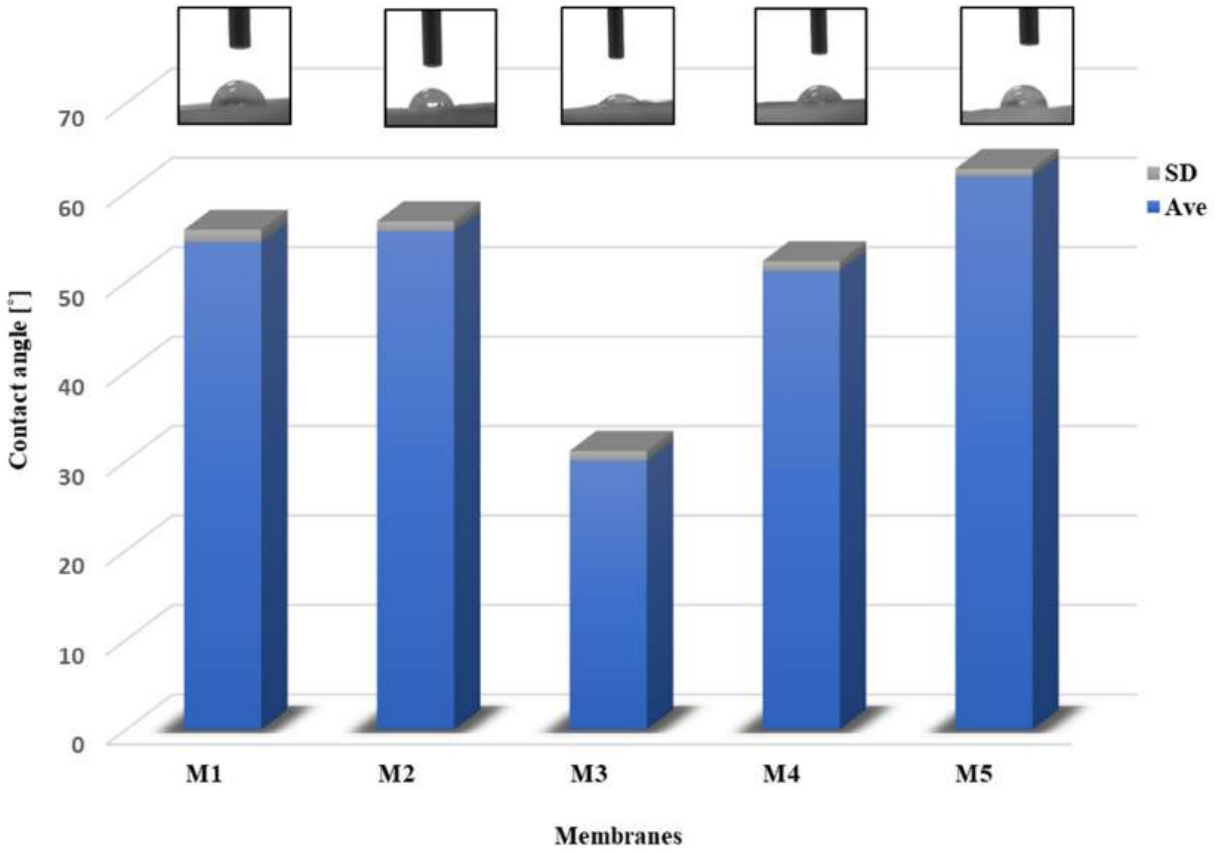

Figure 14. Static water contact angle of membranes. Above the diagram, photos of the surface of the membranes with a water droplet were presented.

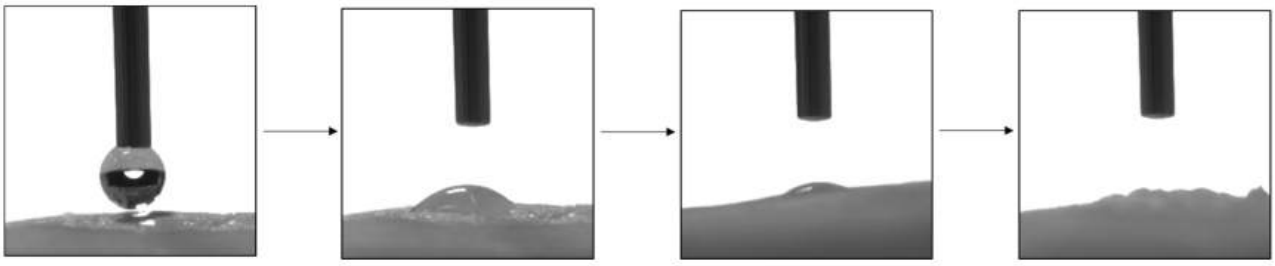

Figure 15. The surface of the M5 scaffold during water contact angle. The presented membrane was after 4 weeks of degradation in SBF fluid.

2.6. Mechanical Properties

It is important to consider the mechanical properties of scaffolds for cartilage regeneration. This is an essential parameter for the proper functioning of the membrane in the joint and should be close to the strength of the natural tissue. Young's modulus value of human articular cartilage in tension is approximately 10 MPa [89,90]. The mechanical tests were performed for each membrane (Figure 16). All tested scaffolds showed good mechanical properties (E > 10 MPa). The reference membranes showed a very high Young's modulus, where the porous scaffolds M3-M4 have a score 3.5 times lower, but they do not fall below 10 MPa. It means that they would certainly withstand the conditions experienced in the knee joint. The PES material showed greater strength, as proven by measurements for M1 and M4 membranes. By changing the weight ratio of PUR/PES (Table 4), the value of Young's Modulus of membranes can be controlled. It could be seen that by increasing the PES polymer, the mechanical strength increased as well. Additionally, it was observed that the less porous membranes had better properties.

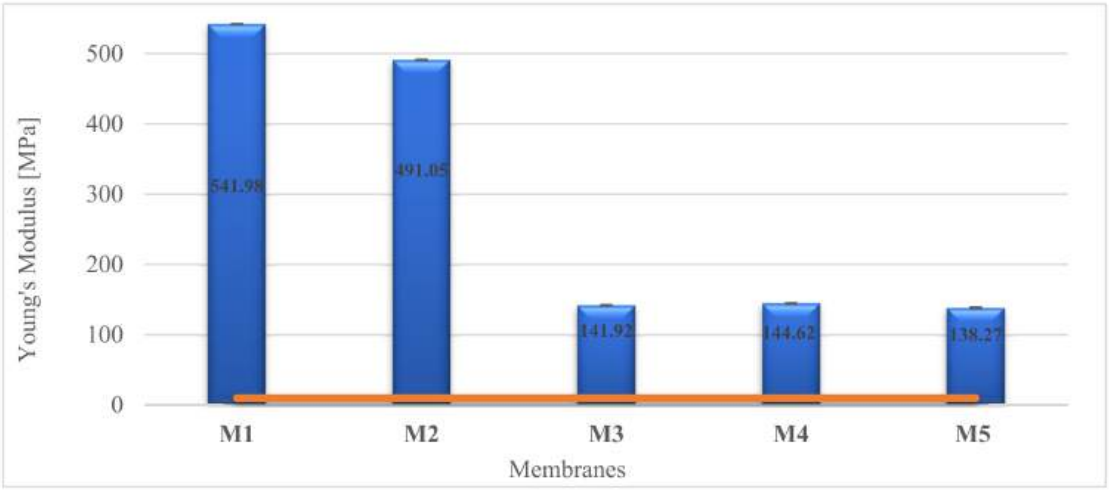

Figure 16. Mechanical properties of membranes. The red line shows the required Young's Modulus for human cartilage.

Table 4. Weight ratios of PES and PUR polymers in the M3–M5 scaffolds.

Scaffold	PES:PUR Weight Ratios
M3	1:1
M4	2:1
M5	1:2

2.7. FT-IR Analysis

The membranes were characterized by FT-IR to study changes after 2 and 4 weeks of degradation. Figure 17 shows the spectra of the membranes before degradation. It can be seen that there were differences in the intensity of peaks corresponding to wavelengths in the 1800–1500 cm^{-1} range (Figure 17, blue square).

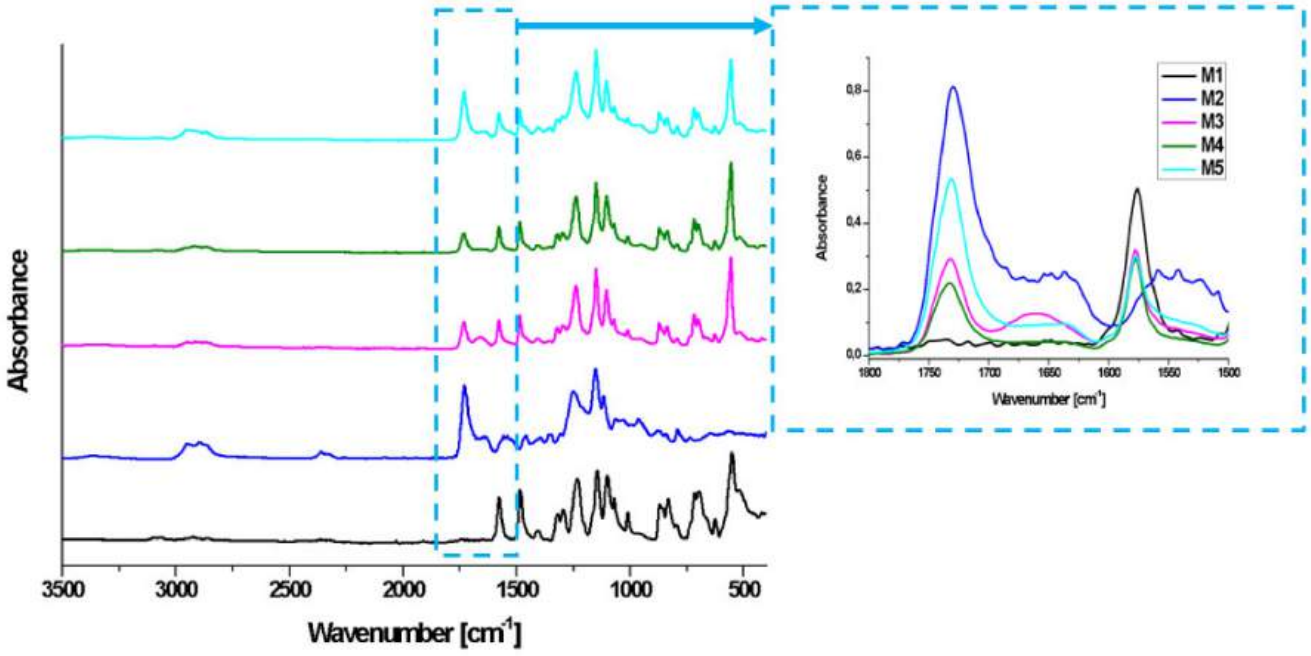

Figure 17. FT-IR analysis of membranes before degradation. In the blue square, the spectra were superimposed and magnified.

The difference in absorbance was observable for the peak at 1730–1740 cm^{-1}, assigned to the C=O functional group derived from ester bonds. The peak had the highest absorbance for membrane M2, while it was not noticeable for M1. The intensity of the peaks decreased with PUR weight ratio (Table 4). The peaks at 1700–1630 cm^{-1} can be attributed to carbamate groups. The peaks in the range of 1600–1570 cm^{-1} represent the aromatic bands, the C-S group characteristic of the PES polymer, and the amine groups, which is occurring in PUR [85,91,92].

Figure 18 shows the spectra of the M1 membranes before and after degradation. There were no visible changes in any of the fluids after 4 weeks of degradation. It indicates that the membrane did not change chemically, only physically—the structure was more brittle, especially after degradation in NaOH.

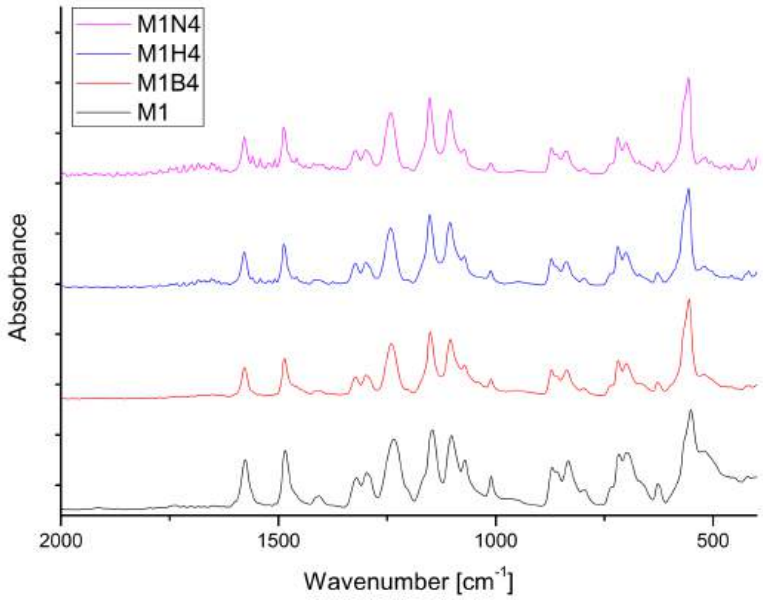

Figure 18. FT-IR spectra of M1 membrane before and after 4 weeks of degradation in each medium.

Changes in the membranes M2–M5 after degradation were noticeable. Both disappearance and increase in the absorbance of peaks at the 1800–1600 cm^{-1} range were observed. The spectra of M2–M5 membranes before and after degradation are presented in the Supplementary Materials. Changes were noted for the peaks at about 1730 cm^{-1} (ester bonds) and in the 1670–1620 cm^{-1} range (carbamate group).

The disappearance of the ester group was visible after two weeks for membranes M2, M4, and M5 in liquid NaOH. After four weeks, it is also noticeable for M3 in NaOH and M5 in HBSS liquid. Reductions in absorbance for the carbonyl group were observed for the M2–M5 membranes [74,76,93].

3. Materials and Methods

3.1. Materials

Chemicals used in our experiments, namely, Polyvinylpyrrolidone (PVP, M_n = 10 kDa), 1–Methyl-2-pyrrolidone (NMP), phosphate-buffered solution (PBS), Pluronic® F127, hydrochloric acid (HCl 70%), sodium bicarbonate ($NaHCO_3$), sodium azide (NaN_3), Tris ($(CH_2OH)_3CNH_3$), phenol red, monopotassium phosphate (KH_2PO_4), D-Glucose, disodium phosphate (Na_2HPO_4), and magnesium sulfate ($MgSO_4$), were acquired from Sigma-Aldrich (Steinheim in Germany). Sodium hydroxide (NaOH), dimethyl sulfoxide (DMSO), N, N-dimethylformamide (DMF), hexane, sodium chloride (NaCl), potassium chloride (KCl), magnesium chloride hexahydrate ($MgCl_2 \cdot 6H_2O$), calcium chloride ($CaCl_2$), potassium hydrogen phosphate trihydrate ($K_2HPO_4 \cdot 3H_2O$), and Sodium sulfate (Na_2SO_4) were purchased from POCh SA (Gliwice in Poland). Ethanol (EtOH 96%) was provided by

Linegal Chemicals (Warsaw in Poland). Polyethersulfone (PES) Ultrason E2020P (Figure 19) was acquired from BASF (Ludwigshafen am Rhein in Germany).

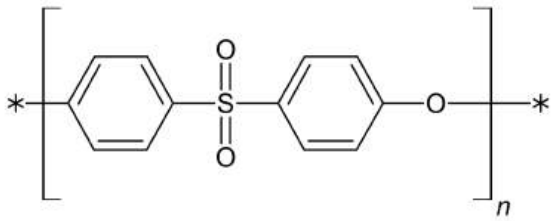

Figure 19. Structural formula of polyethersulfone (PES).

Polyurethane (PUR) (Figure 20), with ≈90% molar content of ester bonds in the structure, was synthesized using methods from articles [60,63,64].

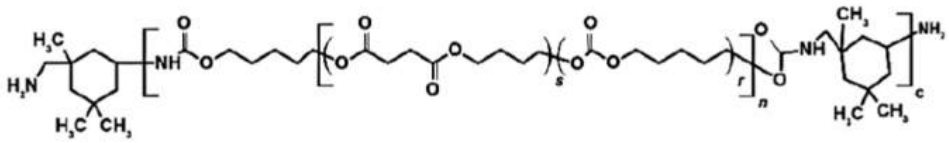

Figure 20. Chemical structure of polyurethane (PUR) [63].

The gelatin (from bovine skin, Type B, ~300 g Bloom, Sigma-Aldrich) nonwovens (Figure 21 were obtained by an electrospinning method in the Institute of Fundamental Technological Research PAS, according to the literature [94,95].

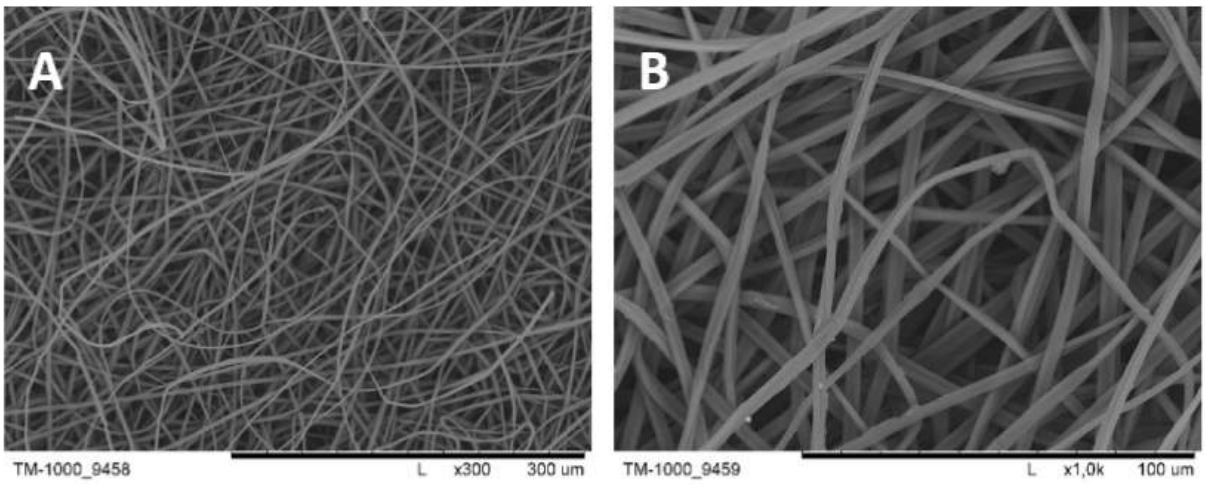

Figure 21. The photomicrographs of pork gelatin nonwovens obtained by an electrospinning method. Magnification: 300× (**A**) and 1000× (**B**).

3.2. Preparation of the Reference Membranes M1 and M2

Preparation of solutions:

- M1: The PES polymer was dissolved in DMF and DMSO (mixed in a ratio of 1:1) to obtain 8.6 wt.% concentration. Then, the 2.5 wt.% PVP 10 kDa and 2.5 wt.% Pluronic F127 were added with constant stirring at room temperature until a solution was achieved.
- M2: The PUR polymer was dissolved in DMF and DMSO (mixed in a ratio of 1:1) to obtain 8.6 wt.% concentration. Then, the 2.5 wt.% PVP 10 kDa and 2.5 wt.% Pluronic F127 were added with constant stirring at room temperature until a solution was achieved.

The M1 and M2 membranes were obtained by the phase method according to the scheme (Figure 22). An appropriately prepared solution was poured onto a glass base.

Both membranes were immersed in the bath with deionized water for up to 24 h. The deionized water (18.2 MΩcm conductivity) was obtained using the arium® comfort apparatus (Sartorius).

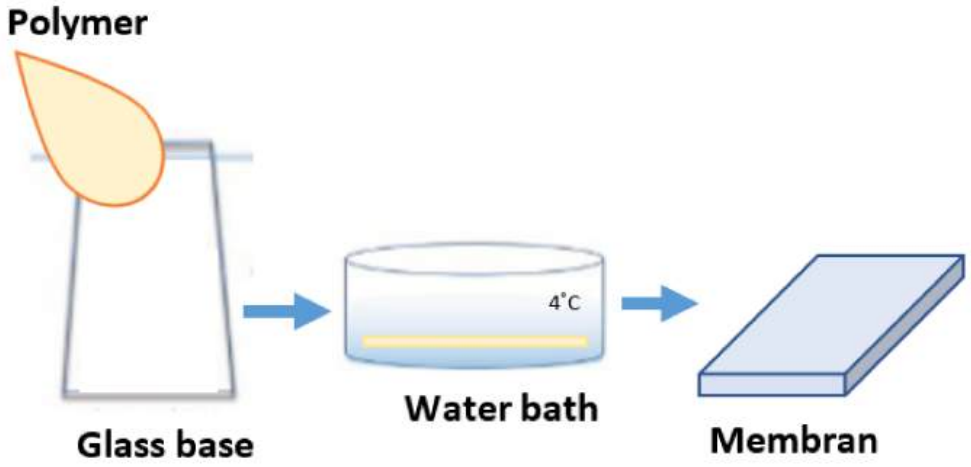

Figure 22. Scheme of preparation of references membrane M1–M2 by the wet-inversion method.

3.3. Preparation of the PUR-PES Scaffolds M3–M5 Using Gelatin Nonwoven

Scaffolds were obtained by combining wet phase inversion and salt leaching methods using different polymers (PES, PUR) weight ratios (Table 4). Solutions were prepared by dissolving the polymer PES, 2.5 wt.% PVP 10 kDa and 2.5 wt.% Pluronic F127 in DMF and DMSO at a ratio of 1:1. Then, PUR was then added to obtain 13.6 wt.% concentration. Three scaffolds (M3–M5) were obtained from the solutions using the appropriate weight ratios of PES and PUR, gelatin nonwovens, and NaCl salt (Figure 23). To obtain NaCl salt with suitable crystals, laboratory grinder FW177 (hemLand) and laboratory sieve with 200 µm mesh were used.

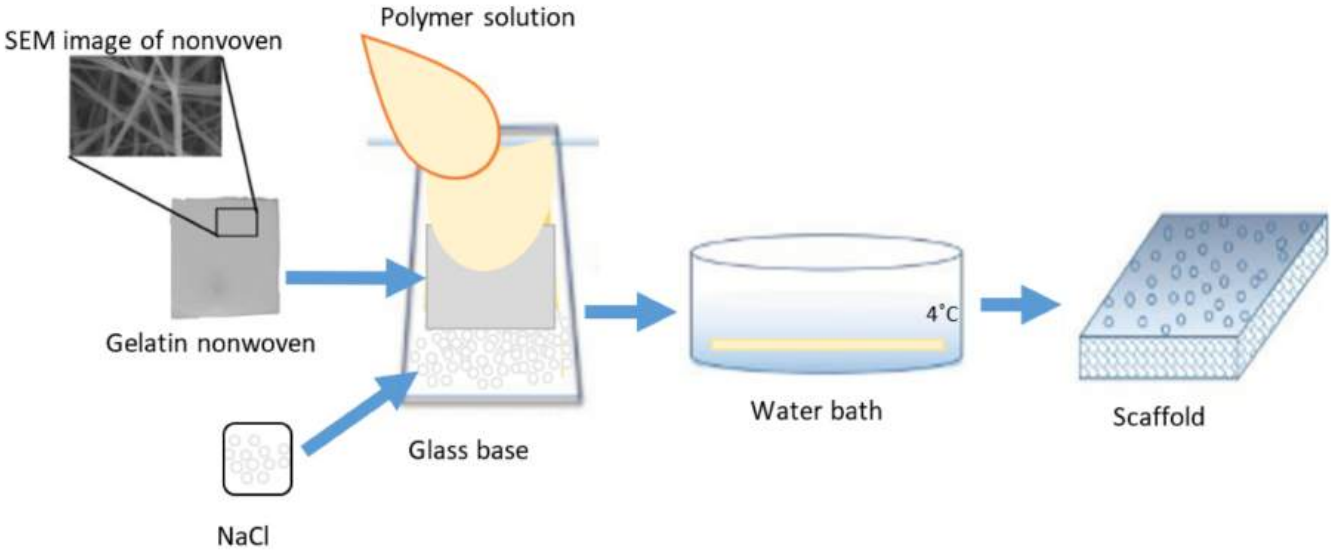

Figure 23. Schema of preparation of the M3–M5 scaffold.

The membranes were obtained as follows: the NaCl salt was spread evenly on the cooled glass base (about 4 °C), then the gelatin nonwoven was laid down, and the appropriate polymer mixture was poured onto it. Next, 2 layers of nonwovens were arranged until they were saturated, and a second layer of membrane-forming solution was added. All layers were pressed with a Teflon roller to remove air bubbles. The received scaffolds were gelled in the bath with deionized water and ice (the temperature of the bath was

about 2 °C). Gelation occurred with simultaneous salt removal. After 12 h, the gelatin was removed by immersing the membrane in a warm deionized water bath (50 °C).

3.4. SEM Observation

The morphology of the top and bottom layers, and cross-section of the membranes before and after degradation were characterized by scanning electron microscope (Hitachi TM–1000, Tokyo, Japan) with an accelerator voltage of 15 kV. The membranes were cut in liquid nitrogen, dried, and then coated with a 7 nm gold layer, using a sputter coater (EMITECH K550X, Warsaw, Poland).

3.5. Estimate of Pores in Scaffolds by MeMoExplorer™ Software

To evaluate changes in the morphology of the cross-section and top layer in the scaffolds (in pore size), selected samples were analyzed using MeMoExplorer™ software (Warsaw, Poland). This program evaluates images obtained from SEM analysis [60,62,80]. The SEM images were taken with microscope magnification of ×300 or ×500. Then, they were analyzed by software which involved contouring of pores surfaces and their evaluation with partitioning them into 8 size classes (Table 5) and calculation of total areas (porosity coefficients).

Table 5. Size classes of pores evaluated by MeMoExplorer™ Software.

j	1	2	3	4	5	6	7	8
Size μm^2	0–3	3–8	8–20	20–80	80–100	100–150	150–300	>300

An average of 30 SEM images were taken for each sample. The received data can be processed statistically to obtain parameters such as average (Ave) and standard deviation (SD). That can be performed by using suitable software such as Origin or Microsoft Excel.

3.6. Degradation of Scaffolds

Scaffolds M1-M5 degradation was performed in three different fluids: in 1 M NaOH (pH = 13.50), Hank's balanced salt solution (HBSS) (pH = 7.54), and in a simulated body fluid (SBF) (pH = 7.31). The SBF and HBSS were chosen for evaluating in vitro biocompatibility as they simulate physiological fluids. Furthermore, an SBF with ion concentrations nearly equal to those of human blood plasma [75,96] (table of ion concentrations is available in Supplementary Materials).

The liquids were prepared in the laboratory according to the method given in the literature [75,96]. The scaffolds were cut into rectangles, which were measured (length, width, and thickness) using a caliper tool and weighed by analytical balance (MATTLER TOLEDO KA-52c, Warsaw, Poland). The shape of the membranes varied due to their different morphology. It was not possible to cut them into samples of similar size. The samples of scaffolds (n = 6) were immersed into plastic bins filled with 40 mL of each liquid for 4 weeks at 36 ± 2 °C in a small multi-purpose incubator CULTURA M, 70700R (Almedica, Krakow, Poland). Every week, samples were washed in deionized water, dried, and weighed, and the pH values of liquids were monitored using an electrolyte-type pH meter (METTLER TOLEDO MP225, Warsaw, Poland). The mass loss was calculated from the following equations (Equation (1)) [97]:

$$\text{Weight loss} = \frac{(M_0 - M_t)}{M_0} \times 100\ \% \quad (1)$$

where M_0 and M_t with subscript 0 and t are mass at the immersion time of 0 and t, respectively. All the values presented were the average of six samples.

3.7. Porosity of Membranes

The porosity of the scaffolds was determined by measuring the mass and dimensions of the scaffolds before and after hydrolysis, as described by Ho et al. [97]. It was calculated with the following formula (Equation (2)):

$$\text{Porosity} = \frac{D_p - D_{ap}}{D_p} \times 100\% \quad (2)$$

where D_p is the density of membranes, which were, respectively, PUR (1.37 g/cm^3), PES (1.25 g/cm^3), M3 (1.31 g/cm^3), M4 (1.33 g/cm^3), and M5 (1.29 g/cm^3); D_{ap} is the apparent density (scaffold mass/apparent scaffold cube volume).

The calculations were carried out in 10 repetitions for both scaffolds before hydrolysis and 7 repetitions after hydrolysis. All data were expressed as average (Ave) ± standard deviation (SD).

3.8. Swelling Ratio

To calculate the saturation of the scaffolds, squares were cut from each scaffold, respectively. The samples were then weighed (W_0) on an analytical balance and immersed in 50 mL bins filled with PBS solution (pH 7.2–7.4). The PBS was prepared by dissolving the tablets in deionized water. The beaker with the scaffolds was set aside for 3 and 24 h, respectively. After this time, the swollen samples were weighed (W_t). The equilibrium swelling ratio (ESR) was then calculated by using the following equation (Equation (3)) [98]:

$$\text{ESR} = \frac{W_t - W_0}{W_0} \quad (3)$$

The 7 repetitions were performed for each membrane.

3.9. Contact Angle Measurement

The static wetting angle of membrane surfaces was analyzed using a DSA25 goniometer, (KRŰSS GmbH). Before the measurements, the membranes were stored in a desiccator. The measurements were carried out at room temperature at 24 ± 2 °C. A 5 µL drop of deionized water was deposited on the test surface. The results were presented as the average of 10 measurements with the standard deviation (Ave ± SD).

3.10. Mechanical Property

The mechanical properties were tested using a materials testing machine (Tiratest 2160, VEB Thuringer Industriewerk Rauenstein, Warsaw, Poland) at 23 ± 2 °C. The sample dimensions were 20 mm × 15 mm × 1–2 mm. The 5 repetitions of dry samples were performed for each membrane.

3.11. FT-IR

The scaffolds were characterized by using the Fourier-transform infrared spectroscopy ALPHA II machine (Platinum- ATR, BRUKER, Warsaw, Poland) with 4 cm^{-1} resolution, averaging for 32 measurements, wavelengths from 4000 to 400 cm^{-1}. The measurements were made using the OPUS 8 software. The graphs were prepared using the OriginPro 8 program.

3.12. Statistical Analysis

All the quantitative data were obtained from at least five samples for analysis. Results were expressed as the average ± standard deviation (Ave ± SD).

4. Conclusions

Currently, the scaffolds are being sought for hyaline cartilage regeneration, which should meet the relevant requirements. In this study, the three scaffolds were prepared from

a mixture of biodegradable polyurethane (PUR) and polyethersulfone (PES). These scaffolds have met the appropriate requirements for cartilage regeneration. The observation with an SEM microscope proved that the internal structure of the membranes forms a network of interconnected pores, while the surface layer is perforated, which creates the possibility for cells to enter the interior. In addition, the analysis of SEM photomicrographs via MeMoExplorer ™ Software showed that the area of pores of >300 um^2 dominated. The scaffolds showed degradation in simulated body fluid. The wettability results showed a hydrophilic nature of scaffolds, especially after degradation. Moreover, an increase in both porosity and pore surface area has been shown for scaffolds after degradation. It is necessary to create space for cellular products such as hyaline cartilage-forming protein. Adequate mechanical properties (>10 MPa) that were shown prove that these membranes will be able to withstand conditions in the knee.

Obtained membranes have shown suitable properties as scaffolds for cartilage engineering. Such membranes can be colonized by autologous/allogeneic chondrocytes (ACI method) or mesenchymal stem cells (MF technique).

Supplementary Materials: The following supporting information can be downloaded at: https://www.mdpi.com/article/10.3390/molecules28073195/s1, Table S1. Ion concentrations of Hank's balanced salt solution (HBSS), simulated body fluid (SBF), and human blood plasma according to ISO 23317; Table S2. The SEM photomicrographs of membranes after 2 and 4 weeks of degradation in SBF, HBSS, and 1 M NaOH fluids; Figure S1. IR spectrum of M2-M5 membranes before and after 2 and 4 weeks of degradation in SBF (B), HBSS (H), and NaOH (N) fluid.

Author Contributions: Conceptualization, M.W. and A.C.; methodology, M.W.; writing—original draft preparation, M.W.; writing—review and editing, M.W. and W.S.; formal analysis, M.W., E.R. and A.C; resources, J.D. and W.S.; visualization, M.W.; supervision, A.C.; funding Acquisition, A.C. All authors have read and agreed to the published version of the manuscript.

Funding: This research was supported by statutory funds of Laboratory of Electrostatic Methods of Bioencapsulation in Nalecz Institute of Biocybernetics and Biomedical Engineering, Polish Academy of Sciences (IBBE PAS).

Institutional Review Board Statement: Not applicable.

Informed Consent Statement: Not applicable.

Data Availability Statement: Not applicable.

Conflicts of Interest: The authors declare no conflict of interest.

References

1. Liu, Y.; Luo, J.; Chen, X.; Liu, W.; Chen, T. *Cell Membrane Coating Technology: A Promising Strategy for Biomedical Applications*; Springer: Singapore, 2019; Volume 11; ISBN 0123456789.
2. Dzobo, K.; Thomford, N.E.; Senthebane, D.A.; Shipanga, H.; Rowe, A.; Dandara, C.; Pillay, M.; Motaung, K.S.C.M. Advances in regenerative medicine and tissue engineering: Innovation and transformation of medicine. *Stem Cells Int.* **2018**, *2018*, 2495848. [CrossRef] [PubMed]
3. Park, K.M.; Shin, Y.M.; Kim, K.; Shin, H. Tissue Engineering and Regenerative Medicine 2017: A Year in Review. *Tissue Eng. Part B Rev.* **2018**, *24*, 327–344. [CrossRef] [PubMed]
4. Vig, K.; Chaudhari, A.; Tripathi, S.; Dixit, S.; Sahu, R.; Pillai, S.; Dennis, V.A.; Singh, S.R. Advances in skin regeneration using tissue engineering. *Int. J. Mol. Sci.* **2017**, *18*, 789. [CrossRef] [PubMed]
5. Tarassoli, S.P.; Jessop, Z.M.; Al-Sabah, A.; Gao, N.; Whitaker, S.; Doak, S.; Whitaker, I.S. Skin tissue engineering using 3D bioprinting: An evolving research field. *J. Plast. Reconstr. Aesthetic Surg.* **2018**, *71*, 615–623. [CrossRef]
6. Nikolova, M.P.; Chavali, M.S. Recent advances in biomaterials for 3D scaffolds: A review. *Bioact. Mater.* **2019**, *4*, 271–292. [CrossRef]
7. Wasyłeczko, M.; Krysiak, Z.J.; Łukowska, E.; Gruba, M.; Sikorska, W.; Kruk, A.; Dulnik, J.; Czubak, J.; Chwojnowski, A. Three-dimensional scaffolds for bioengineering of cartilage tissue. *Biocybern. Biomed. Eng.* **2022**, *42*, 494–511. [CrossRef]
8. Wasyłeczko, M.; Sikorska, W.; Chwojnowski, A. Review of synthetic and hybrid scaffolds in cartilage tissue engineering. *Membranes* **2020**, *10*, 348. [CrossRef]
9. Bružauskaitė, I.; Bironaitė, D.; Bagdonas, E.; Bernotienė, E. Scaffolds and cells for tissue regeneration: Different scaffold pore sizes—Different cell effects. *Cytotechnology* **2016**, *68*, 355–369. [CrossRef]

10. Verma, S.K.; Modi, A.; Singh, A.K.; Teotia, R.; Bellare, J. Improved hemodialysis with hemocompatible polyethersulfone hollow fiber membranes: In vitro performance. *J. Biomed. Mater. Res. Part B Appl. Biomater.* **2018**, *106*, 1286–1298. [CrossRef]
11. Farina, M.; Alexander, J.F.; Thekkedath, U.; Ferrari, M.; Grattoni, A. Cell encapsulation: Overcoming barriers in cell transplantation in diabetes and beyond. *Adv. Drug Deliv. Rev.* **2019**, *139*, 92–115. [CrossRef]
12. Kupikowska-Stobba, B.; Lewińska, D. Polymer microcapsules and microbeads as cell carriers for: In vivo biomedical applications. *Biomater. Sci.* **2020**, *8*, 1536–1574. [CrossRef]
13. Gurtner, G.C.; Werner, S.; Barrandon, Y.; Longaker, M.T. Wound repair and regeneration. *Nature* **2008**, *453*, 314–321. [CrossRef]
14. Oliveira, M.C.; Vullings, J.; van de Loo, F.A.J. Osteoporosis and osteoarthritis are two sides of the same coin paid for obesity. *Nutrition* **2020**, *70*, 110486. [CrossRef]
15. Silverwood, V.; Blagojevic-Bucknall, M.; Jinks, C.; Jordan, J.L.; Protheroe, J.; Jordan, K.P. Current evidence on risk factors for knee osteoarthritis in older adults: A systematic review and meta-analysis. *Osteoarthr. Cartil.* **2015**, *23*, 507–515. [CrossRef]
16. Niemczyk-Soczynska, B.; Zaszczyńska, A.; Zabielski, K.; Sajkiewicz, P. Hydrogel, electrospun and composite materials for bone/cartilage and neural tissue engineering. *Materials* **2021**, *14*, 6899. [CrossRef]
17. Collins, K.H.; Herzog, W.; MacDonald, G.Z.; Reimer, R.A.; Rios, J.L.; Smith, I.C.; Zernicke, R.F.; Hart, D.A. Obesity, metabolic syndrome, and musculoskeletal disease: Common inflammatory pathways suggest a central role for loss of muscle integrity. *Front. Physiol.* **2018**, *9*, 112. [CrossRef]
18. Krishnan, Y.; Grodzinsky, A.J. Cartilage diseases. *Matrix Biol.* **2018**, *71–72*, 51–69. [CrossRef]
19. Walter, S.G.; Ossendorff, R.; Schildberg, F.A. Articular cartilage regeneration and tissue engineering models: A systematic review. *Arch. Orthop. Trauma Surg.* **2019**, *139*, 305–316. [CrossRef]
20. Sophia Fox, A.J.; Bedi, A.; Rodeo, S.A. The basic science of articular cartilage: Structure, composition, and function. *Sport. Health* **2009**, *1*, 461–468. [CrossRef]
21. Zhang, L.; Hu, J.; Athanasiou, K.A. The role of tissue engineering in articular cartilage repair and regeneration. *Crit. Rev. Biomed. Eng.* **2009**, *37*, 1–57. [CrossRef]
22. Armiento, A.R.; Alini, M.; Stoddart, M.J. Articular fibrocartilage—Why does hyaline cartilage fail to repair? *Adv. Drug Deliv. Rev.* **2019**, *146*, 289–305. [CrossRef] [PubMed]
23. Medvedeva, E.V.; Grebenik, E.A.; Gornostaeva, S.N.; Telpuhov, V.I.; Lychagin, A.V.; Timashev, P.S.; Chagin, A.S. Repair of damaged articular cartilage: Current approaches and future directions. *Int. J. Mol. Sci.* **2018**, *19*, 2366. [CrossRef]
24. Kwon, H.; Brown, W.E.; Lee, C.A.; Wang, D.; Paschos, N.; Hu, J.C.; Athanasiou, K.A. Surgical and tissue engineering strategies for articular cartilage and meniscus repair. *Nat. Rev. Rheumatol.* **2019**, *15*, 550–570. [CrossRef] [PubMed]
25. Mirza, U.; Shubeena, S.; Shah, M.S.; Zaffer, B. Microfracture: A technique for repair of chondral defects. *J. Entomol. Zool. Stud.* **2018**, *6*, 1092–1097.
26. Brittberg, M. Symposium Scaffold based Autologous Chondrocyte Implantation: The Surgical Technique. *Asian J. Arthrosc.* **2019**, *4*, 23–26.
27. Zhao, Z.; Fan, C.; Chen, F.; Sun, Y.; Xia, Y.; Ji, A.; Wang, D. Progress in Articular Cartilage Tissue Engineering: A Review on Therapeutic Cells and Macromolecular Scaffolds. *Macromol. Biosci.* **2019**, *20*, 1900278. [CrossRef]
28. Brittberg, M.; Recker, D.; Ilgenfritz, J.; Saris, D.B.F. Matrix-Applied Characterized Autologous Cultured Chondrocytes Versus Microfracture: Five-Year Follow-up of a Prospective Randomized Trial. *Am. J. Sport. Med.* **2018**, *46*, 1343–1351. [CrossRef]
29. Baranowski, M.; Wasyłeczko, M.; Kosowska, A.; Plichta, A.; Kowalczyk, S.; Chwojnowski, A.; Bielecki, W.; Czubak, J. Regeneration of Articular Cartilage Using Membranes of Polyester Scaffolds in a Rabbit Model. *Pharmaceutics* **2022**, *14*, 1016. [CrossRef]
30. Demoor, M.; Ollitrault, D.; Gomez-Leduc, T.; Bouyoucef, M.; Hervieu, M.; Fabre, H.; Lafont, J.; Denoix, J.M.; Audigié, F.; Mallein-Gerin, F.; et al. Cartilage tissue engineering: Molecular control of chondrocyte differentiation for proper cartilage matrix reconstruction. *Biochim. Biophys. Acta Gen. Subj.* **2014**, *1840*, 2414–2440. [CrossRef]
31. Panadero, J.A.; Lanceros-Mendez, S.; Ribelles, J.L.G. Differentiation of mesenchymal stem cells for cartilage tissue engineering: Individual and synergetic effects of three-dimensional environment and mechanical loading. *Acta Biomater.* **2016**, *33*, 1–12. [CrossRef]
32. Eltom, A.; Zhong, G.; Muhammad, A. Scaffold Techniques and Designs in Tissue Engineering Functions and Purposes: A Review. *Adv. Mater. Sci. Eng.* **2019**, *2019*, 3429527. [CrossRef]
33. Takahashi, T.; Ogasawara, T.; Asawa, Y.; Mori, Y.; Uchinuma, E.; Takato, T.; Hoshi, K. Three-Dimensional Microenvironments Retain Chondrocyte Phenotypes During Proliferation Culture. *Tissue Eng.* **2007**, *13*, 1583–1592. [CrossRef]
34. O'Brien, F.J. Biomaterials & scaffolds for tissue engineering. *Mater. Today* **2011**, *14*, 88–95. [CrossRef]
35. Kalkan, R.; Nwekwo, C.W.; Adali, T. The Use of Scaffolds in Cartilage Regeneration. *Eukaryot. Gene Expr.* **2018**, *28*, 343–348. [CrossRef]
36. Gadomska-Gajadhur, A.; Kruk, A.; Ruśkowski, P.; Sajkiewicz, P.; Dulnik, J.; Chwojnowski, A. Original method of imprinting pores in scaffolds for tissue engineering. *Polym. Adv. Technol.* **2021**, *32*, 355–367. [CrossRef]
37. Nava, M.M.; Draghi, L.; Giordano, C.; Pietrabissa, R. The effect of scaffold pore size in cartilage tissue engineering. *J. Appl. Biomater. Funct. Mater.* **2016**, *14*, e233–e239. [CrossRef]
38. Matsiko, A.; Gleeson, J.P.; O'Brien, F.J. Scaffold mean pore size influences mesenchymal stem cell chondrogenic differentiation and matrix deposition. *Tissue Eng. Part A* **2015**, *21*, 486–497. [CrossRef]

39. Koh, Y.G.; Lee, J.A.; Kim, Y.S.; Lee, H.Y.; Kim, H.J.; Kang, K.T. Optimal mechanical properties of a scaffold for cartilage regeneration using finite element analysis. *J. Tissue Eng.* **2019**, *10*, 1–10. [CrossRef]
40. Huang, B.J.; Hu, J.C.; Athanasiou, K.A. Cell-based tissue engineering strategies used in the clinical repair of articular cartilage. *Biomaterials* **2016**, *98*, 1–22. [CrossRef]
41. Ahmadi, F.; Giti, R.; Mohammadi-Samani, S.; Mohammadi, F. Biodegradable Scaffolds for Cartilage Tissue Engineering. *GMJ* **2017**, *6*, 70–80. [CrossRef]
42. Joshi, S.R.; Pendyala, G.S.; Shah, P.; Mopagar, V.P.; Padmawar, N.; Padubidri, M. Scaffolds—The Ground for Regeneration: A Narrative Review. *J. Int. Soc. Prev. Community Dent.* **2020**, *10*, 692–699. [PubMed]
43. Krishani, M.; Shin, W.Y.; Suhaimi, H.; Sambudi, N.S. Development of Scaffolds from Bio-Based Natural Materials for Tissue Regeneration Applications: A Review. *Gels* **2023**, *9*, 100. [CrossRef] [PubMed]
44. Armiento, A.R.; Stoddart, M.J.; Alini, M.; Eglin, D. Biomaterials for articular cartilage tissue engineering: Learning from biology. *Acta Biomater.* **2018**, *65*, 1–20. [CrossRef] [PubMed]
45. Irawan, V.; Sung, T.C.; Higuchi, A.; Ikoma, T. Collagen Scaffolds in Cartilage Tissue Engineering and Relevant Approaches for Future Development. *Tissue Eng. Regen. Med.* **2018**, *15*, 673–697. [CrossRef]
46. Steinwachs, M.R.; Gille, J.; Volz, M.; Anders, S.; Jakob, R.; De Girolamo, L.; Volpi, P.; Schiavone-Panni, A.; Scheffler, S.; Reiss, E.; et al. Systematic Review and Meta-Analysis of the Clinical Evidence on the Use of Autologous Matrix-Induced Chondrogenesis in the Knee. *Cartilage* **2021**, *13*, 42S–56S. [CrossRef]
47. Gobbi, A.; Whyte, G.P. Long-term Clinical Outcomes of One-Stage Cartilage Repair in the Knee with Hyaluronic Acid—Based Scaffold Embedded with Mesenchymal Stem Cells Sourced from Bone Marrow Aspirate Concentrate. *Am. J. Sport. Med.* **2019**, *47*, 1621–1628. [CrossRef]
48. Chen, S.; Chen, W.; Chen, Y.; Mo, X.; Fan, C. Chondroitin sulfate modified 3D porous electrospun nano fiber scaffolds promote cartilage regeneration. *Mater. Sci. Eng. C* **2021**, *118*, 111312. [CrossRef]
49. Zhou, F.; Zhang, X.; Cai, D.; Li, J.; Mu, Q.; Zhang, W.; Zhu, S. Silk fibroin-chondroitin sulfate scaffold with immuno-inhibition property for articular cartilage repair. *Acta Biomater.* **2017**, *63*, 64–75. [CrossRef]
50. Kim, J.S.; Kim, T.H.; Kang, D.L.; Baek, S.Y.; Lee, Y.; Koh, Y.G.; Kim, Y. Il Chondrogenic differentiation of human ASCs by stiffness control in 3D fibrin hydrogel. *Biochem. Biophys. Res. Commun.* **2020**, *522*, 213–219. [CrossRef]
51. Asghari, F.; Samiei, M.; Adibkia, K.; Akbarzadeh, A.; Davaran, S. Biodegradable and biocompatible polymers for tissue engineering application: A review. *Artif. Cells Nanomed. Biotechnol.* **2017**, *45*, 185–192. [CrossRef]
52. Silva, D.; Kaduri, M.; Poley, M.; Adir, O.; Krinsky, N.; Shainsky-roitman, J.; Schroeder, A. Mini Review Biocompatibility, biodegradation and excretion of polylactic acid (PLA) in medical implants and theranostic systems. *Chem. Eng. J.* **2018**, *340*, 9–14. [CrossRef]
53. Janmohammadi, M.; Nourbakhsh, M.S. Electrospun polycaprolactone scaffolds for tissue engineering: A review. *Int. J. Polym. Mater. Polym. Biomater.* **2018**, *68*, 527–539. [CrossRef]
54. Dao, T.T.; Vu, N.B.; Pham, L.H.; Bui, T.; Le, P.T.; Van Pham, P. In Vitro Production of Cartilage Tissue from Rabbit Bone Marrow-Derived Mesenchymal Stem Cells and Polycaprolactone Scaffold. In *Tissue Engineering and Regenerative Medicine*; Springer: Cham, Switzerland, 2017; Volume 1084, pp. 45–60. [CrossRef]
55. Wen, Y.; Dai, N.; Hsu, S. Biodegradable water-based polyurethane scaffolds with a sequential release function for cell-free cartilage tissue engineering. *Acta Biomater.* **2019**, *88*, 301–313. [CrossRef]
56. Hung, K.; Tseng, C.; Hsu, S. Synthesis and 3D Printing of Biodegradable Polyurethane Elastomer by a Water-Based Process for Cartilage Tissue Engineering Applications. *Adv. Healthc. Mater.* **2014**, *3*, 1578–1587. [CrossRef]
57. Mahboudi, H.; Soleimani, M.; Enderami, S.E.; Kehtari, M.; Hanaee- Ahvaz, H.; Ghanbarian, H.; Bandehpour, M.; Nojehdehi, S.; Mirzaei, S.; Kazemi, B. The effect of nanofibre-based polyethersulfone (PES) scaffold on the chondrogenesis of human induced pluripotent stem cells. *Artif. Cells Nanomed. Biotechnol.* **2018**, *46*, 1948–1956. [CrossRef]
58. Płończak, M.; Czubak, J.; Hoser, G.; Chwojnowskl, A.; Kawiak, J.; Dudzińskp, K.; Czumińska, K. Repair of articular cartilage full thickness defects with cultured chondrocytes placed on polysulphonic membrane—Experimental studies in rabbits. *Biocybern. Biomed. Eng.* **2008**, *28*, 87–93.
59. Irfan, M.; Idris, A. Overview of PES biocompatible/hemodialysis membranes: PES-blood interactions and modification techniques. *Mater. Sci. Eng. C* **2015**, *56*, 574–592. [CrossRef]
60. Sikorska, W.; Przytulska, M.; Wasyłeczko, M.; Wojciechowski, C.; Kulikowski, J.L.; Chwojnowski, A. Influence of hydrolysis, solvent and pvp addition on the porosity of psf/pur blend partly degradable hollow fiber membranes evaluated using the memoexplorer software. *Desalination Water Treat.* **2021**, *214*, 114–119. [CrossRef]
61. Ye, H.; Zhang, K.; Kai, D.; Li, Z.; Loh, X.J. Polyester elastomers for soft tissue engineering. *Chem. Soc. Rev.* **2018**, *47*, 4545–4580. [CrossRef]
62. Wasyłeczko, M.; Sikorska, W.; Przytulska, M.; Dulnik, J.; Chwojnowski, A. Polyester membranes as 3D scaffolds for cell culture. *Desalination Water Treat.* **2021**, *214*, 181–193. [CrossRef]
63. Sikorska, W.; Wasyłeczko, M.; Przytulska, M.; Wojciechowski, C.; Rokicki, G.; Chwojnowski, A. Chemical degradation of PSF-PUR blend hollow fiber membranes-assessment of changes in properties and morphology after hydrolysis. *Membranes* **2021**, *11*, 51. [CrossRef] [PubMed]

64. Sikorska, W.; Milner-Krawczyk, M.; Wasyłeczko, M.; Wojciechowski, C.; Chwojnowski, A. Biodegradation process of PSF-PUR blend hollow fiber membranes using escherichia coli Bacteria—Evaluation of changes in properties and porosity. *Polymers* **2021**, *13*, 1311. [CrossRef] [PubMed]
65. Prasanna, S.; Narayan, B.; Rastogi, A.; Srivastava, P. Design and evaluation of chitosan/poly (L-lactide)/pectin based composite scaffolds for cartilage tissue regeneration. *Int. J. Biol. Macromol.* **2018**, *112*, 909–920. [CrossRef]
66. Nofar, M.; Sacligil, D.; Carreau, P.J.; Kamal, M.R.; Heuzey, M.C. Poly (lactic acid) blends: Processing, properties and applications. *Int. J. Biol. Macromol.* **2019**, *125*, 307–360. [CrossRef]
67. Setayeshmehr, M.; Esfandiari, E.; Rafieinia, M.; Hashemibeni, B.; Taheri-Kafrani, A.; Samadikuchaksaraei, A.; Kaplan, D.L.; Moroni, L.; Joghataei, M.T. Hybrid and composite scaffolds based on extracellular matrices for cartilage tissue engineering. *Tissue Eng. Part B Rev.* **2019**, *25*, 202–224. [CrossRef]
68. Zhang, X.; Wu, Y.; Pan, Z.; Sun, H.; Wang, J.; Yu, D.; Zhu, S.; Dai, J.; Chen, Y.; Tian, N.; et al. The effects of lactate and acid on articular chondrocytes function: Implications for polymeric cartilage scaffold design. *Acta Biomater.* **2016**, *42*, 329–340. [CrossRef]
69. Lin, H.; Beck, A.M.; Fritch, M.R.; Tuan, R.S.; Deng, Y.; Kilroy, E.J.; Tang, Y.; Alexander, P.G. Optimization of photocrosslinked gelatin/hyaluronic acid hybrid scaffold for the repair of cartilage defect. *J. Tissue Eng. Regen. Med.* **2019**, *13*, 1418–1429. [CrossRef]
70. Safinsha, S.; Ali, M.M. Composite scaffolds in tissue engineering. *Mater. Today Proc.* **2020**, *24*, 2318–2329. [CrossRef]
71. Bistolfi, A.; Ferracini, R.; Galletta, C.; Tosto, F.; Sgarminato, V.; Digo, E.; Vernè, E.; Massè, A. Regeneration of articular cartilage: Scaffold used in orthopedic surgery. A short handbook of available products for regenerative joints surgery. *Clin. Sci. Res. Rep.* **2017**, *1*, 1–7. [CrossRef]
72. Tan, R.Y.H.; Lee, C.S.; Pichika, M.R.; Cheng, S.F.; Lam, K.Y. PH Responsive Polyurethane for the Advancement of Biomedical and Drug Delivery. *Polymers* **2022**, *14*, 1672. [CrossRef]
73. Xie, F.; Zhang, T.; Bryant, P.; Kurusingal, V.; Colwell, J.M.; Laycock, B. Degradation and stabilization of polyurethane elastomers. *Prog. Polym. Sci.* **2019**, *90*, 211–268. [CrossRef]
74. Cauich-Rodríguez, V.; Chan-Chan, L.H.; Hernandez-Sanchez, F.; Cervantes-Uc, J.M. Degradation of Polyurethanes for Cardiovascular Applications. *Adv. Biomater. Sci. Biomed. Appl.* **2013**, *8*, 51–82. [CrossRef]
75. Kokubo, T.; Takadama, H. How useful is SBF in predicting in vivo bone bioactivity? *Biomaterials* **2006**, *27*, 2907–2915. [CrossRef]
76. Kitahara, S. Effect of Surface Hydrolysis of PLA Film on Apatite Formation in Vitro. *J. Oral Tissue Eng.* **2008**, *6*, 77–87.
77. Shuai, C.; Yu, L.; Yang, W.; Peng, S.; Zhong, Y.; Feng, P. Phosphonic acid coupling agent modification of HAP nanoparticles: Interfacial effects in PLLA/HAP bone scaffold. *Polymers* **2020**, *12*, 199. [CrossRef]
78. Woźniak-Budych, M.J. Polymeric membranes for biomedical applications. *Membr. Technol. Acad. Ind.* **2022**, *15*, 111–140. [CrossRef]
79. Jakutowicz, T. Treatment of articular cartilage damage in rabbits using chondrocyte transplants auto—And allogeneic—A comparati. Ph.D. Thesis, Medical Center for Postgraduate Education, Otwock, Poland, 2016.
80. Przytulska, M.; Kulikowski, J.L.; Wasyłeczko, M.; Chwojnowski, A.; Piętka, D. The evaluation of 3D morphological structure of porous membranes based on a computer-aided analysis of their 2D images. *Desalin. Water Treat.* **2018**, *128*, 11–19. [CrossRef]
81. Sun, L.; Guo, J.; Chen, H.; Zhang, D.; Shang, L.; Zhang, B.; Zhao, Y. Tailoring Materials with Specific Wettability in Biomedical Engineering. *Adv. Sci.* **2021**, *8*, 2100126. [CrossRef]
82. Lee, S.S.; Santschi, M.; Ferguson, S.J. A Biomimetic Macroporous Hybrid Scaffold with Sustained Drug Delivery for Enhanced Bone Regeneration. *Biomacromolecules* **2021**, *22*, 2460–2471. [CrossRef]
83. Ehtesabi, H.; Massah, F. Improvement of hydrophilicity and cell attachment of polycaprolactone scaffolds using green synthesized carbon dots. *Mater. Today Sustain.* **2021**, *13*, 100075. [CrossRef]
84. Aljanabi, A.A.A.; Mousa, N.E.; Aljumaily, M.M.; Majdi, H.S.; Yahya, A.A.; AL-Baiati, M.N.; Hashim, N.; Rashid, K.T.; Al-Saadi, S.; Alsalhy, Q.F. Modification of Polyethersulfone Ultrafiltration Membrane Using Poly(terephthalic acid-co-glycerol-g-maleic anhydride) as Novel Pore Former. *Polymers* **2022**, *14*, 3408. [CrossRef]
85. Arkhangelsky, E.; Kuzmenko, D.; Gitis, V. Impact of chemical cleaning on properties and functioning of polyethersulfone membranes. *J. Membr. Sci.* **2007**, *305*, 176–184. [CrossRef]
86. Shams, M.; Karimi, M.; Jahangir, V.; Mohammadian, M.; Salimi, A. Surface modification of nanofibrous polyethersulfone scaffolds with fluorapatite nanoparticles toward improved stem cell behavior and osteogenic activity in vitro. *Surf. Interfaces* **2023**, *36*, 102512. [CrossRef]
87. Chen, Y.; Etxabide, A.; Seyfoddin, A.; Ramezani, M. Fabrication and characterisation of poly (vinyl alcohol)/chitosan scaffolds for tissue engineering applications. *Mater. Today Proc.* **2023**. [CrossRef]
88. Alosaimi, A.M.; Alorabi, R.O.; Katowah, D.F.; Al-thagafi, Z.T.; Alsolami, E.S.; Hussein, M.A.; Qutob, M.; Rafatullah, M. Review on Biomedical Advances of Hybrid Nanocomposite Biopolymeric Materials. *Bioengineering* **2023**, *10*, 279. [CrossRef]
89. Lai, Y.S.; Chen, W.C.; Huang, C.H.; Cheng, C.K.; Chan, K.K.; Chang, T.K. The effect of graft strength on knee laxity and graft in-situ forces after posterior cruciate ligament reconstruction. *PLoS ONE* **2015**, *10*, e0127293. [CrossRef]
90. Dhandayuthapani, B.; Yoshida, Y.; Maekawa, T.; Kumar, D.S. Polymeric scaffolds in tissue engineering application: A review. *Int. J. Polym. Sci.* **2011**, *2011*, 290602. [CrossRef]
91. Mazurek-Budzyńska, M.; Behl, M.; Razzaq, M.Y.; Nöchel, U.; Rokicki, G.; Lendlein, A. Hydrolytic stability of aliphatic poly(carbonate-urea-urethane)s: Influence of hydrocarbon chain length in soft segment. *Polym. Degrad. Stab.* **2019**, *161*, 283–297. [CrossRef]

92. Belfer, S.; Fainchtain, R.; Purinson, Y.; Kedem, O. Surface characterization by FTIR-ATR spectroscopy of polyethersulfone membranes-unmodified, modified and protein fouled. *J. Membr. Sci.* **2000**, *172*, 113–124. [CrossRef]
93. Cao, X.Y.; Tian, N.; Dong, X.; Cheng, C.K. Polylactide composite pins reinforced with bioresorbable continuous glass fibers demonstrating bone-like apatite formation and spiral delamination degradation. *Polymers* **2019**, *11*, 812. [CrossRef]
94. Denis, P.; Dulnik, J.; Sajkiewicz, P. Electrospinning and Structure of Bicomponent Polycaprolactone/Gelatin Nanofibers Obtained Using Alternative Solvent System. *Int. J. Polym. Mater. Polym. Biomater.* **2015**, *64*, 354–364. [CrossRef]
95. Dulnik, J.; Ko, D.; Denis, P.; Sajkiewicz, P. The effect of a solvent on cellular response to PCL/gelatin and PCL/collagen electrospun nano fibres. *Eur. Polym. J.* **2018**, *104*, 147–156. [CrossRef]
96. Chrzanowski, W.; Ali, E.; Neel, A.; Andrew, D.; Campbell, J. Effect of surface treatment on the bioactivity of nickel—Titanium. *Acta Biomater.* **2008**, *4*, 1969–1984. [CrossRef]
97. Ho, S.T.; Hutmacher, D.W. A comparison of micro CT with other techniques used in the characterization of scaffolds. *Biomaterials* **2006**, *27*, 1362–1376. [CrossRef]
98. Park, H.J.; Min, K.D.; Lee, M.C.; Kim, S.H.; Lee, O.J.; Ju, H.W.; Moon, B.M.; Lee, J.M.; Park, Y.R.; Kim, D.W.; et al. Fabrication of 3D porous SF/β-TCP hybrid scaffolds for bone tissue reconstruction. *J. Biomed. Mater. Res. Part A* **2016**, *104*, 1779–1787. [CrossRef]

PUBLIKACJA 4

Three-dimensional scaffolds for bioengineering

of cartilage tissue,

Monika Wasyłeczko, Zuzanna Joanna Krysiak, Ewa Łukowska, Marcin Gruba, Wioleta Sikorska, Aleksandra Kruk, Judyta Dulnik, Jarosław Czubak, Andrzej Chwojnowski

Biocybernetics and Biomedical Engineering **2022**, 42, 494– 511.
https://doi.org/10.1016/j.bbe.2022.03.004
IF: 5,687
MNiSW: 200

BIOCYBERNETICS AND BIOMEDICAL ENGINEERING 42 (2022) 494–511

Available at www.sciencedirect.com

ScienceDirect

journal homepage: www.elsevier.com/locate/bbe

Original Research Article

Three-dimensional scaffolds for bioengineering of cartilage tissue

Monika Wasyłeczko [a,*], *Zuzanna Joanna Krysiak* [a,b], *Ewa Łukowska* [a], *Marcin Gruba* [c], *Wioleta Sikorska* [a], *Aleksandra Kruk* [a,d], *Judyta Dulnik* [e], *Jarosław Czubak* [c], *Andrzej Chwojnowski* [a]

[a] *Nałeôcz Institute of Biocybernetics and Biomedical Engineering, Polish Academy of Sciences, KsieôciaTrojdena 4 str., 02-109 Warsaw, Poland*
[b] *International Center of Electron Microscopy for Material Science, Faculty of Metals Engineering and Industrial Computer Science, AGH University of Science and Technology, Cracow, Poland*
[c] *Gruca Orthopedic and Trauma Teaching Hospital, Centre of Postgraduate Medical Education, Konarskiego 13 str., 05-400 Otwock, Poland*
[d] *Faculty of Chemistry Warsaw University of Technology, Noakowskiego 3 str., 00-664 Warsaw, Poland*
[e] *Institute of Fundamental Technological Research, Polish Academy of Sciences, Pawińskiego 5B str., 02-106 Warsaw, Poland*

ARTICLE INFO

Article history:
Received 15 October 2020
Received in revised form
7 March 2022
Accepted 9 March 2022
Available online 17 March 2022

Keywords:
3D-scaffolds
Membrane structure
Polyethersulfone
Poly(L-lactide)
Chondrocyte culture
Cartilage regeneration

ABSTRACT

The cartilage tissue is neither supplied with blood nor innervated, so it cannot heal by itself. Thus, its reconstruction is highly challenging and requires external support. Cartilage diseases are becoming more common due to the aging population and obesity. Among young people, it is usually a post-traumatic complication. Slight cartilage damage leads to the spontaneous formation of fibrous tissue, not resistant to abrasion and stress, resulting in cartilage degradation and the progression of the disease. For these reasons, cartilage regeneration requires further research, including use of new type of biomaterials for scaffolds. This paper shows cartilage characteristics within its most frequent problems and treatment strategies, including a promising method that combines scaffolds and human cells. Structure and material requirements, manufacturing methods, and commercially available scaffolds were described. Also, the comparison of poly(L-lactide) (PLLA) and polyethersulfone (PES) 3D membranes obtained by a phase inversion method using nonwovens as a pore-forming additives were reported. The scaffolds' structure and the growth ability of human chondrocytes were compared. Scaffolds' structure, cells morphology, and protein presence in the membranes were examined with a scanning electron microscope. The metabolic activity of cells was tested with the MTT assay. The structure of the scaffolds and the growth capacity of human chondrocytes were compared. Obtained results showed higher cell activity and protein content for PES scaffolds than for PLLA.

* Corresponding author at: Nałeôcz Institute of Biocybernetics and Biomedical Engineering, Polish Academy of Sciences, Department of Biomaterials and Biotechnological Systems, KsieôciaTrojdena 4 str., Room 142, 02-109 Warsaw, Poland.
E-mail addresses: mwasyleczko@ibib.waw.pl (M. Wasyłeczko), elukowska@ibib.waw.pl (E. Łukowska), wsikorska@ibib.waw.pl (W. Sikorska), akruk@ch.pw.edu.pl (A. Kruk), jdulnik@ippt.pan.pl (J. Dulnik), jarek@czubak.neostrada.pl (J. Czubak), achwoj@ibib.waw.pl (A. Chwojnowski).
https://doi.org/10.1016/j.bbe.2022.03.004

The PES membrane had better mechanical properties (e.g. ripping), greater chondrocytes proliferation, and thus a better secretion of proteins which build up the cartilage structure.

1. Introduction

Up to date, the effective treatment of organ failure still has not been found, as the regeneration process is complex. There are insufficient medical procedures and pathogenesis mechanisms are not fully explained. In addition, there is limited knowledge of the pharmacological and technical needs and the necessary adaptation to the specific conditions of the patient during the course of a given disease. Therefore, new therapies are still challenging. Organ transplantation, as an ideal option, suffers from the limited availability of donor organs. Techniques to replace organ function *in situ* by inserting complex artificial materials into damaged areas have been investigated in recent years and turned out to be promising. However, implanted foreign organs may fail due to rejection, inflammatory reactions, or insufficient compliance to lifelong immunosuppression [1–3]. Tissue engineering (TE) offers innovative concepts and promising solutions for tissue repair and regeneration. The combination of various fields of science, such as medicine, physiology, biotechnology, and material science, allows to open up new therapeutic perspectives [4–6].

Recent investigations have shown the possibility to produce biohybrid tissues and organs, which can either restore, maintain, or improve a given tissue or organ [4,5,7–9]. Tissue engineering is used in many medical areas with failing organs or tissues, such as musculoskeletons, skin, liver, heart, kidney, or even neurology [5,7,10–24]. Apart from tissue maintenance, TE can be applied for drug delivery systems (DDS), e.g., for supporting diseases such as diabetes [25,26] or cancer [27]. Furthermore, TE is essential in organs with a limited regenerative capacity [4], such as cartilage tissue with neither vascularity nor innervations [28]. For this purpose, the most promising approach is the use of scaffolds, which can be colonized with either mesenchymal stem cells (MSCs) or autologous chondrocytes. Such bio-implants have already been successfully applied in patients [28–30]. Scaffolds' structure plays an important role in supporting cell attachment and proliferation [7,31–34]. Adequate 3D structures and mechanical parameters adapted to the native tissue are targets for bioengineers [33,35,36]. Thus, TE offers promising tools for regenerative medicine.

This paper presents a description of articular cartilage and associated problems. Further, the methodology of cartilage regeneration is discussed, including the requirements for scaffolds. In addition, two types of scaffolds obtained by our team and the experiments with them are discussed.

2. Scaffolds for cartilage tissue engineering

2.1. *Characteristics of articular cartilage tissue*

Cartilage is a connective tissue composed of chondrocytes with a diameter of about 20 μm that produces the extracellular matrix (ECM) [37–39]. It is classified into three types: hyaline cartilage, fibrocartilage, and elastic cartilage. The hyaline articular cartilage (AC) is highly specialized connective tissue that allows low-friction joint movement, absorbs the biochemical forces, and stabilizes the joint. It covers and protects the ends of bones and allows smooth motion. Moreover, it prevents the bones' abrasion and absorbs shocks and forces acting on the joints [37,39]. The AC is rich in water and contains many biological components, such as collagen II, chondroitin sulfate, and hyaline cartilage acid (HA), while the total chondrocyte volume is about 2%. However, cartilage cannot transfer nutrients to cells due to a lack of blood supply and a neural system. Thus, the AC cannot repair itself [37,39,40]. Therefore, scientists are continuously searching for the treatment of damaged cartilage.

2.2. *Problems, diseases, and clinical strategies for the treatment of articular cartilage*

Cartilage deformity can affect people of all ages. Osteoarthritis (OA) or cartilaginous tumor are frequently caused by injuries, age and genetic determinants, unhealthy lifestyle, and obesity. The typical symptoms are pain, limiting the range of movement, lead to swelling and stiffness [40–45]. OA is the most common disease in the locomotive system. It develops due to a disturbance in AC's quality, quantity and can affect joints in the knees, fingers, hip, or spine. OA leads to a deterioration in the quality of life and, most importantly, to disability. The disease progresses with age, and mainly women are exposed [40,42,44].

Regenerative medicine aims to reproduce hyaline cartilage at the chondral lesion. Regeneration results are weak in traditional clinical methods, as the fibrocartilage or hyaline-like cartilage is exposed to further degenerative changes [46,47]. Despite many therapeutical approaches in medicine, currently, there is no effective treatment for OA. Clinical methods focus mainly on pain treatment, which is unsatisfactory in the long run [47]. Recently developed methods for AC treatment are: microfracture, osteochondral transplantation, chondroplasty surgery, mosaicplasty. The most promising one is based on autologous chondrocyte implantation (ACI) or by using mesenchymal stem cells (MSCs) [28-30,46,48,49]. The microfracture method is currently preferred to other techniques. It is based on the sub-cartilage stimulation of the bone marrow. The defective cartilage is filled with a clot composed of MSCs (an appropriate tissue regeneration environment). Unfortunately, the regenerated site consists of fibrocartilage instead of hyaline cartilage [49]. More promising clinical methods are cell-based approaches. They are based either on one- or two-step surgical procedures. Initially, this method was very invasive and was based on two steps. The first step involves an arthroscopy followed by a biopsy from a healthy area of the cartilage. Subsequently, chondrocytes

are isolated and proliferated in the laboratory. In the second step, the cultured cells are reimplanted beneath a periosteal patch that has previously been taken from the patient's tibia bone [50–52]. A more modern and less invasive technique turned out to be autologous matrix-induced chondrogenesis (AMIC). AMIC is a one-step procedure that combines microfracture with an application of a 3D scaffold. It protects and stabilizes the initial blood clot and ensures space for the developing chondrocytes from stem cells [53,54]. This method uses different types of scaffolds made mostly from natural polymers. AMIC is safer than the microfracture method, as it avoids surgical intervention in healthy tissue [54,55]. Further advances in cartilage tissue engineering have led to the matrix–induced autologous chondrocyte implantation (MACI) technique. It is similar to AMIC except that chondrocytes are cultured *in vitro* on appropriate scaffolds, and the obtained bioimplant is placed in the cartilage defect site. Results have shown that it is one of the most promising cartilage regeneration methods [56–59]. Unfortunately, there is currently no method that would restore hyaline cartilage. Nevertheless, the most promising approach is to combine current techniques with the use of cartilage tissue engineering, including scaffolds, cells (chondrocytes or MSCs), and biological components, like growth factors, to restore hyaline cartilage [30,46,60–63].

2.3. *Scaffolds for cartilage tissue engineering: requirements, materials, and methodologies*

2.3.1. *Requirements for scaffolds*

The role of scaffolds is to create a 3D structure, similar or better than the native hyaline cartilage, to enhance chondrocytes or MSCs growth [30,64–66]. Scaffolds need to have a 3D structure with appropriate pores diameters. Materials used for scaffold production should be biocompatible, have adequate mechanical strength, and undergo controlled biodegradation. They should also possess a highly porous volume fraction with an interconnected pore network to promote cell spreading, attachment, and proliferation. Porous network provides diffusion of oxygen and nutrients, and allows metabolic products removal [30,36,64,65,67,68]. An appropriate and optimal diameter for macropores should be between 100 and 250 μm or over 300 μm. Pore dimension of 100–250 μm prevents the dedifferentiation of chondrocytes into fibroblasts. Further, pores with a diameter larger than 300 μm are necessary for the chondrogenesis of MSCs [30,36,67–74]. Scaffolds must possess proper morphology, flexibility, sufficient mechanical strength, and adequate stiffness during cell cultivation and after implantation into the human body. They have to provide enough space for ECM formation and prevent chondrocytes' dedifferentiation into fibroblast-like cells [36,63,65–67,70,71,75-77]. When cultivated on 2D-surfaces, such as on Petri-dishes, chondrocytes lose their characteristic phenotype [59,71].

The final morphology of scaffolds mainly depends on pore precursors and the methods of their manufacturing. Nonclassical blowing agents that guarantee macropore formation are gelatin, polyvinylpyrrolidone (PVP), or cellulose nonwovens [78–82]. Scanning electron microscopy (SEM) can examine the scaffolds and pore sizes' structure (SEM) [83]. SEM micrographs can be analyzed by the MeMoExplorer™ software [84,85]. It provides precise information about pore size dimensions by the contour assessment of the pores, what is applicable for sponge-type scaffolds [86,87], and works well for sponge-type membranes [88].

2.3.2. *Materials for scaffolds*

The scaffolds should be made from biocompatible and biodegradable material with appropriate mechanical parameters. Polymer materials should be degradable into non–inflammatory and non-toxic products in the host organism and should undergo an easy removal from the body. Biomaterials need to be resistant to the body's corrosive conditions, such as varying temperatures and pH. The most common materials are natural, synthetic polymers or their combinations (hybrid materials) [30,36,67,70,89–93]. Preferred natural materials are collagen, chitosan, alginate, or hyaluronic acid due to their biocompatibility and biodegradability. Their properties are comparable to native tissues. Unfortunately, they are soluble in an aqueous environment thus, quickly lose their mechanical strength. Moreover, their premature resorption may lead to a loss of scaffold shape and size during cultivation or after implantation to the body [30,65,70,89,91,94]. The most popular synthetic materials for scaffolds are polyesters, such as polylactide (PLA), polyglycolide (PGA), polycaprolactone (PCL), or their copolymers [70,89,93–97]. Due to the chiral nature of lactic acid, several forms of PLA exist: poly-L-lactide (PLLA), poly-D-lactide (PDLA), and poly-D, L-lactide (PDLLA) [98]. PLA degrades into L/D forms of lactic acid, which is transformed into water and carbon dioxide. However, only the L-lactic acid enantiomer is naturally present in the human body as a metabolite [99,100]. Other examples of synthetic materials are polysulfone [101] and polyethersulphone (PES) [81,102,103]. PES is biocompatible and has a high chemical resistance and good mechanical strength [102,103]. Many synthetic polymers have been approved by the Food and Drug Administration (FDA) [65,97,104]. Polymers' degradation time and mechanical properties can be controlled by using them in different relative proportions, as blends or copolymers. Many degrade into monomers or oligomers, which are metabolized in the organism due to their low molecular weight [88,91,93,98,105–107]. The main disadvantage of synthetic materials is their hydrophobic nature leading to reduced cell adhesion and premature degradation, resulting in brittleness [66,92,98,105]. Additionally, degradation is frequently followed by forming acidic components toxic for cells and stimulating inflammatory reactions in the body [66,108]. Hybrid materials combine the advantages of natural and synthetic materials, which allows for obtaining structures with appropriate biological and mechanical properties with good degradation times [65,68,90,92].

2.3.3. *Methods of scaffolds production*

The appropriate form and structure of the scaffolds depend on the proper method of production. This section will list and briefly describe the most common manufacturing methods of scaffolds [35,66,109,110].

Phase inversion is one of the most applied methods for membrane production. The membranes of the desired shape

are formed using either an appropriate temperature or a polymer non-solvent. Thus, several types of the method can be distinguished from thermal-induced phase separation (TIPS) and non-solvent-induced phase separation (NIPS) [33,35,66]. In NIPS, the shaped mold is immersed in a non-solvent (gelling bath), followed by a phase inversion where the solvent from the polymer solution diffuses into the gelling bath. Before use, the formed scaffold is dried to remove the solvent and non-solvent [66,111]. A variant of this method is adding a pore precursor to a previously prepared polymer solution, promoting micro-and macropore formation (for more information, see section 2.3.1.). Then, the pore precursors are removed in the gelling bath or an additional liquid bath [79–82,110,112].

On the other hand, the TIPS method applies different temperatures, and during this process, the temperature of the polymer solution is lowered, which causes phase separation. The low temperature polymer phase is then removed by freezing the solution, followed by a freeze-drying process. In this method, pore morphology can be easily modified by selecting the appropriate thermodynamic parameters of the process [66,69,113–115].

The other method is electrospinning, where a polymer solution is forced through a needle and exposed to an electric field. Thanks to these electrostatic forces between needle and collector, it is possible to obtain fibrous material with various fiber diameters [66,109]. In addition, scaffolds obtained by this method show good flexibility, mechanical properties, and high porosity [116–120].

Rapid prototyping (RP) techniques represent a more advanced method. The most popular RP methods are 3D-printing [2,121–125], selective laser sintering (SLS) [2,126,127], or fused deposition modeling (FDM) [2,128,129]. With RP techniques, natural and synthetic polymers, including cells and biological factors, can be used. Scaffolds can be manufactured with precise and controllable designs with adequate mechanical properties [2,66,109,122–125,130,131]. Some materials such as natural polymers are thermally or pH-dependent, very sensitive, and cannot be used in every method mentioned. However, hybrid scaffolds with desired properties are available using combinations of the above mentioned methods [132-134].

2.3.4. *Scaffolds in cartilage tissue engineering*

Scaffolds for cartilage tissue can be formed as sponges, nonwovens, hydrogels, or combinations thereof [66,135]. Hydrogels are popular in cartilage engineering. Unfortunately, their solubility in aqueous solutions results in a low mechanical strength, which affects later handling. Therefore, only stable synthetic and hybrid scaffolds will be mentioned here and described in this section [136,137].

Commercial scaffolds currently available for patients use the AMCI and MACI methods. In these technique the collagen is preferentially used [46,71,94,138–140]. Due to its disadvantages, the collagen structure often does not meet the appropriate requirements. The gelly framework of collagen rather leads to the formation of non-valuable fibrocartilage rather than hyaline cartilage [46,65,70,90,91,94,138]. Synthetic or hybrid materials are also used for scaffold manufacturing. BioSeed® – C (Biotissue) is an example of such a synthetic scaffold. The product consists of PGA, PLA, and poly-p-dioxanone (PDS) [138]. It has been shown that postoperative values are improved, and results from 4 years of clinical trials have proven a good treatment outcome for cartilage defects [141]. Chondrotissue® (Biotissue) is another example of a commercial hybrid scaffold. It is made of PGA and HA by a freeze–drying method and subsequently enriched with autologous platelet rich plasma (PRP) or serum-containing platelets [138]. The clinical outcomes from a 5 years study showed good results for the one-step cure treatment with the Chondrotissue® membrane [142].

In many studies, promising results are obtained with synthetic and hybrid scaffolds. In Table 1, synthetic and hybrid scaffolds dedicated to cartilage regeneration and passed preclinical studies with good results are shown.

3. Experimental section

3.1. *Materials and devices*

Chemicals used in our experiments: Polyvinylpyrrolidone (PVP, M_n = 10 kDa), 1–Methyl-2-pyrrolidone (NMP), chloroform ($CHCl_3$), collagenase type II, trypan blue, thiazolyl blue tetrazolium bromide (98% MTT assay), collagen from bovine Achilles tendon, glutaraldehyde (25%), phosphate buffer solution (PBS), hydrochloric acid (HCl 70%), sodium bicarbonate ($NaHCO_3$), Dulbecco's modified Eagle's medium–high glucose with 4500L-glutamine (DMEM), fetal bovine serum (FBS), penicillin–streptomycin (10 000 U/mL), L-glutamine (200 mM), and amphotericin (250 μg) were acquired from Sigma-Aldrich. Cupric sulfate ($CuSO_4{\cdot}5H_2O$), sodium hydroxide (NaOH), ammonia solution (NH_4OH 25%), nitric acid solution (HNO_3 70%), dimethyl sulfoxide (DMSO), N, N-dimethylformamide (DMF), 1,4-dioxane were purchased from POCh SA. Poly-L-lactide (PLLA, M_n = 86 kDa) was acquired from Nature Works NW 2003D.

Qualitative filter paper (cellulose paper no. 1 and no. 3) was purchased from Whatman®. NucBlue, live ready probes reagent (Hoechst 33342) was acquired from Thermo Fisher Scientific (Gibco). Methanol (MeOH) and ethanol (EtOH 70%, and 96%) were provided by Linegal Chemicals. The deionized water (18.2 MΩcm conductivity) was obtained using the Mili-Q apparatus.

According to the literature, the porcine gelatin nonwoven was obtained by an electrospinning method applied in the Institute of Fundamental Technological Research PAS, Warsaw [154,155]. The cartilage was taken from the surgical waste of 50–71-year-old patients hospitalized in the Gruca Orthopaedic and Trauma Teaching Hospital, Department of Traumatology and Orthopaedics in Otwock. The Medical Centre obtained the consent of the Medical Ethics Committee for Postgraduate Education branch Otwock (number 57/PB/2014 from the 15th of July 2014 year).

The analytical methods were performed using the following devices: scanning electron microscope (Hitachi TM–1000) with an accelerator voltage of 15 kV, sputter coater (EMITECH

Table 1 – Scaffolds for cartilage tissue regeneration.

Study	Material	Method	Cells, animal model	Results
Conoscenti et al. [69]	PLLA	Phase inversion	human articular chondrocytes	Scaffold with high porosity and pore size of about 100 μm. It promoted the secretion of chondrogenic genes and was better than the PLLA scaffold with larger pores (~200 μm)
Dudziński et al. [81], Płończak et al. [143–145]	PES	Phase inversion	human articular chondrocytes rabbit model	Obtained results indicated that PES scaffolds are effective in cartilage treatment. Scaffolds showed better results during *in vivo* outcomes compared to commercially available Chondro-Guide® scaffolds
Tsai et al. [146]	PUR	Phase inversion	Human articular chondrocytes and human MSCs	Scaffolds with a porosity of ~ 97%, the pore sizes of 126–186 μm. Chondrocytes grew well, and human MSCs indicated great chondrogenic gene expression in PUR scaffold than PLA scaffolds.
Sharifi et al. [117]	GEL, CS, PCL	Electrospinning and cross-linking	Human bone mesenchymal stem cells (BM-MSCs)	The study showed the chondrogenesis without using a differential medium. Gene expression of collagen type II proved the differentiation of seeded hMSCs to chondrocytes in hybrid scaffolds without using any external chondrogenic differentiation factors. The best results came for scaffolds containing the highest GEL-CS content. The study showed promising outcomes with the potential for future study in cartilage tissue engineering.
Prasanna et al. [107]	CH, PC, PLLA, EDC, CS, NHS	Phase inversion and cross-linking	Rabbit model	Scaffold with a porosity of ~84%, pore size from 50 to 170 μm, and adequate mechanical strength. The outcomes showed the suitability of the scaffold for cartilage tissue regeneration.
Liao et al. [147]	CMSA, PECA, GO	Phase inversion	Rabbitarticular chondrocytes and rat model	Scaffold with a porosity of ~70% and a mean 175.2 μm pore size. Good results have been obtained in both *in vitro* and *in vivo* studies.
Setayeshmehr et al. [148]	DCM, PVA, fibrin	Phase inversion and cross-linking	Human adipose-derived mesenchymal stromal cells (ASCs)	Scaffold with apore size of about 120 μm and porosity of about 89%. The scaffold can be considered a promising membrane for cartilage tissue engineering applications.
He et al.[149]	PLCL, COL	3D-printing	Rabbit articular chondrocyte	Scaffold with a controlled structure with a porosity of ~ 85% and pore size ~ 450 μm. Membrane with good flexibility and mechanical properties. Study with promising results for tissue cartilage engineering.
Rofiqoh et al. [150]	PLGA, COL	Phase inversion and cross-linking	Bovine articular chondrocytes (BACs) mouse model	The membrane has high porosity of ~ 98% and large spherical pores of about 440 μm. The *in vitro* and *in vivo* studies showed promising results with high potential for future work on cartilage regeneration.
Nogami et al. [151]	PLGA, ECM	SCPL	Rat mesenchymal stem cells (MSCs) and rat model	Scaffold with a porosity of 90%. The *in vitro* study showed promising results with the proper differentiation of MSCs. The *in vivo* outcomes indicated the regeneration of tissue hyaline cartilage. Thus, scaffold seems to have the potential for cartilage tissue regeneration.
Kamath et al. [152]	EGCG, PCL, ENP	SCPL	Human articular chondrocytes	Membrane with a pore size of less than 300 μm. Results showed a synthetic scaffold with the addition of EGCG - plant of a potent chondrogenic drug, which was loaded into albumin nanoparticles (ENP). Scaffold with potential for future study for cartilage regeneration.
So et al. [153]	PCL, CS	FDM	BM-MSCs	Scaffold with a pore size of ~ 390 μm and porosity of ~ 60%. Firstly, the scaffold was treated with alkaline. Then during culture, the medium was supplemented with CS that induced chondrogenic differentiation of BM-MSCs.

CH-chitosan; COL-collagen; GEL-gelatin; PUR-polyurethane; PC-pectin based; PDS-poly-p-dioxanone; CS-chondroitin sulfate; CSMA-methacrylated chondroitin sulfate; HA-hyaluronic acid; PEG-poly (ethylene glycol); PCL-polycaprolactone; PLA-polylactic acid; PLLA-poly (L-lactide); PGA-poly(glycolic acid); PES-polyethersulfone; PLGA-polylactic-co-glycolic acid; DCM-devitalized costal cartilage matrix; PVA-poly(vinyl alcohol; ECM-Extracellular matrix; EDC-1-ethyl-3-(3-dimethylaminopropyl) carbodiimide; NHS-N-hydroxysuccinimide; PLCL-poly(l-lactide-co-ε-caprolactone); SCPL-solvent casting and particulate leaching method; AC-acryloyl chloride; CMSA-methacrylated chondroitin sulfate; GO-graphene oxide; PECA-poly(ethylene glycol) methyl ether-ε-caprolactone-acryloyl chloride; EGCG-Epigallocatechin-3-gallate, ENP-albumin nanoparticles; FDM-fused deposition modeling.

K550X), CHNS analyzer (Elementar, Vario EL III), multi-well spectrophotometer (Synergy HT, BioTek Instruments), UV light in a fluorescent microscope (OLYMPUS IX71).

3.2. Preparation of the PES scaffold

The PES scaffold was obtained according to the method presented in previous works [81,156,157]. All components and the polymer solution were kept under anhydrous conditions. The membrane forming solution was prepared by dissolving PES and PVP polymers (mixed in ration 3:1) in DMF and NMP solvents (mixed in ratio 1:1) with constant stirring under a nitrogen atmosphere to 17 wt%. The chromatography paper (Whatman no. 3) was saturated with a polymer solution for 30 min and placed on Whatman no.1, which was saturated with DMF. For gelation, the membrane was immersed in the bath with deionized water for up to 12 h. To dissolve the cellulose, it was placed in the copper hydroxide ammonia complex (Schweizer's reagent) and then in a 5% (v/v) solution of nitric (V) acid to remove copper oxide. Next, the membrane was rinsed with deionized water until it achieved a neutral reaction. Finally, the prepared scaffolds were stored in polyethylene bags filled with 70% ethanol.

3.3. Preparation of the PLLA scaffolds

The PLLA scaffold was fabricated according to the method that has been presented in previous works [158,159]. In this method, it is important to protect the gelatin nonwoven from water to prevent its dissolving. The PLLA and PVP (mixed in ratio 2:1) polymers were dissolved in chloroform with constant stirring to obtain 6 wt% in solution. The gelatin nonwoven was placed on the polymer solution layer. Next, another portion of the solution was poured on it, and the second slice of nonwoven was placed on the top. The received membrane was gelled in the bath with methanol at room temperature. The gelatin was removed by immersing the membrane in a hot deionized water bath (about 60 °C). The scaffolds were stored in 70% ethanol.

3.4. Chondrocytes isolation

The following procedures were performed under sterile conditions in a laminar flow cabinet. The tissue taken from the patient was kept in PBS to prevent drying. First, the cartilage tissue was cut into small slices. Then, it was rinsed three times with PBS and supplemented with medium (DMEM containing 10% (v/v) of FBS, 1.5% (v/v) of the penicillin–streptomycin solution, 1% (v/v) of L-glutamine solution, and 0.1% (v/v) of amphotericin B). Next, the cartilage was digested in 0.2 wt% of collagenase type II solution with a complete medium for 16 h in the incubator (37 °C, 5% CO_2). After that time, the obtained samples were filtered (pore size: 0.7 μm) and centrifuged at 5 °C at 1000 rpm for 5 min. The supernatant was discarded, and the obtained pellet was suspended in 2 mL medium. Before cell counting with the Neubauer chamber, the cells were stained with a 0.5 wt% solution of trypan blue.

3.5. Chondrocytes culture

The sterile scaffolds were cut into round pieces of 15 mm diameter. They were rinsed three times with PBS and supplemented medium, and then placed directly into 24-well plates. Sterile poly(tetrafluoroethylene) rings were used to immobilize the membranes on the bottom of the wells. The chondrocytes were seeded on the scaffold's perforated layer with a concentration of $1–7{\cdot}10^5$ cells/well. The cell cultures were carried out in the incubator at 37 °C and in an atmosphere with a 5% concentration of CO_2. The medium was exchanged twice a week.

3.6. Hoechst dye staining procedures

Chondrocytes cultured on PLLA and PES scaffold for 72 h, 3, and 7 weeks were fixed with a solution of 2.5% glutaraldehyde in PBS and incubated at 5 °C for 1 h. The solution was discarded, and one drop of Hoechst dye and 500 μL of PBS were added to each membrane. The samples were observed under UV light in a fluorescent microscope (OLYMPUS IX71).

3.7. Recovery of protein from scaffolds

PLA and PES scaffolds after 3 and 7 weeks of cultivation were treated with a 2.5% glutaraldehyde solution in PBS and then were incubated at 5 °C for 1 h. Next, fixed PLLA and PES scaffolds were dissolved in chloroform or DMF mixed with NMP in ratio 1:1, respectively. The samples were kept in the solvent for 2 h with constant stirring. Then, obtained residue with a new portion of the solvent was centrifuged at 4 °C at 900 rpm for 2 min, it was repeated 3 times. Next, samples were centrifuged 3 times in deionized water and were left to dry.

3.8. SEM observation

The PLLA and PES samples were immersed in ethanol for at least 15 min and then put into liquid nitrogen to cut into pieces. Afterward, the samples were dried and coated with a 7 nm layer of gold using a sputter coater [83]. The top, bottom layer, cross-section of the PLLA, and PES scaffolds were observed with a microscope. Additionally, the pore size and thickness of the scaffolds were measured. Before SEM observation, samples from cell culture were fixed with 2.5% glutaraldehyde, and the procedure was followed as shown for PLLA and PES membranes.

3.9. Metabolic activity of cells

The MTT assay was used to examine cell proliferation. This colorimetric assay is based on reducing a yellow tetrazolium salt (3-(4,5-dimethylthiazol-2-yl)-2,5-diphenyltetrazolium bromide or MTT) to purple formazan crystals by metabolically active cells. Metabolic activity of cells seeded on PLLA, and PES membranes was studied using the MTT assay after 24 h, 72 h, 8 days, 2, and 3 weeks of culture. First, the scaffolds were gently removed from the culture wells and transferred to a new plate to separate cells on the scaffolds from cells that

had grown at the bottom of the well. Next, the scaffolds were treated with 0.25 μg/μl MTT for 2 h (37 °C, 5% CO_2). Next, the formazan crystals were dissolved by DMSO mixed with acidified ethanol (1:1) for 45 min. The 100% DMSO solvent was also used as a control. Then, the obtained solutions were transferred into a 96-well plate. The absorbance was measured by a multi-well spectrophotometer (Synergy HT, BioTek Instruments) at 570 nm.

3.10. *Elemental analysis*

Elemental analysis was used to check the PLLA and PES scaffolds' elemental composition before (reference samples) and after chondrocytes culture (7 weeks). The samples were fixed and dried as previously described. The protein content was assessed by multiplying the determined nitrogen content to a protein conversion factor of 6.25. Two analyses were performed for each sample.

3.11. *The porosity of the scaffolds*

The porosity of the scaffolds was determined by measuring the mass and dimension of the scaffolds, as described by Ho et al. [160], and calculated using the following formula (Eq. (1)):

$$Porosity = \frac{D_p - D_{ap}}{D_p} \hat{A} \cdot 100\% \quad (1)$$

With D_p : density of PES (1.37 g/cm^3) and PLLA (1.24 g/cm^3), D_{ap} : apparent density (scaffold mass / apparent scaffold cube volume). The calculations were carried out in 10 repetitions.

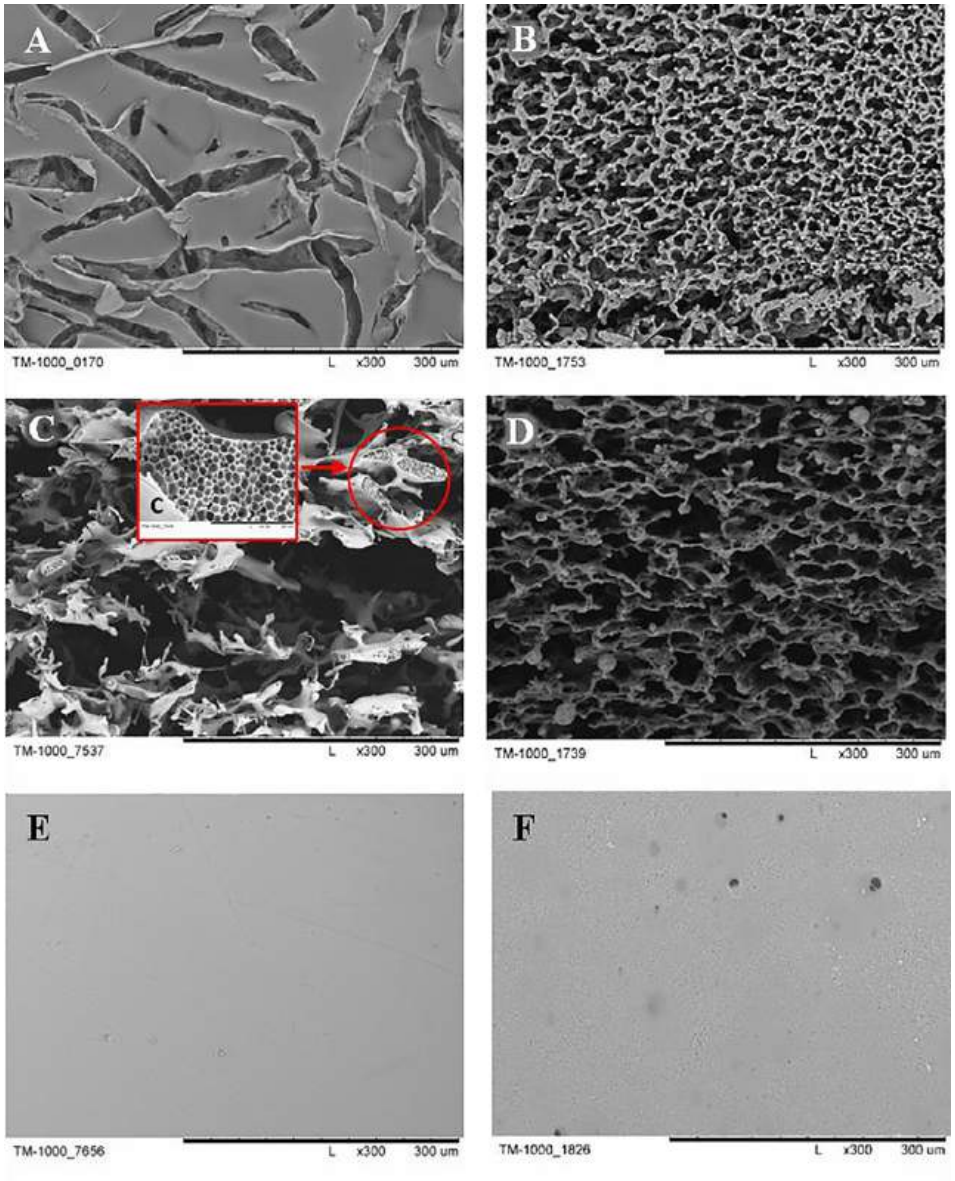

Fig. 1 – SEM photomicrographs of scaffolds. A – perforated skin layer of PES scaffold; B – perforated skin layer of PLLA scaffold; C – a cross-section of PES scaffold; c- micropores structure of PES scaffold; D – a cross-section of PLLA scaffold; E–dense bottom layer of PES scaffold; F–the dense bottom layer of PLLA scaffold. Scale bars: A, B, C, D, E, F- 300 μm, c- 20 μm.

4. Results

4.1. *Characterization of PLLA and PES scaffolds*

The SEM micrographs of both scaffolds present an irregular structure with macropores (Fig. 1). The thickness of both scaffolds was about 400–600 μm. Membranes show a perforated top layer (Fig. 1A, B). The top layer of the PLLA membrane contains numerous pores with sizes from 20 to 60 μm (Fig. 1B). In the PES scaffold, the perforation gaps range from 10 to 60 μm, whereby its length often exceeds 1 mm (Fig. 1A). The interior of both scaffolds shows a three-dimensional network of interconnected macropores (Fig. 1C, D). For PLLA, scaffold pores range between 20 and 100 μm diameter (Fig. 1D) and PES from 60 to 300 μm (Fig. 1C). The bottom skin layer of both membranes was dense (Fig. 1E, F). Furthermore, the addition of PVP also affects the morphology of micropores (Fig. 1c). The porosity of PLLA and PES membranes was determined from Eq. (1) and has reached 98.1% and 98.5%, respectively.

4.2. *Observation of cells during cultivation*

During cultivation, the cells were observed on the edges of both scaffolds by an inverted microscope. The cells appear to be round, with a diameter ranging from 10 to 20 μm (Fig. 2). Moreover, they are connected by the ECM, which indicates that both PLLA and PES membranes enhance chondrocyte development and ECM production.

Another test performed during cell culture was nuclei staining with the Hoechst dye. The nuclei detected under a fluorescent microscope were round or slightly elongated (Fig. 3). The staining was done after 72 h, 3 weeks, and 7 weeks. After 3 weeks, on the PES scaffold, relatively more stained nuclei are found (Fig. 3B, 3b) in comparison to experiments with the PLLA membrane (Fig. 3A, 3a). Unfortunately, after 3 weeks on a PLLA scaffold, fewer nuclei than staining after 72 h could be detected. Nuclei are not evenly distributed and appear small aggregates (brighter areas) (Fig. 3D-E). The cell nuclei are visible in both scaffolds even after 7 weeks (Fig. 3C, F). The PLLA membrane observation showed a reduced number of stained nuclei compared to experiments with the PES membranes.

Samples after cell culture were evaluated with SEM to determine cells' distribution with their metabolic products on the investigated scaffolds (Fig. 4). Results show that the cells were spread and attached to both scaffolds. On both perforated surfaces, cells and their products are visible (Fig. 4 A-B). There are numerous cells with their products in the cross-section of PES and PLLA scaffolds after 2 and 3 weeks. Furthermore, the cells are interconnected by ECM (Fig. 4 A-D). Moreover, visible cells form small aggregates (some examples are marked with white circles in Fig. 4). Also, single stretched cells are visible (Fig. 4 E, F).

4.3. *Metabolic activity of the cells seeded on PES and PLLA scaffolds*

The MTT assay was done after 24 and 72 h, 8 days, 2 and 3 weeks of cultivation. The metabolic activity of cells with the PES scaffold was higher than with the PLLA scaffold (Figs. 5, 6). The decrease in the absorbance value in the 2nd and 3rd week of cultivation on PLLA scaffolds was most likely due to the significant progress of degradation of these scaffolds (Fig. 5). The differences in seeding density on mem-

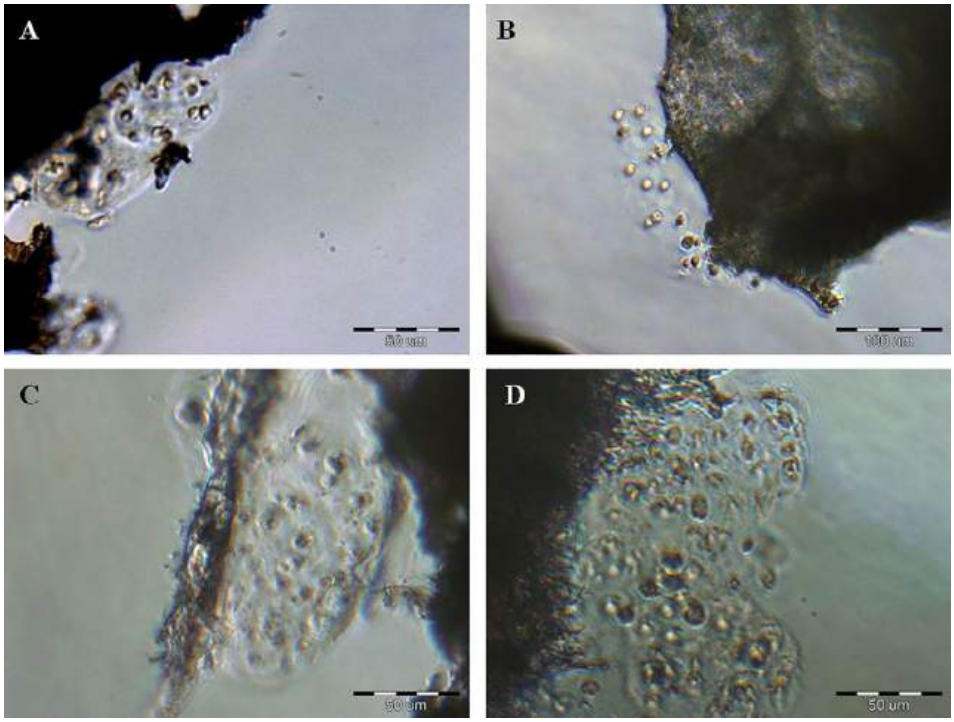

Fig. 2 – The cells on the edges of scaffolds. A, C – PES scaffold respectively after 1 and 2 weeks of cultivation; B, D – PLLA scaffold respectively after 1 and 2 weeks of cultivation. Scale bars: A, C, D – 50 μm, and B – 100 μm.

branes were so insignificant that they can be ignored. However, it should be pointed out that these experiments are preliminary and the results of the MTT assay are only illustrative and have been included to show the overall trend.

4.4. *Elemental analysis*

The nitrogen content was checked before and after 7 weeks of cultivation for both scaffolds using an elemental analyzer. The obtained nitrogen value was respectively 7.55% for PES and 2.27% for PLLA scaffold. It means 47.26% and 14.16% content of protein for PES and PLLA scaffold, respectively. The protein to mass membrane ratio was found between 0.90 and 0.16 for the PES and PLLA membranes. Thus, PES scaffold showed a significant increase in nitrogen in contrast to PLLA.

4.5. *Recovery of cells and their products from scaffolds*

To recover the cells and their product from scaffolds, they were dissolved in an appropriate solvent. The SEM images of recoveries from scaffolds, native cartilage, and Hoechst dye staining are presented in Fig. 7. The surfaces are rough and irregular (Fig. 7 D-E, G-H), and resemble native cartilage (Fig. 7 A-B). The presence of cells in the residue was confirmed by Hoechst staining. The cells' nuclei (white spots) are visible in Fig. 7 C, F, I. Photos show recoveries stained by Hoechst after 3 weeks of culture on PES (Fig. 7H) and PLLA (Fig. 7I). For comparison, native cartilage was also stained (Fig. 7C). Cells are evenly distributed and appear in groups (Fig. 7 C, F, I). However, cells are not sharp due to their presence in different planes, making it impossible to catch the correct severity during the experiment.

5. Discussion

PLLA and PES scaffolds characterized in this study show a perforated skin layer with pores with a diameter of more than 20 μm. It allows chondrocytes to penetrate the membrane structure. The interior of both membranes shows a network of interconnected macropores (Fig. 1). It provides an appropri-

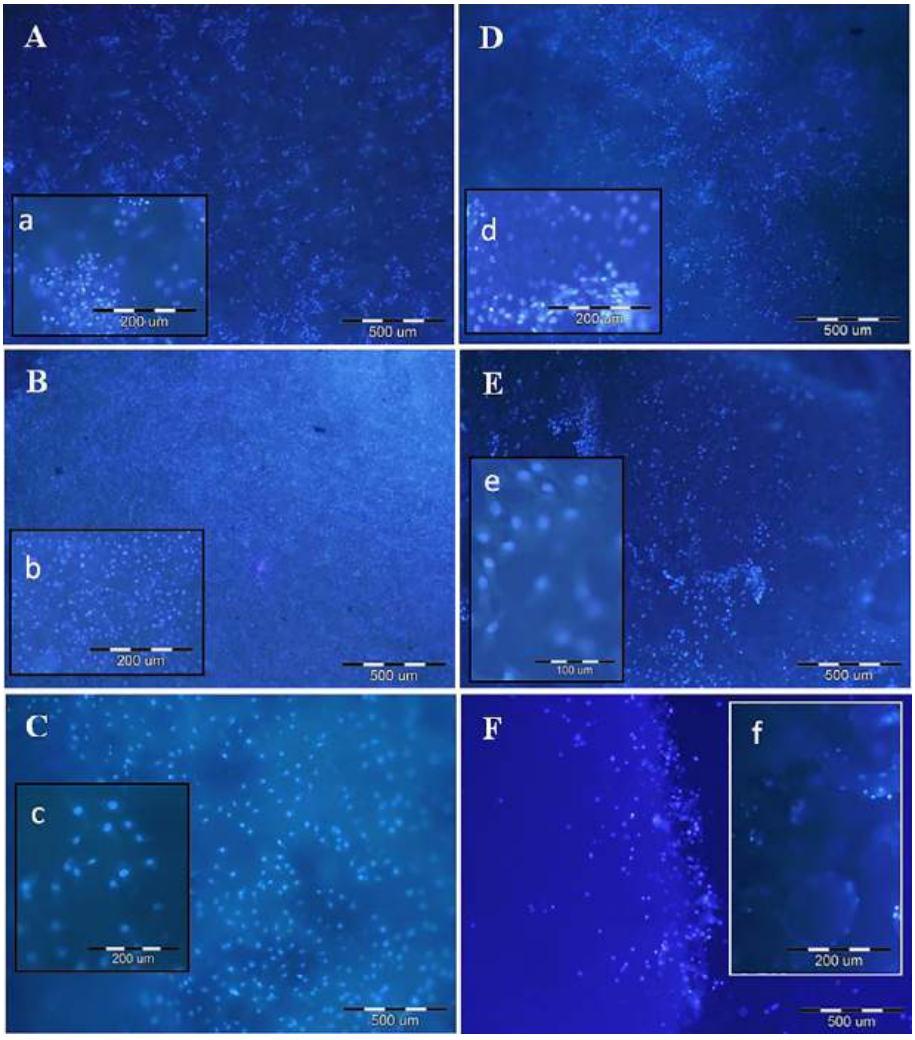

Fig. 3 – Hoechst staining of cell nuclei using UV light. A, B, C–PES scaffolds respectively after 72 h,3 weeks and 7 weeks; D, E, F–PLLA scaffolds respectively after 72 h, 3 weeks, and 7 weeks. Pictures of a-f show the approximation of A-F images. Scale bars: A-F – 500 μm, a-d, f – 200 μm, and e – 100 μm.

ate environment for the migration, proliferation, and adhesion of chondrocytes, thus allowing ECM production. Additionally, the micropore structure assures oxygen transport, nutritious and metabolic products (Fig. 1C). The bottom skin layer is dense, preventing cells from getting out of the scaffolds (Fig. 1E, F) [33,36,161].

Numerous tests were performed to assess isolated chondrocytes growth in PLLA and PES scaffolds. Cells attachment to the edges of the membrane was observed by an optical microscope (Fig. 2), whereas cell morphology was studied with a SEM (Fig. 4). The cells visible in Fig. 2 and Fig. 4 are connected by ECM and show a spherical shape. Their shape may indicate that their phenotype was kept [38]. The cross-section's SEM image suggests that the cells have penetrated the membranes, where they could develop and produce proteins (Fig. 4C-F). Cell occurred in groups of 2 to 3 what proves their capacity to proliferate.

To visualize cells within scaffolds, Hoechst dye staining was performed. The test showed many nuclei (white points in Fig. 3). Cells were growing at the different depth levels of scaffolds, and thus, many cells were not equally in focus. This implies that the cells can penetrate the 3D structure of the membrane. PES scaffolds showed an increase in cell number and an even distribution. In contrastto observations with PLLA membranes, cell growth could not be detected, although cells could form aggregates. Further, after seven weeks of chondrocyte cell culture on the PLLA membrane, only a few nuclei have been noticed (Fig. 3F). The viability and prolifera-

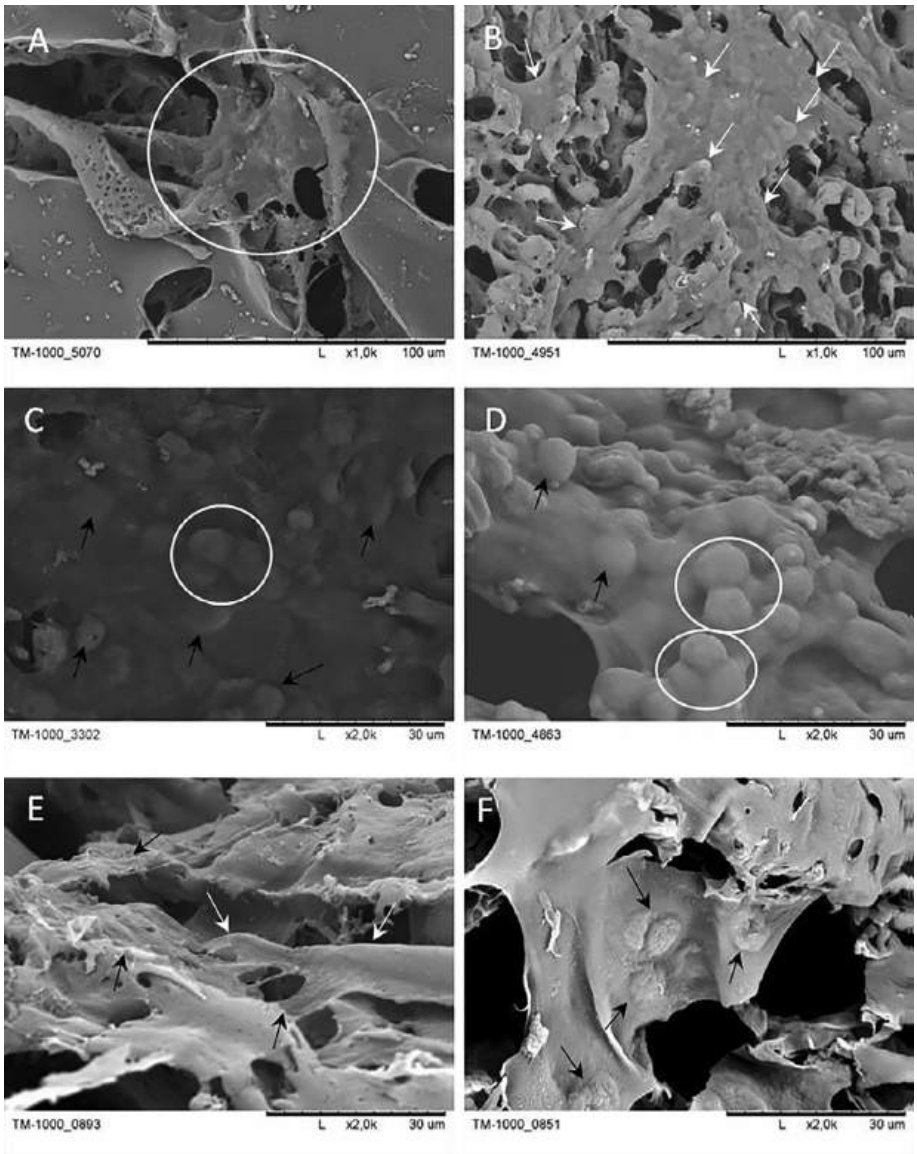

Fig. 4 – The SEM micrographs of cross-sections and the perforated top layers of scaffolds during cultivation. A, B – perforated surfaces of PES (A) and PLLA (B) scaffolds after 2 weeks of cultivation. The cells and ECM are marked in a white circle (A) and white arrows (B). C, D – the cross-sections of PES (C) and PLLA (D) scaffolds after 2 weeks of cultivation. Dividing cells are marked in a white circle, black arrows indicate some cells. E, F- the cross-sections of PES (E) and PLLA scaffolds after 3 weeks. White and black arrows indicate cells with their products. Scale bars: A, B – 100 μm, and C-F – 30 μm.

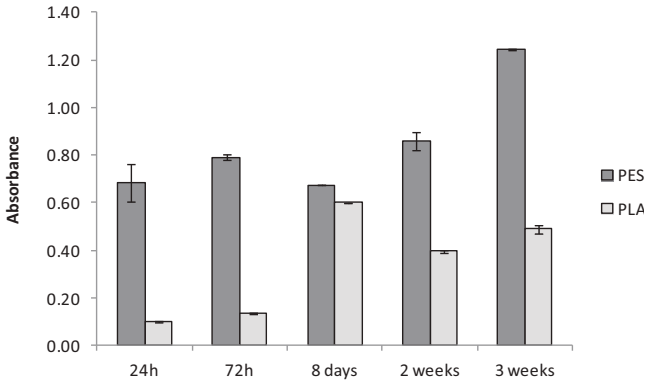

Fig. 5 – Experiment 1. Comparison of MTT assay results for chondrocyte cultures on PES and PLLA scaffolds. The seeding density was for the PES membranes $3.4 \cdot 10^5$ cells/well and for the PLLA membranes $2.5 \cdot 10^5$ cells/well (24-well plate). Negative control – scaffold without cells immersed in complete medium - has been subtracted.

tion of chondrocytes were examined with the MTT assay after 24, 72 h, 8 days, 2 weeks, and 3 weeks of cultivation (Figs. 5, 6). Higher absorbance values were obtained for PES scaffolds compared to PLLA scaffolds. This effect does not ultimately rule out the possibility of using PLLA scaffolds for cartilage renewal purposes. Lower values may be the result of the progressive degradation of PLLA during the experiment. PES scaffolds were easy to handle throughout the experiments, whereas the PLLA membranes became crunchy and brittle after 2–3 weeks. Therefore, it was difficult to transfer PLLA membranes to a new plate for MTT assay. However, the results of the MTT assay support the conclusions drawn from the other studies described in this paper. At the end of the culture period, elemental analysis was performed for both types of scaffolds, PES and PLLA. Nitrogen was found in a higher percentage of PES membranes. After thoroughly washing the culture medium from the scaffold, the source of nitrogen was the cells and proteins produced by the cells (PLLA

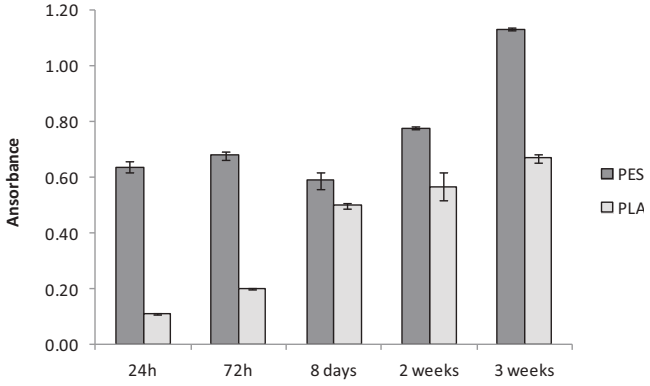

Fig. 6 – Experiment 2. Comparison of MTT assay results for chondrocyte cultures on PES and PLLA scaffolds. The seeding density was for the PES membranes $6.6 \cdot 10^5$ cells/well and for the PLLA membranes $3.3 \cdot 10^5$ cells/well (24-well plate). Negative control - scaffold without cells immersed in complete medium - has been subtracted.

and PES do not contain nitrogen). The nitrogen content is an objective and reliable indicator of the amount of proteins in the tested sample. Therefore, we believe that PES membranes provide a better environment for chondrocytes' growth and protein production. Numerous attempts to remove cells from the membranes, e.g., did not yield positive results for their counting (like trypsinization). For this purpose, the scaffolds had to be dissolved with an appropriate solvent. Unfortunately, this procedure might have damaged the protein. The SEM results obtained from recoveries have shown similarities to the native cartilage structure (Fig. 7). Besides, recoveries and native cartilage were stained with Hoechst dye to confirm cells' presence (Fig. 7 C, F, I), which finally proved the method's efficiencyfor protein recovery.

The results show PES scaffolds advantage over PLLA. It is possible to obtain an appropriate structure with this PES material using various methods. Another advantage of the PES scaffold represents the sulfate groups [-SO_2] in the polymer chain. These groups are also found in the hyaline cartilage matrix (chondroitin-sulfate). Thus, chondrocytes had a similar environment to their natural matrix [162]. Further, the scaffolds can be sterilized with all currently available sterilization techniques, such as with ethanol, gamma-rays, or β-irradiation, by autoclave and then is easy to store. This may also explain why the PES scaffolds have been successfully applied for cartilage regeneration in rabbits [81,143].

PLLA scaffolds can be obtained by various methods, from simple phase inversion to 3D-techniques. The PLLA polymer is commonly used for medical applications and is well described in many papers. Furthermore, PLLA has been chosen due to its degradation to.

L–lactic acid, which naturally occurs in the body [163]. Unfortunately, due to the short degradation time of PLLA, scaffolds have shown to be unstable and even crumbled after 2 weeks of chondrocyte culture. Moreover, in the third week of cultivation, a decrease in cells' viability was noticed (Table 1). Furthermore, the cell number decreased after 7 weeks of culture (Fig. 3 F). This can be explained by the negative effect of lactic acid on chondrocytes and reduced material structure due to degradation [108].

For our study, we have selected isolated chondrocytes. A chondrocyte cell line was not used because such cells are possibly more resistant to the artificial environment and scaffold-internal conditions during culture. Isolated cells can show the actual results. As a result of the cooperation between our institute and the local hospital, we could obtain material from various patients. This has undoubtedly increased the reliability of the study.

This study has several limitations. First, the article only presents preliminary research. Second, the statistics were not made due to the study's basic assumptions to exclusively prove that it is possible to carry out a human chondrocytes culture with artificially designed membranes. Finally, the number of cells obtained after isolation was too small to perform many repetitions. Further, cells from different donors have been used for the same experiments, such that their dataset may not support statistical relevance. Finally, cells have not been further multiplied due to maintaining the proper phenotype of chondrocytes [67,71,77]. Tests confirming the chondrocyte phenotype were not performed. More

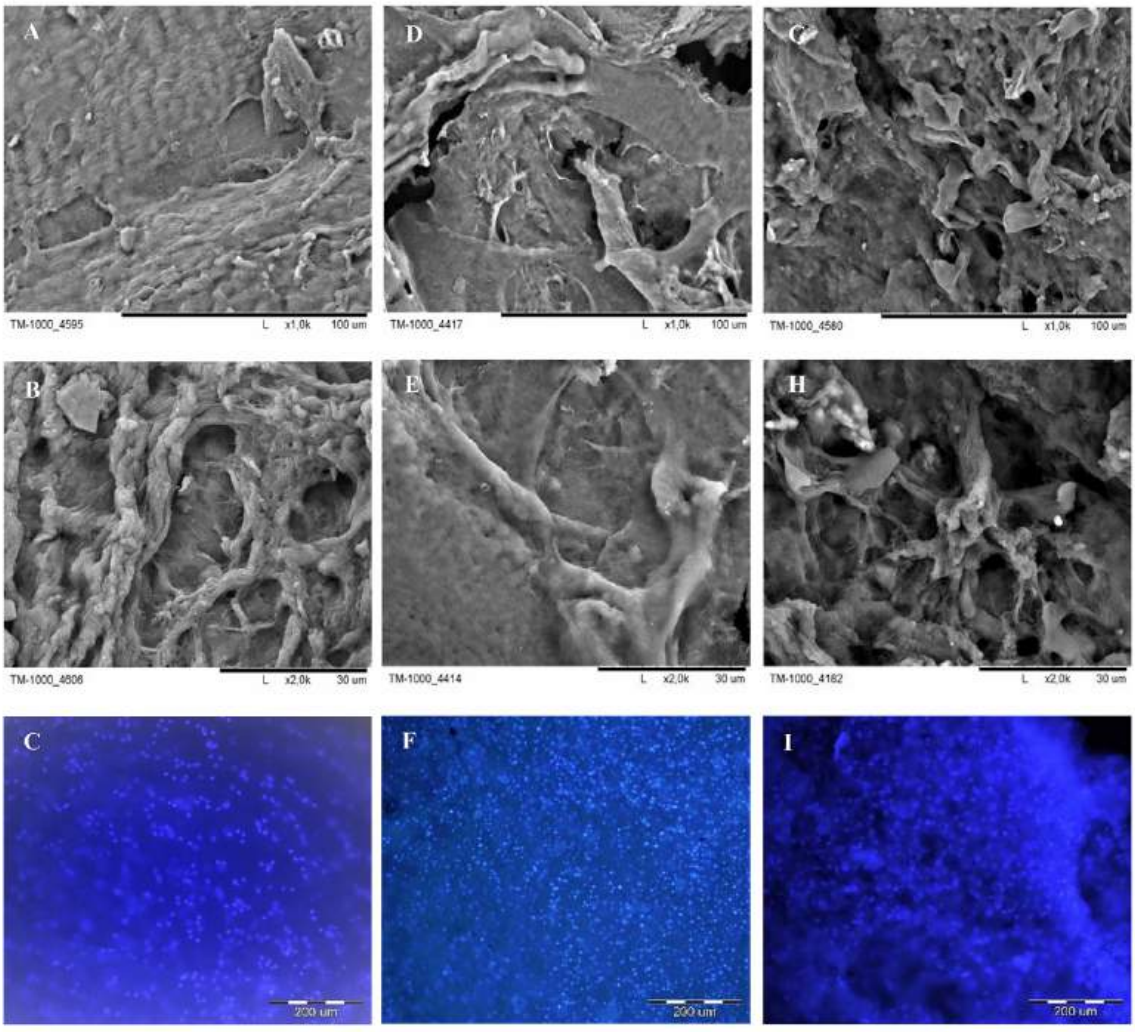

Fig. 7 – The SEM micrographs of native cartilage and recoveries were obtained from scaffolds and their staining with Hoechst. A-B –native cartilage; D-E – the recoveries from PES scaffold after 3 and 7 weeks; G-H –the recoveries from PLLA scaffold after 3 and 7 weeks. The nuclei staining with Hoechst dye respectively for C – native cartilage, F – recoveries from PES scaffold after 3 weeks of cultivation, I – recoveries from PLLA scaffold after 3 weeks of culture. Scale bars: C, F, I – 200 μm, A, D, C – 100 μm and B, E, H – 30 μm.

detailed studies will have to be conducted and shown in perspective.

6. Conclusions

Many people suffer from cartilage diseases, like osteoarthritis, that provide disability. Unfortunately, there is still no proper method available for hyaline cartilage regeneration. The most promising tissue cartilage engineering method is implanting the scaffold with or without cells (autologous chondrocytes or MSCs). Commercial scaffolds do not provide satisfactory results because the properties of the regenerated tissue material are rather closer to fibrocartilage than to hyaline cartilage. New approaches and solutions are desperately needed, and that hybrid scaffolds based on synthetic polymers may provide hope in this respect. As shown here in our experiments, the combination of natural with synthetic materials ensures proper chondrogenesis, the preservation of cell phenotype, and good mechanical properties. Choosing appropriate cells and additives, like growth factors, will be helpful in future experiments. Altogether, there is a need for a new method in cartilage regeneration to obtain hyaline cartilages in damaged areas.

The scaffolds made of PES and PLLA have a perforated top layer, dense bottom layer, and highly porous structure inside. Such a 3D construct mimics native tissue and thus enhances chondrocyte proliferation and ECM formation. Both polymers are known to form their biocompatibility. Here, it was examined by the proliferation MTT assay and nuclei staining with Hoechst. Cells observation with an inverted microscope and SEM showed that they kept their round shape and proved ECM production, which indicates that PES and PLLA scaffolds create a structure suitable for chondrocyte culture. PES was less brittle than PLLA and had a longer degradation time, so

cell number within this membrane was greater. Moreover, elemental analysis has presented significantly higher nitrogen content in the PES scaffold. In both materials, recoveries after polymer dissolution had a structure similar to the native tissue. Our study demonstrated PES great advantage over PLLA for chondrocytes *in vitro* culture and showed a perspective for future *in vivo* experiments.

Fundings

This research was supported by statutory funds of Laboratory of Semipermeable Membranes and Bioreactors in Nalecz Institute of Biocybernetics and Biomedical Engineering, Polish Academy of Sciences (IBBE PAS).

Declarations of interest.

None.

CRediT authorship contribution statement

Monika Wasyłeczko: Conceptualization, Data curation, Methodology, Validation, Writing – review & editing. **Zuzanna Joanna Krysiak:** Methodology, Data curation, Writing – review & editing. **Ewa Łukowska:** Methodology, Validation, Writing – review & editing. **Marcin Gruba:** Resources. **Wioleta Sikorska:** Writing – review & editing. **Aleksandra Kruk:** Resources. **Judyta Dulnik:** Resources. **Jarosław Czubak:** Resources. **Andrzej Chwojnowski:** Conceptualization, Supervision, Funding acquisition.

REFERENCES

[1] Giwa S, Lewis JK, Alvarez L, Langer R, Roth AE, Church GM, et al. The promise of organ and tissue preservation to transform medicine. Nat Biotechnol 2017;35(6):530–42. https://doi.org/10.1038/nbt.3889.

[2] Yan Q, Dong H, Su J, Han J, Song B, Wei Q, et al. A review of 3D printing technology for medical applications. Engineering 2018;4:729–42. https://doi.org/10.1016/j.eng.2018.07.021.

[3] Popoola J, Greene H, Kyegombe M, MacPhee IA. Patient involvement in selection of immunosuppressive regimen following transplantation. Patient Preference Adherence 2014;8:1705–12. https://doi.org/10.2147/PPA.S38987.

[4] Dzobo K, Thomford NE, Senthebane DA, Shipanga H, Rowe A, Dandara C, et al. Advances in regenerative medicine and tissue engineering: innovation and transformation of medicine. Stem Cells Int 2018;2018:1–24. https://doi.org/10.1155/2018/2495848.

[5] Park KM, Shin YM, Kim K, Shin H. Tissue engineering and regenerative medicine 2017: a year in review. Tissue Eng - Part B 2018;24(5):327–44. https://doi.org/10.1089/ten.teb.2018.0027.

[6] Messner F, Guo Y, Etra JW, Brandacher G. Emerging technologies in organ preservation, tissue engineering and regenerative medicine: a blessing or curse for transplantation ? Transpl Int 2019;32:673–85. https://doi.org/10.1111/tri.13432.

[7] Scarritt ME, Pashos NC, Bunnell BA. A review of cellularization strategies for tissue engineering of whole organs. Front Bioeng Biotechnol 2015;3:1–17. https://doi.org/10.3389/fbioe.2015.00043.

[8] Mir TA, Iwanaga S, Kurooka T, Toda H, Sakai S. Biofabrication offers future hope for tackling various obstacles and challenges in tissue engineering and regenerative medicine: a perspective. Int J Bioprinting 2019;5(1):1–11.

[9] Murphy SV, Atala A. Organ engineering - combining stem cells, biomaterials, and bioreactors to produce bioengineered organs for transplantation. BioEssays 2012;35(3):163–72. https://doi.org/10.1002/bies.201200062.

[10] Tang X, Qin Y, Xu X, Guo D, Ye W, Wu W, et al. Fabrication and in vitro evaluation of 3D printed porous polyetherimide scaffolds for bone tissue engineering. Biomed Res Int 2019;2019:1–8. https://doi.org/10.1155/2019/2076138.

[11] Sasaki J-I, Hashimoto M, Yamaguchi S, Itoh Y, Yoshimoto I, Matsumoto T, et al. Fabrication of biomimetic bone tissue using mesenchymal stem cell-derived three- dimensional constructs incorporating endothelial cells. PLoS ONE 2015;10(6):1–17. https://doi.org/10.1371/journal.pone.0129266.

[12] Mazza G, Al-Akkad W, Rombouts K, Pinzani M. Liver tissue engineering: from implantable tissue to whole organ engineering. Hepatol Commun 2017;2(2):131–41. https://doi.org/10.1002/hep4.1136.

[13] Hussein KH, Saleh T, Ahmed E, Kwak H, Park K, Yang S, et al. Biocompatibility and hemocompatibility of efficiently decellularized whole porcine kidney for tissue engineering. J Biomed Mater Res A 2018;106(7):2034–47. https://doi.org/10.1002/jbm.a.36407.

[14] Zhang D, Wei G, Li P, Zhou X. Urine-derived stem cells: a novel and versatile progenitor source for cell-based therapy and regenerative medicine. Genes Dis 2014;1:8–17. https://doi.org/10.1016/j.gendis.2014.07.001.

[15] Perán M, García MA, Lopez-ruiz E, Jiménez G, Marchal JA. How can nanotechnology help to repair the body? Advances in cardiac, skin, bone. Cartilage Nerve Mater 2013;6:1333–59. https://doi.org/10.3390/ma6041333.

[16] Yeung P, Cheng KH, Yan CH, Chan BP. Collagen microsphere based 3D culture system for human osteoarthritis chondrocytes. Sci Rep 2019;9:1–14. https://doi.org/10.1038/s41598-019-47946-3.

[17] Kirby GTS, Mills SJ, Cowin AJ, Smith LE. Stem cells for cutaneous wound healing. Biomed Res Int 2015;2015:1–11. https://doi.org/10.1155/2015/285869.

[18] Ciechanowska A, Ladyzynski P, Hoser G, Sabalinska S, Kawiak J, Foltynski P, et al. Human endothelial cells hollow fiber membrane bioreactor as a model of the blood vessel for in vitro studies. J Artif Organs 2016;19(3):270–7. https://doi.org/10.1007/s10047-016-0902-0.

[19] Boyce ST, Lalley AL. Tissue engineering of skin and regenerative medicine for wound care. Burns Trauma 2018;6(4):1–10. https://doi.org/10.1186/s41038-017-0103-y.

[20] Tarassoli SP, Jessop ZM, Al-Sabah A, Gao N, Whitaker S, Doak S, et al. Skin tissue engineering using 3D bioprinting: an evolving research field. J Plastic Reconstructive Aesth Surg 2018;71:615–23. https://doi.org/10.1016/j.bjps.2017.12.006.

[21] Lewis PL, Green RM, Shah RN. 3D-printed gelatin scaffolds of differing pore geometry modulate hepatocyte function and gene expression. Acta Biomater 2018;69:63–70. https://doi.org/10.1016/j.actbio.2017.12.042.

[22] Moreira R, Velz T, Alves N, Gesche VN, Malischewski A, Schmitz-Rode T, et al. Tissue-engineered heart valve with a tubular leaflet design for minimally invasive transcatheter implantation. Tissue Eng Part C 2015;21(6):530–40. https://doi.org/10.1089/ten.tec.2014.0214.

[23] Kinasiewicz A, Dudziński K, Chwojnowski A, Weryński A, Kawiak J. Three-dimensional culture of hepatocytes on spongy polyethersulfone membrane developed for cell

transplantation. Transpl Proc 2007;39:2914–6. https://doi.org/10.1016/j.transproceed.2007.08.061.
[24] Kinasiewicz A, Śmietanka A, Dudziński K, Chwojnowski A, Gajkowska B, Weryński A. Spongy polyethersulfone membrane for hepatocyte cultivation: studies on human hepatoma C3A cells. Artif Organs 2008;32(9):747–52. https://doi.org/10.1111/j.1525-1594.2008.00600.x.
[25] Farina M, Alexander JF, Thekkedath U, Ferrari M, Grattoni A. Cell encapsulation: overcoming barriers in cell transplantation in diabetes and beyond. Adv Drug Deliv Rev 2019;139:92–115. https://doi.org/10.1016/j.addr.2018.04.018.
[26] Liu Y, Luo J, Chen X, Liu W, Chen T. Cell membrane coating technology: a promising strategy for biomedical applications. Nano-Micro Lett 2019;11:1–46. https://doi.org/10.1007/s40820-019-0330-9.
[27] Plichta A, Kowalczyk S, Kamiński K, Wasyłeczko M, Wieôckowski S, Oleôdzka E, et al. ATRP of methacrylic derivative of camptothecin initiated with PLA toward three-arm star block copolymer conjugates with favorable drug release. Macromolecules 2017;50:6439–50. https://doi.org/10.1021/acs.macromol.7b01350.
[28] Walter SG, Ossendorff R, Schildberg FA. Articular cartilage regeneration and tissue engineering models: a systematic review. Arch Orthop Trauma Surg 2018;139(3):305–16. https://doi.org/10.1007/s00402-018-3057-z.
[29] Kwon H, Brown WE, Lee CA, Wang D, Paschos N, Hu JC, et al. Surgical and tissue engineering strategies for articular cartilage and meniscus repair. Nat Rev Rheumatol 2019;15:550–70. https://doi.org/10.1038/s41584-019-0255-1.
[30] Zhao Z, Fan C, Chen F, Sun Y, Xia Y, Ji A, et al. Progress in articular cartilage tissue engineering: a review on therapeutic cells and macromolecular scaffolds. Macromol Biosci 2019;1900278:1–13. https://doi.org/10.1002/mabi.201900278.
[31] Orłowska J, Kurczewska U, Derwińska K, Orłowski W, Orszulak-Michalak D. The use of biodegradable polymers in design of cellular scaffolds. Posteôpy Higieny Medycyny Doświadczalnej 2015;69:294–301. https://doi.org/10.5604/17322693.1142717.
[32] Pina S, Ribeiro VP, Marques CF, Maia FR, Silva TH, Reis RL, et al. Scaffolding strategies for tissue engineering and regenerative medicine applications. Materials 1824;2019 (12):1–42. https://doi.org/10.3390/ma12111824.
[33] Bružauskaitė I, Bironaitė D, Bagdonas E, Bernotienė E. Scaffolds and cells for tissue regeneration: different scaffold pore sizes—different cell effects. Cytotechnology 2016;68:355–69. https://doi.org/10.1007/s10616-015-9895-4.
[34] Chwojnowski A, Wojciechowski C, Dudziński K, Łukowska E. Polysulphone and polyethersulphone hollow fiber membranes with developed inner surface as material for bio-medical applications. Biocybernetics Biomed Eng 2009;29:47–59.
[35] Zhao P, Gu H, Mi H, Rao C, Fu J, Turng LS. Fabrication of scaffolds in tissue engineering: a review. Front Mech Eng 2018;13:107–19. https://doi.org/10.1007/s11465-018-0496-8.
[36] Loh QL, Choong C. Three-dimensional scaffolds for tissue engineering applications: role of porosity and pore size. Tissue Eng Part B: Rev 2013;19:485–502. https://doi.org/10.1089/ten.teb.2012.0437.
[37] Sophia Fox AJ, Bedi A, Rodeo SA. The basic science of articular cartilage: structure, composition, and function. Sports Health Orthopaedics 2009;1(6):461–8. https://doi.org/10.1177/1941738109350438.
[38] Archer CW, Francis-West P. The chondrocyte. Int J Biochem Cell Biol 2003;35:401–4. https://doi.org/10.1016/S1357-2725(02)00301-1.
[39] Grassel S, Aszodi A. Cartilage. Volume 1: Physiology and Development. Switzerland: Springer; 2016.
[40] Krishnan Y, Grodzinsky AJ. Cartilage diseases. Matrix Biol 2018;71–72:51–69. https://doi.org/10.1016/j.matbio.2018.05.005.
[41] Collins AT, Kulvaranon ML, Cutcliffe HC, Utturkar GM, Smith WAR, Spritzer CE, et al. Obesity alters the in vivo mechanical response and biochemical properties of cartilage as measured by MRI. Arthritis Res Ther 2018;20:1–9. https://doi.org/10.1186/s13075-018-1727-4.
[42] Appleton CT. Osteoarthritis year in review 2017: biology. Osteoarthritis Cartilage 2018;26:296–303. https://doi.org/10.1016/j.joca.2017.10.008.
[43] Yeung P, Zhang W, Wang XN, Yan CH, Chan BP. A human osteoarthritis osteochondral organ culture model for cartilage tissue engineering. Biomaterials 2018;162:1–21. https://doi.org/10.1016/j.biomaterials.2018.02.002.
[44] Guilak F, Nims RJ, Dicks A. Osteoarthritis as a disease of the cartilage pericellular matrix. Matrix Biol 2018;71-72:40–50. https://doi.org/10.1016/j.matbio.2018.05.008.
[45] Merkely G, Ackermann J, Lattermann C. Articular cartilage defects: incidence, diagnosis, and natural history. Operative Tech Sports Med 2018;26:156–61. https://doi.org/10.1053/j.otsm.2018.06.008.
[46] Medvedeva EV, Grebenik EA, Gornostaeva SN, Telpuhov VI, Lychagin AV, Timashev PS, et al. Repair of damaged articular cartilage: current approaches and future directions. Int J Mol Sci 2018;19(2366):1–23. https://doi.org/10.3390/ijms19082366.
[47] Armiento AR, Alini M, Stoddart MJ. Articular fibrocartilage - Why does hyaline cartilage fail to repair? Adv Drug Deliv Rev 2019;146:289–305. https://doi.org/10.1016/j.addr.2018.12.015.
[48] Liu Y, Zhou G, Cao Y. Recent progress in cartilage tissue engineering — our experience and future directions. Engineering 2017;3:28–35. https://doi.org/10.1016/J.ENG.2017.01.010.
[49] Mirza U, Shubeena S, Shah MS, Zaffer B. Microfracture: a technique for repair of chondral defects. J Entomol Zool Stud 2018;6(5):1092–7.
[50] Brittberg M, Lindahl A, Nilsson A, Ohlsson C, Isaksson O, Peterson L. Treatment of deep cartilage defect in knee with autologous chondrocyte transplantation. N Engl J Med 1994;331:889–95. https://doi.org/10.1056/NEJM199410063311401.
[51] Kraeutler MJ, Belk JW, Purcell JM, McCarty EC. Microfracture versus autologous chondrocyte implantation for articular cartilage lesions in the knee: a systematic review of 5-year outcomes. Am J Sports Med 2018;46:995–9. https://doi.org/10.1177/0363546517701912.
[52] Minas T, Von Keudell A, Bryant T, Gomoll AH. The John Insall Award: a minimum 10-year outcome study of autologous chondrocyte implantation knee. Clin Orthop Relat Res 2014;472:41–51. https://doi.org/10.1007/s11999-013-3146-9.
[53] Gao L, Orth P, Cucchiarini M, Madry H. Autologous matrix-induced chondrogenesis: a systematic review of the clinical evidence. Am J Sports Med 2019;47:222–31. https://doi.org/10.1177/0363546517740575.
[54] Schiavone Panni A, Del Regno C, Mazzitelli G, D'Apolito R, Corona K, Vasso M. Good clinical results with autologous matrix-induced chondrogenesis (Amic) technique in large knee chondral defects. Knee Surg Sports Traumatol Arthrosc 2018;26:1130–6. https://doi.org/10.1007/s00167-017-4503-0.
[55] Lee YHD, Suzer F, Thermann H. Autologous matrix-induced chondrogenesis in the knee: a review. Cartilage 2014;5:145–53. https://doi.org/10.1177/1947603514529445.
[56] Erickson BJ, Strickland SM, Gomoll AH. Indications, techniques, outcomes for matrix-induced autologous chondrocyte implantation (MACI). Oper Tech Sports Med 2018;26:175–82. https://doi.org/10.1053/j.otsm.2018.06.002.

[57] Dunkin BS, Lattermann C. New and emerging techniques in cartilage repair: Matrix-induced autologous chondrocyte implantation. Oper Tech Sports Med 2013;21:100–7. https://doi.org/10.1053/j.otsm.2013.03.003.
[58] Brittberg M. Scaffold based autologous chondrocyte implantation: the surgical technique. Asian J Arthroscopy 2019;4(1):23–6. https://doi.org/10.13107/aja.2456-1169.v04i01.006.
[59] Cao C, Zhang Y, Ye Y, Sun T. Effects of cell phenotype and seeding density on the chondrogenic capacity of human osteoarthritic chondrocytes in type I collagen scaffolds. J Orthop Surg Res 2020;15(120):1–11.
[60] Fahy N, Alini M, Stoddart MJ. Mechanical stimulation of mesenchymal stem cells: implications for cartilage tissue engineering. J Orthop Res 2018;36:52–63. https://doi.org/10.1002/jor.23670.
[61] Mastrolia I, Foppiani EM, Murgia A, Candini O, Samarelli AV, Grisendi G, et al. Challenges in clinical development of mesenchymal stromal/stem cells: concise review. Stem Cells Transl Med 2019;8(11):1135–48. https://doi.org/10.1002/sctm.19-0044.
[62] Li X, Liang Y, Xu X, Xiong J, Ouyang K, Duan L, et al. Cell-to-cell culture inhibits dedifferentiation of chondrocytes and induces differentiation of human umbilical cord-derived mesenchymal stem cells. Biomed Res Int 2019;2019:1–11. https://doi.org/10.1155/2019/5871698.
[63] Okubo R, Asawa Y, Watanabe M, Nagata S, Nio M. Proliferation medium in three-dimensional culture of auricular chondrocytes promotes effective cartilage regeneration in vivo. Regenerative Ther 2019;11:306–15. https://doi.org/10.1016/j.reth.2019.10.002.
[64] Bruzauskaite I, Bironait D, Bagdonas E, Bernotiene E. Scaffolds and cells for tissue regeneration : different scaffold pore sizes — different cell effects. Cytotechnology 2015;68:355–69. https://doi.org/10.1007/s10616-015-9895-4.
[65] Kalkan R, Nwekwo CW, Adali T. The use of scaffolds in cartilage regeneration. Eukaryotic Gene Express 2018;28(4):343–8.
[66] Eltom A, Zhong G, Muhammad A. Scaffold techniques and designs in tissue engineering functions and purposes: a review. Adv Mater Sci Eng 2019;2019:1–14. https://doi.org/10.1155/2019/3429527.
[67] Irawan V, Sung TC, Higuchi A, Ikoma T. Collagen scaffolds in cartilage tissue engineering and relevant approaches for future development. Tissue Eng Regenerative Med 2018;15:673–97. https://doi.org/10.1007/s13770-018-0135-9.
[68] Panadero JA, Lanceros-Mendez S, Ribelles JLG. Differentiation of mesenchymal stem cells for cartilage tissue engineering: individual and synergetic effects of three-dimensional environment and mechanical loading. Acta Biomater 2016;33:1–12. https://doi.org/10.1016/j.actbio.2016.01.037.
[69] Conoscenti G, Schneider T, Stoelzel K, Carfi Pavia F, Brucato V, Goegele C, et al. PLLA scaffolds produced by thermally induced phase separation (TIPS) allow human chondrocyte growth and extracellular matrix formation dependent on pore size. Mater Sci Eng, C 2017;80:449–59.
[70] Demoor M, Ollitrault D, Gomez-Leduc T, Bouyoucef M, Hervieu M, Fabre H, et al. Cartilage tissue engineering: molecular control of chondrocyte differentiation for proper cartilage matrix reconstruction. Biochim Biophys Acta - General Subjects 2014;1840(8):2414–40. https://doi.org/10.1016/j.bbagen.2014.02.030.
[71] Huang BJ, Hu JC, Athanasiou KA. Cell-based tissue engineering strategies used in the clinical repair of articular cartilage. Biomaterials 2016;98:1–22. https://doi.org/10.1016/j.biomaterials.2016.04.018.
[72] Zhao Y, Tan K, Zhou Y, Ye Z, Tan WS. A combinatorial variation in surface chemistry and pore size of three-dimensional porous poly(ε-caprolactone) scaffolds modulates the behaviors of mesenchymal stem cells. Mater Sci Eng, C 2016;59:193–202. https://doi.org/10.1016/j.msec.2015.10.017.
[73] Nava MM, Draghi L, Giordano C, Pietrabissa R. The effect of scaffold pore size in cartilage tissue engineering. J Appl Biomater Funct Mater 2016;14:e223–9. https://doi.org/10.5301/jabfm.5000302.
[74] Matsiko A, Gleeson JP, O'Brien FJ. Scaffold mean pore size influences mesenchymal stem cell chondrogenic differentiation and matrix deposition. Tissue Eng - Part A 2015;21:486–97. https://doi.org/10.1089/ten.tea.2013.0545.
[75] Lai YS, Chen WC, Huang CH, Cheng CK, Chan KK, Chang TK, et al. The effect of graft strength on knee laxity and graft in-situ forces after posterior cruciate ligament reconstruction. PLoS ONE 2015;10:1–11. https://doi.org/10.1371/journal.pone.0127293.
[76] Koh YG, Lee JA, Kim YS, Lee HY, Kim HJ, Kang KT. Optimal mechanical properties of a scaffold for cartilage regeneration using finite element analysis. J Tissue Eng 2019;10:1–10. https://doi.org/10.1177/2041731419832133.
[77] Depends C, Anderer U. Tissue specific differentiation of human chondrocytes depends on cell microenvironment and serum selection. Cells 2019;8(934):1–15.
[78] Dulnik J, Sajkiewicz P. Characterization of biocomponent polycaprolactone/gelatin electrospun nanofibres crosslinked with EDC/NHS. Eng Biomater 2019;153:26.
[79] Chwojnowsk A, Kruk A, Wojciechowski C, Łukowska E, Dulnik J, Sajkiewicz P. The dependence of the membrane structure on the nonwoven forming the macropores in the 3D scaffolds preparation. Desalin Water Treat 2017;64:324–31. https://doi.org/10.5004/dwt.2017.11394.
[80] Kruk A, Gadomska-gajadhur AA, Dulnik J. Preparation of biodegradable semi-permeable membranes as 3D scaffolds for cell cultures preparation of biodegradable semi-permeable membranes as 3D scaffolds for cell cultures. Desalin Water Treat 2017;64:317–23. https://doi.org/10.5004/dwt.2016.11415.
[81] Dudziński K, Chwojnowski A, Gutowska M, Płończak M, Czubak J, Łukowska E, et al. Three dimensional polyethersulphone scaffold for chondrocytes cultivation - the future supportive material for articular cartilage regeneration. Biocyber Biomed Eng 2010;30:65–76.
[82] Gadomska-Gajadhur A, Kruk A, Ruśkowski P, Sajkiewicz P, Dulnik J, Chwojnowski A. Original method of imprinting pores in scaffolds for tissue engineering. Polym Adv Technol 2021;32:1–13. https://doi.org/10.1002/pat.5091.
[83] Chwojnowski A, Wojciechowski C, Nowak J, Kupikowska-stobba B, et al. Studies on the structure of semi-permeable membranes by means of SEM problems and potential sources of errors. Biocyber Biomed Eng 2012;32(1):51–64. https://doi.org/10.1016/S0208-5216(12)70032-3.
[84] Andrzej C, Malgorzata P, Diana W, Juliusz K, Cezary W. Membranes ' porosity evaluation by computer-aided analysis of sem images – a preliminary study. Biocyber Biomed Eng 2012;32(4):65–75. https://doi.org/10.1016/S0208-5216(12)70050-5.
[85] Przytulska M, Kruk A, Kulikowski JL, Wojciechowski C, Gadomska-Gajadhur A, Chwojnowski A. Comparative assessment of polyvinylpyrrolidone type of membranes based on porosity analysis. Desalin Water Treat 2017;75:18–25. https://doi.org/10.5004/dwt.2017.20586.
[86] Kulikowski JL, Przytulska M, Chwojnowski A. Computer - aided analysis of micro - morphological structure of porous membranes. Biomed Eng Online 2018;17:1–15. https://doi.org/10.1186/s12938-018-0481-9.

[87] Przytulska M, Kulikowski JL, Wasyłeczko M, Chwojnowski A, Pieôtka D. The evaluation of 3D morphological structure of porous membranes based on a computer-aided analysis of their 2D images. Desalin Water Treat 2018;128:11–9. https://doi.org/10.5004/dwt.2018.22569.
[88] Sikorska W, Wojciechowski C, Przytulska M, Rokicki G, Wasyłeczko M, Kulikowski JL, et al. Polysulfone–polyurethane (PSf-PUR) blend partly degradable hollow fiber membranes: preparation, characterization, and computer image analysis. Desalin Water Treat 2018;128:383–91. https://doi.org/10.5004/dwt.2018.23101.
[89] Nikolova MP, Chavali MS. Recent advances in biomaterials for 3D scaffolds: a review. Bioact Mater 2019;4:271–92. https://doi.org/10.1016/j.bioactmat.2019.10.005.
[90] Ahmadi F, Giti R, Mohammadi-Samani S, Mohammadi F. Biodegradable scaffolds for cartilage tissue engineering. Galen Med J 2017;6:70–80. https://doi.org/10.22086/GMJ.V6I2.696.
[91] Armiento AR, Stoddart MJ, Alini M, Eglin D. Biomaterials for articular cartilage tissue engineering: learning from biology. Acta Biomater 2018;65:1–20. https://doi.org/10.1016/j.actbio.2017.11.021.
[92] Setayeshmehr M, Esfandiari E, Rafieinia M, Hashemibeni B, Taheri-kafrani A, Samadikuchaksaraei A. Hybrid and composite scaffolds based on extracellular. Tissue Eng Part B 2019;25:202–24. https://doi.org/10.1089/ten.teb.2018.0245.
[93] Jafari M, Paknejad Z, Rad MR, Motamedian SR, Eghbal MJ, Nadjmi N, et al. Polymeric scaffolds in tissue engineering: a literature review. J Biomed Mater Res - Part B Appl Biomater 2017;105(2):431–59. https://doi.org/10.1002/jbm.b.33547.
[94] Jeuken RM, Roth AK, Peters RJRW, van Donkelaar CC, Thies JC, van Rhijn LW, et al. Polymers in cartilage defect repair of the knee: current status and future prospects. Polymers 2016;8:1–30. https://doi.org/10.3390/polym8060219.
[95] Ulery BD, Nair LS, Laurencin CT. Biomedical applications of biodegradable polymers. J Polym Sci, Part B: Polym Phys 2011;49:832–64. https://doi.org/10.1002/polb.22259.
[96] Daranarong D, Techaikool P, Intatue W, Daengngern R, Thomson KA, Molloy R, et al. Effect of surface modification of poly(L-lactide-co-ε-caprolactone) membranes by low-pressure plasma on support cell biocompatibility. Surf Coat Technol 2016;306:328–35.
[97] Ye H, Zhang K, Kai D, Li Z, Loh XJ. Polyester elastomers for soft tissue engineering. Chem Soc Rev 2018;47:4545–80. https://doi.org/10.1039/c8cs00161h.
[98] Nofar M, Sacligil D, Carreau PJ, Kamal MR, Heuzey MC. Poly (lactic acid) blends: processing, properties and applications. Int J Biol Macromol 2019;125:307–60. https://doi.org/10.1016/j.ijbiomac.2018.12.002.
[99] Shuai C, Li Y, Wang G, Yang W, Peng S, Feng P. Surface modification of nanodiamond: toward the dispersion of reinforced phase in poly-L-lactic acid scaffolds. Int J Biol Macromol 2019;126:1116–24. https://doi.org/10.1016/j.ijbiomac.2019.01.004.
[100] He Y, Wang WR, Ding JD. Effects of L-lactic acid and D, L-lactic acid on viability and osteogenic differentiation of mesenchymal stem cells. Chin Sci Bull 2013;58:2404–11. https://doi.org/10.1007/s11434-013-5798-y.
[101] Filimon A, Olaru N, Doroftei F, Logigan C, Dunca S. Design of biological active surface based on functionalized polysulfones by electrospinning. Proceedings 2019; 41:1–8. https://doi.org/10.3390/ecsoc-23-06495.
[102] Irfan M, Idris A. Overview of PES biocompatible/hemodialysis membranes: PES-blood interactions and modification techniques. Mater Sci Eng, C 2015;56:574–92. https://doi.org/10.1016/j.msec.2015.06.035.
[103] Mahboudi H, Soleimani M, Enderami SE, Kehtari M, Hanaee-Ahvaz H, Ghanbarian H, et al. The effect of nanofibre-based polyethersulfone (PES) scaffold on the chondrogenesis of human induced pluripotent stem cells. Artif Cells Nanomed Biotechnol 2018:1–9.
[104] Lam ATL, Reuveny S, Oh SKW. Human mesenchymal stem cell therapy for cartilage repair: review on isolation, expansion, and constructs. Stem Cell Res 2020;44. https://doi.org/10.1016/j.scr.2020.101738 101738.
[105] Xu Y, Kim C, Saylor DM, Koo D. Polymer degradation and drug delivery in PLGA-based drug – polymer applications: a review of experiments and theories. Society For Biomater 2016;105(6):1692–716. https://doi.org/10.1002/jbm.b.33648.
[106] Jiang L, Xu L, Ma B, Ding H, Tang C. Effect of component and surface structure on poly (L-lactide-co-ε- caprolactone) (PLCA)-based composite membrane. Compos B 2019;174. https://doi.org/10.1016/j.compositesb.2019.107031 107031.
[107] Prasanna S, Narayan B, Rastogi A, Srivastava P. Design and evaluation of chitosan/poly (L-lactide)/ pectin based composite scaffolds for cartilage tissue regeneration. Int J Biol Macromol 2018;112:909–20. https://doi.org/10.1016/j.ijbiomac.2018.02.049.
[108] Zhang X, Wu Y, Pan Z, Sun H, Wang J, Yu D, et al. The effects of lactate and acid on articular chondrocytes function: implications for polymeric cartilage scaffold design. Acta Biomater 2016;42:329–40. https://doi.org/10.1016/j.actbio.2016.06.029.
[109] Dutta RC, Dey M, Dutta AK, Basu B. Competent processing techniques for scaffolds in tissue engineering. Biotechnol Adv 2017;35:240–50. https://doi.org/10.1016/j.biotechadv.2017.01.001.
[110] Lu T, Li Y, Chen T. Techniques for fabrication and construction of three-dimensional scaffolds for tissue engineering. Int J Nanomed 2013;8:337–50.
[111] H, Kim J, Shin K, Koh Y, Hah MJ, et al. Production of Poly(ε-Caprolactone)/Hydroxyapatite composite scaffolds with a tailored macro/micro-porous structure, high mechanical properties, and excellent bioactivity. Materials 10(10):1-13. https://doi.org/10.3390/ma10101123.
[112] Plisko TV, Penkova AV, Burts KS, Bildyukevich AV, Dmitrenko ME, Melnikova GB, et al. Effect of Pluronic F127 on porous and dense membrane structure formation via non-solvent induced and evaporation induced phase separation. J Membr Sci 2019;580:336–49. https://doi.org/10.1016/j.memsci.2019.03.028.
[113] Mannella GA, Conoscenti G, Pavia FC, La CV, Brucato V. Preparation of polymeric foams with a pore size gradient via Thermally Induced Phase Separation (TIPS). Mater Lett 2015;160:31–3. https://doi.org/10.1016/j.matlet.2015.07.055.
[114] Sultana N, Hassana MI, Ridzuana N, Ibrahima Z, Soonc CF. Fabrication of gelatin scaffolds using thermally induced phase separation technique. Int J Eng 2018;31:1302–7.
[115] Buzarovska A, Gualandi C, Parrilli A, Scandola M. Effect of TiO2 nanoparticle loading on Poly(L-lactic acid) porous scaffolds fabricated by TIPS. Compos B 2015;81:189–95. https://doi.org/10.1016/j.compositesb.2015.07.016.
[116] Semitela Â, Girão AF, Fernandes C, Ramalho G, Bdikin I, Completo A, et al. Electrospinning of bioactive polycaprolactone-gelatin nanofibres with increased pore size for cartilage tissue engineering applications. J Biomater Appl 2020;35:471–84. https://doi.org/10.1177/0885328220940194.
[117] Sharifi F, Irani S, Azadegan G, Pezeshki-modaress M. Co-electrospun gelatin-chondroitin sulfate/polycaprolactone nanofibrous scaffolds for cartilage tissue engineering. Bioactive Carbohydrates Dietary Fibre 2020;22:100215. https://doi.org/10.1016/j.bcdf.2020.100215.
[118] Zhou Y, Chyu J, Zumwalt M. Recent progress of fabrication of cell scaffold by electrospinning technique for articular

cartilage tissue engineering. Int J Biomater 2018;2018:1–10. https://doi.org/10.1155/2018/1953636.
[119] Canton TT, Kunert LR, Suellen B, Ana I, Serafini P. Nonwoven membranes for tissue engineering: an overview of cartilage, epithelium, and bone regeneration. J Biomater Sci Polym Ed 2019;30:1026–49. https://doi.org/10.1080/09205063.2019.1620592.
[120] Girão AF, Semitela Â, Ramalho G, Completo A, Marques PAAP. Mimicking nature-fabrication of 3D anisotropic electrospun polycaprolactone scaffolds for cartilage tissue engineering applications. Compos B 2018;154:99–107. https://doi.org/10.1016/j.compositesb.2018.08.001.
[121] Li K, Wang D, Zhao K, Song K, Liang J. Electrohydrodynamic jet 3D printing of PCL/PVP composite scaffold for cell culture. Talanta 2020;211:1–11. https://doi.org/10.1016/j.talanta.2020.120750.
[122] Baena JM, Jiménez G, López-Ruiz E, Antich C, Griñán-Lisón C, Perán M, et al. Volume-by-volume bioprinting of chondrocytes-alginate bioinks in high temperature thermoplastic scaffolds for cartilage regeneration. Exp Biol Med 2019;244:13–21. https://doi.org/10.1177/1535370218821128.
[123] Markstedt K, Mantas A, Tournier I, Martínez Ávila H, Hägg D, Gatenholm P. 3D bioprinting human chondrocytes with nanocellulose – alginate bioink for cartilage tissue engineering applications. Biomacromolecules 2015;16:1489–96. https://doi.org/10.1021/acs.biomac.5b00188.
[124] Daly AC, Freeman FE, Gonzalez-fernandez T, Critchley SE, Nulty J, Kelly DJ. 3D bioprinting for cartilage and osteochondral tissue engineering. Adv Healthcare Mater 2017;6:1–20. https://doi.org/10.1002/adhm.201700298.
[125] Seung J, Sang H, Jung H, Lee H, Hong H, Jin Y, et al. 3D-printable photocurable bioink for cartilage regeneration of tonsil-derived mesenchymal stem cells. Additive Manuf 2020;33:101136. https://doi.org/10.1016/j.addma.2020.101136.
[126] Wu J, Yang R, Zheng J, Pan L, Liu X. Fabrication and improvement of PCL/alginate/PAAm scaffold via selective laser sintering for tissue engineering. Micro Nano Lett 2019;14(8):852–5. https://doi.org/10.1049/mnl.2018.5806.
[127] Chen C, Shyu VB, Chen J, Lee M. Selective laser sintered poly-ε-caprolactone scaffold hybridized with collagen hydrogel for cartilage tissue engineering. Biofabrication 2014;6(1):1–11. https://doi.org/10.1088/1758-5082/6/1/015004.
[128] Longley R, Ferreira AM, Gentile P. Recent approaches to the manufacturing of biomimetic multi-phasic scaffolds for osteochondral regeneration. Mol Sci 2018;19(6):1–17. https://doi.org/10.3390/ijms19061755.
[129] Benwood C, Anstey A, Andrzejweski J, Misra M, Mohanty AK. Improving the impact strength and heat resistance of 3D printed models: structure, property, and processing correlationships during fused deposition modeling (FDM) of poly(lactic acid). Am Chem Soc Omega 2018;3(4):4400–11. https://doi.org/10.1021/acsomega.8b00129.
[130] Cheng A, Schwartz Z, Kahn A, Li X, Shao Z, Sun M, et al. Advances in porous scaffold design for bone and cartilage tissue engineering and regeneration. Tissue Eng Part B 2019;25(1):14–29. https://doi.org/10.1089/ten.TEB.2018.0119.
[131] Abdelaal OAM, Darwish SMH. Review of rapid prototyping techniques for tissue engineering scaffolds fabrication. Adv Struct Mater 2013;29:33–54. https://doi.org/10.1007/978-3-642-31470-4.
[132] Chen W, Xu Y, Liu Y, Wang Z, Li Y, Jiang G, et al. Three-dimensional printed electrospun fiber-based scaffold for cartilage regeneration. Mater Des 2019;179:107886.
[133] Xu T, Binder KW, Albanna MZ, Dice D, Zhao W, Yoo JJ, et al. Hybrid printing of mechanically and biologically improved constructs for cartilage tissue engineering applications. Biofabrication 2013;5(1):1–10. https://doi.org/10.1088/1758-5082/5/1/015001.
[134] Garrigues NW, Little D, Sanchez-adams J, Ruch DS, Guilak F. Electrospun cartilage-derived matrix scaffolds for cartilage tissue engineering. J Biomed Mater Res Part A 2014;102:3998–4008. https://doi.org/10.1002/jbm.a.35068.
[135] Correa D, Lietman SA. Articular cartilage repair: current needs, methods and research directions. Semin Cell Dev Biol 2017;62:67–77. https://doi.org/10.1016/j.semcdb.2016.07.013.
[136] Hoffman AS. Hydrogels for biomedical applications. Adv Drug Deliv Rev 2012;64:18–23. https://doi.org/10.1016/j.addr.2012.09.010.
[137] Janoušková O. Synthetic polymer scaffolds for soft tissue engineering department of biological models. Physiol Res 2018;67(2):335–48. https://doi.org/10.33549/physiolres.933983.
[138] Bistolfi A, Ferracini R, Galletta C, Tosto F, Sgarminato V, Digo E, et al. Regeneration of articular cartilage: scaffold used in orthopedic surgery. A short handbook of available products for regenerative joints surgery. Clin Sci Res Rep 2017;1:1–7. https://doi.org/10.15761/CSRR.1000101.
[139] Urbanek O, Kołbuk D, Wróbel M. Articular cartilage: new directions and barriers of scaffolds development – review. Int J Polym Mater Polym Biomater 2019;68:1–15. https://doi.org/10.1080/00914037.2018.1452224.
[140] Brittberg M, Recker D, Ilgenfritz J, Saris DBF. Matrix-Applied characterized autologous cultured chondrocytes versus microfracture: five-year follow-up of a prospective randomized trial. Am J Sports Med 2018;46:1343–51. https://doi.org/10.1177/0363546518756976.
[141] Kreuz PC, Müller S, Freymann U, Erggelet C, Niemeyer P, Kaps C, et al. Repair of focal cartilage defects with scaffold-assisted autologous chondrocyte grafts. Am J Sports Med 2011;39:1697–706. https://doi.org/10.1177/0363546511403279.
[142] Siclari A, Mascaro G, Kaps C, Boux E. A 5-year follow-up after cartilage repair in the knee using a platelet- rich plasma-immersed polymer-based implant. Open Orthop J 2014;8:346–54.
[143] Płończak M, Czubak J, Hoser G, Chwojnowskl A, Kawiak J, Dudzińskp K, et al. Repair of articular cartilage full thickness defects with cultured chondrocytes placed on polysulphonic membrane - experimental studies in rabbits. Biocyber Biomed Eng 2008;28:87–93.
[144] Płończak M, Czubak J. Culture of human autologous chondrocytes on polysulphonic membrane – preliminary studies. Biocyber Biomed Eng 2012;32(3):63–7. https://doi.org/10.1016/S0208-5216(12)70042-6.
[145] Płończak M. The value of autogenous cartilage cell transplants in the experimental treatment of articular cartilage defects in rabbits [in Polish]. In: doctoral thesis, Poland: Otwock; 2008.
[146] Tsai M, Hung K, Hung S, Hsu S. Evaluation of biodegradable elastic scaffolds made of anionic polyurethane for cartilage tissue engineering. Colloids Surf, B 2015;125:34–44. https://doi.org/10.1016/j.colsurfb.2014.11.003.
[147] Liao J, Qu Y, Chu B, Zhang X, Qian Z. Biodegradable CSMA/PECA/graphene porous hybrid scaffold for cartilage tissue engineering. Sci Rep 2015;9879:1–16. https://doi.org/10.1038/srep09879.
[148] Setayeshmehr M, Esfandiari E, Hashemibeni B, Tavakoli AH, Rafienia M, Samadikuchaksaraei A, et al. Chondrogenesis of human adipose-derived mesenchymal stromal cells on the [devitalized costal cartilage matrix/poly(vinyl alcohol)/fibrin] hybrid scaffolds. Eur Polym J 2019;118:528–41. https://doi.org/10.1016/j.eurpolymj.2019.04.044.

[149] He Y, Liu W, Guan L, Chen J, Duan L, Jia Z, et al. A 3D-printed PLCL scaffold coated with collagen type I and its biocompatibility. Biomed Res Int 2018;2018:1–10. https://doi.org/10.1155/2018/5147156.
[150] Rofiqoh N, Putri E, Wang X, Chen Y, Li X, Kawazoe N, et al. Preparation of PLGA-collagen hybrid scaffolds with controlled pore structures for cartilage tissue engineering. Prog Nat Sci: Mater Int 2020;30:642–50. https://doi.org/10.1016/j.pnsc.2020.07.003.
[151] Nogami M, Kimura T, Seki S, Matsui Y, Yoshida T, Koike-Soko C, et al. A human amnion-derived extracellular matrix-coated cell-free scaffold for cartilage repair- in vitro and in vivo studies. Tissue Eng Part A 2016;22(7-8):680–8. https://doi.org/10.1089/ten.TEA.2015.0285.
[152] Kamath SM, Jaison D, Krishna S, Sridhar K, Kasthuri N, Gopinath V, et al. In vitro augmentation of chondrogenesis by Epigallocatechin gallate in primary Human chondrocytes - sustained release model for cartilage regeneration. J Drug Deliv Sci Technol 2020;60. https://doi.org/10.1016/j.jddst.2020.101992.
[153] So C, Silva JC, Fernandes PR, Lobato C, Manuel J, Cabral S, et al. Chondrogenic differentiation of mesenchymal stem / stromal cells on 3D porous poly (ε -caprolactone) scaffolds: effects of material alkaline treatment and chondroitin sulfate supplementation. J Biosci Bioeng 2020;129:756–64. https://doi.org/10.1016/j.jbiosc.2020.01.004.
[154] Denis P, Dulnik J, Sajkiewicz P. Electrospinning and structure of bicomponent polycaprolactone/gelatin nanofibers obtained using alternative solvent system. Int J Polymeric Mater Polymeric Biomater 2015;64:354–64. https://doi.org/10.1080/00914037.2014.945208.
[155] Dulnik J, Ko D, Denis P, Sajkiewicz P. The effect of a solvent on cellular response to PCL/gelatin and PCL/collagen electrospun nano fibres. Eur Polym J 2018;104:147–56. https://doi.org/10.1016/j.eurpolymj.2018.05.010.
[156] Chwojnowski A, Kruk A, Wojciechowski C, Łukowska E, Dulnik J, Sajkiewicz P. The dependence of the membrane structure on the non-woven forming the macropores in the 3D scaffolds preparation. Desalin Water Treat 2017;64:324–31. https://doi.org/10.5004/dwt.2017.11394.
[157] Chwojnowski A, Dudziński K. Method for producing semipermeable polysulfone and polyethersulfone membranes and their applications, PL 211793 B1, 2012.
[158] Kruk A, Gadomska-Gajadhur A, Ruśkowski P, Chwojnowski A, Dulnik J, Synoradzki L. Preparation of biodegradable semi-permeable membranes as 3D scaffolds for cell cultures. Desalin Water Treat 2017;64:317–23. https://doi.org/10.5004/dwt.2017.11415.
[159] Gadomska-Gajadhur A, Kruk A, Synoradzki L, Chwojnowski A. Patent PL 229497 B1; Method for producing three-dimensional polylactide scaffolds, 2015.
[160] Ho ST, Hutmacher DW. A comparison of micro CT with other techniques used in the characterization of scaffolds. Biomaterials 2006;27:1362–76. https://doi.org/10.1016/j.biomaterials.2005.08.035.
[161] Oh SH, Kim TH, Il IG, Lee JH. Investigation of pore size effect on chondrogenic differentiation of adipose stem cells using a pore size gradient scaffold. Biomacromolecules 2010;11:1948–55. https://doi.org/10.1021/bm100199m.
[162] van Susante JLC, Pieper J, Buma P, van Kuppevelt TH, van Beuningen H, van der Kraan PM, et al. Linkage of chondroitin-sulfate to type I collagen scaffolds stimulates the bioactivity of seeded chondrocytes in vitro. Biomaterials 2001;22:2359–69. https://doi.org/10.1016/S0142-9612(00)00423-3.
[163] Narumi K, Furugen A, Kobayashi M, Otake S, Itagaki S, Iseki K. Regulation of monocarboxylate transporter 1 in skeletal muscle cells by intracellular signaling pathways. Biol Pharm Bull 2010;33:1568–73. https://doi.org/10.1248/bpb.33.1568.

PUBLIKACJA 5

Intraarticular Implantation of Autologous Chondrocytes Placed on Collagen or Polyethersulfone Scaffolds: An Experimental Study in Rabbits

Maciej Płończak, **Monika Wasyłeczko**, Tomasz Jakutowicz, Andrzej Chwojnowski, Jarosław Czubak

Polymers **2023**, 15, 2360.
https://doi.org/10.3390/polym15102360
IF: 4,967,
MNiSW: 100

polymers

MDPI

Article

Intraarticular Implantation of Autologous Chondrocytes Placed on Collagen or Polyethersulfone Scaffolds: An Experimental Study in Rabbits

Maciej Płończak [1,*], Monika Wasyłeczko [2], Tomasz Jakutowicz [3], Andrzej Chwojnowski [2] and Jarosław Czubak [4]

[1] Mazovia Regional Hospital John Paul II, 08-110 Siedlce, Poland
[2] Nałęcz Institute of Biocybernetic and Biomedical Engineering, Polish Academy of Sciences, 02-109 Warsaw, Poland; mwasyleczko@ibib.waw.pl
[3] Department of Neurosurgery and Children Traumatology, Medical University of Warsaw, 02-091 Warsaw, Poland; jakutowicztom@gmail.com
[4] Department of Orthopedics, Pediatric Orthopedics and Traumatology, Centre of Postgraduate Medical Education, Gruca Orthopaedic and Trauma Teaching Hospital, 05-402 Otwock, Poland
* Correspondence: maciej.plonczak@interia.pl

Abstract: Hyaline cartilage has very limited repair capability and cannot be rebuilt predictably using conventional treatments. This study presents Autologous Chondrocyte Implantation (ACI) on two different scaffolds for the treatment of lesions in hyaline cartilage in rabbits. The first one is a commercially available scaffold (Chondro–Gide) made of collagen type I/III and the second one is a polyethersulfone (PES) synthetic membrane, manufactured by phase inversion. The revolutionary idea in the present study is the fact that we used PES membranes, which have unique features and benefits that are desirable for the 3D cultivation of chondrocytes. Sixty-four White New Zealand rabbits were used in this research. Defects penetrating into the subchondral bone were filled with or without the placement of chondrocytes on collagen or PES membranes after two weeks of culture. The expression of the gene encoding type II procollagen, a molecular marker of chondrocytes, was evaluated. Elemental analysis was performed to estimate the weight of tissue grown on the PES membrane. The reparative tissue was analyzed macroscopically and histologically after surgery at 12, 25, and 52 weeks. RT-PCR analysis of the mRNA isolated from cells detached from the polysulphonic membrane revealed the expression of type II procollagen. The elementary analysis of polysulphonic membrane slices after 2 weeks of culture with chondrocytes revealed a concentration of 0.23 mg of tissue on one part of the membrane. Macroscopic and microscopic evaluation indicated that the quality of regenerated tissue was similar after the transplantation of cells placed on polysulphonic or collagen membranes. The established method for the culture and transplantation of chondrocytes placed on polysulphonic membranes resulted in the growth of the regenerated tissue, revealing the morphology of hyaline-like cartilage to be of similar quality to collagen membranes.

Keywords: autologous chondrocyte implantation; cartilage regeneration; cartilage tissue engineering; collagen scaffold; osteochondral defects; rabbit; polyethersulfone scaffold; regenerative medicine

Citation: Płończak, M.; Wasyłeczko, M.; Jakutowicz, T.; Chwojnowski, A.; Czubak, J. Intraarticular Implantation of Autologous Chondrocytes Placed on Collagen or Polyethersulfone Scaffolds: An Experimental Study in Rabbits. *Polymers* **2023**, *15*, 2360. https://doi.org/10.3390/polym15102360

Academic Editors: Yadong Tang and Lu Jiang

Received: 30 March 2023
Revised: 15 May 2023
Accepted: 16 May 2023
Published: 18 May 2023

1. Introduction

Articular cartilage (AC) is the tissue that covers the long bones ends. It provides sufficient structural stability to transfer heavy loads between bones. It is strong, frictionless for load-bearing surfaces, and protects the subchondral bone. Unfortunately, it can be distorted, leading to adverse complications [1–3]. AC cannot regenerate because of the absence of nerves and blood vessels, and the poor mitogenic force of chondrocytes. Left untreated, damage to cartilage causes pain, stiffness, movement limitation, and disappearance of joint function. This can lead to diseases, including osteoarthritis, or even disability [1,2,4–7].

Available treatments do not do much to rebuild the quality and efficiency of the joint surface. The commonly used treatment methods of AC are microfracture (MF) and cell-based techniques, such as autologous chondrocyte implantation (ACI) or mosaicplasty [4,8–10]. The limited ability of AC to reclaim has received clinical awareness and interest in recent times. Many trials, like implantation of the periosteum, cells, or osteochondral fragments, have been performed in pre-clinical (animals model) or even in clinical attempts [11,12]. The MF technique provides infiltration of the mesenchymal stem cells from the bone marrow (subchondral bone perforation), whereby a blood clot fills in the damage. This provides a suitable environment for AC regeneration [13,14]. In the ACI method, the isolated chondrocytes from the host are placed on a scaffold and cultured in an incubator. After some weeks, the obtained bio-implant is transplanted. Achieving hyaline or hyaline-like repair by ACI for damaged AC is very promising. Research evidence shows that the transplantation of chondrocytes with membranes (scaffolds or matrices) obtained from natural or synthetic biomaterials can improve the quality of AC [4,9,10,15–18]. Unfortunately, in the MF and ACI techniques, the regeneration is composed mainly of fibrocartilage. It has less favorable biomechanical properties than hyaline cartilage, and can be exposed to further damage. Furthermore, experimental evidence shows better results with the ACI than with the MF method [10,19,20]. Thus, researchers and doctors are still searching for a more promising method of AC regeneration, among which the most promising one is to use cells with biomaterials (bioimplants) [1,4,8,9,16–18,21,22].

The membranes (scaffolds) must be spatial, with interconnected pore structures. They should be biocompatible, and possess sufficient stiffness, mechanical stability, and shape properties to withstand stresses during culture and after implantation [16,23–27]. Scaffold materials should be biocompatible, biodegrade to non-harmful components in the organism, and be resistant to body conditions such as pH and temperature. Therefore, it is necessary to choose appropriate biomaterials—synthetic or natural polymers, or their combination (hybrid materials) [9,16,25,26,28–32]. Natural polymers, such as collagen, hyaluronic acid (HA), chondroitin sulfate (CS), chitosan (CH), and fibrin [9,33–37], are distinguished by their high biocompatibility and bioactivity. Natural materials have features similar to those of human tissues, so they exist naturally in the human organism. Due to their origin, they stimulate cell adhesion and ECM production. Despite their many advantages, they have significant disadvantages. In the aqueous environment, they quickly lose mechanical properties (hydrolysis). The scaffold loses suitable properties for cell culture (supporting cells). In addition, methods for obtaining scaffolds from these materials are limited due to their lack of resistance to process parameters, like high temperature or pressure [9,16,24–28,33]. Synthetic polymers: polycaprolactone (PCL), polyurethane, polylactic acid (PLA), and polyethersulfone (PES) [21,31,38–43] are more diverse and promising. Compared to natural materials, they can be used to produce a variety of membrane structures using different methods. They have appropriate mechanical, physical, and chemical properties. Many of them degrade to non-toxic components in the body. In addition, the mechanical properties and degradation time of the scaffolds can be controlled through appropriate combinations of these polymers—copolymers or blends [16,27–29,33,44–47]. Hybrid scaffolds should also be briefly introduced. They combine the advantages of synthetic and natural biomaterials. This makes it possible to obtain scaffolds with appropriate mechanical properties, bio-functionality, and the ability to regulate degradation [16,25,26,30].

The purpose of the study was to evaluate the effect of autologous chondrocyte transplantation, placed on polyethersulfone (PES) or commercial, collagen Chondro-Guide scaffolds, in the treatment of lesions in hyaline cartilage in rabbits. An effective technique of isolation and culture of chondrocytes was established. Rabbits were divided into five groups. Full-thickness lesions were produced, and the scaffolds were used with or without autologous chondrocytes. As a control, non-filled cavities were used. The macroscopic and microscopic appearance of the tissue in the damaged region of the AC surface as a result of regeneration was evaluated. In the end, the chondrogenic potential of the cells cultured in vitro on a non-absorbable PES membrane was compared with that

of cells cultured in vitro on an absorbable collagen scaffold. The regenerated tissue was observed over time, up to 52 weeks. The novelty of this study lies in the use of the synthetic PES membrane, which was used here for the first time on an animal model (rabbits). In addition, it is compared with a commercial membrane made of collagen. Studies show that the PES membrane was able to achieve its task, and can be used for further research.

2. Materials

2.1. Membranes

The semipermeable, porous membrane was made of a polyethersulfone (PES) (Figure 1). Polymer is biocompatible, and is used in tissue engineering [38,42,48].

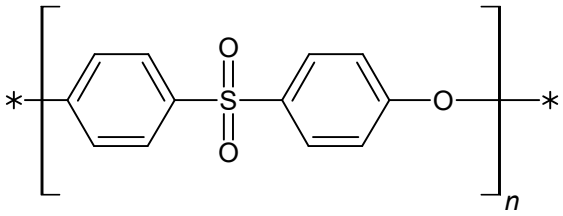

Figure 1. The chemical formula of the polyethersulfone, where n = 50–80.

The PES scaffold was designed and manufactured in cooperation with chemists from the Institute of Biocybernetics and Biomedical Engineering of the Polish Academy of Sciences in Warsaw. The choice of this material was determined by its favorable biomechanical properties, like chemical resistance and the possibility of forming a membrane using easy methods. It was obtained by the wet inversion phase technique according to the previous work [38,49,50]. Figure 2 shows the cross-section and the top and bottom layers of the PES and Chondro-Gide scaffolds. The top layer of the PES scaffold is perforated, while the bottom layer is smooth and compacted. This is necessary for scaffolds, as it allows cells to enter the membrane and be retained inside.

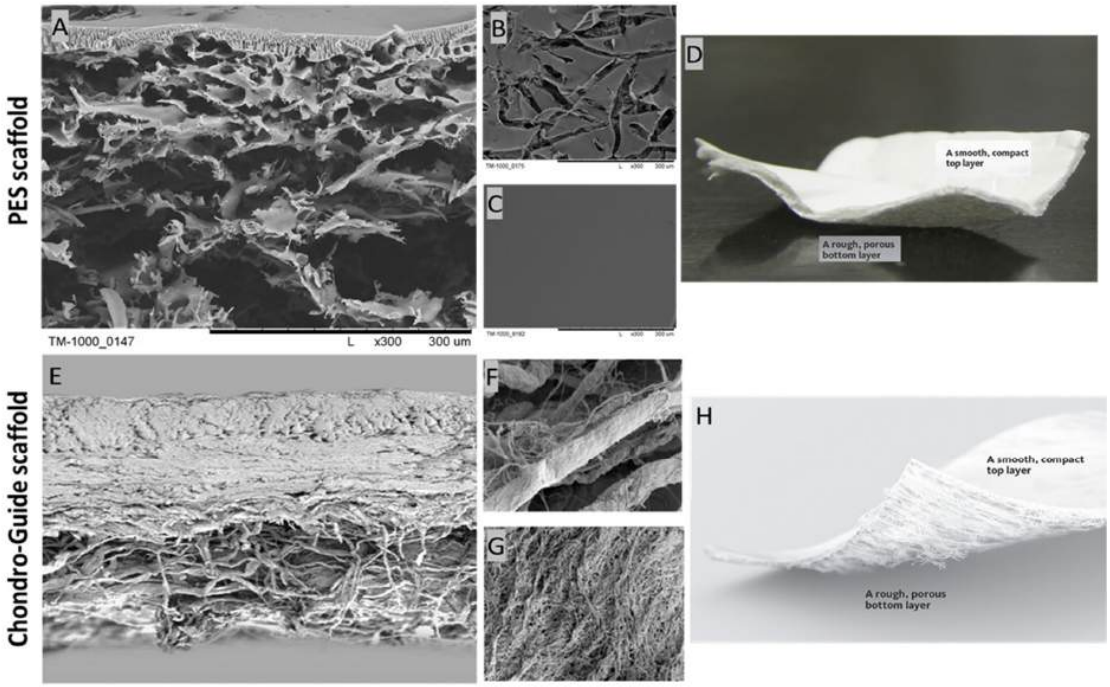

Figure 2. SEM photomicrographs of the PES scaffold: (**A**) cross-section; (**B**) bottom layer; (**C**) top layer; and the Chondro-Gide scaffold: (**E**) cross-section; (**F**) top layer; (**G**) bottom layer. Photos of the PES scaffold (**D**) and the Chondro-Gide scaffold (**H**). Adapted from [51], Geistlich. Magnification: (**A**–**C**) ×300; (**E**) ×100; (**F**,**G**) ×1500.

A Chondro-Gide membrane was used to comparatively evaluate the chondrogenic potential of the PES membrane (Figure 2). A commercial scaffold manufactured by the Swiss company Geistlich Pharma AG was employed. According to the information provided by the company, it is a collagen membrane made of type I and III collagen of porcine origin. It has a two-layer structure, comprised of a compact layer and a porous layer. The compact layer has a smooth surface visible on one side of the membrane, and the spongy layer is characterized by its rough surface. Due to the materials used, the Chondro-Gide is absorbable. The arrangement of collagen fibers increases the membrane's resistance to tearing. The proteolytic enzyme collagenase is responsible for membrane resorption, and the resulting breakdown products are denatured at 37 °C. The resulting oligopeptides are broken down into individual amino acids. Membrane manufacturers have also described its immunogenic properties as being very low [51].

2.2. Rabbits

The right and left knees of 64 White New Zealand rabbits, weighing 2–3.5 kg and aged 4 months, were used for this study. They were kept in an animal house on the premises of the Miroslaw Mossakowski Institute of Experimental and Clinical Medicine of the Polish Academy of Sciences in Warsaw, under standard environmental conditions: air humidity 50 ± 10%, temperature 24 °C ± 2 °C. The animals were kept in separate cages, where they were able to move freely, both before and after treatment.

In all of the knee joints, grade IV defects on the articular surface were produced (Figure 3).

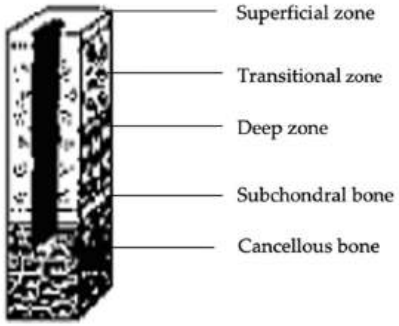

Figure 3. Articular cartilage loss exceeding the subchondral bone—grade IV cartilage damage according to the ICRS scale Adapted from [52], InTech, 2011.

Operational joints were divided into five groups:

1. Full-thickness defect with implanted chondrocytes placed on a collagen membrane: 28 knees.
2. Full-thickness defect and chondrocytes implanted on a PES membrane: 30 knees.
3. Full-thickness lesion and implantation of a collagen membrane without cells: 25 knees.
4. Full-thickness defect and implantation of a PES membrane without cells: 26 knees.
5. Full-thickness defect without any implant, allowing cells from the bone marrow to infiltrate the regenerated tissue: 13 knees.

The choice of research material was justified by the following facts: the morphological and functional similarity of rabbit and human articular cartilage; the relatively low cost of purchase and culture; ease of performing general anesthesia; the ubiquity of the use of rabbits for experimental studies on articular cartilage; and the global literature, providing the possibility of comparing our results with the work of other authors.

This research received the approval of the First Warsaw Ethical Commission for Experiments on Animals of the M. Nencki Institute of Experimental Biology of the Polish Academy of Sciences in Warsaw, through Opinion No. 349/2004.

3. Methods

3.1. Chondrocyte Isolation and Culture Techniques

For Group I and II rabbits, articular cartilage slices were taken from the non-weight-bearing area of the articular surface. Cartilage fragments were collected from the marginal region of the lateral and medial condyles of the rabbits' femurs. They were transported to the laboratory in sterile tubes containing about 1.5 mL of saline solution (0.9% NaCl), where cell isolation and culture were carried out. The cell isolation process was initiated less than two hours after the time at which the tissue was collected. They were cut into slices approximately 1 mm thick using a surgical blade (No. 12) under the sterile conditions of a laminar chamber. The cartilage mass was then washed several times with saline solution and placed in a sterile tube containing 0.25% of collagenase type II solution with culture medium (RPMI with DNAase at a concentration of 7.2 g/L (17.6 units/g), 10% FBS serum, and 1.5% 100 × diluted antibiotics (Streptomycin and Penicillin)). Then, the sample was shaken for 12 h in the incubator (37 °C, 5% CO_2). Subsequently, the obtained samples were centrifuged at 5 °C and 1000 rpm for 5 min. The supernatant was discarded, and the obtained pellets were suspended in 2 mL medium. Before cell counting with the Bürker chamber, the cells were stained with a 0.5% solution of trypan blue. Then, the cells were placed on a PES or collagen membrane with a diameter of 5 mm in a six-well cell culture plate. Supplementary medium was added to each well. Cells were incubated at 37 °C and 5% CO_2. Implantation was performed 14 days after the biopsy.

3.2. Identification of Procollagen Type II

Total mRNA was isolated from the cultured cells according to Chomczyński's method [53]. The obtained mRNA was reverse transcribed (RT-PCR) to obtain cDNA. Then, the cDNA was amplified by PCR, and the product was identified by electrophoresis. The expression of the gene encoding procollagen type II, which is a molecular marker of chondrocytes, was evaluated. Due to the presence of type I and III collagen in the collagen membrane, the test was performed using the PES membrane. The expression of the gene encoding procollagen type II, a molecular marker of chondrocytes, was evaluated only in the second group of rabbits, with implanted chondrocytes placed on a PES membrane. For collagen II, the PCR conditions differed with respect to the primer attachment temperature, which was 61 °C. All PCR reactions were carried out using a Perkin Elmer 9600 machine. The reaction products were developed by electrophoresis on a 1.5% agarose gel, and the resulting product was stained with ethidium bromide.

The primer sequences used for DNA amplification by PCR were as follows:

- Collagen I (5′ starter—5′-CCAGATTGAGACCCTCCTCA-3′, 3′starter—5′-ATGCAAT GCTGTTCTTGCAG-3′)
- Collagen II (5′ starter—5′-GGGGTCCTTTAGGTCCTACG-3′, 3′starter—5′-AGTCGCTG GTGCTGCTGAC-3′)

3.3. Elemental Analysis

To estimate the mass of the tissue grown on the PES membrane after culture, elemental analysis was performed at the Department of Analytical Chemistry, Faculty of Chemistry, Warsaw University of Technology. The tissue mass of the 5-mm-diameter PES membrane slices were determined on the basis of nitrogen (N) content. The test was performed before (reference samples) and after chondrocyte culture (2 weeks). The post-culture samples were fixed with 2.5% glutaraldehyde and dried. Protein was assessed by multiplying the determined nitrogen content by a protein conversion factor of 6.25. Eight analyses were performed—four for the reference samples and four for scaffolds after culture. Due to the composition of the Chondro-Gide membrane (type I, III collagen), these tests were performed only for the PES scaffold.

3.4. SEM Observation

The PES samples were immersed in ethanol for about 15 min. They were then broken into pieces in liquid nitrogen. The samples prepared in this way were dried and coated with a 7 nm layer of gold using a sputtering machine.

3.5. Implantation of Grafts

The surgical procedures were performed under aseptic conditions in the operating room. Subsequent surgeries were performed on the rabbits in Groups I, II, III, IV, and V under combined general anesthesia, using 30 mg/kg ketamine hydrochloride and 2 mg/kg xylazine administered intramuscularly. The rabbits were placed in a supine position, and the surgery was performed on both knees. After shaving and sterile prepping of the lower limbs, an anteromedial parapatellar arthrotomy was performed in the knee. Each patella was dislocated laterally, and a cylindrical osteochondral defect penetrating the subchondral bone was made on the patellar groove of the femur. The defect was 5 mm in diameter and 4 mm in depth. In Group I, II, III, and IV rabbits, the defect was filled with PES or collagen membrane, which was rolled up and attached by press fitting. In Group V rabbits (control group), the defect was left empty. In Group I and II rabbits, autologous chondrocytes were implanted on both kinds of membranes into the defect. In Group III and IV rabbits, membranes without cells were used. The knee wound was closed in layers with 4–0 vicryl sutures. After the operation, all animals were allowed to walk freely in cages without splinting. The rabbits were terminated with an overdose of phenobarbital sodium salt at 12, 25, and 52 weeks after the operation.

3.6. Macroscopic Evaluation

The filling level of the defect relative to the surrounding healthy tissue, the degree of integration, and the regularity of the surface were evaluated macroscopically. For this purpose, the International Cartilage Repair Society (ICRS) cartilage repair assessment scale was used (Figure 4) [54].

	Criteria	Points
Degree of defect repair	Level with surrounding cartilage	4
	75% repair of defect depth	3
	50% repair of defect depth	2
	25% repair of defect depth	1
	0% repair of defect depth	0
Integration to border zone	Complete integration with surrounding cartrilage	4
	Demarcating border < 1mm	3
	¾ of graft integrated, ¼ with a notable border > 1mm	2
	½ of graft integrated with surrounding cartilage, ½ with a notable border > 1mm	1
	From no contact to ¼ of graft integrated with surrounding cartilage	0
Macroscopic appearance	Intact smooth surface	4
	Fibrillated surface	3
	Small, scattered fissure or cracks	2
	Several, small or few but large fissures	1
	Total degeneration of grafted area	0

Figure 4. International Cartilage Repair Society (ICRS) cartilage repair assessment tool. Adapted from [54], Oxford University Press, 2019.

3.7. Microscopic Analysis

Decalcified material was embedded in Paraplast PLUS paraffin (Sigma Aldrich, Poznań, Poland). The blocks were cut in the frontal plane onto slides using a microtome, to a thickness of 4 µm. Paraffin sections were stained by the routine hematoxylin–eosin method. Samples from several areas of the regeneration were selected for microscopic evaluation. The reparative tissue was analyzed histologically. The cell morphology, regularity of surface, integrity of the structure, thickness, integration with surrounding cartilage, cellularity, and necrosis were studied by microscopic analysis on the basis of the O'Driscoll scale (Table 1) [55,56].

Table 1. Criteria and scale for evaluating microscopic images of articular cartilage regeneration according to O'Driscoll [55,56].

Category	Subcategory	Characteristic	Score
1. Nature of predominant tissue	Cellular morphology	Hyaline articular cartilage	4
		Young hyaline cartilage	3
		Incompletely differentiated mesenchyme	2
		Fibrous cartilage	1
		Fibrous tissue or bone	0
2. Structural characteristics	Surface regularity	Smooth and intact	3
		Superficial horizontal lamination	2
		Fissures 25–100% of the thickness	1
		Severe disruption including fibrillation	0
	Structural integrity	Normal	2
		Slight disruption including cysts	1
		Severe disintegration	0
	Thickness	100% of normal adjacent cartilage	2
		50–99% of normal cartilage	1
		0–50% of normal cartilage	0
	Bonding to the adjacent cartilage	Bonded at both ends of graft	2
		Bonded at one end or partially at both ends	1
		Not bonded	0
3. Freedom from cellular changes of degeneration	Hypocellularity	Normal cellularity	3
		Slight hypocellularity	2
		Moderate hypocellularity	1
		Severe hypocellularity	0
	Degenerative changes	None	2
		Moderate	1
		Significant changes	0
4. Subchondral bone reconstruction		100%	2
		50–99%	1
		<50%	0

3.8. Statistical Analysis

For macroscopic and microscopic data analysis, the arithmetical mean, standard deviation (SD), and median value were evaluated. The Mann–Whitney test was used to

compare the scores of the experimental groups. A significance level of 0.05 was used for the statistical analysis.

4. Results

4.1. The Number of Cells

Cells obtained by enzymatic isolation were counted in a Bürker chamber. Approximately 1–1.5 × 10^5 viable cells were obtained after each isolation. An equal number of cells were transferred to scaffolds in six-well plates.

After 14 days of culture, images were taken using an inverted microscope. Figure 5 shows cells that were attached to the edge of the membrane.

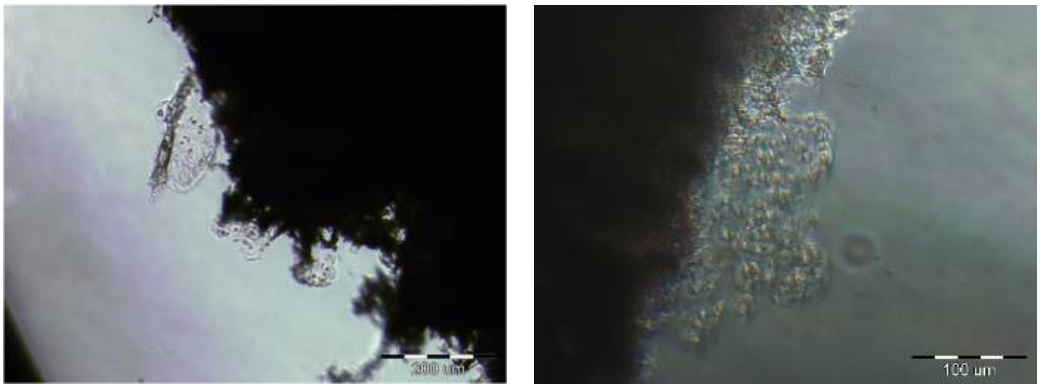

Figure 5. The cells on the edges of the PES scaffolds after 2 weeks of cultivation. Scale bars: left image—200 µm; right image—100 µm.

The presence of cells on the PES membranes was confirmed via SEM microscopy (Figure 6). Cells with an intercellular matrix are noticeable on the PES scaffold, as indicated by the red arrows.

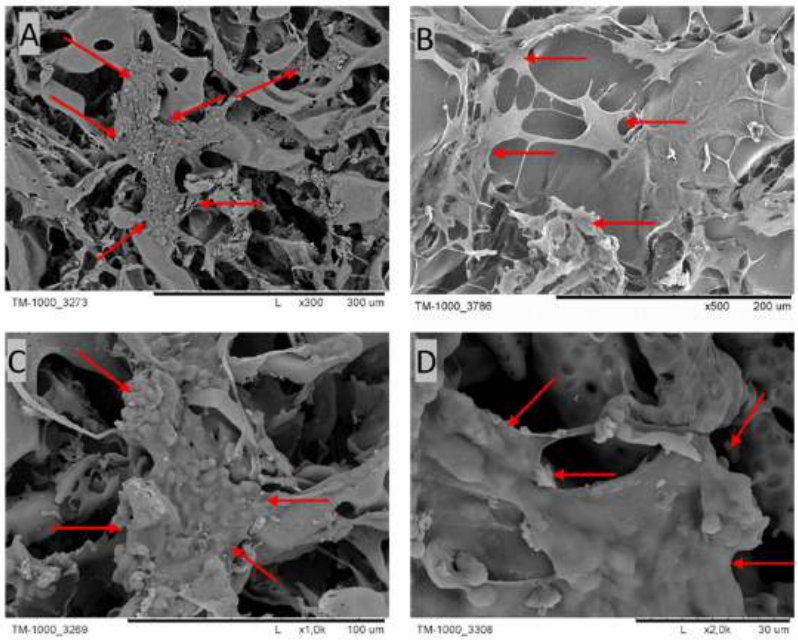

Figure 6. SEM micrographs of cross-sections and the top layers of PES scaffolds after 4 weeks of culture. The red arrows indicate cells with their ECM. Scale bars: (**A**) 300 µm; (**B**) 200 µm; (**C**) 100 µm; (**D**) 30 µm.

4.2. RT-PCR for mRNA of Type II Collagen

Because of the material composing Chondro-Gide (collagen type I and III), the RT-PCR test was only performed for the PES scaffolds. The test was carried out after 2 weeks of cultivation. The analysis of the mRNA isolated from the cells from the bottom of the culture plate and the PES membrane revealed thick bands corresponding to 145 base pairs (bp). There was no band at 352 bp. These data indicate the expression of type II procollagen without exon 2 (type IIB collagen), which is characteristic of cartilage. The bands at 400 bp appearing in the RT-PCR for mRNA, which was extracted from the cells detached from the culture flask and the PES membrane, indicated the expression of type I procollagen. However, the thickness of the bands was greater for cells detached from the bottom of the culture flask (Figure 7).

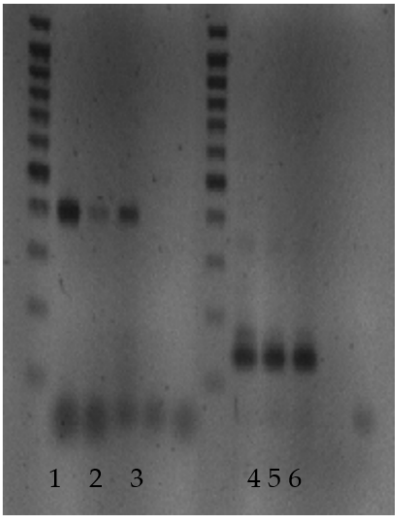

1. type-I collagen, cells from the culture flask
2. type-I collagen, cells from membrane
3. type-I collagen, cells from membrane
4. type-II collagen, cells from the culture flask
5. type-II collagen, cells from membrane
6. type-II collagen, cells from membrane

Figure 7. RT-PCR analysis of the mRNA isolated from the cells detached from the bottom of the culture plate and PES membrane.

4.3. Elementary Analysis

The elementary analysis was carried out only for the PES scaffolds. The problem here was the same as in the case of RT-PCR analysis. Collagen types I/III contain nitrogen, so the results would not be correct. The PES membrane slices after 2 weeks of culture with chondrocytes revealed a concentration of about 0.23 $\pm$ 0.035 mg of tissue on one part of the membrane (Table 2).

Table 2. Tissue mass content from PES scaffolds after 14 days of culture.

Number of PES Scaffold	Tissue Mass Content [mg]
1	0.28
2	0.19
3	0.25
4	0.21

4.4. Macroscopic Evaluation

After 12, 28, and 54 weeks, most of the operated knee joints had normal contouring and preserved a full range of motion. According to the ICRS scale (Figure 4), a diagram was made (Figure 8). Each group of rabbits was considered in turn, and they were divided into subgroups on the basis of the number of points obtained. Data from the macroscopic evaluation indicated that 57% of Group I scored 9 to 11 points, and 43% scored 6 to 8 points. For Group II, 60% of the samples scored 9 to 11 points, 17% scored 6 to 8 points, and 23% scored 3 to 5 points. In Group III, 20% of the samples scored 9 to 11 points, 56% scored 6

to 8 points, and 24% scored 3 to 5 points. In Group IV, 34% of cases scored 9 to 11 points, 46% scored from 6 to 8 points, and 20% scored 3 to 5 points. For samples in Group V, 75% scored less than 3 points and 25% scored 3 to 5 points (Figure 8). The mean scores in Group I, II, III, IV, and V were 8.6, 8.1, 6.9, 7.3, and 1.6, respectively.

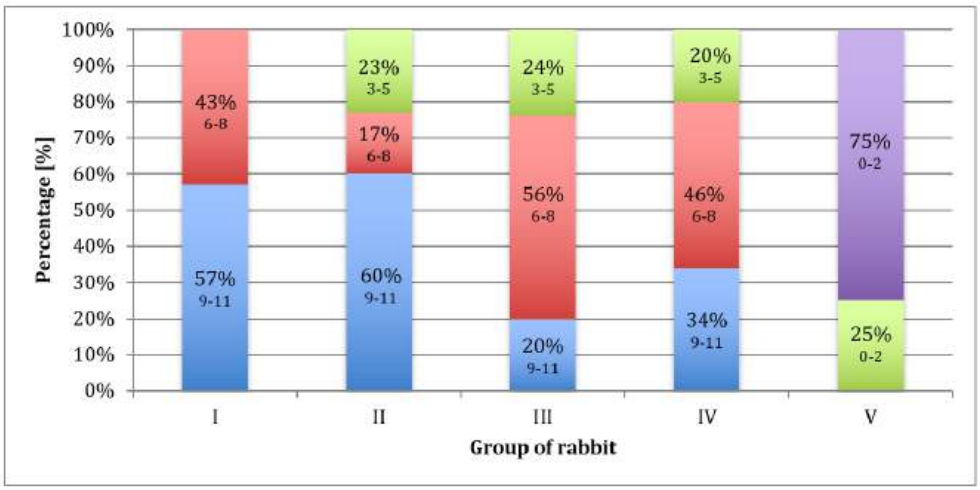

Figure 8. Percentage of rabbits that scored 9–11 (blue), 6–8 (red), 3–5 (green), and less than 3 (purple) points upon macroscopic evaluation after 52 weeks, according to the ICRS scale.

Table 3 shows the parameters calculated by adding up all the scores obtained by the rabbit groups.

Table 3. The parameters calculated by adding up all the grades achieved by the groups of rabbits.

	12 Weeks					25 Weeks					52 Weeks				
Groups	**I**	**II**	**III**	**IV**	**V**	**I**	**II**	**III**	**IV**	**V**	**I**	**II**	**III**	**IV**	**V**
mean	8.3	8.6	6.8	8	1.7	8.2	7.3	7	7.2	1.8	9.4	8.5	7	6.8	1.5
SD	1.5	2.8	1.3	2.4	1	1.7	2.6	1.3	2	1.3	1.5	2.5	2.1	2.1	1.1
median value	8	10	7	9	2	8	9	7	7	2	9	8.5	7	7	1.5

There were statistical differences ($p < 0.05$) between Groups I and III and between Groups I and IV in the 52 weeks of observation (Table 4). Samples in Group V were excluded from the statistical analysis due to failure of the Mann–Whitney test criteria.

Table 4. Comparison of rabbits from Groups I, II, III, and IV: sum ratings based on the Mann–Whitney test.

Groups	**Level of Statistical Significance of the Differences between Groups. Highlighted Fields Indicate Statistically Significant Differences ($p \leq 0.05$)**		
	12 Weeks	**25 Weeks**	**52 Weeks**
I/II	0.369	0.462	0.473
I/III	0.083	0.178	0.030
I/IV	0.930	0.354	0.029
II/III	0.083	0.534	0.178
II/IV	0.514	0.806	0.131
III/IV	0.312	0.962	0.962

The distribution of results was similar in all observation periods (Table 5).

Table 5. Results of the test to determine significant differences between the observation times (Mann–Whitney test).

Groups	Level of Statistical Significance of the Difference between Observation Times Highlighted Fields Indicate Statistically Significant Differences ($p \leq 0.05$)		
	12 Weeks ↔ 25 Weeks	**12 Weeks ↔ 52 Weeks**	**25 Weeks ↔ 52 Weeks**
I	0.895	0.153	0.178
II	0.174	0.910	0.385
III	0.834	0.962	0.885
IV	0.596	0.470	0.700

In Group I, 65% of the evaluated regenerates, and in Group II, 70% of the evaluated regenerates were filled with tissue with a 75–100% degree of similarity to the surrounding cartilage. In Groups III and IV, a similar amount of cavity-filling tissue was found in 39% and 57%, respectively, while in Group V, most cavities remained unfilled or were only 25% filled. Figure 9 shows images of the regenerates for Group II (Figure 9A—a cavity completely filled with tissue) and Group V (Figure 9B—a cavity slightly filled with cartilage), respectively.

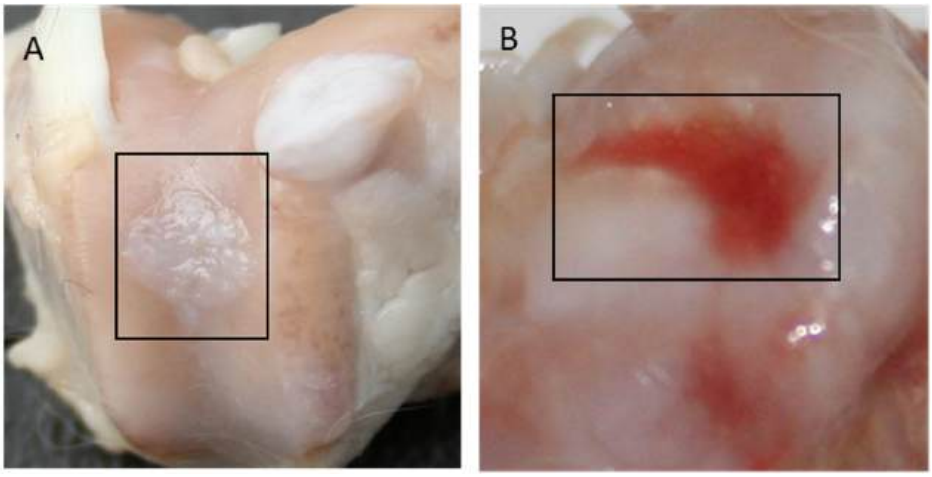

Figure 9. Gross appearance of the cartilage defect at 52 weeks after implantation for Group II (**A**) and Group V (**B**).

4.5. Microscopic Evaluation

Each group of rabbits was considered in turn, and they were divided into subgroups on the basis of the number of points obtained according to the O'Driscoll scale (Table 1). Evaluation of the data indicated that 43% of samples in Group I scored 16 to 20 points, and 57% scored 12 to 15. In Group II, 54% of the samples scored 16 to 20 points, 17% scored 12 to 15 points, 16% scored 8 to 11 points, and 13% scored 0 to 7 points. In Group III, 28% of the samples scored 16 to 20 points, 44% scored 12 to 15 points, 26% scored 8 to 11 points, and 2% scored 0 to 7 points. In Group IV, 35% of cases scored 16 to 20 points, 27% scored 12 to 15 points, 31% scored 8 to 11 points, and 7% scored 0 to 7 points. For Group V, 92% of the samples scored less than 7 points and 8% scored 8 to 11 points (Figure 10). The mean scores in Group I, II, III, IV, and V were 15, 13.6, 13, 13, and 4, respectively.

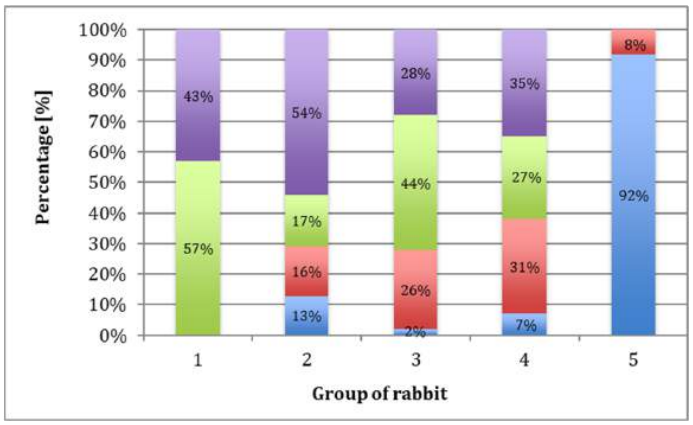

Figure 10. Percentage of rabbits that scored 16–20 (purple), 12–15 (green), 8–11 (red), and less than 7 (blue) points based on microscopic evaluation after 52 weeks, according to the O'Driscoll scale.

In Group I rabbits, the average score was 15 (Table 6). There was a statistically significant improvement in the quality of regenerates during the longest observation period compared to the shortest. The best quality of regenerated tissues was observed after a one-year healing period, with 70% of results being very good. There was also a significant advantage in the results in Group I compared to those in Group IV after a one-year observation period (Table 7). In Group II rabbits, the average score was 13.6 (Table 6). There was no significant difference in the quality of the regenerates due to the length of the observation period (Table 8), nor were there significant differences between this and the other groups (Table 7). In Group III, the average score was 13 (Table 6). Extending the observation period did not significantly improve the quality of the regenerates (Table 8). As in Group II, there were no significant differences between IV and the other groups (Table 7). In Group IV, the average score was 13 (Table 6). The length of the observation period did not significantly affect the quality of the regenerates (Table 8). After a one-year observation period, the regenerate scores were significantly lower than that of Group I (Table 7). In Group V (the control group), the average score was 4 (Table 6), with 90% of the scores not exceeding 8 on the O'Driscoll scale (Figure 11A), and the length of the healing period did not significantly affect regeneration. In groups, I, II, III, and IV, tissue similar to mature hyaline cartilage predominated. In Group V, regenerates composed of fibrocartilage predominated (Figure 11D), accounting for 56%.

Table 6. The parameters were calculated by summing the grades achieved by the rabbit groups.

	12 Weeks					25 Weeks					52 Weeks				
Groups	**I**	**II**	**III**	**IV**	**V**	**I**	**II**	**III**	**IV**	**V**	**I**	**II**	**III**	**IV**	**V**
mean	14	14	13	14	4	15	13	13	12	4	16	14	13	13	4
SD	1.5	6	3	4.4	1.2	1.7	4.7	2.9	3.4	2.2	2.1	4.3	4.1	3.2	1.1
median value	14	16	13.5	15	3	15	14.5	14.5	12	3	16.5	14.5	13	13.5	4.5

Table 7. Comparison between rabbit Groups I, II, III, and IV: sum ratings using the Mann–Whitney test.

Groups	**The Level of Statistical Significance of Differences Between Groups. Highlighted Fields Indicate Statistically Significant Differences ($p \leq 0.05$)**		
	12 Weeks	**25 Weeks**	**52 Weeks**
I/II	0.221	0.462	0.326
I/III	0.441	0.441	0.066

Table 7. *Cont.*

Groups	The Level of Statistical Significance of Differences Between Groups. Highlighted Fields Indicate Statistically Significant Differences ($p \leq 0.05$)		
	12 Weeks	**25 Weeks**	**52 Weeks**
II/III	0.198	0.756	0.391
II/IV	0.596	0.744	0.424
III/IV	0.564	0.501	0.885

Table 8. The results of the test to determine the significant differences between the observation times (Mann–Whitney test).

Groups	Level of Statistical Significance of the Difference between the Observation Times Highlighted Fields Indicate Statistically Significant Differences ($p \leq 0.05$)		
	12 Weeks ↔ 25 Weeks	**12 Weeks ↔ 52 Weeks**	**25 Weeks ↔ 52 Weeks**
I	0.233	0.018	0.121
II	0.307	0.650	0.406
III	0.431	0.847	0.847
IV	0.536	0.847	0.700

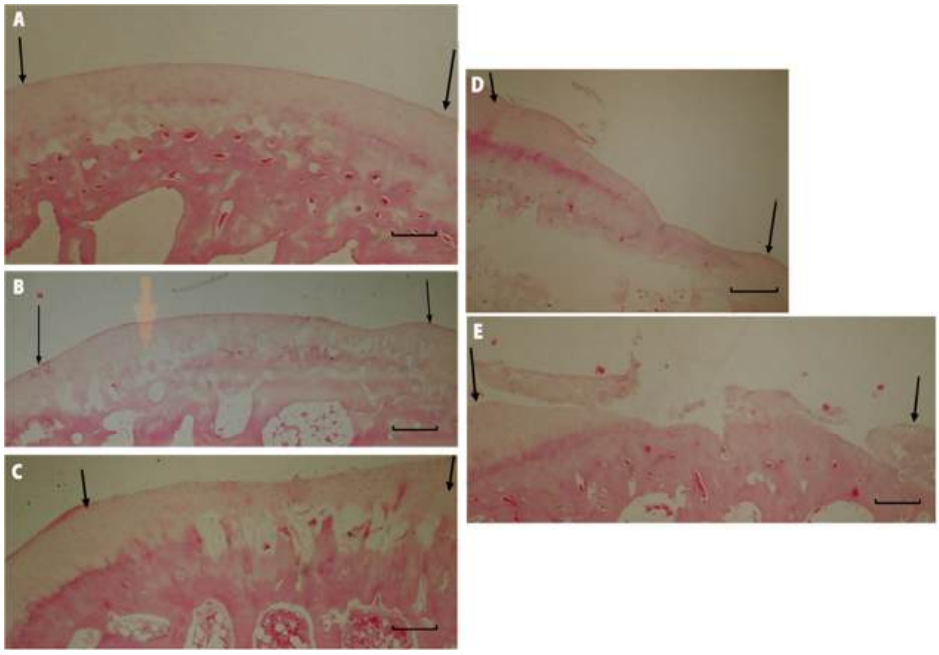

Figure 11. Microscopic imagines of histological samples of the cartilage of the studied groups. (**A**) Group I after 52 weeks of observation. The defect is bonded at both ends of graft (marked with arrows), the surface is smooth and intact, the thickness of the regenerated tissue is 100% that of normal cartilage, 50–99% of the subchondral bone is reconstructed. (**B**) Group II after 52 weeks of observation. The defect is well integrated, the surface is smooth, the thickness is 50–99% of normal cartilage, and more than 50% of the subchondral bone is reconstructed. (**C**) Group III after 52 weeks of observation. The surface of the regenerated tissue is smooth, the cartilage is well integrated, the thickness is 50–99% of normal cartilage, but less than 50% of subchondral bone is reconstructed. (**D**) Group IV after 52 weeks of observation. The surface of the defect is irregular, the margins of the defect are well integrated, the thickness is 50% of normal cartilage, and 100% of the subchondral bone is reconstructed. (**E**) Group V after 52 weeks of observation. The defect has disintegrated. Magnification x50.

In Groups I and II, 70% were regenerated with normal cellularity (Figure 12A). In Group V, regenerates with necrotic features predominated (Figure 12B). There were no significant differences in the results among any of the described groups that were dependent on the length of the observation period.

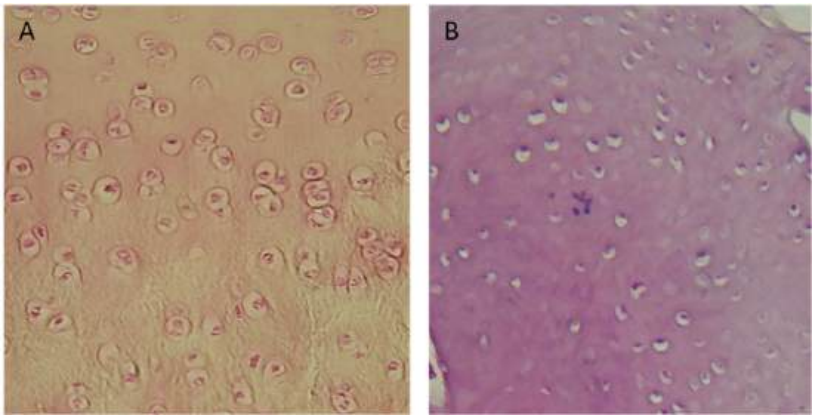

Figure 12. Microscopic images: (**A**) cell-rich regenerate, visible isogenic groups of cells (Group I); (**B**) Significant necrosis of regenerate, visible empty cavities. Magnification: (**A**) ×100; (**B**) ×200.

Group I and II rabbits showed mostly complete regeneration of subchondral bone, with an increase in the number of normal results over longer periods of observation (Figure 13A). In Groups III and IV, subchondral bone regeneration occurred to a similar degree as in Groups I and II, but no improvement in regeneration scores was observed over longer observation periods. Group V was dominated by regenerates in which regeneration of the subchondral layer did not exceed 50% (Figure 13B).

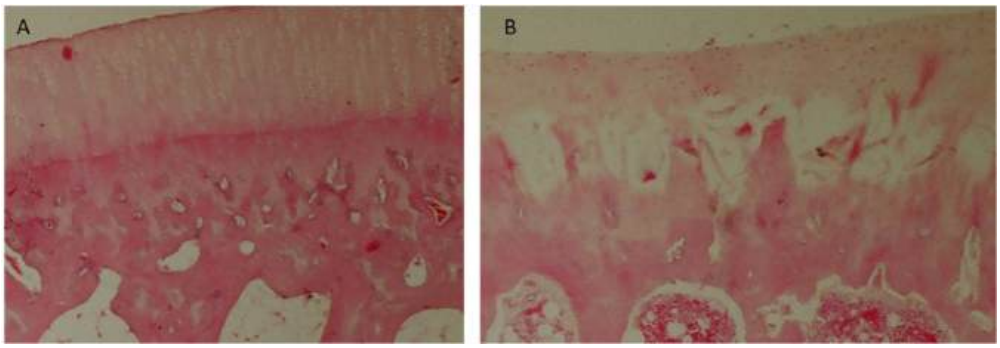

Figure 13. Microscopic images: (**A**) cell-rich regenerate, visible isogenic groups of cells (Group I); (**B**) significant necrosis of regenerate, visible empty cavities (Group III). Magnification: (**A**) ×100; (**B**) ×200.

5. Discussion

Various types of three-dimensional (3-D) matrices have been used for the regeneration of articular cartilage defects in research work carried out over the last fifty years. These include both natural and synthetic materials [57–59]. This is the first report describing the effectiveness of chondrocyte transplantation placed on a polyethersulfone (PES) membrane. In this study, a synthetic PES matrix was used for the first time to regenerate deep defects of the articular cartilage in rabbit knee. The properties of PES membranes were compared with commercially available collagen membranes used in the treatment of articular cartilage defects in humans.

The PES scaffold used in our research was produced based on collaboration between chemists and orthopedic surgeons. The desired features of the scaffold are:

- Sterile and non-cytotoxic;

- Preservable without losing its properties;
- Allows culturing of cells in a 3-D structure [60–62];
- Biodegradable after 6 months.

PES, which is a semipermeable membrane, possesses a pore system and a large inner surface that promotes cell migration and attachment. Due to its wide-meshed interconnecting pores, extensive contact between cells is possible. The porous, spongy structure of the membrane, with its interconnecting pores, promotes the development of collagen fibrils. The specific structure of the PES membrane and its durability (it is a non-absorbable polymer) protects the formation of vulnerable tissue, on one hand, while on the other hand it enables the complete disintegration of the scaffold after about six months, allowing undisturbed development of the cartilage. PES membranes contain sulfate groups [SO_2] attached to the main chain of the polymer. These groups in the membranes mimic similar sulfate groups in the negatively charged glycosaminoglycan chains of the hyaline cartilage matrix. In this study, the PES membrane does not have a skin layer, which on one hand could be a significant obstacle to cell penetration, and cells would stick to the surface of the membrane and would not penetrate inside it. On the other hand, such an epidermal layer could protect joint-transplanted cells from escaping into the joint or from the impact of bone marrow-derived immune cells on the forming cartilage in allogeneic chondrocyte grafts.

The PES membrane has a higher resistance to tearing than collagen in an aqueous environment. This semipermeable material can be held in position by sutures and/or tissue glue, preventing membrane migration under mechanical loading.

The Chondro-Gide collagen membrane is a two-layer structure. The more compact layer—corresponding to the epidermal layer of the membrane—is a reinforcing layer, ensuring the strength of the carrier, and protecting the cells inhabiting the membrane from escaping into the synovial fluid, as well as against mechanical injuries. The less compact, spongy layer, made of collagen fibers with a loose structure, is inhabited by cells. The collagen structure stimulates chondrocytes cultivated in vitro to adopt cartilage metabolism and produce type II collagen and proteoglycans, according to the information provided by the manufacturer of the membrane. The arrangement of the collagen fibers increases the membrane's resistance to tearing, allowing it to be attached with surgical sutures, and preventing it from detaching from the joint surface when the joint is subjected to loading. The Chondro-Gide collagen membrane covering the defect of the joint surface, attached to the margins of the defect with surgical sutures and sealed with tissue glue, can serve as a barrier for the suspension of tissue culture cells introduced under its surface. This method of collagen membrane implantation is currently being used in the treatment of defects of the human cartilage surface. Brittberg reported the treatment of full-thickness defects of cartilage in the knee with chondrocyte transplantation with monolayer culture. This method seems to be suitable for the treatment of cartilage defects with autologous chondrocytes, but there is a risk that cells transplanted in suspension may leak out of the defect due to joint motion [63].

In the described research, collagen and PES scaffolds were placed in six-well cell culture plates to enable their colonization by cells, cell proliferation within the spatial structure of these membranes, and the production of a cartilage matrix containing type II collagen and proteoglycans during culture. A similar method of cultivating cartilage cells on collagen scaffolds was described by Behrens et al. [64].

Our observations showed that the collagen membrane, in aqueous environments such as tissue culture, lost its biomechanical properties, taking on the consistency of a gel, preventing its transfer during culture and implantation into the joint. Compared to the PES scaffold, whose properties did not change under the influence of the environment, collagen seems to be less useful as a cell carrier.

Cartilage fragments taken from rabbit knee joints were exposed to a proteolytic enzyme to isolate the cells. Following Brittberg [65], collagenase and deoxyribonuclease were used for the enzymatic isolation of cartilage cells according to the current knowledge. Despite existing reports on the use of trypsin for the isolation of chondrocytes [66], due to its

cytotoxic effect, described by Moskalewski [67], it was not used in the experiment. After 12 h of isolation, about 1.5–2 $\times$ 10^5 cells were obtained from one rabbit, which is half the value reported by Brittberg [65]. After 4 days of culture, most of the cells were attached to the bottom of the culture plate or settled on the membranes. Cells attached to the bottom changed shape from spherical to spindle-like, similar to fibroblasts. At 14 to 21 days after the beginning of cultivation, as a result multiple divisions, a single layer of cells was formed at the bottom of the six-well cell culture plate. Similar observations have been made by other researchers [65].

A major problem with the regeneration of cartilage by autologous chondrocyte implantation is the dedifferentiation of chondrocytes during monolayer culture, resulting in cells with a fibroblast-like phenotype. These cells produce fibrous tissue instead of hyaline cartilage. Matmati et al. described the use of heat-inactivated allogeneic serum (HIFBS) in a monolayer expansion of bovine chondrocytes to generate cells with differentiated phenotypes [68]. In our study, the three-dimensional arrangement of the PES membrane under in vitro conditions enhanced cell proliferation, and the dedifferentiation of chondrocytes to a fibroblast phenotype was not observed.

According to Benya and Schaffer [69], the chondrocytes isolated from the matrix are phenotypically unstable and dedifferentiate under monolayer culture conditions. They take a form similar to that of mesenchymal progenitor cells or prechondrogenic precursor cells, which are similar to fibroblasts. The effect of their metabolism is the production of proteoglycans and type I and III collagen, which are not characteristic of cartilage [70]. The re-envelopment of the extracellular matrix restores the cells to their chondrocytic form. It is highly probable that the isolation and dedifferentiation of chondrocytes in vitro is a way to obtain a large number of mesenchymal cells that, when implanted into the joint, continue the production of the cartilage matrix started in culture for as long as they do not redifferentiate [71].

In the elementary analysis and after taking pictures of the membranes by means of electron microscopy, two weeks after the start of culture, the presence of tissue on the PES scaffold was observed. The available literature does not contain information on the cultivation of any cells on a PES membrane; therefore, the results described in this study can be regarded as innovative. The average tissue mass of about 0.23 mg on each fragment of membrane with a diameter of 0.5 cm, as well as the electron microscopy images of both the surface and the inside of the membrane after cell culture, prove that the sulfone polymer is a material that provides adequate conditions for the newly formed tissue. It enables undisturbed growth of cells in the 3-D environment, which may reduce the potential for chondrocytes to assume a form similar to fibroblasts, which is characteristic of cultures in a single layer at the bottom of the six-well plate.

The collagen structure of the Chondro-Gide membrane and the nitrogen content made it difficult to perform an elementary analysis of this membrane. Its protein chemical composition makes it impossible to objectively analyze the nitrogen content, on the basis of which the amount of protein on the PES scaffold was estimated. No cells were isolated from the collagen membrane in order to estimate their number, despite the attempts made. The cells isolated and propagated in vitro expressing the gene encoding type II B collagen, which is a molecular marker of cartilage tissue [72,73], were characterized by a metabolism typical for chondrocytes. The expression of the type I collagen gene, specific for fibroblasts, proves that the cells were dedifferentiated in culture and took on a form similar to prechondrogenic fibroblast-like mesenchymal cells [69,70]. According to some authors, the cultivation of cartilage cells at the bottom of the culture flask causes their irreversible dedifferentiation, and stops the production of type II collagen and proteoglycans [74].

Culturing chondrocytes on a porous PES membrane creates spatial conditions for proliferating cells that are completely different from those that are possible when cultured in a single layer. It can be assumed that cartilage cells undergo less dedifferentiation under the conditions created by the porous sulfone polymer. The significantly lower intensity of the bands at the level of 400 base pairs, i.e., the lower expression of the type I collagen

gene for cells collected from the PES scaffold in comparison to the cells from the bottom of the wells in the culture plate, may indicate the preserved metabolism characteristic of cartilage tissue.

Summarizing the macroscopic evaluation, the advantage in terms of the points obtained by Groups I and II over III and IV is visible. The average results and the frequency of very good results were both higher in these groups. There is a subtle advantage, although not statistically confirmed, of the scores obtained in the group in which cells were transplanted on a collagen membrane compared to the group where PES was used as a carrier. The statistical analysis did not confirm a significant advantage in terms of the points obtained for Group I over II; however, a significant difference was shown between Group I rabbits and both groups when using only membranes—PES and collagen—in the longest observation period of fifty-two weeks. There were also no significant differences between the quality of regenerates after transplantation of empty membranes, apart from a very slight advantage to the results obtained for Group IV—the PES scaffold—compared to III—the collagen membrane. The results obtained for the control group (V), not included in the statistical analysis, were significantly worse than those obtained for the groups after cell implantation on membranes and empty membranes.

In the microscopic assessment of cartilage surface repair, analysis of the sum of the scores obtained in individual groups indicated a slight advantage in the results obtained for Group I after the transplantation of cartilage cells placed on collagen material compared to Groups II, III and IV, in which the described results were similar to each other. There were no statistical differences between these groups: only in Group I was there a statistically significant improvement in the results after the longest period of observation. In the group left to heal spontaneously (V), the regeneration of damage in the cartilaginous surface had not occurred even after the longest observation period. The differences in results between Groups I, II, III and IV were less pronounced than those reported by Brittberg et al. [65]. He noted and statistically confirmed the advantage of the quality of regenerates in the group of animals in which chondrocytes were transplanted compared the group receiving periosteum transplantation. The difference described may be related to the poorer regenerative potential of the periosteum compared to collagen and PES scaffolds.

Pulkkinen et al. [75] tested a recombinant human type II collagen (rhCII) gel combined with autologous chondrocytes as a scaffold for cartilage repair in rabbits in vivo. Similar to our studies, cultivation for 2 weeks prior to transplantation into a lesion with a diameter of 4 mm created in the rabbit's femoral trochlea. After 6 months, the repair tissue in both groups filled the lesion, but with rhCII repair, the filling was more complete. The O'Driscoll grading showed no significant differences between rhCII repair and spontaneous repair, with both presenting lower quality than intact cartilage. When rhCII was used to repair cartilage defects, the repair quality was histologically incomplete, but still, the rhCII repair showed moderate mechanical characteristics, which were a slight improvement over those following spontaneous repair.

Allogenic chondrocytes may be rejected by the defect as a result of the immune response. Articular cartilage is thought to have low immunogenicity, because the cellular antigens of chondrocytes are covered by the extracellular matrix. However, once chondrocytes have been isolated from the extracellular matrix, they do show immunogenicity [76]. The chondrocytes used in our experimental model were autologous and immunogenic rejection could not be induced.

To overcome the disadvantages of autologous osteochondral transplantation in the treatment of deep osteochondral defects, Schleicher I. et al. developed two biphasic scaffolds—a hydroxyapatite/collagen scaffold and an allogenous sterilized bone/collagen scaffold—and tested their integration in a sheep model. A moderate lowering of the surface, smaller defect size, fewer immune-competent cells in the specimens, and significant upregulation of collagen II and SOX-9 messenger ribonucleic acid expression on the surface of the allogenous sterilized bone/collagen scaffold compared with the hydroxyapatite/collagen scaffold were observed [77]. Recent tissue-engineering approaches, including gene delivery,

have been proposed for the regeneration of cartilage tissue [78]. Odabas S. and Co. investigated genetically modified cells with plasmid-encoding bone morphogenetic protein-7 (BMP-7) implanted into gelatin-oxidized dextran scaffolds in the regeneration of auricular cartilage defects in New Zealand (NZ) white rabbits.

6. Conclusions

The established method for the isolation and culturing of chondrocytes is adequate to provide a sufficient number of cells that can be used as a transplant. Autologous chondrocyte transplantation resulted in the growth of the regenerated tissue, revealing a morphology similar to hyaline-like cartilage. The quality of the regenerated tissue after the transplantation of the PES membrane was similar to that for the collagen membrane. The RT-PCR analysis of mRNA isolated from the chondrocytes cultured on the PES scaffolds showed the expression of type II procollagen. Elemental analysis of PES membrane slices after 2 weeks of culture with chondrocytes showed a concentration of 0.23 mg of tissue per membrane section. Macroscopic and microscopic evaluation indicated that the quality of the regenerated tissue was similar after the transplantation of cells placed on PES or collagen membranes. The regenerated tissue in the full-thickness defects reached maturity after 12 weeks, and exhibited a hyaline cartilage morphology even after 52 weeks.

Author Contributions: Conceptualization, M.P., A.C. and J.C.; Methodology, M.P., T.J. and A.C.; Validation, M.P.; Formal analysis, M.P.; Investigation, M.P.; Resources, M.P., M.W. and A.C.; Data curation, M.P.; Writing—original draft, M.P. and M.W.; Writing—review & editing, M.W. and T.J.; Supervision, A.C. and J.C. All authors have read and agreed to the published version of the manuscript.

Funding: This study was supported by Scientific Research Grants Nos. 2P05C 044 29 and N518 4058 33 from the Ministry of Science and Higher Education of Poland.

Institutional Review Board Statement: Not applicable.

Data Availability Statement: Not applicable.

Conflicts of Interest: The authors declare no conflict of interest.

References

1. Zhang, L.; Hu, J.; Athanasiou, K.A. The role of tissue engineering in articular cartilage repair and regeneration. *Crit. Rev. Biomed. Eng.* **2009**, *37*, 1–57. [CrossRef] [PubMed]
2. Sophia Fox, A.J.; Bedi, A.; Rodeo, S.A. The basic science of articular cartilage: Structure, composition, and function. *Sport. Health* **2009**, *1*, 461–468. [CrossRef] [PubMed]
3. Armstrong, C.G.; Mow, V.C. Variations in the intrinsic mechanical properties of human articular cartilage with age, degeneration, and water content. *J. Bone Jt. Surg. Ser. A* **1982**, *64*, 88–94. [CrossRef]
4. Walter, S.G.; Ossendorff, R.; Schildberg, F.A. Articular cartilage regeneration and tissue engineering models: A systematic review. *Arch. Orthop. Trauma Surg.* **2019**, *139*, 305–316. [CrossRef] [PubMed]
5. Krishnan, Y.; Grodzinsky, A.J. Cartilage diseases. *Matrix Biol.* **2018**, *71–72*, 51–69. [CrossRef] [PubMed]
6. Oliveira, M.C.; Vullings, J.; van de Loo, F.A.J. Osteoporosis and osteoarthritis are two sides of the same coin paid for obesity. *Nutrition* **2020**, *70*, 110486. [CrossRef]
7. Temenoff, J.S.; Mikos, A.G. Review: Tissue engineering for regeneration of articular cartilage. *Biomaterials* **2000**, *21*, 431–440. [CrossRef]
8. Kwon, H.; Brown, W.E.; Lee, C.A.; Wang, D.; Paschos, N.; Hu, J.C.; Athanasiou, K.A. Surgical and tissue engineering strategies for articular cartilage and meniscus repair. *Nat. Rev. Rheumatol.* **2019**, *15*, 550–570. [CrossRef]
9. Zhao, Z.; Fan, C.; Chen, F.; Sun, Y.; Xia, Y.; Ji, A.; Wang, D. Progress in Articular Cartilage Tissue Engineering: A Review on Therapeutic Cells and Macromolecular Scaffolds. *Macromol. Biosci.* **2019**, *20*, 1900278. [CrossRef]
10. Medvedeva, E.V.; Grebenik, E.A.; Gornostaeva, S.N.; Telpuhov, V.I.; Lychagin, A.V.; Timashev, P.S.; Chagin, A.S. Repair of damaged articular cartilage: Current approaches and future directions. *Int. J. Mol. Sci.* **2018**, *19*, 2366. [CrossRef]
11. Homminga, G.N.; Bulstra, S.K.; Kuijer, R.; van der Linden, A.J. Repair of sheep articular cartilage defects with a rabbit costal perichondrial graft. *Acta Orthop.* **1991**, *62*, 415–418. [CrossRef] [PubMed]
12. O'Driscoll, S.W.; Salter, R.B. The repair of major osteochondral defects in joint surfaces by neochondrogenesis with autogenous osteoperiosteal grafts stimulated by continuous passive motion. An experimental investigation in the rabbit. *Clin. Orthop. Relat. Res.* **1986**, *208*, 131–140. [CrossRef]

13. Armiento, A.R.; Alini, M.; Stoddart, M.J. Articular fibrocartilage-Why does hyaline cartilage fail to repair? *Adv. Drug Deliv. Rev.* **2019**, *146*, 289–305. [CrossRef] [PubMed]
14. Mirza, U.; Shubeena, S.; Shah, M.S.; Zaffer, B. Microfracture: A technique for repair of chondral defects. *J. Entomol. Zool. Stud.* **2018**, *6*, 1092–1097.
15. Brittberg, M. Symposium Scaffold based Autologous Chondrocyte Implantation: The Surgical Technique. *Asian J Arthrosc.* **2019**, *4*, 23–26. [CrossRef]
16. Wasyłeczko, M.; Sikorska, W.; Chwojnowski, A. Review of synthetic and hybrid scaffolds in cartilage tissue engineering. *Membranes* **2020**, *10*, 348. [CrossRef]
17. Xue, X.; Hu, Y.; Deng, Y.; Su, J. Recent Advances in Design of Functional Biocompatible Hydrogels for Bone Tissue Engineering. *Adv. Funct. Mater.* **2021**, *31*, 2009432. [CrossRef]
18. Tamaddon, M.; Gilja, H.; Wang, L.; Oliveira, J.M.; Sun, X.; Tan, R.; Liu, C. Osteochondral scaffolds for early treatment of cartilage defects in osteoarthritic joints: From bench to clinic. *Biomater. Transl.* **2020**, *1*, 3–17.
19. Follow-up, F.; Randomized, P.; Brittberg, M.; Recker, D.; Ilgenfritz, J. Matrix-Applied Characterized Autologous Cultured Chondrocytes Versus Microfracture. *Am. J. Sport. Med.* **2018**, *46*, 1–9. [CrossRef]
20. Kon, E.; Gobbi, A.; Filardo, G.; Delcogliano, M.; Zaffagnini, S.; Marcacci, M. Arthroscopic second-generation autologous chondrocyte implantation compared with microfracture for chondral lesions of the knee: Prospective nonrandomized study at 5 years. *Am. J. Sport. Med.* **2009**, *37*, 33–41. [CrossRef]
21. Baranowski, M.; Wasyłeczko, M.; Kosowska, A.; Plichta, A.; Kowalczyk, S.; Chwojnowski, A.; Bielecki, W.; Czubak, J. Regeneration of Articular Cartilage Using Membranes of Polyester Scaffolds in a Rabbit Model. *Pharmaceutics* **2022**, *14*, 1016. [CrossRef] [PubMed]
22. Lam, A.T.L.; Reuveny, S.; Oh, S.K.W. Human mesenchymal stem cell therapy for cartilage repair: Review on isolation, expansion, and constructs. *Stem Cell Res.* **2020**, *44*, 101738. [CrossRef] [PubMed]
23. Huang, B.J.; Hu, J.C.; Athanasiou, K.A. Cell-based tissue engineering strategies used in the clinical repair of articular cartilage. *Biomaterials* **2016**, *98*, 1–22. [CrossRef] [PubMed]
24. Demoor, M.; Ollitrault, D.; Gomez-Leduc, T.; Bouyoucef, M.; Hervieu, M.; Fabre, H.; Lafont, J.; Denoix, J.M.; Audigié, F.; Mallein-Gerin, F.; et al. Cartilage tissue engineering: Molecular control of chondrocyte differentiation for proper cartilage matrix reconstruction. *Biochim. Biophys. Acta Gen. Subj.* **2014**, *1840*, 2414–2440. [CrossRef]
25. Ahmadi, F.; Giti, R.; Mohammadi-Samani, S.; Mohammadi, F. Biodegradable Scaffolds for Cartilage Tissue Engineering GMJ. *Gmj* **2017**, *6*, 70–80. [CrossRef]
26. Kalkan, R.; Nwekwo, C.W.; Adali, T. The Use of Scaffolds in Cartilage Regeneration. *Eukaryot. Gene Expr.* **2018**, *28*, 343–348. [CrossRef]
27. Eltom, A.; Zhong, G.; Muhammad, A. Scaffold Techniques and Designs in Tissue Engineering Functions and Purposes: A Review. *Adv. Mater. Sci. Eng.* **2019**, *2019*, 3429527. [CrossRef]
28. Armiento, A.R.; Stoddart, M.J.; Alini, M.; Eglin, D. Biomaterials for articular cartilage tissue engineering: Learning from biology. *Acta Biomater.* **2018**, *65*, 1–20. [CrossRef]
29. Jeuken, R.M.; Roth, A.K.; Peters, R.J.R.W.; van Donkelaar, C.C.; Thies, J.C.; van Rhijn, L.W.; Emans, P.J. Polymers in cartilage defect repair of the knee: Current status and future prospects. *Polymers* **2016**, *8*, 219. [CrossRef]
30. Setayeshmehr, M.; Esfandiari, E.; Rafieinia, M.; Hashemibeni, B.; Taheri-Kafrani, A.; Samadikuchaksaraei, A.; Kaplan, D.L.; Moroni, L.; Joghataei, M.T. Hybrid and composite scaffolds based on extracellular matrices for cartilage tissue engineering. *Tissue Eng. Part B Rev.* **2019**, *25*, 202–224. [CrossRef]
31. Chen, S.; Chen, X.; Geng, Z.; Su, J. The horizon of bone organoid: A perspective on construction and application. *Bioact. Mater.* **2022**, *18*, 15–25. [CrossRef]
32. Sun, C.; Kang, J.; Yang, C.; Zheng, J.; Su, Y.; Dong, E.; Liu, Y.; Yao, S.; Shi, C.; Pang, H.; et al. Additive manufactured polyether-ether-ketone implants for orthopaedic applications: A narrative review. *Biomater. Transl.* **2022**, *3*, 116–133. [CrossRef] [PubMed]
33. Irawan, V.; Akon, T.S.; Toshiyuki, H. Collagen Scaffolds in Cartilage Tissue Engineering and Relevant Approaches for Future Development. *Tissue Eng. Regen. Med.* **2018**, *15*, 673–697. [CrossRef] [PubMed]
34. Lin, H.; Beck, A.M.; Fritch, M.R.; Tuan, R.S.; Deng, Y.; Kilroy, E.J.; Tang, Y.; Alexander, P.G. Optimization of photocrosslinked gelatin/hyaluronic acid hybrid scaffold for the repair of cartilage defect. *J. Tissue Eng. Regen. Med.* **2019**, *13*, 1418–1429. [CrossRef] [PubMed]
35. Mittal, H.; Sinha, S.; Singh, B.; Kaur, J.; Sharma, J.; Alhassan, S.M. Recent progress in the structural modification of chitosan for applications in diversified biomedical fields. *Eur. Polym. J.* **2018**, *109*, 402–434. [CrossRef]
36. Chen, S.; Chen, W.; Chen, Y.; Mo, X.; Fan, C. Chondroitin sulfate modified 3D porous electrospun nano fi ber scaffolds promote cartilage regeneration. *Mater. Sci. Eng. C* **2021**, *118*, 111312. [CrossRef]
37. Zhou, F.; Zhang, X.; Cai, D.; Li, J.; Mu, Q.; Zhang, W.; Zhu, S. Silk fibroin-chondroitin sulfate scaffold with immuno-inhibition property for articular cartilage repair. *Acta Biomater.* **2017**, *63*, 64–75. [CrossRef]
38. Wasyłeczko, M.; Krysiak, Z.J.; Łukowska, E.; Gruba, M.; Sikorska, W.; Kruk, A.; Dulnik, J.; Czubak, J.; Chwojnowski, A. Three-dimensional scaffolds for bioengineering of cartilage tissue. *Biocybern. Biomed. Eng.* **2022**, *42*, 494–511. [CrossRef]

39. Wasyłeczko, M.; Sikorska, W.; Przytulska, M.; Dulnik, J.; Chwojnowski, A. Polyester membranes as 3D scaffolds for cell culture. *Desalination Water Treat.* **2021**, *214*, 181–193. [CrossRef]
40. Silva, D.; Kaduri, M.; Poley, M.; Adir, O.; Krinsky, N.; Shainsky-roitman, J.; Schroeder, A. Mini Review Biocompatibility, biodegradation and excretion of polylactic acid (PLA) in medical implants and theranostic systems. *Chem. Eng. J.* **2018**, *340*, 9–14. [CrossRef]
41. Wen, Y.T.; Dai, N.T.; Hsu, S. Hui Biodegradable water-based polyurethane scaffolds with a sequential release function for cell-free cartilage tissue engineering. *Acta Biomater.* **2019**, *88*, 301–313. [CrossRef] [PubMed]
42. Mahboudi, H.; Soleimani, M.; Enderami, S.E.; Kehtari, M.; Hanaee-Ahvaz, H.; Ghanbarian, H.; Bandehpour, M.; Nojehdehi, S.; Mirzaei, S.; Kazemi, B. The effect of nanofibre-based polyethersulfone (PES) scaffold on the chondrogenesis of human induced pluripotent stem cells. *Artif. Cells Nanomed. Biotechnol.* **2018**, *46*, 1948–1956. [CrossRef] [PubMed]
43. Wu, S.; Wu, X.; Wang, X.; Su, J. Hydrogels for bone organoid construction: From a materiobiological perspective. *J. Mater. Sci. Technol.* **2023**, *136*, 21–31. [CrossRef]
44. Sikorska, W.; Milner-Krawczyk, M.; Wasyłeczko, M.; Wojciechowski, C.; Chwojnowski, A. Biodegradation process of PSF-PUR blend hollow fiber membranes using escherichia coli Bacteria—Evaluation of changes in properties and porosity. *Polymers* **2021**, *13*, 1311. [CrossRef] [PubMed]
45. Sikorska, W.; Wasyłeczko, M.; Przytulska, M.; Wojciechowski, C.; Rokicki, G.; Chwojnowski, A. Chemical degradation of PSF-PUR blend hollow fiber membranes-assessment of changes in properties and morphology after hydrolysis. *Membranes* **2021**, *11*, 51. [CrossRef]
46. Jiang, L.; Xu, L.; Ma, B.; Ding, H.; Tang, C. Effect of component and surface structure on poly (L-lactide-co-ε-caprolactone) (PLCA)-based composite membrane. *Compos. Part B* **2019**, *174*, 107031. [CrossRef]
47. Nofar, M.; Sacligil, D.; Carreau, P.J.; Kamal, M.R.; Heuzey, M.C. Poly (lactic acid) blends: Processing, properties and applications. *Int. J. Biol. Macromol.* **2019**, *125*, 307–360. [CrossRef]
48. Azadbakht, M.; Madaeni, S.S.; Sahebjamee, F. Biocompatibility of polyethersulfone membranes for cell culture systems. *Eng. Life Sci.* **2011**, *11*, 629–635. [CrossRef]
49. Dudziński, K.; Chwojnowski, A.; Gutowska, M.; Płończak, M.; Czubak, J.; Łukowska, E.; Wojciechowski, C. Three dimensional polyethersulphone scaffold for chondrocytes cultivation-The future supportive material for articular cartilage regeneration. *Biocybern. Biomed. Eng.* **2010**, *30*, 65–76.
50. Chwojnowski, A.; Dudziński, K. Method for producing semipermeable polysulfone and polyethersulfone membranes and their applications. Patent: PL 211793 B1, 2012.
51. Steinwachs, M. Collagen Membrane for Articular Cartilage Repair: Chondro-Gide. Geistlich Company: Freiburg, Germany.
52. Harris, J.D.; Flanigan, D.C. Management of knee articular cartilage injuries. In *Modern Arthroscopy*; Dragoo, J.L., Ed.; InTech: Rijeka, Croatia, 2011; Volume 6, pp. 103–128. [CrossRef]
53. Chomczynski, P. A reagent for the single-step simultaneous isolation of RNA, DNA and proteins from cell and tissue samples. *BioTechniques* **1993**, *15*, 532–537.
54. Cai, H.; Wang, P.; Xu, Y.; Yao, Y.; Liu, J.; Li, T.; Sun, Y.; Liang, J.; Fan, Y.; Zhang, X. BMSCs-assisted injectable Col i hydrogel-regenerated cartilage defect by reconstructing superficial and calcified cartilage. *Regen. Biomater.* **2019**, *7*, 35–45. [CrossRef] [PubMed]
55. O'Driscoll, S.W.; Marx, R.G.; Beaton, D.E.; Miura, Y.; Gallay, S.H.; Fitzsimmons, J.S. Validation of a simple histological-histochemical cartilage scoring system. *Tissue Eng.* **2001**, *7*, 313–320. [CrossRef]
56. Metineren, H.; Dülgeroğlu, T.C. Regenerative effect of platelet-rich fibrin on articular cartilage defects in an experimental rat model. *Eur. Res. J.* **2018**, *5*, 299–305. [CrossRef]
57. Speer, D.P.; Chvapil, M.; Volz, R.G.; Holmes, M.D. Enhancement of healing in osteochondral defects by collagen sponge implants. *Clin. Orthop. Relat. Res.* **1979**, *144*, 326–335. [CrossRef]
58. Minns, R.J.; Muckle, D.S. Mechanical and histological response of carbon fibre pads implanted in the rabbit patella. *Biomaterials* **1989**, *10*, 273–276. [CrossRef] [PubMed]
59. AR, C. Arthroplasties using compressed ivalon sponge. *South. Med. J.* **1960**, *53*, 957–960.
60. Burmester, G.R.; Menche, D.; Merryman, P.; Klein, M.; Winchester, R. Application of monoclonal antibodies to the characterization of cells eluted from human articular cartilage. Expression of Ia Antigens in Certain Diseases and Identification of an 85-kD Cell Surface Molecule Accumulated in the Pericellular Matrix. *Arthritis Rheum.* **1983**, *26*, 1187–1195. [CrossRef]
61. Lance, E.M.; Kimura, L.H.; Manibog, C.N. The expression of major histocompatibility antigens on human articular chondrocytes. *Clin. Ortopaedics Relat. Res.* **1993**, *291*, 266–282. [CrossRef]
62. Moskalewski, S.; Kawiak, J. Cartilage Formation after Homotransplatation of Isolated Chondrocytes.pdf. *Transplantation* **1965**, *3*, 737–747. [CrossRef]
63. Moskalewski, S.; Osiecka-Iwan, A.; Hyc, A. Cartilage produced after transplantation of syngeneic chondrocytes is rejected in rats presensitized with allogeneic chondrocytes. *Cell Transplant.* **2001**, *10*, 625–632. [CrossRef]
64. Behrens, P.; Bitter, T.; Kurz, B.; Russlies, M. Matrix-associated autologous chondrocyte transplantation/implantation (MACT/MACI)-5-year follow-up. *Knee* **2006**, *13*, 194–202. [CrossRef] [PubMed]
65. Brittberg, M.; Nilsson, A.; Lindahl, A.; Ohlsson, C.; Peterson, L. Rabbit articular cartilage defects treated with autologous cultured chondrocytes. *Clin. Orthop. Relat. Res.* **1996**, *326*, 270–283. [CrossRef]

66. Katsube, K.; Ochi, M.; Uchio, Y.; Maniwa, S.; Matsusaki, M.; Tobita, M.; Iwasa, J. Repair of articular cartilage defects with cultured chondrocytes in Atelocollagen gel. Comparison with cultured chondrocytes in suspension. *Arch. Orthop. Trauma Surg.* **2000**, *120*, 121–127. [CrossRef] [PubMed]
67. Oliver, R. *Yearbook of Cell and Tissue Transplatation*; Lanz, R.P., Chick, W.L., Eds.; Kulwer Academic: Hingham, MA, USA, 2021; ISBN 9789401065603.
68. Matmati, M.; Ng, T.F.; Rosenzweig, D.H.; Quinn, T.M. Protection of bovine chondrocyte phenotype by heat inactivation of allogeneic serum in monolayer expansion cultures. *Ann. Biomed. Eng.* **2013**, *41*, 894–903. [CrossRef]
69. Benya, P.D.; Shaffer, J.D. Dedifferentiated chondrocytes reexpress the differentiated collagen phenotype when cultured in agarose gels. *Cell* **1982**, *30*, 215–224. [CrossRef] [PubMed]
70. Benya, P.D.; Padilla, S.R.; Nimni, M.E. Independent regulation of collagen types by chondrocytes during the loss of differentiated function in culture. *Cell* **1978**, *15*, 1313–1321. [CrossRef] [PubMed]
71. Tgfb-, E.; Verhaar, J.A.N. Optimization of chondrocyte expansion in culture. *Acta Orthop. Scand.* **1999**, *70*, 55–61.
72. Barone, L.M. LEESA M. BARONE, Genzyme Tissue Repair. Ph.D. Thesis, Cambridge, MA, USA, 1999.
73. Im, G.I.; Kim, D.Y.; Shin, J.H.; Hyun, C.W.; Cho, W.H. Repair of cartilage defect in the rabbit with cultured mesenchymal stem cells from bone marrow. *J. Bone Jt. Surg. Ser. B* **2001**, *83*, 289–294. [CrossRef]
74. Von der Mark, K.; Gauss, V.; von der Mark, H.; Müller, P. Relationship between cell shape and type of collagen synthesized as chondrocytes lose their cartilage phenotype in culture. *Nature* **1977**, *267*, 531–532. [CrossRef]
75. Pulkkinen, H.J.; Tiitu, V.; Valonen, P.; Jurvelin, J.S.; Rieppo, L.; Töyräs, J.; Silvast, T.S.; Lammi, M.J.; Kiviranta, I. Repair of osteochondral defects with recombinant human type II collagen gel and autologous chondrocytes in rabbit. *Osteoarthr. Cartil.* **2013**, *21*, 481–490. [CrossRef]
76. Moskalewski, S.; Osiecka-iwan, A.; Jozwiak, J. Mechanical Barrier as a Protection Against Rejection of Allogeneic Cartilage Formed in Joint Surface Defects in Rats. *Cell Transplant.* **2000**, *9*, 349–357. [CrossRef] [PubMed]
77. Schleicher, I.; Lips, K.S.; Sommer, U.; Schappat, I.; Martin, A.P.; Szalay, G.; Hartmann, S.; Schnettler, R. Biphasic scaffolds for repair of deep osteochondral defects in a sheep model. *J. Surg. Res.* **2013**, *183*, 184–192. [CrossRef] [PubMed]
78. Odabas, S.; Feichtinger, G.A.; Korkusuz, P.; Inci, I.; Bilgic, E.; Yar, A.S.; Cavusoglu, T.; Menevse, S. Auricular cartilage repair using cryogel scaffolds loaded with BMP-7-expressing primary chondrocytes. *J. Tissue Eng. Regen. Med.* **2013**, *7*, 831–840. [CrossRef] [PubMed]

PUBLIKACJA 6

Regeneration of Articular Cartilage Using Membranes of Polyester Scaffolds in a Rabbit Model

Maciej Baranowski, **Monika Wasyłeczko**,
Anna Kosowska, Andrzej Plichta, Sebastian Kowalczyk,
Andrzej Chwojnowski, Wojciech Bielecki,
Jarosław Czubak

Pharmaceutics **2022**, 14, 1016.
https://doi.org/10.3390/pharmaceutics14051016
IF: 6,321
MNiSW: 140

pharmaceutics

MDPI

Article

Regeneration of Articular Cartilage Using Membranes of Polyester Scaffolds in a Rabbit Model

Maciej Baranowski [1,*], Monika Wasyłeczko [2], Anna Kosowska [3], Andrzej Plichta [4], Sebastian Kowalczyk [4], Andrzej Chwojnowski [2], Wojciech Bielecki [5] and Jarosław Czubak [1]

1 Department of Orthopedics, Pediatric Orthopedics and Traumatology, Gruca Orthopaedic and Trauma Teaching Hospital, Centre of Postgraduate Medical Education, Konarskiego 13, 05-400 Otwock, Poland; czubakjarek@gmail.com
2 Nalecz Institute of Biocybernetics and Biomedical Engineering PAS, Księcia Trojdena 4, 02-109 Warsaw, Poland; mwasyleczko@ibib.waw.pl (M.W.); achwojnowski@ibib.waw.pl (A.C.)
3 Department of Histology and Embryology, Medical University of Warsaw, Chałubińskiego 5, 02-004 Warsaw, Poland; akosowska@wum.edu.pl
4 Faculty of Chemistry, Warsaw University of Technology, 3 Noakowskiego Str., 00-664 Warsaw, Poland; andrzej.plichta@pw.edu.pl (A.P.); skowalczyk@ch.pw.edu.pl (S.K.)
5 Department of Pathology and Veterinary Diagnostics, Faculty of Veterinary Medicine, Warsaw University of Live Sciences, Nowoursynowska 159c, 02-787 Warsaw, Poland; wojciech_bielecki@sggw.edu.pl
* Correspondence: maciekbar@gmail.com; Tel.: +48-22-779-4031

Abstract: One promising method for cartilage regeneration involves combining known methods, such as the microfracture technique with biomaterials, e.g., scaffolds (membranes). The most important feature of such implants is their appropriate rate of biodegradation, without the production of toxic metabolites. This study presents work on two different membranes made of polyester (L-lactide-co-ε-caprolactone-PLCA) named "PVP and "Z". The difference between them was the use of different pore precursors—polyvinylpyrrolidone in the "PVP" scaffold and gelatin in the "Z" scaffold. These were implemented in the articular cartilage defects of rabbit knee joints (defects were created for the purpose of the study). After 8, 16, and 24 weeks of observation, and the subsequent termination of the animals, histopathology and gel permeation chromatography (GPC) examinations were performed. Statistical analysis proved that the membranes support the regeneration process. GPC testing proved that the biodegradation process is progressing exponentially, causing the membranes to degrade at the appropriate time. The surgical technique we used meets all the requirements without causing the membrane to migrate after implantation. The "PVP" membrane is better due to the fact that after 24 weeks of observation there was a statistical trend for higher histological ratings. It is also better because it is easier to implant due to its lower fragility then membrane "Z". We conclude that the selected membranes seem to support the regeneration of articular cartilage in the rabbit model.

Keywords: scaffolds; regenerative medicine; cartilage tissue engineering; articular cartilage; poly(L-lactide-co-ε-caprolactone); rabbit; cartilage regeneration

check for updates

Citation: Baranowski, M.; Wasyłeczko, M.; Kosowska, A.; Plichta, A.; Kowalczyk, S.; Chwojnowski, A.; Bielecki, W.; Czubak, J. Regeneration of Articular Cartilage Using Membranes of Polyester Scaffolds in a Rabbit Model. *Pharmaceutics* **2022**, *14*, 1016. https://doi.org/10.3390/pharmaceutics14051016

Academic Editors: Ionela Andreea Neacsu and Bogdan Stefan Vasile

Received: 24 April 2022
Accepted: 5 May 2022
Published: 8 May 2022

Publisher's Note: MDPI stays neutral with regard to jurisdictional claims in published maps and institutional affiliations.

1. Introduction

The articular surfaces of the bones are covered with articular cartilage (AC), which is made of hyaline cartilage connective tissue. Hyaline cartilage prevents the abrasion of bones, is resistant to friction, and facilitates movement. So, it is necessary to enable proper movement [1,2]. The cells of cartilage, chondrocytes, produce an extracellular matrix (ECM), which is mainly made of collagen II and proteoglycans. Chondrocytes are located in small spaces in the ECM, called lacunae. These spaces do not allow their migration to damaged sites. Musculoskeletal ailments caused by cartilage damage are common and they are also more often recognized. Most cartilage damage occurs as a result of trauma, an unhealthy lifestyle, or various diseases, such as osteoporosis or autoimmune disorders.

They can damage the cartilage, causing pain, stiffness, movement limitations, and even disability. This can be direct trauma to the cartilage—most often a sharp strike to a bone or repeated microtrauma, the overload causing gradual damage. Repeated damage leads to the formation of defects on the surface. AC lacks blood supply and the neural system, so it has limited regenerative capacity. Moreover, the regenerate process becomes less effective as the human body ages. Leaving defects untreated leads to the development of a degenerative disease [1–9].

Treatment techniques currently used include microfractures (MF), mosaicplasty, osteochondral allograft transplantation, and autologous chondrocyte implantation. Microfractures are now the gold standard of treatment. This technique consists in making the defect within the cartilage damage deep enough to cause the outflow of mesenchymal stem cells (MSC) from the bone marrow. However, due to the specific structure of cartilage (lack of blood vessels, layered structure), none of the abovementioned techniques achieves satisfactory results. The resulting regenerated tissue is often of poor quality: is fibrous-like cartilage, or does not have an appropriate layered structure; therefore, it has reduced mechanical resistance. Some techniques are complex and time-consuming, making them unavailable for many patients. Another problem is the size of the defect. The larger the defect, the more difficult it is to repair with known techniques. Currently, research is focused on combining the microfracture technique with the simultaneous use of scaffolds (3D membranes) to improve the regenerative capacity of cartilage [10–25]. A scaffold is a spatial structure that takes the form of membranes, hydrogels, or nonwovens. Such an implant can be colonized by autologous chondrocytes or mesenchymal stem cells (MSCs). It serves as a temporary matrix that provides a suitable environment for cells that guarantee success in the cartilage regeneration process [16,26–29]. Such scaffolds have already been successfully applied in patients [10,26].

The ideal biomaterial should enable the transport of nutrients to chondrocytes and allow the elimination of metabolites; it should also be completely biodegradable and biocompatible. The degradation products should be non-toxic, non-inflammatory, and mechanically neutral (with adequate softness, stiffness, and roughness). These materials should also be resistant to the conditions in the body, such as pH and body temperature for a certain period. Membranes should have an appropriate microstructure (porosity, pore size, pore shape) [28] and allow for the formation of functional gap junctions and interaction with other cells and the extracellular matrix. The asymmetry of the membrane structure is extremely important—one surface of the membrane should have numerous and large pores, while the opposite surface should have as few and as small pores as possible. This prevents the cells from escaping from the substrate. The size of the pore is properly defined in the purpose of the research, among other things, as is the kind of cells for which the membranes are intended. For example, working with chondrocytes requires smaller pores than working with stem cells for chondrogenesis or with osteoblasts. However, the most important parameters are: biodegradation time; non-toxic, soft metabolites; and a safe degradation process without inflammatory reactions [10,13,16,27–39].

Materials for an implant are mainly made of synthetic or natural polymers or a combination of both (hybrid materials) Currently, commercial scaffolds for cartilage regeneration are made primarily of collagen. Due to defects in the natural polymers, these scaffolds do not meet the appropriate requirements (their rapid hydrolysis, low mechanical stability) that lead to the regenerated tissue being non-valuable fibrocartilage rather than hyaline cartilage [13,16,26–28,37,40]. Unlike natural materials, polyesters provide good mechanical properties and can be used to produce a variety of scaffold shapes using many techniques. They are biocompatible with good mechanical strength that hydrolyze into harmless components that are metabolized in the body and are easily removed from the organism [27,37,41–43]. Currently, research is focused on synthetic polymers, such as polycaprolactone (PCL) and poly (L-lactic acid) (PLLA). Various proportions and combinations of these biodegradable polymers can be used to achieve the desirable surface, mechanical, and structural properties [41,44–47]. Synthetic polyesters, such as poly(L-

lactide-ε-caprolactone) copolymers, are biocompatible and completely bioresorbable. Their degradation products are non-toxic to cells and the major route of the first stage of degradation is hydrolysis. The degradation pathway is through monomers that are elastic and they do not damage the articular surface. The second stage of degradation is the conversion of the monomer to carbon dioxide and water. When polylactide membranes are broken down, lactic acid is formed, which induces inflammation. On the one hand, however, the use of a lactic acid copolymer reduces the concentration of lactic acid in the decomposition products; on the other, it allows the glass transition temperature of the copolymer to be lowered and, ultimately, by disturbing the regularity of the PLA structure, it accelerates the decomposition process [48,49]. An important advantage of co-polyester PLCA structures is that they do not lose their strength in the aquatic environment, and their mechanical and biological durability is significantly greater than that of the collagen substrate. The fact that caprolactone, which is part of the copolymer, has been used for many years to coat absorbable surgical sutures, is an argument in favor of the selected membranes [50]. Individual polyesters differ in biodegradation time—the rule is that the longer the carbon chain, the longer the decomposition time. Due to this mechanism, we can roughly estimate the time it takes for the entire substrate to convert to water and carbon dioxide [51–53]. Such membranes can be used in medicine where scientists and doctors are still looking for new scaffolds for the treatment of articular cartilage.

The literature describes many methods for obtaining synthetic and hybrid scaffolds for tissue engineering. One of the most frequently used membrane preparation techniques is wet phase inversion. The properly formed polymer solution is immersed in a coagulation bath containing a non-solvent of the polymer. Due to the solvent and non-solvent exchange, the phase inversion takes place that gives a membrane. In these techniques, membranes with different porosities and pore sizes can be obtained. Furthermore, in this method, the pore precursor can be added to a previously prepared polymer solution or during membrane formation. It can promote the formation of larger pore sizes and higher porosity. The pore precursors are eventually removed from the scaffold using a suitable solvent (porogen leaching) [54–57].

In this article, we report an animal model study using two scaffolds made of polyester (L-lactide-co-ε-caprolactone) (PLCA). The membranes were prepared by the wet phase inversion method. The difference between them was the use of different pore precursors. It has been hypothesized that the stem cells will colonize the membranes; after that, these cells will differentiate and form hyaline cartilage. The aim was to describe the effect of using the MF method with novel and promising scaffolds to regenerate hyaline cartilage in a rabbit model. The study was conducted in three different time frames using the microscopic examination. Microanalytic studies of origin membranes and extracted residue were carried out as well in order to find out the rate of the molar mass change of PLCA during in vivo therapy. We also evaluated the practical aspects of implantation and surgical techniques.

2. Materials and Methods

2.1. Materials

2.1.1. Membranes

Scaffolds were obtained from the Institute of Biocybernetics and Biomedical Engineering (BBE) of Polish Academy of Sciences. Both scaffolds were made of PLCA by the wet inversion phase method. The difference was the use of various nonwovens as macroporous precursors. Membranes were obtained according to the method presented in previous work [25].

In the first case, the macropore precursor was a nonwoven fabric made of polyvinylpyrrolidone 1.3 MDa (PVP). We named it "PVP" (Figure 1). It was received as follows: the PLCA and Pluronic polymers with 4:1 were dissolved in dioxane with constant stirring to obtain 10 wt.% concentration. Next, a polymer mixture was poured onto the glass base and then the PVP nonwoven layer was laid. Then another portion of polymers was poured on the nonwoven and again a second slice of nonwoven and third layer of membrane forming

solution were added. All layers were pressed and the air was removed using a Teflon roller. The received membrane was gelled in a bath with deionized water with ice (about 4 °C). The prepared membranes were stored in 70% ethanol. It is important to protect the PVP nonwoven from water to prevent its dissolving.

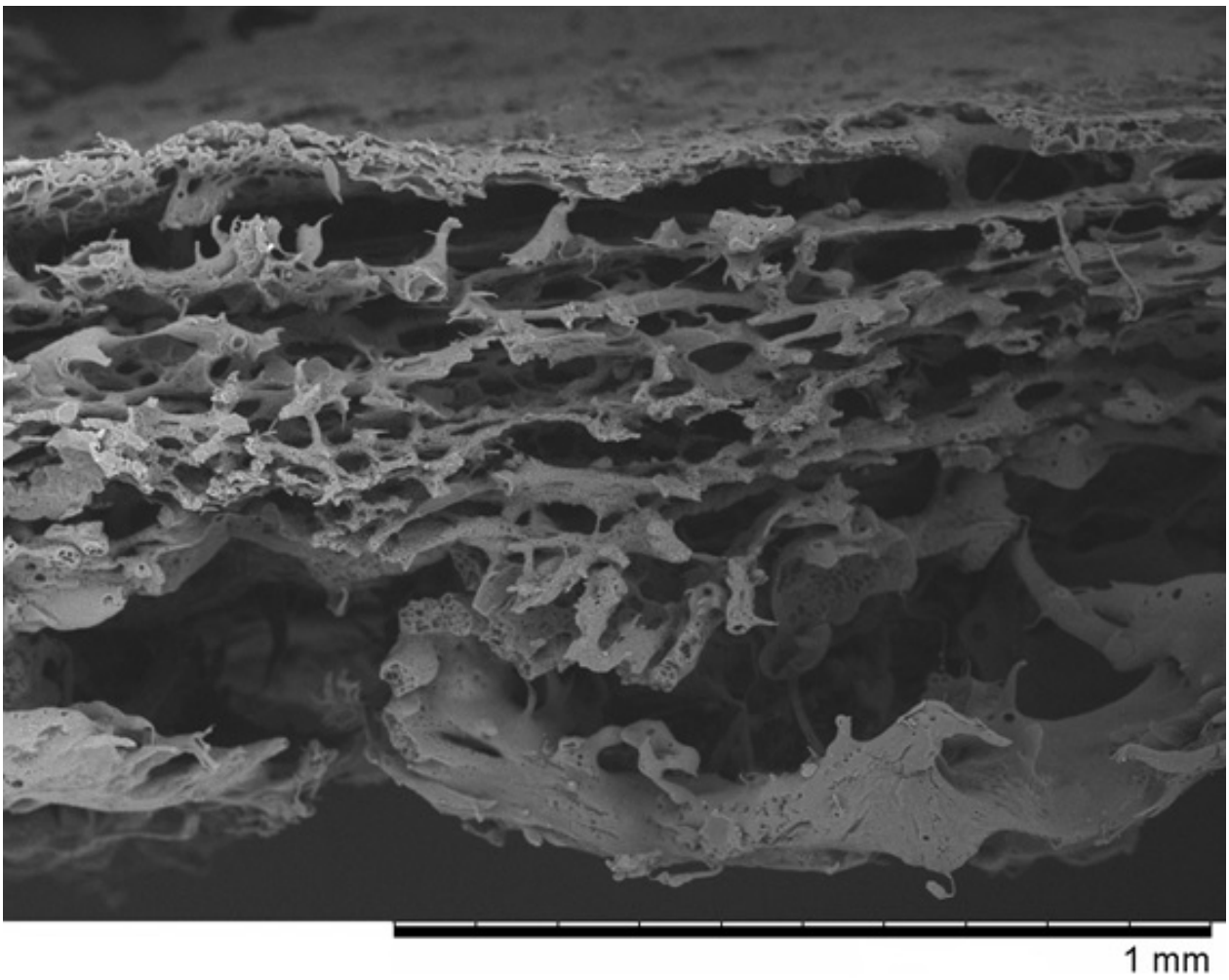

Figure 1. The SEM photomicrographs of the "PVP" membrane.

In the second case, the macropore precursor was a nonwoven fabric made of gelatin. We named it "Z" (Figure 2). It was obtained in a similar way to the previous membrane. The PLCA and PVP 10 kDa polymers with 4:1 ratio were dissolved in chloroform with constant stirring to obtain 10 wt.% concentration. The scaffold was made analogous to "PVP" preparation. The only difference was that the gelation bath contained cooled methanol at 4 °C and the obtained membrane was treated with warm water (50 °C) to removed gelatin nonwoven. Similarly to "PVP" membrane, scaffolds were stored in 70% ethanol. The gelatin nonwoven needs to be protected from water.

The SEM micrographs of "PVP (Figure 1) and "Z" (Figure 2) scaffolds present an irregular structure with macropores and a three-dimensional network of interconnected macropores from 20 to even 500 μm in diameter. Both scaffolds have perforated skin layers that allow cells to enter them. Furthermore, the addition of extra pore precursors of polymers Pluronic ("PVP") and PVP 10 kDa ("Z") affects the microporous morphology of the membranes. It ensures access to oxygen, nutritious substances, or allows for the removal of metabolic products from the interior of scaffolds. The average thickness of both scaffolds is about 700–1200 μm. According to biomedical applications, the porosity and pore size of scaffolds are critical factors. In the previous study, the degradation rate and

porosity of membranes (before and after hydrolysis) were measured [25]. To determine the degradation rate of scaffolds, PBS and Hank's balanced salt solution (HBSS) fluids were used. The hydrolysis time was 5 weeks for "PVP" and 4 weeks for "Z" due to their faster destructions at 37 °C. The loss of weight was observed for both membranes in the range from 17 to 72 of weight percentage. We have also observed that the decrease in pH was not rapid—that should not have a negative effect on the body, such as the occurrence of inflammation. Results showed that both membranes were characterized by high porosity, about 95%. After degradation, this value increased, especially for "Z" in HBSS.

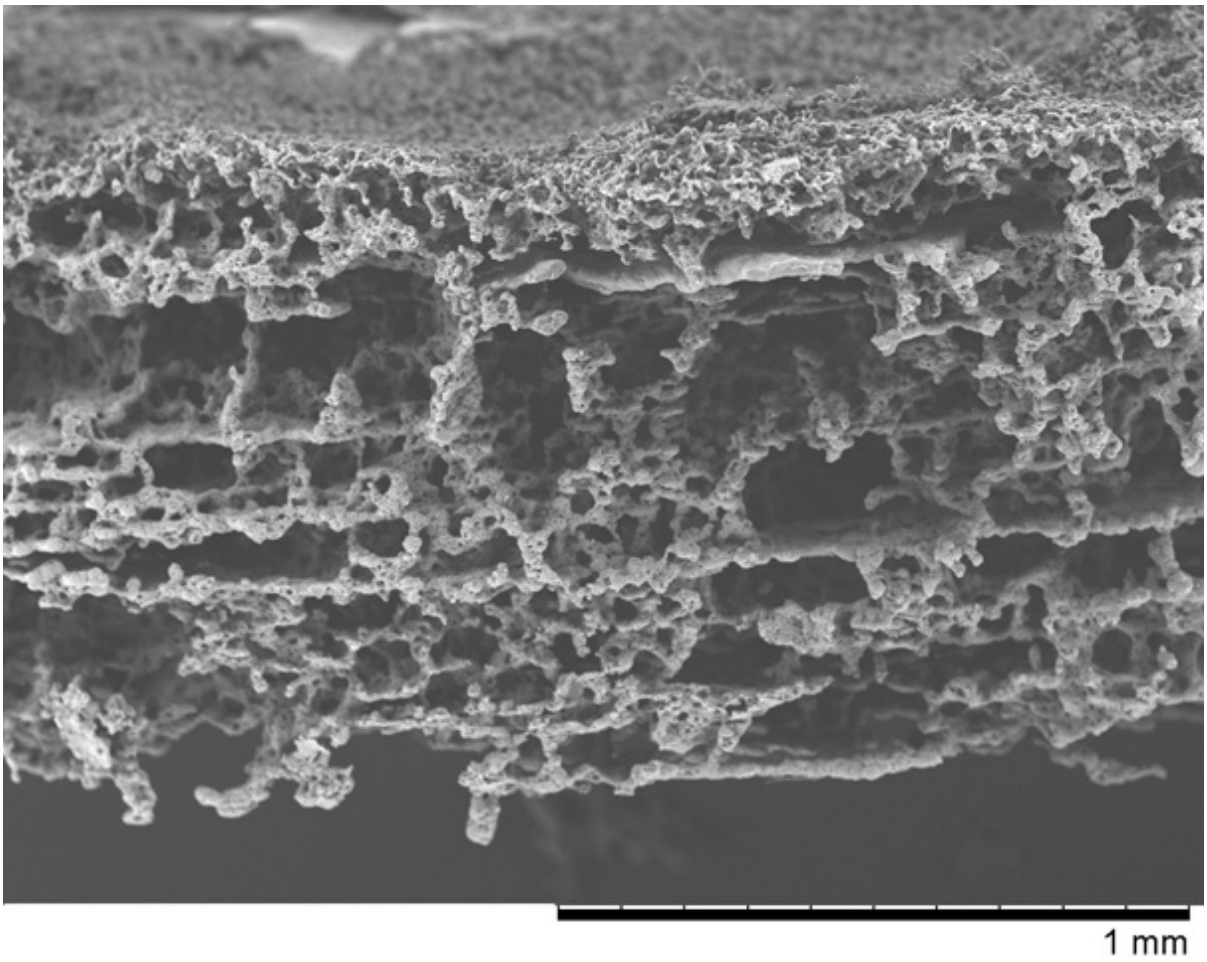

Figure 2. The SEM photomicrographs of the "Z" membrane.

2.1.2. Rabbits

We used 27 white New Zealand male rabbits, weighing about 3–4 kg, and aged about 4 months. Before the start of the study, the animals were habituated to the new environment and caretakers. During the experiment, the rabbits were weighed weekly. The animals were kept under standard environmental conditions: air humidity 55 ± 10%, temperature 21 °C ± 2 °C, 15 air changes per hour, circadian rhythm (light/ dark)12/12 h. All activities performed on animals were in accordance with the principles of occupational health and safety in the laboratory and good laboratory practice. The participants in the study were properly trained and have many years of experience in this field. We split the animals into three groups. In all the knee joints of all the animals, we performed grade IV defects on the articular surface, according to the Outerbridge scale [58]. In group I, defects were created with the simultaneous implantation of a membrane made of a copolymer (L-lactide-co-caprolactone) "PVP". After implantation, we waited for 8 weeks (observing 7 defects), 16 weeks (7 defects), and 24 weeks (7 defects). Then the joint was removed

and the regenerate was assessed. In group II, defects were created with the simultaneous implantation of a membrane "Z". After implantation, we waited for 8 weeks (observing 7 defects), 16 weeks (7 defects), and 24 weeks (7 defects). In group III (control group), defects were created and no other action was taken. After surgery, we waited for 8 weeks (observing 4 defects), 16 weeks (4 defects), and 24 weeks (4 defects).

2.2. Methods

We conducted the study, taking into account the International Cartilage Repair Society (ICRS) recommended guidelines for histological endpoints for cartilage repair studies in animal models and clinical trials [59].

2.2.1. Implantation

All surgical procedures were performed under aseptic conditions of the operating room at the Animal Breeding Laboratory of the Medical University of Warsaw. The surgical operations were performed according to the scheme (Figure 3):

(a) We administered general anesthesia intramuscularly (xylazine and ketamine—dose calculated according to the animal's body weight; ketamine—0.4 mg/kg, xylazine 0.5 mg/kg).
(b) We shaved the area to be operated.
(c) We placed the animal on the side opposite the one to be operated, with the limb in abduction. Skin decontamination with iodine solution. We covered the operating area with sterile drapes, which were attached to the skin.
(d) We prepared the scaffold (membrane "PVP" or "Z"—depending on group). Under sterile conditions, we removed the membrane immersed in alcohol in transport packaging and placed the membrane in sterile petri dishes filled with a 0.9% NaCl solution. Rinsed the membranes twice at 10-min intervals with a 0.9% NaCl solution (to get rid of alcohol). For each animal, membranes were prepared in a separate petri dish. This point was omitted in the control group (where no membrane was used).
(e) Skin incision on the lateral side at the level of the knee joint, then the incision of subcutaneous tissue and the joint capsule. Dislocation of the kneecap to the medial side, providing access to the articular surface of the femur. We created 2 defects located symmetrically at both condyles (each condyle had one defect) of the femur (load bearing area), using a chisel (Figure 3). Defect (0.1 cm^2) of cartilage and bone to a depth of 3 mm. Confirming a full-depth defect penetrating the bone marrow by the occurrence of bleeding from the base of the defects.
(f) We rinsed the defects with sterile 0.9% NaCl solution and dried them (to get rid of any debris). We cut a scaffold to the size of the defect and inserted a scaffold inside the defect so that the more porous surface of the membrane was in direct contact with the bone marrow.
(g) After filling the defects with membranes, we applied the tissue glue (TisselLyo) to the surface of the defects according to the manufacturer's instructions.
(h) We waited for the adhesive to bond with the surrounding tissues. We moved back the kneecap into the correct position. We sutured the articular capsule with a Vicryl 3/0 suture, subcutaneous suture—Vicryl 4/0, skin suture—Ethilon 4/0 (to be removed in 14 days). We covered the postoperative wound with iodoform. Sterile dressing. We applied soft dressing from the ankle to the groin for 24 h.
(i) Postoperative administration of antibiotics (Enrofloxacin) and analgesics (Metamizole) for 2 days.
(j) Due to animal welfare reasons, we operated the second knees of the animals after the previously planned time (8 or 16 weeks, depending on the group).

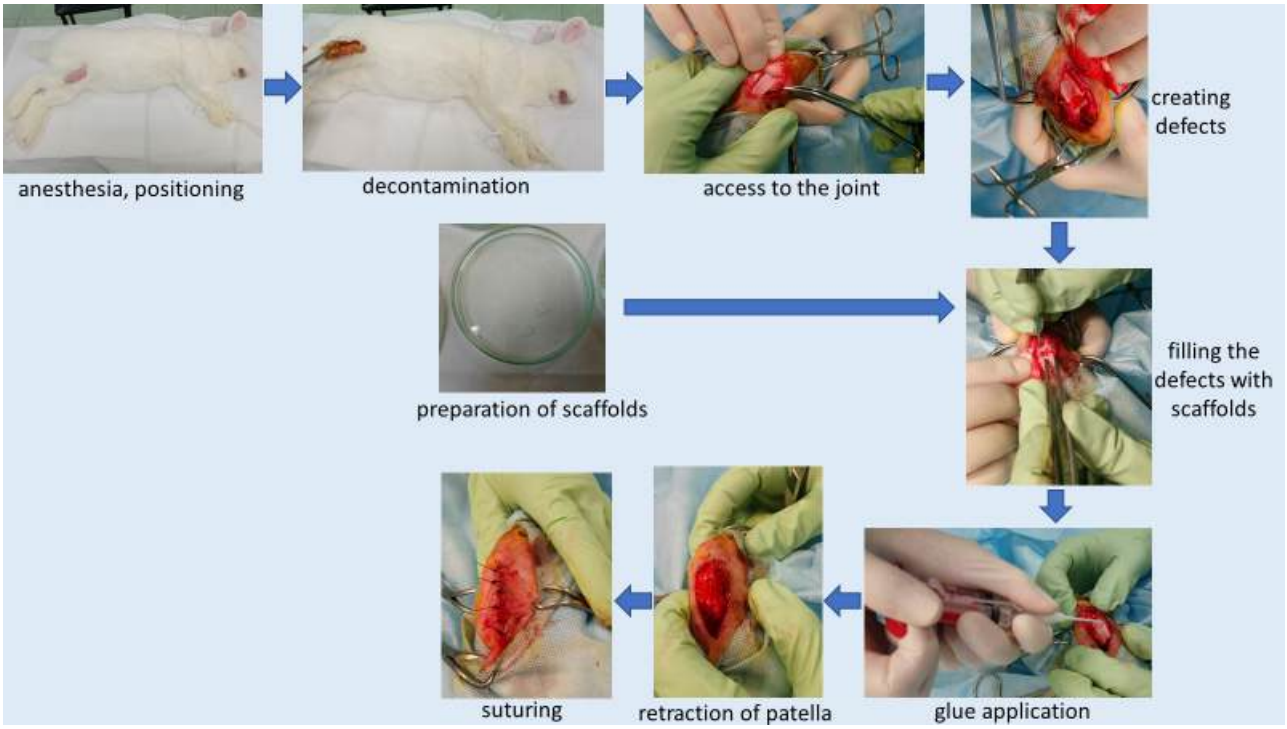

Figure 3. Implantation scheme.

2.2.2. Aftercare

The aftercare was provided in an individual supervision room with electronically controlled temperature, humidity, and exposure time. To ensure maximum comfort and safety for the animals and to minimize the possibility of mistakes, each rabbit had its own separate cage. The animals could move freely around the cage throughout the observation period. Each rabbit had a daily observation card with vital parameters (general and local condition, temperature, body weight), date of surgery, and date of planned termination.

2.2.3. Termination

After the set time of 8, 16, 24 weeks of observation, the rabbits were terminated. Termination procedures were performed according to the scheme (Figure 4):

(a) We administered general anesthesia intramuscularly (dose calculated according to the animal's body weight—ketamine—0.4 mg/kg, xylazine 0.5 mg/kg).
(b) Euthanasia by intravenous administration of Morbital.
(c) We shaved the knee for surgery; disinfection of shaved areas.
(d) Access to the knee joint (skin and deeper tissues were cut, as in the case of surgery). Extraction of the distal femur. Marked the place of defects/membrane insertion with ink. Cut the condyles from the rest of the bone and placed in a sterile transport container for further examination. Lateral condyle was taken to the histopathology examination, medial condyle to GPC.

2.2.4. Gel Permeation Chromatography (GPC)

GPC is the analytical technique that allows to detect and characterize qualitatively polymer chains soluble in eluent used. It provides number and weight average molar masses and the dispersity index of polymers. The chains of various lengths are separated on the gel column with respect to their hydrodynamic radii and the time of elution is correlated with molar masses at the peak of narrow polystyrene standards. The measurement was carried out with the system by Viscotek composed of GPC max and TDA 305, equipped with Jordi Lab DVB column (mixed bed) and refractometer. Dichloromethane was used as

eluent with a flow rate of 1 mL/min at 30 °C. Sample concentration was in the range of 2–4 mg/mL and injection volume was 50 or 150 µL.

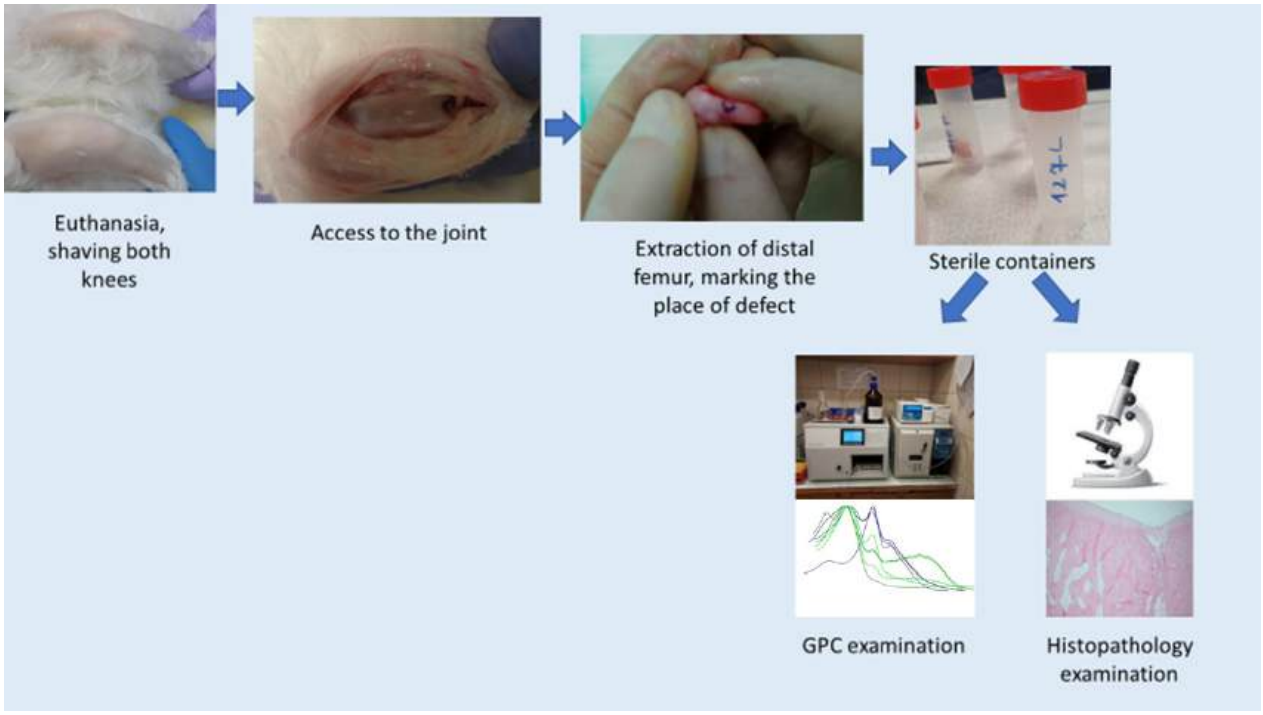

Figure 4. Termination scheme.

Preparation of the material for testing was carried out according to the following scheme:

(a) Scraping and cutting only cavities from previously taken specimens;
(b) Flushing in a physiological saline solution—flushing out physiological fluids;
(c) Rinsing in hexane to extract fats;
(d) Washing in CDCl3 (deuterated chloroform)—deproteinization;
(e) Rinsing in methylene chloride—extraction of membranes (membrane residues);
(f) Filter through a syringe filter with a PTFE membrane, with a porosity of 0.2 µm to get rid of bits of remaining cartilage (insoluble parts).

The GPC test was performed for 5 samples with "PVP" and 5 samples "Z" membrane 8 weeks after implantation; 3 samples with "PVP" and 3 samples "Z" membrane 16 weeks after implantation.

2.2.5. Histopathology

The study was carried out according to the following scheme:

(a) Collected condyles were immersed in 10% formalin.
(b) Descaling—while waiting for the descaling, checks were made on the degree of descaling by trying to puncture the tissue with a needle every few weeks. After decalcification, the damaged areas were more visible.
(c) The decalcified sections were dehydrated and embedded in paraffin (Paraplast sigma).
(d) The material was cut into pieces with a thickness of 4 µm.
(e) Paraffin sections were stained by the routine hematoxylin–eosin method.
(f) The regenerates were evaluated (ICRS microscopic scoring system) under a light microscope by two trained and blinded observers. Each observer rated 1 regenerate 3 times at weekly intervals. The final score is the average of 3 measurements [60].

2.2.6. Statistics

R software with vegan [61], coin [62], and FSA [63] packages was used to answer the research questions. Kendall's *W* coefficient of concordance, Kruskal–Wallis tests with post-hoc Dunn's tests, and Holm's correction for multiple comparisons were performed. Given the small sample size in the study, Kruskal–Wallis *p* values were approximately estimated using 10,000 Monte-Carlo simulations, with bootstrap resampling [64]. Similarly, for Kendall's *W*, 10,000 permutations tests were carried out to estimate null distribution of χ^2 [65]. The significance level was set as $\alpha = 0.05$, while *p* values between 0.05 and 0.1 were treated as tendencies of significance.

3. Results

3.1. Destruction of PLCA Materials in Membranes Analyzed by Means of GPC

The weight average (M_w) and number average (M_n) of molar masses of the initial PCLA copolymer introduced to the membranes were 138,200 g/mol and 78,100 g/mol, respectively. We examined the copolymer material extracted after 8 and 16 weeks of implantation from 16 rabbit joints in total. The average molar masses were measured by means of GPC and calculated with respect to PS standards for all samples. Each sample contained several populations of macromolecules present at fractions. Since the molar mass distributions partially overlapped to facilitate statistical analysis, we decided to calculate the mean values for M_w and M_n for whole multimodal macromolecular distribution of all materials from each sample separately (Table 1). Exemplary, selected molar mass distributions are shown for illustration in Figure 5. Finally, we calculated the mean values of M_w for each type of membrane and implantation period. The data with standard deviation bars are presented in Figure 6.

Table 1. Results of the GPC examination.

Kind of Membrane	Time of Implantation (Weeks)	Sample Nr	Mean Mw
PVP	8	1	5155
PVP	8	2	4816
PVP	8	3	4737
PVP	8	4	1896
PVP [1]	8	5	24,238
PVP	16	1	2387
PVP	16	2	2176
PVP	16	3	2088
Z	8	1	3678
Z	8	2	3167
Z	8	3	3022
Z	8	4	2490
Z	8	5	1432
Z	16	1	2139
Z	16	2	2127
Z	16	3	1663

[1] We reject this sample for statistical reasons—the result of the mean Mw clearly deviates from the other samples.

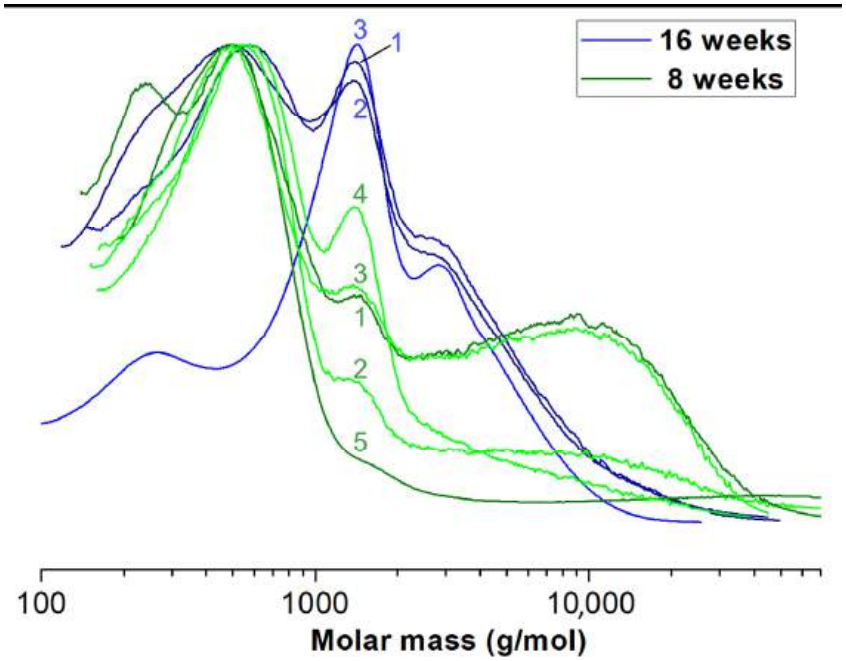

Figure 5. Exemplary molar mass distributions of extracted "PVP" membrane residue.

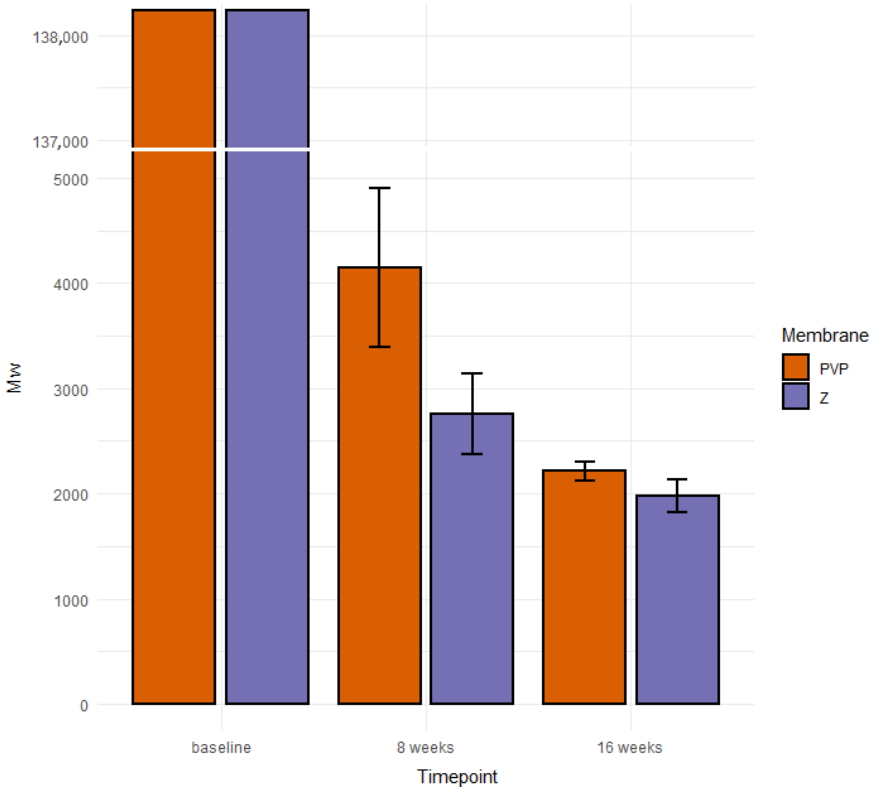

Figure 6. Average values of M_w of PLCA contained in origin membranes and residue materials.

We performed the GPC examination on sections collected only from cavities to prove that the membranes stayed at the primary site of implantation. Because in every sample we detected fractions of polymers, we concluded that membranes remained in the cavities. This confirms that the surgical technique developed by us and used in the study meets the requirements.

3.2. Histopathology

3.2.1. Differences in Membranes Performance

Kruskal–Wallis tests were performed, for ratings provided by each histologist, in each time-point (at 8, 16, or 24 weeks), to examine the differences in recovery between the three groups: a group treated with the membrane PVP (n = 7; the PVP group), a group treated with the membrane Z (n = 7; the Z group), and the control group (n = 4).

3.2.2. Histologist 1

There were no significant differences between studied groups at the 8-week mark—$H(1) = 2.35$, $p = 0.310$, $\varepsilon^2 = 0.14$. However, there was a trend toward a significant difference of ratings at the 16-week mark—$H(1) = 5.53$, $p = 0.057$, $\varepsilon^2 = 0.33$, and a significant difference at the 24-week mark—$H(1) = 5.86$, $p = 0.045$, $\varepsilon^2 = 0.34$. Post-hoc tests at 16 weeks showed a trend for better ratings in the Z group than in the control group—$Z = 2.35$, $p = 0.056$. There were no differences between the PVP group and the control group—$Z = 1.42$, $p = 0.309$, and no differences between the PVP group and the Z group—$Z = 1.08$, $p = 0.278$. At the 24-week mark, there was a trend for higher ratings in the PVP group than in the control group—$Z = 1.97$, $p = 0.099$. No differences between the Z group and the control group—$Z = 0.16$, $p = 0.872$, or between the Z group and the PVP group, $Z = 2.12$, $p = 0.103$, were observed (Figure 7).

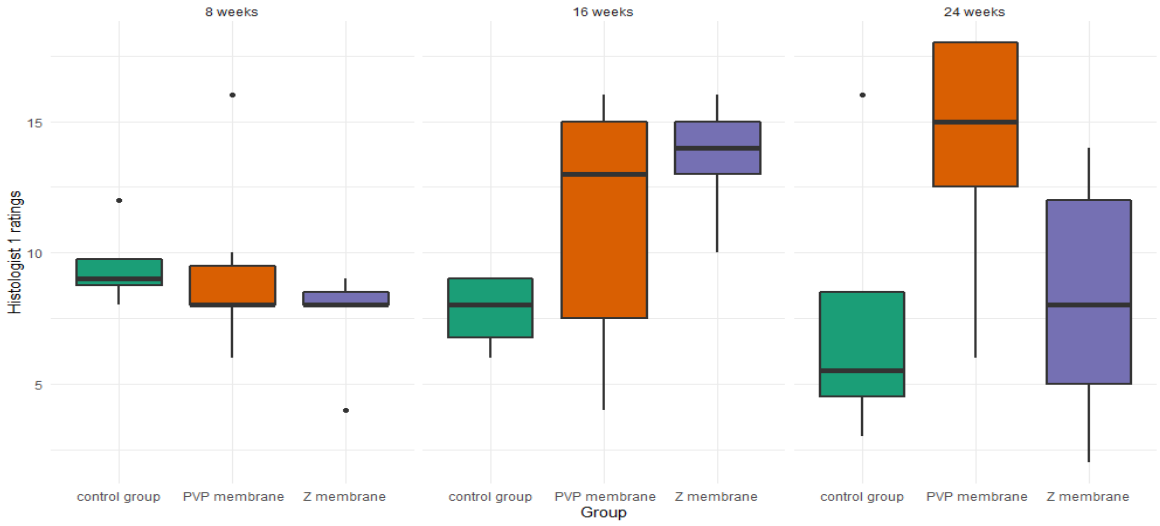

Figure 7. Boxplot of histologist 1 ratings, in the three studied groups, at three time points.

3.2.3. Histologist 2

For histologist 2, there were no differences at the 8-week mark—$H(1) = 1.96$, $p = 0.150$, $\varepsilon^2 = 0.23$ or the 16-week mark—$H(1) = 1.04$, $p = 0.623$, $\varepsilon^2 = 0.06$. However, the Kruskal–Wallis test was significant at the 24-week mark—$H(1) = 9.46$, $p = 0.004$, $\varepsilon^2 = 0.56$. Post-hoc tests for the 24-week mark revealed that histologist 2 rated the healing stage of the membrane PVP—$Z = 2.48$, $p = 0.027$, and the membrane Z—$Z = 2.98$, $p = 0.009$, as superior to the healing properties without a membrane. At the same time there were no differences between the healing properties of the membrane PVP and the membrane Z—$Z = 0.59$, $p = 0.552$ (Figure 8).

It should be noted that the histologic images improve with time when both membranes are used (Figure 9). This proves that the tested scaffolds support cartilage regeneration.

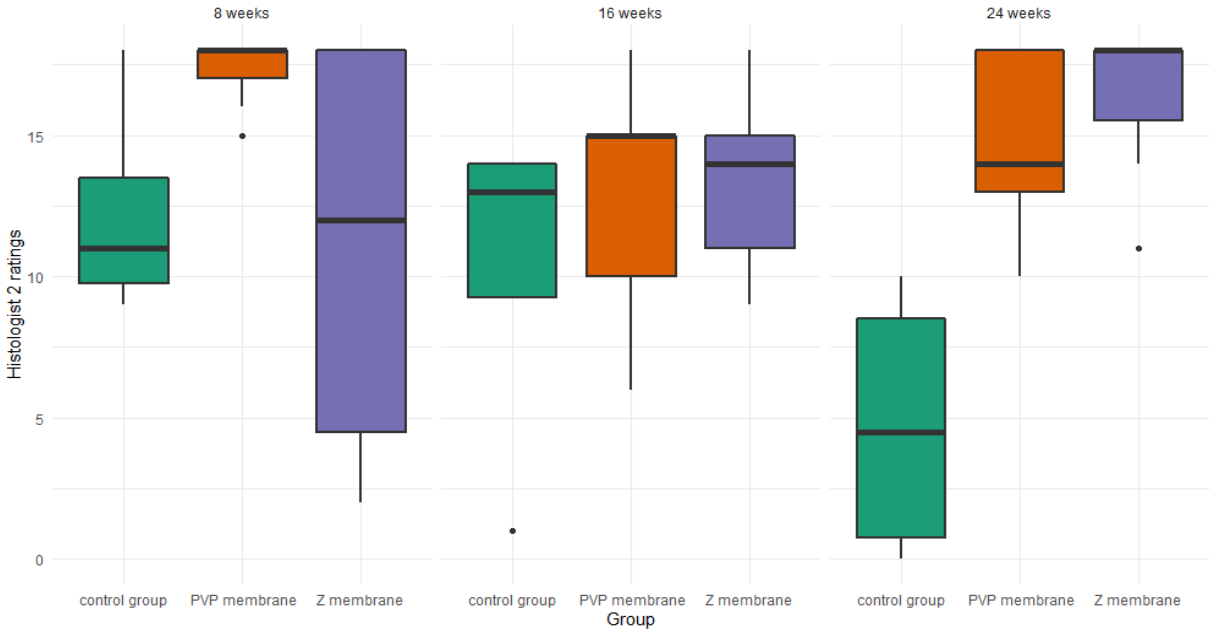

Figure 8. Boxplot of histologist 2 ratings, in the three studied groups, at three time points.

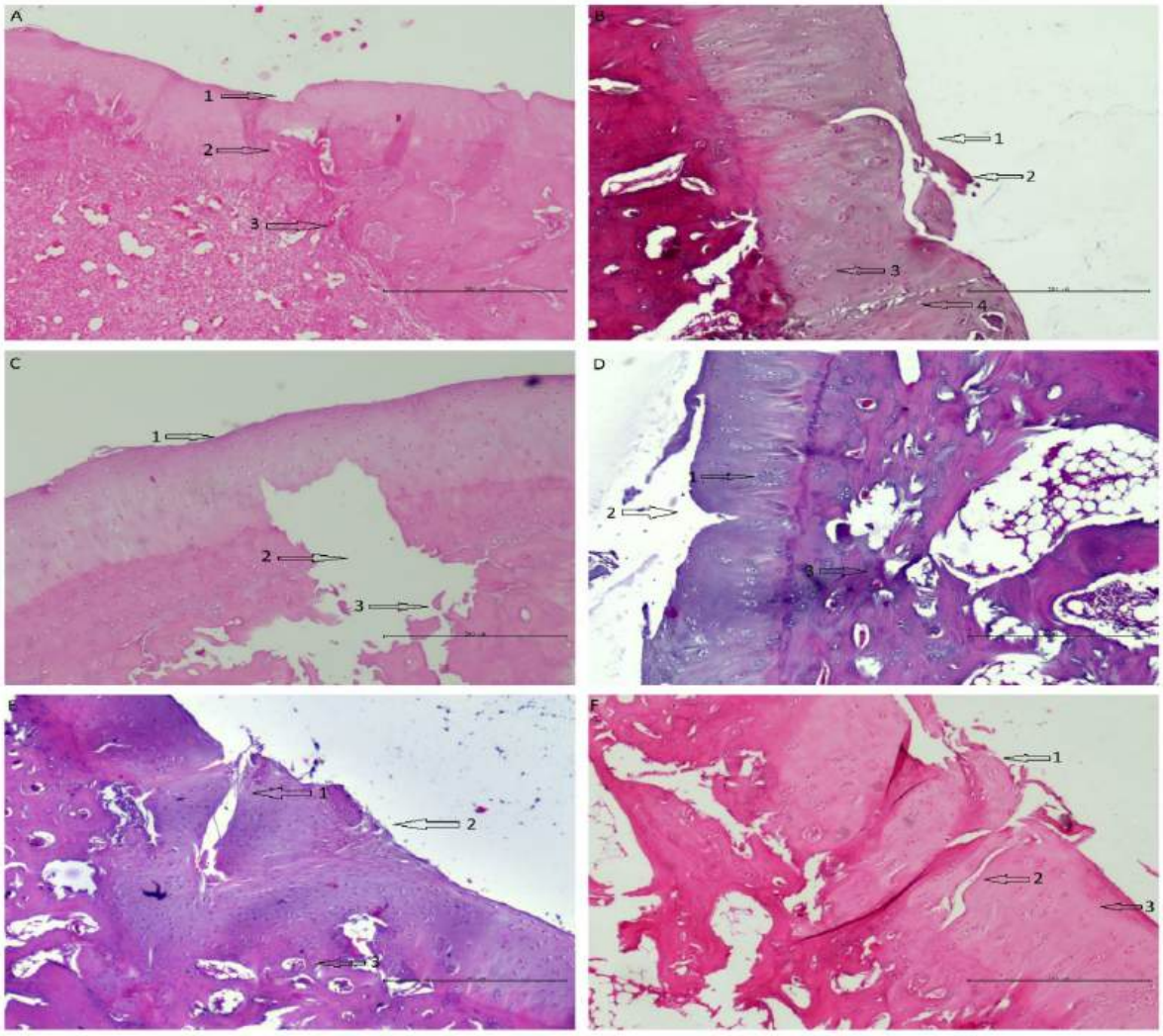

Figure 9. *Cont.*

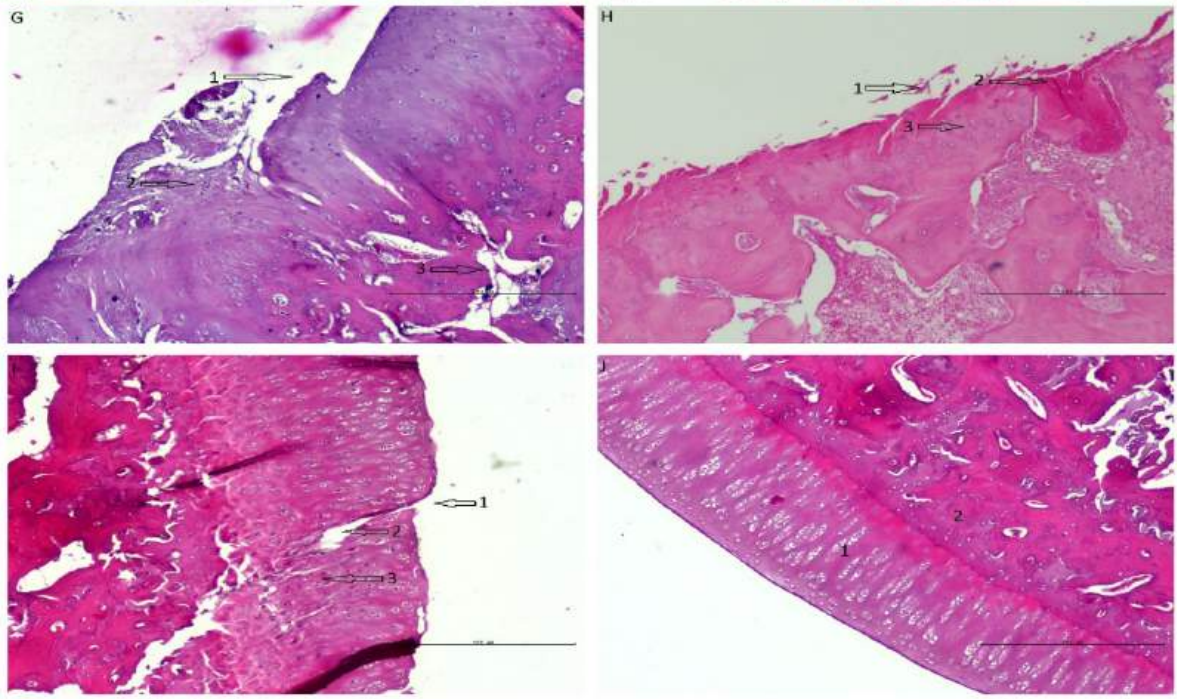

Figure 9. Shows histological samples of the cartilage of the rabbit of the studied groups. The following observations were made by one histologist. (**A**) PVP group after 8 weeks of observation—the defect is easily visible; (1) the surface has irregularities, (2) cells are disorganized, (3) increased remodeling of subchondral bone. (**B**) Z group after 8 weeks of observation—the defect is easily visible; (1) the surface has irregularities, (2) cartilage necrosis, (3) cells are distributed in clusters (4) chondral fracture reaching the subchondral bone. (**C**) Control group after 8 weeks of observation—the defect is easily visible; (1) the surface has irregularities, (2) massive loss of subchondral bone, (3) Bone fractures with the separation of necrotic fragments. (**D**) PVP group after 16 weeks of observation; (1) cells are distributed in clusters, (2) cartilage fracture, the surface has irregularities; (3) porous subchondral bone in some places, otherwise normal. (**E**) Z group after 16 weeks of observation—the defect is easily visible; (1) cells are distributed irregularly, (2) the surface is torn, (3) porous subchondral bone in some places, otherwise normal. (**F**) control group after 16 weeks of observation—the defect is easily visible; (1) the surface is torn, (2) chondral fractures reaching the subchondral bone, (3) cells are distributed irregularly. (**G**) PVP group after 24 weeks of observation; (1) the surface is torn/has irregularities, (2) cartilage fractures, cells are distributed irregularly, (3) increased remodeling of subchondral bone. (**H**) Z group after 24 weeks of observation; (1) the surface is torn, (2) necrosis, (3) cells are distributed in columns. (**I**) Control group after 24 weeks of observation; (1) the surface has irregularities; (2) full thickness chondral fracture; (3) cells are distributed irregularly. (**J**) Histological image of correct hyaline cartilage in rabbit model—(1) cartilage, (2) subchondral bone.

4. Discussion

In our work, we examined scaffolds that have potential use for cartilage tissue engineering. Our scaffolds are characterized by biocompatibility, degradability, and adequate structure. They have perforated top layers with pore diameters of more than 20 µm that allow MSCs to penetrate inside the membrane. The interiors of both membranes (Figures 1 and 2) shows a network of interconnected macropores with an appropriate pore diameter larger than 300 µm, necessary for the chondrogenesis of MSCs [16,66–68]. Their structures provide an appropriate environment for the proliferation, migration, and adhesion of cells. The semipermeable structure assures nutritious, oxygen transport, and metabolic products. Furthermore, the bottom skin layers of the scaffolds are dense, preventing cells from getting out from scaffolds [28].

During the implantation phase, we noticed that membrane "Z" was more fragile and disintegrated easier compared to membrane "PVP". Because of this, it was easier to place

and hold the "PVP" scaffold at the chosen localization (defect). This feature can be of great importance during implantation, not with glue but with threads, e.g., in the human knee.

We created (according to the International Cartilage Repair Society (ICRS) recommended guidelines for histological endpoints for cartilage repair studies in animal models and clinical trials) relatively large (0.1 cm^2) and deep (3 mm) defects (Figure 3), which, especially after the first observation period (8 weeks), could have resulted in the lack of statistical significance of the cartilage regeneration assessments between groups. However, the extended observation time showed that the scores of regenerates without the use of a membrane were worse with each subsequent observation period and the scores of regenerates with membranes improved over time (Figures 7 and 8). We believe that this is because the cartilage in the control group is mechanically weak, despite the fact that, in the histological picture, it was initially similar to the other groups. After some time, it degenerated and had a worse end result. We suspect the reason for that could be the stem cells in the control group having settled only superficially around the defect. Due to all of the above, we believe that the observation times in the rabbit model should be extended to at least 24 or even 36 weeks.

For rabbit welfare reasons, only one knee joint was operated on under each anesthesia. This was followed by a scheduled observation period for the group, during which the animal regained full strength. Only after the observation period was the other knee operated on. Therefore, different membranes were loaded differently during the various observation periods. The movements of the rabbits were not the same after surgery on one limb and again were different after surgery on both limbs. There were also individual characteristics in pain perception and soft tissue recovery and body weight that affected joint loading.

We suspect that PLCA copolymer degrades in the body mostly through the hydrolytic degradation [69]. The resulting lactic and caproic acids, which are naturally occurring products in the body, are subsequently metabolized into CO_2 and H_2O and eliminated from the healthy body. After implantation, the hydrolysis and degradation of polymer starts. In this study, the two stages of degradation were seen after 8 and 16 weeks. In both periods, residual PLCA materials were characterized by means of GPC in order to estimate average values of their molar masses. There was a decrease of mean M_w of both membranes during time (Figure 6).

Different populations of molecules arose in given samples (Figure 5). We do not know why this happened. We assume this was due to limitations of in vivo testing. The decomposition of a polymer molecule begins at its edge and continues deeper into it. What is more, polymers break down from smallest molecules (dispersion). The number of edges may be influenced by the implantation technique (too tight or loose filling of the defect in different individuals). Additionally, the presence of different amount of tissue glue, which initially isolates the membrane from the intra-articular environment, may have an influence. Each rabbit had a different enzymatic activity, each moved differently after the operation of membrane implantation, and each stressed the limb differently. There was also different body weights of animals and individual regenerative properties. Hence, there may have been some irregularities in the breakup. The small percentages of molecules with higher molecular weights than the original were likely contaminants that could not be removed during the preparation of the chromatography samples. Despite so many different variables that were difficult to isolate and study separately, a statistical regularity could be observed with exponential progress in degradation (Figure 6) [70].

One of the PVP 8 samples differed from the others because it only contained two major populations of molecules and a small mass. During the observation of this individual, we did not notice any of its properties that could affect such a result. We believe that he was either individually overactive in enzymes or that we made a laboratory error in preparing the sample (Table 1).

The GPC test carried out each time detected the residual membrane, which shows that, in none of the tested cases, the membrane migrated out of the defect and, thus, the implantation technique was appropriate (Table 1).

In our study, histopathological evaluations varied among histologists (Figures 7 and 8). It follows that the histopathological assessment may not be reproducible. It should be considered whether the ICRS scale requires modifications or corrections. We plan to subject the histopathological samples to further histopathological examinations using other scales. The question remains open as to whether, instead of histopathological tests, a better indicator of cartilage regeneration would be to test the level of glycosaminoglycans or collagen II concentration. Moreover, magnetic resonance imaging (MRI) should be considered when assessing articular cartilage. MRI is relatively non-invasive and can be performed at multiple time points in the same animal, thus enabling long-term follow-up assessments. MRI can show tissue overgrowth and bone edema, which are common complications of cell therapy procedures. Current imaging techniques may indirectly suggest hyaline cartilage formation, but these images are not always directly related to the histological findings [71,72].

The animal model is different from the clinical situation in humans. Humans are treated sometime after the defect develops, whereas, in our study, healthy animal joints were treated immediately after the defect developed. Cartilage regeneration was also affected by the fact that the animals fully loaded the limb immediately after surgery, which is the opposite of how humans recover. Hence, the evaluation of regeneration in humans in the future may be different.

Our work was carried out in accordance with the 3 R-rule (reduction, replacement, refinement). For this reason, we created two defects in one knee joint—one in the medial condyle and one in the lateral condyle, symmetrically (Figure 3). In groups I and II, in each joint, the regenerated defect from the lateral condyle was subjected to a microanalytical examination, the regenerated defect from the medial condyle was subjected to a histopathological examination (Figure 4). In the control group, both defects in each joint were subjected to histopathological examination. The defects in the control group in the same joints differed in terms of assessment, as did the defects in the two different joints. This means that even though the defects were located in the same joint, the regeneration process was different. For this reason, we treated these regenerates as separate statistically accountable values. We believe that since the process of regeneration of two defects in one joint differs, this process is influenced not only by the individual characteristics, the site of the defect (one defect on one condyle symmetrically), and its size (the same in each joint), but also by means that have not yet been recognized. The mechanics themselves and the way rabbits load the joints probably play a major role.

According to the International Cartilage Repair Society (ICRS) recommended guidelines for histological endpoints for cartilage repair studies in animal models and clinical trials, we were looking for any implanted (foreign) material. During preparation of the samples, we did not find any pieces of membranes; moreover, we found no evident residues of previously implanted material in any of the histopathological samples. Based on such results and the GPC examination (Table 1), we assume that this is because the entire polyester has been degraded into the form of very short polymer chains that will be easily and completely degraded in a short time period into the products that can be resorbed by the body.

5. Conclusions

In this work, two types of membranes were tested to demonstrate their effectiveness in supporting the regeneration of articular cartilage in rabbits. The results of microanalytical and histological examinations showed that both scaffolds can support cartilage regeneration. The biodegradation process of the studied membranes is progressing exponentially, causing the membranes to degrade at the appropriate time. The proposed implantation technique is fully sufficient to properly place the scaffolds in the place chosen by the operator. The

"PVP" membrane is better due to the fact that after 24 weeks of observation there was a statistical trend for higher histological ratings. It is also better because it is easier to implant due to its lower fragility then membrane "Z". We can conclude that the selected membranes seem to support the regeneration of articular cartilage in the rabbit model.

Author Contributions: Conceptualization, M.B., A.P., A.C. and J.C.; methodology, M.B., J.C., A.P., A.C. and W.B.; validation, M.B., A.P., S.K. and A.K.; formal analysis, M.B., S.K. and A.P.; investigation, M.B., A.P. and S.K.; resources, M.B., A.P., S.K., A.C. and M.W.; writing—original draft preparation, M.B.; writing—review and editing, M.B., A.P., A.C., M.W. and J.C.; visualization, M.B. and W.B.; supervision, M.B., J.C., A.P., A.K. and A.C.; project administration, M.B. and J.C.; funding acquisition, M.B. and J.C. All authors have read and agreed to the published version of the manuscript.

Funding: This research was funded by the Centre of Postgraduate Medical Education (CMKP), Marymoncka 99/103, 01-813 Warsaw, Poland. Grant number 501-1-18-23-19. The funding source had no involvement in the study design; in the collection, analysis, or interpretation of data; in the writing of the report; and in the decision to submit the article for publication.

Institutional Review Board Statement: The animal study protocol was approved by the Ethics Committee—Second Local Animal Testing Ethics Committee in Warsaw (approval WAW2/078/2018).

Informed Consent Statement: Not applicable.

Data Availability Statement: Not applicable.

Conflicts of Interest: The authors declare no conflict of interest. The funders had no role in the design of the study; in the collection, analyses, or interpretation of data; in the writing of the manuscript, or in the decision to publish the results.

References

1. Chung, C.; Burdick, J.A. Engineering cartilage tissue. *Adv. Drug Deliv. Rev.* **2008**, *60*, 243–262. [CrossRef] [PubMed]
2. Sophia Fox, A.J.; Bedi, A.; Rodeo, S.A. The basic science of articular cartilage: Structure, composition, and function. *Sports Health* **2009**, *1*, 461–468. [CrossRef] [PubMed]
3. Krishnan, Y.; Grodzinsky, A.J. Cartilage diseases. *Matrix Biol.* **2018**, *71–72*, 51–69. [CrossRef] [PubMed]
4. Chen, D.; Shen, J.; Zhao, W.; Wang, T.; Han, L.; Hamilton, J.L.; Im, H.J. Osteoarthritis: Toward a comprehensive understanding of pathological mechanism. *Bone Res.* **2017**, *5*, 16044. [CrossRef]
5. Nauth, A.; McKee, M.D.; Einhorn, T.A.; Watson, J.T.; Li, R.; Schemitsch, E.H. Managing bone defects. *J. Orthop. Trauma* **2011**, *25*, 462–466. [CrossRef] [PubMed]
6. Yeung, P.; Zhang, W.; Wang, X.N.; Yan, C.H.; Chan, B.P. A human osteoarthritis osteochondral organ culture model for cartilage tissue engineering. *Biomaterials* **2018**, *162*, 1–21. [CrossRef] [PubMed]
7. Merkely, G.; Ackermann, J.; Lattermann, C. Articular Cartilage Defects: Incidence, Diagnosis, and Natural History. *Oper. Tech. Sports Med.* **2018**, *26*, 156–161. [CrossRef]
8. Silverwood, V.; Blagojevic-Bucknall, M.; Jinks, C.; Jordan, J.L.; Protheroe, J.; Jordan, K.P. Current evidence on risk factors for knee osteoarthritis in older adults: A systematic review and meta-analysis. *Osteoarthr. Cartil.* **2015**, *23*, 507–515. [CrossRef]
9. Collins, A.T.; Kulvaranon, M.L.; Cutcliffe, H.C.; Utturkar, G.M.; Smith, W.A.R.; Spritzer, C.E.; Guilak, F.; Defrate, L.E. Obesity alters the in vivo mechanical response and biochemical properties of cartilage as measured by MRI. *Arthritis Res. Ther.* **2018**, *20*, 232. [CrossRef]
10. Walter, S.G.; Ossendorff, R.; Schildberg, F.A. Articular cartilage regeneration and tissue engineering models: A systematic review. *Arch. Orthop. Trauma Surg.* **2019**, *139*, 305–316. [CrossRef]
11. Dewan, A.K.; Gibson, M.A.; Elisseeff, J.H.; Trice, M.E. Evolution of autologous chondrocyte repair and comparison to other cartilage repair techniques. *BioMed Res. Int.* **2014**, *2014*, 272481. [CrossRef] [PubMed]
12. Dzobo, K.; Thomford, N.E.; Senthebane, D.A.; Shipanga, H.; Rowe, A.; Dandara, C.; Pillay, M.; Motaung, K.S.C.M. Advances in regenerative medicine and tissue engineering: Innovation and transformation of medicine. *Stem Cells Int.* **2018**, *2018*, 2495848. [CrossRef] [PubMed]
13. Medvedeva, E.V.; Grebenik, E.A.; Gornostaeva, S.N.; Telpuhov, V.I.; Lychagin, A.V.; Timashev, P.S.; Chagin, A.S. Repair of damaged articular cartilage: Current approaches and future directions. *Int. J. Mol. Sci.* **2018**, *19*, 2366. [CrossRef] [PubMed]
14. Armiento, A.R.; Alini, M.; Stoddart, M.J. Articular fibrocartilage—Why does hyaline cartilage fail to repair? *Adv. Drug Deliv. Rev.* **2019**, *146*, 289–305. [CrossRef] [PubMed]
15. Mirza, U.; Shubeena, S.; Shah, M.S.; Zaffer, B. Microfracture: A technique for repair of chondral defects. *J. Entomol. Zool. Stud.* **2018**, *6*, 1092–1097.
16. Zhao, Z.; Fan, C.; Chen, F.; Sun, Y.; Xia, Y.; Ji, A.; Wang, D. Progress in Articular Cartilage Tissue Engineering: A Review on Therapeutic Cells and Macromolecular Scaffolds. *Macromol. Biosci.* **2019**, *20*, 1900278. [CrossRef]

17. Płończak, M.; Czubak, J. Culture of Human Autologous Chondrocytes on Polysulphonic Membrane—Preliminary Studies. *Biocybern. Biomed. Eng.* **2012**, *32*, 63–67. [CrossRef]
18. Kim, Y.S.; Mikos, A.G. Emerging strategies in reprogramming and enhancing the fate of mesenchymal stem cells for bone and cartilage tissue engineering. *J. Control. Release* **2021**, *330*, 565–574. [CrossRef]
19. Knutsen, G.; Isaksen, V.; Johansen, O.; Engebretsen, L.; Ludvigsen, T.C.; Drogset, J.O.; Grøntvedt, T.; Solheim, E.; Strand, T.; Roberts, S. Autologous Chondrocyte Implantation Compared with Microfracture in the Knee: A Randomized Trial. *J. Bone Jt. Surg.—Ser. A* **2004**, *86*, 455–464. [CrossRef]
20. Mastrolia, I.; Foppiani, E.M.; Murgia, A.; Candini, O.; Samarelli, A.V.; Grisendi, G.; Veronesi, E.; Horwitz, E.M.; Dominici, M. Challenges in Clinical Development of Mesenchymal Stromal/Stem Cells: Concise Review. *Stem Cells Transl. Med.* **2019**, *8*, 1135–1148. [CrossRef]
21. Fahy, N.; Alini, M.; Stoddart, M.J. Mechanical stimulation of mesenchymal stem cells: Implications for cartilage tissue engineering. *J. Orthop. Res.* **2018**, *36*, 52–63. [CrossRef] [PubMed]
22. Grässel, S.; Lorenz, J. Tissue-Engineering Strategies to Repair Chondral and Osteochondral Tissue in Osteoarthritis: Use of Mesenchymal Stem Cells. *Curr. Rheumatol. Rep.* **2014**, *16*, 452. [CrossRef] [PubMed]
23. Liu, Y.; Zhou, G.; Cao, Y. Recent Progress in Cartilage Tissue Engineering—Our Experience and Future Directions. *Engineering* **2017**, *3*, 28–35. [CrossRef]
24. Wasyłeczko, M.; Sikorska, W.; Chwojnowski, A. Review of synthetic and hybrid scaffolds in cartilage tissue engineering. *Membranes* **2020**, *10*, 348. [CrossRef] [PubMed]
25. Wasyłeczko, M.; Sikorska, W.; Przytulska, M.; Dulnik, J.; Chwojnowski, A. Polyester membranes as 3D scaffolds for cell culture. *Desalination Water Treat.* **2021**, *214*, 181–193. [CrossRef]
26. Kalkan, R.; Nwekwo, C.W.; Adali, T. The Use of Scaffolds in Cartilage Regeneration. *Eukaryot. Gene Expr.* **2018**, *28*, 343–348. [CrossRef]
27. Eltom, A.; Zhong, G.; Muhammad, A. Scaffold Techniques and Designs in Tissue Engineering Functions and Purposes: A Review. *Adv. Mater. Sci. Eng.* **2019**, *2019*, 3429527. [CrossRef]
28. Bironait, D. Scaffolds and cells for tissue regeneration: Different scaffold pore sizes—different cell effects. *Cytotechnology* **2015**, *68*, 355–369. [CrossRef]
29. Pina, S.; Ribeiro, V.P.; Marques, C.F.; Maia, F.R.; Silva, T.H.; Reis, R.L.; Oliveira, J.M. Scaffolding Strategies for Tissue Engineering and Regenerative Medicine Applications. *Materials* **2019**, *12*, 1824. [CrossRef]
30. Loh, Q.L.; Choong, C. Three-dimensional scaffolds for tissue engineering applications: Role of porosity and pore size. *Tissue Eng.—Part B Rev.* **2013**, *19*, 485–502. [CrossRef]
31. Pompe, W.; Worch, H.; Epple, M.; Friess, W.; Gelinsky, M.; Greil, P.; Hempel, U.; Scharnweber, D.; Schulte, K. Functionally graded materials for biomedical applications. *Mater. Sci. Eng. A* **2003**, *362*, 40–60. [CrossRef]
32. Smidsrød, O. Molecular basis for some physical properties of alginates in the gel state. *Faraday Discuss. Chem. Soc.* **1974**, *57*, 263. [CrossRef]
33. Bretcanu, O.; Samaille, C.; Boccaccini, A.R. Simple methods to fabricate Bioglass®-derived glass-ceramic scaffolds exhibiting porosity gradient. *J. Mater. Sci.* **2008**, *43*, 4127–4134. [CrossRef]
34. Van Tienen, T.G.; Heijkants, R.G.J.C.; Buma, P.; De Groot, J.H.; Pennings, A.J.; Veth, R.P.H. Tissue ingrowth and degradation of two biodegradable porous polymers with different porosities and pore sizes. *Biomaterials* **2002**, *23*, 1731–1738. [CrossRef]
35. Harley, B.A.; Hastings, A.Z.; Yannas, I.V.; Sannino, A. Fabricating tubular scaffolds with a radial pore size gradient by a spinning technique. *Biomaterials* **2006**, *27*, 866–874. [CrossRef]
36. Okubo, R.; Asawa, Y.; Watanabe, M.; Nagata, S.; Nio, M. Proliferation medium in three-dimensional culture of auricular chondrocytes promotes effective cartilage regeneration in vivo. *Regen. Ther.* **2019**, *11*, 306–315. [CrossRef]
37. Armiento, A.R.; Stoddart, M.J.; Alini, M.; Eglin, D. Biomaterials for articular cartilage tissue engineering: Learning from biology. *Acta Biomater.* **2018**, *65*, 1–20. [CrossRef]
38. Zhao, P.; Gu, H.; Mi, H.; Rao, C.; Fu, J.; Turng, L. sheng Fabrication of scaffolds in tissue engineering: A review. *Front. Mech. Eng.* **2018**, *13*, 107–119. [CrossRef]
39. Koh, Y.G.; Lee, J.A.; Kim, Y.S.; Lee, H.Y.; Kim, H.J.; Kang, K.T. Optimal mechanical properties of a scaffold for cartilage regeneration using finite element analysis. *J. Tissue Eng.* **2019**, *10*, 2041731419832133. [CrossRef]
40. Bistolfi, A.; Ferracini, R.; Galletta, C.; Tosto, F.; Sgarminato, V.; Digo, E.; Vernè, E.; Massè, A. Regeneration of articular cartilage: Scaffold used in orthopedic surgery. A short handbook of available products for regenerative joints surgery. *Clin. Sci. Res. Rep.* **2017**, *1*, 1–7. [CrossRef]
41. Ye, H.; Zhang, K.; Kai, D.; Li, Z.; Loh, X.J. Polyester elastomers for soft tissue engineering. *Chem. Soc. Rev.* **2018**, *47*, 4545–4580. [CrossRef] [PubMed]
42. Urbánek, T.; Jäger, E.; Jäger, A.; Hrubý, M. Selectively biodegradable polyesters: Nature-inspired construction materials for future biomedical applications. *Polymers* **2019**, *11*, 1061. [CrossRef]
43. Jiang, L.; Xu, L.; Ma, B.; Ding, H.; Tang, C. Effect of component and surface structure on poly (L -lactide-co- ε—caprolactone) (PLCA) -based composite membrane. *Compos. Part B* **2019**, *174*, 107031. [CrossRef]
44. Nikolova, M.P.; Chavali, M.S. Recent advances in biomaterials for 3D scaffolds: A review. *Bioact. Mater.* **2019**, *4*, 271–292. [CrossRef] [PubMed]

45. Janmohammadi, M.; Nourbakhsh, M.S. International Journal of Polymeric Materials and Electrospun polycaprolactone scaffolds for tissue engineering: A review. *Int. J. Polym. Mater. Polym. Biomater.* **2018**, *68*, 527–539. [CrossRef]
46. Laurent, P. Suitability of a PLCL fibrous scaffold for soft tissue engineering applications: A combined biological and mechanical characterisation. *J. Biomater. Appl.* **2018**, *32*, 1276–1288. [CrossRef] [PubMed]
47. Silva, D.; Kaduri, M.; Poley, M.; Adir, O.; Krinsky, N.; Shainsky-roitman, J.; Schroeder, A. Mini Review Biocompatibility, biodegradation and excretion of polylactic acid (PLA) in medical implants and theranostic systems. *Chem. Eng. J.* **2018**, *340*, 9–14. [CrossRef]
48. Garkhal, K.; Verma, S.; Jonnalagadda, S.; Kumar, N. Fast degradable poly(L-lactide-co-ε-caprolactone) microspheres for tissue engineering: Synthesis, characterization, and degradation behavior. *J. Polym. Sci. Part A Polym. Chem.* **2007**, *45*, 2755–2764. [CrossRef]
49. Herrera-Kao, W.A.; Loría-Bastarrachea, M.I.; Pérez-Padilla, Y.; Cauich-Rodríguez, J.V.; Vázquez-Torres, H.; Cervantes-Uc, J.M. Thermal degradation of poly(caprolactone), poly(lactic acid), and poly(hydroxybutyrate) studied by TGA/FTIR and other analytical techniques. *Polym. Bull.* **2018**, *75*, 4191–4205. [CrossRef]
50. Tomihata, K.; Suzuki, M.; Tomita, N. Handling characteristics of poly(L-lactide-co-ε-caprolactone) monofilament suture. *Bio-Med. Mater. Eng.* **2005**, *15*, 381–391.
51. Jung, Y.; Park, M.S.; Lee, J.W.; Kim, Y.H.; Kim, S.H.; Kim, S.H. Cartilage regeneration with highly-elastic three-dimensional scaffolds prepared from biodegradable poly(l-lactide-co-ε-caprolactone). *Biomaterials* **2008**, *29*, 4630–4636. [CrossRef] [PubMed]
52. Morokov, E.S.; Demina, V.A.; Sedush, N.G.; Kalinin, K.T.; Khramtsova, E.A.; Dmitryakov, P.V.; Bakirov, A.V.; Grigoriev, T.E.; Levin, V.M.; Chvalun, S.N. Noninvasive high-frequency acoustic microscopy for 3D visualization of microstructure and estimation of elastic properties during hydrolytic degradation of lactide and ε-caprolactone polymers. *Acta Biomater.* **2020**, *109*, 61–72. [CrossRef] [PubMed]
53. Sikorska, W.; Wasyłeczko, M.; Przytulska, M.; Wojciechowski, C.; Rokicki, G.; Chwojnowski, A. Chemical degradation of PSF-PUR blend hollow fiber membranes-assessment of changes in properties and morphology after hydrolysis. *Membranes* **2021**, *11*, 51. [CrossRef] [PubMed]
54. Chwojnowski, A.; Kruk, A.; Wojciechowski, C. The dependence of the membrane structure on the non-woven forming the macropores in the 3D scaffolds preparation. *Desalination Water Treat.* **2017**, *64*, 11394. [CrossRef]
55. Dutta, R.C.; Dey, M.; Dutta, A.K.; Basu, B. Competent processing techniques for scaffolds in tissue engineering. *Biotechnol. Adv.* **2017**, *35*, 240–250. [CrossRef]
56. Prasad, A.; Sankar, M.R.; Katiyar, V. State of Art on Solvent Casting Particulate Leaching Method for Orthopedic ScaffoldsFabrication. *Mater. Today Proc.* **2017**, *4*, 898–907. [CrossRef]
57. Plisko, T.V.; Penkova, A.V.; Burts, K.S.; Bildyukevich, A.V.; Dmitrenko, M.E.; Melnikova, G.B.; Atta, R.R.; Mazur, A.S.; Zolotarev, A.A.; Missyul, A.B. Effect of Pluronic F127 on porous and dense membrane structure formation via non-solvent induced and evaporation induced phase separation. *J. Membr. Sci.* **2019**, *580*, 336–349. [CrossRef]
58. Caplan, N.; Kader, D.F. *The Etiology of Chondromalacia Patellae*; Classic Papers in Orthopaedics; Springer: London, UK, 2014; pp. 185–187. [CrossRef]
59. Hurtig, M.B.; Buschmann, M.D.; Fortier, L.A.; Hoemann, C.D.; Hunziker, E.B.; Jurvelin, J.S.; Mainil-Varlet, P.; McIlwraith, C.W.; Sah, R.L.; Whiteside, R.A. Preclinical studies for cartilage repair: Recommendations from the international cartilage repair society. *Cartilage* **2011**, *2*, 137–152. [CrossRef]
60. Rutgers, M.; van Pelt, M.J.P.; Dhert, W.J.A.; Creemers, L.B.; Saris, D.B.F. Evaluation of histological scoring systems for tissue-engineered, repaired and osteoarthritic cartilage. *Osteoarthr. Cartil.* **2010**, *18*, 12–23. [CrossRef]
61. Oksanen, A.J.; Blanchet, F.G.; Friendly, M.; Kindt, R.; Legendre, P.; Mcglinn, D.; Minchin, P.R.; Hara, R.B.O.; Simpson, G.L.; Solymos, P.; et al. Vegan. In *Encyclopedia of Food and Agricultural Ethics*; Springer: Dordrecht, Germany, 2019; pp. 2395–2396. [CrossRef]
62. Hothorn, T.; Van De Wiel, M.A.; Hornik, K.; Zeileis, A. Implementing a class of permutation tests: The coin package. *J. Stat. Softw.* **2008**, *28*, 1–23. [CrossRef]
63. Ogle, D.H.; Doll, J.C.; Wheeler, P.; Dinno, A. FSA: Fisheries Stock Analysis. R Package Version 0.9.1. Available online: https://github.com/fishR-Core-Team/FSA (accessed on 1 July 2021).
64. Kemp, A.W.; Manly, B.F.J. Randomization, Bootstrap and Monte Carlo Methods in Biology. *Biometrics* **1997**, *53*, 1560. [CrossRef]
65. Legendre, P. Species associations: The Kendall coefficient of concordance revisited. *J. Agric. Biol. Environ. Stat.* **2005**, *10*, 226–245. [CrossRef]
66. Panadero, J.A.; Lanceros-Mendez, S.; Ribelles, J.L.G. Differentiation of mesenchymal stem cells for cartilage tissue engineering: Individual and synergetic effects of three-dimensional environment and mechanical loading. *Acta Biomater.* **2016**, *33*, 1–12. [CrossRef] [PubMed]
67. Zhao, Y.; Tan, K.; Zhou, Y.; Ye, Z.; Tan, W.S. A combinatorial variation in surface chemistry and pore size of three-dimensional porous poly(ε-caprolactone) scaffolds modulates the behaviors of mesenchymal stem cells. *Mater. Sci. Eng. C* **2016**, *59*, 193–202. [CrossRef]
68. Matsiko, A.; Gleeson, J.P.; O'Brien, F.J. Scaffold mean pore size influences mesenchymal stem cell chondrogenic differentiation and matrix deposition. *Tissue Eng.—Part A* **2015**, *21*, 486–497. [CrossRef]

69. Jeong, S.I.; Kim, B.; Lee, Y.M.; Ihn, K.J.; Kim, S.H. Morphology of Elastic Poly (L -lactide-co- E -caprolactone) Copolymers and in Vitro and in Vivo Degradation Behavior of Their Scaffolds. *Biomacromolecules* **2004**, *5*, 1303–1309. [CrossRef]
70. In, S.; Kim, B.; Woong, S.; Hyun, J.; Moo, Y.; Hyun, S.; Ha, Y. In vivo biocompatibilty and degradation behavior of elastic poly (l -lactide- co—e -caprolactone) scaffolds. *Biomaterials* **2004**, *25*, 5939–5946. [CrossRef]
71. Ota, Y.; Kamei, N.; Tamaura, T.; Adachi, N.; Ochi, M. Magnetic resonance imaging evaluation of cartilage repair and iron particle kinetics after magnetic delivery of stem cells. *Tissue Eng.—Part C Methods* **2018**, *24*, 679–687. [CrossRef]
72. Koller, U.; Apprich, S.; Schmitt, B.; Windhager, R.; Trattnig, S. Evaluating the cartilage adjacent to the site of repair surgery with glycosaminoglycan-specific magnetic resonance imaging. *Int. Orthop.* **2017**, *41*, 969–974. [CrossRef]

DODATEK I

DEKLARACJE O WSPÓŁAUTORSTWIE PRAC ORGINALNYCH

Prof. dr hab. inż. Andrzej Chwojnowski

Pracownia Elektrostatycznych Metod Bioenkapsulacji

Instytut Biocybernetyki i Inżynierii Biomedycznej im. Macieja Nałęcza

Polskiej Akademii Nauk

Jako osoba nadzorująca prace wykonane w niniejszej rozprawie doktorskiej i kierownik pracowni, w którym doktorat był wykonywany niniejszym deklaruję wkład poszczególnych autorów w następujących publikacjach na podstawie oświadczenia autorstwa CRediT.

1) Monika Wasyłeczko, Wioleta Sikorska and Andrzej Chwojnowski – Review of Synthetic and Hybrid Scaffolds in Cartilage Tissue Engineering, Membranes **2020**, 10(11), 348.

Monika Wasyłeczko: autor korespondencyjny, koncepcja, tekst – wersja oryginalna, pisanie - recenzja i redakcja; **Wioleta Sikorska:** pisanie - recenzja i redakcja; **Andrzej Chwojnowski:** nadzór, pisanie - recenzja i redakcja.

2) Monika Wasyłeczko, Wioleta Sikorska, Małgorzata Przytulska, Judyta Dulnik, Andrzej Chwojnowski - Polyester membranes as 3D scaffolds for cell culture, Desalination and Water Treatment **2021**, 214, 181-193.

Monika Wasyłeczko: autor korespondencyjny, koncepcja, metodologia, tekst – wersja oryginalna, pisanie - recenzja i redakcja, analiza formalna, wizualizacja, walidacja, analiza formalna, badania; **Wioleta Sikorska:** pisanie - recenzja i redakcja; **Małgorzata Przytulska:** oprogramowanie; **Judyta Dulnik:** zasoby; **Andrzej Chwojnowski:** nadzór, koncepcja, metodologia, pozyskanie finansowania

3) Monika Wasyłeczko, Elżbieta Remiszewska, Wioleta Sikorska, Judyta Dulnik, Andrzej Chwojnowski – Scaffolds for Cartilage Tissue Engineering from a Blend of Polyethersulfone and Polyurethane Polymers, Molecules **2023**, 28, 1-25.

Monika Wasyłeczko: autor korespondencyjny, koncepcja, metodologia, tekst – wersja oryginalna, pisanie - recenzja i redakcja, analiza formalna, wizualizacja; **Elżbieta Remiszewska:** analiza formalna; **Wioleta Sikorska:** zasoby, pisanie - recenzja i redakcja; **Judyta Dulnik:** zasoby; **Andrzej Chwojnowski:** nadzór, analiza formalna, pozyskanie finansowania.

4) Monika Wasyłeczko, Zuzanna Joanna Krysiak, Ewa Łukowska, Marcin Gruba, Wioleta Sikorska, Aleksandra Kruk, Judyta Dulnik, Jarosław Czubak, Andrzej Chwojnowski – Three-dimensional scaffolds for bioengineering of cartilage Tissues, Biocybernetics and Biomedical Engineering **2022**, 42, 494– 511

Monika Wasyłeczko: autor korespondencyjny, koncepcja, selekcja danych, metodologia, pisanie - recenzja i redakcja, walidacja; **Zuzanna Joanna Krysiak:** selekcja danych, metodologia, pisanie - recenzja i redakcja; **Ewa Łukowska:** selekcja danych, metodologia, pisanie - recenzja i redakcja; **Marcin Gruba:** zasoby; **Wioleta Sikorska:** pisanie - recenzja i redakcja; **Aleksandra Kruk:** zasoby; **Judyta Dulnik:** zasoby; **Jarosław Czubak:** zasoby; **Andrzej Chwojnowski:** nadzór, koncepcja, pozyskanie finansowania.

5) Maciej Płończak, Monika Wasyłeczko, Tomasz Jakutowicz, Andrzej Chwojnowski, Jarosław Czubak – Intraarticular Implantation of Autologous Chondrocytes Placed on Collagen or Polyethersulfone Scaffolds: An Experimental Study in Rabbits, Polymers **2023**, 15, 2360.

Maciej Płończak: autor korespondencyjny, koncepcja, metodologia, walidacja, analiza formalna, badania, zasoby, selekcja danych, tekst – wersja oryginalna; **Monika Wasyłeczko:** zasoby, tekst – wersja oryginalna, pisanie - recenzja i redakcja; **Tomasz Jakutowicz:** metodologia, pisanie - recenzja i redakcja; **Andrzej Chwojnowski:** nadzór, koncepcja, metodologia, zasoby; **Jarosław Czubak:** nadzór, koncepcja.

6) Maciej Baranowski, Monika Wasyłeczko, Anna Kosowska, Andrzej Plichta, Sebastian Kowalczyk, Andrzej Chwojnowski, Wojciech Bielecki, Jarosław Czubak - Regeneration of Articular Cartilage Using Membranes of Polyester Scaffolds in a Rabbit Model, Pharmaceutics **2022**, 14, 1016

Maciej Baranowski: autor korespondencyjny, koncepcja, metodologia, walidacja, analiza formalna, badania, zasoby, tekst – wersja oryginalna, wizualizacja, nadzór, administracja projektem; **Monika Wasyłeczko:** zasoby, tekst – wersja oryginalna, pisanie - recenzja i redakcja; **Anna Kosowska:** walidacja, nadzór; **Andrzej Plichta:** koncepcja, walidacja metodologia, analiza formalna, badania, zasoby, pisanie - recenzja i redakcja, nadzór; **Sebastian Kowalczyk:** walidacja, analiza formalna, badania, zasoby; **Andrzej Chwojnowski:** koncepcja, metodologia, zasoby, pisanie - recenzja i redakcja, nadzór; **Wojciech Bielecki:** metodologia, wizualizacja; **Jarosław Czubak:** nadzór, koncepcja, metodologia, pisanie - recenzja i redakcja, administracja projektem.

Podpis

Dr n. med. Maciej Płończak

Niniejszym deklaruję swój wkład w następującej publikacji na podstawie oświadczenia autorstwa CRediT.

5) Maciej Płończak, Monika Wasyłeczko, Tomasz Jakutowicz, Andrzej Chwojnowski, Jarosław Czubak – Intraarticular Implantation of Autologous Chondrocytes Placed on Collagen or Polyethersulfone Scaffolds: An Experimental Study in Rabbits, Polymers **2023**, 15, 2360.

Maciej Płończak: autor korespondencyjny, koncepcja, metodologia, walidacja, analiza formalna, badania,zasoby, selekcja danych, tekst – wersja oryginalna

Podpis

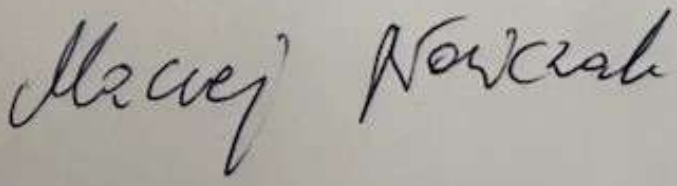

Dr n. med. Maciej Baranowski

Niniejszym deklaruję swój wkład w następującej publikacji na podstawie oświadczenia autorstwa CRediT.

5) Maciej Baranowski, **Monika Wasyłeczko**, Anna Kosowska, Andrzej Plichta, Sebastian Kowalczyk, Andrzej Chwojnowski, Wojciech Bielecki, Jarosław Czubak - Regeneration of Articular Cartilage Using Membranes of Polyester Scaffolds in a Rabbit Model, Pharmaceutics **2022**, 14, 1016

Maciej Baranowski: autor korespondencyjny, nadzór, koncepcja, metodologia, pisanie - recenzja i redakcja, administracja projektem.

Maciej Baranowski

Podpis

Prof. dr hab. n. med. Jarosław Czubak

Niniejszym deklaruję swój wkład w następujących publikacjach na podstawie oświadczenia autorstwa CRediT.

5) Maciej Płończak, **Monika Wasyłeczko**, Tomasz Jakutowicz, Andrzej Chwojnowski, Jarosław Czubak – Intraarticular Implantation of Autologous Chondrocytes Placed on Collagen or Polyethersulfone Scaffolds: An Experimental Study in Rabbits, Polymers **2023**, 15, 2360

Jarosław Czubak: nadzór, koncepcja.

6) Maciej Baranowski, **Monika Wasyłeczko**, Anna Kosowska, Andrzej Plichta, Sebastian Kowalczyk, Andrzej Chwojnowski, Wojciech Bielecki, Jarosław Czubak - Regeneration of Articular Cartilage Using Membranes of Polyester Scaffolds in a Rabbit Model, Pharmaceutics **2022**, 14, 1016

Jarosław Czubak: nadzór, koncepcja, metodologia, pisanie - recenzja i redakcja, administracja projektem.

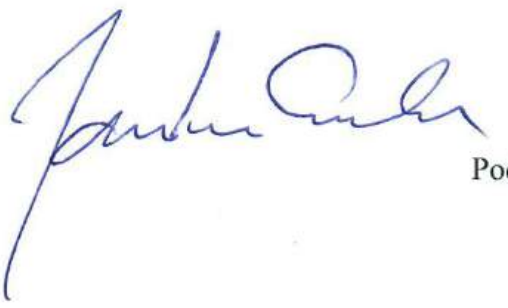

Podpis

DODATEK II

INNE BADANIA NIE UWZGLĘDNIONE W PRACY DYPLOMOWEJ

Artykuły

1) Tomasz Jakutowicz, **Monika Wasyłeczko**, Maciej Płończak, Cezary Wojciechowski, Andrzej Chwojnowski, Jarosław Czubak – Comparative Study of Autogenic and Allogenic Chondrocyte Transplants on Polyethersulfone Scaffolds for Cartilage Regeneration,
International Journal of Molecular Science, 2024, 25, 9075.

IF: 4,9
MNiSW: 140
Publication date: 21 August 2024
DOI: https://doi.org/10.3390/ijms25169075

2) Cezary Wojciechowski, **Monika Wasyłeczko**, Dorota Lewińska, Andrzej Chwojnowski – A Comprehensive Review of Hollow-Fiber Membrane Fabrication Methods across Biomedical, Biotechnological, and Environmental Domains, Molecules, 2024, 29, 2637.
IF: 4,6
MNiSW:140
Publication date: 3 June 2024
DOI: https://doi.org/10.3390/molecules29112637

3) **Monika Wasyłeczko**,Cezary Wojciechowski, Andrzej Chwojnowski – Polyethersulfone Polymer for Biomedical Applications and Biotechnology, International Journal of Molecular Science, 2024, 25, 4233.

IF: 5,6,
MNiSW:140
Publication date: 11 April 2024
DOI: https://doi.org/10.3390/ijms25084233

4) Adam Mirek, Marcin Grzeczkowicz, Habib Belaid, Aleksandra Bartkowiak, Fanny Barranger, Mahmoud Abid, **Monika Wasyłeczko**, Maksym Pogorielov, Mikhael Bechelany, Dorota Lewińska - Electrospun UV-cross-linked polyvinylpyrrolidone fibers modified with polycaprolactone/polyethersulfone microspheres for drug delivery - Biomaterials Advances, 2023, 147l, 213330,

IF= 8,457
MNiSW= 140
Publication date: 9 February 2023
DOI: https://doi.org/10.1016/j.bioadv.2023.213330

5) Wioleta Sikorska, Małgorzata Milner-Krawczyk, **Monika Wasyłeczko**, Cezary Wojciechowski, Andrzej Chwojnowski - Biodegradation Process of PSF-PUR Blend Hollow Fiber Membranes Using *Escherichia coli* Bacteria Evaluation of Changes in Properties and Porosity - *Polymers* 2021, 13, 1311.

IF: 4,967
MNiSW= 100
Publication date: 16 April 2021
DOI: https://doi.org/10.3390/polym13081311

6) Wioleta Sikorska, **Monika Wasyłeczko**, Małgorzata Przytulska, Cezary Wojciechowski, Gabriel Rokicki, Andrzej Chwojnowski - Chemical Degradation of PSF-PUR Blend Hollow Fiber Membranes—Assessment of Changes in Properties and Morphology after Hydrolysis – Membranes 2021, 11, 51.

IF: 4,562

MNiSW= 100

Publication Date:12 January 2021

DOI: https://doi.org/10.3390/membranes11010051

7) Wioleta Sikorska, Małgorzata Przytulska, **Monika Wasyłeczko**, Cezary Wojciechowski, Juliusz L. Kulikowski, Andrzej Chwojnowski -Influence of hydrolysis, solvent and PVP addition on the porosity of PSF/PUR blend partly degradable hollow fiber membranes evaluated using the MeMoExplorer software – Desalination and Water Treatment 2021, 214, 114-119

IF:1.383

MNiSW= 100

Publication Date: May 28, 2020

DOI: https://doi.org/10.5004/dwt.2021.26652

8) Andrzej Chwojnowski, Cezary Wojciechowski, **Monika Wasyłeczko**, Ewa Łukowska, Tomasz Kobiela, Piotr Dobrzyński, Małgorzata Pastusiak, Anna Smola-Dmochowska - Polyethersulfone-co-polyesters blend ultrafiltration membranes for biomedical and biotechnological applications. Preliminary study - Desalination and Water Treatment 2021, 214,86-94

IF: 1,383

MNiSW= 100
Publication Date:25 May 2020
DOI: https://doi.org/10.5004/dwt.2021.26649

9) Wioleta Sikorska, Cezary Wojciechowski, Małgorzata Przytulska, Gabriel Rokicki, **Monika Wasyłeczko**, Juliusz L. Kulikowski, Andrzej Chwojnowski, „Polysulfone–polyurethane (PSf-PUR) blend partly degradable hollow fiber membranes: preparation, characterization, and computer image analysis", *Desalination and Water Treatment*,

IF=1.383
MNiSW= 100
Publication Date: August 27, 2018
DOI: 10.5004/dwt.2018.23101

10) Małgorzata Przytulska, Juliusz Lech Kulikowski, **Monika Wasyłeczko**, Andrzej Chwojnowski, Dariusz Piętka, "The evaluation of 3D morphological structure of porous membranes based on computer-aided analysis of their 2D images", Desalination and Water Treatment 2018, 128, 11-19

IF=1.383
MNiSW= 100
Publication Date: March 26, 2018
DOI: 10.5004/dwt.2018.22569

11) Andrzej Plichta, Sebastian Kowalczyk, Krzysztof Kamiński, **Monika Wasyłeczko**, Stanisław Więckowski, Ewa Olędzka, Grzegorz Nałęcz-Jawecki, Anna Zgadzaj, and Marcin Sobczak, ATRP of Methacrylic Derivative of Camptothecin Initiated with PLA toward Three-Arm Star Block Copolymer Conjugates with Favorable Drug Release, Macromolecules 2017, 50, 6439-6450

IF=5.914
MNiSW= 140
Publication Date (Web): August 31, 2017
DOI: 10.1021/acs.macromol.7b01350

Patenty

1. Współautor patentu: A. Chwojnowski, E, Łukowska, C. Wojciechowski, **M. Wasyłeczko**, W. Sikorska, Z. Krysiak, **PL 238140– 2021-07-12**- Sposób wyodrębniania białka z hodowli komórkowych prowadzonych na rusztowaniach komórkowych (A method of isolating protein from cell cultures carried out on cell scaffolds), udział: 0,20
2. Współautor patentu: A. Chwojnowski, E. Łukowska, C. Wojciechowski, **M. Wasyłeczko**, W. Sikorska, Z. Krysiak, **PL 235794– 2020-10-19** -Sposób wykrywania pozostałości celulozy w półprzepuszczalnych membranach szeroko porowatych (A method for detecting cellulose residues in semipermeable, broad porous membranes), udział: 0,20

3. Współautor patentu: Ewa Łukowska, Anna Szakiel, Michał Markowski, **Monika Wasyłeczko**, Andrzej Chwojnowski, Sylwia Martyniuk, **PL 239461 – 2019-04-2029** Wielowarstwowa membrana poliestrowa i sposób jej wytwarzania (Multilayer polyester membrane and the method of its manufacture), udział: 0,10
4. Współautor patentu: A. Plichta, **M. Wasyłeczko**, T. Jaskulski, **PL 414240 (A1) – 2017-04-10** - Reactive ester derivatives of (S)-(+)-camptothecin and method for producing reactive ester derivatives of (S)-(+)-camptothecin [Reaktywne estrowe pochodne (S)-(+)-kamptotecyny i sposób wytwarzania reaktywnych estrowych pochodnych (S)-(+)-kamptotecyny], udział: 0,333

Konferencje

1. Wrzesień 2019, autor posteru: **M. Wasyłeczko**, E. Łukowska, Z. Krysiak, W. Sikorska, A, Chwojnowski „Biocompatible 3D membrane for cell culture", XV Konferencja Naukowa "Membrany i Procesy Membranowe w Ochronie Środowiska" MEMPEP 2019, Wrocław
2. Wrzesień 2018, współautor posteru pt. Sebastian Kowalczyk, **Monika Wasyłeczko**, Wioleta Sikorska, Andrzej Plichta „Badania nad koniugacją kampototecyny na nośnikach polilaktydowych", 61. Zjazd Naukowy Polskiego Towarzystwa Chemicznego w Krakowie.
3. Wrzesień 2018, współautor wygłoszonego seminarium: Andrzej Plichta, Sebastian Kowalczyk, Krzysztof Kamiński, **Monika Wasyłeczko**, Wioteta Sikorska, Marcin Sobczak, Ewa Olędzka „Badania nad koniugacją i uwalnianiem kamptotecyny z nośników kopolimerowych", 61. Zjazd Naukowy Polskiego Towarzystwa Chemicznego w Krakowie;
4. Czerwiec 2018, współautor wygłoszonego seminarium: MAŁGORZATA PRZYTULSKA, JULIUSZ KULIKOWSKI, **MONIKA WASYŁECZKO**, ANDRZEJ CHWOJNOWSKI, DARIUSZ PIĘTKA "Evaluation of 3D morphological structure of porous membranes based on computer-aided analysis of their 2D images", XII Konferencja Naukowa "Membrany i Procesy Membranowe w Ochronie Środowiska" MEMPEP 2018 w Zakopanym
5. Czerwiec 2018,współautor posteru: W. Sikorska, C. Wojciechowski, M. Przytulska, G. Rokicki, **M. Wasyłeczko**, J.L. Kulikowski, A. Chwojnowski „Polysulfone-polyurethane (PSf-PUR) blend partly degradable hollow fiber membranes: preparation, characterization and computer image analysis"**,** XII Konferencja Naukowa "Membrany i Procesy Membranowe w Ochronie Środowiska" MEMPEP 2018 w Zakopanym
6. Październik 2017, współautor wygłoszonego seminarium: A. Chwojnowski, **M. Wasyłeczko**, Z. Krysiak, E Łukowska „Application of 3D membranes for repair of articular cartilage defects"**,** 157th ICB Seminar on "Nanoparticles and Nanotechnology for Biomedical Engineering, Biotechnology and Medicine" w Warszawie;

7. Październik 2017, współautor wygłoszonego wykładu plenarnego: A. Chwojnowski, **M. Wasyłeczko**, Z. Krysiak, E Łukowska „Zastosowanie membrane półprzepuszczalnych w regeneracji chrząstki", XIV Szkoła Membranowa – „Od badań podstawowych do wdrożenia" w Wiśle;
8. Kwiecień 2017, współautor posteru: W. Sikorska, A. Palińska, C. Wojciechowski, G. Rokicki, **M. Wasyłeczko**, A. Chwojnowski „Receiving semi-permeable membranes from blend of stable and containing groups of esters polymers", V Ogólnopolskie Seminarium „Postępy w Chemii Boroorganicznej" w Radziejowicach;
9. Kwiecień 2017, współautor wygłoszonego wykładu plenarnego: A. Chwojnowski, **M. Wasyłeczko „**Membrany półprzepuszczalne jako rusztowania komórkowe 3D do regeneracji chrząstki", V Ogólnopolskie Seminarium „Postępy w Chemii Boroorganicznej" w Radziejowicach;
10. Październik 2015, współutor posteru: A. Plichta, T. Jaskulski, **M. Wasyłeczko**, BLOCK COPOLYMER CONJUGATES COMPRISING CAMPTOTHECIN AND BIODEGRADABLE PLA SEGMENTS, Knferencja: BIOPOL, 5th International Conference on Biobased and Piodegradable Polymers, 6-9 października 2015, udział: 0,333
11. Maj 2015, współautor posteru: A. Plichta, **M.Wasyłeczko**, A.Kundys, T.Jaskulski, ESTROWE POCHODNE KAMPTOTECYNY JAKO PREKURSORY LEKU IMMOBIOLIZOWANEGO NA MATRYCY POLIMEROWEJ, Konferencja: Chemsession'15, 8.05.2015, udział: 0,250

Nagrody

1. Czerwiec **2021** - Wyróżnienie Dyrektora Instytutu Biocybernetyki i Inżynierii Biomedycznej im. Macieja Nałęcza PAN za wyniki prac naukowych w roku 2020
2. Październik **2018**, **Nagroda Naukowa Drugiego Stopnia** przyznana przez Rektora Warszawskiego Uniwersytetu Medycznego prof. dr hab. N. med. Mirosława Wielgoś za współautorstwo publikacji dotyczącej badań nad innowacyjnym systemem terapeutycznym zawierającym kamptotecynę, mogącym znaleźć zastosowanie w terapii nowotworów:

Projekty

1. Praca magisterska została częściowo zrealizowana w ramach projektu badawczego „Opracowanie implantacyjnych systemów dozowania leku o działaniu antynowotworowym immobilizowanego na matrycy polimerowej" nr 2013/09/B/ST5/03480 finansowanego przez Narodowe Centrum Nauki w ramach konkursu OPUS
2. Praca inżynierska została zrealizowana w ramach projektu „Cukry jako surowce odnawialne w syntezie produktów o wysokiej wartości dodanej", nr POIG.01.01.02-14-102/09. Praca współfinansowana przez Unię Europejską w ramach Europejskiego Funduszu Rozwoju Regionalne